506
C215p
no. 611

c

CONTRIBUTIONS TO EMBRYOLOGY

VOLUME XXXVI
NOS. 242 TO 251

CARNEGIE INSTITUTION OF WASHINGTON PUBLICATION 611
WASHINGTON, D. C.
1957

CONNECTICUT
STATE LIBRARY
JAN 7 1958
HARTFORD
CONNECTICUT

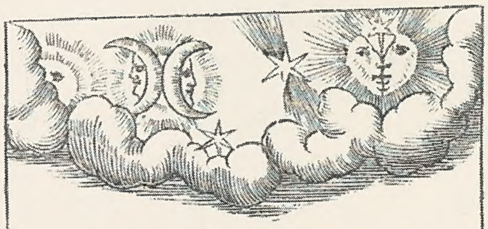

The Beckwith-Browning-Peterson
Teratology Collection

Smithsonian Libraries
2017

CONTRIBUTIONS TO EMBRYOLOGY

VOLUME XXXVI
NOS. 242 TO 251

CARNEGIE INSTITUTION OF WASHINGTON PUBLICATION 611
WASHINGTON, D. C.
1957

This book issued November 15, 1957

THE LORD BALTIMORE PRESS, INC., BALTIMORE, MARYLAND

QM
601
.C66
1915
v.36
SCDIRB

CONTENTS

PAGES

242. METHODS USED BY C. H. HEUSER IN PREPARING AND SECTIONING EARLY EMBRYOS (three plates and twelve text figures) 1–18

Described by Osborne O. Heard

243. THE PRENATAL DEVELOPMENT OF THE HUMAN TEMPOROMANDIBULAR JOINT (two plates) 19–28

Benjamin C. Moffett, Jr.

244. DEVELOPMENTAL HORIZONS IN HUMAN EMBRYOS. DESCRIPTION OF AGE GROUP X, 4 TO 12 SOMITES (two plates and two text figures) 29–39

Chester H. Heuser and George W. Corner

245. THE EARLY DEVELOPMENT OF THE TRACHEA AND ESOPHAGUS IN RELATION TO ATRESIA OF THE ESOPHAGUS AND TRACHEOESOPHAGEAL FISTULA (four plates and eleven text figures) 41–57

E. Ide Smith

246. THE ORIGIN AND DEVELOPMENT OF THE HUMAN EXTRINSIC OCULAR MUSCLES (fourteen plates and two text figures) 59–78

Perry W. Gilbert

247. THE DEVELOPMENT OF THE CRANIAL VENOUS SYSTEM IN MAN, FROM THE VIEWPOINT OF COMPARATIVE ANATOMY (six plates and eighteen text figures) 79–140

Dorcas H. Padget

248. THE DEVELOPMENT OF THE OCCIPITAL AND CERVICAL SEGMENTS AND THEIR ASSOCIATED STRUCTURES IN HUMAN EMBRYOS (four plates) 141–152

E. Carl Sensenig

249. THE FORM AND THE FUNCTIONS OF THE UTERINE BLOOD VESSELS IN THE RHESUS MONKEY (fifteen plates) ... 153–182

George W. Bartelmez

250. CHONDRIFICATION IN THE HANDS AND FEET OF STAGED HUMAN EMBRYOS (one plate) 183–192

Ronan O'Rahilly, D. J. Gray, and Ernest Gardner

251. THE DEVELOPMENT OF THE ADRENAL GLAND IN MAN, WITH SPECIAL REFERENCE TO ORIGIN AND ULTIMATE LOCATION OF CELL TYPES AND EVIDENCE IN FAVOR OF THE "CELL MIGRATION" THEORY (eight plates and seven text figures) 193–210

Roy E. Crowder

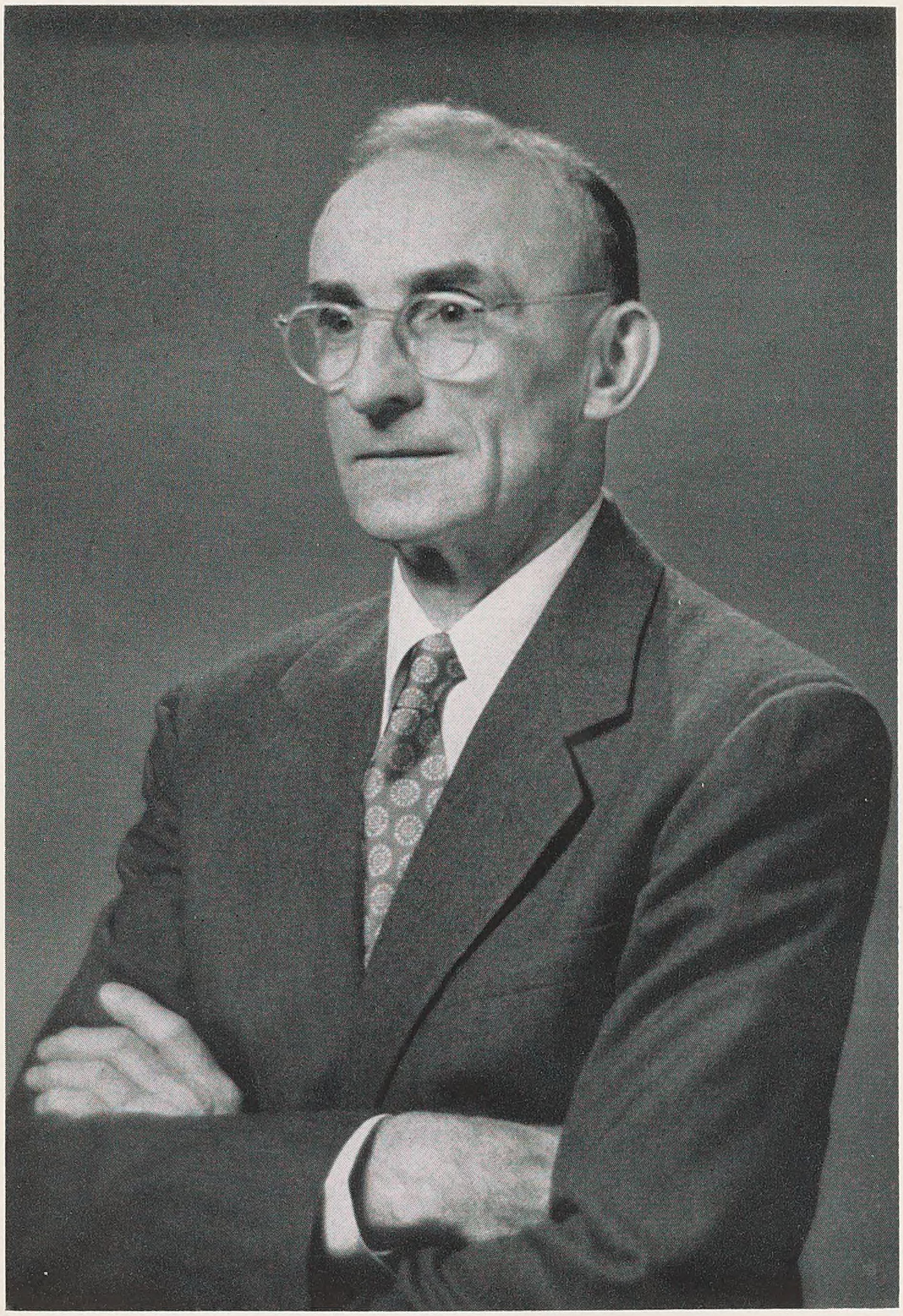

CHESTER H. HEUSER

CONTRIBUTIONS TO EMBRYOLOGY, NO. 242

METHODS USED BY C. H. HEUSER IN PREPARING AND SECTIONING EARLY EMBRYOS

Described by Osborne O. Heard

Department of Embryology, Carnegie Institution of Washington,
Baltimore, Maryland

With three plates and twelve text figures

CONTENTS

PAGE

INTRODUCTION 3

COLLECTION AND PRESERVATION OF EMBRYONIC MATERIAL 3
  Sources and Types 3
  Tubal Pregnancies 4
  Recovery of Segmenting Ova and Unimplanted Blastocysts 4
    Tubal Ova 4
      Identification of the Ovum 5
    Free Blastocysts in the Uterus 5
      Opening and Searching the Uterus 5
    Handling of Ova and Free Blastocysts 5
      Fixation 5
      Dehydration and Temporary Storage 6
      Packing Small Objects for Transport 6
  Discovery and Preparation of Implanted Embryos 6
  Dissection of the Larger Chorions 7
  Dehydration of Embryos with Mechanical Stirring 7
    Closed System 7
    Open System 9

PHOTOGRAPHY 9
  Camera 9
  Photographing Embryos 9
    Illumination 9
  Photographing Free Ova 10
    Photographic Cell 10
    Transferring the Specimen 10
    Cleaning Device 10
    Posing the Ovum 11
    Illumination 11

EMBEDDING 11
  Paraffin 11
    Very Small Objects 11
  Celloidin-Paraffin 12
    Relatively Large Specimens 12
      Boxing 13
      Clearing the Block 13
      Orientation 13
      Reference Marks (Pins) 13
      Correction of the Plane 14
    Very Small Specimens 14
      Boxing 15
      Orientation 15
    Infiltration with Paraffin 15

MOUNTING THE BLOCK 15

SECTIONING 16
  Care of the Knife 16
  Cutting 17
  Mounting the Sections 17

STAINING 18

LITERATURE CITED 18

METHODS USED BY C. H. HEUSER IN PREPARING AND SECTIONING EARLY EMBRYOS

INTRODUCTION

Readers of the Contributions to Embryology have long appreciated the remarkable technical ability of Chester H. Heuser[1] as shown not only in the preparations of early pig and monkey embryos, descriptions of which were published in collaboration with the late G. L. Streeter (1929, 1941), but also in those of human embryos, for example the perfect presomite specimen (Carnegie no. 5960) described by Heuser (1932). When, owing to the enterprise and skill of A. T. Hertig and John Rock, the Department of Embryology was entrusted with a unique series of well preserved human embryos of the first three weeks, it was indeed fortunate that Dr. Heuser was at hand to prepare and section them and, with his unrivaled practical knowledge of very early mammalian embryology, to give advice and counsel on their study.

Visiting colleagues who have seen Dr. Heuser working at the microtome and have observed the many novel details of his technique have often urged that they be described in print. Dr. Heuser's modesty and his desire for perfection, however, have deterred him from rendering this service to his colleagues. Finally, with his consent, the present account was prepared in consultation with other members of the Department. The author, who was associated with Dr. Heuser for many years, has often assisted in the embedding and sectioning of the embryos. In collaboration with Dr. Heuser, and frequently also on his own initiative, he designed and constructed much of the special apparatus used in this work. Dr. Heuser has reviewed the draft of this paper and has given his approval.

While this article was being prepared for press Dr. Heuser reached his seventieth birthday. The Staff of the Department of Embryology of the Carnegie Institution of Washington takes pleasure in presenting it in the Contributions to Embryology, which Dr. Heuser's skill has so greatly enriched, as a tribute on this occasion to the lifelong scientific devotion of a beloved colleague.

COLLECTION AND PRESERVATION OF EMBRYONIC MATERIAL

Sources and Types

Human embryonic material received at the Carnegie laboratory is of three kinds. The first group comprises specimens received from physicians outside of Baltimore, largely in response to periodic appeals circulated by the laboratory. They consist almost entirely of aborted or surgically removed chorions and of Fallopian tubes excised because of tubal pregnancy. The instructions to physicians advise that such specimens be fixed in 10 per cent aqueous formol. Although not the ideal fixative, formol is easily obtained and diluted for use. Specimens are safely kept and shipped in the same fluid without further attention. Furthermore, formol makes the tissues less opaque than do fixatives containing picric acid or mercurial salts, and thus leaves them in more favorable condition for examination and exploration.

The second group comprises specimens obtained by the gynecologists and obstetricians of Baltimore hospitals with whom the laboratory is in close touch. These collaborators are requested to telephone when they have a fresh specimen so that a messenger may be sent to bring the material for immediate attention at the laboratory. Such specimens are fixed, usually in Bouin's picroacetic formol, by the experienced personnel of the laboratory.

The third group comprises specimens obtained by special collaborators thoroughly familiar with the procedures for fixation and subsequent dehydration, who carry out these steps on the fresh material in their own laboratories. In this category are the embryos obtained by Dr. Arthur T. Hertig and Dr. John Rock at the Free Hospital for Women, Brookline, Massachusetts, and sectioned by Dr. Heuser, which have so greatly contributed to our knowledge of human development during the first two weeks.

It will be convenient to discuss first the handling of material already fixed, and the larger specimens which arrive at the laboratory in the fresh condition. These materials include naked embryos and fetuses; chorions of various sizes and in various conditions—intact or torn open; clots and decidual fragments which may contain embryonic tissues; extirpated uteri containing established pregnancies; and Fallopian tubes extirpated because of ectopic pregnancy.

The preliminary exploration of these diverse materials differs so much from specimen to specimen that only general suggestions can be given. The first step is, of course, to free the gestation sac of obscuring tissues, by cautiously opening the uterus, or by dissecting away clots and debris as the case may require. Chorions less than 5 mm. in diameter must usually be studied and handled under the microscope, as will be described below. Larger gestation sacs may be handled by the usual methods employed with biological specimens of ordinary dimensions. Chorionic sacs found in aborted clots or in intra-abdominal clots may simply be washed off with physiological salt solution, freed of adherent organized material as far as is safely possible, studied in a preliminary way, and, if small, fixed by immersion. Chorions 10 mm. or more in diameter should be opened in order to observe the condition of the embryo, and to decide whether to prepare it for sectioning. This statement applies whether the chorionic sac is obtained in an extirpated uterus or as an aborted ovum.

---

[1] Member of the Department of Embryology, Carnegie Institution of Washington, 1921–1950; Research Associate, 1950—. Professor of Microscopic Anatomy, Medical College of Georgia, 1950—.

Tubal Pregnancies

An oviduct (Fallopian tube) containing a gestation sac should always be explored with care, for a good embryo may be present; indeed, it is the tubal pregnancies that offer the best chance of obtaining human embryos in the early somite stages.

A fresh pregnant tube should be dissected at once under physiological salt solution, since fixation adds greatly to the difficulty of exploration by forming adherent, stratified clots about the chorion. If, however, the specimen has been placed in fixing solution by the surgeon or pathologist, the embryologist must do the best he can. With either fresh or fixed material, working under the binocular microscope with finely pointed forceps, needles, and scissors, he cautiously removes a portion of the wall of the oviduct so as to make a window into its lumen, and gently pulls away the clots or, when possible, dislodges them with a stream of salt solution. If chorionic villi are seen, he proceeds with great care to uncover the chorion or to locate the embryo if it has been extruded from the chorionic cavity. With a fixed specimen this operation will require patient, piecemeal removal of the clots, small bits being broken away one at a time with the needle.

The subsequent handling of the embryos will be described below, after the recovery of ova and blastocysts has been discussed.

Recovery of Segmenting Ova and Unimplanted Blastocysts

The special methods used by Dr. Heuser are primarily applicable to the material of the second and third classes mentioned above, that is, specimens obtained from local sources in fresh condition and specimens representing very early pregnancies adequately fixed before shipment to the laboratory.

The procedures to be described are naturally not limited to use with human material, but are for the most part applicable to mammalian embryos in general. In fact, they were largely worked out, in so far as they are original with Dr. Heuser and his co-workers, on other species, as will be realized by those who are familiar with the published reports of his studies, partly in collaboration with the late G. L. Streeter, on the early development of the domestic pig and the rhesus monkey. The only technique specifically designed for human material is that for opening the uterus, and even this was developed by experience with the similar though much smaller uterus of the rhesus monkey.

Tubal Ova

The human ovum, like that of most other mammals, is in the oviduct (Fallopian tube) for about three days after ovulation, and may be recovered by washing out the lumen of the tube.

The excised Fallopian tube should be brought from the operating room in physiological salt solution. The investigator holds it directly over a small dish (embryological watch glass, fig. 1) in which a small amount of the salt solution has been placed. The lumen is then irrigated with salt solution by means of a pipette with a large rubber bulb, inserted into the fimbriated end of the tube. Usually the uterine end is sufficiently contracted to cause distention of the ampulla, so that the spaces between the folds are irrigated; if the end of the tube is not contracted, it may be closed by compressing it between thumb and finger until the ampulla is slightly distended. The egg usually emerges with the first fluid that passes into the dish. The free end of the tube may whip about as the fluid is ejected; hence great care must be taken to keep it over the dish at all times in order not to lose even a drop.

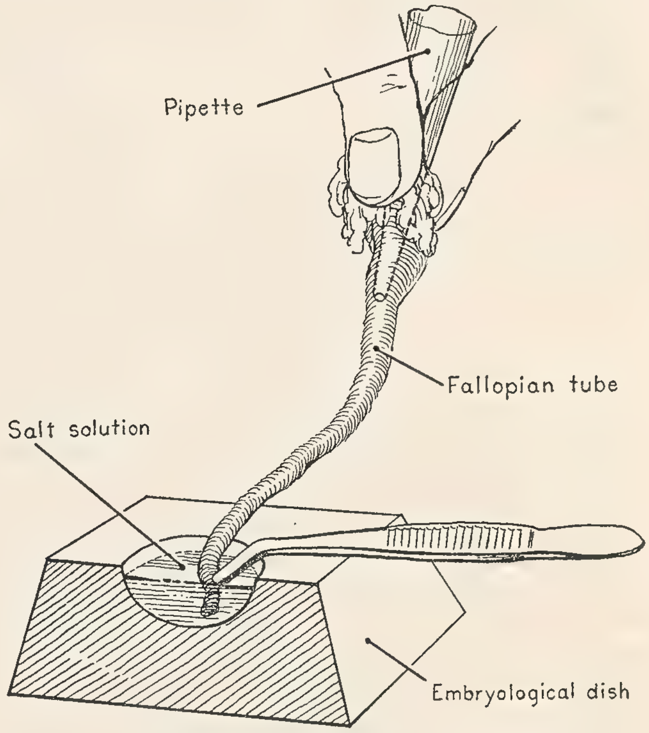

Fig. 1. Method used for recovery of tubal ova.

If the egg is not recovered at the first washing, the process is repeated. The tube may be lightly "milked" downward by the fingers, and finally a fine-pointed

DSI

pipette may be inserted into the narrow lumen of the uterine end and the tube irrigated in the reverse direction.

Identification of the ovum. The fluid in the dish, adequately illuminated from below through the bottom of the dish or by a nearly horizontal beam of light through a side, is now carefully examined under a binocular dissecting microscope at a magnification of about 20 times. The free-lying ovum is usually easy to find. As its specific gravity is slightly greater than that of the salt solution, it sinks, and the microscope should be focused first on the bottom of the dish. If there is too much cellular debris in the fluid, it may be pushed aside with a dissecting needle. The ovum when lying in a clear space in the fluid is usually identifiable, despite its small size, by its round outline, which is more regular and definite than that of any other organic material present, and also by the bright double contour presented by the zona pellucida. Degenerating segmenting ova may lose their spherical form and become ovoid or even lenticular. Often observers have been misled by the presence in tube washings of pseudomorulas formed from epithelial cells rolled into more or less spherical masses. Such masses may suggest a segmenting ovum so strongly as to require sectioning for identification, but with increasing experience it is possible to rule out most of them by inspection at a magnification of 20.

Fixation and dehydration of these very small objects are described below.

Free Blastocysts in the Uterus

The human ovum is free in the uterus from about day 4 to day 6 after ovulation; it may be recovered from the uterine cavity by the following method taught to Dr. Hertig by Dr. Heuser in 1933 and used by Hertig and others ever since (cf. Hertig, Rock, Adams, and Mulligan, 1954) at the Free Hospital for Women, Brookline, Massachusetts. The present description is based on the joint experience of the two laboratories.

Opening and searching the uterus. The uterus is washed with salt solution to remove excess blood and is placed in a flat dish. The myometrium is incised with a scalpel through the areas of attachment of both broad ligaments, on each side, from the cervix to the region of the round ligaments, the muscle of the fundus being left uncut. The incision goes down to the base of the endometrium, which at this stage is left intact. Next, the specimen is immersed in a convenient dish, in physiological salt solution, which is promptly changed if it becomes clouded by blood. The uterine cavity is cautiously entered by incising the endometrium with a scalpel and fine straight scissors, the latter being used chiefly to open the interstitial part of the tubes. The incision is made under a binocular dissecting microscope at a magnification of 3 or 4 and with strong illumination. Hertig has recommended making the first incision into the uterine cavity on the side opposite the recent corpus luteum, so that a free ovum lying near the tubal orifice through which it entered the uterus will sink into the depths of the cavity and not be lost through the first incision. When a small opening has been made, a well rounded pipette with an opening 3 or 4 mm. in diameter is inserted through it, and the fluid in the uterine cavity is pipetted off and placed in an embryological watch glass for examination under the dissecting microscope. Then the uterine cavity may be very gently rinsed by pipetting a little salt solution in and out, the washings being kept for examination. To avoid injuring an implanted embryo, the pipette should never be inserted beyond the edge of the endometrium.

Handling of Ova and Free Blastocysts

All work with ova and blastocysts is done under magnification of not less than 20, and with adequate illumination. Dr. Heuser uses an illuminator constructed in the laboratory, having a 50-watt 6-volt lamp with an adjustable aspheric condenser forming a well defined beam; it is operated from a toy transformer.

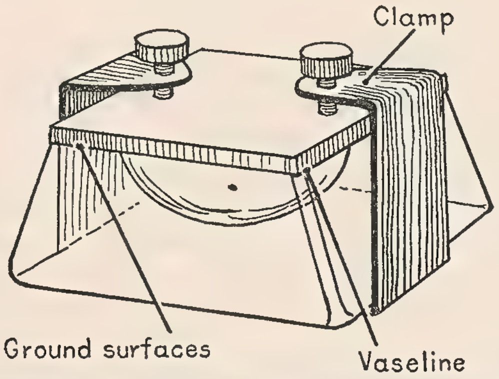

FIG. 2. Method of sealing and storing small specimens in an embryological watch glass with vaseline on ground surfaces.

The specimen under observation is transferred from dish to dish by sucking it into a pipette with a long, slender tip having an orifice at least 1½ times the diameter of the ovum and provided with a small rubber bulb.

Fixation. The specimen is transferred to a dish (embryological watch glass, fig. 2) of clear salt solution. It is fixed by gently flowing a stream of the fixing solution upon it with a pipette while it is under observation in salt solution. Gradually the salt solution is withdrawn as it is replaced by the fixing solution. The fluid mixture may be stirred by a gentle stream of air bubbles from the pipette, the ovum being watched constantly through the microscope.

With such small objects, fixation will be complete in a few minutes; 5 minutes evidently sufficed for the 2-cell egg described by Hertig, Rock, Adams, and Mulligan (1954). The fixing fluid used routinely with the Carnegie human and monkey ova is Bouin's picroacetic formol, which gives good preservation of the nuclei and cytoplasm but tends to dissolve or at least to thin the zona pellucida. Investigators wishing to preserve the zona perfectly would do well to experiment with acid-free fixatives.

Should the ovum stick to the dish because of coagulation of albuminous material on its surface, it is gently freed with a suitably fine hair. A hog's bristle is too large and stiff. For years Dr. Heuser has kept a stock of spines from an anteater skin opportunely provided by a naturalist colleague; these spines have very fine hairlike tips. He has also used a human eyelash, or a hair from a camel's-hair brush. A hair of any sort used in this way must be thoroughly wetted in the alcohol mixture to prevent it from floating unmanageably.

Dr. Hertig once made use of the adhesion by letting it hold the egg in place during preliminary dehydration and transportation from Boston to Baltimore.

Dehydration and temporary storage. These very small specimens are dehydrated by slowly dropping 70 per cent alcohol into the dish and gradually removing the diluted fluid with a pipette, the specimen being kept under observation, until the dish contains alcohol at 70 or 80 per cent concentration. A refinement of this method favored by Dr. Heuser employs two pipettes: the ovum is drawn into the stem of one; with the other, alcohol of higher concentration is added to the dish. The ovum is discharged into the dish and moved about by a pipette-driven stream of the alcohol mixture. This procedure is repeated until the concentration required for temporary storage, photography, and so forth, is reached.

Fixatives other than Bouin's necessitate preliminary washing of the specimen with distilled water, by a similar process of gradual replacement, before dehydration with alcohol.

Ova and blastocysts are best stored in an embryological watch glass with the rim ground flat; a cover of sheet glass made airtight by a layer of vaseline (petroleum jelly) (fig. 2) should be held in place with a spring clip or two small strips of masking tape.

Packing small objects for transport. Ova and blastocysts may be safely transported in glass tubes plugged at both ends with absorbent cotton. Tubes are better than vials because they can be emptied from either end; and cotton is better than cork because it is cleaner and contains no tannin, which might discolor the specimen. The tube should be about 30 mm. long, 6 mm. in diameter. The plugs are prepared by putting wisps of cotton in a dish of alcohol of the same concentration as that in which the specimen is stored. By pressing the cotton against the dish and turning the free ends of the fibers into the center with two pairs of forceps, a smooth, unraveled layer of cotton is formed on the bottom, and this face of the plug is pushed into the tube under alcohol. With a pipette the specimen is introduced well into the alcohol-filled tube, and a second cotton plug is pushed into the other end of the tube. When the plugs are in place there should be no air bubbles in the fluid. The tube is placed in an alcohol-filled stoppered bottle for further storage or transportation.

Discovery and Preparation of Implanted Embryos

If no ovum or blastocyst is recovered in the above steps, or if the clinical history or the appearance of the uterus suggests the presence of an implanted embryo, after the myometrium has been incised as described above (p. 5), the uterine cavity is opened under salt solution by cutting through the endometrium on each side, beginning at the os and working toward the fundus. The anterior half of the uterus is gently pulled away from the posterior half as the lateral cuts progress, in the hope of seeing the implantation site in time to avoid damaging it. This operation of cutting the endometrium and searching the cavity as it is exposed is performed with the aid of a wide-field microscope or a binocular loupe. Finally, the two halves of the uterus are completely separate except for the uncut fundus musculature, which should serve as a temporary hinge, the fundal endometrium being left intact as long as possible in case the implantation site is at the fundus. During the whole process the uterus is completely immersed in physiological salt solution, the fluid serving not only to keep the specimen moist but also to support the delicate embryonic tissues.

When the surface of the entire cavity is revealed, the two halves of the uterus still under fluid are oriented, with their endometrial surfaces uppermost, in the dish in which the dissection was carried out. A beam of light is directed so that it glances across the surface, and the endometrium is carefully examined for a possible small elevation or a local hemorrhage which might mark an implantation site (fig. 13, pl. 1). Once such a site is identified, its salient features are briefly noted and every special feature is sketched. The surface is then flooded with Bouin's fluid while still under salt solution, and when it has been thoroughly fixed, the half uterus is again examined under the microscope for evidence of implantation that may have been missed in the fresh condition. It is finally transferred to a dish of Bouin's fluid without exposure to the air.

It generally will be convenient to transfer the entire half uterus to 35 per cent alcohol and continue the dehydration with alcohol of increasing concentration until a strength suitable for temporary storage (70 to 80 per cent) is reached. At this stage a block containing the implantation site is cut from the half uterus (fig. 29, pl. 3). For this operation a very useful instrument is a suitably fashioned piece of razor blade mounted in a needle holder. The implantation site is photographed before the block is cut out, and the block may again be photographed after removal to show the site from various angles.

Dissection of the Larger Chorions

Chorions 10 mm. in diameter or larger are usually dissected in 80 per cent alcohol. The specimen is placed in a medium-sized Stender dish and is completely covered by the fluid. The bottom of the dish is lined with a sheet of cork cut to fit tightly and forced into place; or a removable piece of cork may be weighted by a square sheet of tinned metal placed under it with the corners of the tin bent over the cork. If the chorion is accompanied by and attached to part of the uterine wall, the specimen is fixed to the cork with fine pins (insect mounting pins are useful for the purpose) inserted through the myometrium. More delicate specimens, like naked chorionic sacs, may be held in position for dissection by means of threads, looped over the specimens and tied either to the pins or to small copper eyelets (wires with a loop at one end) stuck into the cork. With very small specimens, the ends of the threads may be held to the cork by mounds of vaseline. One end is fastened down; the specimen is posed; the thread is gently laid over the object, and pressed into the opposite mound of vaseline. Such mounds may also cradle the specimen. A 5-ml. syringe makes a convenient dispenser for the vaseline (fig. 16, pl. 1). Small blocks of glass, standing alone or supported by vaseline, may also serve as temporary supports.

Before the chorionic sac is opened, an effort is made to locate the embryo and the attachment of the umbilical stalk. Transmitted light is directed on the chorion if it is not too opaque, and gentle pressure is applied here and there over the decidua capsularis, if this is still *in situ,* or over the free surface of the chorion. An area that yields readily to such pressure is presumably safe for incision.

The incision is begun by pricking the tissue with a very fine, very sharp needle, under the dissecting microscope. None but the finest of needles will penetrate the tissue without indenting or damaging it unduly. Only the point of the pricking needle is inserted. When the needle is in position, it is held in one hand, and with the other hand a larger, blunter needle is stroked over the tissue that overlies the inserted point, producing a tiny cut. The fine needle or a favorably shaped piece of razor blade is then advanced and stroked along the incision, and the cutting is continued until the cavity of the chorion is entered. As soon as the orifice is large enough, the cavity is inspected under strong illumination. By means of a small pipette barely inserted within the cavity, loose coagula within the chorion may be gently flushed away with a stream of fluid.

When a short slit has been made it may be held open by small spreaders made from strips of cellophane, so that the hands are freed for further dissection. As soon as the embryo or yolk sac has been located, or when a clear pathway for further safe exploration is discerned, the direction in which the cutting is to proceed is planned, and thereafter the incision may be continued with sharply ground forceps and iridectomy scissors. An incision being made in a small chorion under a relatively high power of the dissecting microscope, and consequently in a restricted visual field, can be directed step by step over the whole distance by choosing under a lower power small landmarks (such as the mouth of an endometrial gland, or a small tag of tissue on the chorion) which lie in the desired direction but within the smaller field. Larger chorions are incised with fine dissecting scissors of the ordinary kind or with a razor blade.

The plan of the opening thus made will naturally be determined by the situation of the embryo in each chorion, the purpose being to open the chorion widely, so as to expose the embryo for photography and to permit excising it intact for sectioning. Usually a circular cut is made, removing a cap which may include half of the chorion. The embryo, if well advanced, is ultimately detached by severing the umbilical cord; the area of attachment containing the body stalk of an early embryo is separated from the rest of the chorion by a small circular cut in the region of the body stalk, on which a few overlying villi are left undisturbed.

Dehydration of Embryos with Mechanical Stirring

Delicate objects and tissues, such as are handled by the embryologist, require very gradual change of the concentration of alcohol in order to avoid damage. The conventional method of transferring the specimen from one dish of alcohol to another of higher concentration consumes overmuch time and attention if the changes are sufficiently gradual. For this reason the Carnegie laboratory has used with success two methods utilizing mechanical stirring and continuous change of alcohol concentration. Specimens small enough to be enclosed in a vial are subjected to mechanical stirring as follows.

Closed System

The specimen, in weak alcohol, is enclosed in a "trap," for example a glass cylinder closed at both ends with linen cloth or with aluminum foil pierced with fine needle holes (figs. 3, 4). The trap is immersed in a closed vial or wide-mouthed bottle (fig. 5) containing alcohol of higher concentration. The bottle is placed on a rack or similar device designed for holding several such vessels (fig. 15, pl. 1), and the rack is slowly rotated by a motor so that the fluids in the jar and in the inner trap are agitated and gradually intermixed through the mesh or needle holes. The advantage of the closed system is that once the specimen is placed in the trap it need not be touched again until dehydration has reached the desired point.

The rate of mixing, which is determined by the size of the holes and the rate of movement, has been arrived at empirically. When mixing is complete, there is no convection current when the two fluids are united at the end of the run. A trap of 10-cc. capacity in a 25-cc. container exchanges within 24 hours. It is convenient, therefore, to replace the alcohol in the container, once a day, with alcohol 5 or 10 per cent stronger. When absolute alcohol and ether-alcohol are reached, several changes of each, rather than one change per day, are required.

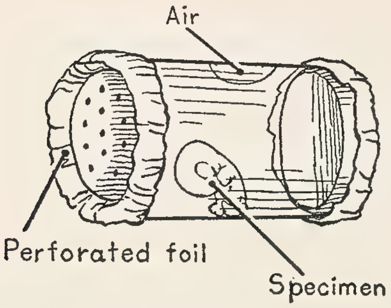

Fig. 3. Specimen trap with perforated foil and air bell.

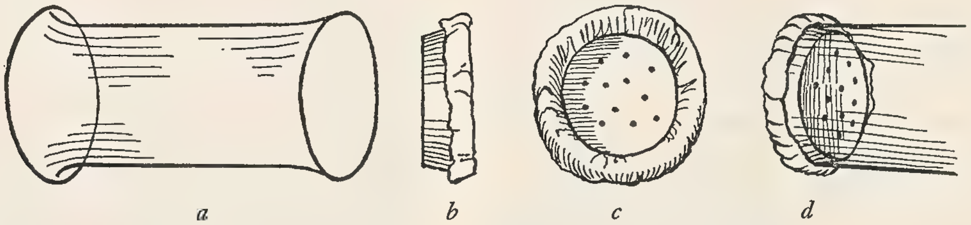

Fig. 4. Elements of a specimen trap: *a,* flared glass tube; *b,* aluminum foil cap viewed in section; *c,* end view of cap; *d,* cap in position on flared end of glass tube.

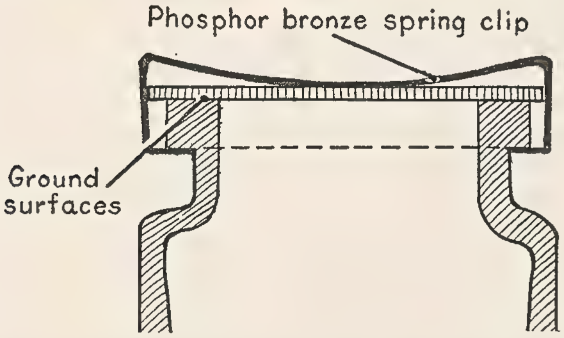

Fig. 5. Wide-mouth specimen bottle with glass closure.

Experience has shown that rotation of the rack bearing the containers at a rate of 2 to 4 times per minute will not traumatize or abrade small embryos. Figure 17 (pl. 1) demonstrates the perfect dehydration, without collapse or distortion, that can be achieved by this method.

To make the trap (fig. 4), a piece of glass tubing of suitable size is chosen; for small embryos in the limb-bud stage, for example, a piece 12 mm. in diameter and 25 mm. long will serve. The ends are flared outward by heating and reaming. Caps are made by crimping disks of aluminum foil down over the smaller end of a cork that fits the tubing easily. While the foil is still on the cork, numerous fine holes are pricked in it with a needle. The cap has the shape of a truncated cone with a skirt at its base. It is pushed into the open tube like a cork, and the skirt is crimped over the flared end. In this way the fine projections about the needle holes are aimed outward, leaving a smooth perforated surface next to the specimen. Before use, caps are thoroughly cleaned with distilled water and alcohol. The volume of the tube is measured for subsequent use in calculating the strength of celloidin during the infiltration process.

For holding a small, delicate embryo, such as one of the early somite stage with attached yolk sac, the vial may be molded by heating and indenting its walls to make rounded supports; or narrow rectangular strips of cellophane, thick enough to be springy, and slightly longer than the inner diameter of the vial, may be sprung into place at the ends of the specimen, to prevent excessive movement. Another method of immobilizing a specimen is shown in figure 6. These contrivances must be fashioned according to the size and shape of each embryo. Thus, when the vial is gently stirred by

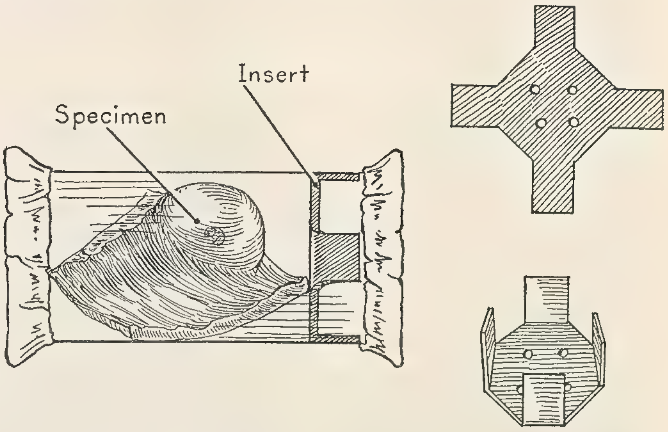

Fig. 6. Trap with plastic insert for immobilizing specimen to prevent injury during dehydration and infiltration.

rotation of the rack, the specimen can move a little, but its weight will not fall upon such delicate structures as the yolk sac or the roof of the fourth ventricle. Fluids entering through the perforated foil at the ends of the vial freely exchange with the fluid in the vial through the spaces around the embryo and the supporting bosses and strips.

The cleaned trap, closed at one end, is placed in a dish containing the specimen in alcohol of known concentration. The specimen is coaxed into the open end, which is then closed. If the transfer is properly made under fluid, there will be no air within the trap; if desired, however, a small bubble may be introduced by a capillary pipette through one of the perforations in the foil or through a mesh of the linen cap.

Open System

In this method, no longer much used, the specimen lies at the bottom of a jar, in an alcohol solution stirred by a motor-driven glass plunger moving in a perforated glass cylinder. Alcohol of a higher percentage drips into the jar at the rate of about one drop per second, the rate being controlled by a plug of cotton packed against indentations in the drip tube.

An intermittent siphon drains excess fluid from the jar. The entire assembly is enclosed in a dust-proof cabinet, except the motor, which is mounted outside. The stirring action is varied by a simple eccentric mechanism on the motor shaft.

This method is subject to loss by evaporation, especially with strong alcohols and alcohol-ether.

PHOTOGRAPHY

Camera

Ova and embryos are photographed with a camera and stand (fig. 14, pl. 1) developed at the Carnegie laboratory to meet its specific requirements. An early form of the apparatus first used by Dr. Heuser has been described and illustrated by Heuser and Streeter (1929); its final form, constructed by O. O. Heard, was reported by Heuser and Heard (1942). The camera is mounted vertically on a hinged support; below it a binocular microscope is so mounted on a pivot that the microscope and camera may be moved alternately in and out of position on the optical axis of the camera. The essential feature of the apparatus is the ability to position the specimen in the pivotal plane. The swinging microscope is set to focus on this plane, and the level of the camera front (lens board) is adjustable. Lens adapters are interchangeable and designed for parfocal adjustment through the range of lenses used, so that, no matter which lens is selected, the camera when in position will be nearly in focus in the same plane.

The specimen, mounted on a stand which can be raised and lowered by a screw, is brought into the focal plane by adjustment of the stand. Thus the specimen may be posed and the lighting arranged with the aid of the microscope (fig. 24, pl. 3). The microscope is then swung away and the camera is swung into position. Now the image of the specimen falls centrally on the photographic plate and is approximately in focus.

To permit stereoscopic photography, the camera is pivoted at its focal point. By this means it can be tilted laterally, without going out of focus, to positions right and left respectively of the vertical, at the proper angle to yield correct stereoscopic fields.

Magnifications from less than 1 to 50 are obtained by means of photographic objectives (for example, Micro-tessars). The camera is provided with stops and template rods to facilitate the use of various lenses to obtain precise magnifications. For magnifications above 50 the compound microscope is used; stereoscopic photography by tilting the camera is then hardly feasible.

Photographing Embryos

For photographing embryos by reflected light, a Stender dish is set in half a Petri dish, which serves as a moat to catch spilled alcohol. If a light background with a shadow of the specimen is desired, a piece of opal glass is placed in the bottom of the dish, and a disk of clear glass is mounted at a short distance above it. It may be convenient to put the opal glass in a small Petri dish inside the Stender dish and let the rim of the Petri dish support the clear glass. The extent of the shadow cast on the opal background depends on the distance between the clear and the opal glass.

The specimen is carefully freed of small specks of dirt and organic debris with a camel's-hair brush and a cleaning pipette as described in the next section. It is put in the Stender dish, which is placed on the focusable stand of the camera mentioned above (fig. 14, pl. 1), and is posed under the binocular microscope of the photographic apparatus. To immobilize and support the embryo, small mounds of vaseline are extruded from a small syringe (fig. 16, pl. 1) onto the glass bottom plate. The vaseline may be built up to the right height and molded with needles until the embryo is in the desired pose. The dish, completely full of alcohol, is then covered by sliding a flat glass plate over it, excluding all air.

Illumination

Two focusable spotlights are desirable, one to provide the general illumination and the other at a somewhat greater distance to balance the shadows and bring out particular details. Diffusing plates of ground glass may be interposed (fig. 24, pl. 3). The use of two lights has replaced a former practice of mounting a curved reflector of white paper in the dish near the specimen, to balance the light of a single lamp. A glancing beam is effective for showing fine details, as on the surface of a blastocyst, or for emphasizing surface modeling of an embryo.

Transmitted light has been used in photographing cleared specimens (to show the skeleton or injected blood vessels, and so forth) with the aid of a special condenser held horizontally in a modified microscope stage.

PHOTOGRAPHING FREE OVA

Photographic Cell

A cell (fig. 7) is prepared from an ordinary slide (1 inch by 3 inches), a square cover slip, and four small glass slips made by cutting a cover slip into narrow strips. A square area somewhat smaller than the whole cover slip is marked off on the middle of the slide by extruding a line of vaseline from a syringe. The small strips of thin glass are pressed down onto the vaseline and covered with a second line of vaseline. The slide is placed in a shallow finger bowl and covered with alcohol of exactly the same concentration as that in which the ovum is stored. The concentration can be tested by adjusting the dilution so that no diffusion currents are produced when a drop of one alcohol mixture is placed in the other. If the two mixtures were not alike, the egg might be lost by spinning away in the diffusion current.

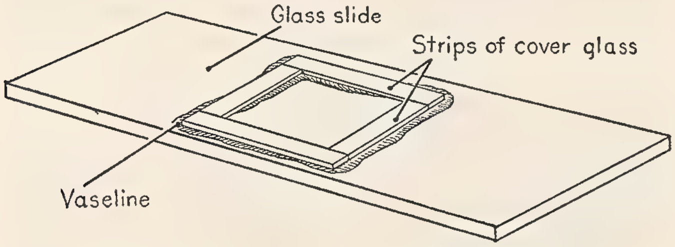

FIG. 7. Special mount for free ova built on a 1 by 3 inch slide, composed of pieces of glass cover slip and vaseline.

Transferring the Specimen

If the ovum is stored in a dish rimmed with vaseline and covered with a glass plate, the lid must be partly slid off (the operator watching the egg through the microscope) so that a little of the fluid can be pipetted off to prevent alcohol and the egg from flowing over the rim of the dish.

Any spicules of dirt near the egg are cautiously removed under the microscope. For transferring ova a glass pipette with a long narrow tip is used. It is chemically cleaned and rinsed with distilled water and with alcohol of the same concentration as that in the dishes. The tip is partly filled with alcohol by suction; it is then put into the dish containing the egg, a drop or two of alcohol is extruded, and under the microscope the tip is brought up to the egg. The egg is sucked into the pipette by lightly releasing the bulb. It is kept in view through the wall of the pipette at all times. If the pipette is chemically clean, the egg will not stick in it; if it does stick, gentle pressure on the bulb may release it. If not, the pipette is scored with a diamond pencil and broken off at a safe distance from the egg, which may then be freed by a hair inserted into the tip.

Before the ovum is transferred to the specially prepared cell, the cell is examined under the microscope to make sure that the area within the square is free from dirt. A cover glass is placed on the end of the slide ready for use; it should be slightly smaller than the width of the slide, to lessen the danger of accidental dislodgment in subsequent handling. The ovum is ejected from the pipette into the cell. The cover glass, picked up with forceps, is held at one side by a needle and gently lowered onto the top of the glass-rimmed square, and is pressed down to ensure that the vaseline seal is complete (fig. 8).

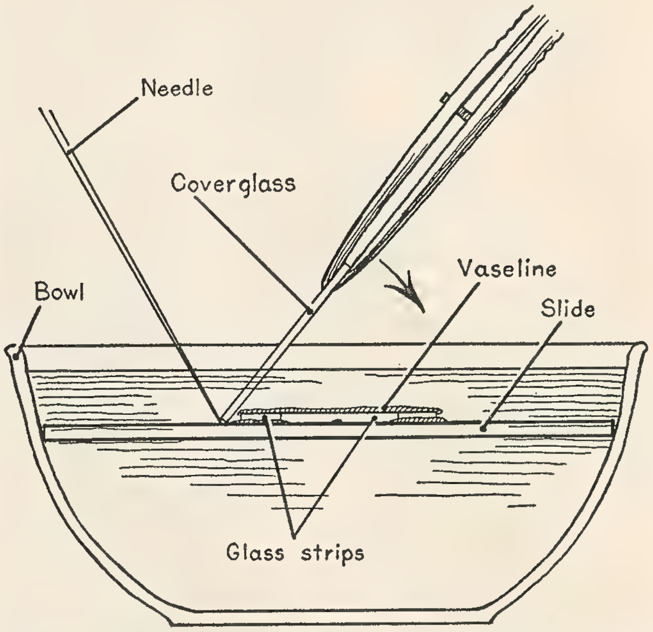

FIG. 8. Method of transferring egg to special mount totally submerged in a glass finger bowl.

The slide may now be lifted out of the bowl. Excess alcohol is blotted off, and the slide is ready to be placed under the photographic microscope. The egg may be kept safely in the cell, for days if necessary, until microscopic study and photography have been completed, by simply reimmersing the cell in the bowl of alcohol when it is not in actual use. The bowl should be covered and sealed with vaseline against evaporation.

Cleaning Device

A useful device for removing small particles of foreign matter from the vicinity of an ovum or from the surface of the specimen itself is a thin-walled glass tube (3-mm. bore), drawn out at one end to form a fine capillary tip which is bent at 45°. The other end, serving as handle, is fitted tightly with a cork and is provided with a rubber tube. With this pipette, particles of debris can be flushed away or picked up by suction. When not in use the delicate pipette is protected by putting it tip down into a 50-cc. bottle so that it is held by the cork.

Posing the Ovum

Positioning very small, round specimens such as segmenting ova and blastocysts presents difficulties, because the specimen is necessarily mounted in a closed cell for photography under the compound microscope. Trial-and-error methods must be used. Experience shows that an egg tends to rest in one position in the cell but can be moved by various means. The slide may be removed from the stage and cautiously jolted or tilted, the result being checked with a hand magnifier. A bubble in the cell may be efficacious in moving the ovum about. A bubble may be deliberately left when the specimen is first mounted in the cell; or, by submerging the slide in the finger bowl and slightly displacing the cover slip, a small air bell may be introduced with the cleaning pipette. When the slide is tilted the bubble will move the egg.

Illumination

Very small objects, like unsegmented and segmenting eggs, are usually best photographed with transmitted light. Sometimes a modified dark-field illumination reveals details of single cells in morulae with as many as 8 cells. Later stages yield better results with reflected light, either vertical or glancing, as determined by trial. A spotlight with focusable beam is essential. Negatives are made with differing poses and illumination in order to record the totality of details that cannot be shown in any one view.

EMBEDDING

PARAFFIN

The ordinary paraffin method has been employed at the Carnegie laboratory for small embryos and will no doubt continue to be used in special cases, although double embedding in celloidin and paraffin is now preferred for the more valuable specimens.

The procedures in paraffin embedding are the conventional ones, except that the apparatus and instruments are adapted to the individual handling of small, delicate, and very valuable specimens requiring accurate orientation for serial sectioning.

Specimens of relatively large size (5 mm. or more) after being photographed are carried through the later stages of dehydration (80 per cent to absolute alcohol) in the mechanical apparatus described above. They are then transferred by hand. Binocular microscopic observation is essential while very small embryos are being transferred from dish to dish; otherwise, there is real danger of losing them. Such transfers may be made by pipette, improvised spoons, or cups so that specimens may at all times be totally submerged and observed with convenient magnifications, as in figure 9. Orientation in the paraffin block is accomplished by the usual method: when the paraffin is on the point of congealing, the specimen is placed in the desired position, in the dish or paper box to be used for embedding, by means of an electrically heated copper needle.

Very Small Objects

Segmenting ova can be more easily kept under observation during transfer through the alcohols and embedding if they are deeply stained with eosin after the *in toto* photographs are made. Drops of alcoholic eosin may be added to the dehydration alcohol at any stage, preferably as soon after photography as possible.

During the infiltration with paraffin and the actual embedding, heated instruments are required, and convenient apparatus (fig. 9) must be at hand to keep the paraffin liquid and at the proper temperature. A brass or copper plate, electrically heated and thermostatically controlled at a constant temperature, is supplemented by overhead heat by radiation from electric bulbs. Over one end of the warm plate a binocular microscope is placed so that the dish and specimen can be observed and all transfers from one fluid to another made directly under the lenses. The eggs are transferred in a pipette wound with resistance wire and heated by electric current closely regulated to keep the contained paraffin at the melting point.

The eggs are embedded beside a small piece of stained tissue which serves as a marker. The piece is cut from some soft tissue large enough to be plainly visible to the unaided eye. It is first embedded in the usual way in a small mass of paraffin which is allowed to harden. When the egg is ready for embedding, the paraffin is melted with an electrically heated copper needle, bent at an angle of 45° a few millimeters behind the working point, until the marker is almost free, and the egg is deposited close to one end of it. If the electric needle is carefully used, there is little danger of superheating the paraffin and thereby injuring the specimen, since it rests upon the congealed paraffin in a layer barely above the melting point. The orientation cannot be accomplished with the copper point of the same electric needle that melts the paraffin because the heat might injure the specimen if the needle should touch it, and moreover the hot needle causes eddies in the melted paraffin which might dislodge the egg from the desired spot. A very useful embedding tool is one provided with two working points, one hot and one warm. It is made by soldering at the bend of the copper point a short piece of fine German silver wire, bent in the same plane but in the opposite direction, so that a gap of 1 or 2 mm. separates the two points. The specimen is oriented with the silver point, which does not conduct the heat as well as copper and is not hot enough to melt the paraffin. Should the paraffin begin to congeal around the egg too soon, the instrument is rotated and the copper point quickly liquefies it again. Sometimes a loop of resistance wire heated by passing the electric current through it is mounted on the arm of a lens holder equipped with a rack and pinion, and so placed as not to touch but to rest just above the embedding mass of paraffin. By regulating the distance between the loop and the specimen, the depth to which the paraffin melts can be controlled; and by manipulation with a needle passed through the loop, the egg can be accurately placed in relation to the marker. As long as the paraffin is melted, the egg can be seen sufficiently well under the microscope to permit placing it in the correct position. The marker can be seen even after the paraffin congeals. The block is secured in the microtome so that the marker lies between the knife and the object. Sections are cut until the first part of the marker is reached, and these are discarded. The remaining part of the block is then cut; the sections containing the specimen itself are located by inspecting the ribbon with a microscope, and these alone are mounted.

CELLOIDIN-PARAFFIN

Relatively Large Specimens

Years of experience in the sectioning of mammalian embryos have resulted in preference for double embedding in celloidin and paraffin. This method protects fragile tissues against the risks of loss of sections and of fragmentation that occur with paraffin alone. A low-melting-point paraffin can be used. Furthermore, the celloidin-paraffin method, as will appear below, is essential in Dr. Heuser's procedure for orientation of embryos. The double embedding facilitates the wet-knife method of sectioning, which reduces compression in cutting.

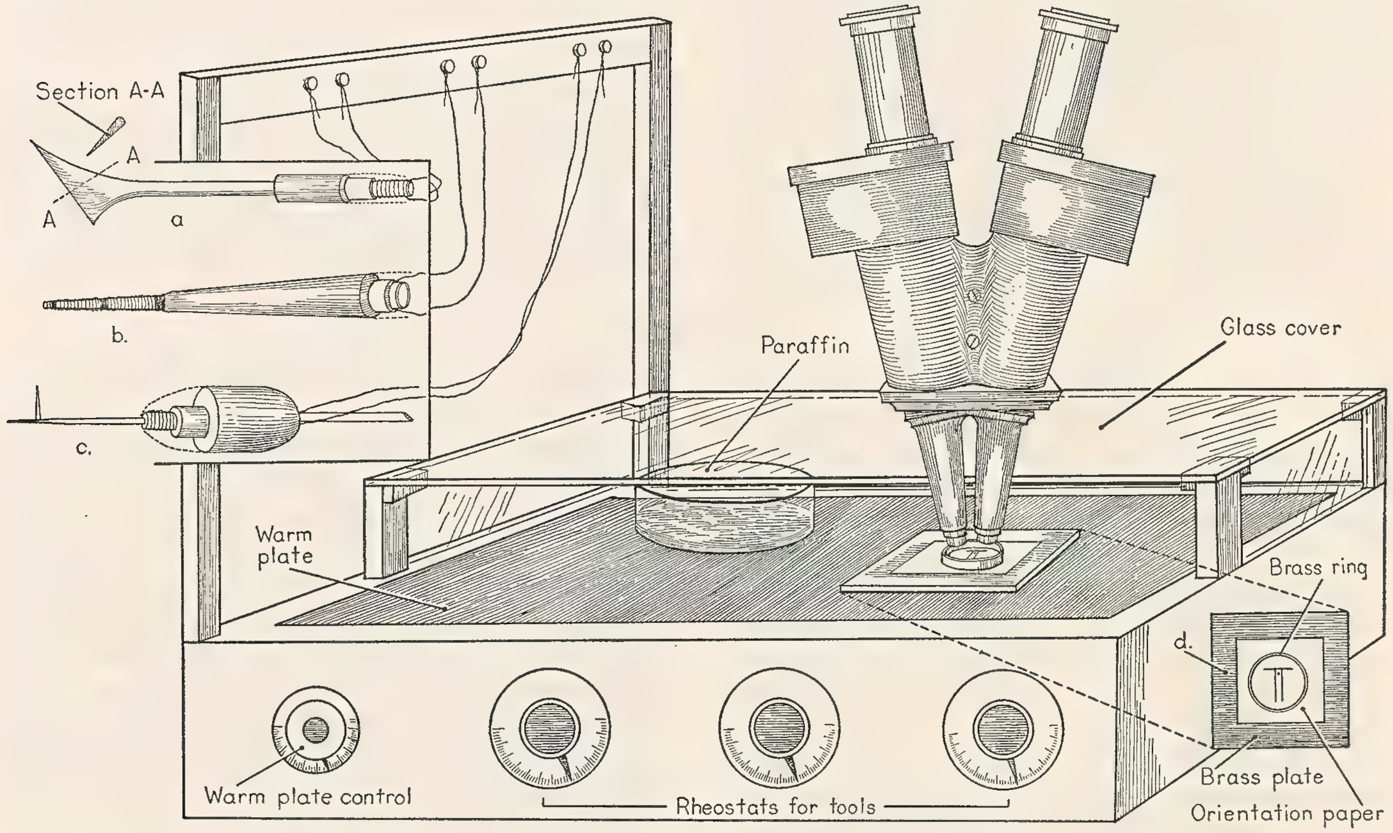

FIG. 9. Warm plate with electrically heated instruments and controls arranged for microscopic examination while specimen is being embedded in paraffin.

Celloidin-paraffin embedding in its practical aspects was introduced to Dr. Heuser in 1931–1932 by a guest investigator, Dr. Peter Mihalik, who had familiarized himself with the method in Europe. Experience has suggested various modifications.

After the specimen has been photographed, it is dehydrated and carried into the ether-alcohol mixture (equal parts ethyl ether and absolute ethyl alcohol) by means of the mechanical agitator described above. At this stage, support of the more delicate embryos by molded vials and by cellophane retaining strips is especially desirable.

Celloidin is added in solid form to the ether-alcohol and allowed to dissolve, so that the concentration is raised very slowly and infiltration is gradual.

The celloidin currently used at the Carnegie laboratory is prepared by the Mallinckrodt Chemical Works, St. Louis 7, Missouri. The chips are washed in absolute alcohol, inspected, dried on filter paper, and stored in a clean glass-covered dish.

The volume of the vessel in which the embryo is to be infiltrated (see next paragraph) having been ascertained, enough of the clean celloidin is weighed out to make an 8 per cent solution when dissolved in the contents of the vial. The proper amount of celloidin is divided into four approximately equal parts for successive addition.

The vessel used by Dr. Heuser is a small, wide-mouthed specimen bottle. The opened end is ground flat and sealed with a glass plate held in position with a metal spring clip. A circular sheet of cellophane is shaped over the small end and the sides of a cork with a hot spatula, to form a basket, which is perforated with numerous holes in its end and wedged into the neck of the bottle. This arrangement is suitable for all except the very smallest specimens, which are more conveniently handled with a miniature rocking device described on page 14. One-fourth of the weighed celloidin is placed in the vessel, to be gradually dissolved in the ether-alcohol as the fluid is gently stirred by the machine. When the first quarter part of the celloidin is dissolved and the embryo is, therefore, in a 2 per cent solution of celloidin, another quarter is added, and so forth until the desired concentration of 8 per cent is reached.

Boxing. A rectangular box, open at the top, is made of cellophane sheeting by folding a piece of the requisite size around a wooden block. The corners of the box are pressed flat with a warm knife blade, any fullness at the sides of the box being pressed toward the corners. The cellophane used at the Carnegie laboratory is du Pont MST-3W; any other transparent plastic sheeting should be tested to make sure that it is not soluble in alcohol-ether or in chloroform. A dish with a neatly fitting cover is chosen, a little larger than the cellophane box, and a small amount of alcohol-ether is placed in it. The cellophane box is put into the dish and is partly filled with 8 per cent celloidin. The embryo may then be transferred to the box from the vial in which it was infiltrated, with a little dipper made of foil. Dr. Heuser prefers, however, to pour the contents of the vial gently into the box, letting the embryo be carried with it. Here again the embryo must be submerged at all stages of the process in order to avoid unequal pressure and consequent deformation.

The dish is covered to allow air bubbles to rise to the surface and be dispelled by the alcohol-ether vapor from the layer in the bottom of the dish. The alcohol-ether is then pipetted off and chloroform is substituted, or the box is lifted to another covered dish containing a little chloroform. When the celloidin begins to congeal under the influence of the chloroform, the box may be tilted and held at various angles, so that the embryo is coaxed into the desired position and finally held there when the celloidin becomes firm enough to prevent it from sinking. Use of a needle or other tool at this stage would introduce ineradicable bubbles and thus ruin the block. There should be clear celloidin on all sides of the embryo to a thickness of 6 mm. or more, to allow for trimming of the block. Considerable time and patience must be devoted to this tedious maneuvering of the specimen into correct position.

Clearing the block. The celloidin block is left in the dish in chloroform vapor until it is hardened throughout, usually overnight. It is then cleared in several changes of cedarwood oil or oil of pine. It may be stored indefinitely in either of these clearing oils.

Orientation. The specimen will, of course, have been oriented in the block as accurately as possible. Orientation is a relatively simple matter if the long axis of the embryo is observable and if the head form, limb buds, and other externally visible features are available as aids. A block of uterine wall containing an implantation site can be oriented with reference to the edges and surface of the block. A small intact chorion, on the other hand, presents no such information. The general position of the early embryo or germ disk within the chorion may be ascertained by observations during the first preparation and subsequent observations of the specimens, for instance by transilluminating the chorion and noting the shadow of the germ disk, body stalk, or yolk sac. By relating this information to small details of the surface, some degree of approximate orientation will have been attained. If no inner structure has been seen, it may be useful to orient the block with reference to the longest axis of the chorion. The germ disk usually but not always lies at the deepest point of the chorionic cavity.

When the block is to be mounted it is studied with the microscope under clearing oil. Trying various powers of the microscope, illuminating the block from various angles, and studying it in many positions, the embryologist takes note of all available clues that may enable him to choose the most advantageous plane of section. In this part of the task previous experience is extremely helpful. Dr. Heuser's conspicuous success in cutting the Hertig-Rock embryos and other early specimens has depended upon his accumulated knowledge of the form of young embryos and their situation within the chorion. Even he, however, is not able to determine the exact plane for sectioning an embryo of the presomite or early somite stage in the intact chorion. Assurance is possible only if the chorionic cavity is opened.

Reference marks (pins). When after careful study the plane of section has been decided upon, it is marked by inserting two pins through the celloidin block at right angles to each other, in planes parallel to the proposed plane of section, far enough apart so that they do not strike each other, and at a safe distance below the embedded embryo (fig. 25, pl. 3).

The pins are the thin, stiff kind employed by insect collectors. The points are shortened by grinding so that they can be pushed through the celloidin without risk of accidental diversion caused by bending of a long, finely tapered point; but the shortened points must be made sharp to avoid cracking or distorting the celloidin. One of the two pins is bent at a right angle near the head to distinguish it from the other.

The block is held with forceps in a dish of clearing oil, and, while the embryo is closely observed under the dissecting microscope, the two pins are pushed through the block, one at a time. If the specimen is not very symmetrical, it may be difficult to place the pins suitably. Dr. Heuser frequently pushes short pins part way into the block as temporary marks before inserting the two long pins.

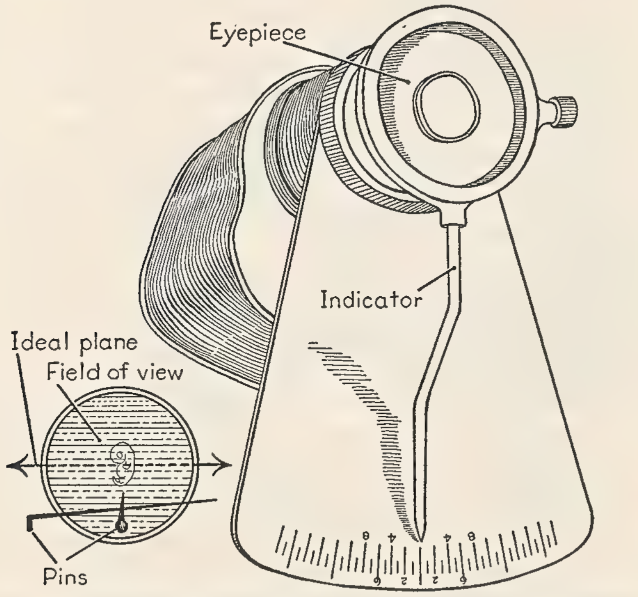

Fig. 10. Wide-field binocular microscope goniometer for measuring the angles of orienting pins in relation to a predetermined plane of section.

Correction of the plane. The placement of the pins is checked by restudy of the block under the dissecting microscope, with reference also to whatever notes and sketches the embryologist has made while choosing the plane of section. After much experience Dr. Heuser has found that he can usually place the pins within 2° to 3° of the desired plane.

Errors in placement must now be measured (as will be described in the next paragraph) and recorded in order that they may be finally corrected when the block is mounted on the carrier of the microtome. If there is an obvious error (6° or more), however, it is best to withdraw the incorrect pin and reinsert it, because compensating for an error of this size by tilting the block may displace the second pin from its position in the correct plane.

Small errors of placement are measured with a special goniometer (fig. 10) consisting of a brass plate mounted on one eye tube of the dissecting microscope just below the eyepiece and projecting fanwise laterally. An arc at the far end is graduated in degrees, and a pointer is fixed to the eyepiece. As the eyepiece is rotated, the amount of rotation is read on the arc. In the eyepiece is a glass disk engraved with a single fiduciary line or a grid of parallel lines. The block being at rest in clearing oil under the microscope, the fiduciary line is placed in the desired plane, then rotated until it is aligned with the pin, and the angular correction is recorded. By another observation at right angles to the first, the error of placement of the second pin is also recorded. The record consists of a careful diagram showing the block, the embryo, the two pins, and the respective corrections. Before the development of the home-made special goniometer, similar corrections were made by projecting the images of the embryo and the pins with a camera lucida onto ruled paper, on which the correction angles could be measured with an ordinary protractor.

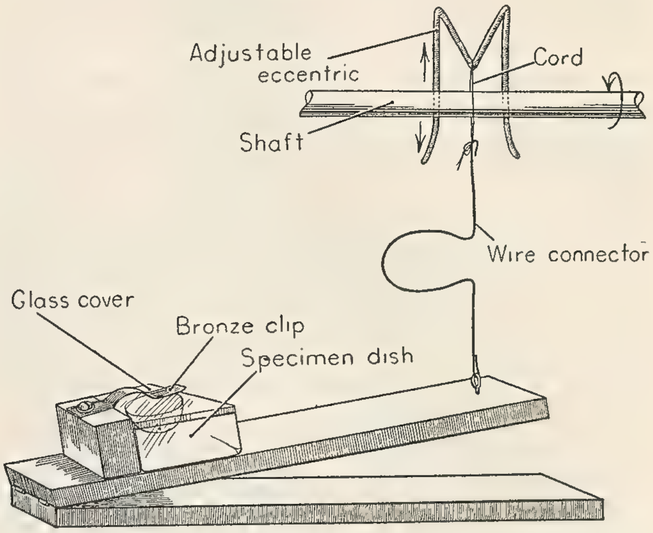

Fig. 11. Device for infiltration by mechanical stirring, with a simple adjustable eccentric and wire connector to facilitate adjustments.

With angles of less than 6° of arc, the subsequent correction of the error of one pin will not materially displace the other pin if it is in the correct plane.

Very Small Specimens

Very small objects (ova and blastocysts) are infiltrated in an embryological watch glass. To the ether-alcohol mixture in which they lie, celloidin is gradually added, either as drops of a thick solution or as small, dry chips. To facilitate solution and uniform mixture the dish is placed on a small motor-driven rocking apparatus resembling a miniature seesaw (fig. 11). The rate and magnitude of rocking are controlled by a cam revolving at a selected speed. The watch glass is provided with a cover tightly clamped to its upper ground surface (fig. 2) and sealed with dilute celloidin. When the desired concentration (8 per cent) is reached, the specimen remains in it for 48 hours, after which it is boxed and the celloidin is hardened.

Boxing. A cellophane box of suitably small size, constructed as described above, is placed in a covered dish containing a little ether-alcohol. The box is filled with celloidin of exactly the same concentration as that finally attained in the dish in which it has been infiltrated; a difference of concentration at this stage might damage a delicate specimen by collapsing or tearing it. To this box the ovum or blastocyst is transferred by a pipette of adequate bore, care being taken to avoid getting bubbles into the celloidin. The dish is covered for a few minutes to allow trapped air to escape. It is not safe to put a drop of ether-alcohol on the surface of the celloidin to dispel bubbles because of the danger of altering the concentration and thus causing collapse of delicate structures.

The alcohol-ether is removed and chloroform is substituted, or the box is transferred to another dish containing chloroform, until the surface has congealed. The tedious but essential task now begins, to get the specimen positioned centrally in the celloidin block, or at least well away from any surface. The method is the same as described above for larger specimens: turning the box over and over, letting the ovum sink in one direction and another until the position is fixed.

If the specimen does not settle rapidly enough, an air bubble may be introduced by pricking the bottom of the box with a needle. The bubble may then be used to push the ovum into a favorable position; once the specimen is in the center of the mass, the bubble will float up and away from it. The location of the specimen (if it is large enough to see clearly) and its preliminary positioning in a suitable plane may be controlled by observation under the dissecting microscope.

When the celloidin is hardened throughout, the box is left in chloroform, usually overnight, and is then cleared in oil of cedarwood or oil of pine.

Orientation. Very small specimens are oriented like larger embryos, the block being trimmed if necessary to a size that will permit observation under sufficiently high powers of the microscope for accurate orientation. Dr. Heuser was able thus to cut sections of the 2-cell Hertig-Rock ovum, Carnegie no. 8698, at right angles to the cleavage plane and through the nuclei of both blastomeres.

If the specimen is so small that it will be invisible after the block is infiltrated with paraffin, a third pin is inserted above it, the distance between specimen and pin being measured with an eyepiece micrometer and recorded. When the microtome knife reaches the track of the pin, the embryologist will know how far he has to go before the object is reached.

Infiltration with Paraffin

When the preliminary orientation procedure has been completed, the celloidin block is roughly trimmed at top and sides with a razor blade. It is then passed through three changes of toluene and one of paraffin-toluene mixture, which is fluid at room temperature. This part of the procedure can be carried out on the mechanical agitator. The actual infiltration in three successive changes of paraffin is done in dishes in the paraffin oven. The block is placed in a small, perforated metal tray suspended from a lever by which it is slowly lifted up and down in the paraffin bath. The lever is operated by a camshaft revolved by an electric motor outside the paraffin oven.

When infiltration is complete, the block is removed from the paraffin bath and put into cold running water to harden the paraffin.

MOUNTING THE BLOCK

The block is now to be mounted on the carrier post of the microtome so that the knife will traverse it in the plane indicated by the two pins. A special post holder (designed and constructed by O. O. Heard), which replaces the usual adjustable holder, permits the specimen to be placed in the predetermined plane. This special holder is an accurately machined metal block with a vertical hole into which the post, a steel cylinder 12.5 mm. in diameter (shown in fig. 12), fits and is clamped by a setscrew, thus being held on the microtome in a fixed vertical position. By means of the apparatus next to be described, the specimen is adjusted to the correct position for cutting, when the celloidin-paraffin block is attached to the post.

The positioning apparatus is shown in figures 26, 27, 28 (pl. 3). It consists of a base (fig. 27), in which the post is held vertically by a setscrew, and of a bracket mounted on an arm clamped to the post after the post is positioned. The bracket carries at the top an arm which terminates in a plate borne on a universal joint by which the plate may be set in any desired plane. In the latest model, Dr. Heuser has fitted a built-in protractor by which the plate may be accurately set at the proper angle.

The celloidin-paraffin block is temporarily attached at its top (the end which is to be struck first by the knife) to the movable plate by embedding short pieces of copper wire in the top of the block and then in a bed of paraffin on the plate.

The position of the plate is now adjusted so that each of the orienting pins is brought into a plane at right angles to the vertical axis of the post: first, the pin is positioned in line with the horizontal line of the protractor; then the small angular correction, called for by the measurements previously made when the pins were inserted, is introduced with the aid of the protractor, the plate being moved so that it deviates from the base line of the protractor by the required angle.

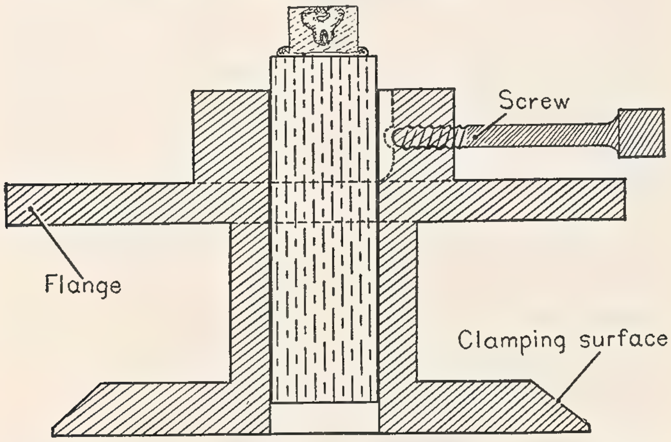

Fig. 12. Special post holder, designed for a no. 860 Spencer Precision microtome, and used in conjunction with goniometer and positioning device shown in figures 21, 22, and 23 (pl. 2).

When the block has been placed accurately, the base is removed. The post, on top of which a layer of high-melting-point paraffin has been fused, is freed by releasing the setscrew on the main arm, and is pushed up until it touches the bottom of the block. To this it is fused by melting the paraffin with a warm needle or small blade.

Before being sectioned, the block is accurately trimmed in a mechanism (devised and constructed by O. O. Heard) consisting essentially of a small sledge microtome modified by fastening a flat metal plate to a sliding knife block. Through a square notch in the front edge of the plate the celloidin-paraffin block is presented for trimming, the post to which the block is fused having been fixed in the object carrier of the microtome. A short microtome knife in a suitable holder is pushed manually along the flat plate to plane off the block as the block is racked upward by the ratchet wheel and screw of the microtome.

The object holder of the microtome is modified so that it bears two sockets for the post. One of them (fig. 18, pl. 2) presents the top of the block for trimming; the other presents the block horizontally, so that its vertical sides may be trimmed (fig. 19, pl. 2). This socket assembly is mounted on a disk which can be rotated through 360°; the disk can be held at 90° intervals by a spring stop, so that accurate trimming of each of the four sides of the block in succession is possible. When the excess celloidin-paraffin has been removed, only enough being left to support the object, one corner of the block is slightly chamfered by a cut at a 45° angle to the sides. The cut serves to mark one corner of each section as a guide in arranging the sections on the slide in case any of them is accidentally turned around or turned over. The diagrams previously made after placement of the pins are consulted in choosing which vertical angle of the block is to be so marked, and the choice is recorded on the diagrams.

The post is taken to the sectioning microtome and fixed in the socket of the rigid carrier block previously mentioned. As a result of the various maneuvers just described, the block is now properly positioned for sectioning in the desired plane.

SECTIONING

The doubly embedded blocks are sectioned on a sliding microtome, by the "water-on-the-knife" method introduced by the late Professor Carl G. Huber, of the University of Michigan. The only previously published description of this valuable method appears to be a brief account by Heuser in McClung's *Handbook of Microscopical Technique* (1929, 1937).

Care of the Knife

The cutting edge of the knife must be well sharpened. The condition of the surfaces as well as of the facets of the knife is also very important, for in the Huber-Heuser method the upper surface must be wet to the very edge, while the lower surface is dry so that water will not flow onto the block. In the practice of the Carnegie laboratory, as will be described in another paper, there is a special reason for keeping the block dry, namely the photographic recording of its upper surface for orientation purposes.

The considerable experience acquired by the author of this article, in the sharpening and surface treatment of microtome knives to meet the above requirements, and also to aid in reducing distortion in section cutting, has been recorded in a recent publication (Heard, 1953).

For cutting serial sections of embryos, the knife is sharpened and surface-treated as outlined in the article just cited. The condition of the edge is checked under the microscope at a magnification of 100, and a record of any small nicks that may remain is made on a strip of paper fastened along the knife. The record is filed with the knife until needed.

The knife is mounted so as to make a slicing cut with the edge at an angle of about 45° with the direction of movement, and at a rake angle of about 60° with the plane of section. With the paper record in position, the knife is set so that nicks will not traverse the block. It is helpful though not absolutely necessary to spread a drop of Mayer's albumen fixative over the portion of the upper surface of the knife that is to be used; it serves as a spreading agent for the fluid used to wet the knife.

CUTTING

The wetting fluid is not actually water, but a 0.1 per cent solution of sodium chromate, which acts as a rust inhibitor also. Three or more small dishes of this solution are at hand to receive the sections as they are cut, and a larger one serves as a reservoir for replenishing the fluid on the knife. Two artist's brushes are provided. One of them, small and finely pointed (fig. 20, pl. 2), is used in handling the sections. A clean sable brush, dipped in water and given a quick shake, acquires a fine point. Incidentally, pointing the brush in the mouth is to be avoided, because it transfers squamous epithelial cells to the sections.

With the larger brush the knife is thoroughly wetted on the upper surface of the portion that will pass through the block. As the knife enters the block and cuts a corner of it, the section will begin to roll up. Dr. Heuser's practice is to rest his left hand (see fig. 20, pl. 2) on an auxiliary post at the level of the knife so that, as he draws the knife toward him, his brush (the smaller one) touches the corner of the block. This contact is maintained until the knife moves forward and barely enters the block. The brush is then raised above the forming section but does not touch it as it slides up the slope of the wet knife. The brush prevents the rolling up of all but a very small part of the section, which can easily be unrolled when the sections are placed on the slide; if, as may happen with thick sections, the tissue-free corner will not unroll, it can be cut off.

If a section rolls up tightly as it is cut because of lack of synchronization of movements, it can be successfully unrolled at once or, if supported in a small dish of water, after all the sections have been cut. When the section is ready to be recovered, it is transferred to a wet but not flooded slide under the dissecting microscope. A free corner of the section is held down with a needle, and the rest is gently unrolled with a pointed sable brush. It is important not to press downward upon the rolled part with the brush, but only against the side of the roll where it bends upward from the flattened portion held down by the needle. If the sections are thick, 10 microns or more, very cautious warming by the heat of a lamp focused upon a rolled-up section will help unroll it.

To lift the section from the knife, where it floats on the wetting fluid, the brush, loaded with fluid, is touched to an edge of the section with a gentle twisting movement, so that the section is lightly wound onto it. By reversing the twist, the section is deposited on the slide or on the surface of the fluid in one of the small dishes previously mentioned (fig. 21, pl. 2). The next section is placed in the next dish, and so on to the third or fourth dish. By this time the assistant will have taken over the first section, leaving its dish free for the next section in order. Recently O. O. Heard has improved this procedure by the introduction of a revolving tray like a "Lazy Susan" to keep the dishes moving in proper sequence.

MOUNTING THE SECTIONS

The assistant picks up each section in turn with a brush and transfers it to a special mounting dish fitted with a metal rack as shown in figure 23 (pl. 2) and figure 30 (pl. 3). This rack is made with two end pieces of brass held together by 3-mm. rods. Two wire clamps hold the slide on a slope partly submerged in the water. Four Nichrome wires under the slide delimit the area within which the sections must be mounted. The slides are 2 by 3 inches (50 by 75 mm.), and the cover slips 43 by 50 mm.; the utilizable area is such as to leave a margin of about 2 mm. between the edge of the cover slip and the nearest points of the sections. If for very small objects a 3 by 1 inch slide (75 by 25 mm.) is used, two slides are placed on the rack and the fluid is brought up partly to cover the upper slide, on which the sections are mounted. The water level in the dish is maintained by a large rubber bulb connected by tubing to a glass siphon (fig. 23, pl. 2). The bulb serves as a reservoir, and the level is held by a clamp on the tubing. Neither bulb nor tube must be allowed to contain air bubbles, which might disturb the sections when the level is changed. Another means of controlling the water level is a reservoir bottle suspended by a rack and pinion device.

The assistant first brings the water level up on the sloping slide to the line along which the upper row of sections is to be mounted. The sections are successively slid with a brush out of the water and onto the slide. When the first row is full, the level is lowered and the second row is mounted, and so forth until the slide is filled. During this process the sections in the upper rows must be kept moist. Dr. Heuser uses a narrow strip of filter paper, dipped in thin celloidin solution (to prevent loose fibers from getting onto the section), and placed on the slide just above the line for the first row of sections. The strip is helpful in aligning the first row, especially of small specimens, and it holds the sections in place when water is added with a brush from time to time along the upper edge of the slide.

A filled slide is replaced by an empty one, and the work goes forward. A team of two persons accustomed to working together can operate with a satisfactory rhythm, but it is helpful to have a second assistant who takes over the freshly mounted slides. He flattens or removes the small corner rolls; checks and, if necessary, adjusts the alignment of the sections; removes air bubbles from under the sections by brushing them out; and sees to it that there is a narrow space between adjacent sections to allow for the small amount of spreading that occurs.

If a second assistant is not available during the sectioning process, the final arrangement of the sections may be postponed. The slides bearing the sections in correct order are stored under Petri dishes until they can be arranged and dried. Recently we have devised moist chambers from cut-off 3-liter reagent bottles, 13 cm. in inside diameter. Racks, designed to hold twenty-five 2 by 3 inch slides, are made of Bakelite and sheet brass to stand upright in Petri dishes. The filled racks and Petri dishes, the latter containing distilled water, are covered by the cut-off bottles. Sections are still movable after three days' storage.

The mounted slides are dried at 44° C. on a thermostatically controlled warm plate protected by a cover from direct air currents and from dust. They are usually left on this plate overnight at 36° C., after which they may be stained. Figure 31 (pl. 3) illustrates one of a sagittal series of sections through a presomite embryo, Carnegie no. 8725, handled by the above technique.

STAINING

For routine purposes a modification of the hematoxylin-eosin staining method is used. It will be outlined here to illustrate the general nature of the staining procedure.

1. Remove paraffin with three changes of xylene.
2. Remove celloidin with absolute alcohol-ether (the usual procedure; celloidin may be allowed to remain if necessary to protect very delicate objects).
3. Dip slides in 1 per cent celloidin, and dry in air briefly until a film has formed; this step prevents washing off the sections.
4. Immerse in alcohol, 70 per cent, or chloroform, to harden the celloidin coating.
5. Change to 95 per cent absolute alcohol, 5 per cent chloroform; the chloroform is necessary to prevent solution of the celloidin coating by the strong alcohol.
6. Rehydrate in alcohol from 80 per cent to 30 per cent by steps of 10 per cent, then distilled water.
7. Stain with Ehrlich's hematoxylin.
8. Rinse in distilled water.
9. Decolorize and sharpen stain in acid alcohol.
10. Rinse in distilled water; turn the sections blue in tap water, or in a weak alkaline solution if local tap water is not sufficiently alkaline.
11. Rinse in distilled water.
12. Dehydrate to 70 per cent alcohol.
13. Counterstain in 1 part eosin, 4 parts phloxine, 500 parts 70 per cent alcohol.
14. Rinse quickly in 95 per cent alcohol (containing 5 per cent chloroform if the celloidin is to be retained).
15. Dehydrate (and differentiate the eosin-phloxine stain) in absolute alcohol.
16. Immerse in absolute alcohol-ether if celloidin coating is to be removed; otherwise, pass directly to xylene, 2 or 3 changes.
17. Mount with Clarite, and dry overnight at 36° C.

The foregoing account, simplified as it is, represents the major effort of a professional career devoted to embryology. The quality of the morphological reports in the Contributions to Embryology is largely founded on the painstaking procedures originated or perfected by Dr. Heuser. It is hoped that this account will make his methods for handling, preserving, and preparing early and delicate specimens available to fellow biologists who have not had the opportunity to profit by watching him at work and observing his skill and precision.

The author acknowledges with thanks the editorial assistance of Dr. George W. Corner in preparing this article for publication.

LITERATURE CITED

Because the author was not familiar with all the sources, written and verbal, from which Dr. Heuser obtained information on which various parts of his technique may have been based, the latter should not be held responsible for omissions in the following list.

Heard, O. O. 1931. A photographic method of orienting serial sections for reconstruction. Anat. Rec., vol. 49, pp. 59–70.

——— 1953. The influence of surface forces in microtomy. Anat. Rec., vol. 117, pp. 725–739.

Hertig, A. T., J. Rock, E. C. Adams, and W. J. Mulligan. 1954. On the preimplantation stages of the human ovum: a description of four normal and four abnormal specimens ranging from the second to the fifth day of development. Carnegie Inst. Wash. Pub. 603, Contrib. to Embryol., vol. 35, pp. 199–220.

Heuser, C. H. 1932. A presomite human embryo with a definite chorda canal. Carnegie Inst. Wash. Pub. 433, Contrib. to Embryol., vol. 23, pp. 251–267.

——— and O. O. Heard. 1942. A vertical stereocamera for biological photography. Jour. Biol. Photog. Assoc., vol. 11, pp. 5–12.

——— and G. L. Streeter. 1929. Early stages in the development of pig embryos, from the period of initial cleavage to the time of the appearance of limb-buds. Carnegie Inst. Wash. Pub. 394, Contrib. to Embryol., vol. 20, pp. 1–30.

——— ——— 1941. Development of the macaque embryo. Carnegie Inst. Wash. Pub. 525, Contrib. to Embryol., vol. 29, pp. 15–55.

Huber, G. C. 1901. Studies on the neuroglia. Amer. Jour. Anat., vol. 1, pp. 45–61.

McClung, C. E. (ed.) 1929. Handbook of microscopical technique, for workers in both animal and plant tissues. 495 pp. New York.

——— 1937. Handbook of microscopical technique, for workers in both animal and plant tissues. 2d ed. 698 pp. Oxford.

PLATES

Plate 1

Fig. 13. Surface view of an early implantation after fixation in Bouin's fluid. Carnegie no. 8004. × 1.5. Arrow indicates implantation site.

Fig. 14. Vertical camera specially designed for embryological photography. Heuser and Heard (1942).

Fig. 15. Mechanical stirring device, used for gradual dehydration and infiltration.

Fig. 16. Vaseline dispenser with embryological watch glass and ground-glass cover.

Fig. 17. Presomite human embryo, caudal aspect. Note uncollapsed yolk sac and attachment to chorionic wall. Carnegie no. 8725. × 11.5. Compare with figure 31 (pl. 3).

13

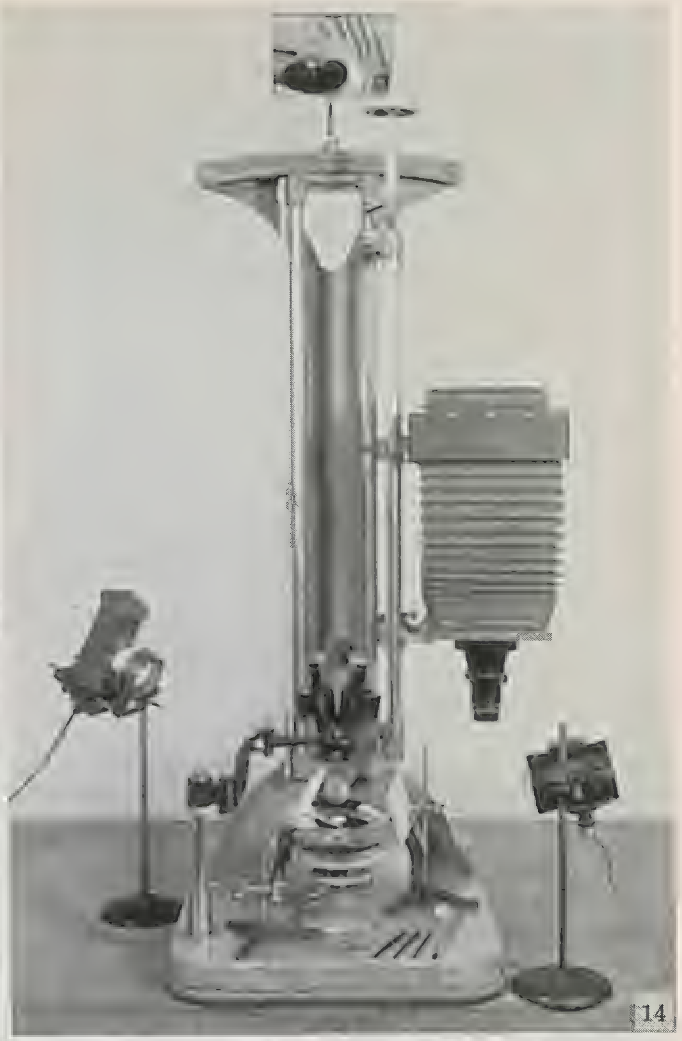

14

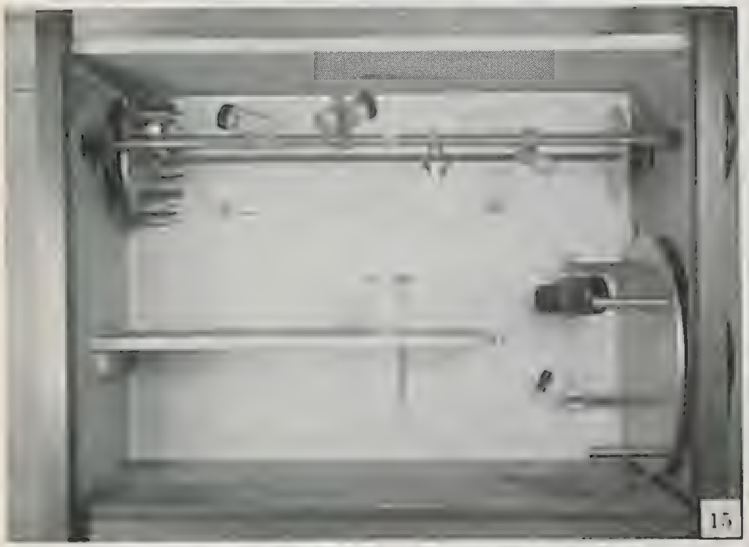

15

16

17

PLATE 2

FIG. 18. Block-trimming device arranged for trimming the upper surface.

FIG. 19. Block positioned for trimming the sides. One of the four notches is shown at the arrow tip.

FIG. 20. Sectioning by "water-on-the-knife" method. Note how the fine-pointed brush prevents the section from rolling at the beginning of the cut, also the "water" on the upper facets of the treated microtome knife.

FIG. 21. Transferring section from "water" film on microtome knife to one of the small dishes.

FIG. 22. Arranging sections on the slides in the mounting dish.

FIG. 23. Mounting dish with inclined rack and siphon.

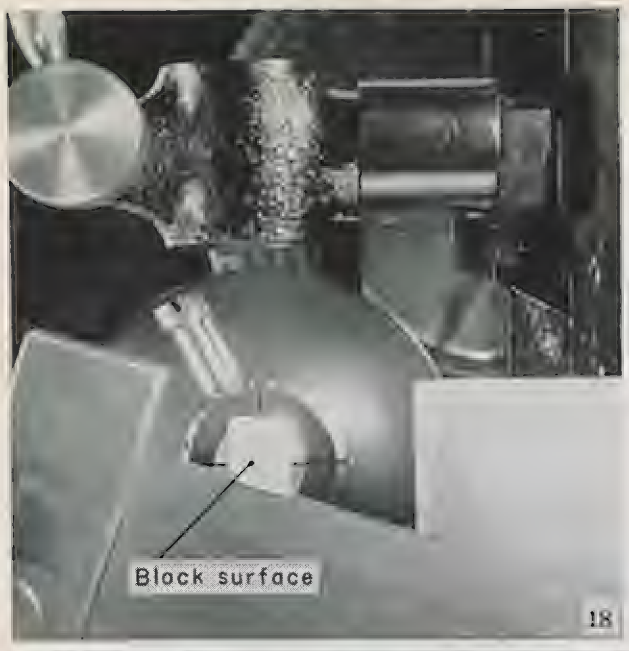

18

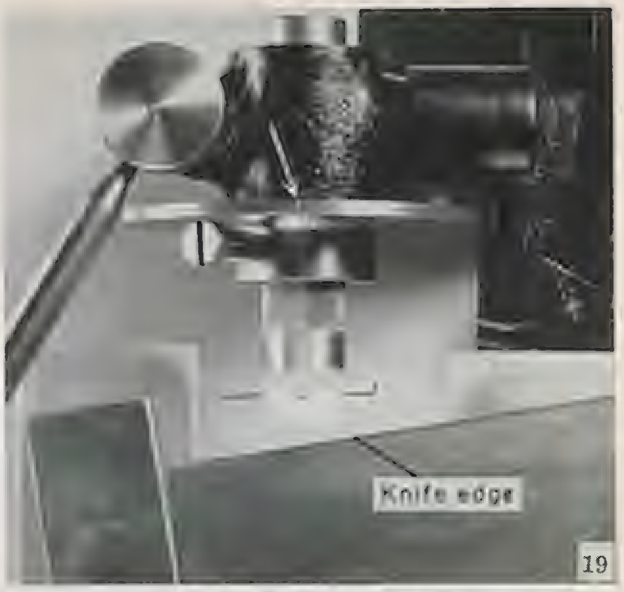

19

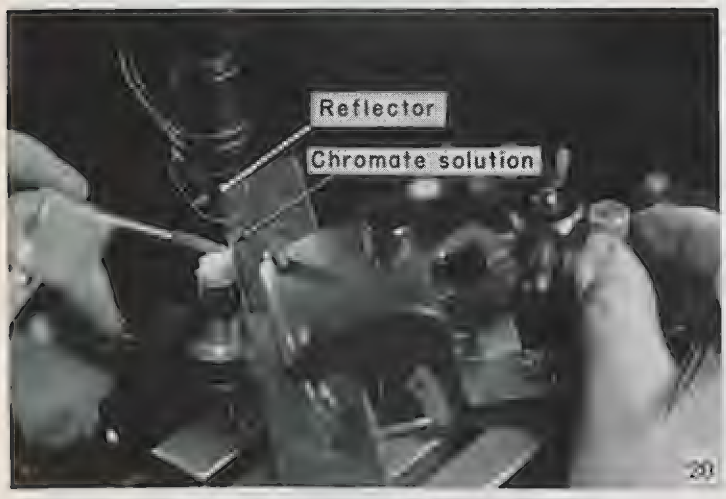

20

21

22

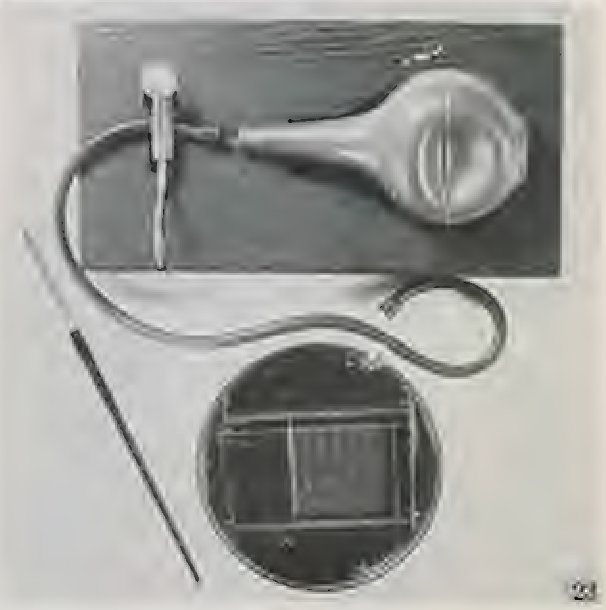
23

PLATE 3

FIG. 24. Arrangement of specimen with the aid of a binocular microscope. The prefocused binocular microscope is in the working position.

FIG. 25. Celloidin-embedded specimen with orienting pins. × 5.25.

FIGS. 26, 27, 28. Device for positioning double-embedded specimens, used to carry over and fix the angles determined by the goniometer shown in figure 18. Figures 26 and 28 are side elevations; figure 27, plan view.

FIG. 29. Area of implantation excised after fixation. Carnegie no. 7700. × 6.8. Twelve days' implantation.

FIG. 30. Close-up view of mounting dish with metal inclined rack.

FIG. 31. Sagittal section of Carnegie no. 8725. × 30. See figure 17 (pl. 1), demonstrating results obtained by these procedures.

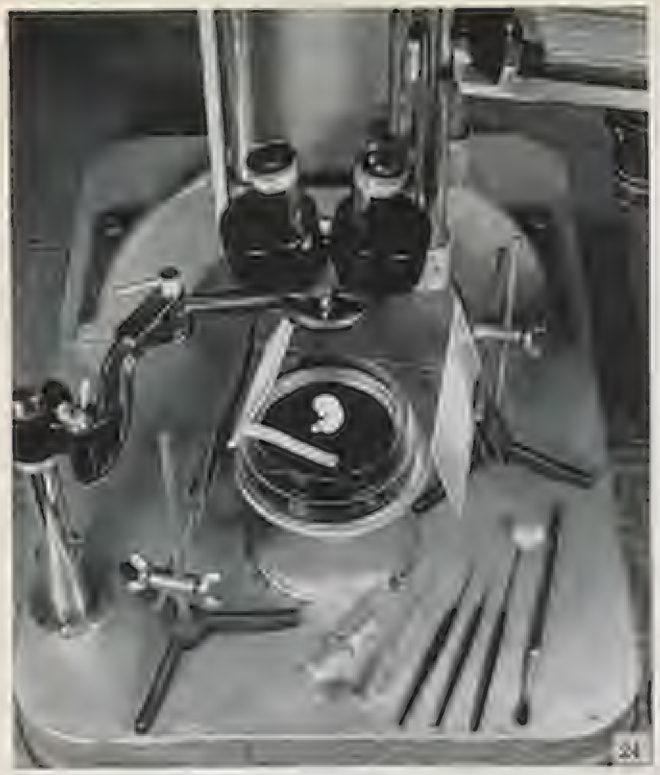

24

25

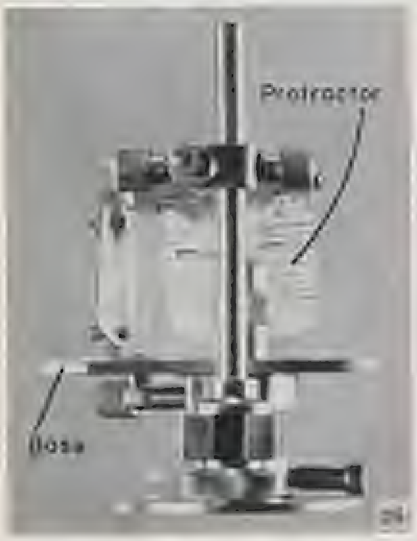

26

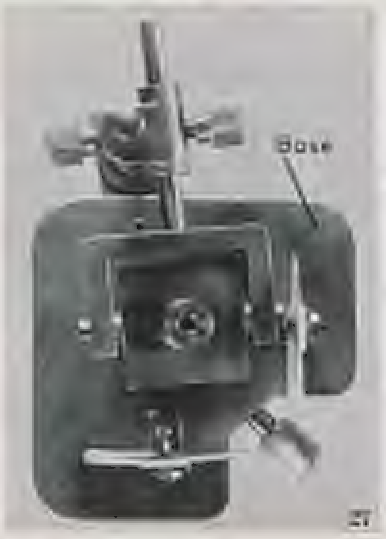

27

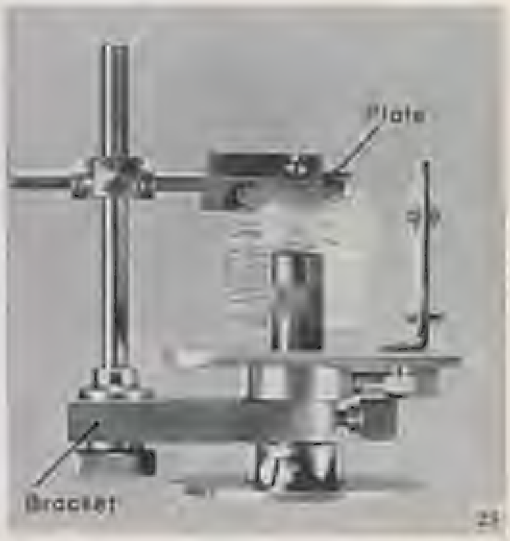

28

29

30

31

CONTRIBUTIONS TO EMBRYOLOGY, NO. 243

THE PRENATAL DEVELOPMENT OF THE HUMAN TEMPOROMANDIBULAR JOINT

Benjamin C. Moffett, Jr.

School of Dentistry and Medical College of Alabama, Birmingham

With two plates

CONTENTS

PAGE

Introduction 21

Anatomy of the Temporomandibular Joint in the Adult 21

Prenatal Development 22

- Embryonic Rudiments 22
  - Developing Mandible 22
  - Origin of Articular Disk 22
- Fetal Development 24
  - Relations to Adjacent Structures 24
  - First Appearance of the Condylar Cartilage 24
  - Passage of External Pterygoid Tendon and Disk to Malleus 24
  - Development of Articular Blood Supply 24
  - Growth of Condyle and Formation of Joint Cavity 25
  - Development of Joint Capsule 25
  - Meckel's Cartilage 25
  - Skeletal Components 26

Discussion 26

- Time of Development 26
- Articular Disk 26
- Mechanical Theories of Joint Formation 27
- Joint Interzones 27

Summary 28

Literature Cited 28

THE PRENATAL DEVELOPMENT OF THE HUMAN TEMPOROMANDIBULAR JOINT

INTRODUCTION

The least dispensable synovial joint in man is the articulation between the upper and lower jaws, the temporomandibular joint. This articulation is also in many respects unique, exhibiting such special anatomical characteristics as a complete intra-articular disk formed by the modification of an intercepted tendon, two synovial cavities, fibrocartilaginous articular surfaces, and tooth-bearing skeletal components. The temporomandibular joint is the only articulation which has both hinge and sliding movements.

This joint is a relatively new structure, existing only in mammals. It appeared late in evolution when the early jaw joint was incorporated into the middle ear (Gaupp, 1911). What the temporomandibular joint lacks in phylogenetic antiquity, however, it makes up in importance. The movements of the lower jaw in such vital functions as speech, mastication, and respiration all take place at the temporomandibular joint. If this articulation is injured during childhood or if it develops abnormally, the result will often be an extreme underdevelopment of the lower jaw and face, causing severe malocclusion and other dental problems, disturbed digestion and respiration, and possibly psychological complications.

The temporomandibular joint has been and still is the subject of a great many clinical investigations because of its intimate functional relationship with the occlusion of the teeth. There are many controversies in the literature about this and other aspects of the temporomandibular joint. It is surprising to find, however, that no embryological evidence has been brought to bear on these controversial issues. A partial explanation is the fact that a careful search has disclosed only three major sources of information on the embryology of the human temporomandibular joint.

Kjellberg (1904) described the temporomandibular joint in 5 human fetuses, the smallest one having a crown-rump length of 55 mm. He observed in 3 of these specimens that some of the fiber bundles of the external pterygoid muscle pass into the articular disk of the temporomandibular joint and then continue posteriorly between the squama and the tympanic bone to attach to the head of the malleus. He concluded that the passage of the external pterygoid muscle between the temporal squama and the mandibular condyle on its way to the malleus accounts for the formation of the articular disk.

Vinogradoff (1910) studied the development of the temporomandibular joint in 9 human fetuses, beginning with a 35-mm. specimen. He concentrated on the histological changes that occur in the condyle and zygomatic process of the temporal bone during fetal life. His description of the other joint components is vague. He presents no evidence of a connection between the external pterygoid muscle and the malleus.

More recently Harpman and Woollard (1938) made a specific study of the tendon of the external pterygoid muscle; they confirmed Kjellberg's original finding that in the human fetus this muscle does contribute to the origin of the articular disk or meniscus by passing posteriorly between the squama and the condyle to the malleus.

Macalister (1955) has described some of the histological modifications that occur in the prenatal development of the temporomandibular joint.

Although these authors were limited to a small number of specimens, their descriptions do show that the embryology of the temporomandibular joint differs in some respects from that of the more commonly studied synovial joints. Before such a comparison can be made, however, further investigation of the embryology of this joint is required. This need for detailed information led to a study of the temporomandibular joint components in human embryos and fetuses at the Department of Embryology, Carnegie Institution of Washington. The investigation was supported by a grant from the fellowship fund of the Carnegie Institution of Washington and by the Department of Anatomy, Medical College and School of Dentistry, University of Alabama. I wish to express my gratitude to Dr. George W. Corner for his generous assistance during this investigation; to Mr. Richard Grill for the accompanying photomicrographs; and to Drs. Earl O. Butcher, E. Carl Sensenig, and William L. Straus for the stimulating encouragement and interest they have shown in this project.

ANATOMY OF THE TEMPOROMANDIBULAR JOINT IN THE ADULT

The fully developed temporomandibular joint is a freely movable synovial joint between the condyle of the mandible and the articular eminence of the temporal bone. A fibrous joint capsule lined with synovial tissue surrounds the articular surfaces of the two bones. Inside the joint is an intra-articular disk or meniscus which separates the condyle from the articular eminence of the temporal bone. The articular disk is attached around its entire periphery to the joint capsule. The synovial cavity is thus divided into two separate spaces:

a superior joint cavity between the disk and the temporal bone; and a smaller, inferior joint cavity between the disk and the condyle of the mandible.

One of the muscles acting upon the joint is the external pterygoid muscle, which is inserted on the anterior surface of the neck of the condyle and on the anteromedial portion of the articular capsule and disk. When the mouth is widely opened or the lower jaw is protruded, this muscle pulls the condyle and disk forward, so that they slide downward along the sloping posterior surface of the articular eminence. As the mouth is closed, the external pterygoid muscle normally relaxes and the condyle and disk return to their former resting position higher up on the posterior surface of the articular eminence.

The central portion of the articular disk is compressed between the condyle and the articular eminence and contains neither blood vessels nor nerves. The function of the disk is generally regarded to be to stabilize and help to lubricate the incongruent articular surfaces of the condyle and articular eminence. Some of the controversy that still continues over the temporomandibular joint centers about the anatomy and function of the articular disk. A knowledge of the embryology of this joint may, in addition to its inherent value, help resolve these controversial questions.

PRENATAL DEVELOPMENT

The development of the temporomandibular joint was studied in a series of 46 human embryos and fetuses from the Carnegie Collection, ranging from 23 to 350 mm. crown-rump length. The specimens were sectioned in the frontal, sagittal, and transverse planes as indicated in table 1. In fetuses larger than 80 mm., the region of the temporomandibular joint was removed and only this part of the specimen was sectioned.

Embryonic Rudiments

The rudiments of the human temporomandibular joint make their embryonic appearance in the last two stages, xxii and xxiii, of Streeter's (1951) developmental horizons.

Developing mandible. In embryo no. 6832 (stage xxii, 25.8 mm.) the region of the future joint was recognized with great difficulty, because most of the joint components were not yet in existence and the muscles had not differentiated sufficiently to serve as landmarks. Identification was established by tracing distally the masseteric and auriculotemporal nerves, which enclose the developing joint anteroposteriorly.

The mandible is the only joint component present at this stage. There is no condyle, its place being occupied by the upper end of the osseous lamella, which constitutes the mandible. Meckel's cartilage already extends from the middle-ear region to the mid-line of the future chin, where it meets the distal end of the contralateral first branchial bar. This cartilage passes posteromedially to the future temporomandibular joint and appears on the medial side of the developing mandible. No other parts of the joint can be identified in this embryo.

Origin of articular disk. The origin of the articular disk is associated with the appearance of the external pterygoid and masseter muscles, which are recognizable in a stage-xxii embryo (no. 6701, 24 mm.). In a frontal section (fig. 1, pl. 1) through the region corresponding to the anterior portion of the future condyle, the disk is seen as a vague layer of mesenchyme extending laterally across the superior border of the external pterygoid muscle to the medial side of the masseter. The developing disk is separated from the condensation of mesenchyme which becomes the zygomatic process of the temporal bone by a large area of sparse cells, the precursor of the superior joint cavity. In contrast, the inferior joint cavity is preceded by only a very narrow zone of cells, because the articular disk, even in its early development, rests closely on the mandible. In this specimen an attachment of the external pterygoid muscle to the mandible could not be identified. The muscle, however, could be followed back to the posterior end of Meckel's cartilage.

An embryo of stage xxiii (no. 86, 30 mm.) shows the further development of the articular disk. In frontal section (fig. 2, pl. 1), the upper surface of the developing condyle faces laterally. Lying against this surface is a dark band of cells which gives rise to the articular disk. The external pterygoid muscle joins the medial side of the condyle at its approximate site of attachment in the fully developed joint. The muscle does not end at this point, however. It passes posteriorly along the medial side of the condyle and joins the band of cells forming the articular disk. The cells giving rise to the articular disk and to the external pterygoid tendon continue from this point posterosuperiorly to attach to that portion of Meckel's cartilage which becomes the malleus. This attachment of the mesenchymal layer and the external pterygoid tendon[1] to the malleus is a constant feature, seen in all specimens up to and including a 140-mm. fetus.

In this 30-mm. embryo, membrane-bone spicules make their appearance in the zygomatic process and squama of the temporal bone. The articular disk is still separated from the temporal bone by a large area of sparse cells which are giving up their round form to become elongated. The joint capsule is not yet recognizable.

---

[1] The term tendon is used here in a morphological rather than a histological sense; at this stage it consists only of undifferentiated mesenchyme.

TABLE 1

Human embryos and fetuses of the Carnegie Collection used in this study

Age group (gestation age)	Specimen no.	Crown-rump length (mm.)	Thickness of sections (microns)	Plane of section *	Figure	Plate
xxii (44–46 days)	6701	24	20	F	1	1
	6832	25.8	20	F		
xxiii (46–48 days)	86	30	50	F	2	1
	756A	27	50	F		
	1199	26	40	F		
	5725	23	25	F		
	7425	27	20	F		
10 weeks	972	37	50	S		
	1318	37	100	F	3	1
	4415	37	20	T		
	362	39	50	S		
	1597B	39	100	S		
	1611A	39.4	50	F		
	224	40	50–100	S		
	6658	40	40	S		
11 weeks	1826	40.5	50–100	T		
	6236	40.5	40	T		
	886	43	100	F		
	95	46	100	S	4	1
	1686	46	100	S		
	4475	48	20	T		
	3143	49	40	T		
	5652	49	40	F	5	1
	96	50	100	S	6	1
	184	50	50	S		
	538	50	100	F		
	965	50	100	F		
	1537	50	100	S		
	2331	50	40	F		
12 weeks	448	52	25–100	S		
	3990	54	20	T	7	2
	858	57.25	200	T	8	2
	4229	58	20	T		
	907	60	200	S		
	1183	60	200	F		
13 weeks	1656	67	200	S		
	4291	69	100	T		
14 weeks	6581	75†	20	S	9	2
	1455	78.5	50	S	10, 11	2
	172	80	100	T		
15 weeks	1858	100†	20	F, S		
18 weeks	928B	140†	20	S		
22 weeks	8634	180†	20	S		
26 weeks	625	220†	20	S	12	2
31 weeks	62	270†	20	S		
39 weeks	61	350†	20	S		

* F, frontal or coronal; S, sagittal; T, transverse.

† Specimen loaned by Department of Embryology, Carnegie Institution of Washington; sectioned and stained at Department of Anatomy, Medical College and School of Dentistry, University of Alabama.

Fetal Development

Relations to adjacent structures. In a frontal section through a 37-mm. fetus, no. 1318 (fig. 3, pl. 1), the condyle is still merely a condensation of mesenchyme around the upper end of the osseous lamella forming the mandible. The articular disk and external pterygoid tendon are shown continuing posteriorly to their attachment on the malleus. The structures in immediate relation to the medial side of the temporomandibular joint are demonstrated in this section. Directly inferior to the external pterygoid muscle is the internal maxillary artery cut in cross section. The middle meningeal artery is seen in longitudinal section running superiorly between the condyle and the otic ganglion. The two portions of the auriculotemporal nerve which surround the middle meningeal artery are visible, as are also the inferior alveolar and lingual nerves.

First appearance of the condylar cartilage. No further development of the joint components was noticed until the condylar cartilage appeared in a 46-mm. fetus, no. 95. The cartilage is located at the upper end of the osseous lamella, which forms the posterior border of the mandible. In sagittal section (fig. 4, pl. 1), the growth of this cartilage appears to be directed superiorly and somewhat anteriorly. The condylar cartilage has not grown sufficiently to force the disk into contact with the superior articular element. Immediately above the condyle, between it and the disk, is the external pterygoid tendon cut almost in cross section as it curves laterally to attach to the malleus. The auriculotemporal nerve has been cut obliquely, passing between Meckel's cartilage and the posterior surface of the condyle.

The articular disk appears to be elevated from the condyle because this section is close to the external pterygoid muscle, which comes between the mesenchymal portion of the disk and the medial part of the condyle. The relationship is better understood by referring to the frontal section (fig. 5, pl. 1) of a 49-mm. fetus, no. 5652. The articular disk lies directly on the condyle except in the area occupied by the external pterygoid tendon. This frontal section illustrates several important points about the articular disk:

1. The disk is associated developmentally with the mandible and the muscles of mastication, specifically the external pterygoid and the masseter.

2. The major portion of the articular disk is derived from a mesenchymal layer which, anterior to the joint, extends from the external pterygoid muscle to the masseter muscle, and, after passing over the condyle, continues posteriorly in company with an extension of the external pterygoid muscle to attach to the developing malleus.

3. The posterior extension of the external pterygoid muscle does in fact contribute to the formation of the articular disk, as is shown in the other figures.

Passage of external pterygoid tendon and disk to malleus. The actual passage of the external pterygoid tendon from the condyle to the malleus can be seen in a sagittal section (fig. 6, pl. 1) of the temporomandibular joint in a 50-mm. fetus, no. 96. The tendon runs obliquely from the upper posterior part of the condyle to the posterior surface of Meckel's cartilage. In adjacent sections Meckel's cartilage changes its direction and position slightly so that the pterygoid tendon is actually attached to the lateral side of the malleus. A short segment of the articular disk extends posteriorly above the upper end of the external pterygoid tendon and parallel to the membrane bone that forms the zygomatic process of the temporal bone. This part of the disk when followed posteriorly joins the external pterygoid tendon and travels in common with it to the malleus.

The attachment of the developing disk to Meckel's cartilage can be seen also in superior view by looking down on a transverse or horizontal section (fig. 7, pl. 2) through the joint in a 54-mm. fetus, no. 3990. Here the tendon of the external pterygoid muscle passes over the medial side of the condyle and then turns, proceeding to the lateral side of Meckel's cartilage, on its way to the head of the malleus. The contribution from the disk over the lateral part of the condyle is more readily visible a few sections higher, where it joins this tendon as a somewhat more deeply stained band of cells.

Development of articular blood supply. The specimen just discussed, a 54-mm. fetus, no. 3990, also illustrates certain features in the development of the blood supply to the temporomandibular joint. These features will be described here because they have a bearing on a paper soon to be published on the blood supply in the fully developed joint. In a horizontal section (fig. 7, pl. 2) through the joint, many blood vessels, mostly veins, are seen in the area enclosed on three sides by the sectioned disk, the lateral surface of the condyle, and the external pterygoid tendon lateral to Meckel's cartilage. When followed inferiorly these blood vessels are seen to run vertically against the posterolateral aspect of the condyle and mandibular ramus. At varying levels along the ramus they join the superficial temporal artery and vein, the posterior facial vein and the external carotid artery. The same vessels when traced superiorly are seen to shift slightly to a closer association with Meckel's cartilage. They remain on the lateral side of this cartilage, gradually diminishing in number as they give off branches which surround the developing malleus and incus. They apparently terminate on the ossicles in the region of the middle ear.

At the level shown, these blood vessels give off branches which run anteriorly in the articular disk and on the external pterygoid tendon to anastomose with capillaries coming from the anterior surface of the joint. This capillary anastomosis, extending anteroposteriorly completely across the articular disk, is shown in a horizontal section (fig. 8, pl. 2) through a 57.25-mm. fetus, no. 858, in which the vascular system was injected with India ink. The level of section corresponds to that shown in figure 7, and passes through the disk and pterygoid tendon immediately above the condyle.

Growth of condyle and formation of joint cavity. As the condyle grows, its articular surface and shape undergo marked changes. In a 30-mm. embryo, before the appearance of a condylar cartilage (fig. 2, pl. 1), the articular surface of the condyle faces directly laterally, almost in a vertical plane. The articular disk and the articular surface of the zygomatic process of the temporal bone are parallel to that of the condyle.

In a 49-mm. fetus, no. 5652, the condylar cartilage has shaped the articular surface of the condyle into a hemisphere, as seen in a frontal section (fig. 5, pl. 1) through the center of the cartilage. The articular disk flattens this contour and makes it congruous with the articular surface being formed by the squama and zygomatic process of the temporal bone. The plane of the articular surfaces has shifted to approximately 45° from the vertical. The joint cavities have not yet appeared in this specimen, and there is no actual contact between the two articulating elements.

In five out of the six 50-mm. fetuses studied, the condyle and disk are not in contact with the temporal bone and the joint cavities are not yet formed. The sixth specimen shows an area of sparse cells between the disk and the temporal bone which appears to be developing a cavity. Contact between the disk and temporal bone is made in the 60-mm. fetuses. The sections in these specimens were too thick, however, to show the presence of joint cavities. In a 75-mm. fetus, no. 6581, sagittal section (fig. 9, pl. 2), the inferior joint cavity is present and the superior cavity is being formed.

Development of joint capsule. The articular capsule of the temporomandibular joint is first recognizable in 50-mm. fetuses in the form of faint cellular condensations along the medial and lateral sides of the joint, connecting the two skeletal components. The articular disk merges peripherally with these capsular condensations and thus obtains an attachment to the temporal bone and mandible. The joint is still not bounded anteroposteriorly by a capsule in the 75-mm. fetus. Before the formation of the capsule posterior to the joint, the articular disk transfers its attachment from Meckel's cartilage to the temporal bone and mandible. This transfer results from a narrowing of the Glaserian fissure and an approximation of Meckel's cartilage to the posterior part of the neck of the condyle. An early phase in the transfer to the temporal bone is seen in a sagittal section (fig. 10, pl. 2) through the lateral portion of the temporomandibular joint in a 78.5-mm. fetus, no. 1455. The articular disk here extends posteriorly, following the contours of the zygomatic process of the temporal bone, a relation which results from the approximation of the two articular elements and from the persisting attachment of the disk to Meckel's cartilage. As the articular disk accompanies Meckel's cartilage through the Glaserian fissure into the middle ear, the disk comes in contact with the anterior wall of the fissure. At this point the cells of the disk are becoming attached to the temporal bone. This attachment limits the superior joint cavity posteriorly and forms the superior attachment of the developing articular capsule on the anterior lip of the Glaserian fissure posterior to the temporomandibular joint.

The inferior attachment of the disk and articular capsule on the posterior surface of the neck of the condyle results from a similar transfer involving the external pterygoid tendon, the mandible, and Meckel's cartilage. In figure 10 (pl. 2), the external pterygoid tendon is visible on the posterior surface of the condyle and again just inferior to Meckel's cartilage as the tendon continues toward its insertion on the malleus. Further medially in a sagittal section through the middle of the condyle in the same specimen the tendon forms an attachment to the mandible (fig. 11, pl. 2). Here the external pterygoid tendon passes through a narrow space between the mandible and Meckel's cartilage and appears to be attaching itself to the neck of the condyle. From this point, cells are seen extending superiorly toward the attachment of the disk on the temporal bone. At this stage, however, there is not a complete capsule posterior to the joint; the development of the capsule in this region proceeds very slowly.

In a 140-mm. fetus the articular disk still passes through a narrow Glaserian fissure to be inserted on the malleus. Some of the cells are attached, however, to the anterior lip of the fissure. Meckel's cartilage is now constricted as it passes through the fissure, but it is still continuous with the malleus. In a 180-mm. fetus, the disk ends at the Glaserian fissure and the joint is definitely enclosed posteriorly by a capsule. The joint cavities are sharply bounded by synovial tissue. Synovial villi with adipose subsynovial tissue project into the anterior and posterior ends of the cavities.

The attachments of the disk to the temporal bone and condyle are shown in sagittal section through the joint of a 220-mm. fetus, no. 625 (fig. 12, pl. 2). This section passes through the medial part of the condyle. The external pterygoid muscle is seen merging with the anterior part of the disk. The Glaserian fissure is still open.

Meckel's cartilage. Before the first components of the temporomandibular joint became visible in a stage-xxii embryo, Meckel's cartilage extended all the way from the base of the skull to the future chin, this relation being maintained during the entire development of the temporomandibular joint. The cartilage serves, therefore, as a supporting framework around which the mandible develops, and as a strut which holds the lower jaw in place until the temporomandibular joint has formed. It plays a direct role in the formation of the temporomandibular joint through its association with the external pterygoid tendon and the mesenchymal portion of the articular disk. Meckel's cartilage also carries blood vessels through the Glaserian fissure which vascularize the developing malleus and incus. These vessels can be seen in 57- to 180-mm. fetuses.

At 220 mm., when the temporomandibular joint can be considered developed, Meckel's cartilage still extends through the Glaserian fissure. The portion of Meckel's cartilage extending between the mandible and the skull, however, is very thin, and in a 270-mm. fetus it becomes recognizable as the sphenomandibular ligament. Kjellberg (1904) presents an interesting historical summary of information on this and other derivatives of Meckel's cartilage. At 270 mm. the superior attachment of the sphenomandibular ligament appears to be on the medial end of the temporal bone, the sphenoid bone being directly adjacent to this point. The Glaserian fissure is practically closed at this stage. In the 350-mm. fetus, the superior attachment of the sphenomandibular ligament is on the sphenoid bone just lateral and posterior to the foramen spinosum.

Skeletal components. The mandibular fossa develops its final contours only during postnatal life, with the appearance of the articular eminence of the temporal bone. A slight concavity present in the 180-mm. and larger fetuses is due only to a slight prominence or projection at the posterior border of the fossa.

During its development the condylar cartilage shows a peculiarity which has been described by Vinogradoff (1910). In the 140-mm. fetus and on through the 350-mm. fetus, peglike processes, which Vinogradoff likens to "crampons," occur at first in the lateral portion of the condyle. Then they appear also on the medial side, and finally all over the articular surface of the condylar cartilage. Vinogradoff says that these "crampons" serve to anchor the fibrous articular surfaces in the temporomandibular joint to the condyle and to the temporal bone.

DISCUSSION

Time of Development

The first significant fact brought out by this study is the relatively late embryonic development of the temporomandibular joint as compared with the larger joints of the extremities. During the last stage, xxiii, of embryonic development, all the major components of the elbow, hip, and knee joints "are present in a form and arrangement closely resembling the adult" (Gardner, 1952). In this same embryonic stage, however, the temporomandibular joint is still rudimentary in comparison with the fully developed joint; the condylar cartilage, joint cavities, synovial tissue, and articular capsule have not yet appeared, and the skeletal elements—mandible and temporal bone—are not in contact. All the components of the temporomandibular joint except the articular eminence of the temporal bone are present in the 220-mm. fetus. The joint does not assume its typical adult contours, however, until the articular eminence has completed its development during the twelfth year of age (Humphreys, 1932).

Articular Disk

The development of the articular disk is worthy of discussion in order to correct some common misstatements about this structure. The articular disk of the temporomandibular joint should not be regarded as forming from tissue which is caught or pinched between the mandible and the temporal bone by upward growth of the condyle, as Keith (1948) states. This erroneous concept can be traced to Vinogradoff (1910) and to other investigators who did not study embryos young enough to show the early development of the disk. Actually, the articular disk can be identified as a mesenchymal and muscular derivative of the first branchial arch, which appears earlier than the condyle, long before the mandible comes in contact with the temporal bone. If the disk were to develop as stated by Keith, disturbances in its formation would undoubtedly result in specific congenital anomalies which have in fact never been reported. The only known developmental anomaly of the temporomandibular joint is the absence of one or both condyles—a very rare condition.

The development of the temporomandibular intra-articular disk resembles certain processes seen in other joints and yet in other respects appears to be a unique phenomenon. For instance, a small medial portion of the disk is derived from the posterior extension (referred to as a tendon) of the external pterygoid muscle. This passage of a muscle tendon through a synovial joint is similar to the situation described in the human shoulder joint by Gardner and Gray (1953), in which the tendon of the long head of the biceps brachii muscle develops *in situ* in the extrablastemal tissue of the glenohumeral joint. These situations differ, however, in that the external pterygoid tendon becomes incorporated into the disk and later in fetal life loses its attachment to the malleus. Development here does not proceed rapidly from the primordial state to a form and arrangement characteristic of the adult. The disk passes through the intermediate stages described here and by other investigators. The temporomandibular joint does truly seem to have a developmental stage in which it resembles the normal structure of lower forms where the jaw joint occurs between the os quadratum and os articulare. Its relatively late appearance as a new structure in evolution supports this conclusion, which as far as is known applies to no other joint.

In describing the fully developed temporomandibular joint, the term articular disk is frequently limited to the fibrous, hard, glistening portion of the intra-articular tissue. This definition excludes a considerable quantity of less-dense connective tissue, vascularized and innervated, which connects the fibrous portion of the disk on all sides to the joint capsule. Developmentally, there is no basis for this distinction. During fetal life the entire disk is vascularized. Only after the central portion of the disk is compressed between the condyle and temporal bone does this portion become avascular. In the fully developed joint the peripheral portions of the disk still retain their blood and nerve supply, the distribution of which will be described in later papers. The complete vascularization of the disk seen in the fetus indicates that both the vascular and avascular portions in the fully developed joint should be included in the definition of the articular disk.

MECHANICAL THEORIES OF JOINT FORMATION

The formation of intra-articular disks is explained by several investigators as resulting from the absence of pressure exerted on the undifferentiated mesenchyme between the developing bones. Whillis (1940) says that relief of pressure on the joint disk in the ulnar-triquetral joint by the ulnar styloid process results in a nonchondrified disk which becomes stretched and incorporated in the medial ligament of the wrist joint. He cites the clavicle as another example by saying that the centers of ossification that appear in the early development of the clavicle lead to a slowing in the growth of the precartilage. This relief of pressure on the mesenchyme removes the stimulus for chondrification, and the disks become modified to form the articular disks of the sternoclavicular and acromioclavicular joints. Prentiss (1918) had already proposed this explanation in connection with the development of the knee and temporomandibular joints. The embryonic human knee joint contains at first a complete meniscus separating the femur from the tibia. Prentiss says that at birth the central portion of this meniscus or disk has disappeared, undoubtedly because of pressure exerted on the disk by powerful muscular pull across the joint. When in postnatal life great pressure is brought to bear on this joint by standing, etc., the disk continues its retrograde changes until only semilunar cartilages remain.

Prentiss explains the development and also the pathology of the temporomandibular articular disk by this concept of the effect of pressure. He says that eruption of the teeth and, earlier, the presence of the large alveolar processes of the jaws prevent the condyles from pressing against the temporal articular surfaces. The disk, therefore, is not obliterated by pressure. The finding reported here that the condyle and disk are separated from the temporal bone during the early development of this joint favors this hypothesis. An observation familiar to anatomists and dentists is mentioned by Prentiss: with the loss of the teeth and resorption of the alveolar processes, the disk is subjected to increased pressure, and it degenerates, disappearing partially or almost completely.

Another hypothesis that interprets joint formation on a mechanical basis is presented by Carey (1922). He postulated that joints are the mechanical resultants of the opposed actions of accelerated growth centers of the segmental skeleton; the contours of the opposed surfaces forming a joint are dependent upon the intensity of the force of interstitial growth on the cross-sectional area of the segments forming the joint and upon the resistances to the growth of each skeletal segment. As an example Carey cites the hip joint, where the head of the femur advances farther into the acetabulum because the femur has a greater longitudinal growing force than the acetabulum.

Both these suppositions—that pressure determines the fate of an articular disk, and that it establishes the contours of the joint surfaces—are compatible with the development of the temporomandibular joint. They must remain hypothetical, however, until experimental evidence determines whether a cause-and-effect relation exists between these conditions in the embryo as it appears to do in pathological changes of the temporomandibular joint.

JOINT INTERZONES

Considerable attention has been given by many investigators (see Gardner, 1950) to the question, Are articular structures derived from a blastemal interzone? Much evidence has been offered from the study of the joints of the extremities to indicate that either the blastema or the mesenchyme, or both, may be the source of articular structures. The temporomandibular joint consists of membrane-bone skeletal components that are not connected by a blastemal interzone. A condylar growth-cartilage appears later in one of the skeletal components, but there is no indication in this joint of a continuous blastema which chondrifies and becomes segmented. The interzone appears to be mesenchymal, and through it the external pterygoid tendon passes to contribute to the formation of the articular disk, which as stated before is a derivative of the first branchial arch. The late evolutionary development of the temporomandibular joint, and the fact that its skeletal components are membrane-bone elements of the skull and first branchial arch, result in a developmental pattern which differs from that seen in the joints of the extremities.

SUMMARY

1. The temporomandibular joint develops from the membranous portion of the temporal bone; from skeletal, muscular, and mesenchymal derivatives of the first branchial arch; and from a mesenchymal interzone.

2. The rudiments of the temporomandibular joint appear in the last stages of embryonic development. The joint passes slowly through a developmental stage in which it resembles the normal structure of lower forms where the jaw joint occurs between the os quadratum and os articulare. Its development is essentially complete in the 220-mm. fetus.

3. The articular disk develops early from muscular and mesenchymal derivatives of the first branchial arch. It consists mainly of a mesenchymal layer which passes between the external pterygoid and masseter muscles and then extends posteriorly over the developing condyle to attach to the part of Meckel's cartilage that becomes the malleus. A small medial segment of the disk is formed by the tendon of the external pterygoid muscle, which is also attached to the malleus.

4. The articular disk maintains its attachment to the malleus until fetal development of the joint is completed. It then takes part in the formation of the posterior joint capsule by becoming attached to the anterior lip of the Glaserian fissure and to the mandible.

5. Meckel's cartilage plays an important role in the development of the temporomandibular joint by (*a*) forming a framework around which the mandible develops; (*b*) acting as a strut which holds the lower jaw in place until the temporomandibular joint is formed; (*c*) providing an attachment for the developing articular disk.

6. Developmental differences between the temporomandibular joint and the joints of the extremities are described, and mechanical theories of joint formation are discussed.

LITERATURE CITED

Carey, E. J. 1922. Direct observations on the transformation of the mesenchyme in the thigh of the pig embryo (*Sus scrofa*), with especial reference to the genesis of the thigh muscles, of the knee- and hip-joints, and of the primary bone of the femur. Jour. Morphol., vol. 37, pp. 1–77.

Gardner, E. 1950. Physiology of movable joints. Physiol. Rev., vol. 30, pp. 127–176.

——— 1952. The anatomy of joints. Amer. Acad. of Orthopaed. Surgeons Instructional Course Lectures, vol. 9, pp. 149–170.

——— and D. J. Gray. 1953. Prenatal development of the human shoulder and acromioclavicular joints. Amer. Jour. Anat., vol. 92, pp. 219–276.

Gaupp, E. 1911. Beiträge zur Kenntnis des Unterkiefers der Wirbeltiere. Anat. Anz., vol. 39, pp. 609–666.

Harpman, J. A., and H. H. Woollard. 1938. The tendon of the lateral pterygoid muscle. Jour. Anat., vol. 73, pp. 112–115.

Humphreys, H. 1932. Age changes in the temporomandibular joint and their importance in orthodontics. Internat. Jour. Orthodontia Oral Surgery and Radiography, vol. 18, pp. 809–815.

Keith, A. 1948. Human embryology and morphology. 6th ed. 690 pp. Baltimore.

Kjellberg, K. 1904. Beiträge zur Entwicklungsgeschichte des Kiefergelenks. Gegenbaurs Morphol. Jahrb., vol. 32, pp. 159–184.

Macalister, A. D. 1955. The development of the human temporomandibular joint. A microscopic study. Australian Jour. Dent., vol. 59, pp. 21–27.

Prentiss, H. J. 1918. A preliminary report upon the temporomandibular articulation in the human type. Dent. Cosmos, vol. 60, pp. 505–512.

Streeter, G. L. 1951. Developmental horizons in human embryos. Description of age groups xix, xx, xxi, xxii, and xxiii. Carnegie Inst. Wash. Pub. 592, Contrib. to Embryol., vol. 34, pp. 165–196.

Vinogradoff, A. 1910. Développement de l'articulation temporo-maxillaire chez l'homme dans la période intra-utérine. Internat. Monatsschr. f. Anat. u. Physiol., vol. 27, pp. 490–523.

Whillis, J. 1940. The development of synovial joints. Jour. Anat., vol. 74, pp. 277–283.

ABBREVIATIONS USED IN PLATES

a. d., articular disk
a. n., auriculotemporal nerve
c., condyle
c. c., condylar cartilage
e. p. m., external pterygoid muscle
e. p. t., external pterygoid tendon
g. f., Glaserian fissure
i. a. n., inferior alveolar nerve
i. j. c., inferior joint cavity
i. m. a., internal maxillary artery
l. n., lingual nerve
m., mandible
mall., malleus
m. c., Meckel's cartilage
m. m., masseter muscle
m. m. a., middle meningeal artery
o. g., otic ganglion
s. j. c., superior joint cavity
t., temporal bone

PLATES

PLATE 1

FIG. 1. Frontal section of right temporomandibular joint of embryo no. 6701, 24 mm., age group xxii; thickness 20 microns. Shows mesenchymal portion of disk associated with masseter and external pterygoid muscles. Note large distance separating disk and mandible from temporal bone. × 45.

FIG. 2. Frontal section (inclined posteriorly) of right temporomandibular joint of embryo no. 86, 30 mm., age group xxiii; thickness 50 microns. Shows external pterygoid tendon and mesenchymal portion of disk extending posteriorly toward attachment to Meckel's cartilage. × 45.

FIG. 3. Frontal section (inclined posteriorly) of right temporomandibular joint of fetus no. 1318, 37 mm.; thickness 100 microns. Shows disk and external pterygoid tendon extending toward malleus. Note structures adjacent to joint. × 60.

FIG. 4. Sagittal section of temporomandibular joint of fetus no. 95, 46 mm.; thickness 100 microns. Shows condylar cartilage and relation of disk and external pterygoid tendon to medial part of condyle. × 45.

FIG. 5. Frontal section of left temporomandibular joint of fetus no. 5652, 49 mm.; thickness 40 microns. Shows relation of disk to condyle and temporal bone. × 45.

FIG. 6. Sagittal section of right temporomandibular joint of fetus no. 96, 50 mm.; thickness 100 microns. Shows passage of external pterygoid tendon from condyle to malleus. × 45.

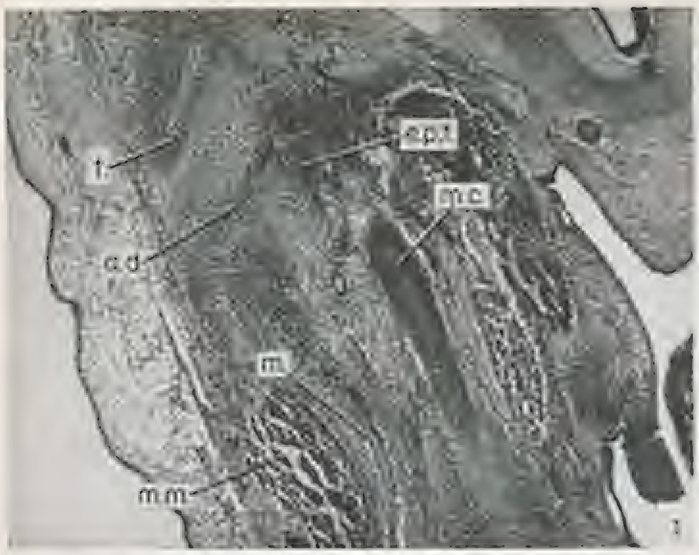
e.p.t
t
m.c
a.d
m
m.m
1

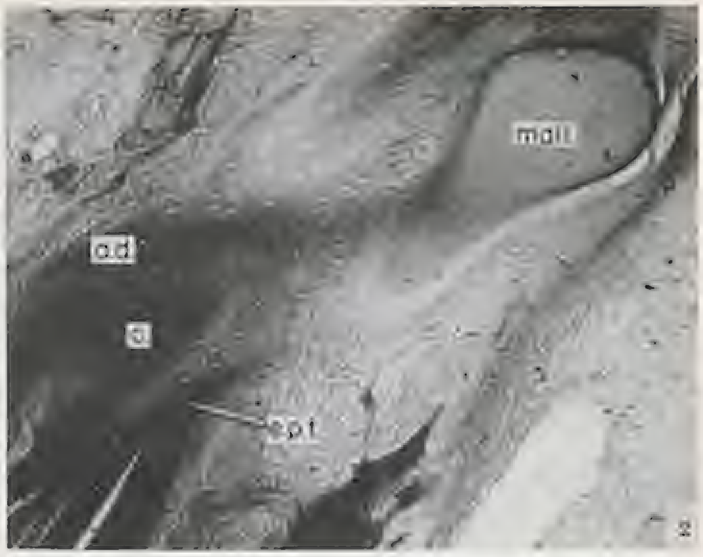
mall
a.d
c
e.p.t
2

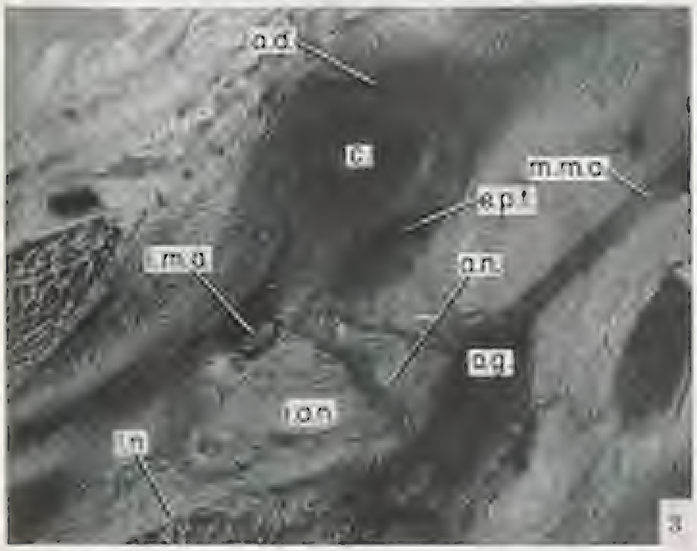
a.d
c
m.m.c
e.p.t
i.m.a
a.n
a.g
i.a.n
l.n
3

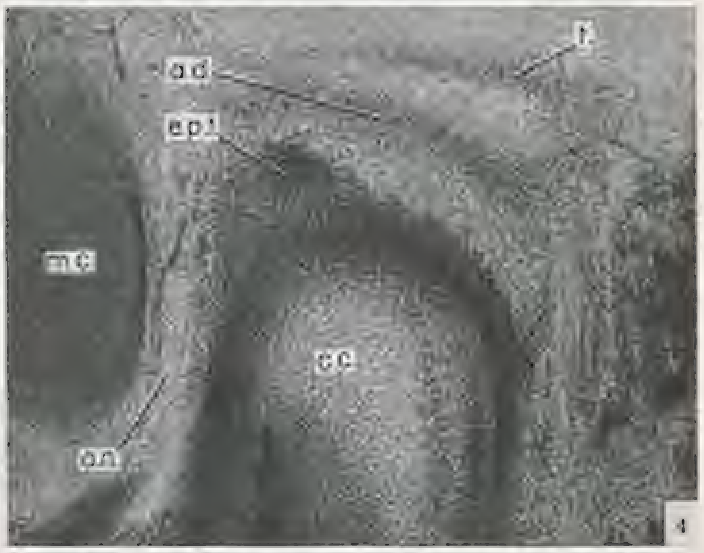
t
a.d
e.p.t
m.c
c.c
a.n
4

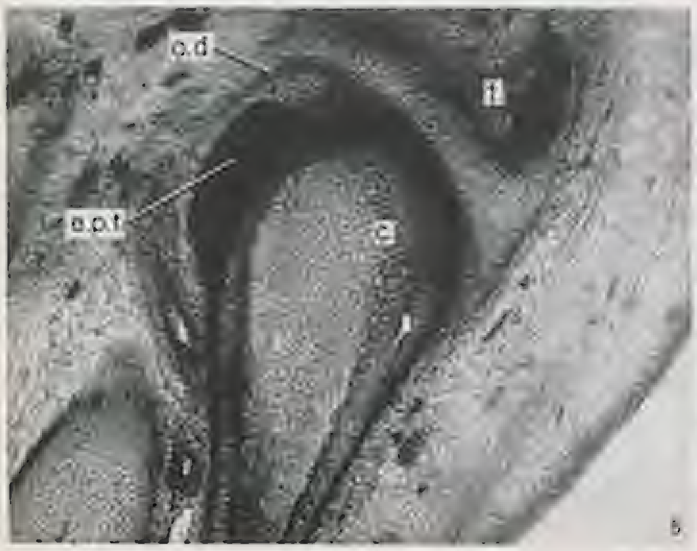
a.d
t
e.p.t
c
5

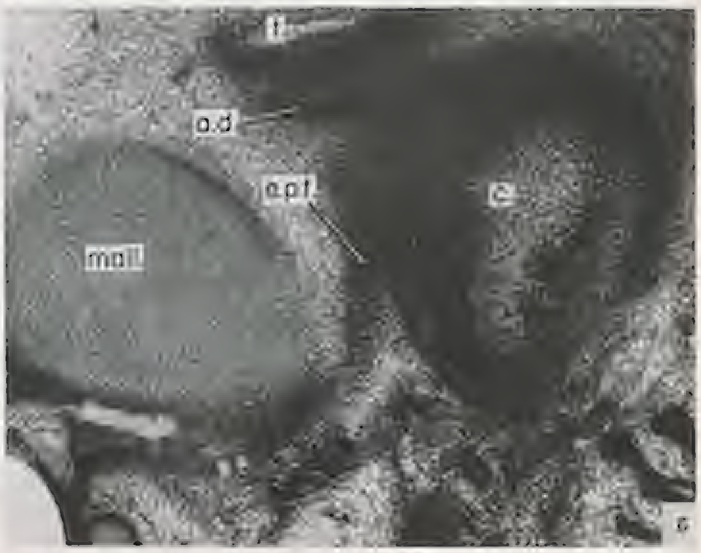
t
a.d
e.p.t
c
mall
6

PLATE 2

FIG. 7. Transverse section of left articular disk and condyle of fetus no. 3990, 54 mm.; thickness 20 microns. Shows passage of external pterygoid tendon to Meckel's cartilage. Note adjacent blood vessels. × 45.

FIG. 8. Transverse section of left articular disk and condyle of fetus no. 858, 57.25 mm.; thickness 200 microns. Shows vascular anastomosis (injected with India ink) extending through disk anteroposteriorly. × 45.

FIG. 9. Sagittal section of temporomandibular joint of fetus no. 6581, 75 mm.; thickness 20 microns. Shows inferior joint cavity formed; superior joint cavity forming in central portion. × 36.

FIG. 10. Sagittal section of left temporomandibular joint of fetus no. 1455, 78.5 mm.; thickness 50 microns. Shows attachment of disk to anterior wall of Glaserian fissure. × 45.

FIG. 11. Sagittal section of left temporomandibular joint of fetus no. 1455, 78.5 mm.; thickness 50 microns. Section is medial to that in figure 10. Shows external pterygoid tendon in narrow space between condyle and Meckel's cartilage. × 45.

FIG. 12. Sagittal section of left temporomandibular joint of fetus no. 625, 220 mm.; thickness 20 microns. Disk is attached posteriorly to the temporal bone in the Glaserian fissure, which is still open. × 11.8.

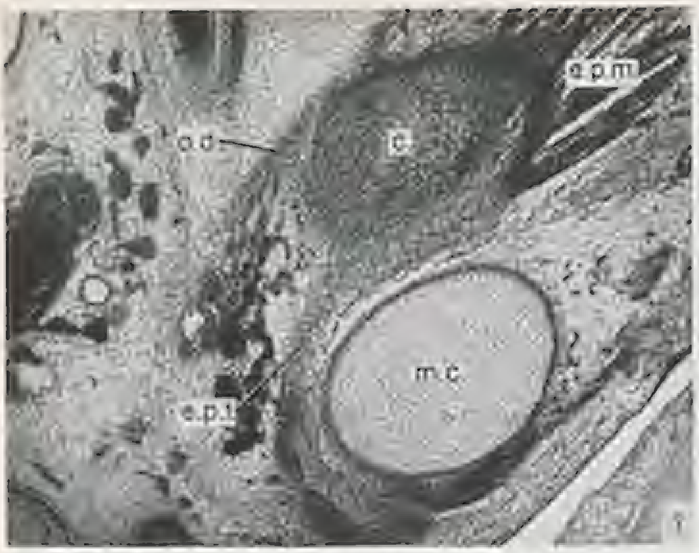
e.p.m.
a.d.
c
m.c.
e.p.t.
7

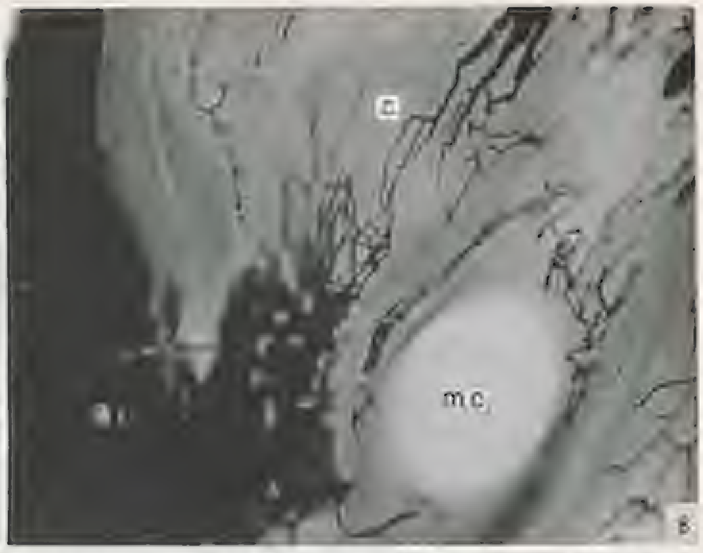
a
m.c.
8

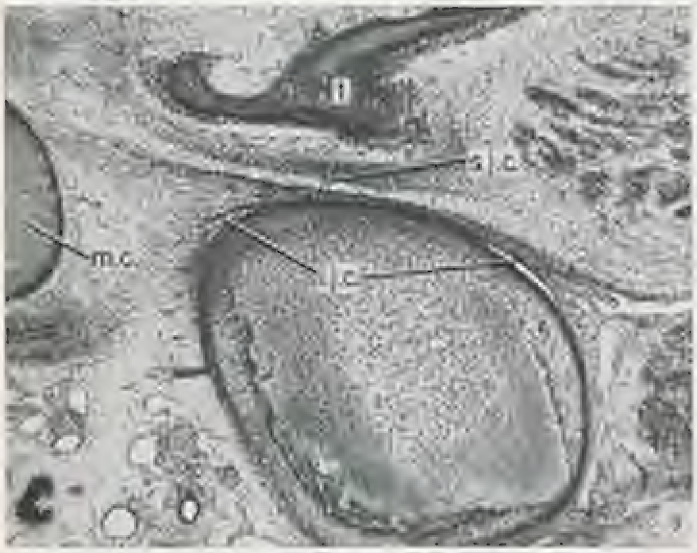
t
a.j.c.
m.c.
j.c.
9

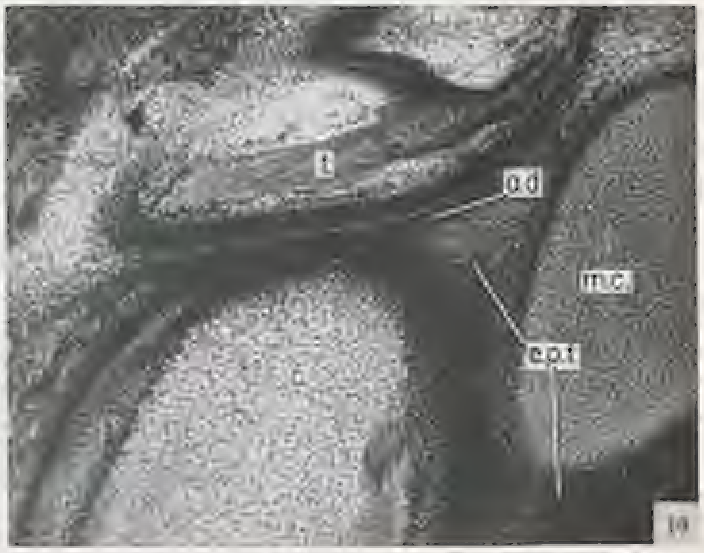
t
a.d.
m.c.
e.p.t.
c
10

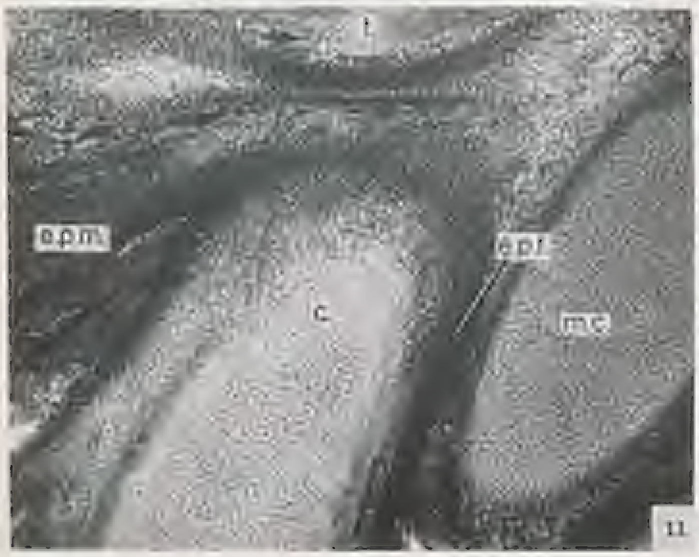
t
e.p.m.
e.p.t.
c
m.c.
11

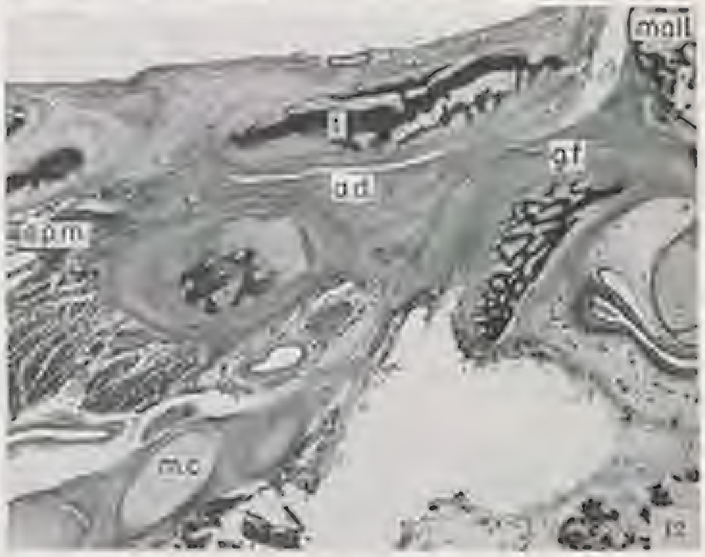
mall.
t
a.f.
a.d.
e.p.m.
m.c.
12

CONTRIBUTIONS TO EMBRYOLOGY, NO. 244

DEVELOPMENTAL HORIZONS IN HUMAN EMBRYOS

Description of Age Group X, 4 to 12 Somites

Chester H. Heuser and George W. Corner

Department of Microscopic Anatomy, Medical College of Georgia, Augusta, and
Department of Embryology, Carnegie Institution of Washington,
Baltimore, Maryland

With two plates and two text figures

CONTENTS

PAGE

INTRODUCTION 31

AGE GROUP X, 4 TO 12 SOMITES 31

External Form, Size, and Age 31

Coelomic Tract 34

Heart 34

Nervous System 35

Notochord and Primitive Streak 35

Nephrogenic Tissue 36

Normal Embryos in Carnegie Collection Belonging in Age Group X 36

Embryos of Horizon X Described or Usefully Cited in the Literature, Including the Present Chapter 36

LITERATURE CITED 38

DEVELOPMENTAL HORIZONS IN HUMAN EMBRYOS

Description of Age Group X, 4 to 12 Somites[1]

INTRODUCTION

For convenience in classifying human embryos as to state of structural organization and age, the late George L. Streeter (1945, 1948, 1949, 1951) set up 23 age groups to indicate levels of development from the fertilized egg to embryos measuring 30 mm. in length, or approximately 47 days old. Beginning with stage xi, ovulation age 24 ± 1 days, Dr. Streeter carried the work forward through the remaining older groups. In preparing a survey of embryos of the first 3 weeks of development, it is convenient to begin with the oldest specimens of the period and thus consider the age group immediately preceding the one first completed by Dr. Streeter.

AGE GROUP X, 4 TO 12 SOMITES

External Form, Size, and Age

The most conspicuous event during age group x is the fusion of the neural folds. In the younger specimens the neural groove is open through its whole length. Fusion of the folds begins at about the stage of 7 somites, and by the end of the period the neural tube is closed from the otic region of the rhombencephalon to about the level of the latest-formed somite. Other important changes of form occur during stage x. The embryo progressively elongates, and the yolk sac continues to expand. At the same time the cranial portion of the neural folds grows forward and becomes distinctly elevated; the tail fold appears at the beginning of the period and overrides the yolk sac, and finally the whole embryo rises above the level of the yolk sac. The visceral components of the head begin to appear. Toward the end of the period, the increasing size of the heart makes the pericardial region a prominent feature of the external form.

The task of compiling for the "Horizons" series a survey of this stage has been lightened by free use of the admirable study of human embryos, covering a slightly longer period of development (2 to 16 somites), that was published by Bartelmez and Evans in 1926. Their study, which was concerned chiefly with the early development of the nervous system, included all relevant embryos then in the Carnegie and the University of Chicago Collections, and incorporated references to specimens in other laboratories. Since it appeared, 3 additional embryos of stage x have been acquired by the Carnegie Collection; the University of Chicago specimens have been deposited there; and 5 embryos have been described from other laboratories. In all, counting both fully described specimens and those that have merely been cited incidentally, about 36 embryos having 4 to 12 pairs of somites are known to have been examined by the embryologists of the world. Of these, 13 are now in the Carnegie Collection (including 2 which are not good enough for use in the "Horizons"), and 6 more are represented there by tracings, photographs, or models. Four of the remainder have been described in monographic form (Orts Llorca, 1934; Politzer, 1930; Schenck, 1954; Sternberg, 1927), so that they can be compared in almost all details with those available at the Department of Embryology in Baltimore. Arey's (1938) comprehensive study of the first somite in human embryos has also been very useful for the present undertaking.

Unfortunately, only one specimen of this period has been received, in the unfixed condition or recently preserved, at the Carnegie laboratory since the development there of expert photographic methods such as produced the superb photographs which Streeter was able to present with his account of horizon xi.

Representative specimens of this age group are illustrated in figures 1 and 2. These outlines, showing the dorsal aspect and the median longitudinal section of each specimen, are enlarged to the same scale. As pointed out by Bartelmez and Evans (1926), the cranial flexure is present in all embryos of this period. A dorsal flexure may or may not be present. The curvature of the dorsal profile varies from a gentle convexity through all degrees of concavity from the least possible curve to a deep, sharp kink. Bartelmez and Evans (1926) and Streeter (1942) have discussed the significance of this variation as seen in human and rhesus embryos of the early somite stages. On the whole, the evidence indicates that, whereas extreme dorsal flexion must be regarded as an artifact, anything from a gentle convexity to a moderate dorsal concavity must be considered normal.

The modeling of the head shows certain significant features. At about the stage of 7 somites the optic sulcus appears as a shallow groove on the external surface of the forebrain (fig. 1). It becomes much more prominent as it extends rostrally in later specimens, but at the end of this stage (no. 3707, 12 somites) the optic primordium, as seen in sections, is still only a thickened ectodermal plate indented by the sulcus.

In discussing the visceral regions of the head we are forced to depend, for lack of good photographs of the youngest stages, upon the evidence afforded by the

---

[1] The studies of C. H. Heuser were supported in part by a research grant, RG-4222, from the National Institutes of Health, U. S. Public Health Service.

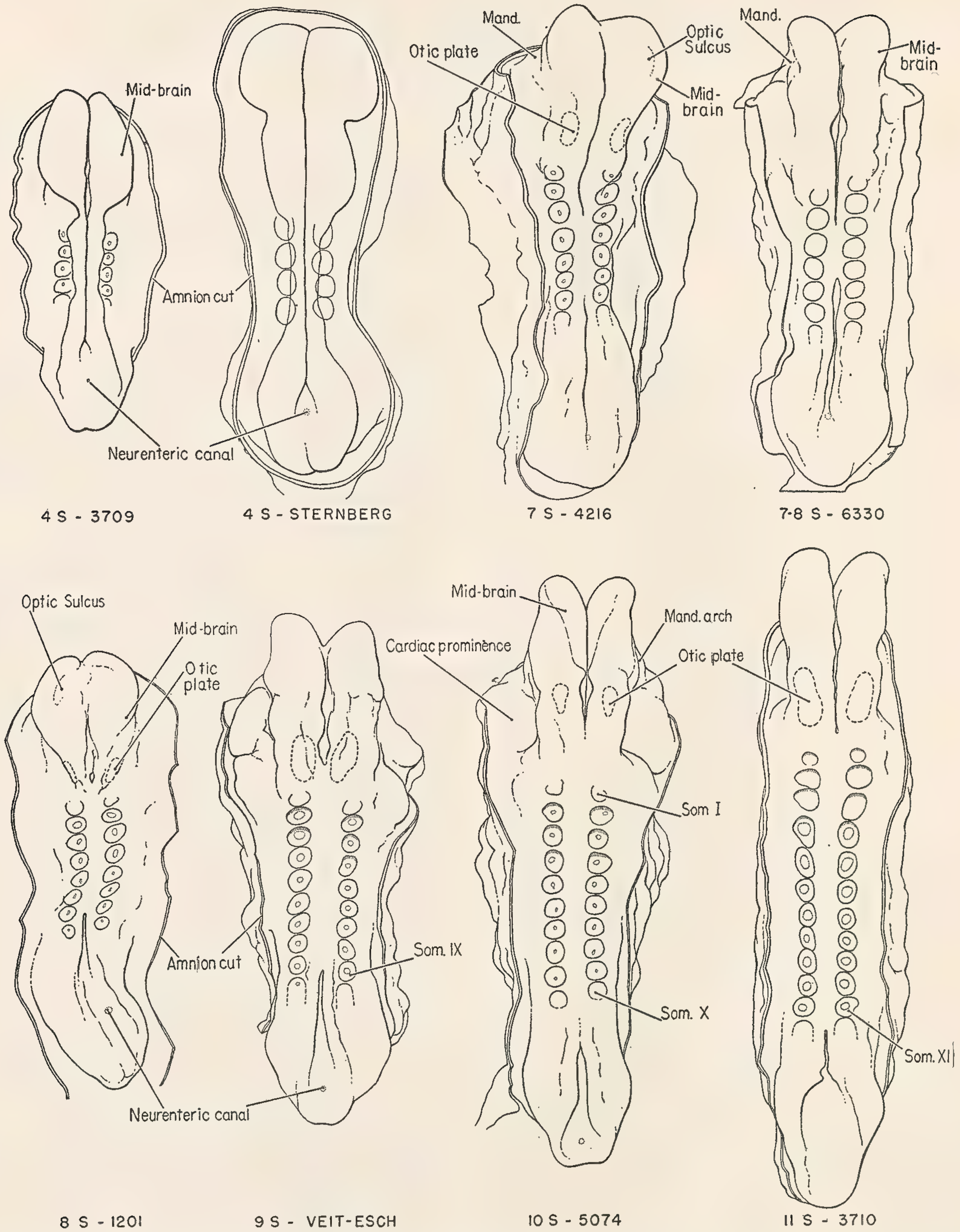

FIG. 1, x. Outline drawings showing, in dorsal view, 8 embryos belonging in age group x. The number of somite pairs and the collection number are given for each specimen. The neural folds still gaping apart or separated from each other in the 4-somite specimens come together, and the fusion rapidly spreads forward into the region of the hindbrain and backward about as far as the last somites formed; the anterior and posterior neuropores shrink, but they are still relatively large in the oldest members of the group. The pericardial region, relatively small in the 4-somite embryos, is prominent in embryos of 10 or more somites. The tracing of one 4-somite embryo was made from figures by Sternberg; no. 6330 and Veit-Esch were drawn from models in Baltimore. The others are drawings based on models and figures by Bartelmez and Evans (1926); Payne (1925); Corner (1929). All figures × 35.

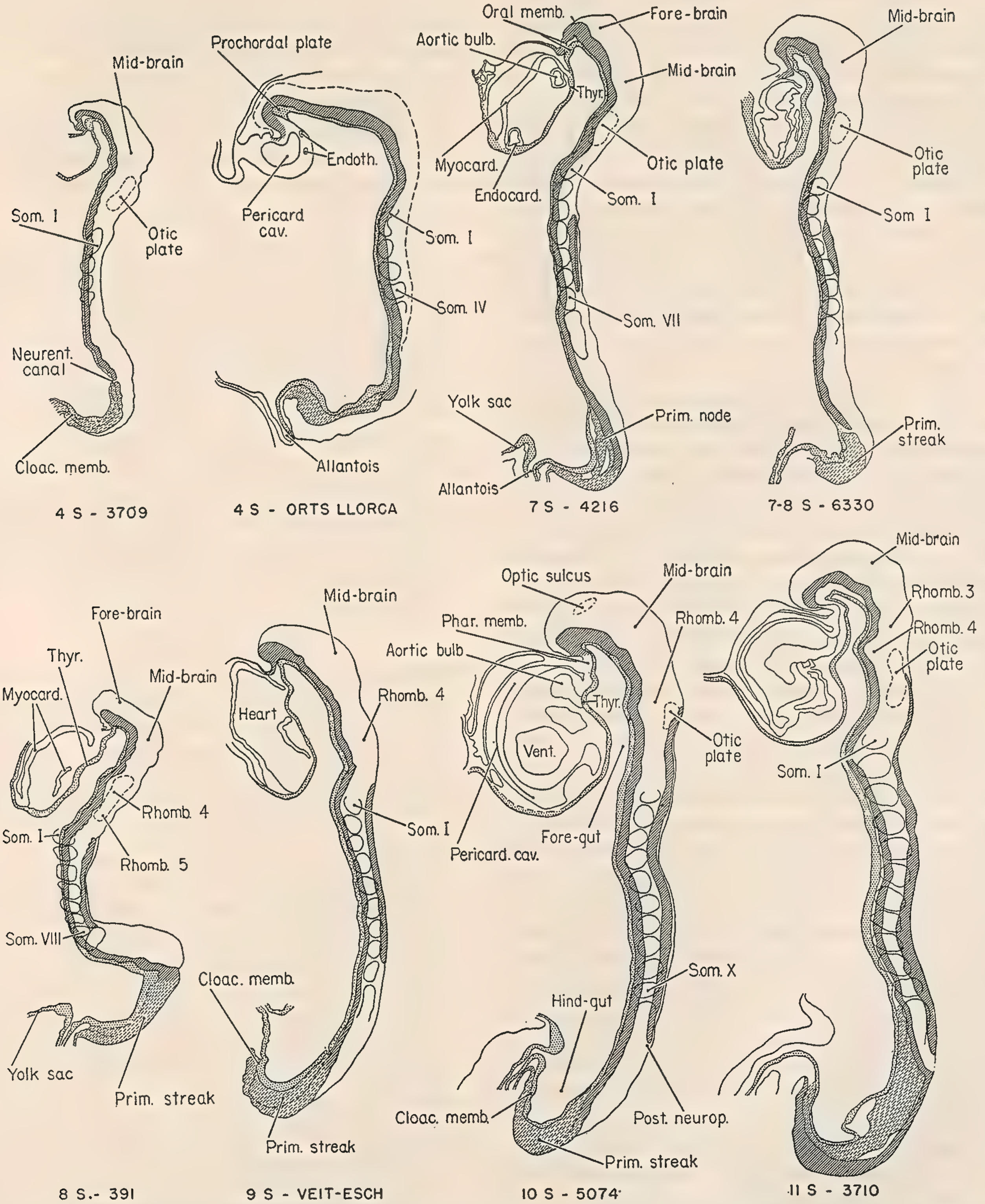

Fig. 2, x. Outline drawings of mid-sagittal sections of embryos belonging in age group x. The head fold is prominent in all the specimens shown, and the tail fold is just beginning to appear in the 4-somite embryo; the hindgut shows the first sign of separating from the yolk sac. The line of fusion of the neural folds lengthens rapidly after the 7-somite stage. In the older embryos the general form of the body is greatly influenced by the enlarging heart and pericardial cavity.

The drawing of one 4-somite embryo was slightly modified from a figure by Orts Llorca (1934); data for the Veit-Esch embryo were obtained from a model in Baltimore, and from a figure by Florian and Völker (1929). No. 6330 was drawn from a model. The others are drawings based on models and figures by Bartelmez and Evans (1926); Payne (1925); and Corner (1929). All figures × 35.

models. In the 4-somite stage, of which 3 modeled specimens are available for comparison, the sides of the head region appear fairly smooth, without swellings to indicate the location of the mandibular and hyoid areas. At the stage of 7 somites the mandibular area is clearly visible as a rounded swelling (no. 4216, Payne, 7 somites; no. 6330, 7 to 8 somites). As Bartelmez and Evans (1926) have described, the hyoid area becomes distinctly visible externally in the models of the Veit embryo (no. 4251, 9 somites); it is perhaps beginning to appear in no. 6330. The maxillary process, recognized by Bartelmez and Evans (1926) as clearly present in the Veit embryo, is scarcely distinguishable on the external surface of the models until about the end of the period (no. 3710, 11 somites).

Swellings at the site of the first and second branchial pouch are evident in the Veit embryo just caudal to the mandibular area and hyoid areas, respectively. At 9 somites the first branchial groove is seen as a distinct depression. In the 11-somite embryos, as far as can be made out from the two available modeled specimens, the second branchial furrow is not yet visible on the surface.

The dimensions of the chorion, recorded in only 8 of the specimens in the Carnegie list, are variable, because of differences in preparation and handling. One chorion has an average diameter (the mean of the largest and smallest diameters) of 19 mm. The average diameter of the other chorions falls between 8 and 15 mm. The dimensions of 6 specimens recorded in published accounts fall within the same range.

The reported size of the embryo itself, expressed by the greatest length, is of no great informational value, for various reasons which have been well set forth by Bartelmez and Evans (1926, pp. 17–18). The lengths of the embryos of this stage in the Carnegie records, omitting those known to be badly flexed, are from 2.0 to 2.7 mm., with one exception, no. 3710, which measured 3.6 mm. in formol and 3.0 mm. as modeled. The clinical histories do not provide useful information about the age of the embryos in this group; as Streeter pointed out in his remarks about the age limits of subsequent horizons, the best estimate is obtained by matching the specimens against macaque embryos of known ovulation age at a similar stage of development. Three such macaque embryos in the Carnegie Comparative Collection having 5 to 9 somites are listed (C 418, C 474, C 649), and 2 of them, 21 to 23 days old, are illustrated by Heuser and Streeter (1941). If the human embryos are of comparable age, an ovulation age of 22 days can be tentatively assigned to horizon x. The fact that an 11-somite monkey embryo (C 495) had an ovulation age of 24¾ days must be kept in mind as a warning that the age estimates for *Macaca mulatta* and the comparison with human embryos are based on limited material having an as yet unknown range of variability.

In summary, the characteristics of this age group are: fusion of the neural folds is imminent or in progress; the optic sulcus is present; the mandibular and hyoid bars begin to be visible externally; 4 to 12 pairs of mesodermal somites are present; the embryo in most cases is between 1.5 and 2.0 mm. long; the average diameter of the chorion is between 8 and 15 mm. The ovulation age of the group is estimated to be 22 ± 1 days.

Coelomic Tract

The pericardial cavity is present as a horseshoe-shaped cavity in the earliest embryos of this group (horizon x) (Orts Llorca; Sternberg; no. 3709), all of 4 somites. The future pleural and peritoneal spaces are represented only by small discontinuous cavities in the mesoblastic sheet; these spaces gradually coalesce, and at the 7-somite stage the passage thus formed opens more or less freely into the extraembryonic coelom. The process of cavitation of the mesoblast now continues, as the body wall and gut differentiate, until, in the later embryos of horizon xi, an extensive coelomic space is formed. Streeter (1942) has interestingly discussed the primitive coelom as a means for access of nutritive fluid to the embryonic tissues before the development of the blood vessels.

Heart

Goss (1938), extrapolating to the human species his observations on the first beating of the heart in rat embryos, states that the human heart must begin to beat at about the 3-somite stage, that is, the end of horizon ix. This event is followed in horizon x by marked changes of form by which the organ becomes ultimately an effective pump. The development has been very carefully described in an article by C. L. Davis (1927), with excellent illustrations by J. F. Didusch, to which the reader is referred for details. Here need be given only a summary with confirmatory mention of specimens obtained since Davis wrote.

Three distinct steps in the development of the heart can be recognized in this horizon. The first, seen at the stage of 4 somites, is illustrated by Davis in his figure 12 (no. 3709) and figure 16 ("Klb"). The endocardial rudiment of the heart at this stage is a plexus of delicate vessels lying on the foregut. It consists of two parallel channels interconnected by two or more small transverse vessels. This condition is matched by all the other 4-somite embryos available for comparison (no. 2795; Orts Llorca; Sternberg), except that in Sternberg's figure the endocardium is represented as consisting largely of discontinuous spaces, probably because of the difficulty of reconstructing collapsed channels from serial sections.

The myocardial wall of the heart, as illustrated by Davis, also shows traces of origin from two tubes. Transverse sulci mark off the regions of the aortic bulbs, ventricles, and atria.

In the second step (stage of 7 to 8 somites, illustrated by Davis' fig. 17 [no. 4216], fig. 20 [no. 4439], and fig. 22 [no. 391]), the two endothelial tubes have fused in the regions of the aortic bulb and bulbus cordis, and also progressively in the ventricular region; the fusion becomes complete at the 8-somite stage, the atria still being left paired. The single ventricular tube thus formed is at first practically straight, then assumes the gentle beginnings of an S curve. Embryos that have become available since Davis' work (no. 6330, 7 or 8 somites; Politzer, 8 somites; West, no. 4983, 8 somites) all agree closely with the foregoing account.

The enveloping myocardial wall is also a single tube as far as the ventricular region, but distinct bulges, to the left cranially and to the right caudally, give evidence of the imminent curving while the endocardium is as yet scarcely curved.

The third step is the definite appearance of the S curve of the bulbus cordis and ventricular endocardial tube. The curvature, which is not marked in some of the 9-somite embryos (Eternod "Du Ga," no. 4439; Wilson H. 98, no. 7251), is apparent in the 9-somite Veit specimen, no. 4251, and well developed in no. 5074 (10 somites). Davis illustrates it in the 12-somite embryo no. 3707.

In the myocardial wall, deep sulci separate the bulbar region from the twisted ventricular segment, and the latter from the right atrium.

The heart is ready to begin the propulsion of blood through the pathways that are becoming available by the formation of the first and second aortic arches at about the end of horizon x.

Nervous System

The nervous system, because of its simplicity at this period, offers few salient features that are useful in the classificatory description at which these Horizons aim. The elevation of the head fold has been mentioned in the introductory paragraph.

The otic placode (otic plate or disk) could probably be seen by direct inspection of intact embryos of the horizon in the unfixed condition or after recent formol fixation. As Bartelmez (1922) showed, the otic placode appears very early in development and affords an excellent landmark for analyzing the early embryonic brain. It has been identified in sections in all phases of this horizon, early and late. In the oldest specimen, no. 3707, the plate is perhaps just beginning to show the invagination, preparatory to formation of the otic cyst, which is characteristic of horizon xi.

As to the closure of the neural groove, some of the newer specimens help to throw light upon the time of this event and the level at which it begins. The earliest embryo, as defined by a precise count of the somites, in which closure of the folds is under way is the 6-somite Huber embryo, Michigan no. 71. Professor Arey states (personal communication) that in this specimen the neural folds are in relatively close relation throughout most of the somite region. Actual fusion extends from the middle of somite 2 to the middle of somite 3. If, as Bartelmez supposes (personal communication), the West embryo, no. 4923, has only 5 or 6 somites instead of 8 as tentatively counted by West, it would be the earliest known embryo showing closure. The 6-somite Farris embryo, no. 8244, has a completely open neural groove. The embryo "Ludwig" (Streiter, 1951), ostensibly of 7 somites, is out of line with all others of comparable somite number; the extensive closure of the neural tube, taken into account with other advanced features, throws doubt on the somite count.

The level at which fusion begins is evidently variable. Bartelmez and Evans (1926) located it at about the 4th somite, basing their conjecture on an apparently impending closure at that level in the Pfannenstiel embryo of 5 or 6 somites, and also on retrospective calculation from no. 4216 (7 somites), in which the tube is closed from the middle of the 3d to the middle of the 6th pair of myotomes. In Politzer's 8-somite embryo, the fusion, which must have begun at about the same level, has reached two somites farther caudally, extending from the middle of the 3d to the middle of the 8th myotome. (This statement takes account of Arey's correction of the somite count; compare his article of 1938 and the list of embryos, page 37 of the present paper.) West's embryo has only a short closure opposite the 6th somite. Since the first contact occurs wherever the curving edges of the infolding ridges meet, it is to be expected that, when additional specimens having 6 or 7 somites are obtained, some scattering of the level of first contact from the 2d to the 7th somite will be found.

The rate of spread of the closure in both directions was tabulated by Bartelmez and Evans (1926). As they point out, the caudal extension of the closure proceeds at about the same rate as the formation of new somites, so that the margin of the posterior neuropore is usually opposite the latest pair of somites. Rostrally, progress is slower and apparently more variable. At the end of the period of horizon x, no. 3707, closure has reached well into the hindbrain region (rhombomere 3). The 10-somite embryo no. 5074, which may now be added to the tabulation, is no exception, the closed part of the neural tube reaching from the caudal end of the 10th somite to the level of the otic plate.

Notochord and Primitive Streak

By the time embryos are 3 weeks old, the cephalic region has greatly increased in size, and in all members of horizon x the primitive node and streak are limited to the relatively short caudal part of the body. At the headward limit of the primitive streak the embryonic node is about at the entrance of the hindgut. Florian (1934) illustrates this point in a diagram in which one of the youngest embryos of stage x, Sternberg's Vienna A, is included. This condition persists throughout the period of horizon x, existing in all the embryos available for comparison by study of the sections or by published descriptions. In the embryos of this age group tabulated by Bartelmez and Evans (1926), the length of the primitive streak was found to be 25 per cent of the total length of the embryo at the 4-somite stage (no. 3709), and to decrease to 18 per cent at the 11-somite stage (no. 3710). From the diagram of Florian (1934), a similar calculation can be made which gives a somewhat smaller proportionate length: about 14 per cent of the length of the embryo in the Veit-Esch embryo (9 somites) and Bi XI (10 somites).

The general picture of the notochord, which differs from specimen to specimen only in lengthwise dimension and in details of cellular structure, is that of a chordal plate or bar of cells beginning at the anterior end of the foregut and running caudally until it merges with the primitive streak. During most of its length the notochord is embedded in the dorsal endoderm, but in many embryos of horizon x it becomes clearly separate from the gut wall, and for a short distance (a few sections) forms a distinct rodlike structure which ultimately joins the primitive streak.

Nephrogenic Tissue

At horizon x the nephric structures first appear. This occurrence has very recently been reviewed by Torrey (1954), who had at his disposal all the Carnegie embryos listed herewith. Nephric structures are absent in the 7-somite embryo (no. 4216), as stated by Payne and confirmed by Torrey. Embryos with 8 somites are the youngest that are known to show such rudiments. The specimen (no. 391) described by Dandy (1910), and embryo no. 6330, possess primitive segment stalks with characteristic nephrocoels and variable connections (peritoneal funnels) with the coelomic epithelium, but other parts of the nephrons develop later. Confirming Corner (1929), Torrey places the first formation of a definitive nephron at the 10-somite stage (no. 5074). The Corner embryo, in addition to the structures named above, shows the rudiments of pronephric tubules in the form of elevations from the dorsal walls of the nephrotomes and the beginning of a solid nephric ridge.

Normal Embryos in Carnegie Collection Belonging in Age Group X

The embryos available for this study are listed in the accompanying table. In the 3d column, E. gives the greatest length of the embryo and Ov. is the average diameter (the mean of the greatest and least diameters) of the chorion. The grade of the embryo, "Poor," "Good," or Excellent ("Exc."), refers to the total grade of the specimen, and includes both its original quality and the condition of the mounted sections. The cutting medium was either paraffin (P) or a combination of celloidin and paraffin (C-P). All sections were cut in a transverse plane.

Embryos of Horizon X Described or Usefully Cited in the Literature, Including the Present Chapter

4 somites, Carnegie Collection no. 3709, Baltimore (University of Chicago H. 279). Characterized, with outline sketches, by Bartelmez and Evans (1926).

4 somites, Histologisch-Embryologisches Institut, Embryo A, Vienna. Fully described by Sternberg (1927).

4 somites, Histologisch-Embryologisches Institut, Embryo Ca, Vienna. Fully described by Orts Llorca (1934).

4 to 5 somites, Florian's Embryo Bi II. The whereabouts of this, the following embryo, and the 10-somite Bi XI (see below) are not known; Florian's collection has not been found since his death during World War II. The embryo Bi II was briefly characterized by Studnička (1929), cited and partly illustrated by Florian (1928, 1930).

4 to 5 somites, Florian's Embryo Bi III. (See note on previous embryo.) Briefly characterized by Studnička (1929) and cited by Florian (1928).

4 to 5 somites, Carnegie Collection no. 2795, Baltimore. Cited and briefly characterized by Bartelmez and Evans (1926). The specimen is distorted and somewhat macerated.

5 somites, Anatomisches Institut, Zurich, GM 1954. Described and illustrated by Schenck (1954).

5 to 6 somites, Pfannenstiel "Klb" (originally at Giessen; was in Keibel's Institute at Freiburg i. B. about 1911, may now be in Berlin). This well known embryo is no. 3 in the Keibel and Elze Normentafel (1908). Models by Kroemer (1903). A partial set of tracings made by H. M. Evans is in the Carnegie Collection, no. 5463.

6 somites, Carnegie Collection no. 8244, Baltimore. Somewhat distorted; histologically fair.

6 somites, University of Michigan no. 71, Ann Arbor. Briefly described by Arey and Henderson (1943). A full description in an unpublished doctoral dissertation is in the files of L. B. Arey at Northwestern University, Chicago.

6 somites, Carnegie Collection no. 8818, Baltimore (University of Chicago H. 338). Pathological; not used in present study. Listed here because cited by Bartelmez and Evans (1926).

6 to 7 somites, His' Embryo "SR." Cited by His (1880) and by Bartelmez and Evans (1926). Has been studied only in the gross.

6 to 7 somites, Embryo LM, present location unknown. Cited here from manuscript notes at Carnegie laboratory, made from Russian text of Burow (1928). Condition said to be poor.

7 somites, Carnegie Collection no. 4216, Baltimore. Described by Payne (1925), and very frequently cited.

7 (?) somites, Embryo "Ludwig," Berlin. Described by Streiter (1951). This specimen, which is somewhat macerated, is in certain characteristics considerably in advance of others of similar somite number.

7 or 8 somites, Carnegie Collection no. 6330, Baltimore (University of Chicago H. 1404). Extensive manuscript notes on this specimen, made under the supervision of G. W. Bartelmez, are in the files of the Carnegie laboratory.

8 somites, Dublin. Described by West (1930); see also Arey (1938). Photographs and models are in the Carnegie Collection, no. 4923. Bartelmez (personal communication) thinks that this distorted embryo had only 5 or 6 somites.

List of Embryos

Serial no.	Paired somites	Size (mm.)	Grade	Fixation	Cutting medium	Thinness (microns)	Stain	Date, donor, and remarks
391	8	E., 2 Ov., 14	Good	Formol	P	10	Al. coch.	1907, R. W. Pearce, Albany, N. Y. Monograph by W. E. Dandy
1201	8	E., 2 Ov., 14.4	Good	Formol	P	8	H.-Or. G.	1915, A. B. Streedain, Chicago (University of Chicago H. 87)
2795	4–5	E., 2 Ov., . . .	Poor	Alcohol	P	6	Al. coch. Or. G.	1919, H. H. Cushing, Philadelphia
3707	12	E., 1.5 Ov., . . .	Good	Formol	P	12.5	Iron H.	1921, R. T. Legge, Berkeley, Calif. (University of Calif. H. 197)
3709	4	E., 1.74 Ov., 14.8	Poor	Formol	P	10	Erythrosin	1921, J. P. Spooner, Peru, Ind. (University of Chicago H. 279)
3710	11	E., 3.6 Ov., 19.0	Good	Formol	C–P	10	H.-Or. G.	1921, E. Rice, Chicago (University of Chicago H. 392)
4216	7	E., 2 Ov., 9.8	Good	Formol	P	15	?	1923, F. Payne, Bloomington, Ind. Monograph by F. Payne
5074	10	E., 3.3 Ov., 10.8	Exc.	Bouin	P	10	Al. coch.	1925, T. Jameson, Rochester, N. Y. (University of Rochester H. 10). Monograph by G. W. Corner
6330	7–8	E., 2.83 Ov., . . .	Good	?	C–P	5	Ehr. H.	1931, S. S. Schochet, Chicago (University of Chicago H. 1404)
8244	6	E., 1.55 Ov., 8.5	Good	Alcohol	C–P	8	H.-E. Phloxine	1944, E. J. Farris, Philadelphia
8970	12	E., . . . Ov., ca. 8	Good	Zenker	P	5	Various, chiefly carmine	1952, E. Hirsch, Chicago (University of Chicago H. 637)

8 somites, Carnegie Collection no. 391, Baltimore. Described by Dandy (1910) and frequently cited (cf. Bartelmez and Evans, 1926, with additional illustrations). There were neither camera drawings nor photographs of the intact specimen, and therefore the reconstructions are not entirely satisfactory. The plaster models now at the Carnegie laboratory were made by O. O. Heard under the supervision of Bartelmez for the paper by Bartelmez and Evans (1926). The apparent lack of fusion of the neural folds described by Dandy is an artifact produced by a crack.

8 somites, Carnegie Collection no. 1201, Baltimore (University of Chicago H. 87). Described briefly by Evans and Bartelmez (1917); cited, with illustrations, by Bartelmez and Evans (1926).

8 somites, Embryologisches Institut, Embryo Ct, Vienna. Fully described by Politzer (1930). Arey (1938) counts 8 paired somites in this embryo instead of 7 as stated by Politzer.

9 somites, University of Cambridge, Department of Anatomy H. 98. Photographs and models in Carnegie Collection, no. 7251. Described by J. T. Wilson (1914). Cited by Bartelmez and Evans (1926), who consider it slightly abnormal in form though good histologically.

9 somites, Embryo "Esch 1," Marburg. Elaborately described by Veit and Esch (1922), and cited, with illustrations, by Bartelmez and Evans (1926), who count 9 somites instead of 8 as stated by the original authors. Photographs and models are in the Carnegie Collection, no. 4251.

9 somites, Embryo "Du Ga," Geneva. Described by Eternod (1896); models by Ziegler were distributed commercially. Cited by Bartelmez (1922) and Bartelmez and Evans (1926), with illustrations. Tracings made by H. M. Evans at Geneva and models are in the Carnegie Collection, no. 4439.

About 9 somites, Embryo Unger, Keibel Collection, Freiburg i. B., no. 4 of Keibel and Elze (1908). Listed by Bartelmez and Evans (1926).

9 somites, Embryo "Jacobsen," formerly at Kiel (Graf

Spee's collection was destroyed in World War II). Described by von Spee (1887). Listed by Bartelmez and Evans (1926) as having "at least" 9 somites.

9 somites, Embryo Ca of Orts Llorca, Madrid. Various details described by Mari Martínez (1950) and Martínez Rovira (1953).

9 to 10 somites, Embryo R. Meyer 335 (Professor Robert Meyer's collection was purchased by the late Dr. Hedwig Frey and bequeathed by him to the Anatomisches Institut, University of Zurich). Listed by Bartelmez and Evans (1926), and cited by Felix (1912).

10 somites, Carnegie Collection no. 5074, Baltimore (University of Rochester H. 10). Fully described by Corner (1929), and subjected to volumetric analysis by Boyden (1940).

10 somites, Grosser's Embryo Schw2 (present location unknown). Briefly described, without illustrations, by Treutler (1931). Preservation said to be not altogether satisfactory.

10 somites, Florian's Embryo Bi XI. (*See note on Bi II above.*) Briefly described, with illustrations, by Politzer and Sternberg (1930); cited and partly illustrated by Florian (1930).

10 somites, Anatomy Department, University of South Wales, Cardiff. Partly described and illustrated by Baxter and Boyd (1939).

11 somites, Carnegie Collection no. 3710, Baltimore (University of Chicago H. 392). Cited by Bartelmez (1922) and Bartelmez and Evans (1926).

11 somites, Embryo T 152, University of Toronto, Department of Anatomy. Cited by Arey (1938).

11 somites, Embryo G-dt, Uppsala. Described by Holmdahl (1943) as having 11 well differentiated somite pairs, with beginning delimitation of 4 more.

11 to 12 somites, Carnegie Collection no. 8970, Baltimore (University of Chicago H. 637). Somewhat damaged. Cited, with illustrations, by Bartelmez (1922) and Bartelmez and Evans (1926).

12 somites, Carnegie Collection no. 3707, Baltimore (University of California H. 197). "Legge embryo." Cited, with illustrations, by Bartelmez and Evans (1926). The coital history accompanying this specimen, which was declared to be reliable, would give it an ovulation age of either 18 or 39 days; the former seems too little, and the latter is much too long.

12 somites, Litzenberg embryo, University of Minnesota, Minneapolis. Briefly described by J. C. Litzenberg (1933); characterized and subjected to volumetric analysis by Boyden (1940), who counts 12 somites instead of 13 to 14 as in the original description. Photographs and model in Carnegie Collection, no. 6740.

12 somites, M. 24, University of Michigan, Ann Arbor. Cited by Arey (1938).

LITERATURE CITED

Arey, L. B. 1938. The history of the first somite in human embryos. Carnegie Inst. Wash. Pub. 496, Contrib. to Embryol., vol. 27, pp. 233–269.

——— and J. W. Henderson. 1943. The Huber six-somite human embryo (no. 71). Anat. Rec., vol. 85, p. 295.

Bartelmez, G. W. 1922. The origin of the otic and optic primordia in man. Jour. Comp. Neurol., vol. 34, no. 2, pp. 201–232.

——— and H. M. Evans. 1926. Development of the human embryo during the period of somite formation, including embryos with 2 to 16 pairs of somites. Carnegie Inst. Wash. Pub. 362, Contrib. to Embryol., vol. 17, pp. 1–67.

Baxter, J. S., and J. D. Boyd. 1939. Observations on the neural crest of a ten-somite human embryo. Jour. Anat., vol. 73, pp. 318–326.

Boyden, E. A. 1940. A volumetric analysis of young human embryos of the 10- and 12-somite stage. Carnegie Inst. Wash. Pub. 518, Contrib. to Embryol., vol. 28, pp. 157–191.

Burow, W. S. 1928. A human embryo in the first month of embryonic life. Med. Jour. Irkutsk, vol. 6, pp. 71–79. (Title and text in Russian; no illustrations.)

Corner, G. W. 1929. A well-preserved human embryo of 10 somites. Carnegie Inst. Wash. Pub. 394, Contrib. to Embryol., vol. 20, pp. 81–102.

Dandy, W. E. 1910. A human embryo with seven pairs of somites, measuring about 2 mm. in length. Amer. Jour. Anat., vol. 10, pp. 85–109.

Davis, C. L. 1927. Development of the human heart from its first appearance to the stage found in embryos of 20 paired somites. Carnegie Inst. Wash. Pub. 380, Contrib. to Embryol., vol. 19, pp. 245–284.

Eternod, A. C. F. 1896. Sur un œuf humain de 16.3 mm. avec embryon de 2.11 mm. (utérus et annexes). Actes de la Soc. Helvet. des sci. natur., vol. 79, pp. 164–169.

Evans, H. M., and G. W. Bartelmez. 1917. A human embryo of 7 to 8 somites. Anat. Rec., vol. 11, pp. 355–356.

Felix, W. 1912. The development of the urinogenital organs. *In* F. Keibel and F. P. Mall (eds.), *Manual of human embryology*, vol. 2, chap. 19, pp. 752–979. Philadelphia.

Florian, J. 1928. La gouttière primitive, le canal de Lieberkühn et la plaque chordale chez deux embryons humains (Bi II, Bi III) avec quatre somites. Compt. rend. de l' Assoc. des anat., vol. 23, pp. 154–162.

——— 1930. The formation of the connecting stalk and the extension of the amniotic cavity towards the tissue of the connecting stalk in young human embryos. Jour. Anat., vol. 64, pp. 454–476.

——— 1934. Ein Schema der Entwicklung der Axialgebilde des menschlichen Embryos bis in das Stadium von 10 Urwirbelpaaren. Biologia Generalis, vol. 50, pp. 533–544.

——— and O. Völker. 1929. Ueber die Entwickelung des Primitivstreifens, der Kloakenmembran und der Allantois beim Menschen. Ztschr. f. mikrosk.-anat. Forsch., vol. 16, pp. 75–100.

Goss, C. M. 1938. The first contractions of the heart in rat embryos. Anat. Rec., vol. 70, pp. 505–524.

Heuser, C. H., and G. L. Streeter. 1941. Development of the macaque embryo. Carnegie Inst. Wash. Pub. 525, Contrib. to Embryol., vol. 29, pp. 15–55. Reprinted in *Embryology of the Rhesus Monkey* (*Macaca mulatta*), Carnegie Inst. Wash. Embryology Reprint Volume I.

His, W. 1880. Anatomie menschlicher Embryonen: 1, Embryonen des ersten Monats. F. C. W. Vogel, Leipzig, 184 pp.

Holmdahl, D. E. 1943. Beitrag zur Kenntnis der Entwicklung des Blutgefassystems und Blutes beim Menschen. Nebst einem Exkurs über die Entstehung der Neuralleiste. Eine Studie mit Ausgangspunkt von einem frühen, operativ gewonnen, menschlichen Embryo G-dt, 1.7 mm., mit 11

(-15) Somitenpaaren. Ztschr. f. mikrosk.-anat. Forsch., vol. 54, pp. 219-296.

Keibel, F., and C. Elze. 1908. Normentafel zur Entwickelungsgeschichte des Menschen. Jena. 314 pp., 6 plates.

Kroemer, P. 1903. Wachsmodell eines jungen menschlichen Embryo. Verh. d. deutsch. Gesellsch. f. Gynäkol., Wurzburg, p. 537.

Litzenberg, J. C. 1933. A young human ovum of the early somite period. Amer. Jour. Obstet. and Gynecol., vol. 26, pp. 519-529.

Mari Martínez. 1950. Embrión humano (Ca) con nueve pares de segmentos primitivos. Contribución al estudio de las primeras fases de la diferenciación somítica en el embrión humano. Arch. españ. de morfol., vol. 8, no. 9, pp. 225-242.

Martínez Rovira, José. 1953. Estudio de la notocorda ("Chorda dorsalis") en un embrión humano de nueve pares de somitos. Arch. españ. de morfol., vol. 10, pp. 179-191.

Orts Llorca, F. 1934. Beschreibung eines menschlichen Embryo mit 4 Urwirbelpaaren. Ztschr. f. Anat. u. Entwick., vol. 103, pp. 765-792.

Payne, F. 1925. General description of a 7-somite human embryo. Carnegie Inst. Wash. Pub. 361, Contrib. to Embryol., vol. 16, pp. 115-124.

Politzer, G. 1930. Ueber einen menschlichen Embryo mit sieben Urwirbelpaaren. Ztschr. f. Anat. u. Entwick., vol. 93, pp. 386-428.

——— and H. Sternberg. 1930. Ueber die Entwicklung der ventralen Körperwand und des Nabelstranges beim Menschen. Ztschr. f. Anat. u. Entwick., vol. 92, pp. 279-376.

Rodríguez Maffiotte, C. 1954. Estudio del embrión humano Ca de nueve pares de somitos. Acta Med. Tenerife (Santa Cruz), 3/suppl., 1, 24 pp.

Schenck, R. 1954. Beschreibung eines menschlichen Keimlings mit 5 Ursegmentpaaren. Acta Anat., vol. 22, pp. 236-271.

von Spee, F. 1887. Ueber einen menschlichen Embryo von 2.69 mm. längstem geraden Durchmesser. Mitth. f. d. Vereines Schleswig-Holsteiner Aerzte, part 11, no. 8.

Sternberg, H. 1927. Beschreibung eines menschlichen Embryo mit vier Ursegmentpaaren, nebst Bemerkungen über die Anlage und früheste Entwicklung einiger Organe beim Menschen. Ztschr. f. Anat. u. Entwick., vol. 82, pp. 142-240.

Streeter, G. L. 1942. Developmental horizons in human embryos. Description of age group xi, 13 to 20 somites, and age group xii, 21 to 29 somites. Carnegie Inst. Wash. Pub. 541, Contrib. to Embryol., vol. 30, pp. 211-245.

——— 1945. Developmental horizons in human embryos. Description of age group xiii, embryos about 4 or 5 millimeters long, and age group xiv, period of indentation of the lens vesicle. Carnegie Inst. Wash. Pub. 557, Contrib. to Embryol., vol. 31, pp. 27-63.

——— 1948. Developmental horizons in human embryos. Description of age groups xv, xvi, xvii, and xviii, being the third issue of a survey of the Carnegie Collection. Carnegie Inst. Wash. Pub. 575, Contrib. to Embryol., vol. 32, pp. 133-203.

——— 1949. Developmental horizons in human embryos. A review of the histogenesis of cartilage and bone. Carnegie Inst. Wash. Pub. 583, Contrib. to Embryol., vol. 33, pp. 149-167.

——— 1951. Developmental horizons in human embryos. Description of age groups xix, xx, xxi, xxii, and xxiii, being the fifth issue of a survey of the Carnegie Collection. Carnegie Inst. Wash. Pub. 592, Contrib. to Embryol., vol. 34, pp. 165-196.

The cited five papers by Streeter have been reprinted in Carnegie Inst. Wash. Embryology Reprint Volume II, 1951.

Streiter, A. 1951. Ein menschlicher Keimling mit 7 Urwirbelpaaren (Keimling Ludwig). Ztschr. mikrosk.-anat. Forsch., vol. 57, pp. 181-248.

Studnička, F. K. 1929. Ueber den Zusammenhang des Cytoplasmas bei jungen menschlichen Embryonen. Ztschr. f. mikrosk.-anat. Forsch., vol. 18, pp. 553-656.

Torrey, T. W. 1954. The early development of the human nephros. Carnegie Inst. Wash. Pub. 603, Contrib. to Embryol., vol. 35, pp. 175-197.

Treutler, K. 1931. Ueber das wahre Alter junger menschlicher Embryonen. Anat. Anz., vol. 71, pp. 245-258.

Veit, O., and P. Esch. 1922. Untersuchung eines in situ fixierten, operativ gewonnenen menschlichen Eies der vierten Woche. Ztschr. f. Anat. u. Entwick., vol. 63, pp. 343-414.

West, C. M. 1930. Description of a human embryo of eight somites. Carnegie Inst. Wash. Pub. 407, Contrib. to Embryol, vol. 21, pp. 25-35.

Wilson, J. T. 1914. Observations upon young human embryos. Jour. Anat. and Physiol., vol. 48, pp. 315-351.

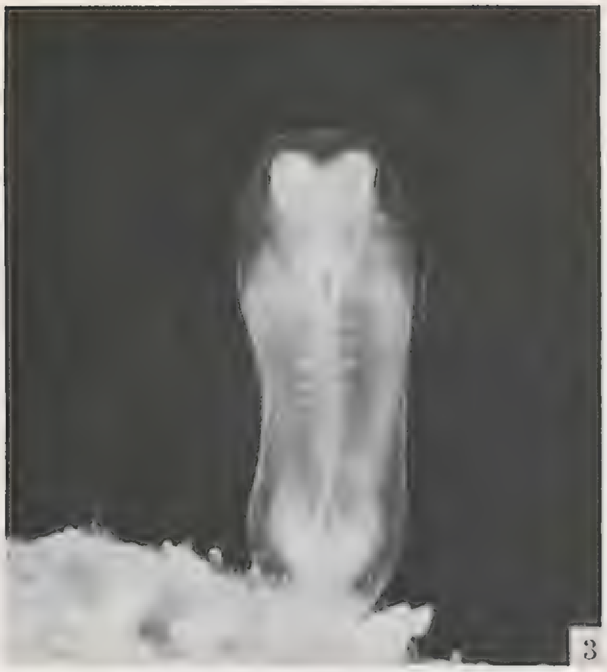
3

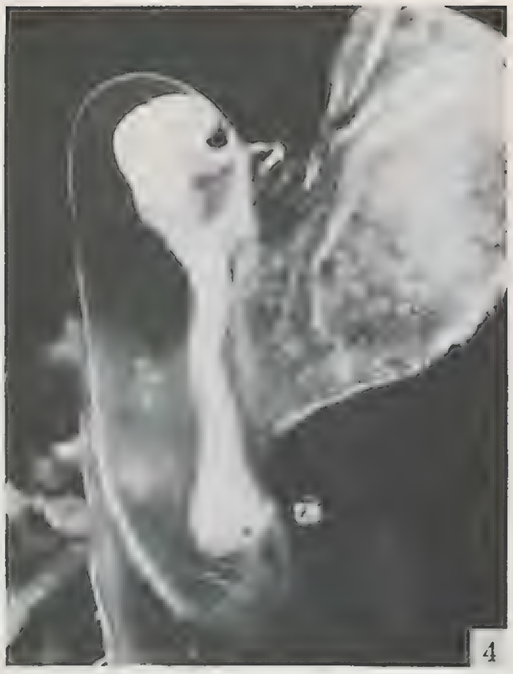
4

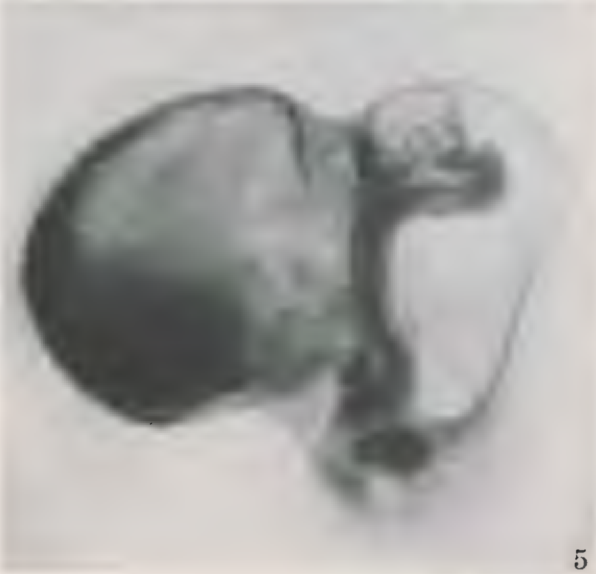
5

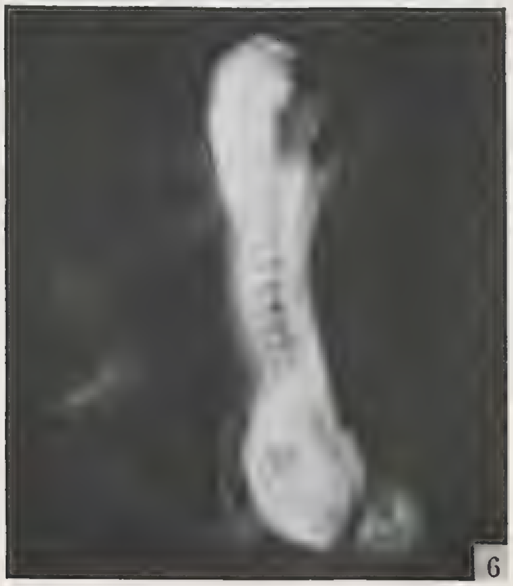
6

Photographs of 3 embryos with 7 to 11 pairs of somites. In the dorsal view of no. 6330 (fig. 3), the neural folds are well shown both in the brain and in the spinal-cord regions. The folds are actually fused in a short region of the embryo as indicated in the outline sketches of the same specimen (figs. 1 and 2). The mandibular arch is clearly seen in the lateral view, figure 4. The 9-somite embryo, H. 98 (Wilson, 1914), figure 5, has an unusually abrupt upward bending of the front third of the body. The relations of heart, yolk sac, and other details are well shown.

Fig. 3. Embryo no. 6330. × 20.
Fig. 4. Embryo no. 6330. × 20.
Fig. 5. Embryo H. 98. × 30.
Fig. 6. Embryo no. 3710. × 20.

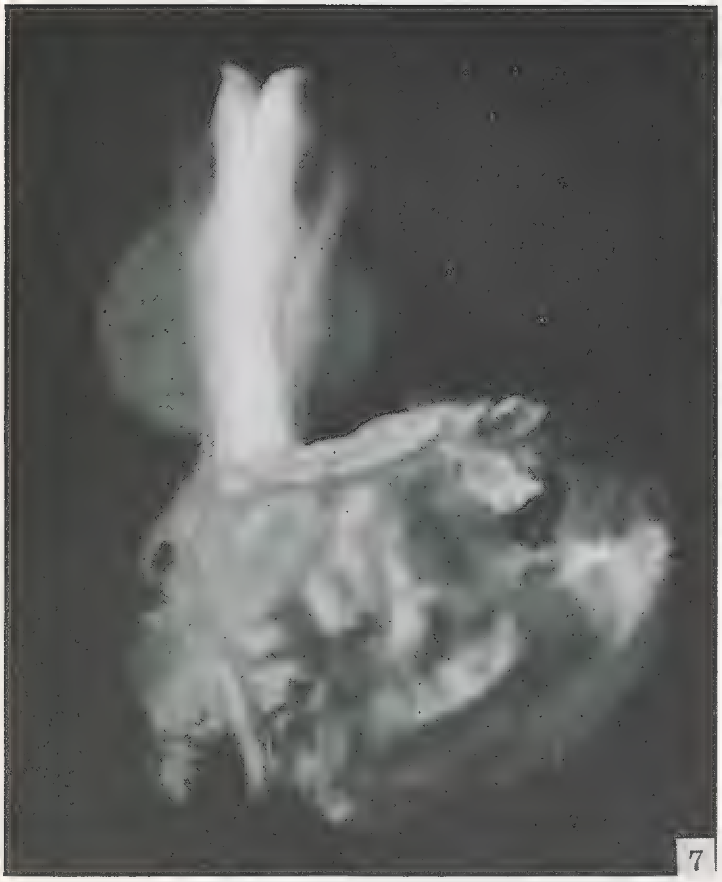

7

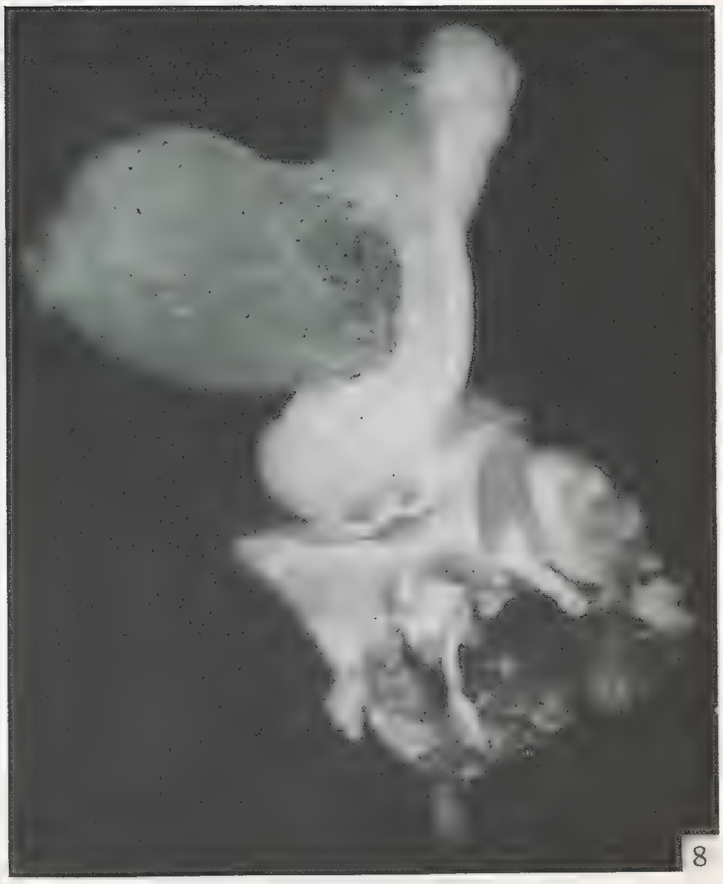

8

Photographs of the 10-somite embryo no. 5074, made after most of the amnion had been cut off. The general body form and structural details of the embryo are well shown in both the dorsal and lateral views. The neural closure extends a short distance caudal to the last somite, to the level of the otic segment of the hindbrain. The pericardial cavity is quite large in this specimen; in figure 8 the heart itself is faintly visible through the thin, semitransparent body wall.

Fig. 7. Embryo no. 5074. × 20.

Fig. 8. Embryo no. 5074. × 20.

CONTRIBUTIONS TO EMBRYOLOGY, NO. 245

THE EARLY DEVELOPMENT OF THE TRACHEA AND ESOPHAGUS IN RELATION TO ATRESIA OF THE ESOPHAGUS AND TRACHEOESOPHAGEAL FISTULA

E. Ide Smith

Department of Embryology, Carnegie Institution of Washington, Baltimore, Maryland

With four plates and eleven text figures

CONTENTS

PAGE

Introduction 43

Normal Development of the Trachea and Esophagus in Man 44

- Horizon X, 21 to 23 Days, 4 to 12 Somites 44
- Horizon XI, 24 to 26 Days, 13 to 20 Somites 44
- Horizon XII, 25 to 27 Days, 21 to 29 Somites 46
- Horizon XIII, 27 to 29 Days, Embryos about 4 to 5 mm. Long 46
- Horizon XIV, 29 to 31 Days, Embryos about 6 to 7 mm. Long 47
- Horizon XV, 30 to 32 Days, Embryos about 7 to 8 mm. Long 48
- Horizon XVI, 32 to 34 Days, Embryos about 8 to 11 mm. Long 49
- Horizon XVII, 34 to 36 Days, Embryos about 11 to 14 mm. Long 49
- Horizon XVIII, 36 to 38 Days, Embryos about 14 to 16 mm. Long 49

Description of Abnormal Embryos 50

Hypothetical Explanations of the Anomaly 53

- Epithelial Occlusion 53
- Intraembryonic Pressure 53
- Differential Growth 53

Discussion 54

Conclusions 56

Literature Cited 56

THE EARLY DEVELOPMENT OF THE TRACHEA AND ESOPHAGUS IN RELATION TO ATRESIA OF THE ESOPHAGUS AND TRACHEOESOPHAGEAL FISTULA[1]

INTRODUCTION

Among the important congenital abnormalities now amenable to surgical correction is atresia of the esophagus, with or without tracheoesophageal fistula. Estimates of the frequency of the condition vary from Ingalls and Prindle's (1949) report of 6 cases in 30,497 live births at the Boston Lying-In Hospital to the statement by Belsey and Donnison (1950) that it occurs as often as 1 in 800 pregnancies. The common variations of this abnormality have been classified by Vogt (1929) as shown in figure 1. The most frequently seen type, more than 90 per cent of all cases, is that designated as III*b,* in which the upper esophageal pouch ends blindly and a fistulous tract leads from the trachea to the lower esophageal segment.

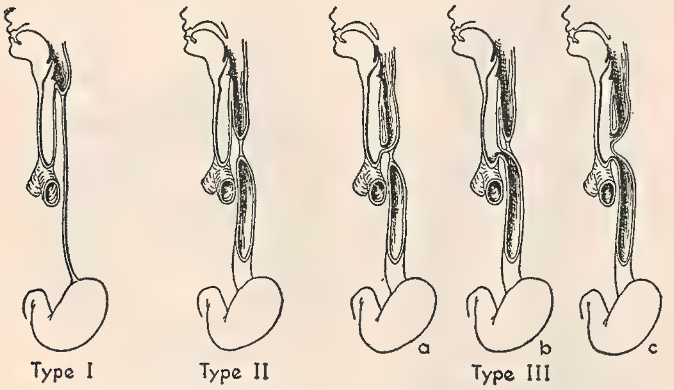

FIG. 1. Vogt's classification of atresia of the esophagus. Type I, atresia of entire esophagus. Type II, atresia of a segment of the esophagus with defined upper and lower esophageal pouches. Type III, atresia of the esophagus with tracheoesophageal fistula: *a,* fistula between the upper esophageal segment and the trachea; *b,* fistula between the lower esophageal segment and the trachea; *c,* fistulae between both esophageal segments and the trachea. From Leven *et al.,* Ann. Surg., vol. 136, p. 704, 1952.

Esophageal atresia with tracheoesophageal fistula was first described in 1696 by Thomas Gibson, whose interesting account is quoted by Ingalls and Prindle (1949). The condition has always aroused considerable interest, and reviews of the subject have been published by Keith (1910), Plass (1919), Rosenthal (1931), Gage and Ochsner (1936), and Lanman (1940). The problem of tracheoesophageal fistula without esophageal atresia has been extensively reviewed by Ferguson (1951).

The possibility of definitive treatment by division of the fistula and simultaneous primary end-to-end anastomosis of the esophageal pouches, originally suggested by the anatomist Sir Arthur Keith, in 1910, set a goal toward which surgeons struggled through the next thirty years. In 1939, working independently, Leven (1941) and then Ladd (1944) had the first successes of any sort with infants with a type III*b* atresia of the esophagus. Both infants were handled by multiple-stage procedures: primary gastrostomy to permit feeding, ligation of the tracheoesophageal fistula in the chest, and exteriorization of the upper pouch in the neck. Keith's idea of a primary ligation of the fistula and simultaneous esophageal anastomosis was pioneered by Lanman (1940) and by Shaw (1939), but the first success was attained in 1941 by Haight and Towsley (1943). Since that time various improvements have raised the survival rate in recent years in some clinics above 60 per cent.

While the surgery of congenital abnormalities has been advancing rapidly in the past twenty-five years, our knowledge of the basic processes leading to the production of these same abnormalities has not kept pace. Just as investigations into the basic physiology, pathology, and bacteriology of infectious-disease processes have furthered the prevention and therapy of these diseases, so may an understanding of the basic processes in the causation of congenital abnormalities be expected ultimately to indicate the means of treating them or preventing their occurrence.

The once widely accepted view of Mall (1908) that all anomalies of human development result from faulty implantation of the embryo due to maternal disease was succeeded by a general tendency to assume that all congenital anomalies result from genetic causes inherent in the fertilized ovum. This view, as E. S. J. King (1948) has commented, hindered research by perpetuating the belief that congenital anomalies must be accepted as accomplished facts, and that their causes and the path of their development can never be traced.

In recent years, the hope that abnormalities of development may ultimately be explainable in terms of developmental physiology has been encouraged by several lines of investigation, including the analysis of differentiation, as exemplified, for instance, by the organizer theory of Spemann (1928) and the production of embryonic anomalies by various experimental means. It is now clear that the immediate cause of any anomaly of development is a disturbance of growth at a critical time in the differentiation of the embryonic tissues. Such disturbance may result from the action of unfavorable genes; from environmental causes such as trauma, the action of toxins, certain viruses, nutritional deficiencies, and various other harmful agents; or from combinations of genetic and environmental factors.

---

[1] This investigation was begun during the author's tenure of the Halsted Fellowship of the Department of Surgery, Johns Hopkins University, under the direction of Dr. Alfred Blalock, Director of the Department of Surgery, and with the co-operation and invaluable assistance of Dr. George W. Corner and Dr. Chester H. Heuser of the Department of Embryology of the Carnegie Institution of Washington.

Hypotheses concerning the causes of abnormal growth must be consistent with the principles of physiological embryology now being developed from experimental studies, and they must rest upon the morphological features of normal development. In the study of any particular anomaly, the path of normal development must be clearly defined and, as far as material is available, must be compared with that of embryos which exhibit the anomaly. In this way, the time of first departure from the normal may be ascertained, and the investigator may be able to discover whether the abnormality results from deficiency or cessation of development, or from a local excess in the growth of tissues such as has been suggested by Patten (1953) as a possible explanation of embryonic abnormalities. At present, human embryological material is available in quantities and in excellence of preparation hitherto not known, and so a re-evaluation of the clinically accepted concepts of abnormal development becomes possible. Such a re-evaluation of the nature of tracheoesophageal anomalies is the aim of the present paper.

NORMAL DEVELOPMENT OF THE TRACHEA AND ESOPHAGUS IN MAN

The development of the human trachea and esophagus has been described by Lewis (1912), by Grosser (1912), and by Puiggrós-Sala (1937). The development of the respiratory system in the pig was investigated by Flint (1907). A monograph by Hjortsjö (1945) on the development of the respiratory system in the cat has been published. The later phases of pulmonary development have been described by Wells and Boyden (1954). Johns (1952) has described the development of the esophageal epithelium.

The rich material of the Carnegie Collection of human embryos now permits a more precise account of the early development of the trachea and esophagus and a much more accurate statement of the relation of the stages of this process to the general development and age of the embryo than have previously been possible. The following account is based on a survey of 112 embryos in horizons x to xv, from which 58 specimens were selected for detailed study. Streeter's comments in his Horizon articles (1942, 1945, and 1948) on various phases of development, and his previously published descriptions of the individual embryos as cited, have been freely drawn upon.

Horizon X, 21 to 23 Days, 4 to 12 Somites

At horizon x, the first primordium of the respiratory system is seen in the mid-line of the ventral wall of the foregut between the thyroid primordium cranially and the anterior intestinal portal caudally. A cellular proliferation produces a ridge on the external surface of the foregut and a corresponding mid-line groove, the laryngotracheal sulcus, on the internal surface. The ridge widens as it extends caudally. A slight furrow is seen in this region in the 8-somite Dandy (1910) embryo, no. 391. In the 10-somite Corner (1929) embryo, no. 5074 (fig. 2), this laryngotracheal sulcus is well defined. Whereas the lining cells of the foregut are single-layered and in some areas almost squamous, in the laryngotracheal sulcus the lining consists of 2- to 3-cell layers, and the cells appear transitional or almost columnar with a striated border suggesting possible ciliation. They are surrounded by undifferentiated mesenchyme.

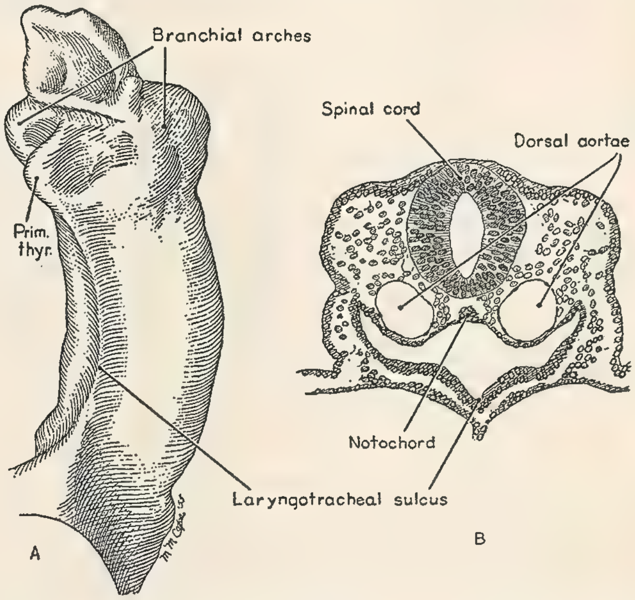

Fig. 2. *A,* the ventrolateral aspect of a model of the foregut of embryo no. 5074, horizon x, showing the earliest pulmonary primordium, the laryngotracheal sulcus, between the thyroid and the anterior intestinal portal. Drawing by Mary M. Cope. ×75. *B,* section 2-2-3, same embryo, at the level of the laryngotracheal sulcus. The notochord forms a portion of the thin dorsal wall of the foregut. The differentiation of the cells of the ventral wall of the foregut is noted. ×100.

Horizon XI, 24 to 26 Days, 13 to 20 Somites

The next stage of development is well illustrated by two embryos of horizon xi, no. 6344 and no. 2053 (Davis, 1923). In figure 3, the foregut has increased in length as the embryo has grown. The laryngotracheal groove has elongated. A definite thickening of the ventral wall of the foregut is present cephalad to the liver primordium. Number 6344 has a laryngotracheal groove 168 microns long, which begins just caudal to the thyroid primordium as a shallow furrow and ends with a knoblike thickening of the endodermal wall. The groove lies directly

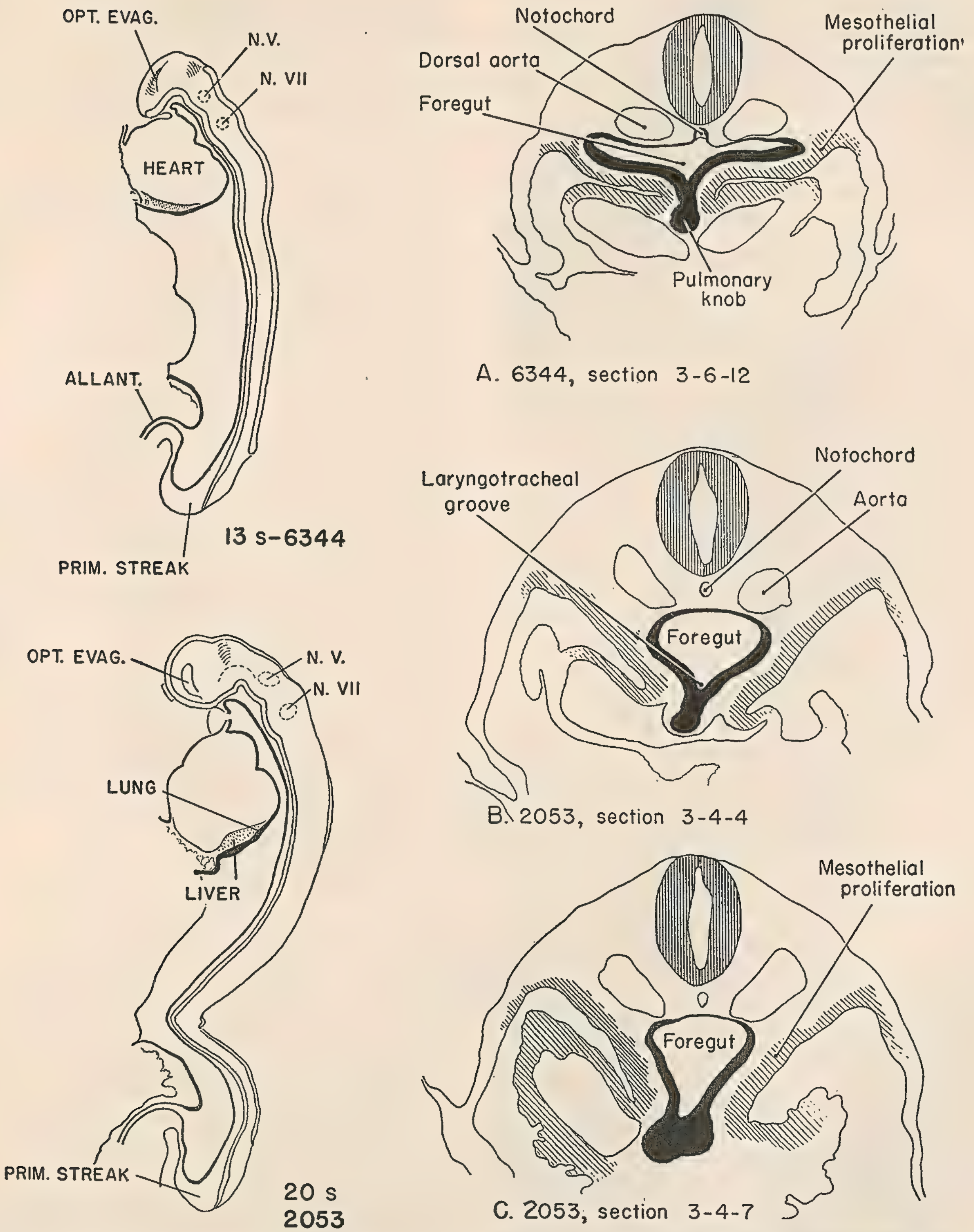

A. 6344, section 3-6-12

B. 2053, section 3-4-4

C. 2053, section 3-4-7

FIG. 3. Left, profile reconstructions of the gut tract (×30) in two embryos in horizon xi (no. 6344, 13 somites; no. 2053, 20 somites). *A, B, C* are drawings (×100) of transverse sections through the developing respiratory primordium to show the relation of the pulmonary knob or the lung bud to the surrounding structures. These sections show the knoblike appearance of the lung bud, which is bilobular in section *C*. The profile reconstructions are adapted from Streeter, 1942, figure 1, xi. The transverse sections in this and following horizon composites were drawn from the actual sections by Mary M. Cope.

in the dorsal mesocardium and laterally is in contact with the coelomic cavities. The ventral and lateral walls of the foregut are 3 to 4 cells in depth; in contrast, the dorsal wall is only 1 cell thick. The nuclei of the cells of the future respiratory system have grouped themselves ventrally, and numerous mitoses are seen.

In a later example of horizon xi, the Davis embryo (no. 2053) of 20 somites, a well marked laryngotracheal groove extends from the contracted caudal end of the pharynx to a point just cephalad to the liver diverticulum, and ends in a bilobular swelling separated from the liver by a shallow transverse sulcus. The groove is separated from the dorsal digestive tract by a longitudinal sulcus running from the cephalic portion of the laryngotracheal groove. The respiratory primordium lies cranial to the liver, caudal to the thyroid, dorsal to the sinus venosus, and ventral to the descending aortae, spinal cord, and notochord (sections *A, B, C* of fig. 3). The microscopic appearance is little changed from that of no. 6344.

Horizon XII, 25 to 27 Days, 21 to 29 Somites

Figure 4 shows the characteristic state of the endodermal tract of embryos of horizon xii. In no. 5056, an early representative of the period, there is a knoblike lung bud adjacent to the sinus venosus. On transverse section, the notochord, previously an integral part of the dorsal wall of the foregut, has moved farther dorsalward between the paired aortae. The long axis of the growing foregut has become oriented in a dorsoventral direction. Separation of the respiratory and digestive tracts, as described below, is beginning. Small sprouts of vessels can be seen forming the pulmonary vasculature. In no. 5923, the lung bud has become more prominent and separation has progressed. The ventral wall of the foregut reaches a thickness of 7 to 8 cells, whereas the dorsal wall is only 3 or 4 cells thick. Small vascular twigs are present. Below the point of separation of the trachea and esophagus, the wall of the esophagus thickens and the caliber of the lumen diminishes.

The early formation of the tracheoesophageal septum was studied carefully, for it seemed crucial in the development of a tracheoesophageal fistula. Although the septum is often pictured as resulting from the "pinching-off" of the lung bud from the foregut, this explanation does not appear to be correct. Ridges of endodermal cells develop from the lateral walls at the caudal end of the lung-bud region of the foregut. The union of these proliferating ridges, within the lumen of the foregut, divides it into a ventral respiratory and a dorsal digestive portion. At this point there is seen no evidence of external pressure upon the foregut, no condensation of mesenchyme, no indentation of the basement membrane indicative of a "pinching-off." (See fig. 14, pl. 1; figs. 16, 17, pl. 2.) This interpretation of the manner of separation is in keeping with modern concepts of embryonic organization. Hjortsjö (1945) has described a similar tracheoesophageal division in the cat. After division by the cellular ridges, the innermost cells in the core of the septum apparently undergo necrosis, to form coalescent vacuoles (fig. 17, pl. 2); finally the basement membrane collapses, and mesenchyme passively fills the space so vacated.

A second feature of this horizon and the next, which was subjected to a careful investigation, is the presence of lateral esophageal grooves as described by Lewis (1912) and Forssner (1907). Figure 5 shows the caudal and dorsal course described for these grooves running from just dorsal to the tracheoesophageal ridges to the dorsal wall of the esophagus. The internal ridges thus produced are similar in histological structure to the ridges forming the tracheoesophageal septum. Their importance lies in the fact that overgrowth could well result in a type III*b* abnormality as illustrated on the right in figure 5. In the light of Patten's suggestion (1953) that excessive development, as well as deficient growth, may precipitate abnormalities, these ridges are of considerable interest. Definite evidence of them was found in at least 6 embryos of horizon xii studied (nos. 1062, 4245, 4736, 4759, 7724, 5035). This second ridge of endodermal cells can be seen in figures 13 and 15 (pl. 1). A sagittal section from no. 7724 (fig. 15, pl. 1) shows evidence of a well developed lateral esophageal groove. It is of interest to note the manner in which the protruding mass of this groove occludes the lumen of the esophagus dorsally, while a communication between the respiratory tree and the lower esophagus still exists. A similarity can be seen between this section and that of the Harvard embryo shown in figure 23 (pl. 4).

Horizon XIII, 27 to 29 Days, Embryos about 4 to 5 mm. Long

Figure 6 illustrates the continued development of the lung, trachea, esophagus, and stomach. In transverse sections, the trachea and primary bronchi can be distinguished. In the older embryos of this horizon, that part of the respiratory tract cephalad to the bifurcation of the bronchi certainly seems to represent the future trachea, and not the lung bud as claimed by some authors whose descriptions imply that the trachea appears at a much later time.

Embryos of horizon xiii indicate clearly the semi-independence of the various growth phases involved: branching of the bronchial tree, formation of the tracheoesophageal septum, and lengthening of the trachea and esophagus. Figure 7 exemplifies this point. Three lung buds are shown in which the cranial extent of tracheoesophageal separation has been marked. Despite a comparable degree of bronchial development, three different levels of tracheoesophageal separation are seen.

A marked diminution in the diameter of the esophagus just caudal to the tracheoesophageal separation is noted. This finding has also been reported by Johns (1952) as occurring in all embryos between 5 mm. and 23 mm. It would appear that the elongation of the esophagus causes a reduction in its diameter. In no. 836, the esophagus narrows at one point to such an extent that no lumen is visible in the sections. Microscopic evidences of the endodermal formation of the tracheoesophageal septum, however, continue to be found. Numerous cells are seen to be migrating from the lining of the coelomic cavity to contribute to the supporting structures of the trachea and esophagus (fig. 6).

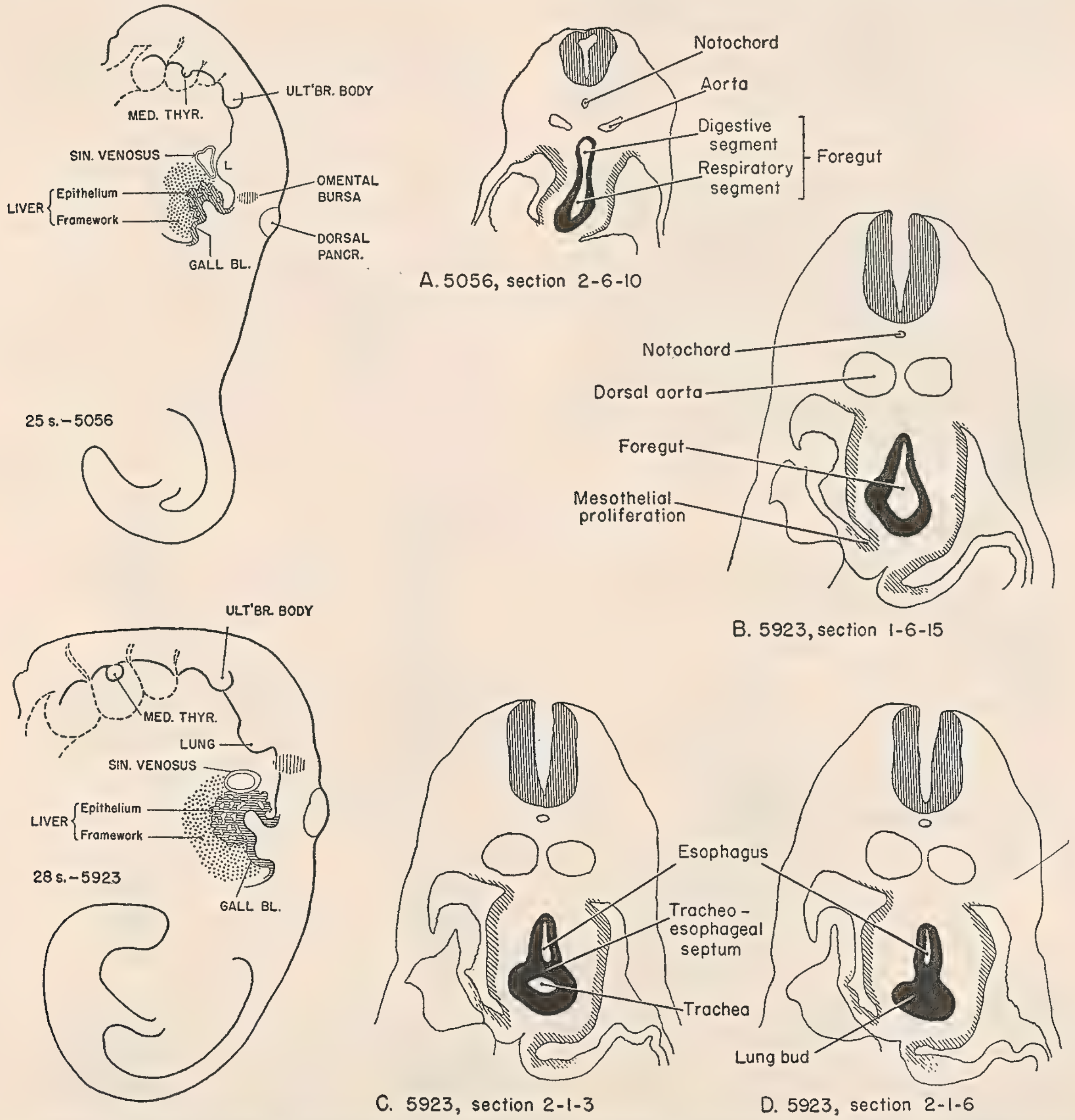

A. 5056, section 2-6-10

B. 5923, section 1-6-15

C. 5923, section 2-1-3

D. 5923, section 2-1-6

Fig. 4. Left, profile reconstructions (×35) of the gut tracts in two embryos from horizon xii (no. 5056, 25 somites; no. 5923, 28 somites). *A* is a transverse section (×50) of the respiratory region in an early embryo of this horizon. *B, C, D* are transverse sections (×50) at three levels to show the shape of the lung bud in a later embryo in the same horizon. There is an increase in mesenchymal activity in the cells adjacent to the coelomic cavity. The epithelial nature of the division of the respiratory and digestive tubes is shown clearly in the last three transverse sections. Profile reconstruction from Streeter, 1942, figure 2, xii.

Horizon XIV, 29 to 31 Days, Embryos about 6 to 7 mm. Long

Figure 8 shows the endodermal tract of horizon xiv. In front of the esophagus, a definite trachea with two primary bronchi is present. The bronchi begin to curve backward. As Streeter (1945) has pointed out, the right bronchus tends to be longer and directed downward, the left bronchus being more horizontal and shorter. Further, the growing ends of the bronchi are bulbous, as is characteristic of centers of active cell proliferation. In the older members of the series, secondary foci of proliferation can be seen which have become free of the dominance of the growing tip. They mark sites

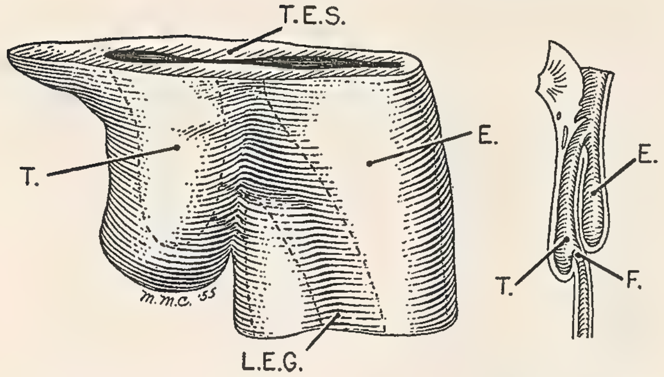

Fig. 5. Left, drawing of the foregut of a 4-mm. human embryo in the region of the developing lung bud, showing the location of the lateral esophageal groove (*L. E. G.*) in relation to the tracheoesophageal septum (*T. E. S.*) and the lumen of the trachea (*T.*) and of the esophagus (*E.*). Overdevelopment of the internal ridges of this groove would occlude the esophagus along the line of the groove. Maintenance of a communication between the trachea and the esophagus, as indicated in the drawing by the region outlined by a broken line, would result in a picture similar to a type III*b* atresia of the esophagus with a tracheoesophageal fistula (*F.*) as illustrated on the right. From Keibel and Mall, *Manual of Human Embryology*, volume 2, figures 237 and 238.

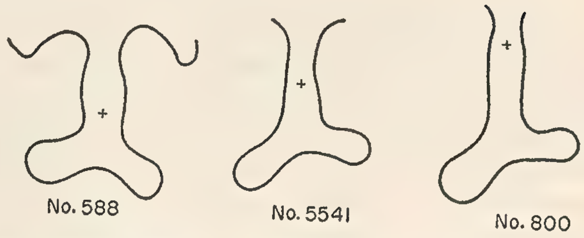

Fig. 7. Three embryos of horizon xiii, showing the disparity of bronchial branching and tracheoesophageal separation. + marks the level at which the trachea and esophagus have a common lumen. ×65. From Streeter, 1945, figure 1, xiii.

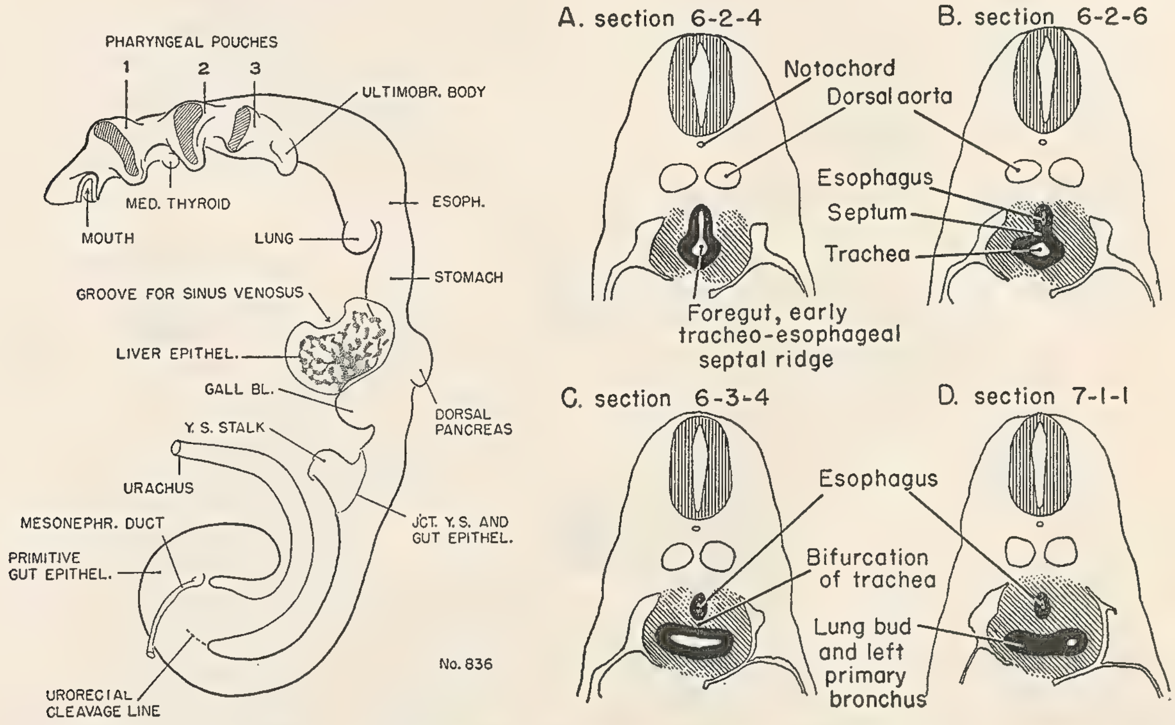

Fig. 6. Left, profile reconstruction (×30) of the gut tract in an embryo of horizon xiii, no. 836. *A, B, C, D* are drawings (×30) of transverse sections of this embryo at the level of the respiratory primordium. From the surrounding mesenchyme the supporting connective tissue and muscle layers begin differentiation. The profile reconstruction is taken from Streeter, 1945, figure 1, xiii.

where secondary bronchi are to branch off. Such secondary foci do not occur in the trachea, which, it is evident, is already specialized in its own way. Likewise, the early steps in specialization of the larynx can be seen.

Figure 9 illustrates the microscopic appearance of the lung and esophagus at this stage. There is an inner epithelial tube surrounded by a richly vascularized mesenchymal zone, which in turn is partly enclosed by mesothelium facing the coelomic spaces. The lumen of the esophagus remains small. The beginning pulmonary blood supply is more clearly defined. The small arterial twigs descend from the sixth aortic arch with irregular bilateral channels. A small common pulmonary vein drains into the left atrium. (See no. 721, fig. 9, in horizon xv.)

The remaining four stages, horizons xv to xviii, were not studied in detail, having been sufficiently described by Streeter in the Horizons series, from which the following paragraphs are abstracted.

Horizon XV, 30 to 32 Days, Embryos about 7 to 8 mm. Long

Figure 10, xv, shows the developing trachea, bronchi, and esophagus in this horizon. Definite secondary bronchi are present. Figure 9 and figure 18 (pl. 3) show that the supporting frameworks of the trachea and the esophagus are distinct, one from the other. As noted in the previous horizon, pulmonary vessels can be recognized, and a plexus of capillaries surrounds the primary bronchi.

Horizon XVI, 32 to 34 Days, Embryos about 8 to 11 mm. Long

Figure 10, xvi, illustrates the continued differentiation and elongation of the trachea and the esophagus. Separation of the two components is almost complete. Figure 19 (pl. 3) shows further differentiation of the supporting structures.

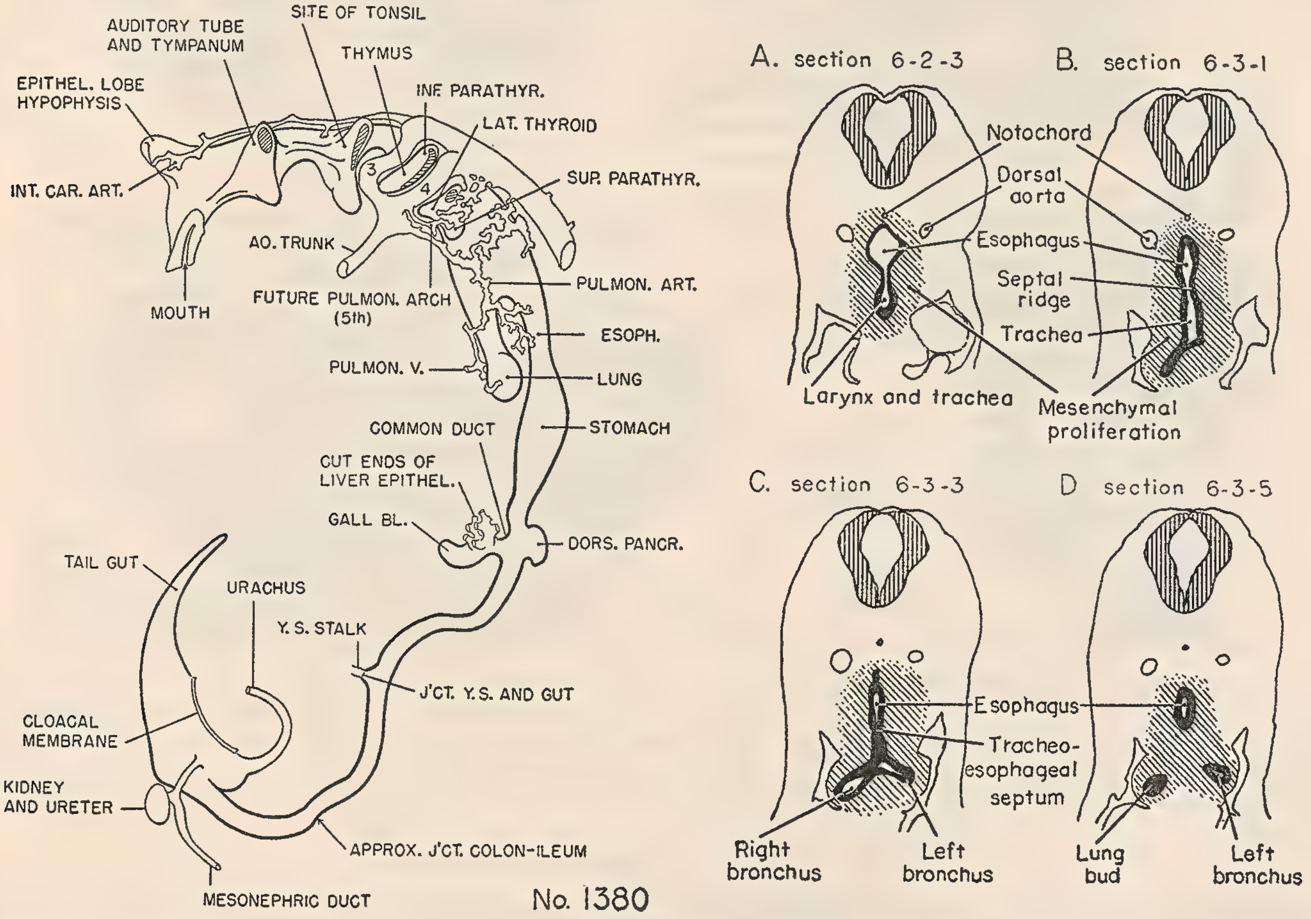

Fig. 8. Left, profile reconstruction of the gut tract and developing vasculature from an embryo of horizon xiv, no. 1380. ×35. *A, B, C, D* are drawings of frontal sections showing the trachea, primary bronchi, and esophagus. ×20. Profile reconstruction from Streeter, 1945, figure 1, xiv.

Horizon XVII, 34 to 36 Days, Embryos about 11 to 14 mm. Long

The endodermal tract of this embryo is shown in figure 10, xvii. Separation of lung and trachea from the foregut is essentially complete. A definite larynx is seen. Differentiation of the lung into five lobes has begun. Figure 20 (pl. 3) exhibits the microscopic structure. Elsewhere condensations of mesenchyme foreshadowing the tracheal cartilages can be identified.

Horizon XVIII, 36 to 38 Days, Embryos about 14 to 16 mm. Long

Figure 21 (pl. 3) illustrates the microscopic structure of the trachea and the esophagus at horizon xviii. Mesenchymal condensation about the trachea is marked. Submucosal and muscular layers can be identified about the esophagus. The aorta, pulmonary arteries, and vagus nerves are also visible.

From these studies of normal embryos, the following conclusions have been reached concerning the development of the trachea and the esophagus. The epithelium, termed by Streeter "the dictator tissue of the lung," is truly the initiator and governor of the formation of the tracheoesophageal septum. The mesenchyme throughout plays only a passive role. Angiogenesis occurs in response to epithelial growth. The original laryngotracheal groove, which is seen as early as the 10-somite stage, is probably the direct primordium of the pulmonary system. The critical period of development with respect to the occurrence of atresia and fistula probably begins at this stage or perhaps earlier.

Through horizons xii to xiv, three crucial phases of development occur concomitantly: rapid elongation of the trachea and the esophagus, division of the trachea from the esophagus, and bronchial budding. That these somewhat independent processes may be competitive has been suggested.

In horizon xv, definite separation has occurred, and the supporting tissues of the trachea and esophagus are present.

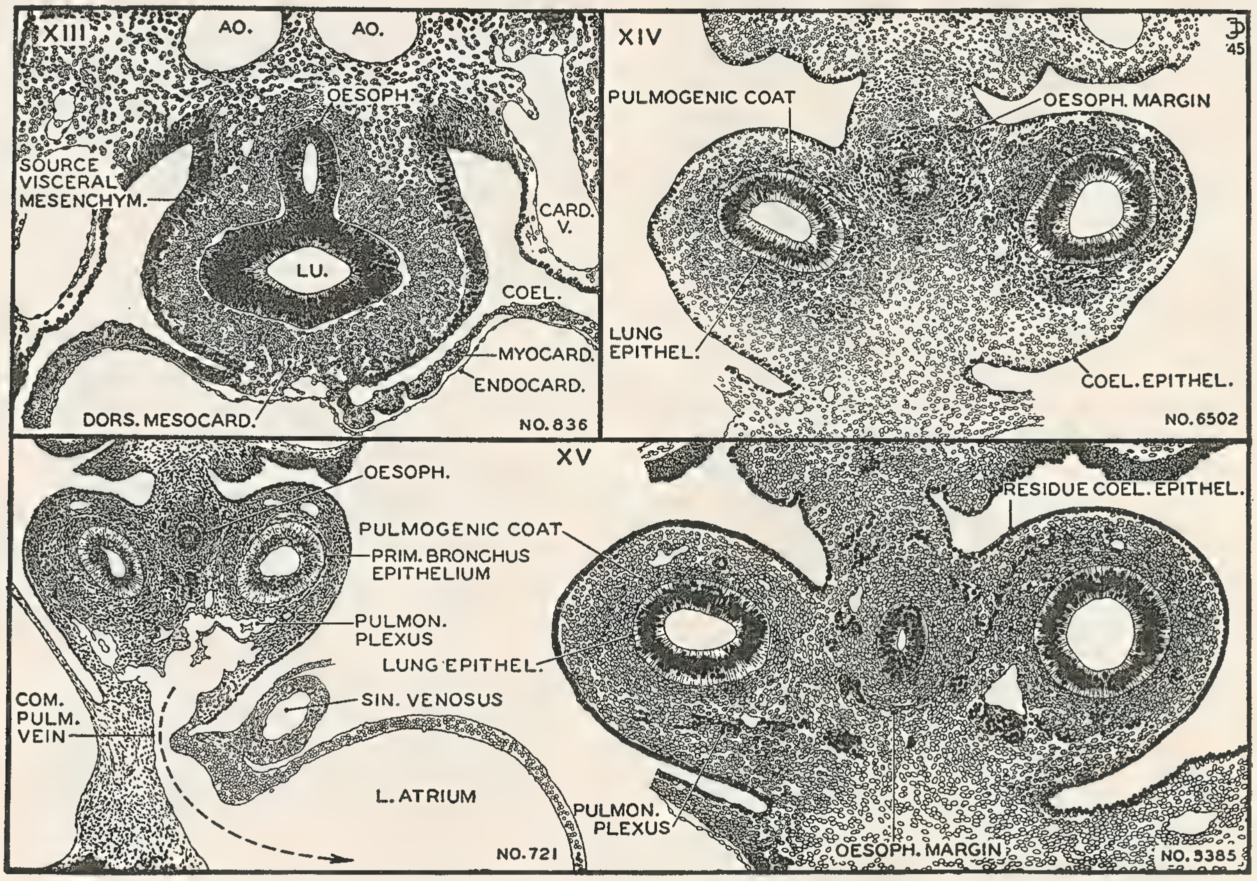

FIG. 9. Drawings of sections taken through the respiratory and esophageal regions in horizons xiii, xiv, and xv to show the differentiation of the supporting tissues of the lung and esophagus. In horizon xiii is still seen the proliferating coelomic epithelium which is the source of the supporting tissues of the pulmonary and esophageal regions. In horizon xiv, further organization of the mesenchyme occurs, and angiogenesis is seen about the esophagus. Continued vascular development is seen in horizon xv with the appearance of a common pulmonary vein. Embryo no. 721 is ×50; the remaining sections are ×100. Drawings by J. F. Didusch from Streeter, 1945, figure 4, xv.

DESCRIPTION OF ABNORMAL EMBRYOS

Five early human embryos with esophageal atresia have been reported. We have fortunately been able to study the microscopic sections of three of them.

1. Gladstone (1935) demonstrated an embryo of 19-mm. crown-rump length to the Anatomical Society of Great Britain and Ireland. From his description, this specimen belongs to horizon xix (39±1 days). The embryo had a blind cranial esophageal pouch, and from the dorsal aspect of the trachea, just above the bifurcation, a tracheoesophageal fistula led to the patent end of a distal segment of esophagus continuous with the stomach. The anomaly is, therefore, type III*b*. The size of the cranial esophagus diminished as it terminated in imperfectly developed epithelial and muscular coats. Among other abnormalities present was defective development of the vascular system with persistence of the right dorsal aorta giving rise to a retroesophageal subclavian artery, while the right common carotid artery arose directly from the arch of the aorta. Other malformations included absence of the posterior nares, abnormal development of the occipitocervical region of the skull and vertebral column, and an abnormal development of the brain. Gladstone reported evidence of impaired nutrition and a diseased condition of the tissues, affecting particularly the muscular and endothelial walls of the heart and blood vessels. He believed that the atresia of the esophagus and the tracheoesophageal fistula could not be explained simply as due to the development of a retroesophageal subclavian artery. In view of the multiplicity and extent of the developmental defects exhibited by this embryo, Gladstone suggested that "the evidence appeared to be in favour of the anomalies being primarily due to some general cause, e.g., a diseased condition of the chorion and embryo interfering with the normal development, rather

than to a local cause such as pressure of a persistent right dorsal aorta on the oesophagus and trachea." Our efforts to locate this embryo in order to borrow it for study were not successful.

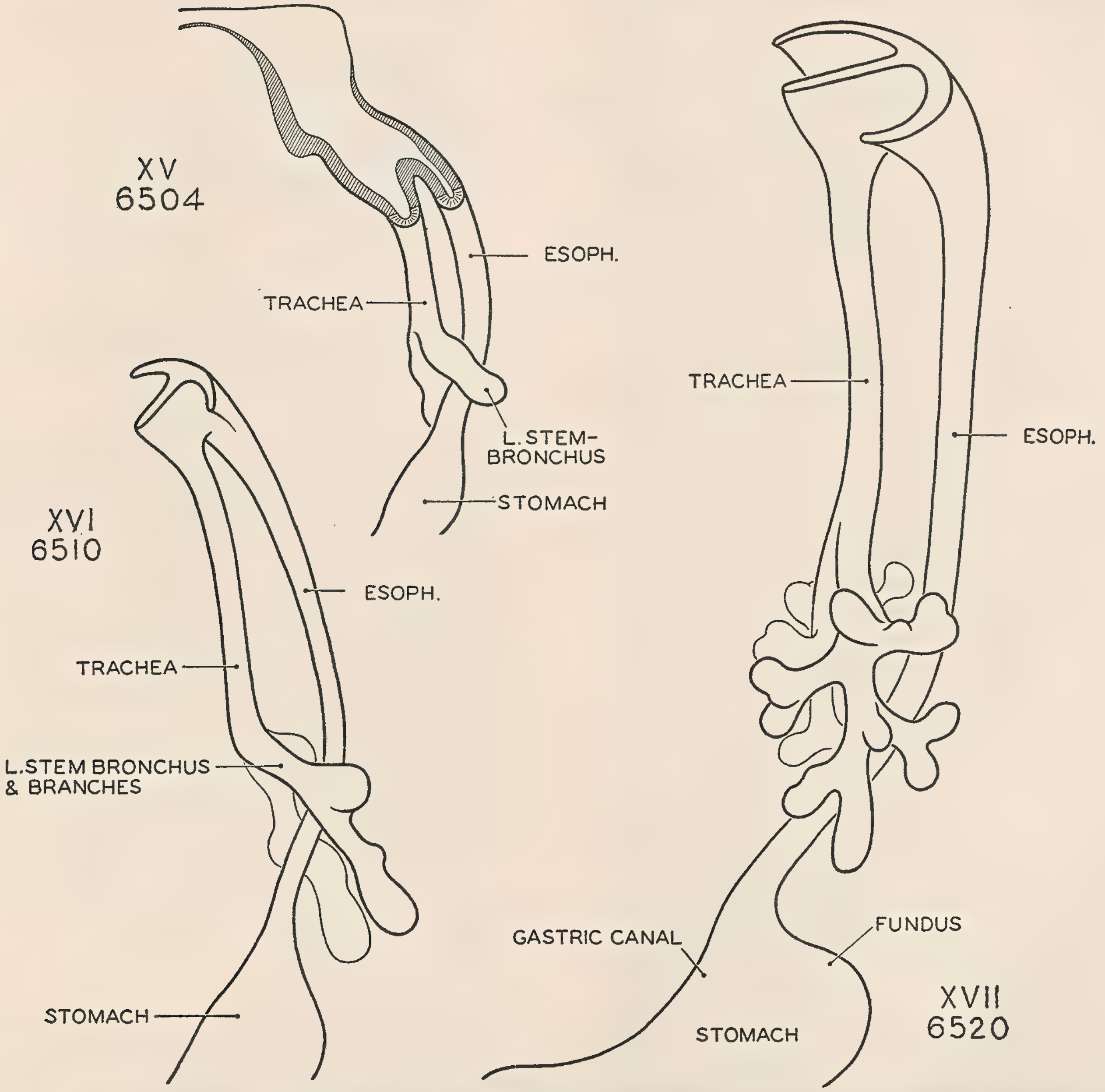

Fig. 10. Profile reconstructions of the respiratory system, esophagus, and stomach in embryos of horizons xv (no. 6504), xvi (no. 6510), and xvii (no. 6520). There is continued branching of the bronchial tree with dorsal inclination of the bronchi. The larynx is differentiated. The narrowness of the esophagus in horizon xvi is to be noted. ×45. Profile reconstructions from Streeter, 1945, figure 5, xv; figure 5, xvi; figure 6, xvii.

2. Ysander (1925), in an inaugural dissertation on double monsters, described an 8-mm. double monster embryo, lent by Dr. Robert Meyer. Efforts to trace the present whereabouts of this embryo were not successful. Through the kindness of Dr. John Naeslund of Uppsala, Sweden, we were able to obtain the original monograph. Notes on the specimen are filed in the Carnegie Collection (no. 9334). This embryo, whose endodermal tract is shown in figure 22 (pl. 4), has two esophagi, both of which become atretic at the level of the atria. Beginning at the level of the carinae of both tracheae, there are fistulae continuous with what appear to be caudal esophageal segments opening into a large common stomach. Although the total length is 8 mm., the embryo is obviously stunted, because other features place it in an older age group. The form of the upper and lower lung buds, the presence of pigment about the lens, and the development of secondary bronchi would place it in horizon xvi (33 days, 8 to 11 mm.). The presence of a foramen ovale secundum suggests an even greater age. The detailed description of the esophagus is as follows (with minor verbal emendations):

> At first the two oesophagi run in the ordinary way immediately behind their respective tracheae, and appear to be

normal, both as regards the structure of the walls and the width of the lumen. 25 mm. below the commencement of the trachea in the case of the left component, and 20 mm. in the case of the right component (measured on the model), the oesophagi suddenly come to an end. Without any demonstrable dilatation the epithelial tube ends blindly, and is continued downwards as a strand of mesenchyme, which soon becomes lost in the thin posterior wall of the peri-tracheal mesenchyme. . . . This, however, is not the last trace of the oesophagi, for out of the tracheal bifurcation of each component a tube projects, which is lined with epithelium. Further down, this tube curves downwards and inwards toward the centre of the double monster, where, at a distance of 23 mm. in case of the left component, and 19 mm. in case of the right component, from the bifurcation (measured on the model), it opens up into a large common ventriculus, thus proving itself to be the true continuation of the oesophagus, the course of which was interrupted by the obliteration.

In anticipation of a discussion of the causes of tracheo-esophageal fistulae, several observations about this monster are of interest. The lungs are normally developed for the corresponding stage of development. The heart is enlarged, although the points of esophageal obliteration lie cranial to the heart. The upper segment of the esophagus is continuous with the trachea through the mesenchymal condensation. The fistulae do not exhibit the narrowing seen in other specimens. Ysander made no mention of any epithelial occlusion. In relation to this specimen, a report by Panse and Gierlich (1949) is of interest. In each of a pair of identical twins, one a stillborn anencephalic monster and the other an externally normal newborn who lived only a few hours, a Vogt type III*b* esophageal atresia was found at postmortem examination.

3. The late Dr. F. T. Lewis described (1912) an 18.1-mm. embryo in the Harvard Collection which gives evidence of a Vogt type III*b* atresia of the esophagus and also a retroesophageal right subclavian vessel. This embryo was first described by Minot (1910) and was estimated to be about 40 days of age; it is classified as horizon xix. Although otherwise normal, the embryo exhibits epithelial occlusion in the duodenum and anus. The lungs appear to have developed to a stage consistent with the length and age of the embryo. A model, figure 23 (pl. 4), clearly shows the dilatation of the caudal esophagus compared with the extreme narrowness of the fistulous tract shortly after it leaves the trachea. Through the kindness of Dr. Lewis, the sections of this embryo were made available for examination. Memoranda and notes are filed in the Carnegie Collection (no. 9335).

4. Gruenwald (1940) reported a 9-mm. human embryo with a type III*b* atresia of the esophagus. On the basis of development, length, and estimated age, this embryo would be classified as belonging to horizon xvi. The lung buds appear to be somewhat retarded in growth for an embryo of that horizon. The case is remarkable in that the lower segment of the esophagus arises from the upper third of the trachea, 630 microns above the bifurcation. The upper segment is only 140 microns long. The embryo shows agenesis of both ureteric buds and hypoplasia of the right umbilical artery. As in the preceding specimen, the esophagus is extremely narrow in the section closest to the trachea.

Fluss and Poppen (1951) have suggested that the upper pouch of the esophagus in this embryo represents a pharyngeal diverticulum, the connection between esophagus and trachea, described by Gruenwald as the fistula, being simply the common foregut normal at this stage. They suggest that the trachea may not be differentiated to the same extent as the lung bud and larynx. Such an interpretation is not in accord with the descriptions based on adequate material, as outlined above in the section on normal development, which show that in horizons xv to xvi a definite trachea, separated significantly from the esophagus, exists and will shortly be followed by development of the larynx.

5. Another embryo with an atresia of the esophagus was reported by Professor M. Yamasaki of Tohoku University, Sendai, Japan, in 1933. We are greatly indebted to Professor Yamasaki for generously lending the specimen for study, and to Colonel Carl F. Tessmer of the Medical Corps, U. S. Army (attached to the Atomic Bomb Casualty Commission), for facilitating its temporary transfer to Baltimore. Models and other records are preserved in the Carnegie Collection (no. 8731). The embryo, measuring 8.5 mm., had abnormalities of other regions, including the nervous system, the face, and the spinal column. The embryo is classified as belonging to horizon xvi because of pigmentation of the eye vesicle, incipient phalangeal rays on the hand plate, separation of the lens vesicle, and the presence of primordia of the cochlear duct and of the pancreas. The head is small; the cervical curvature is slight; and the heart does not appear to be enlarged. The trachea and lungs seem somewhat retarded in comparison with other embryos of horizon xvi.

On examination, an upper esophageal pouch is seen to end blindly (figs. 24, 25, pl. 4). The larynx begins just below the thyroid pouch. At this point, the epithelial lining is of fairly uniform thickness, approximately three cell layers. Few mitoses are present. Beyond the separation of the trachea and esophagus, there is a definite zone of condensation about the cranial portion of the trachea which is well differentiated from the condensation about the dorsal gut. The cells about the trachea and in the more cranial portion have elongated nuclei, in contrast with the rounded nuclei of the cells of the wall of the gut. The wall of the cranial esophagus is formed of two layers of oblong cells. The trachea, at the point of bifurcation, has a finger-like projection of epithelium and surrounding connective tissue which is directed toward a more caudal blind stump of esophagus that enters the stomach (fig. 26, pl. 4). Yamasaki postulates that this embryo with a type II atresia of the esophagus developed along the same pathway as an embryo with a type III*b* atresia of the esophagus with a tracheoesophageal fistula and differs only in the development of an atretic segment in the mid-portion of the fistula. Thinning of the fistulous tract in this same region has been noted both in the Harvard embryo and in the Gruenwald embryo which were described above.

The embryo also shows an overgrowth of the duodenal mucosa. The pneumatoenteric recess is present, but does not seem large enough to cause changes by pressure. Both 4th aortic arches are present, but without exaggeration of size.

HYPOTHETICAL EXPLANATIONS OF THE ANOMALY

The many hypotheses suggested to explain the origin of atresia of the esophagus and tracheoesophageal fistula reflect the basic lack of understanding of the origin of all congenital defects. The hypotheses can be divided into the following groups.

Epithelial Occlusion

Kreuter (1905) suggested that a physiological occlusion of the lumen of the esophagus, which had been described in the 19- to 20-mm. stage, might lead to atresia if recanalization did not occur. Subsequent work has led to some doubt whether complete occlusion of the lumen occurs. The present investigation has revealed little evidence of epithelial occlusion in horizons x to xv, although narrowing of the esophagus in the region just caudal to the bifurcation of the trachea was noted, reducing the caliber of the esophageal lumen. (See horizon xiii, no. 836.) Johns (1952) has noted vacuolization in the esophageal epithelium in the 13- to 16-mm. stage (horizons xvii to xviii). Neither of these findings, however, appears to correspond to a "solid" stage of esophageal development suggested by Kreuter. The occurrence of esophageal atresia in embryos considerably younger than the 19- to 20-mm. group, in which epithelial occlusion is stated to occur, points to some earlier cause. Epithelial occlusion also fails to explain the frequent accompaniment of a tracheoesophageal fistula.

Intraembryonic Pressure

Pressure of the heart. It has been suggested by Schmitz (1923) that enlargement of the embryonic heart combined with marked dorsal curvature in the cervical region may displace the esophagus and trachea dorsally, the esophagus being pinched off against the vertebral column. As the embryo subsequently enlarges, the cranial segment is pulled free. Although several of our specimens had signs of cardiac enlargement, esophageal atresia and tracheoesophageal fistula have been known to occur in acardiac or microcardiac monsters. This fact, combined with general objections to hypotheses dependent upon pressure, leads the present author to question this general explanation.

Pressure from abnormal vessels. The frequent association of a retroesophageal right subclavian artery with tracheoesophageal fistulae and esophageal atresia has led to the speculation by Fluss and Poppen (1951) and others that the abnormally persistent caudal portion of the right dorsal aorta, passing dorsal to the esophagus, may press upon it and cause an atresia. Against this hypothesis is the finding of esophageal atresia in two embryos at an early stage of development when the vessel in question appears too small to exert significant pressure. The presence of an abnormal vessel, though frequent and of considerable surgical importance, is not a constant feature of esophageal atresia. The presence of a retroesophageal artery in the Gladstone and Harvard embryos would seem to represent the simultaneous occurrence of a related, but not causative, anomaly.

Pressure by the pneumatoenteric recesses. Broman (1904) suggested pressure from the pneumatoenteric recesses as the cause of the abnormality. These recesses are connected with the pericardial cavity and with the chorionic cavity at one stage of development. The presence of excess fluid, accentuated by the movements of the heart, was thought to cause pressure against the dorsal portion of the foregut with pinching-off of the digestive tube. These recesses, however, develop somewhat later than the stages indicated as critical by this study, that is, horizons xi to xv.

Despite the continued arguments for the causation of defective growth by abnormal pressures on developing structures, considerable doubt exists as to the importance of mechanical pressure. The disturbance of spatial relations thus produced might influence growth by altering the concentration or locus of action of "organizers," but mechanical pressure *per se* seems to be an unlikely cause of malformations. The extremely gelatinous nature of the embryo in these early stages would appear to permit considerable displacement of developing structures.

Differential Growth

Hypotheses of the third group are based on biochemical and physical alterations, caused by unknown factors, of the complex integration of growth necessary to normal development. Yamasaki (1933) has stated that "according to my interpretation the dysfunction of active cellular proliferation is to be looked upon as the primary and fundamental reason for the abnormal development of the lung buds while other factors, such as the abnormal heart size, play only a contributory role in the process."

He called attention to the difference between the thin dorsal layer of cells and the rather profuse epithelium on the ventral side of the primitive foregut. Clinical experience showing esophageal atresia to be far more common than tracheal atresia, which is in fact exceedingly rare, can be correlated with this finding. Yamasaki went on to postulate that the rapid growth of the trachea and pulmonary primordium uses up so much of the "growth potential," as expressed in available cells, that the posterior digestive segment cannot provide enough cellular material to complete the esophagus.

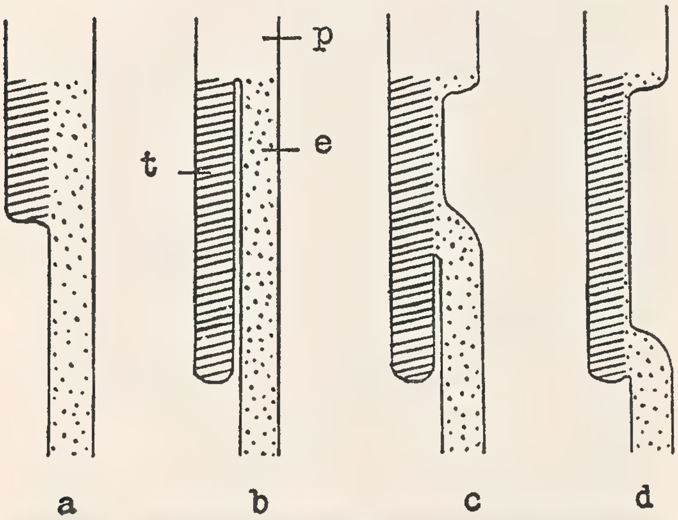

FIG. 11. *a,* lung bud and trachea ventrally (shaded) and esophageal tissue dorsally (stippled). *b,* normal development of the trachea (*t*) and the esophagus (*e*) caudal to the pharynx (*p*), showing synchronized growth and continuity of the esophagus. *c,* rapid elongation of the trachea, resulting in a thinning-out of the segment of the esophagus along the dorsal wall so that a communication or fistula is left. *d,* with elongation of the trachea the fistula comes to occupy a position near the bifurcation. From Gruenwald (1940), figure 3.

Gruenwald (1940) suggested a similar chain of events in that a delay in separation accompanying a rapid elongation of the trachea may carry the developing digestive tube caudalward so rapidly that it loses the ability to differentiate into a separate and normal esophagus over the distance which the trachea has grown (fig. 11). With a decrease in the rate of growth of the trachea, the cranial segment of the digestive tract may begin to differentiate, and may even make up the growth difference and overlap the lower segment. He points to the presence of esophageal tissue on the dorsal wall of the trachea, or of muscular bands passing from the upper segment of the esophagus to the trachea, as evidence that esophageal tissue stretched thin by rapid elongation of the trachea is present on the dorsal wall of the respiratory tree. Our study has substantiated the semi-independent nature of the processes of elongation and tracheoesophageal division.

Rosenthal (1931), whose views reflect the experienced judgment of G. L. Streeter, with whom he discussed his cases, believed the defect to be caused by faulty union of the epithelial ridges which divide the foregut internally. He pointed out, without attempting a detailed explanation, that some alteration from a truly craniocaudal division, causing the growth to be directed dorsalward, might divide the foregut in such a way as to produce the abnormality under discussion. The possibility that epithelial ridges of the lateral esophageal groove play this role was not mentioned.

DISCUSSION

It has been the purpose of this investigation to elucidate the early development of the pulmonary and esophageal portions of the foregut in the early human embryo, and to attempt to clarify the abnormal processes which lead to esophageal atresia and tracheoesophageal fistula. A complete solution to these problems is still lacking, but the morphological analysis presented above makes it possible to question and possibly discard some of the hypotheses and to suggest lines of evidence from which an explanation may ultimately be attained.

As illustrated by the specimens brought together in this study, abnormalities in the differentiation of the trachea and esophagus are well established as early as horizon xvi or xvii (fifth week of embryonic life). The disturbances of embryonic development which cause the anomalies must, therefore, be looked for at earlier stages. The observations on normal embryos reported above show that the tracheopulmonary primordium is distinguishable as early as 21 days after fertilization. At least as early as this, possibly earlier, the tissues are sufficiently differentiated to respond to specific organizer actions. Anatomical defects of the type we are considering must have their beginnings at this and the immediately preceding stages. Disturbances acting much earlier, for example before horizon x or xi (fourth week), would in all probability result in more widespread defects. A later disturbance, after horizon xviii, say, would require deterioration of structures already well developed. At such later stages, the specific developmental phases of the trachea and esophagus have passed their period of greatest vulnerability to disturbance. Explanations of esophageal atresia caused by disturbances after this critical period call for a high degree of coincidence to account for the rather constant anatomical appearance of the abnormality.

Among the morphological points brought out by this investigation which suggest in what direction we must look for the site of the primary organizational defect, the most crucial is the apparent importance of the epithelium of the foregut as the determining factor in the separation of the trachea from the esophagus. The mesenchyme seems to have only a passive role in this process. The possibility of epithelial imbalance results from the apparent independence in timing shown by elongation of the trachea and esophagus, bronchial branching, and tracheoesophageal separation. The defects in question thus appear to arise from disturbances in the differentiation and growth pattern of the epithelial lining of the foregut at the time when separation of the trachea and esophagus is impending or is in its earliest stages.

The hypothesis that the abnormality is caused by abnormal intraembryonic pressures has very little morphological support. Many investigators have stressed that the embryonic tissues appear most susceptible to injury, and consequent abnormality, when they are undergoing the most rapid and complex development. During horizons x to xv, three rapid and complex major changes are occurring: elongation and growth; separation of the trachea from the foregut; and branching and growth of the bronchial tree. At this time, abnormalities may come about either as the result of retardation of growth or as the result of excessive growth in certain portions of the developing structure; in fact, probably both are involved. The concept of "tissue availability," suggested by Gruenwald and Yamasaki, seems useful in analyzing the sequence of events. The present investigation suggests that the development of both esophageal atresia and tracheoesophageal fistula may involve hyperplasia of the lateral esophageal ridges. The atresia would seem to result from the too rapid elongation of the trachea, combined with diminution in esophageal substance such that the esophagus "cannot make ends meet," as suggested by Gruenwald. The thickened tissue of the wall of the lateral esophageal groove provides cellular material for the continuation of the esophagus, at this point, with the development of a fistula. Lesions of type II may arise, as suggested by Yamasaki, from a failure of the fistula to persist or to develop. The tenuous nature of the fistula was noted in the Harvard embryo. Where no suggestion of a fistulous tract exists, we would assume only the factor of too rapid a respiratory elongation without abnormal development of lateral esophageal grooves. Fistulae without atresia and defects of type III*c* would appear to be due to localized or limited failure of the developing tracheoesophageal ridges, perhaps caused by imbalance between tracheoesophageal division and elongation.

The similarities between esophageal atresia and imperforate anus, and between tracheoesophageal and urogenital fistulae, are striking. Atresia of the ventral and secondarily developing system is rare in both the former regions; and the urogenital septum resembles the tracheoesophageal septum in many respects. In a brief study, the mechanism of separation appeared to be similar, that is, epithelial division rather than pressure from the ingrowth of mesenchymal bars. The frequent occurrence of a fistula from the blind "inner" segment to the ventral respiratory or urogenital system follows much the same pattern.

Although the time of onset of the disturbance can be determined within close limits, and its morphological stages can at least be subjected to reasonable conjecture, the causal factors that actually operate in individual human cases, by interfering with the growth process at the critical time, remain to be determined by clinical study.

Evidence for genetic causation of these defects in man is scanty in spite of their relative frequency in newborn infants. Three cases have been reported in which the abnormality occurred in more than one pregnancy in the same family, in each instance in the same generation (Mackenzie, 1884; Grieve and McDermott, 1939; Lanman, 1940). In the first of these reports, three children of the same father but by different mothers had the abnormality. In another case mentioned previously (Panse and Gierlich, 1949), both of a pair of twins were affected; and Ysander (1925) described the anomaly in both portions of a double monster. Ingalls and Prindle (1949), in reviewing 107 cases of esophageal atresia at the Boston Children's Hospital, found no evidence of a genetic element in their origin. As yet, no geneticist has observed a strain of laboratory animals carrying these defects, such as are now well known in connection with many other anomalies.

TABLE 1

MATERNAL PRENATAL FACTORS IN 87 CASES OF ESOPHAGEAL ATRESIA WITH TRACHEOESOPHAGEAL FISTULA

Acute infections or metabolic disturbances in first trimester	6
Chronic disease	12
Hydramnios	20
Antepartum bleeding	6

From cases of Children's Hospital, Boston, and Boston Lying-In Hospital. Ingalls and Prindle: Esophageal atresia with tracheoesophageal fistula.

Possible environmental causes of malformations can be studied in two ways: beginning with malformed infants and studying the pregnancy of the mothers; or beginning with mothers who have a suspicious complication in pregnancy and determining the outcome, as has been done in studies on German measles. Table 1 gives prenatal data from a group of 87 cases of the Boston Lying-In Hospital and the Boston Children's Hospital. The rather high proportion of various disturbances of pregnancy, coupled with a high incidence of prematurity, suggests that the embryonic abnormalities were part of a picture of generally inadequate gestation. Ingalls and Prindle also remarked on the frequent incidence of early bleeding from the uterus in the prenatal history of the cases. Such inadequacy, however, could result either from genetic weakness of the embryo or from a disturbance of gestation due to causes operating through the maternal environment. That this is a generalized factor is suggested by the frequent occurrence of associated abnormalities as shown in table 2.

Experimental evidence for the causation of these particular defects by environmental agencies is almost entirely lacking. Warkany *et al.* (1948) have reported one rat fetus in a group born to a vitamin-A-deficient mother in which a tracheoesophageal fistula was present. In view of the repeated production of various other common defects, such as spina bifida, cleft palate, and cardiac lesions, by a wide variety of traumatic and toxic agents, it is to be expected that, sooner or later, carefully timed experiments will result in the production of tracheoesophageal defects.

In the present state of knowledge, we can only suppose that tracheoesophageal defects of the human embryo may result from either genetic or environmental causes or from a combination of both, such as a maternal infection or nutritional deficiency acting upon a genetically weak embryonic tissue.

As stated above, the time at which any injurious stimulus or agent is acting upon the embryo seems to be of more importance than the specific nature or quantitative amount of the noxious agent. For example, defective genes, X rays, cortisone treatment, and vitamin deficiency might all produce the same abnormality if applied at the same period of development. It is to be hoped that the present study, by defining the time at which the human embryo becomes susceptible to defects of organization of the trachea and the lower esophagus, may assist clinicians in studying prenatal histories in the search for their specific environmental causes.

TABLE 2

Associated abnormalities found in 233 babies who had esophageal atresia

Congenital heart disease	24
Malformation of anus or rectum	23
Meckel's diverticulum	10
Atresia or stenosis of small intestine	7
Malrotation of colon and intestines	4
Coarctation of aorta	4
Vertebral anomalies	4
Stenosis of ureter	4
Annular pancreas	2
Mongolism	2
Pyloric stenosis	2
Duplication of stomach	2
Absence of kidney	2
Horseshoe kidney	2
Harelip and cleft palate	2
Hypospadias	2
Hypoplasia of kidneys	1
Diaphragmatic hernia	1
Agenesis of lung	1
Stenosis of bronchi	1
Septate vagina and bicornuate uterus	1
Pseudohermaphroditism	1
Club foot	1
Various minor anomalies	7

From Gross: The surgery of infancy and childhood.

CONCLUSIONS

1. A review of the normal development of the trachea and esophagus from horizon x to horizon xviii (23 to 38 days after ovulation) shows that the critical period at which congenital atresia of the esophagus and tracheoesophageal fistula must begin to develop is in horizons x to xvi.

2. The earliest observed embryonic cases are in horizon xvi or xvii.

3. Study of five embryonic specimens showing these defects, three of which have been examined by the present author, suggests that the mechanism of their production is a growth defect of the esophagus and trachea, coupled with overgrowth of the epithelium which bulges into the foregut over the lateral esophageal ridges.

4. In the present state of knowledge, the causation of these defects must tentatively be ascribed to genetic defects or disturbances of the maternal environment (infectious diseases, toxic conditions, or nutritional disturbances during pregnancy) acting at a critical period in the organization of the trachea and esophagus.

LITERATURE CITED

Belsey, R. H. R., and C. P. Donnison. 1950. Congenital atresia of the oesophagus. Brit. Med. Jour., vol. 2, pp. 324–328.

Broman, I. 1904. Die Entwickelungsgeschichte der Bursa omentalis und ähnlicher Rezessbildungen bei den Wirbeltieren. 611 pp. Wiesbaden.

Corner, G. W. 1929. A well-preserved human embryo of 10 somites. Carnegie Inst. Wash. Pub. 394, Contrib. to Embryol., vol. 20, pp. 81–101.

Dandy, W. E. 1910. A human embryo with seven pairs of somites measuring about 2 mm. in length. Amer. Jour. Anat., vol. 10, pp. 85–108.

Davis, C. L. 1923. Description of a human embryo having twenty paired somites. Carnegie Inst. Wash. Pub. 332, Contrib. to Embryol., vol. 15, pp. 1–51.

Ferguson, C. F. 1951. Congenital tracheoesophageal fistula not associated with atresia of the esophagus. Laryngoscope, vol. 61, pp. 718–766.

Flint, J. M. 1907. The development of the lungs. Amer. Jour. Anat., vol. 6, pp. 1–165.

Fluss, Z., and K. J. Poppen. 1951. Embryogenesis of tracheoesophageal fistula and esophageal atresia. Arch. Pathol., vol. 52, pp. 168–181.

Forssner, H. 1907. Die angeborenen Darm- und Ösophagusatresien. Anat. Hefte, vol. 34, pp. 1–163.

Gage, M., and A. Ochsner. 1936. The surgical treatment of congenital tracheo-esophageal fistula in the new-born. Ann. Surg., vol. 103, pp. 725–737.

Gladstone, R. J. 1935. Exhibit of lantern slides of 19 mm. embryo. *In* Proceedings of the Anatomical Society of Great Britain and Ireland. Jour. Anat., vol. 70, pp. 198–199.

Grieve, J. G., and J. G. McDermott. 1939. Congenital atresia of the oesophagus in two brothers. Canadian Med. Assoc. Jour., vol. 41, pp. 185–186.

Gross, R. E. 1953. The surgery of infancy and childhood: its principles and techniques. 1000 pp. Philadelphia.

Grosser, O. 1912. The development of the respiratory apparatus. *In* Keibel and Mall (eds.), Manual of human embryology, vol. 2, chap. 17, pp. 473–493. Philadelphia.

Gruenwald, P. 1940. A case of atresia of the esophagus combined with tracheo-esophageal fistula in a 9-mm. human embryo, and its embryological explanation. Anat. Rec., vol. 78, pp. 293–302.

Haight, C., and H. A. Towsley. 1943. Congenital atresia of the esophagus with tracheoesophageal fistula. Extrapleural ligation of fistula and end-to-end anastomosis of esophageal segments. Surg., Gynecol. and Obstet., vol. 76, pp. 672–688.

Hjortsjö, C. H. 1945. De epiteliala lunganlagens tidiga morfogenes hos *Felis catus* L. Monograph. 184 pp. Lund.

Ingalls, T. H., and R. A. Prindle. 1949. Esophageal atresia with tracheoesophageal fistula. Epidemiologic and teratologic implications. New England Jour. Med., vol. 240, pp. 987–995.

Johns, B. A. E. 1952. Developmental changes in the oesophageal epithelium in man. Jour. Anat., vol. 86, pp. 431–442.

Keith, A. 1910. A demonstration on constrictions and occlusions of the alimentary tract of congenital or obscure origin. Brit. Med. Jour., vol. 1, pp. 301–305.

King, E. S. J. 1948. Lecture I: Significance of modern embryology in pathology. Med. Jour. Australia, vol. 2, pp. 705–710.

Klebs, E. 1869. Handbuch der pathologischen Anatomie. Vol. 1, p. 164. Berlin.

Kreuter, E. 1905. Die angeborenen Verschliessungen und Verengerungen des Darmkanals im Lichte der Entwicklungsgeschichte. Deut. Ztschr. f. Chir., vol. 79, pp. 1–89.

Ladd, W. E. 1944. The surgical treatment of esophageal atresia and tracheoesophageal fistulas. New England Jour. Med., vol. 230, pp. 625–637.

Lanman, T. H. 1940. Congenital atresia of the esophagus. Arch. Surg., vol. 41, pp. 1060–1083.

Leven, N. L. 1941. Congenital atresia of the esophagus with tracheoesophageal fistula. Jour. Thor. Surg., vol. 10, pp. 648–657.

Lewis, F. T. 1912. The development of the oesophagus. *In* Keibel and Mall (eds.), Manual of human embryology, vol. 2, chap. 17, pp. 355–368. Philadelphia.

Mackenzie, M. 1884. A manual of diseases of the throat and nose. Vol. 2. Diseases of the oesophagus, nose, and nasopharynx. 400 pp. New York.

Mall, F. P. 1908. A study of the causes underlying the origin of human monsters. (Third contribution to the study of the pathology of human embryos.) Jour. Morphol., vol. 19, pp. 3–368.

Minot, C. S. 1910. A laboratory text-book of embryology. 2d ed., rev. 402 pp. Philadelphia.

Panse, F., and J. Gierlich. 1949. Zur Pathogenese der Anencephalie. Virchow's Arch. f. pathol. Anat. u. Physiol., vol. 316, pp. 135–148.

Patten, B. M. 1953. Embryological stages in the establishing of myeloschisis with spina bifida. Amer. Jour. Anat., vol. 93, pp. 365–396.

Plass, E. D. 1919. Congenital atresia of the esophagus with tracheo-esophageal fistula: associated with fused kidney. A case report and survey of the literature on congenital anomalies of the esophagus. Johns Hopkins Hosp. Reports, vol. 18, pp. 259–286.

Puiggrós-Sala, J. 1937. Ueber die Entwicklung der Lungenanlage des Menschen. Ztschr. f. Anat. u. Entwicklungsgesch., vol. 106, pp. 209–225.

Rosenthal, A. H. 1931. Congenital atresia of the esophagus with tracheo-esophageal fistula. Arch. Pathol., vol. 12, pp. 756–772.

Schmitz, J. A. 1923. Ueber die formale Genese der Oesophagusmissbildungen. Virchow's Arch. f. pathol. Anat. u. Physiol., vol. 247, pp. 278–293.

Schridde, H. 1908. Ueber die Epithelproliferationen in der embryonalen menschlichen Speiseröhre. Virchow's Arch. f. pathol. Anat. u. Physiol., vol. 191, pp. 178–192.

Shaw, R. 1939. Surgical correction of congenital atresia of the esophagus with tracheo-esophageal fistula. Case Report. Jour. Thor. Surg., vol. 9, pp. 213–219.

Spemann, H. 1928. Croonian Lecture of 1927: Organizers in animal development. Proc. Roy. Soc. London, B, vol. 102, pp. 177–187.

Streeter, G. L. 1942. Developmental horizons in human embryos. Description of age group xi, 13 to 20 somites, and age group xii, 21 to 29 somites. Carnegie Inst. Wash. Pub. 541, Contrib. to Embryol., vol. 30, pp. 211–245.

——— 1945. Developmental horizons in human embryos. Description of age group xiii, embryos about 4 or 5 millimeters long, and age group xiv, period of indentation of the lens vesicle. Carnegie Inst. Wash. Pub. 557, Contrib. to Embryol., vol. 31, pp. 27–63.

——— 1948. Developmental horizons in human embryos. Description of age groups xv, xvi, xvii, xviii, being the third issue of a survey of the Carnegie Collection. Carnegie Inst. Wash. Pub. 575, Contrib. to Embryol., vol. 32, pp. 133–203.

Vogt, E. C. 1929. Congenital esophageal atresia. Amer. Jour. Roent., vol. 22, pp. 463–465.

Warkany, J., C. B. Roth, and J. G. Wilson. 1948. Multiple congenital malformations: a consideration of etiologic factors. Pediatrics, vol. 1, pp. 462–471.

Wells, L. J., and E. A. Boyden. 1954. The development of the bronchopulmonary segments in human embryos of horizons xvii-xix. Amer. Jour. Anat., vol. 95, pp. 163–202.

Yamasaki, M. 1933. Ein menschlicher Embryo von 8.5 mm Scheitel-Steisslänge mit fehlerhaften und ungewöhnlichen Bildungen. Arb. aus dem Anat. Inst. d. Kaiserlich-Japanischen Universität z. Sendai, vol. 15, pp. 27–59.

Ysander, F. 1925. Human diplo-terata. Inaugural dissertation. Uppsala.

PLATE 1

FIG. 12. Photomicrograph showing the endodermal proliferation characteristic of the pulmonary knob in horizon xi. The lateral and ventral walls of the foregut are thicker than the dorsal wall. The ventral and lateral epithelium has a transitional appearance; the dorsal epithelium is more cuboidal. Embryo no. 2053, section 3-4-7, ×100.

FIG. 13. Photomicrograph of the foregut, showing the presence of a second endodermal ridge, the lateral esophageal groove, dorsal to the tracheoesophageal ridge. In this section the right ridge is more prominent, though serial sections confirm the presence of both a right and a left ridge. Again, the disparity in the thickness of the ventral and dorsal walls is noted. Embryo no. 5035, section 2-1-15, ×400.

FIG. 14. Photomicrograph showing the early tracheoesophageal separation as shown by horizon xii. The ventral respiratory segment shows a characteristically thick endodermal wall. The endodermal ridges between the respiratory and digestive portions have joined without an indentation of the basement membrane as might be expected from a "pinching-off." Although an indentation is seen on the right coelomic surface, no condensation of mesenchyme is present. The primarily endodermal nature of the tracheoesophageal separation is well illustrated. Embryo no. 6144, section 2-3-8, ×200.

FIG. 15. Sagittal section taken in the plane of the primary bronchus, showing the manner in which the lateral esophageal groove, by medial overgrowth, would tend to block the lumen of the upper esophagus. The remaining sections of this embryo show the lumen of both trachea and esophagus to be patent. Definite lateral esophageal grooves running dorsally and caudally narrow the esophagus markedly. The communication in this section is between a bronchus, at the level of the bifurcation, and the esophagus. Embryo no. 7724, section 2-2-13, ×100.

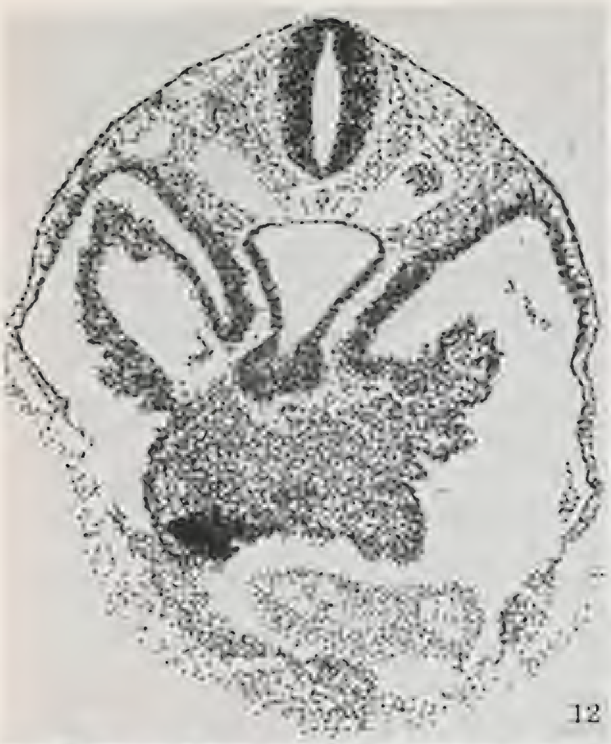

12

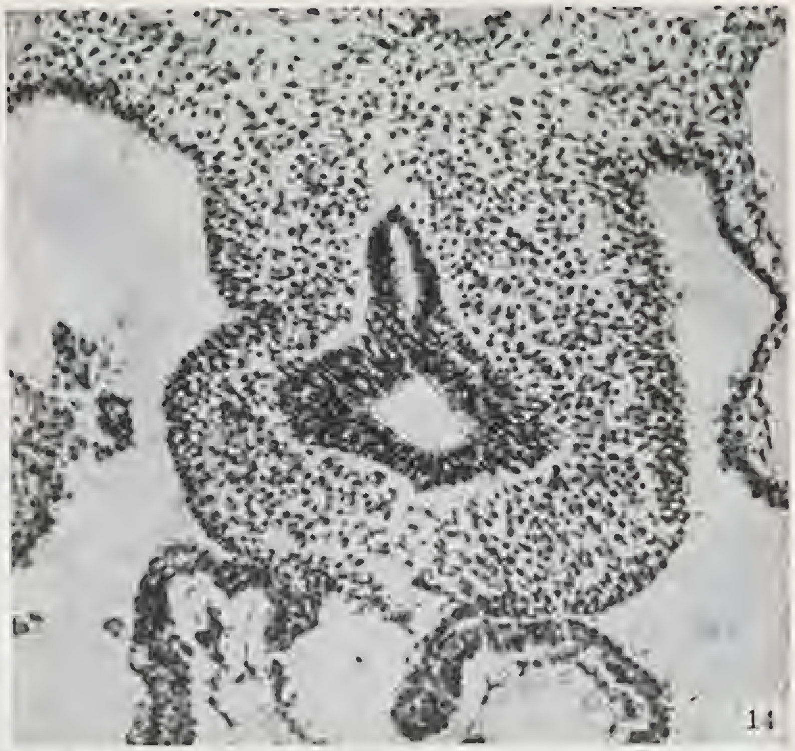

14

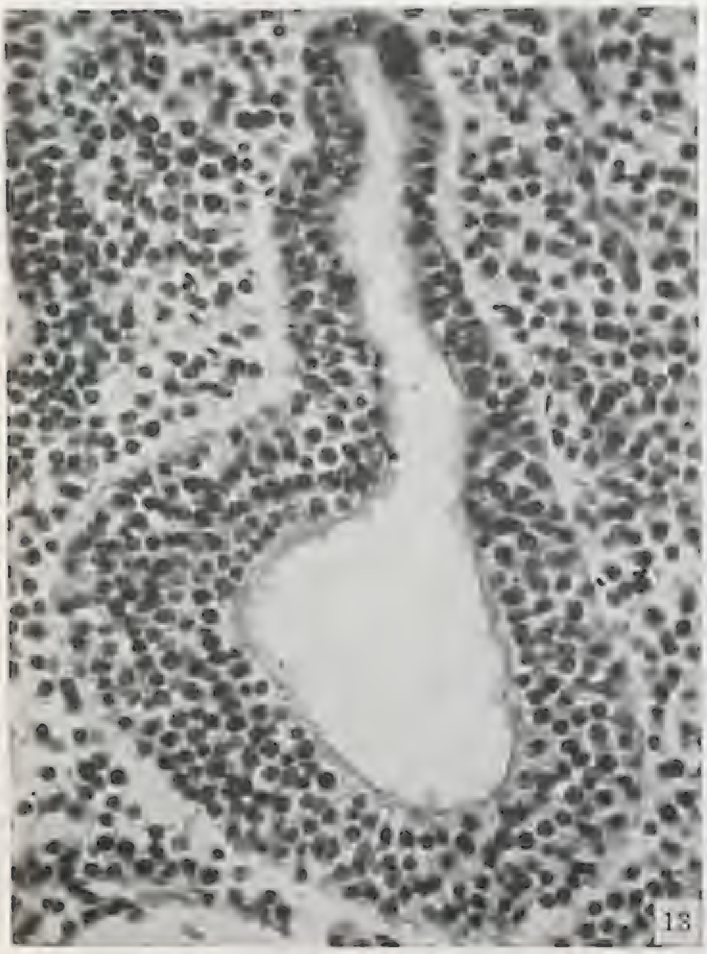

13

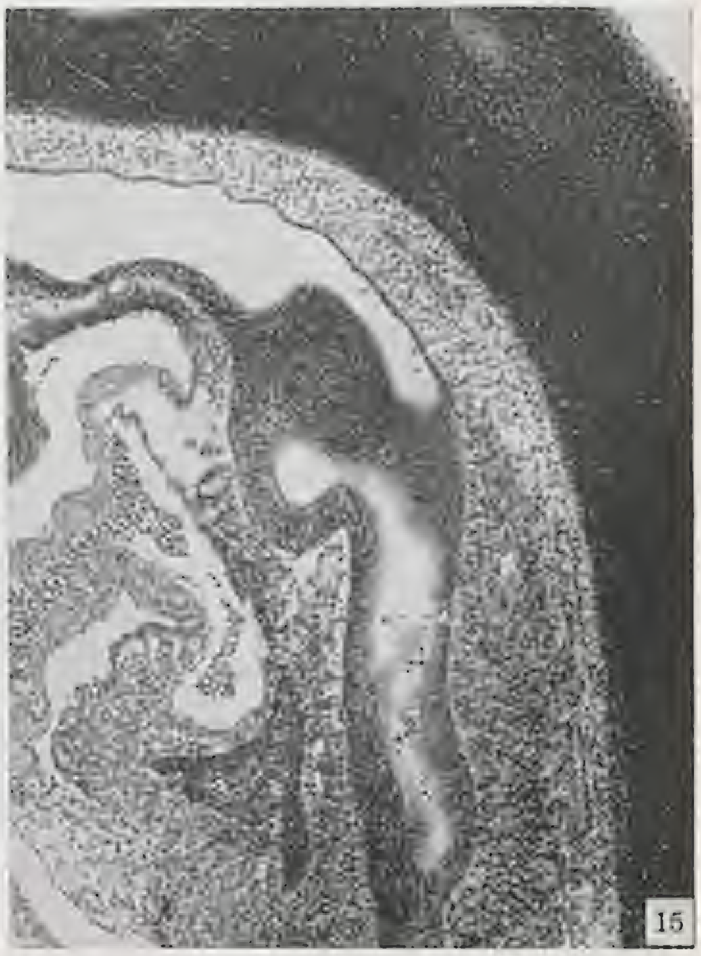

15

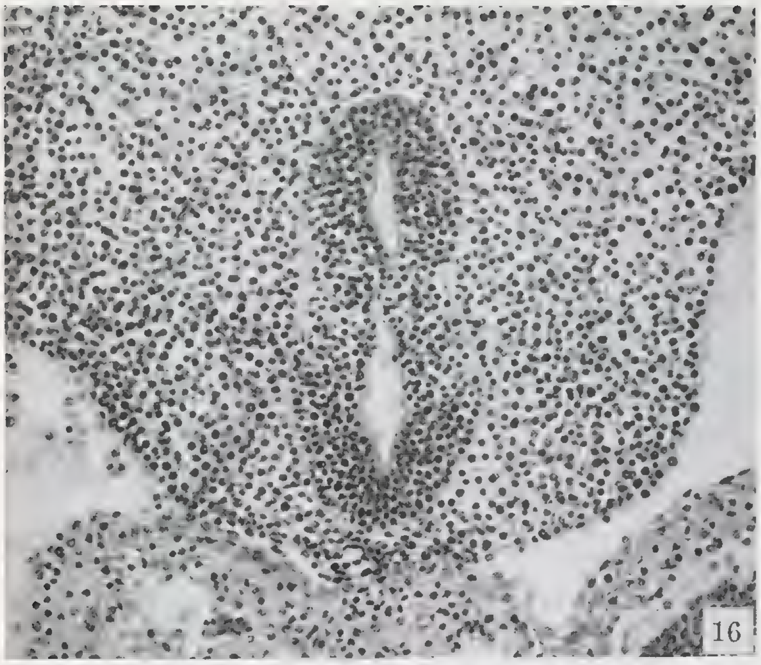

FIG. 16. Photomicrograph to show the tracheoesophageal separation in horizon xiii. Although there is a slight indentation in the left basement membrane, endodermal division is present without evidence of mesenchymal pressure or condensation. Embryo no. 5541, section 2-7-1, × 200.

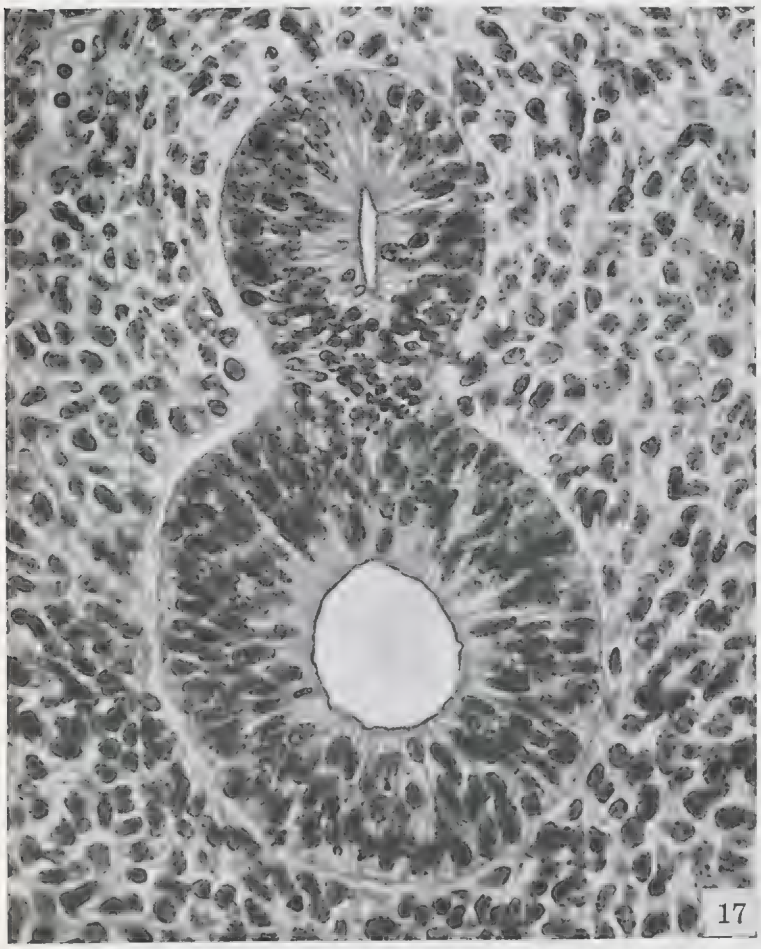

FIG. 17. Photomicrograph showing a later stage in tracheoesophageal separation than that of figure 16. There is evidence of necrosis in the central cells of the endodermal septum, and indentation of the external basement membrane is present. Various stages of tracheoesophageal separation can be seen in the same embryo as one progresses cranially in the region of the tracheoesophageal septum. Embryo no. 8119, section 3-4-7, × 400.

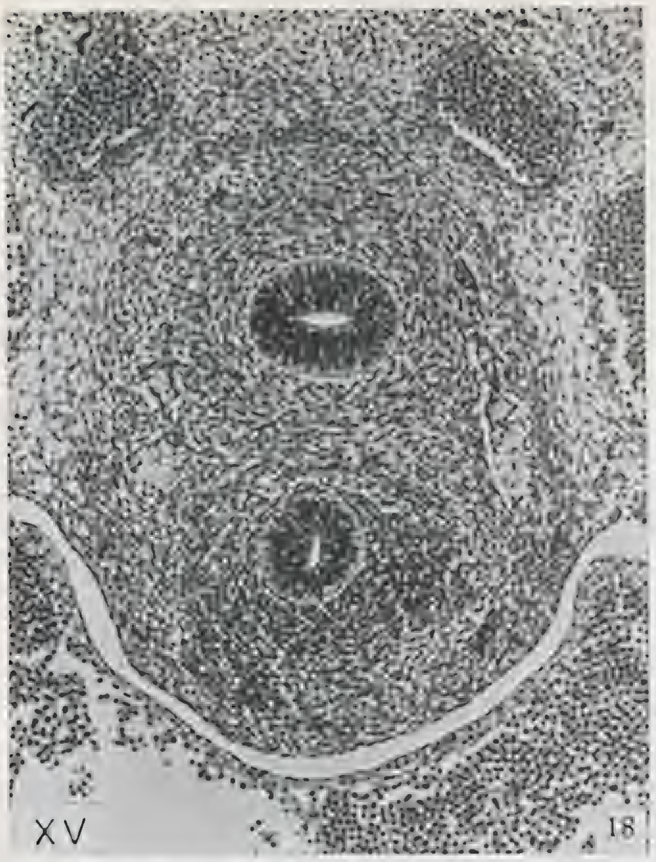

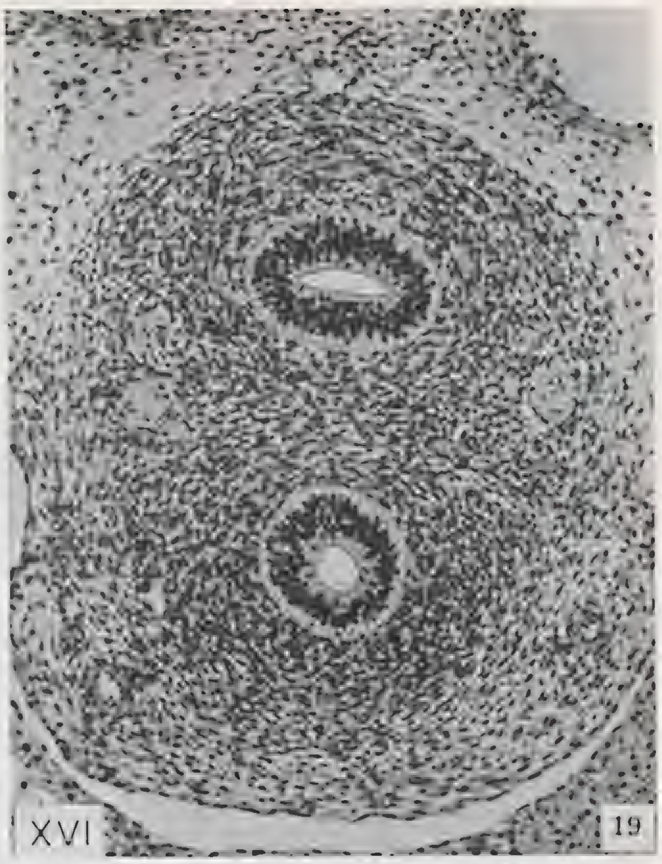

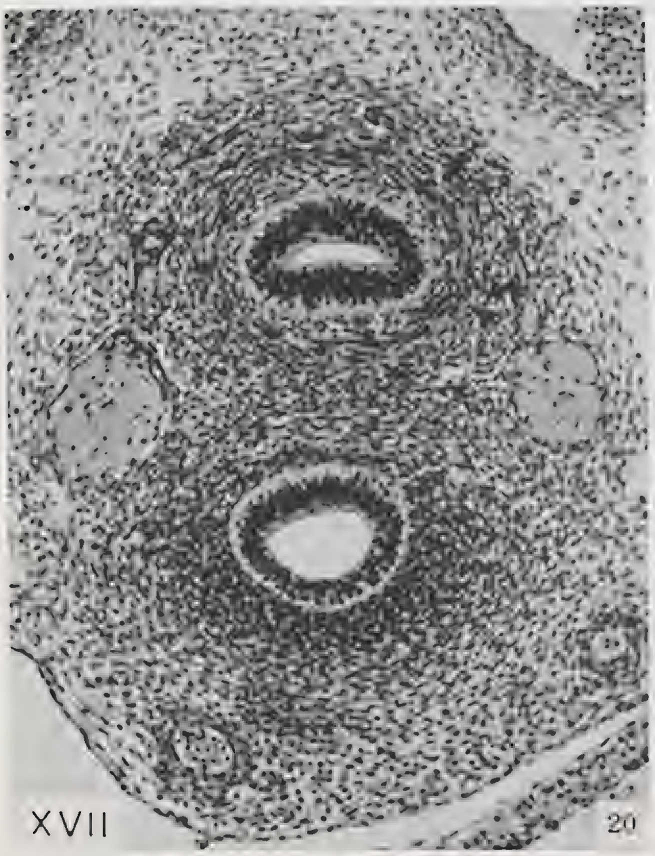

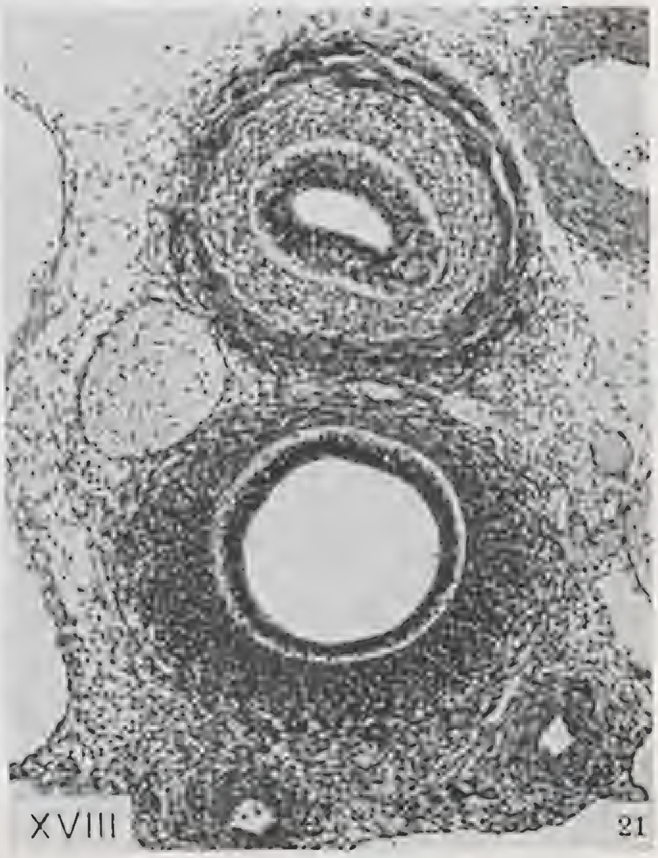

Four photomicrographs of sections at comparable levels through the esophagus and trachea in horizons xv through xviii. All are shown at the same enlargement, × 150. There is a progressive increase in the size of the lumen and in differentiation of the supporting structures of the trachea and esophagus. By horizon xviii, definitive mucosal, submucosal, and muscular layers can be seen in the esophagus. Atresia of the esophagus with a tracheoesophageal fistula would probably occur before this stage of development. Note the large vagus nerves, the pulmonary arteries, and the aorta. From Streeter, 1945, plate 3, xv.

Fig. 18. Embryo no. 3512, section 12-4-6.
Fig. 19. Embryo no. 6519, section 21-4-3.
Fig. 20. Embryo no. 6521, section 30-2-5.
Fig. 21. Embryo no. 4430, section 17-4-5.

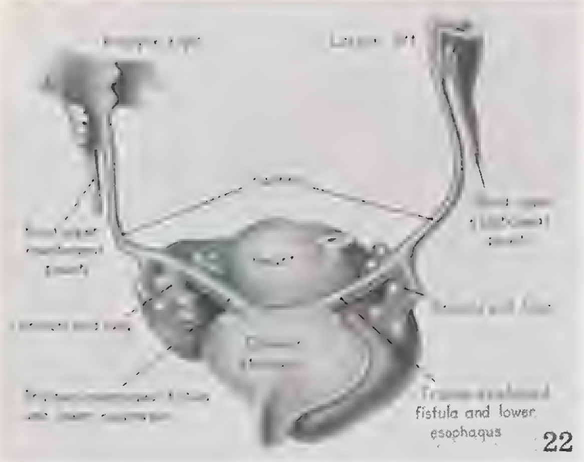

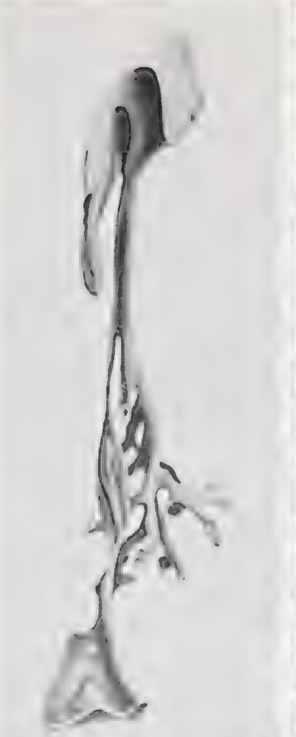

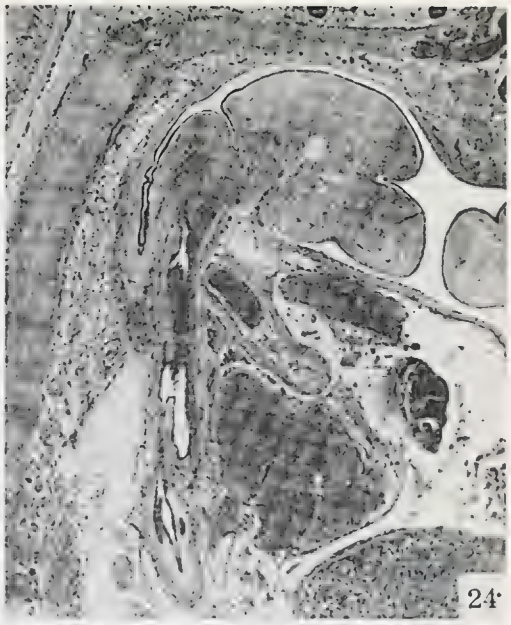

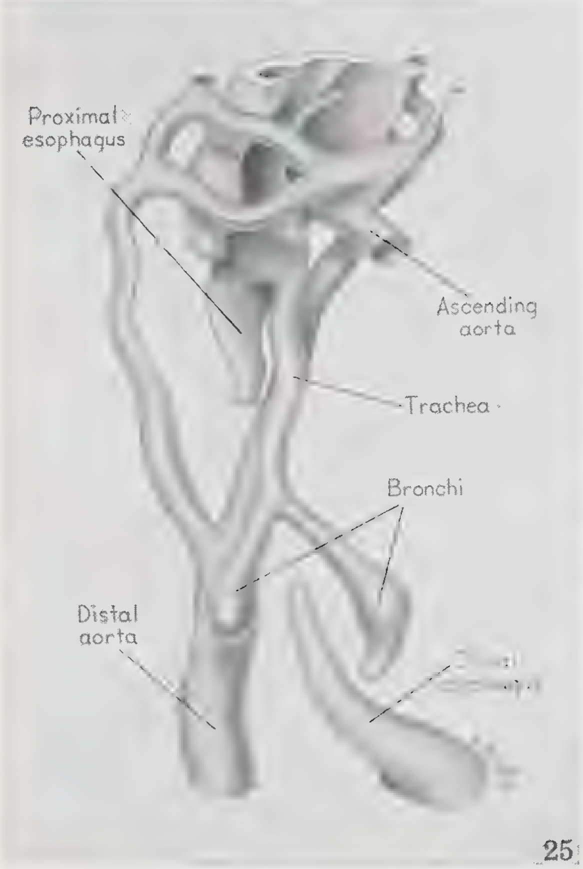

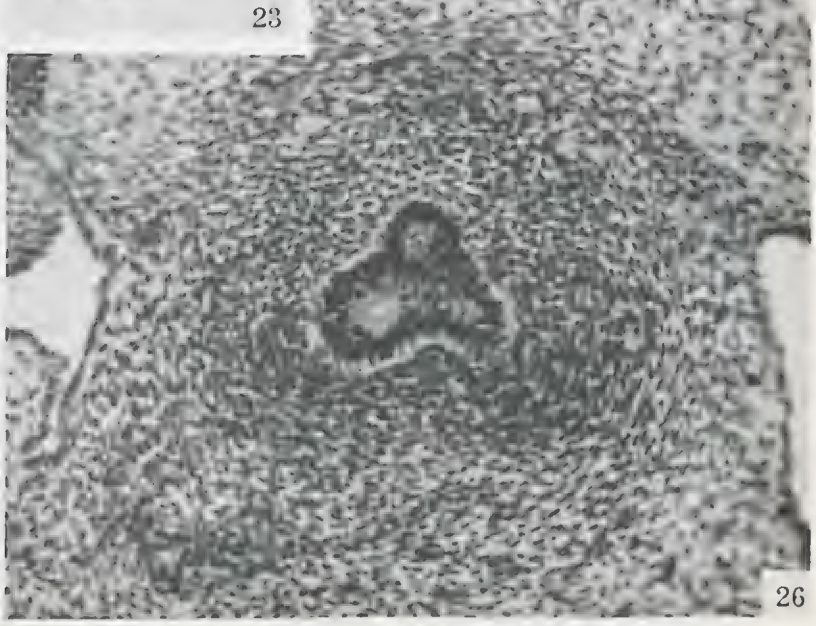

FIG. 22. Model of the upper endodermal tract and cardiovascular system of the double monster described by Ysander. Both upper esophageal pouches end blindly. Fistulae can be seen connecting both tracheae with the lower esophageal pouches and common stomach. Drawing by Mary M. Cope from an illustration in the original monograph. ×15.

FIG. 23. Model of the endodermal tract of the Harvard 18.1-mm. human embryo with type III*b* atresia of the esophagus. The tenuous nature of the lower esophagus is shown. Copied from a photograph of the model made by Dr. Albert F. Boretti, which was given to the present author by the late Professor Frederick T. Lewis.

FIG. 24. Photomicrograph showing a sagittal section through the respiratory and esophageal regions of the Harvard 18.1-mm. human embryo. The lumen of the blind upper pouch, the trachea, and the fistula to the lower esophagus can be seen. Note the degree of organization of the supporting structures about the esophagus and the trachea. In appearance this section is strikingly similar to the sagittal section in figure 15. (Harvard Collection Series 1129, section 171, carried as Carnegie no. 9335.) From Ingalls and Prindle, figure 3.

FIG. 25. Drawing of a model of the endodermal tract of the Yamasaki embryo. The blind upper esophageal segment is seen along with the aortic arches. The orientation of the lower esophageal segment toward the bifurcation of the trachea is quite clear, corresponding to the course of the lower segment in the type III*b* atresia of the esophagus. The atretic region of the esophagus matches closely the narrow portion of the esophagus noted in figure 23. The small dorsal diverticulum from the trachea seen in figure 26 lies on the far side of the tracheal bifurcation in this view. Drawing by Mary M. Cope from a model (Carnegie no. 8731) made at the Carnegie Institution, Department of Embryology, by Mary M. Cope and O. O. Heard from the sections of this embryo, lent by Dr. Yamasaki.

FIG. 26. Photomicrograph of the Yamasaki embryo (Carnegie no. 8731, section 27-6), showing the diverticulum which arises from the dorsal side of the trachea at the site of its bifurcation. This diverticulum points toward the lower esophageal segment seen in figure 25. ×200.

CONTRIBUTIONS TO EMBRYOLOGY, NO. 246

THE ORIGIN AND DEVELOPMENT OF THE HUMAN EXTRINSIC OCULAR MUSCLES

Perry W. Gilbert

Department of Embryology, Carnegie Institution of Washington, Baltimore, Maryland,
and Department of Zoology, Cornell University, Ithaca, New York

With fourteen plates and two text figures

CONTENTS

PAGE

Introduction 61

Acknowledgments 63

Material and Methods 63

The Prechordal Plate and the Origin of the Premandibular Condensations 63

The Maxillomandibular Mesoderm 67

The Development of the Lateral Rectus 68

The Development of the Superior Oblique 70

The Fate of the Premandibular Condensations 71

Discussion 74

Summary 76

Literature Cited 77

Abbreviations Used in Figures 78

THE ORIGIN AND DEVELOPMENT OF THE HUMAN EXTRINSIC OCULAR MUSCLES

INTRODUCTION

Few muscles in vertebrates have been more challenging to the comparative anatomist than those that move the eyeball, yet, interestingly enough, few muscles have, during their evolution, remained more conservative. In all the vertebrates, the superior rectus, the medial rectus, the inferior rectus, and the inferior oblique are innervated by the oculomotor nerve, the superior oblique is supplied by the trochlear nerve, and the lateral rectus by the abducens nerve.[1] A seventh eyeball muscle, the retractor bulbi, found in several groups of vertebrates, is, like the lateral rectus, supplied by the abducens nerve.

The uniform appearance of these muscles throughout the different classes of vertebrates, and their consistent innervation, lead one to anticipate some uniformity in their pattern of development. Marked similarity has indeed been found in elasmobranchs, reptiles, and birds, in which groups the eyeball muscles consistently arise from the walls of three pairs of head cavities or from homologous solid condensations. In these vertebrates, the four eyeball muscles innervated by the oculomotor nerve arise from the walls of the premandibular head cavity; the superior oblique arises from the walls of the mandibular head cavity or from a homologous solid condensation; and the abducens musculature arises, at least in part, from the hyoid head cavity or condensation. A comprehensive review of eyeball-muscle development in these groups may be found in the papers of Adelmann (1927), Edgeworth (1935), and Wedin (1949); specific groups have been treated fairly exhaustively by the following: *elasmobranchs,* Balfour (1878), Dohrn (1904), Lamb (1902), Marshall (1881), Neal (1918), Platt (1891), Wedin (1949), van Wijhe (1883); *reptiles,* Filatoff (1907), Johnson (1913), Orr (1887), Wedin (1953*a*); *birds,* Adelmann (1926, 1927), Rex (1900, 1905), Wedin (1953*b*).

As for the Metatheria, the eyeball muscles have been intensively studied embryologically in *Trichosurus* and other marsupials by Fraser (1915); Gilbert (1954) has investigated their early development in the opossum, *Didelphys virginiana.* In both *Trichosurus* and *Didelphys,* the oculomotor muscles arise from the wall of a well defined premandibular cavity situated on each side of the head, whereas the superior oblique and the abducens muscles are derived from distinct primordia which may be homologized with the mandibular and hyoid condensations of lower vertebrates. The extrinsic ocular muscles in marsupials thus arise from three separate primordia, as they do in elasmobranchs, reptiles, and birds.

In placental mammals, accounts of the ontogeny of the eyeball muscles have been conflicting and, until recently, incomplete. Basing their observations on relatively late stages of development, Reuter (1897) and Keil (1906) believed that all the extrinsic ocular muscles of the pig arise from a single condensation of mesoderm adjacent and caudal to the optic stalk. Lešer (1925), after observing early stages of the ground squirrel, bat, rabbit, dog, mouse, and guinea pig, concluded that the eyeball muscles of these mammals likewise originate from a single condensation on each side of the head.

On the other hand, Corning (1899) found in rabbit embryos of 12 and 17 somites a solid pair of premandibular condensations arising from the prechordal plate, which he suggested are the source of the oculomotor muscles. He was unable to find in these early stages the primordia of the superior oblique and abducens muscles, but believed that they arise independently of those innervated by the oculomotor. Bonnet (1901) likewise found, in a 16-somite dog embryo, a pair of mesodermal condensations derived from a medial mass of cells at the anterior end of the notochord intimately associated with the roof of the preoral gut. Bonnet called these condensations rudimentary head cavities (*Kopfhöhlenrudimenten*), but did not follow their fate. His illustration leaves no doubt that these masses are premandibular condensations of prechordal-plate origin.

The investigations of Corning and Bonnet suggested that an examination of mammalian embryos younger than those that were available to Keil and Reuter, and more critically studied than those of Lešer, might well reveal the true origin of the eyeball musculature in placental mammals and, at the same time, determine whether in this group the extrinsic ocular muscles arise from a single primordium or from three distinct but closely apposed primordia such as are found in elasmobranchs, reptiles, birds, and marsupials.

---

[1] The innervation of the extrinsic ocular muscles in certain cyclostomes is somewhat unusual in that the abducens nerve appears to supply both the lateral rectus and inferior rectus muscles. P. Fürbringer (1875) first noted this condition in the lamprey, *Petromyzon marinus;* his observations were subsequently confirmed by M. Fürbringer (1897), Corning (1900), and Cords (1929). Addens (1933) cleared up this apparent inconsistency when he showed that "the III nucleus of petromyzonts, in contradistinction to that of all other vertebrates, which is always single, consists of two widely separated divisions, viz., a large rostral part, situated at about the same place as the single nucleus in gnathostomes, and a small caudal part lying far backward, viz., at the caudal level of the V root." The root arising from the caudal division of the III nucleus does not join that arising from the rostral division, but issues separately from the brain as a part of cranial nerve VI. Addens proposed, therefore, the name "oculomotor-abducens" for this composite nerve of petromyzonts, and showed that the oculomotor portion innervates the inferior rectus whereas the abducens portion supplies the lateral rectus.

With this in mind, the author (Gilbert, 1947) examined 225 cat embryos, in stages ranging from 10 somites to 55 mm., and studied the origin and development of the extrinsic ocular muscles. It was found that the oculomotor muscles arise from a pair of premandibular condensations of prechordal-plate origin, and that the eyeball muscles innervated by the IVth and VIth nerves arise from separate condensations in the maxillomandibular mesoderm. It was concluded that "the origin, relations, and fate of the 3 condensations giving rise to the eye muscles in the cat indicate clearly their homology with the so-called premandibular, mandibular, and hyoid eye-muscle anlagen of lower vertebrates." Is it possible that the eyeball muscles of other placental mammals, including man, follow a similar pattern in their development?

References to the origin and development of the extrinsic ocular muscles in man are to be found in the texts of Mann (1928) and Wolff (1940). Mann states (p. 254) that "the eye muscles in man seem, at their earliest stage, to be represented by a single undifferentiated mass. The earliest trace of these muscles in man can be seen at 7 mm. when they are represented by a massed condensation in the paraxial mesoderm surrounding the optic vesicle." Wolff reaches a similar conclusion, reporting that the primordia of the human eyeball muscles at first "form one mass which Lewis (1910) found was supplied by the 3rd nerve only. Later (at 9 mm.) when the 4th and 6th nerves enter, this mass divides into separate muscles."

To the author's knowledge, Lewis (1910) was the first investigator to study and describe the early development of the human extrinsic ocular muscles. Unfortunately, only a limited number of human embryos was available to him when he made his study; for this reason he was unable to investigate the very early stages, which would have thrown more light on this problem. Lewis' widely quoted statement concerning the origin of the eyeball musculature in man is as follows:

> It has commonly been assumed that the muscles of the orbit are derived from anterior head somites; the first somite giving rise to the Mm. levator palpebrae superioris, rectus superior, rectus internus, rectus inferior, and obliquus inferior, supplied by the N. oculomotorius; the second, to M. obliquus superior, supplied by the N. trochlearis; and the third, to the M. rectus lateralis, supplied by the N. abducens. Anterior head somites have, however, never been observed in man or mammals. Zimmermann (1898) [actually, 1899, P.W.G.] observed in a 3.5-mm. embryo several small head cavities in the region where later the eye muscles develop. It is uncertain even that they represent rudimentary head somites, and no connection has been established between them and the eye muscles. On the contrary, the observations of Reuter (1897) on the pig and my own observations on human embryos, which follow here, show that all the eye muscles arise from a common premuscle mass, which occupies, both in the pig and in man, the same general position in the early embryo. This common premuscle mass is first to be recognized in human embryos of about 7 mm. in length (fig. 367). It consists of a lens-shaped mass of condensed mesenchyme, outlined from the surrounding mesenchyme by a capillary network over its surface. This premuscle mass lies dorsal to the optic stalk, between it and the ganglion Gasseri, and medial to the optic cup. The N. ophthalmicus passes in front of and lateral to the mass, and the N. maxillaris behind and lateral to it. At this stage only the N. oculomotorius enters the anterior end of the muscle mass. The Nn. trochlearis and abducens do not appear until later.
>
> In a 9-mm. embryo the eye premuscle mass occupies much the same position as in the earlier stage, lying on the dorsal side of the optic stalk and medial to the N. ophthalmicus and maxillaris (Figs. 368, 369). It has enlarged somewhat and extends along the caudal side of the optic stalk. It also begins to show cleavage into separate muscle masses, each supplied by its respective nerve. The N. trochlearis now enters the anterior portion of the mass which later forms the rudiment of the M. obliquus superior. The N. abducens enters the caudal end of the mass, which has begun to extend out along the path of the nerve and also shows indications of separation from the rest of the mass which lies closer to the optic stalk and into which the N. oculomotorius runs. The muscle mass at this stage has no very distinct attachment either to the precartilage or to the sclera, but there exists a direct continuity with the mesenchyme from which these structures differentiate.
>
> In an 11-mm. embryo the premuscle mass has still farther enlarged and partially split into the rudiments supplied by the three nerves. The anlagen lie on the dorsal and caudal sides of the optic nerve and for the most part medial to the eyeball (Figs. 370, 379). They are continuous laterally with the primitive sclera, which is now beginning to form as a definite condensation of the mesenchyme about the eyeball, and medially with the precartilaginous tissue about the optic nerve. The M. rectus lateralis has extended farther out along the path of the N. abducens and has as yet no skeletal attachment. The N. ophthalmicus passes above these muscle masses and nearly at right angles to them.
>
> As differentiation progresses the muscle mass of the N. oculomotorius gradually extends around the optic nerve and splits into the various muscles supplied by this nerve. In a 14-mm. embryo all the orbital muscles are to be distinguished and have nearly the adult relations to the bulbus oculi. The M. obliquus inferior, however, does not completely separate off from the M. rectus inferior until a later stage.

Recently, in a doctoral thesis, Carnicer (1950) described the origin and development of the extrinsic ocular muscles of three placental mammals, *Lepus, Mus,* and *Homo.* He believes that mesenchymal thickenings, the primordia of the eyeball muscles, arise *in situ* about the distal ends of cranial nerves III, IV, and VI, and is of the opinion that the nerves in some way are responsible for the appearance of the eye-muscle primordia. He ignores the fact that the eye-muscle primordia in both cat and man are evident before the cranial nerves III, IV, and VI make their appearance. Although he does not state clearly the number of mesenchymal thickenings, he gives the impression that there is but a single mass on each side of the head which thickens unevenly to form the eye-muscle primordia.

Carnicer's conclusions are based on an examination of the following material: *Lepus* (6 specimens: 10, 11, 11 to 13, 13, 15, 15 to 18 days), *Mus* (6 specimens: 10, 12, 12, 15, 16, 16 to 17 days), *Homo* (4 specimens: 2 to 4 weeks, 5 to 6 weeks, 2 months, 3 to 4 months). The youngest human embryo he examined appears to belong to late horizon xiv or early horizon xv, for the lens vesicle has nearly closed off from the surface ectoderm. Insufficient data are given for the other human embryos to permit assignment to a specific horizon, but, from their condition, it must be concluded that two and possibly all three are much too old to be of value in reaching any conclusions as to the origin and early development of the eyeball musculature. Even the youngest human embryo he examined, belonging to horizon xiv to xv, hardly provides an acceptable starting point for such a study. Moreover, the paucity of material with which Carnicer worked, not only in man, but also in the mouse and rabbit, would provide a serious handicap even for an experienced investigator. It is not surprising, therefore, that Carnicer's study does little to elucidate the early ontogeny of the mammalian eyeball musculature.

It should be remembered that the observations of Lewis (1910) and Carnicer (1950) on the eyeball muscles of man, like those of Reuter (1897) and Keil (1906) on the eye muscles in the pig, were made on embryos belonging to relatively late stages of development. The present study, based on a younger and much more extensive series of human embryos than was available to Lewis and Carnicer, reveals that: (1) transitory head cavities do exist in a premandibular condensation on each side of the head, and that this condensation subsequently gives rise to the extrinsic ocular muscles innervated by the oculomotor nerve; (2) the premandibular condensations are formed by cells proliferated from the prechordal plate; (3) the superior oblique and lateral rectus muscles arise from separate primordia adjacent to the premandibular condensations; (4) the eyeball muscles in man, therefore, do not arise from "a common premuscle mass," but rather from three separate primordia on each side of the head; (5) the development of the extrinsic ocular muscles in man follows a pattern which conforms in essential features with that found in elasmobranchs, reptiles, birds, marsupials, and the cat.

ACKNOWLEDGMENTS

Much of this investigation was conducted at the Department of Embryology, Carnegie Institution of Washington, in Baltimore, Maryland, during a sabbatic leave from Cornell University. It was made possible in part through a generous research grant from the Carnegie Institution of Washington; to both that Institution and Cornell University the author is most grateful. The author wishes to express his appreciation to Dr. George W. Corner, Director of the Department of Embryology of the Carnegie Institution of Washington, for his many kindnesses and for the privileges of the laboratory. It is also a pleasure to thank Dr. Chester H. Heuser and Dr. Robert K. Burns, of the Carnegie laboratory, and Dr. Howard B. Adelmann, of the Cornell University Department of Zoology, for their helpful advice and interest in this problem. The author is grateful to the late Mr. James Didusch and to Mrs. Mary M. Cope for the skillful preparation of the illustrations; their patience and care in the execution of those drawings based on the plastic and plaster reconstructions are particularly appreciated. To Mr. O. O. Heard and Mrs. Cope the author is indebted for assistance in making the plaster and plastic models, and to Mr. Richard Grill for the preparation of the photomicrographs.

MATERIAL AND METHODS

The material for this study consisted of approximately 100 human embryos (table 1), ranging in size from presomite to 32+ mm. All the embryos belong to the collection of the Department of Embryology, Carnegie Institution of Washington. The fact that these embryos, largely through the efforts of the late Dr. George L. Streeter, are arranged in the collection according to their developmental age (horizon) contributes immeasurably to the ease and efficiency with which a study of this kind can be pursued.[2] Paper, plastic, and plaster reconstructions of important stages in the development of the eyeball muscles were made.

THE PRECHORDAL PLATE AND THE ORIGIN OF THE PREMANDIBULAR CONDENSATIONS

In most, and possibly all, fishes, amphibians, reptiles, and birds, the eyeball muscles innervated by the oculomotor nerve arise from mesoderm derived from the prechordal plate. Parker (1917) found this to be true in marsupials also, and the author has pointed out the significance of the prechordal plate in this connection in the cat (Gilbert, 1947) and opossum (Gilbert, 1954). An understanding of the prechordal plate is, therefore, of

---

[2] For a description of horizons xi to xxiii, consult Streeter (1942, 1945, 1948, 1951).

TABLE 1

Human embryos of the Carnegie Collection utilized in studying the development of the extrinsic ocular musculature

Horizon	Approximate age (days)	Embryo number	Somites, or crown-rump length (mm.)*	Plane of section †	Thickness of sections (microns)
x	22±1	4216	(7)	T	15
		5074	(10)	T	10
xi	24±1	2053	(20)	T	10
		4529	(14)	T	10
		6050	(19)	FT	10
		6344	(13)	T	6
		6784	(17)	T	6
		7611	(16)	T	8
		8005	(16)	T	8
xii	26±1	486	(21)	T	10
		4245-7	ca. (24)	T	10
		4736	(26)	F	10
		4784	(23)	T	10
		6097	(25)	T	10
		6144	(27)	T	10
		7724	ca. (29)	S	8
		7852	(25)	T	10
		7999	ca. (28)	T	10
		8505A	(24)	T	8
		8505B	(23)	S	8
xiii	27±1	463	3.9	F	10
		588	4.0	F	15
		836	4.0	T	15
		6473	5.0	F	6
		7433	5.2	F	8
		7618	4.8	F	10
		8119	5.3	T	8
		8239	4.3	S	8
		8581	4.8	S	8, 10
xiv	29±1	1620	6.6	S	20
		6428	7.0	F	6, 10
		6500	4.9	S	10
		6503	6.3	F	10
		6830	5.5	F	8
		6848	7.8	F	10
		7394	7.2	T	8
		8141	7.3	F	8
xv	31±1	241	6.0	T	10
		810	7.0	S	20
		1006	9.0	F	20
		1091	7.2	F	20
		3385	8.3	T	20
		4602	9.3	S	15
		6506	7.5	F	10
xvi	33±1	163	9.0	T	20
		617	7.0	T	15
		1197	10.0	S	20
		5515	12.0	T	10
		6507	9.0	F	8
		6509	8.1	F	10
		6511	8.1	S	10
		6513	7.2	F	10
		6516	10.5	S	8
		6517	10.5	T	8
		6750	10.0	T	10
		7115	9.7	F	10
		7629	11.5	F	10
		7804	9.5	T	10
		7897	12.2	T	10
		8112	10.9	F	8
		8179	11.9	F	10
xvii	35±1	6258	14.0	T	10
		6519	10.8	S	8
		6631	13.0	F	10
		8118	12.6	F	10
xviii	37±1	1909	14.6	F	20
		4430	13.4	T	15
		6522	13.2	F	10
		6524	11.7	T	10
		6528	13.4	F	8
		6529	15.6	F	10
		6533	12.5	S	6, 8, 10
		8097	15.5	T	10
		8235	14.0	S	10
xix	39±1	409	18.0	T	20
		1390	18.0	S	20
		5609	18.0	F	25
		6824	18.5	S	12
xx	41±1	431	19.0	S	20
		4059	21.6	F	15
		6202	21.0	S	20
		6426	21.5	T	20
		8157	20.8	F	20
xxi	43±1	4960	22.0	T	15
		7254	22.5	T	20
		7392	22.7	T	20
		8553	22.0	T	12
xxii	45±1	4304	25.0	T	20
		4339	24.5	T	15
		6701	24.0	F	20
		8394	25.3	T	20
xxiii	47±1	4289	32.2	T	15, 20
		4525	30.0	S	20
		4570	30.7	T	15
		5154	32.0	T	20
		5725	23.0	F	25
		7425	27.0	F	20
Unclassified	ca. 9 weeks	5017	32.2	S	40
Unclassified	ca. 9 weeks	9226	31.0	T	10

---

* Number of somites given in parentheses.

† T, transverse; F, frontal; S, sagittal.

paramount importance in ascertaining the origin of the oculomotor eyeball musculature.

The prechordal plate is a median mass of cells, located at the anterior end of the notochord; it appears in early embryos as an integral part of the roof of the foregut.[3] From it, prechordal mesoderm is proliferated laterally. According to Adelmann (1922), it is to be regarded as "an essentially mesodermal structure" which participates in the marked bilateral growth of the embryonic head. "The extent to which this bilateral growth occurs and the stage of development at which it is initiated," Adelmann believes, "probably differs to some extent in different forms, and this may account for the variations in the extent to which the prechordal plate is developed in various forms. Marked bilateral growth occurring early in development would cause a less noticeable medial accumulation of material anterior to the notochord. This may possibly account for the poorly developed prechordal plate which has been described in mammals."

The prechordal or prochordal plate has been described by Heuser (1932) in a presomite human embryo (no. 5960) having an ovulation age of approximately 18 days. Traced forward from the anterior end of the notochord, the plate, according to Heuser, "is found to gradually increase in thickness until in its middle portion as many as eight rows of nuclei can be counted. However, the dorsal surface is very irregular, since cells are being given off to the surrounding tissue and some of them should no doubt be classified as mesodermal cells." One would surmise, therefore, that the prechordal plate has, at this early stage, already begun to proliferate prechordal mesoderm. Heuser further noted that the plate "becomes thinner and broader in the anterior part; in the first six sections it is composed of two layers of cells. The front end of the prochordal [prechordal] plate can be definitely located in section 205, since in front of it the entoderm abruptly changes to a layer of one cell thick. Sections through the plate, especially in its middle portion, show irregular outlines with bulgings from the ventral surfaces into the cavity of the yolk-sac. Ridges and grooves thus appear on the ventral surface of the plate."

Until more material is available that is sectioned and stained to show the prechordal plate clearly, it will not be possible to follow in detail its cytological development in the human embryo. Glimpses of what is going on in this area may be obtained, however, by examining the prechordal region of human embryos ranging from 7 to 20 somites.

In a 7-somite human embryo (no. 4216), the youngest examined in this study, the neural folds have met in the region between somites 3 and 7; otherwise, the central nervous system is widely open dorsally, and the trough-like brain has differentiated into three primary divisions. The head is slightly bent in the region of the midbrain so that the forebrain is directed toward the yolk sac. The optic sulcus is just beginning to form, and traces of the otic plate can be seen. The heart, the dorsal aorta, and the first pair of aortic arches have appeared. Only in the region immediately ahead of the primitive streak does the notochord exist as an independent structure, lying between the floor of the neural tube and the endoderm of the gut roof. Anterior to this region the notochord appears as a thickened plate of cells on the dorsal wall of the gut.

The prechordal plate of this 7-somite embryo was first noted by Payne (1925), who described it as "a thickened mass of cells continuous dorsally and posteriorly with the notochord, and extending caudally along the ventral surface of the gut for a short distance. Dorsally, it is in contact with the ectoderm of the neural groove but is not fused with it." The author has verified the presence of this mass of cells, 15 to 20 in number, and is in full agreement with Payne's interpretation. The structure Payne describes corresponds closely to the prechordal plate from which prechordal mesoderm is proliferated in slightly older embryos.

As development proceeds, the cephalic flexure in the region of the midbrain becomes more and more pronounced, so that, in embryos with 10 to 13 somites, the long axis of the forebrain forms a right angle with that of the hindbrain. Concomitantly with the bending of the brain, the prechordal portion of the roof of the foregut in contact with the brain is bent ventrally, the prechordal plate becoming vertical in the process. Transections through this region of the head are, therefore, most unfavorable for observing the prechordal plate at this stage, since it appears in only one or two sections between the ventral (now posteriorly directed) floor of the forebrain and the lumen (originally dorsal) of the foregut. This is probably one reason why the prechordal plate of young mammalian embryos has so often been overlooked. In the 10-somite embryo (no. 5074), for example, the prechordal plate appears in two 10-micron sections only, crowded in between the floor of the forebrain and the anterior wall of the foregut (fig. 3, pl. 1). Posteriorly, the prechordal plate is continuous with the notochord, which is still embedded in the roof of the gut throughout most of its length. At this stage, the prechordal plate consists of about 35 to 40 cells. These cells can be clearly delimited from the forebrain anteriorly, but not from the cells that will ultimately line the roof of the foregut. Determination of the caudal limit of the prechordal plate is also difficult, for the cells blend imperceptibly with the tip of the notochord.

---

[3] Several investigators have confused the prechordal plate with an extensive area of endoderm (and mesoderm?), known as the protochordal plate, located at the anterior end of the notochord of early embryos which develop from yolk-rich eggs or eggs which behave as if they were yolk-rich. Some workers have employed the term prochordal plate for protochordal plate, whereas others have used it in a more restricted sense as a synonym for prechordal plate. A discussion of the difference between prechordal, prochordal, and protochordal plate lies beyond the scope of this paper; the subject has been treated by Parker (1917), Hill and Tribe (1924), and Adelmann (1922, 1926).

With its expansion restricted by the floor of the forebrain, the prechordal plate, of necessity, can proliferate prechordal mesoderm only laterally over the "knee" of each aorta. For a short time the prechordal mesoderm appears as a thin lamina of cells anterior to the first aortic arch of each side. As more and more prechordal mesoderm is proliferated, it forms a globular mass of cells cranial and lateral to the "knee" of each aorta. These masses of prechordal mesoderm are known as the premandibular condensations; they abut against the maxillomandibular mesoderm laterally, and from the beginning are connected with each other across the mid-line by a thin lamina or bridge of mesodermal cells of prechordal-plate origin. The development of the premandibular condensations in the human embryo is illustrated schematically in figure 1.

A pair of small premandibular condensations first appears in human embryos of 14 somites between the "knee" of the aorta and the floor of the forebrain (fig. 6, pl. 1). As development proceeds, and an internal carotid artery grows forward from the "knee" of each aorta, the premandibular condensations, connected by a narrow bridge of prechordal mesoderm, increase in size and occupy a position above and external to each internal carotid artery. By the 19-somite stage (figs. 7, 8, pl. 1), each premandibular condensation is well developed and occupies a position adjacent and lateral to the internal carotid artery, and somewhat above and medial to the optic vesicle. Laterally, the premandibular condensations abut against, and almost imperceptibly blend with, the maxillomandibular mesoderm; medially, they remain joined across the mid-line by a solid transverse bridge of cells.

In the stage that immediately follows (20 to 30 somites), lateral expansion of the head in this region continues, and the premandibular condensations enlarge. During this period of rapid growth of the head as a whole, small epithelium-lined spaces, the head cavities, appear in the premandibular condensations. It is remarkable that, of all the placental mammals that have been thus far studied, man is the only one in which premandibular head cavities have been found. Their origin, structure, and fate in the human embryo are, therefore, of special interest.

In this study, head cavities were observed in a total of ten human embryos belonging to horizons xii, xiii, and xiv (table 2). Nine of the embryos belong to horizon xii or xiii and range in size from 24 somites to 5.2 mm.[4] An embryo of 28 somites (no. 7999), belonging to horizon xii, about 26 days of age, may be considered as representative. In this embryo (figs. 32, 33, pl. 8), three small cavities appear in the premandibular condensation of the right side, and one somewhat larger head cavity is located in the left premandibular condensation. The lumen of this last cavity is about equal in diameter to the height of the single layer of columnar epithelial cells surrounding it, and occupies a position in the premandibular condensation about 40 microns above the internal carotid artery. The entire head cavity, including its wall of radially arranged columnar epithelial cells, measures about 40 microns by 45 microns, and is only slightly greater in diameter than that of the internal carotid artery at this level. The three head cavities located along the upper cranial border of the right premandibular condensation of embryo no. 7999 are arranged in an oblique row which parallels the floor of the forebrain. The most caudal and medial of the three head cavities on this side has the largest lumen, and, like its somewhat larger fellow on the left, is situated about 40 microns above the internal carotid artery.

In certain embryos, for example no. 7724, the ventral wall of a head cavity may actually abut against the dorsal wall of the internal carotid artery (fig. 27, pl. 7). In others, for example no. 8239, a small head cavity is found some distance (about 30 microns) medial to the internal carotid artery in the tapered medial end of the premandibular condensation near its junction with the bridge. For the most part, however, head cavities, when present, are situated in the premandibular condensation above or lateral to the level of the internal carotid artery. A glance at table 2 reveals no uniformity in their location or number, and they have been as frequently encountered on the right side of the head as on the left.

The head cavities in the human embryo are never as large as those in many reptiles and birds. They resemble very closely, however, early stages in the development of these structures in both the turtle and the chick; that is, they appear as small isolated lumina, lined with cuboidal or columnar epithelium, in the premandibular condensations. In reptiles and some birds, it will be recalled, the separate lumina eventually coalesce to form one or more larger cavities on each side, from the walls of which the oculomotor eyeball muscles presently arise. But, in man, no such fusion of separate lumina to form a large single cavity has been observed.

It cannot yet be stated whether head cavities develop in the premandibular condensations of all human embryos. Certainly many of the embryos belonging to horizons xii and xiii in the Carnegie Collection do not possess them. Although it is possible that these embryos never did have, or never would have developed, head cavities, it is more likely that cavities do form with some regularity in embryos of horizons xii and xiii, last but a few hours, and then become crowded out by the rapid multiplication of cells in the premandibular condensations. It is probable, therefore, that the head cavities vanish as suddenly as they appear, and by the time the human embryo reaches its 30th day no trace of these transient structures can be found.

---

[4] Two of these embryos were not mentioned by Gilbert (1952), for they were added to the collection in 1954. They are nos. 8505A (24 somites) and 8581 (4.8 mm.).

TABLE 2

Human embryos of the Carnegie Collection demonstrating head cavities

Horizon	Embryo no.	Size of embryo	Plane of section *	Head cavities, right	Head cavities, left	Total head cavities	Slide, row, section
xii	4736	26 som.	F	1	2	3	2-5-3, 4, 5, 6, 7
xii	6097	25 som.	T	0	1	1	1-4-2
xii	7724	ca. 29 som.	S	1	4	5	2-1-6, 8, 12; 2-3-11, 12
xii	7999	ca. 28 som.	T	3	1	4	2-1-11, 12
xii	8505A	24 som.	T	0	1	1	2-7-8; 3-1-1
xiii	463	3.9 mm.	F	1	0	1	5-2-5, 6, 7
xiii	7433	5.2 mm.	F	3	1	4	2-3-15; 3-1-1, 2
xiii	8239	4.3 mm.	S	1	1	2	2-3-7; 3-1-8
xiii	8581	4.8 mm.	S	1	1	2	1-6-4; 2-4-4
xiv	6830	5.5 mm.	F	1	0	1	4-3-1, 2, 3

* F, frontal; S, sagittal; T, transverse.

THE MAXILLOMANDIBULAR MESODERM

In embryos belonging to horizon xi, a diffuse mass of mesenchymal cells, situated just beneath the surface ectoderm at the upper end of the mandibular arch and maxillary process, can be distinguished. For convenience, this mass is referred to as the maxillomandibular mesoderm. Part of its medial surface adjoins the developing premandibular condensation; anteriorly, it crowds against the optic vesicle, and ventrally it is continuous with the somewhat denser mesoderm of the mandibular arch. At this stage a prominent cephalic flexure exists in the region of the midbrain, so that the forebrain forms an angle of about 90° with that of the hindbrain. It is important to bear in mind that at this time the maxillomandibular mesoderm crowds against the caudal surface of the optic vesicle that is evaginating from the cephalic end of the forebrain. As development proceeds (horizon xii), the cephalic flexure becomes more prominent, and the angle formed by the long axis of the forebrain with that of the hindbrain becomes more acute (see Streeter, 1942, p. 241, fig. 7). During this period the maxillomandibular mesoderm becomes more compact; because of the ventral rotation of the forebrain, its cranial end now lies adjacent to the dorsocaudal surface of the optic vesicle (figs. 30, 31, pl. 7).

The cephalic flexure continues to increase in prominence in embryos of horizon xiii; from the dorsocranial border of the maxillomandibular mesoderm an arm of cells extends forward over the optic vesicle. Since the head is expanding rapidly in this region, the arm of maxillomandibular mesoderm above the optic vesicle keeps pace and moves laterally as well as cranially. The caudal portion of the maxillomandibular mesoderm, lying in a region expanding less rapidly, curves, therefore, into a plane lying medial to its cranially directed arm. The position of the maxillomandibular mesoderm relative to the optic vesicle and premandibular condensation at this stage is illustrated schematically in figure 1.

In embryos belonging to late horizon xiii, a condensation appears in the caudal and more medial portion of the maxillomandibular mesoderm, medial to the Gasserian ganglion and vena capitis medialis. A homologous condensation found in cat embryos at a comparable stage of development has been termed the VIth condensation, and from it arise the retractor bulbi and lateral rectus muscles, both innervated by cranial nerve VI. Since man lacks a retractor bulbi muscle, this condensation in the human embryo will be referred to as the lateral rectus primordium. Anteriorly, this condensation abuts against the premandibular condensation, and at later stages is very difficult to delimit from it.

Shortly after the primordium of the lateral rectus becomes established, a second condensation appears in the maxillomandibular mesoderm. This condensation, the primordium of the superior oblique, is first observed in embryos of horizon xiv in the cranial arm of maxillomandibular mesoderm that has extended forward above the eye. It is somewhat smaller and less dense than the lateral rectus primordium, and occupies a position between the vena cerebralis anterior and the dorsocranial surface of the optic cup. Situated between the Gasserian ganglion and optic cup, and lateral to the bifurcation in the vena capitis medialis, a more diffuse mass of mesodermal cells connects the condensations for the superior oblique and lateral rectus muscles. This mass of cells, which Fraser (1915) has termed the "intermediate mass" in *Trichosurus* and Adelmann (1927) the "intermediate region" in the chick, abuts medially against the premandibular condensation and is continuous ventrally with the denser mesoderm of the mandibular arch. These relations are illustrated schematically in figures 1 and 2.

While the superior oblique and lateral rectus primordia are increasing in density, the intermediate mass adjacent to the caudal surface of the optic cup spreads forward above and below the outer margin of the eye, beneath the surface ectoderm. In this mesoderm around the periphery of the optic cup there appear in older embryos, belonging to horizon xiv, four faint condensations, each approximately equal in diameter to that of the lens vesicle, which is in the process of invagination. These peripheral condensations, first described by the author (Gilbert, 1947) in the cat, and termed the superior, anterior, inferior, and posterior peripheral condensations, are believed to contribute to the formation of the scleral coat of the eye, and they mark the points of insertion on the sclera of the four rectus muscles which, at a later period, grow out into them. The peripheral condensations in the human embryo are less dense than in the cat, and are most readily observed in parasagittal sections through the eye in embryos belonging to horizons xv, xvi, and xvii. The position of the four condensations relative to the eye and the superior oblique primordium, in embryos of horizons xv and xvi, is illustrated in figures 2, 52 (pl. 11), and 53 (pl. 11). Because of the lack of material suitably sectioned and the lack of density of those condensations in the human embryo, their fate could not be followed as clearly as it was in the cat. However, since in the time of their appearance and in their location relative to the periphery of the optic cup they agree with the similar condensations found in the cat, we may assume that they probably have the same fate.

Before discussing the subsequent development of the lateral rectus and superior oblique muscles, the relation of these two eye-muscle primordia to the premandibular condensation (from which the oculomotor eyeball muscles develop) in the human embryo and in other vertebrates deserves comment. There is a striking similarity in these three separate and distinct eyeball-muscle primordia at this stage of development (lens vesicle invaginating and closing off or closed off from surface ectoderm) in mammals, birds, reptiles, and elasmobranchs. The premandibular condensations of the mammal are directly comparable to the premandibular head cavities of birds, reptiles, and elasmobranchs. In all groups, a solid transverse band or hollow cross canal at first connects the premandibular condensation or cavity of the right side with its fellow on the left. This transverse connection passes above the internal carotid arteries and across the confined area between the cranial tip of the notochord and the floor of the forebrain. The maxillomandibular mesoderm, exclusive of the lateral rectus primordium, is similar with respect to location and fate to the mandibular head cavity or homologous condensation of birds,[5] reptiles, and elasmobranchs. Finally, the VIth condensation of the cat or lateral rectus primordium of man has its counterpart in the hyoid cavity or condensation in the embryonic head of lower vertebrates. In both cat and man, this eyeball-muscle primordium, in its relations to the eye, first pharyngeal pouch, Gasserian ganglion, superior oblique primordium, and premandibular condensation, bears a conspicuous resemblance to the hyoid condensation of birds and the hyoid head cavity of reptiles and elasmobranchs.

THE DEVELOPMENT OF THE LATERAL RECTUS

The earliest primordium of the lateral rectus, it will be recalled, is situated caudal and slightly dorsal to the premandibular condensation and medial to the maxillary division of the Gasserian ganglion in embryos belonging to horizon xiii. Although poorly defined in embryos of this horizon, the lateral rectus condensation quickly increases in density, and in several embryos of horizon xiv it is easily recognized. Its shape is roughly ovoid; its long axis extends cephalocaudally; and its total volume is approximately one-third that of the premandibular condensation. As development proceeds (horizon xv), the lateral rectus condensation, while retaining its confluence with the intermediate mass of the maxillomandibular mesoderm, increases in density and size as it swings craniolaterally across the dorsocaudal surface of the premandibular condensation, through the fork in the vena capitis medialis formed by its bifurcation into the vena cerebralis anterior and the vena orbitalis inferior. The abducens nerve, which has emerged by several rootlets from the floor of the hindbrain, extends forward ventrally and laterally, and penetrates the dorsocaudal surface of the lateral rectus condensation. The ophthalmic nerve has, in the meantime, become conspicuous above, and cranial to, the distal end of the lateral rectus condensation; the maxillary nerve now extends ventrally behind the distal end of the condensation into the maxillary process. Medially, a portion of the lateral rectus condensation appears to be confluent with the premandibular condensation, and, were it not for the fact that the oculomotor nerve, which has grown ventrally from the midbrain, now passes between the premandibular and lateral

[5] Variation exists among vertebrates as to which end of the superior oblique primordium grows medially and eventually attaches to the orbital wall. In *Chelydra* (Johnson, 1913), the cranial end of the superior oblique primordium swings medially during development and eventually attaches to the orbital wall. On the other hand, in *Torpedo* (Wedin, 1949), chick (Adelmann, 1927), *Ardeá* (Wedin, 1953*b*), *Trichosurus* (Fraser, 1915), cat (Gilbert, 1947), and man, the caudal end of the superior oblique primordium grows medially to gain insertion on the wall of the orbit, whereas the cranial end eventually inserts on the sclera.

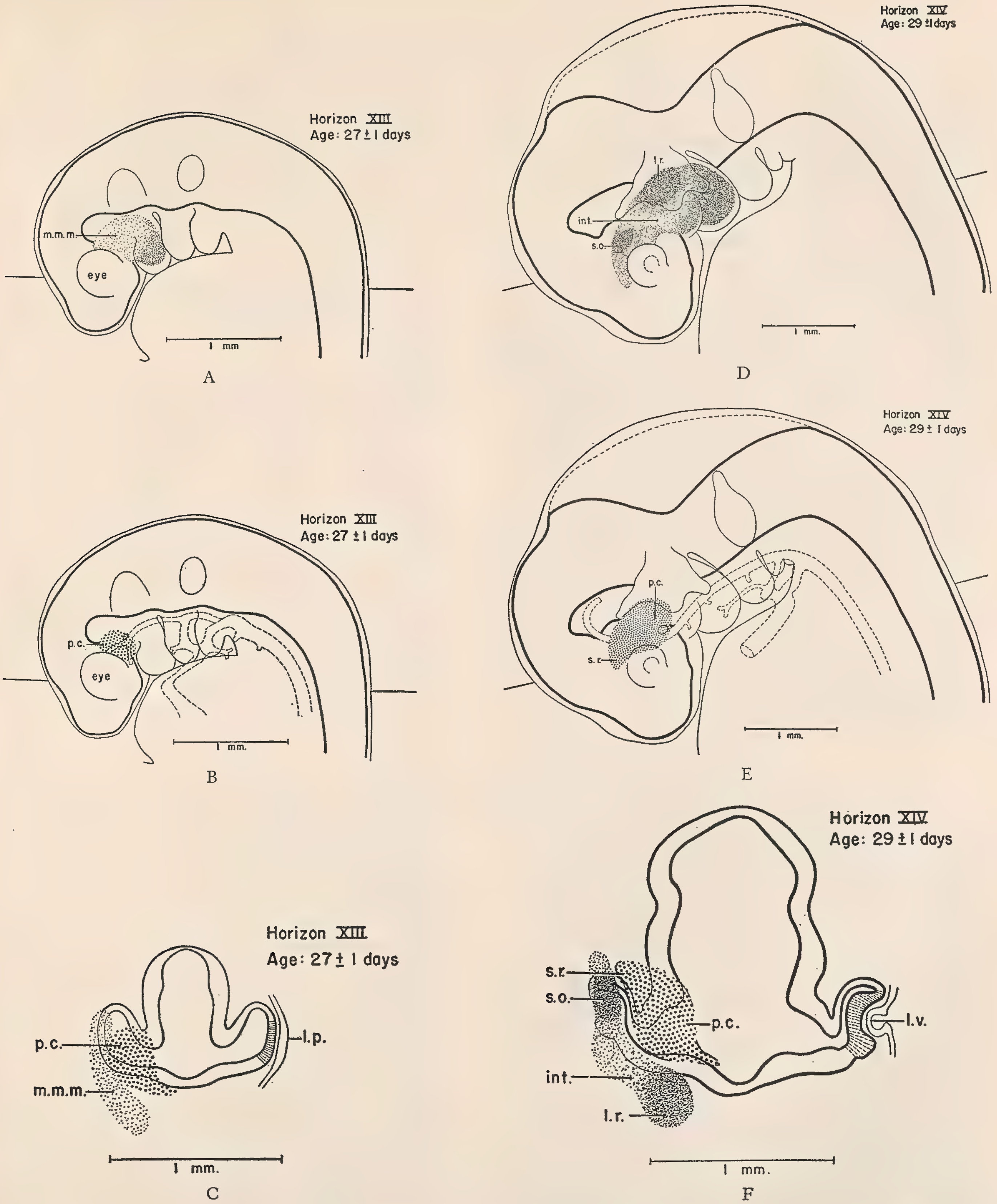

FIG. 1. Diagrams, based on reconstructions of embryos of horizons xiii and xiv, illustrating the relations of the maxillomandibular mesoderm (figs. A, D) and the premandibular condensation (figs. B, E) to the brain, eye vesicle, Gasserian ganglion, and mandibular arch. Figures C and F represent transections through the brain of embryos of horizons xiii and xiv respectively at the levels indicated in figures A and D; the maxillomandibular mesoderm and premandibular condensation have been superimposed on the left side; the developing eye is illustrated on the right side of each transection.

In embryos of horizon xiii a prominent pear-shaped premandibular condensation (*p. c.*) is situated dorsal and caudal to the medial surface of each optic vesicle and is in contact laterally with the maxillomandibular mesoderm (*m. m. m.*). The rapid expansion of the head anterior to the end of the foregut, in embryos of horizons xi and xii, is reflected not only in the growth of the premandibular condensations but also in the lateral movement of the maxillomandibular mesoderm above the expanding optic vesicles, so that in embryos of horizon xiii the caudal portion of the maxillomandibular mesoderm, situated in a region which has expanded less rapidly, lies in a plane some distance medial to its cranial portion above the eye.

In embryos of horizon xiv, a small process, the primordium of the superior rectus (*s. r.*), extends forward and outward from the dorsolateral border of the premandibular condensation. The primordium of the superior oblique (*s. o.*) and that of the lateral rectus (*l. r.*) have appeared as condensations in the cranial and caudal portions of the maxillomandibular mesoderm respectively, and are connected by a more diffuse area of maxillomandibular mesoderm known as the intermediate mass (*int.*).

rectus condensations, it would be difficult, if not impossible, to distinguish one condensation from the other. It is not surprising, therefore, that earlier investigators, when examining embryos of this and older stages, failed to distinguish the two condensations and believed them to be one.

In embryo no. 3385, a typical representative of horizon xv, the lateral rectus condensation is well defined, and its relation to the premandibular condensation, principal nerves, and blood vessels of the head is readily ascertained. The caudal and more medial end of the condensation is situated midway between the internal carotid artery and that portion of the vena capitis medialis which lies adjacent and medial to the root of the maxillary nerve. A few sections cranial to its caudal end, the lateral rectus condensation receives the abducens nerve, and from this point proceeds cranially and laterally along the dorsocaudal face of the premandibular condensation, from which it is separated for a short distance by the oculomotor nerve, and thence laterally in front of the fork in the vena capitis medialis into the diffuse "intermediate mass" of maxillomandibular mesoderm. To what extent this mass, situated between the roots of the ophthalmic and maxillary nerves, participates in forming the distal end of the lateral rectus is difficult to ascertain. At horizon xv the "intermediate mass" is less dense than the medial portion of the lateral rectus condensation, and is so situated that the lateral rectus condensation would have to grow through it in the next few days, or receive a contribution from it, before reaching the eyeball. In the cat, it was concluded that the latter phenomenon takes place, and, from the limited material at hand for horizon xv, it appears probable that the "intermediate mass" makes some contribution to the distal end of the lateral rectus in man also.

By horizon xvi, the lateral rectus condensation is sufficiently dense to be traced from its caudomedial extremity forward and laterally in front of the fork in the vena capitis medialis to the posterior peripheral condensation on the outer margin of the optic cup (figs. 47–50, pl. 10). The relation of the lateral rectus condensation at subsequent stages (horizons xvii, xix, xxiii) to the other eye-muscle primordia, the eyeball, and the ophthalmic and maxillary nerves is illustrated in plates 4, 5, and 6. The lateral rectus has a well defined insertion in embryos of horizon xix, and its proximal (origin) end becomes clearly separated from the other extrinsic ocular muscles in embryos of horizon xx. Muscle fibers appear in the lateral rectus condensation as early as horizon xx; Bartelmez (personal communication) has recently found, in teased preparations of this muscle, that Q, J, and Z lines are present in the myofibrillae of a 25-mm. embryo (no. 5635) belonging to horizon xxii.

THE DEVELOPMENT OF THE SUPERIOR OBLIQUE

The superior oblique primordium, it will be recalled, appears first as a condensation in an arm of maxillomandibular mesoderm extending from the upper end of the mandibular arch forward over the dorsal surface of the optic vesicle, close to the surface ectoderm. The condensation is first visible slightly dorsal and medial to the superior peripheral condensation in older embryos of horizon xiv (fig. 1). At this stage the superior oblique condensation is less dense and somewhat smaller than the lateral rectus primordium, and considerably smaller than the premandibular condensation. The ophthalmic nerve lies close to the superior oblique condensation, if not actually embedded in it.

During the next 6 days (horizons xv to xvii), the head continues to expand rapidly, the ophthalmic nerve divides into frontal and nasociliary branches, the optic stalk lengthens, and the optic vesicle increases markedly in diameter. Concomitantly with the enlargement of the optic vesicle, and possibly as a result of it, the caudal end of the superior oblique primordium shifts medially, retaining an intimate association with the frontal branch of the ophthalmic. In an embryo of horizon xvii (no. 6258), the superior oblique primordium has become more elongated and is crescentic (fig. 16, pl. 4). Its center lies medial and cranial to the superior peripheral condensation, and its cranial (insertion) end bends downward and backward (in the region of the future trochlea), almost touching the periphery of the optic vesicle between the superior and anterior peripheral condensations. The caudal end of the superior oblique primordium is situated in a plane medial to that of its cranial end, and is penetrated by the trochlear nerve, the last of the eye-muscle nerves to appear, at a point immediately ventral and lateral to the vena cerebralis anterior.

The relation of the frontal branch of the ophthalmic to the superior oblique primordium is of interest at this stage. As the caudal end of the superior oblique condensation moves medially, it passes obliquely above the frontal nerve. More anteriorly, the frontal nerve still retains intimate contact with the ventral surface of the superior oblique, and emerges lateral to it in the region where the trochlea will presently form. The caudal half of the superior oblique condensation, therefore, "pivots" medially on the dorsal surface of the frontal nerve.

Four days later (horizon xix, no. 5609), the caudal end of the superior oblique primordium has grown much farther medially and caudally, practically reaching the point where it will ultimately become attached to the orbital wall (fig. 20, pl. 5). The progressive growth medially of the caudal portion of the superior oblique primordium, especially pronounced in embryos of horizons xix and xx, is shown in table 3 for a series of representative sagittally sectioned embryos belonging to horizons xvi to xx. In each case, the number of sections in which a portion of the superior oblique primordium appears has been counted and multiplied by the thickness of the section to give the lateromedial (transverse) extent of the condensation. The frontal division of the ophthalmic nerve now lies dorsal to that portion of the superior oblique about which the trochlea will soon form; the nasociliary division lies ventral to it.

TABLE 3

Transverse extent of superior oblique primordium

Horizon	Embryo	Length of embryo (mm.)	Transverse extent of superior oblique (microns)
xvi	1197	10.0	160
xvii	6519	10.8	224
xviii	6533	12.5	300
xix	1390	18.0	640
xx	431	19.0	880

By the time the human embryo is 42 days old (horizon xx), striated fibers are recognizable in the superior oblique muscle, which extends from its narrow tendon of origin on the anterior margin of the optic foramen forward along the dorsomedial wall of the orbit, terminating anteriorly in a round tendon which, after passing through the developing trochlea (figs. 73, 74, pl. 14), is deflected ventrally, laterally, and caudally beneath the superior rectus to its insertion on the sclera on the equator of the eyeball. The frontal nerve at this stage extends forward midway between the bellies of the superior oblique and levator palpebrae superioris muscles. As the two eyes move forward, the frontal nerve comes to lie directly above the levator palpebrae superioris. During this period, the angle formed by the proximal and distal portions of the superior oblique tendon at the trochlea (trochlear angle) becomes more acute.

It is interesting that the trochlear angle appears in the superior oblique condensation as early as horizon xvii, and in a sense anticipates the formation of a trochlea which does not become evident until 5 or 6 days later (horizon xx). From the beginning, the trochlear angle is obtuse; even in an embryo of horizon xix, just before the trochlea appears, it is about 120°. After the U-shaped trochlea forms about the superior oblique tendon and becomes attached to the developing frontal bone near the anterior margin of the orbit, the trochlear angle becomes progressively more acute. This increase in the acuity is probably the result of the forward growth of the portion of the frontal bone to which the trochlea is attached. Thus the trochlear angle, which was about 120° in horizon xix, becomes about 95° in horizon xxii (fig. 75, pl. 14), about 80° in horizon xxiii (fig. 24, pl. 6), and about 55° in adult man.

THE FATE OF THE PREMANDIBULAR CONDENSATIONS

The early history of the premandibular condensations and the development of small, transitory, epithelium-lined head cavities within them, in embryos belonging to horizons xii to xiv, has already been sketched. Each condensation is formed from mesodermal cells proliferated laterally from the prechordal plate; as the head expands, each condensation, which from the beginning is connected with its fellow by a solid transverse bridge of mesoderm, rapidly enlarges. In early embryos belonging to horizon xiv, each pear-shaped premandibular condensation is well developed and anteriorly almost reaches the caudomedial surface of the optic vesicle, its tapered medial end passing above the internal carotid artery; caudally, it is in contact with, and difficult to delimit from, the primordium of the lateral rectus. At this time the premandibular condensations are about twice the size of the lateral rectus primordium (described above) and are still connected across the mid-line by a rather tenuous transverse bridge of mesodermal cells which, in the mid-plane, is in contact with the cranial tip of the notochord.

In older embryos of horizon xiv, the middle of the transverse bridge ruptures, and the two premandibular condensations are no longer connected. During this period, when the lens vesicle is invaginating, a small bud of mesodermal cells (the primordium of the superior rectus) appears on the dorsolateral portion of the premandibular condensation, and extends forward and laterally toward the upper surface of the optic vesicle to the level of the fork in the vena capitis medialis (fig. 35, pl. 8).

During the next 2 days (horizon xv), the lens vesicle closes off from the surface ectoderm, and cranial nerve III and the frontal branch of the ophthalmic nerve appear. The superior rectus primordium is closely apposed to the caudomedial surface of the superior oblique condensation, from which it may with some difficulty be distinguished, since the frontal nerve usually passes between these two condensations. In slightly older embryos (horizon xvi), the superior rectus primordium extends cranially and laterally as a rather dense arm of cells and establishes a diffuse connection with the superior peripheral condensation. Proximally, the frontal branch of the ophthalmic nerve passes above the superior rectus primordium, and the nasociliary branch passes below it near its junction with the parent premandibular condensation. The oculomotor nerve has grown down between the caudal face of the premandibular condensation and the cranial border of the lateral rectus primordium (now supplied by the abducens nerve), and is

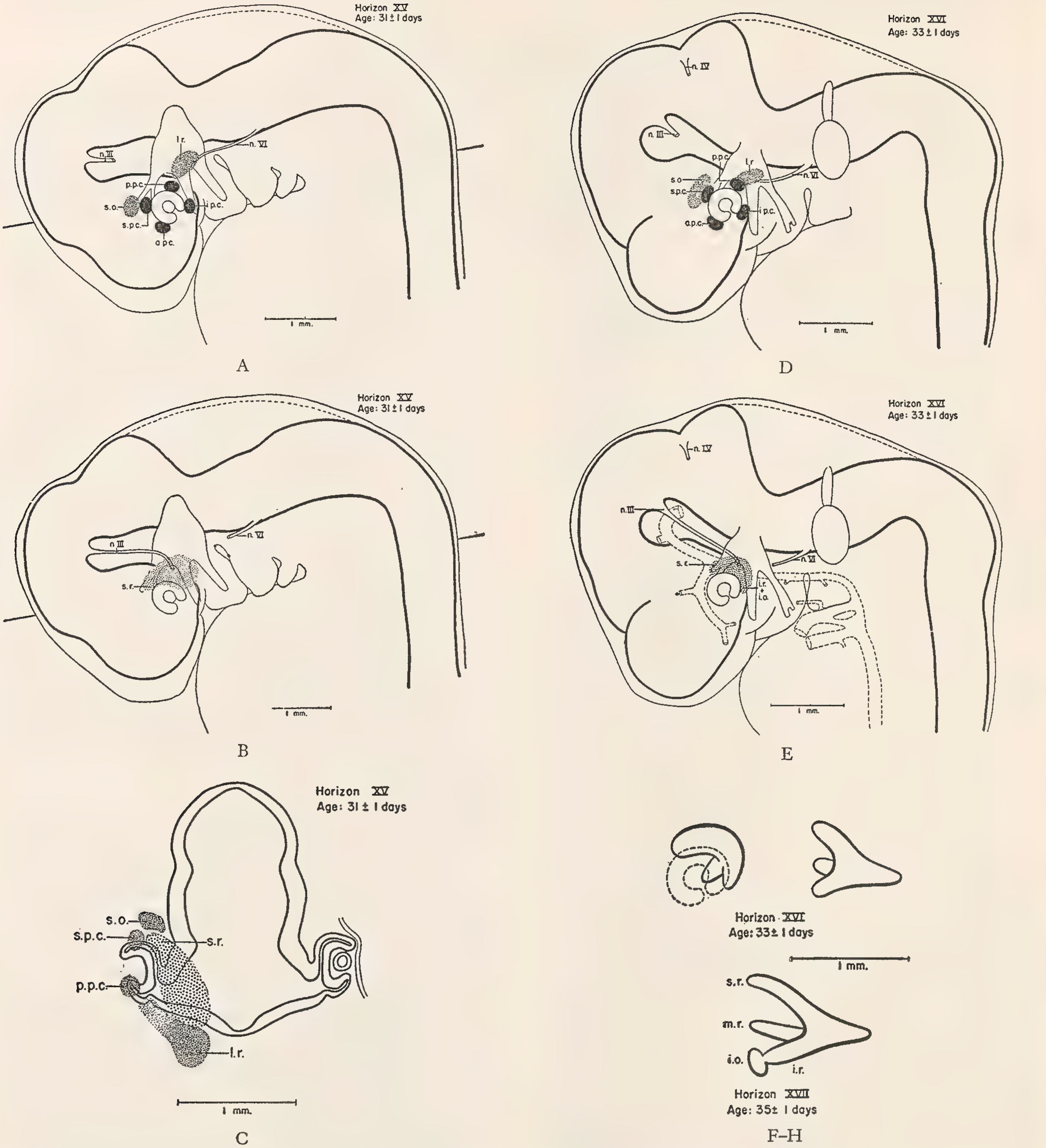

FIG. 2. Diagrams, based on reconstructions of embryos of horizons xv, xvi, and xvii, illustrating the relations of the derivatives of the maxillomandibular mesoderm (figs. A, D) and the premandibular condensation (figs. B, E) to the brain, eye vesicle, Gasserian ganglion, and mandibular arch. Figure C represents a transection through the brain of an embryo of horizon xv at the level indicated in figure A. The derivatives of the maxillomandibular mesoderm and the premandibular condensation have been superimposed on the left side; the developing eye is illustrated on the right side of the transection.

In addition to the superior oblique and the lateral rectus primordia, four other condensations appear in embryos of horizon xv in the maxillomandibular mesoderm. These condensations, situated around the outer rim of the optic vesicle (figs. A, B, C), are known as the superior (*s. p. c.*), inferior (*i. p. c.*), anterior (*a. p. c.*), and posterior (*p. p. c.*) peripheral condensations, and they anticipate in a sense the insertion points of the four rectus muscles on the eyeball and probably contribute to the formation of the sclera. At this stage, cranial nerves III and VI have grown from the brain into their respective eye-muscle primordia; the lens vesicle has pinched off from the surface ectoderm.

In embryos of horizon xvi (figs. D–G), the superior oblique and lateral rectus condensations have elongated, and, in addition to the superior rectus, two other processes, the primordium of the medial rectus (*m. r.*) and the common primordium of the inferior rectus and inferior oblique (*i. r.+i. o.*), project laterally from the premandibular condensation. In figures F and G, the premandibular condensation and associated eye-muscle primordia, illustrated in figure E, are viewed from lateral and caudal aspects, respectively. A distinct inferior oblique primordium first appears in embryos of horizon xvii (fig. H), and remains intimately attached for some time to the distal end of the inferior rectus.

of considerable assistance in delimiting these two intimately associated condensations. In fact, were it not for our knowledge of the early independent origins of these two condensations, it would be extremely difficult to separate them at this time, and one might easily, as did Lewis (1910), erroneously consider them to be one.

The superior rectus continues to increase in density, and in embryos of horizon xvii (fig. 16, pl. 4) establishes a firm connection with the superior peripheral condensation. Although the superior rectus is not yet clearly delimited from the premandibular condensation proximally, it is supplied by a branch of the oculomotor nerve. By the time the embryo attains a crown-rump length of 19 to 20 mm. (horizon xx), muscle fibers appear in the superior rectus; its insertion on that portion of the sclera formerly occupied by the superior peripheral condensation is clearly defined; and its attachment medially to the developing sphenoid bone immediately above the optic foramen now closely adjoins that of the lateral rectus. It will be recalled that in the adult all four rectus muscles attach to a funnel-shaped tendinous ring, known as the annulus of Zinn, which encloses the optic foramen.

In embryos of horizons xxii and xxiii, a thin muscular sheet, the levator palpebrae superioris, splits off from the dorsomedial surface of the superior rectus and grows forward into the upper eyelid. The levator palpebrae superioris in an embryo of horizon xxiii (figs. 23, 24, pl. 6; fig. 72, pl. 13) is situated adjacent and lateral to the frontal nerve and immediately above and slightly medial to the belly of the superior rectus. As the eyes move forward, the frontal nerve ultimately comes to lie above the levator palpebrae superioris, which in turn comes to occupy a position immediately above the superior rectus.

In older embryos of horizon xv, while the superior rectus is growing forward toward the superior peripheral condensation, a broad bulge develops on the ventrolateral surface of the premandibular condensation and extends laterally as far as the fork in the vena capitis medialis. Presently, in embryos of horizon xvi, two buds appear on the outer surface of the bulge. The more cranial bud, the primordium of the medial rectus, at first consists of a small, diffuse cluster of cells projecting craniolaterally for two or three 10-micron sections. It soon increases in density, and stretches forward beneath the optic stalk toward the anterior peripheral condensation on the outer margin of the optic vesicle. In embryo no. 6258 of horizon xvii, the medial rectus primordium has extended cranially and ventrolaterally until its distal end is continuous with the anterior peripheral condensation (figs. 16, 17, pl. 4). The nasociliary branch of the ophthalmic nerve passes immediately above and cranial to the point where the medial rectus joins its peripheral condensation. For some time the proximal end of the medial rectus is indistinguishable from the proximal ends of the other rectus muscles; it is not until horizon xix that a clearly defined origin for this muscle may be detected on the orbital wall. The medial rectus first receives a branch of the oculomotor nerve in embryos of horizon xix; muscle fibers are observable in this muscle soon thereafter (horizon xx).

The second and more caudal bud that develops on the bulging ventrolateral surface of the premandibular condensation in embryos of horizon xvi is destined to form the inferior rectus and inferior oblique muscles. From the beginning, the primordium of the inferior rectus is more dense and better defined than that of the medial rectus. It grows laterally, and in younger embryos of horizon xvii its distal end, which now nearly reaches the inferior peripheral condensation, becomes conspicuously expanded to form the primordium of the inferior oblique. At this stage, a branch of the oculomotor nerve extends along the primordium of the inferior rectus almost up to the inferior oblique condensation, if it does not actually enter it. Medially, ventrally, and caudally, the compact inferior oblique primordium is bounded by branches of the vena orbitalis inferior. Proximally, the inferior oblique condensation is continuous with that of the inferior rectus; in sagittally sectioned embryos, it is impossible to delimit the two primordia. In embryos sectioned frontally, however, the fate of the inferior oblique and inferior rectus condensations may be easily followed.

In older embryos of horizon xvii, the primordium of the inferior oblique has become ovoid, and its long axis is situated at approximately right angles to that of the inferior rectus (figs. 14, 17, pl. 4). The inferior rectus primordium has grown laterally between the inferior oblique and the optic cup to reach the inferior peripheral condensation. In embryos of horizons xviii and xix, the inferior oblique retains intimate contact with the inferior rectus primordium even after the latter has reached its peripheral condensation (fig. 65, pl. 12; figs. 68, 69, pl. 13); it is not until horizon xx, at which time the inferior oblique becomes attached to the eyeball, that all connection with the inferior rectus is lost. At this time a well defined branch of the oculomotor nerve can be traced to the inferior oblique; shortly thereafter (late horizon xx), muscle fibers appear in both the inferior oblique and inferior rectus, and separate attachments (origins) on the orbital wall are distinguishable. The inferior oblique becomes attached to the floor of the orbit near its outer medial rim, whereas the proximal end of the inferior rectus takes origin on the wall of the orbit immediately below the optic foramen, adjacent and caudal to the origin of the medial rectus.

DISCUSSION

There can be little doubt that the pattern of development of the extrinsic eye muscles of man is very similar to that of the cat, marsupials, birds, reptiles, and most, if not all, anamniotes. Although minor differences in detail do exist in the above groups, the extrinsic eye muscles uniformly arise on each side of the head from three well defined primordia. This, of course, runs counter to the conclusions of most investigators who have studied the development of these muscles in placental mammals. But, as was pointed out in the introduction, most investigators have failed to examine critically very young mammalian embryos, and have thus been misled by the condition in older embryos, in which the three pairs of extrinsic eye-muscle primordia have already reached a rather advanced stage of development and have become so intimately associated with one another that it is difficult to distinguish among them. At the time when Lewis (1910) worked on the development of the eyeball muscles of man, he was badly handicapped by the lack of carefully prepared younger stages (of horizons x to xiv), and thus could scarcely have distinguished separate primordia for the lateral rectus, superior oblique, and oculomotor muscles in a 7-mm. human embryo, the youngest he examined.

The present study has led to the conclusion that two of the eye-muscle primordia (superior oblique and lateral rectus) in man arise in the maxillomandibular mesoderm, and that the third primordium (the premandibular condensation), from which the four oculomotor eye muscles develop, arises from the prechordal plate.

The striking similarity in the relation of the three eye-muscle primordia in man to that observed in the chick, turtle, and shark deserves comment. This similarity is emphasized when figure 1 presented here for man is compared with Adelmann's (1927) text figure 2 for the chick, Johnson's (1913) figure 19 for the turtle, and Scammon's (1911) text figure 20 for the shark. The premandibular condensations of man are directly comparable to the premandibular head cavities of the chick, turtle, and shark, which in all these forms arise from a similar source, the prechordal plate. The maxillomandibular condensation of man, exclusive of the lateral rectus primordium, bears a striking resemblance to an equivalent portion of the maxillomandibular mesoderm in the chick and to the mandibular head cavity of the turtle and shark. Finally, the lateral rectus primordium of man closely resembles the primordium of the abducens musculature in the chick and the hyoid head cavity of the turtle and shark in its relation to the other eye-muscle primordia and to the first pharyngeal pouch.

In both man and the chick, the superior oblique primordium is continuous caudally with a more diffuse mesodermal condensation, the intermediate mass, which in turn is continuous caudomedially with the lateral rectus condensation (man) or the primordium of the abducens musculature (chick). The intermediate mass in man is believed to contribute to the distal (insertion) end of the lateral rectus, and to be, undoubtedly, homologous with "muscle E" of elasmobranchs, first described by Platt (1891). Platt noted that muscle E arises from the ventromedian wall of the mandibular head cavity and, after early reaching an advanced stage of development, rather quickly degenerates and disappears. Lamb (1902) confirmed Platt's conclusion concerning the fate of muscle E, but, like Platt, provided no convincing proof that muscle E degenerates. Johnson (1913) assumed that muscle E degenerates in the turtle, but he, also, supplied no proof for this assumption; Wedin (1953*a*) came to no decision concerning the fate of muscle E in the alligator. Fraser (1915) concluded that the intermediate mass "apparently" degenerates in marsupials.

On the other hand, Dohrn (1904) and Neal (1918) were of the opinion, now widely accepted, that in the shark the 2d head somite (mandibular head cavity) is divisible into two portions, a dorsal one from which the superior oblique is derived, and a ventral one (muscle E of Platt) which contributes to the distal end of the lateral rectus. Thus the lateral rectus muscle of the shark, according to the convincing evidence of Dohrn and Neal, has a dual origin, the proximal end being formed from the hyoid head cavity (3d somite), and the distal end from the ventral portion (muscle E) of the mandibular head cavity (2d somite). On this point, Neal (1918) wrote as follows:

> Of the disintegration or degeneration of the muscle cells of muscle E there is not the slightest evidence. On the contrary, in the stages during which degeneration has been said to occur, the embryonic muscle cells of both elements of the external [lateral] rectus muscle undergo similar progressive differentiation as elongated spindle-shaped muscle fibers. In both, myofibrillae are visible in *Squalus* embryos of forty-five millimeters and transverse striae in embryos of one hundred millimeters.

Adelmann (1927) considered a comparable dual origin of the lateral rectus in the chick probable, in which the primordium of the abducens musculature is regarded as the homologue of the hyoid head cavity of the shark, and the intermediate mass of maxillomandibular mesoderm is considered to be the counterpart of the ventral portion (muscle E) of the shark's 2d or mandibular somite. Precisely how much of the distal end of the lateral rectus is formed in the chick from the intermediate mass, Adelmann did not determine, but he was convinced that the intermediate mass contributes to the formation of this muscle.

In the cat (Gilbert, 1947), the intermediate mass of maxillomandibular mesoderm forms the distal part of the lateral rectus, whereas the proximal portion of the muscle is derived from a more medial and caudal condensation in the maxillomandibular mesoderm referred to as the VIth condensation. This conclusion concerning the dual origin of the lateral rectus muscle in the cat agrees in all essential respects with the findings presented here for man. Thus, in those forms in which the fate of muscle E, or its counterpart, the intermediate mass of maxillomandibular mesoderm, has been intensively studied in a closely graded series of embryos, it has been found to contribute to the formation of the distal end of the lateral rectus muscle rather than to degenerate.

McAlpine (1955) believed the mesoderm of branchial arches I and II to be of neural-crest origin, on the basis of its relatively high level of alkaline glycerophosphatase activity. "Branchial arch I also receives," according to McAlpine, "a significant contribution of cells from the lateral head ectoderm and neural tube rostral to a dorsoventral plane through the region of the hypophysis." He is of the opinion "that the extrinsic ocular muscles, as well as the tunics of the eye, are of similar origin." This premature and rather startling conclusion, based on a single staining reaction in one mammal, is difficult to reconcile with the way in which the eye muscles develop in lower vertebrates such as elasmobranchs and certain reptiles, in which the muscles form as hollow invaginations or solid outgrowths of the walls of the head cavities which are definitely not derived from the neural crest. Although it is possible that neural-crest elements mingle with the maxillomandibular mesoderm in mammals, McAlpine's implication that the premandibular condensations come from this source also, rather than from the prechordal plate, is most improbable, and certainly, without conclusive evidence, impossible to accept.

A consideration of the origin and early development of the vertebrate eye muscles is hardly complete without some reference to head cavities. These structures, and the role they play in the formation of the extrinsic eye muscles of lower vertebrates, have been reviewed elsewhere (Gilbert, 1952). Like the eyeball muscles themselves, these cavities are of considerable interest to the student of phylogeny, for they are well developed in elasmobranchs and many reptiles, in which groups the primordia of the six extrinsic ocular muscles typically arise from the walls of three well developed pairs of head cavities. The four eyeball muscles innervated by the oculomotor nerve arise from the walls of a conspicuous premandibular head cavity, while the superior oblique arises from the mandibular head cavity wall, and the lateral rectus, in whole or in part, takes origin from the epithelium lining the hyoid head cavity. Although premandibular head cavities are usually encountered in birds, mandibular head cavities are less common. A well developed mandibular head cavity is present in the heron (Wedin, 1953*b*); several smaller cavities which collectively may represent the mandibular head cavity were described by Rex (1905) for the gull; a mandibular head cavity is absent in the chick and robin (Adelmann, 1926). Hyoid head cavities, with one possible exception (Rex, 1905), have never been observed in birds.

Among mammals, premandibular head cavities have been found in several marsupials, including *Macropus ruficollis, Perameles nasuta, Phascolarctos cinereus, Phascolomys mitchelli,* and *Trichosurus vulpecula* by Fraser (1915), and more recently they were observed and described in the opossum, *Didelphys virginiana,* by Gilbert (1954). In no marsupial thus far studied have mandibular or hyoid head cavities been found, but homologous solid condensations which give rise to the superior oblique and abducens musculature have been clearly demonstrated.

The fact that the human embryo is the only placental mammal in which head cavities have as yet been found is, therefore, of great interest. These spaces, first pointed out, but misinterpreted, by Zimmerman (1899) in a single human embryo of 4.5 mm., have been found, half a century later, in ten human embryos in the Carnegie Collection. They never attain the conspicuous size that they do in the lower vertebrates, and are restricted to the premandibular condensations from which the four oculomotor eyeball muscles arise. They probably last but a few hours in man, and vanish as suddenly as they appear when the embryo is only 26 to 28 days of age. Because the cavities are of such small size and last so short a time, it is not surprising that they have been so long overlooked. There is little doubt that the head cavities of man are comparable to early stages in the development of the head cavities of lower vertebrates (see Gilbert, 1952), and probably arise for the same dynamic reasons.

To appreciate the dynamic factors involved in the production of head cavities, we must recall that one of the most salient features of early development is the rapid growth and expansion of the forebrain and eyes. It is precisely at this time that the head cavities of lower vertebrates and the eye-muscle primordia of mammals appear and increase markedly in size. Adelmann's (1926) comments in this connection are particularly cogent:

> That great expansion is characteristic of the head region has been stressed by Kingsbury and myself (1924) elsewhere. It is also supported by studies on the development of the neural tube (Bartelmez, 1923; Adelmann, 1925). Professor Kingsbury has suggested that the expansion of the mesoderm occurring coincident with the expansion of the head may conceivably take two forms—either epithelial or mesenchymal. If the expansion is epithelial in nature, head cavities are the result. It is perhaps not insignificant in this connection that the premandibular cavities should be most persistent, since they arise in a place where one would ex-

pect the bilateral expansion of material to be most marked. In the chick the expansion of the premandibular head cavities seems to be directly related to the release from restraint or confinement of neighboring parts. The sudden expansion of the mesoderm keeping pace with the shiftings and expansions of the head as a whole, and the expanding mesoderm taking an epithelial habitus, the head cavities result.

Wedin (1955) reached a somewhat similar conclusion in accounting for the origin of head cavities. "The deciding factor in the formation of head cavities," according to Wedin, "probably is the demand for space which during a certain phase of development is placed on the rostral mesenchyme." Or, to put it another way, head cavities probably arise and enlarge, as both Adelmann (1926) and Wedin (1955) imply, because there is potential space to be filled.

The question may now be raised whether the assumption of an epithelial or mesenchymal habitus by the expanding mesoderm is related to differences in proliferation rate. We might speculate, for example, that a low rate of proliferation would necessitate the epithelial type, the cells quickly arranging themselves as an epithelium about a space and thus forming head cavities, as in elasmobranchs and reptiles. If, on the other hand, the mesodermal cells behind and medial to the optic vesicle proliferate rapidly, solid mesenchymal condensations, such as the primordia of the superior oblique and abducens musculature of birds and marsupials or the premandibular condensations and the superior oblique and lateral rectus primordia of placental mammals, would result.

Attempts have been made from time to time to assign the eye-muscle primordia, or the head cavities which foreshadow these primordia, to segments or metameres in the head; a voluminous literature related to this subject now exists. Recently this matter was extensively treated by Wedin (1955), who concluded that "the morphogenesis of the head structures investigated [neuromeres, neural crest, head cavities, extrinsic eye muscles, and pharyngeal gut] lend no support to the theory that the vertebrate head has a metameric organization."

There has been no mention in our discussion thus far of the segmentation of the head in the human embryo, and any inference that the extrinsic-eye-muscle primordia are in any way related to head segments has been deliberately avoided, for it would only serve to obscure the principal thesis of this study. Instead, emphasis has repeatedly been placed on the striking similarity that exists in the general pattern of development of these muscles in man, cat, marsupials, birds, reptiles, and most, if not all, anamniotes. The widespread concept that all the extrinsic eye muscles of placental mammals, including man, arise from a single primordium on each side of the head should now definitely be abandoned.

SUMMARY

1. The extrinsic ocular muscles of man arise from three independent but closely apposed mesenchymal condensations situated on each side of the head. These condensations are homologous with the premandibular, mandibular, and hyoid head cavities of lower vertebrates.

2. The eyeball muscles innervated by the oculomotor nerve arise from a pair of premandibular condensations derived from the prechordal plate. The right and left premandibular condensations are from the beginning (horizon xi) connected across the mid-line by a solid bridge of prechordal mesoderm. Subsequently the bridge becomes tenuous (horizon xiii), then ruptures (horizon xiv), and ultimately disappears (horizon xv).

3. Small epithelium-lined spaces briefly appear in the premandibular condensations in embryos of horizons xii to xiv. The spaces never coalesce to form larger cavities such as are found in lower vertebrates, and are interpreted as being rudimentary head cavities, collectively homologous with the premandibular head cavities of elasmobranchs, reptiles, birds, and marsupials. To date, man is the only placental mammal known to possess premandibular head cavities.

4. Each premandibular condensation subsequently gives rise to three processes, the primordia of the four oculomotor eyeball muscles, which grow craniolaterally toward the optic vesicle. The primordium of the superior rectus first appears in embryos of horizon xiv; that of the medial rectus and the common primordium of the inferior rectus and inferior oblique, in embryos of horizon xvi.

5. Laterally each premandibular condensation adjoins a diffuse mass of mesenchymal cells known as the maxillomandibular mesoderm, which extends from the dorsal portion of the mandibular arch upward and forward over the eye.

6. Two condensations subsequently appear in the maxillomandibular mesoderm: (*a*) The more caudal and medial condensation, the primordium of the lateral rectus, is first found in embryos of horizon xiii. It grows cranially and laterally along the caudolateral face of the premandibular condensation and reaches the periphery of the optic vesicle in embryos of horizon xvi. (*b*) A second condensation, the primordium of the superior oblique, first appears in embryos of horizon xiv in an arm of maxillomandibular mesoderm above the optic vesicle. As the superior oblique condensation grows craniolaterally toward the periphery of the optic vesicle, its caudal end swings medially toward the developing orbital wall. At its distal end the superior oblique primordium bends sharply in embryos of horizon xvii and grows ventrally, laterally, and caudally to its insertion on the eyeball. About the bend in the distal end of the

superior oblique tendon, the trochlea begins to form in embryos of horizon xx, and is conspicuously, but not completely, developed 7 days later (horizon xxiii).

7. In embryos of horizon xiv, four peripheral condensations appear in the maxillomandibular mesoderm beneath the surface ectoderm about the periphery of the optic vesicle. Toward these peripheral condensations the four rectus muscles grow, and eventually become inserted into them. It is believed that the peripheral condensations contribute to the formation of the sclerotic coat of the eyeball.

8. The levator palpebrae superioris arises by delamination from the dorsomedial portion of the superior rectus muscle in embryos of horizon xxi to xxiii.

9. The eye-muscle nerves grow from the brain into their respective condensations in the following sequence: oculomotor (horizon xv), abducens (horizon xv), trochlear (horizon xvi).

10. The origin and development of the extrinsic ocular muscles in man thus follow a pattern which conforms in essential features with that found in the cat, marsupials, birds, reptiles, and elasmobranchs.

LITERATURE CITED

Addens, J. L. 1933. The motor nuclei and roots of the cranial and first spinal nerves of vertebrates. Part I. Introduction. Cyclostomes. Ztschr. f. Anat. u. Entwicklungsgesch., vol. 101, pp. 307–410.

Adelmann, H. B. 1922. The significance of the prechordal plate: an interpretative study. Amer. Jour. Anat., vol. 31, pp. 55–101.

——— 1925. The development of the neural and cranial ganglia of the rat. Jour. Comp. Neurol., vol. 39, pp. 19–171.

——— 1926. The development of the premandibular head cavities and the relations of the anterior end of the notochord in the chick and robin. Jour. Morphol., vol. 42, pp. 371–439.

——— 1927. The development of the eye muscles of the chick. Jour. Morphol., vol. 44, pp. 29–87.

Balfour, F. M. 1878. A monograph on the development of elasmobranch fishes. London.

Bartelmez, G. W. 1923. The subdivisions of the neural folds in man. Jour. Comp. Neurol., vol. 35, pp. 231–247.

Bonnet, R. 1901. Beiträge zur Embryologie des Hundes. Erste Fortsetzung. Anat. Hefte, vol. 16, pp. 231–332.

Carnicer, F. C. 1950. Origen y desarrollo embriológico de la musculatura extrínseca del ojo. Arch. españ. de morfol., vol. 8, pp. 75–107.

Cords, E. 1929. Die Kopfnerven der Petromyzonten. Ztschr. f. d. Ges. Anat., Abt. I, vol. 89, pp. 201–249.

Corning, H. K. 1899. Ueber die Entwicklung der Kopf- und Extremitätenmuskulatur bei Reptilien. Morphol. Jahrb., vol. 28, pp. 28–104.

——— 1900. Ueber die vergleichende Anatomie der Augenmuskulatur. Morphol. Jahrb., vol. 29, pp. 94–140.

Dohrn, A. 1904. Studien zur Urgeschichte des Wirbelthierkörpers. 23, Die Mandibularhöhle der Selachier. 24, Die Prämandibularhöhle. Mitteil. Zool. Stat. Neapel., vol. 17, pp. 1–294.

Edgeworth, F. H. 1935. The cranial muscles of vertebrates. 493 pp. Cambridge.

Filatoff, D. 1907. Die Metamerie des Kopfes von *Emys lutaria.* Zur Frage über die korrelative Entwicklung. Morphol. Jahrb., vol. 37, pp. 289–396.

Fraser, E. A. 1915. The head cavities and development of the eye muscles in *Trichosurus vulpecula,* with notes on some other marsupials. Proc. Zool. Soc. London, III, pp. 299–346.

Fürbringer, M. 1897. Ueber die spino-occipitalen Nerven der Selachier und Holocephalen und ihre vergleichende Morphologie. Festschr. f. Gegenbaur, vol. 3, pp. 349–788. Leipzig.

Fürbringer, P. 1875. Untersuchungen zur vergleichenden Anatomie der Muskulatur des Kopfskeletes der Cyclostomen. Ztschr. f. Naturwiss., vol. 9, pp. 1–93.

Gilbert, P. W. 1947. The origin and development of the extrinsic ocular muscles in the domestic cat. Jour. Morphol., vol. 81, pp. 151–193.

——— 1952. The origin and development of the head cavities in the human embryo. Jour. Morphol., vol. 90, pp. 149–187.

——— 1954. The premandibular head cavities in the opossum, *Didelphys virginiana.* Jour. Morphol., vol. 95, pp. 47–76.

Heuser, C. H. 1932. A presomite human embryo with a definite chorda canal. Carnegie Inst. Wash. Pub. 433, Contrib. to Embryol., vol. 23, pp. 251–267.

Hill, J. P., and M. Tribe. 1924. The early development of the cat (*Felis domestica*). Quart. Jour. Microsc. Sci., vol. 68, pp. 513–602.

Johnson, C. E. 1913. The development of the prootic head somites and eye muscle in *Chelydra serpentina.* Amer. Jour. Anat., vol. 14, pp. 119–185.

Keil, R. 1906. Beiträge zur Entwickelungsgeschichte des Auges vom Schwein, mit besonderer Berücksichtigung des Verhaltens der fötalen Augenspalte. Anat. Hefte, vol. 32, pp. 1–87.

Kingsbury, B. F., and H. B. Adelmann. 1924. The morphological plan of the head. Quart. Jour. Microsc. Sci., vol. 68, pp. 239–285.

Lamb, A. B. 1902. The development of the eye muscles in *Acanthias.* Amer. Jour. Anat., vol. 1, pp. 185–202.

Lešer, O. 1925. Development of the extra-ocular muscles in some mammals. Brit. Jour. Ophthalmol., vol. 9, pp. 154–161.

Lewis, W. H. 1910. The development of the muscular system. *In* Keibel and Mall (eds.), Manual of human embryology, vol. 1, pp. 505–508. Philadelphia.

Mann, I. C. 1928. The development of the human eye. 312 pp. Cambridge.

Marshall, A. M. 1881. On the head cavities and associated nerves of elasmobranchs. Quart. Jour. Microsc. Sci., vol. 21, pp. 72–97.

McAlpine, R. J. 1955. Observations on the cranial neural crest and the head mesoderm in the developing rat as revealed by the alkaline phosphatase technique. Anat. Rec., vol. 121, p. 337.

Neal, H. V. 1918. The history of the eye muscles. Jour. Morphol., vol. 30, pp. 433–453.

Orr, H. 1887. Contribution to the embryology of the lizard. Jour. Morphol., vol. 1, pp. 311–372.

Parker, K. M. 1917. The development of the hypophysis cerebri, pre-oral gut, and related structures in the Marsupialia. Jour. Anat., vol. 51, pp. 181–249.

Payne, F. 1925. General description of a 7-somite human embryo. Carnegie Inst. Wash. Pub. 361, Contrib. to Embryol., vol. 16, pp. 115–124.

Platt, J. B. 1891. A contribution to the morphology of the vertebrate head, based on a study of *Acanthias vulgaris.* Jour. Morphol., vol. 5, pp. 79–112.

Reuter, K. 1897. Ueber die Entwickelung der Augenmuskulatur beim Schwein. Anat. Hefte, vol. 9, pp. 365–387.

Rex, H. 1900. Zur Entwicklung der Augenmuskeln der Ente. Arch. f. mikrosk. Anat., vol. 57, pp. 229–271.

——— 1905. Ueber das Mesoderm des Vorderkopfes der Lachmöwe (*Larus ridibundus*). Morphol. Jahrb., vol. 33, pp. 107–347.

Scammon, R. E. 1911. Normal plates of the development of *Squalus acanthias. In* Keibel, Normentafeln zur Entwicklungsgeschichte der Wirbeltiere, vol. 12. 140 pp. Jena.

Streeter, G. L. 1942. Developmental horizons in human embryos. Description of age group xi, 13 to 20 somites, and age group xii, 21 to 29 somites. Carnegie Inst. Wash. Pub. 541, Contrib. to Embryol., vol. 30, pp. 211–245.

——— 1945. Developmental horizons in human embryos. Description of age group xiii, embryos about 4 or 5 millimeters long, and age group xiv, period of indentation of the lens vesicle. Carnegie Inst. Wash. Pub. 557, Contrib. to Embryol., vol. 31, pp. 27–63.

——— 1948. Developmental horizons in human embryos. Description of age groups xv, xvi, xvii, and xviii, being the third issue of a survey of the Carnegie Collection. Carnegie Inst. Wash. Pub. 575, Contrib. to Embryol., vol. 32, pp. 133–203.

——— 1951. Developmental horizons in human embryos. Description of age groups xix, xx, xxi, xxii, and xxiii, being the fifth issue of a survey of the Carnegie Collection. Carnegie Inst. Wash. Pub. 592, Contrib. to Embryol., vol. 34, pp. 165–196.

van Wijhe, J. W. 1883. Ueber die Mesodermsegmente und die Entwickelung der Nerven des Selachierkopfes. 50 pp. Amsterdam.

Wedin, B. 1949. The anterior mesoblast in some lower vertebrates. 225 pp. Lund.

——— 1953*a*. The origin and development of the extrinsic ocular muscles in the alligator. Jour. Morphol., vol. 92, pp. 303–335.

——— 1953*b*. The development of the eye muscles in *Ardea cinerea* L., Acta Anat., vol. 18, pp. 30–48.

——— 1955. Embryonic segmentations in the head. Malmö.

Wolff, E. 1940. The anatomy of the eye and orbit including the central connections, development, and comparative anatomy of the visual apparatus. 2d ed. 374 pp. London.

Zimmerman, K. W. 1899. Ueber Kopfhöhlenrudimente beim Menschen. Arch. f. mikrosk. Anat., vol. 53, pp. 481–484.

ABBREVIATIONS USED IN FIGURES

ao., aorta
ao. a. I, aortic arch I
ao. a. II, aortic arch II
ao. a. III, aortic arch III
a. p. c., anterior peripheral condensation
c. g., ciliary ganglion
fb., forebrain
fg., foregut
fr. n., frontal nerve
g. V, Gasserian ganglion
hb., hindbrain
h. c., head cavity
i. c. a., internal carotid artery
int., intermediate mass
i. o., inferior oblique
i. p. c., inferior peripheral condensation
i. r., inferior rectus
l. p., lens placode
l. p. s., levator palpebrae superioris
l. r., lateral rectus
l. v., lens vesicle
m. a., mandibular arch
mand. V, mandibular branch of cranial nerve V
max. V, maxillary branch of cranial nerve V
mb., midbrain
m. m. m., maxillomandibular mesoderm
m. r., medial rectus
n., notochord
n. III, oculomotor nerve
n. IV, trochlear nerve
n. VI, abducens nerve
nc. n., nasociliary nerve
op. s., optic stalk
op. v., optic vesicle
op. V, ophthalmic branch of cranial nerve V
p. b., prechordal bridge
p. c., premandibular condensation
p. pl., prechordal plate
p. p. c., posterior peripheral condensation
s. o., superior oblique
s. p. c., superior peripheral condensation
s. r., superior rectus
t., trochlea
v. c. a., vena cerebralis anterior
v. c. m., vena capitis medialis
v. o. i., vena orbitalis inferior

PLATES

PLATE 1

FIG. 3. Transection through the head of a 10-somite embryo. The plane of section passes through the prechordal plate. No. 5074, section 1-3-4, × 100.

FIG. 4. Transection through the head of a 10-somite embryo. The plane of section passes through the cranial end of the foregut. No. 5074, section 1-3-5, × 100.

FIG. 5. Oblique transection through the head of a 14-somite embryo. The plane of section passes through the cranial end of the notochord. No. 4529, section 1-6-6, × 100.

FIG. 6. Oblique transection through the head of a 14-somite embryo. The plane of section passes through the prechordal plate, from which prechordal mesoderm has been proliferated laterally to form a small club-shaped premandibular condensation ahead of the knee of the left aorta. No. 4529, section 1-6-8, × 100.

FIG. 7. No. 6050, section 3-5-10, × 100.

FIG. 8. No. 6050, section 3-5-11, × 100.

Two consecutive transections through the head of a 19-somite embryo. The premandibular condensations are larger than in embryos of 14 somites, and are still connected across the mid-line by a transverse bridge of prechordal mesoderm. To emphasize their limits, both the bridge and the premandibular condensations are shaded. Actually, the contrast with the surrounding mesoderm is not so great as shown here, and, in some embryos, the limits of the premandibular condensations can be determined only after prolonged study.

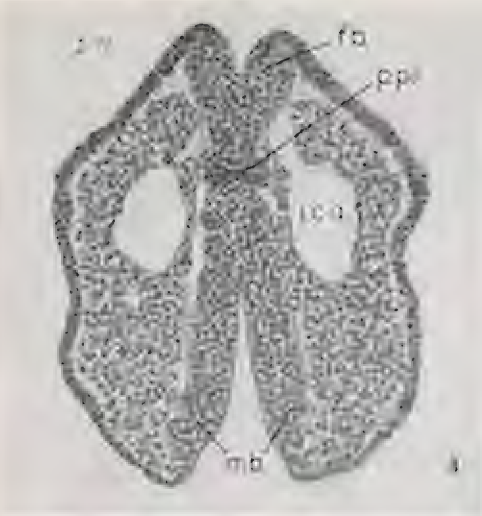
fb
ppl
ica
mb
3

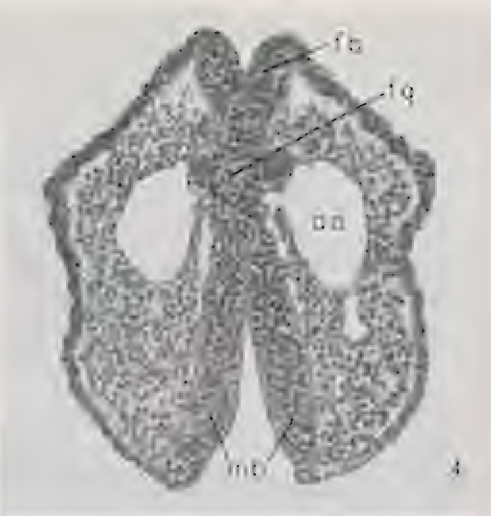
fb
fg
aa
mb
4

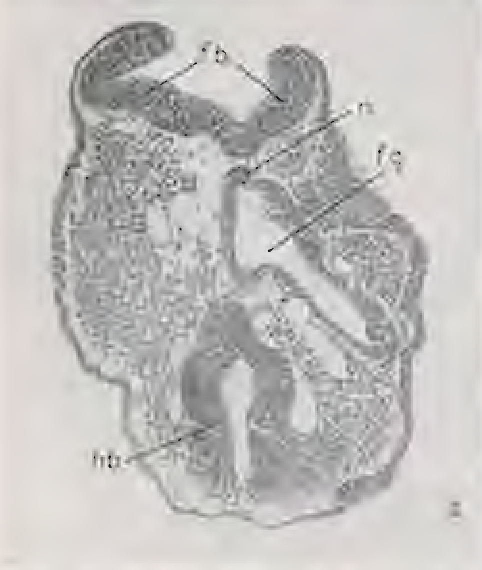
fb
n
aa
fg
hb
5

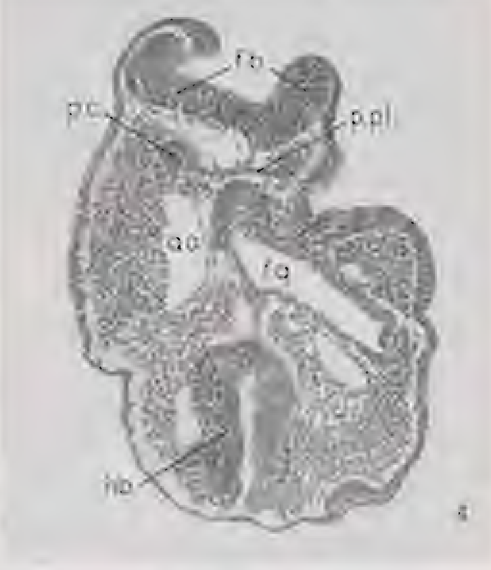
fb
pc
ppl
aa
fg
hb
6

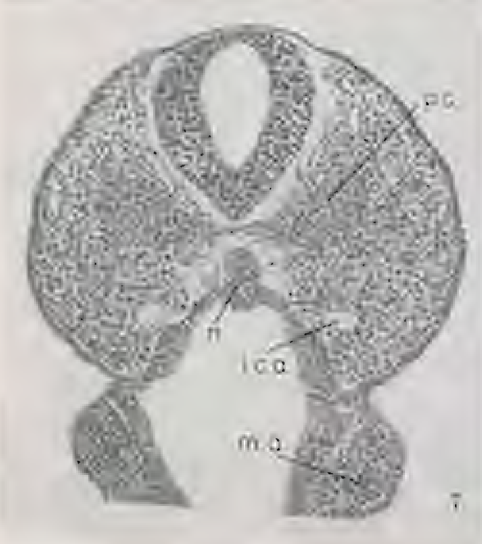
pc
n
ica
m.a
7

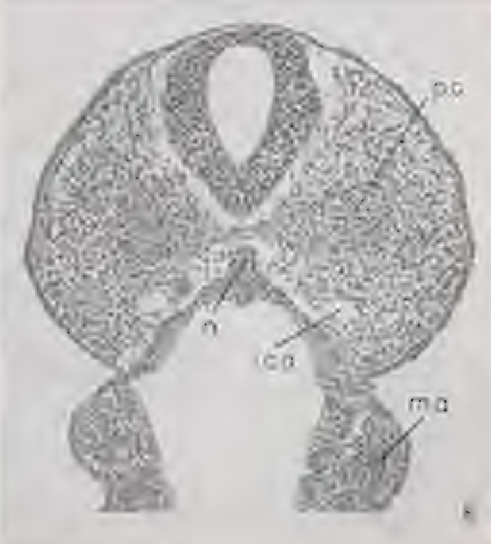
pc
n
ica
ma
8

PLATE 2

FIG. 9. Based on a plastic reconstruction of a part of the head of a 26-somite embryo sectioned frontally; the observer is looking caudally toward the cranial tip of the notochord. No. 4736, × 100.

FIG. 10. Head of the same embryo, looking cranially toward the floor of the forebrain. × 100.

The premandibular condensations containing small epithelium-lined head cavities are located above and slightly lateral to the internal carotid arteries, and are connected by a conspicuous transverse bridge of prechordal mesoderm that lies between the anterior end of the notochord and the floor of the forebrain.

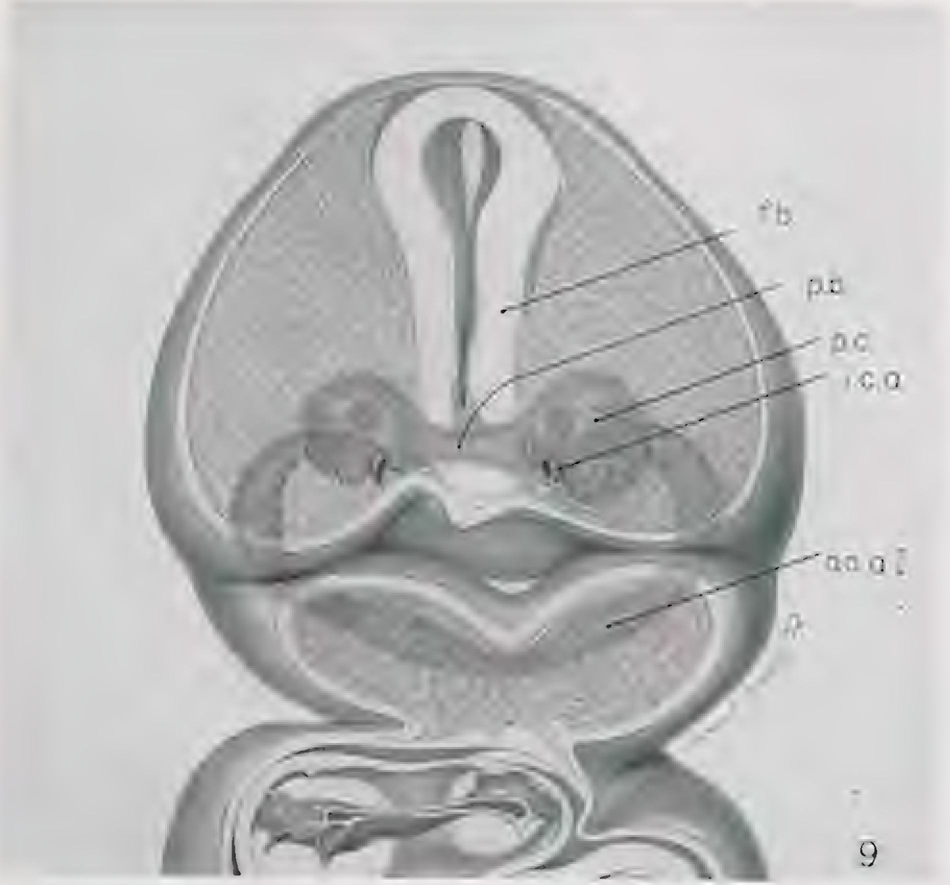

9

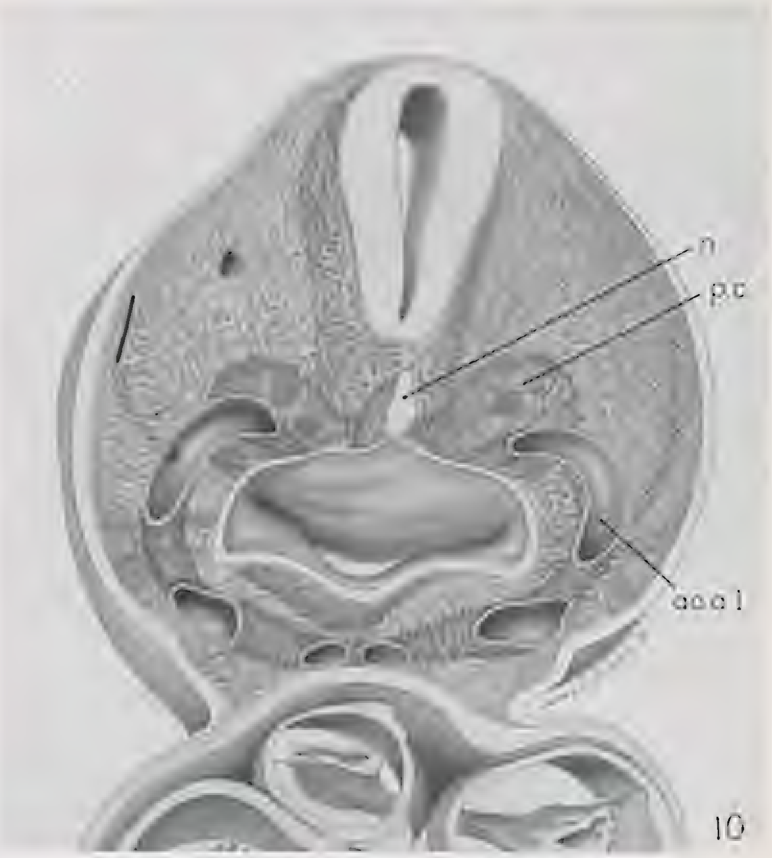

10

PLATE 3

FIG. 11. Based on a plastic reconstruction of the left side of the head of a 29-somite embryo sectioned sagittally; the external surface is nearest the observer. Note the premandibular condensation slightly dorsal and caudal to the optic vesicle, and lateral to the internal carotid artery. Only two of the four head cavities in the left premandibular condensation can be seen. No. 7724, ×60.

FIG. 12. Left side of the head of the same embryo. The median sagittal plane is nearest the observer. Note the transverse bridge of prechordal mesoderm connecting the left and right premandibular condensations.

FIG. 13. Details of the epithelium that lines one of the head cavities. No. 4736, section 2-5-3, ×500.

11

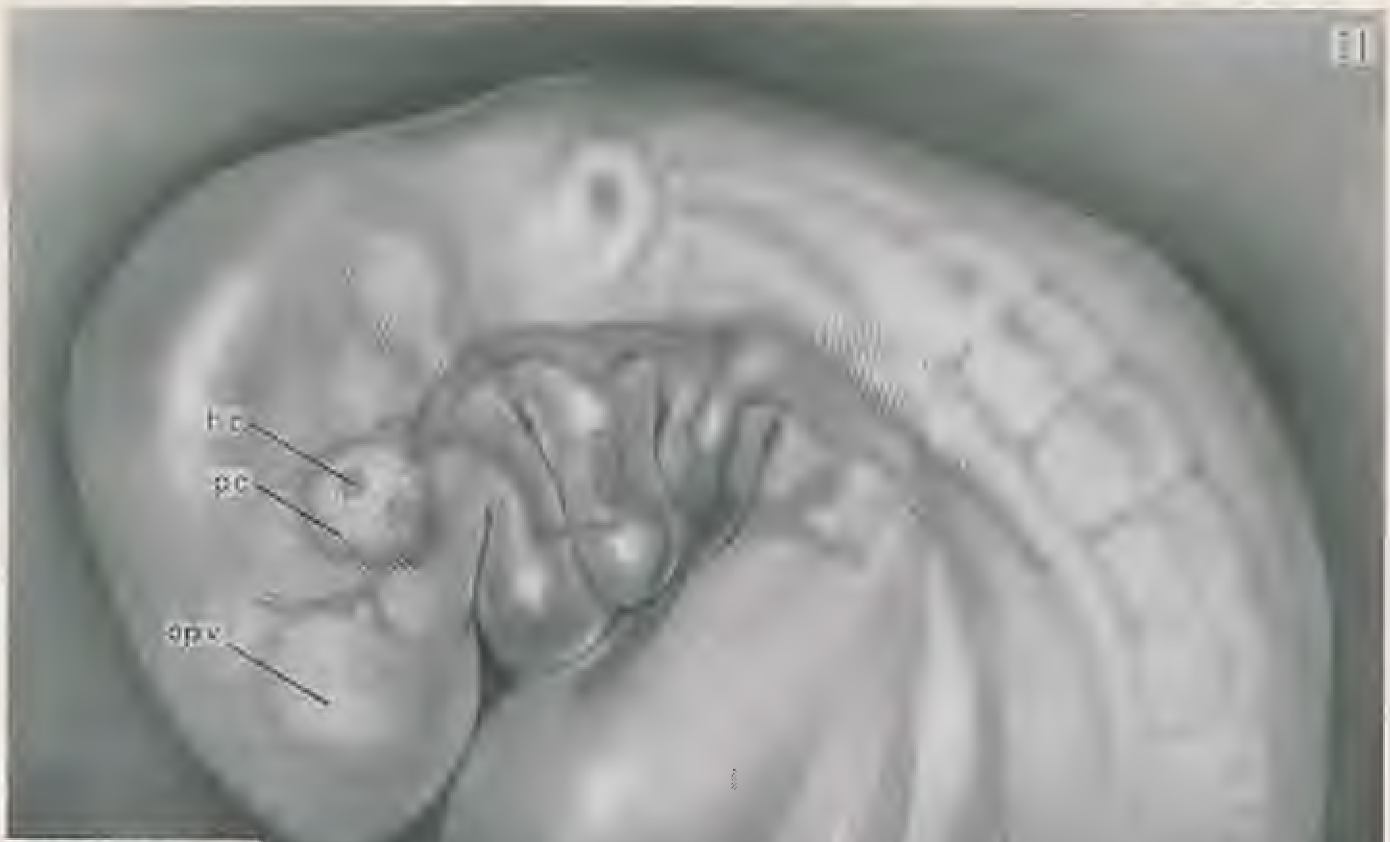

13

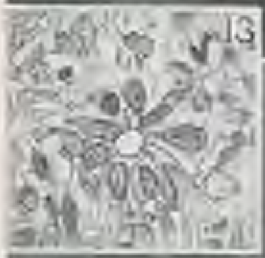

12

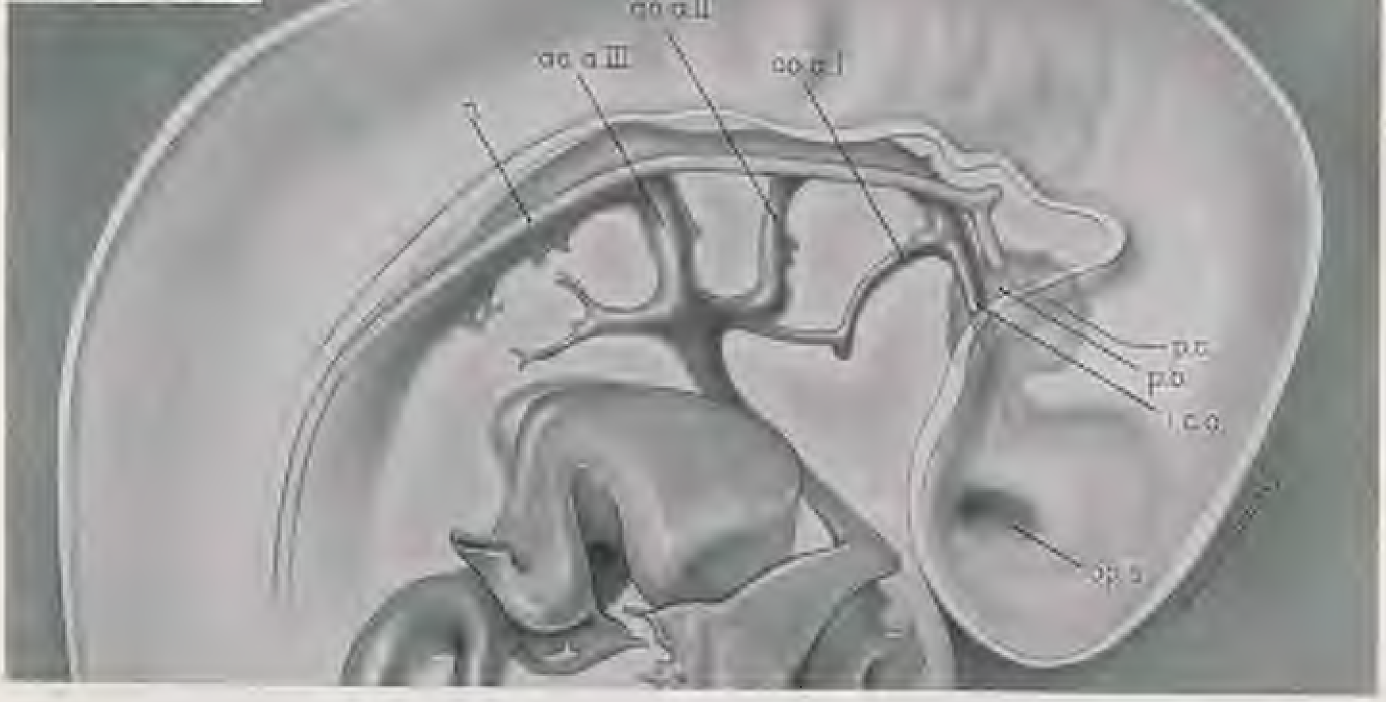

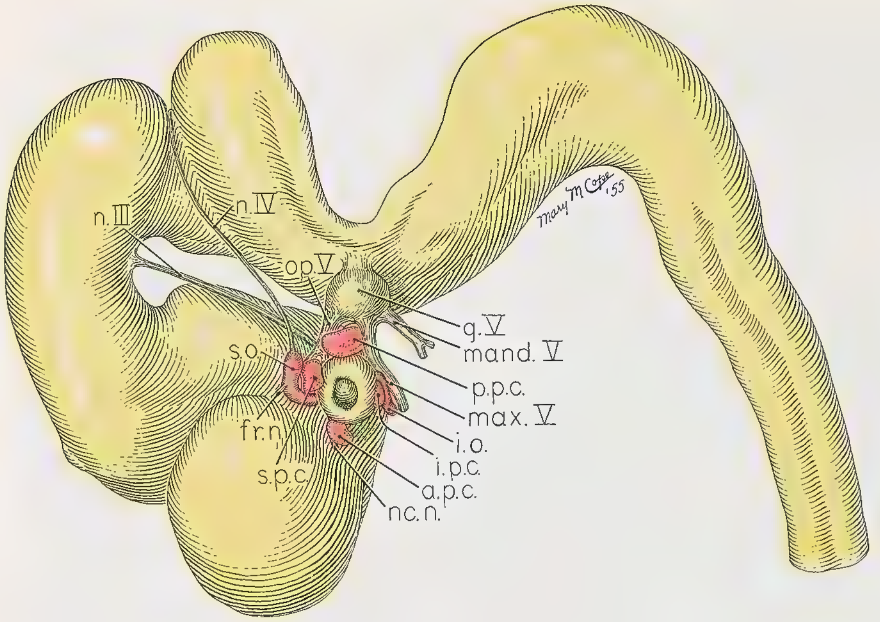

Fig. 14.

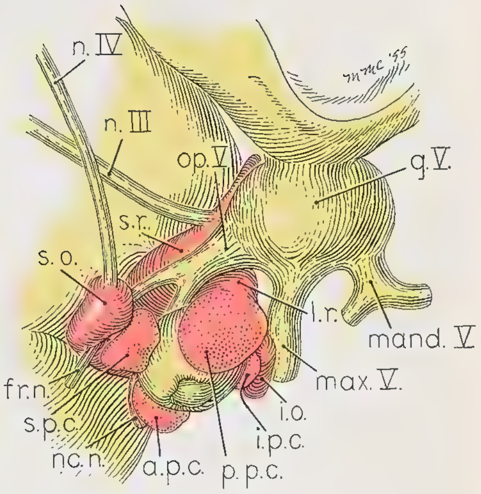

Fig. 15.

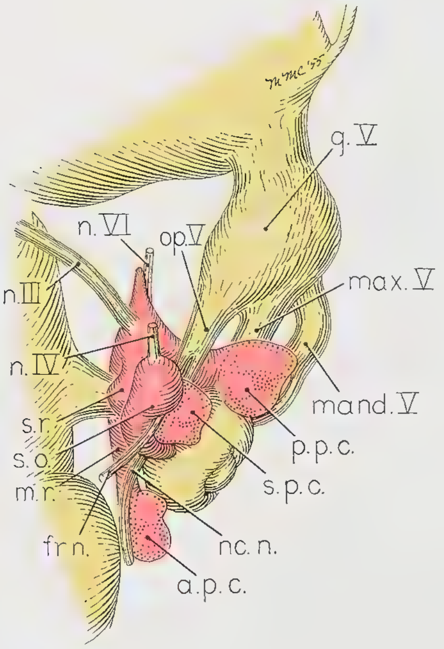

Fig. 16.

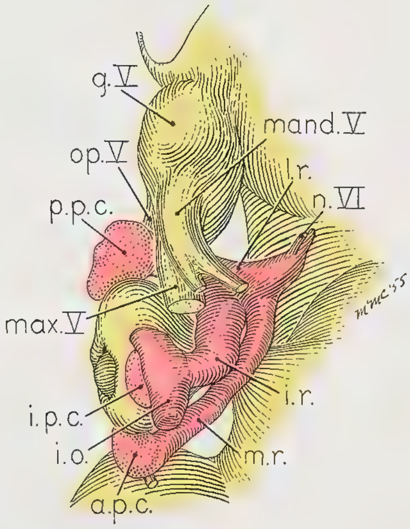

Fig. 17.

Four drawings of a model of the eye, eye-muscle primordia, and associated nerves, of embryo no. 6258, horizon xvii.

Fig. 14. The eye-muscle primordia of embryo no. 6258 are superimposed on the brain of another embryo, no. 6520, of approximately the same age and size. The relation of the principal branches of cranial nerve V to the four peripheral condensations into which the four rectus muscles grow is illustrated. Lateral aspect. × 15.

Fig. 15. A portion of the brain, the eye, principal nerves, peripheral condensations, and the eye-muscle primordia. Dorsolateral aspect. No. 6258, × 30.

Fig. 16. Dorsocranial aspect of the same model illustrated in figure 15. × 30.

Fig. 17. Ventrocaudal aspect of the same model illustrated in figure 15. × 30.

Attention is called to the four peripheral condensations, about the outer margin of the optic vesicle, into which the primordia of the four rectus muscles have grown. Cranial nerves III, IV, and VI have reached their respective eye-muscle primordia; the primordium of the inferior oblique has appeared as a conspicuous condensation at the distal end of the inferior rectus; a prominent bend (at the point where the trochlea will subsequently develop) has appeared near the distal end of the superior oblique primordium, and the proximal end of the superior oblique has begun to shift medially.

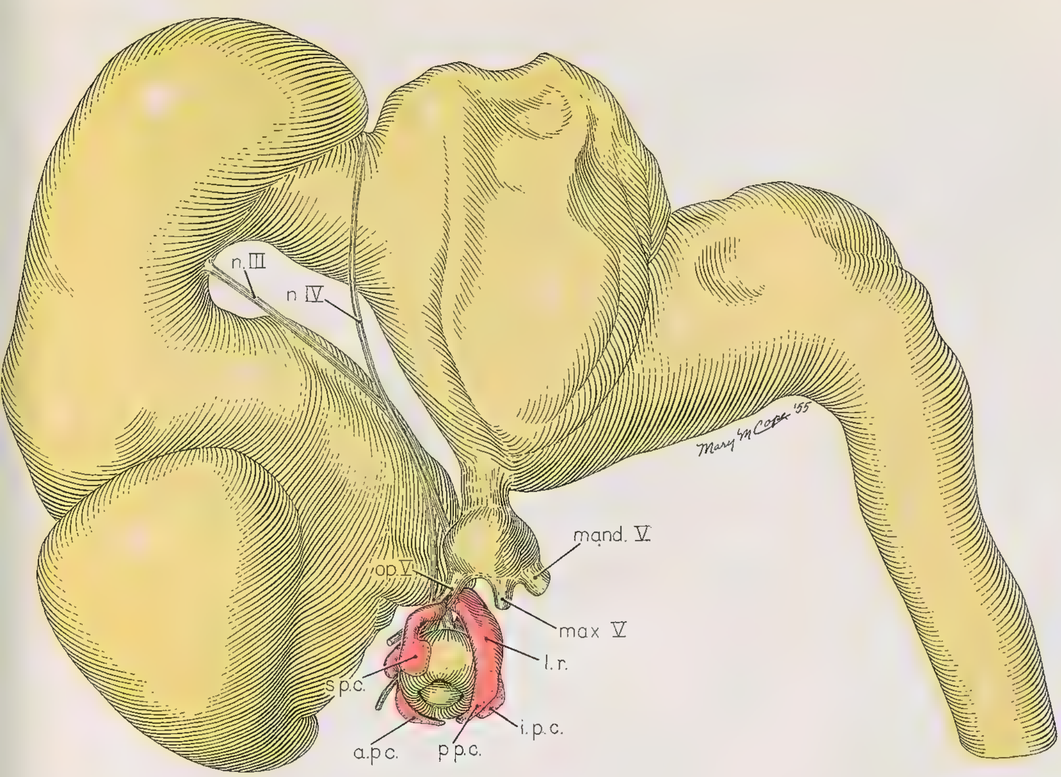

FIG. 18.

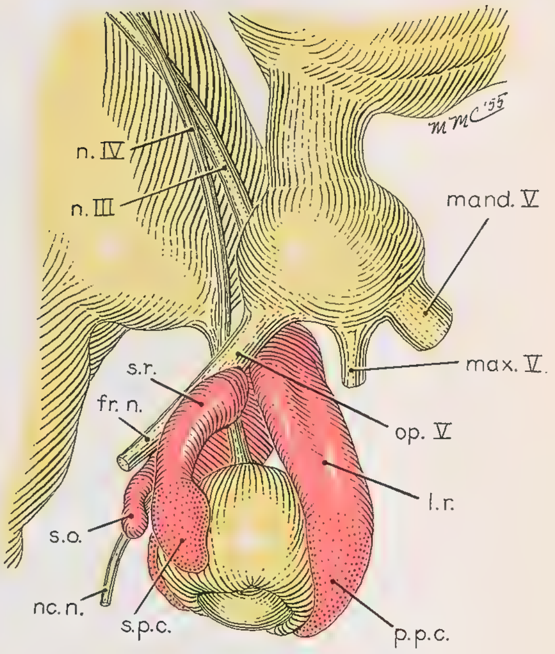

FIG. 19.

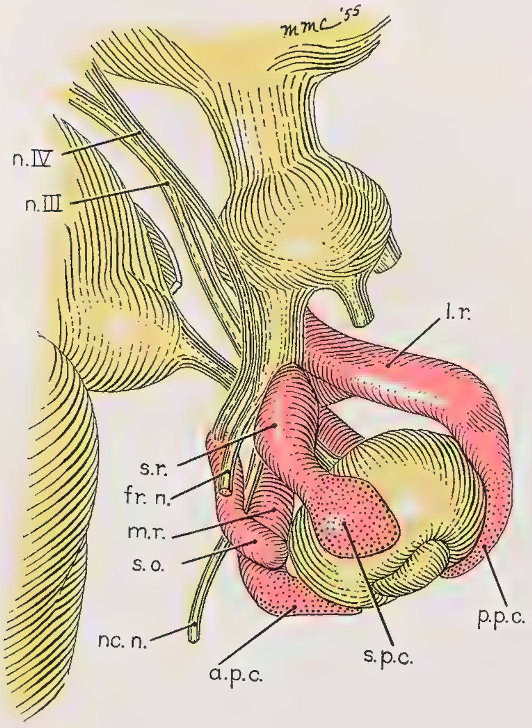

FIG. 20.

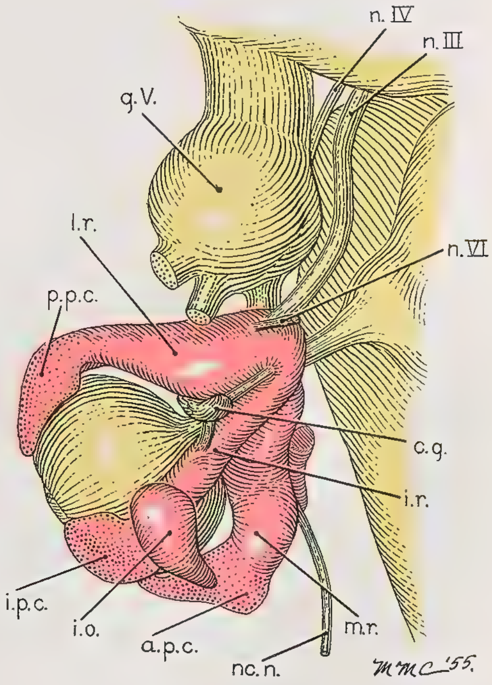

FIG. 21.

Four drawings of a model of the eye, eye-muscle primordia, and associated nerves of embryo no. 5609, horizon xix.

FIG. 18. The eye-muscle primordia of embryo no. 5609 are superimposed on the brain for orientation; the relation of the principal branches of cranial nerve V to the four peripheral condensations into which the four rectus muscles have grown is illustrated. Lateral aspect. × 15.

FIG. 19. A portion of the brain, the eye, principal nerves, peripheral condensations, and the eye-muscle primordia. Dorsolateral aspect. No. 5609, × 30.

FIG. 20. Dorsocranial aspect of the model illustrated in figure 19. × 30.

FIG. 21. Ventrocaudal aspect of the same model illustrated in figure 19. × 30.

Four peripheral condensations are still present at this stage, and with these the primordia of the four rectus muscles have intimately fused. The inferior oblique primordium has become more elongated, and its long axis lies at roughly a right angle to that of the inferior rectus, with which it still retains a tenuous connection. The bend, anticipating a trochlea, at the distal end of the superior oblique primordium is more prominent, and the proximal end of the superior oblique has grown farther medially toward its future origin on the orbital wall.

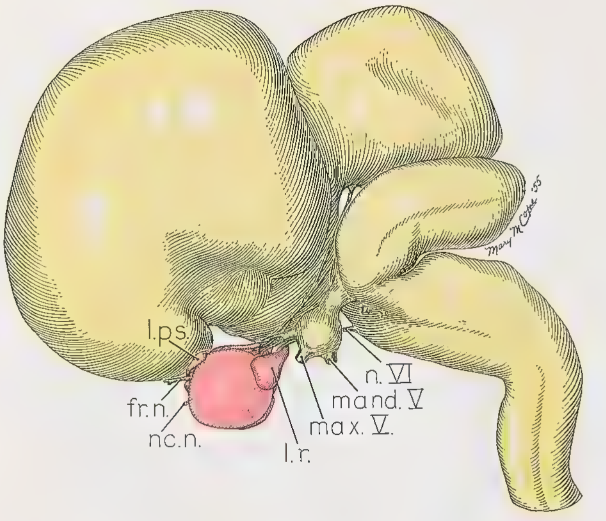

FIG. 22.

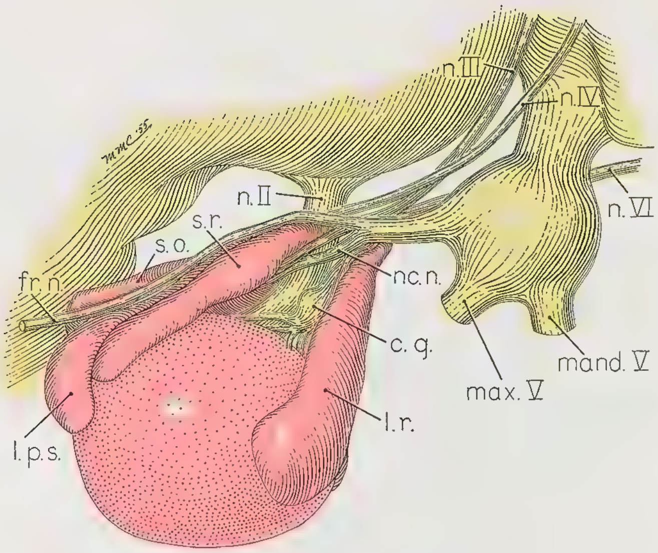

FIG. 23.

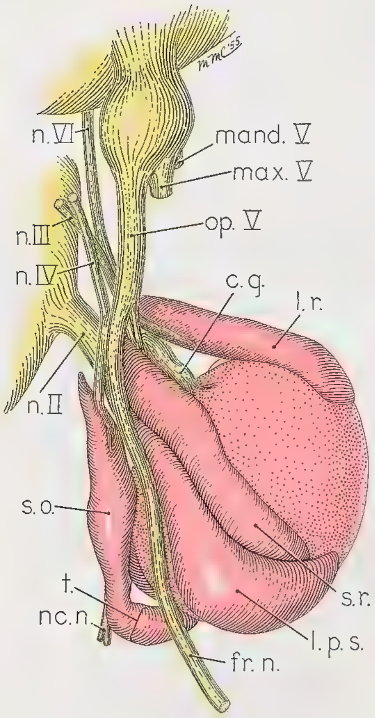

FIG. 24.

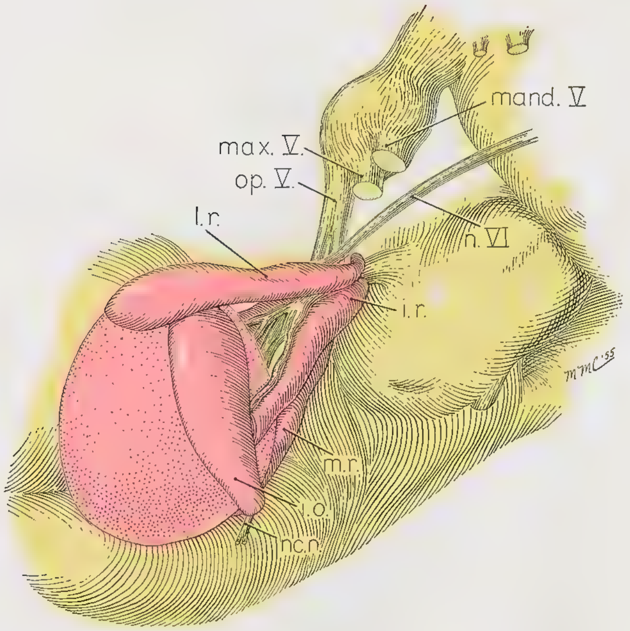

FIG. 25.

Four drawings of a model of the eye, eye muscles, and associated nerves of embryo no. 5154, horizon xxiii.

FIG. 22. The eye muscles of embryo no. 5154 are superimposed on the brain for orientation; the relation of the principal branches of cranial nerve V to the eye muscles, which now have well defined insertions on the sclera, is illustrated. The peripheral condensations are no longer recognizable, for they have contributed to the formation of the sclera. Lateral aspect. ×5.

FIG. 23. A portion of the brain, the eye, principal nerves, and the eye muscles. Dorsolateral aspect. No. 5154, ×17.

FIG. 24. Dorsocranial aspect of the same model illustrated in figure 23. ×17.

FIG. 25. Ventrocaudal aspect of the same model illustrated in figure 23. ×17.

A sclerotic coat, to which the peripheral condensations have contributed, now covers the eyeball; muscle fibers have appeared in all six eye muscles, and all have well defined origins on the orbital wall and insertions on the sclera; a trochlea has begun to develop at the bend in the tendon of insertion of the superior oblique; a thin sheet of muscle, the levator palpebrae superioris, has split off from the dorsomedial surface of the superior rectus, and extends outward into the upper eyelid.

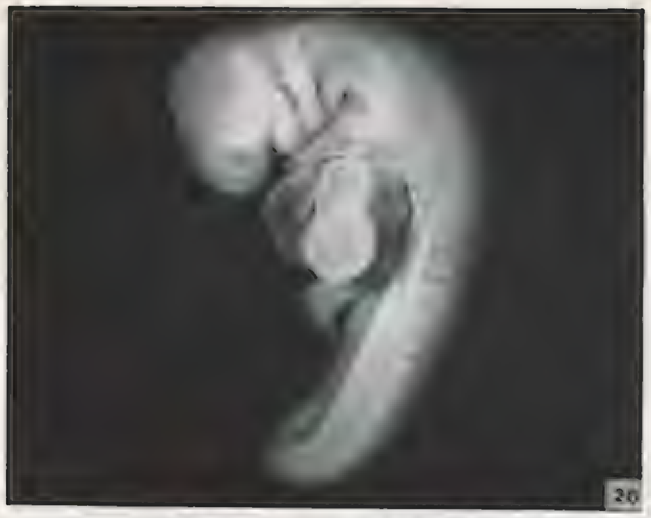

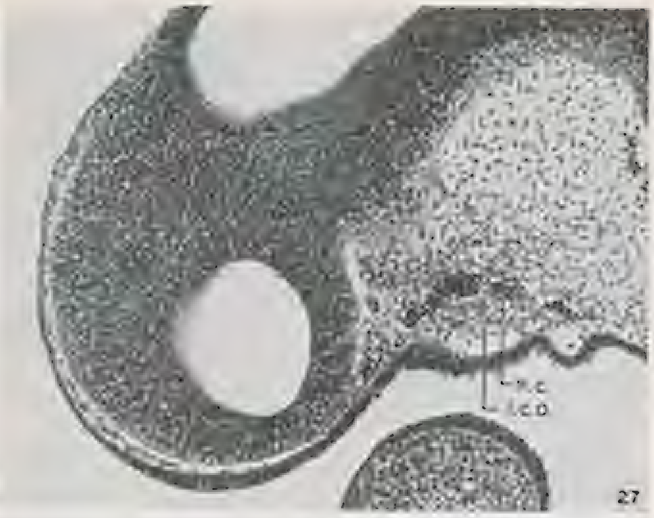

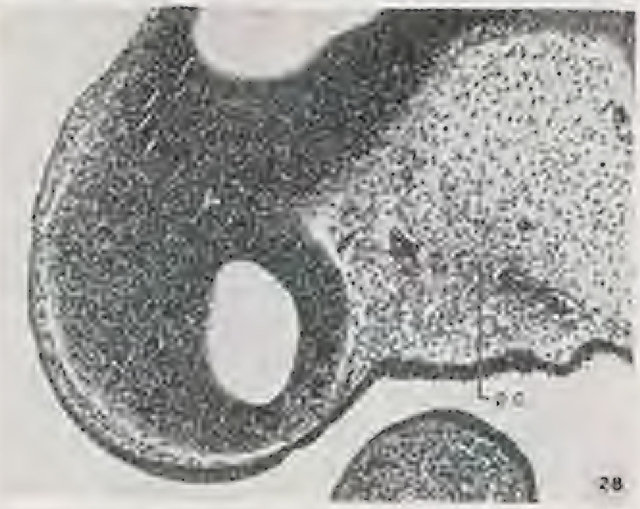

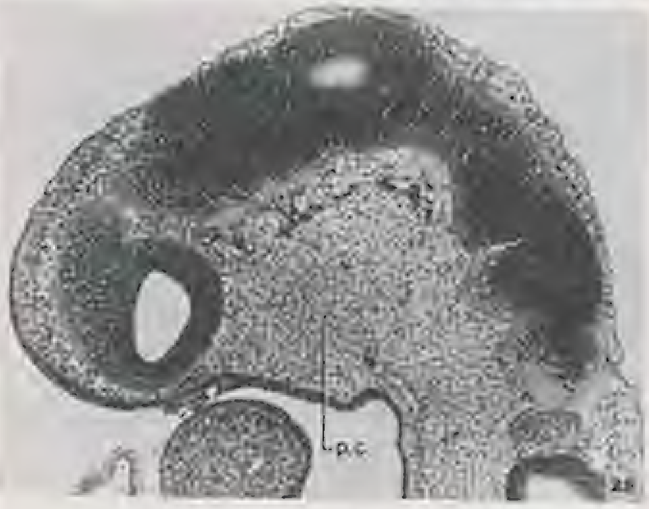

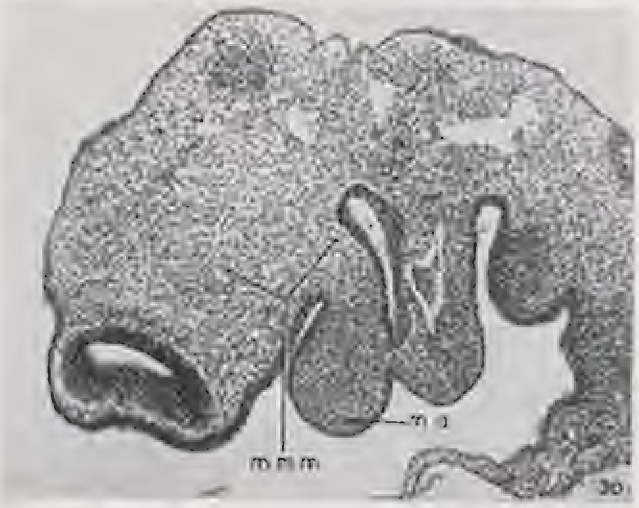

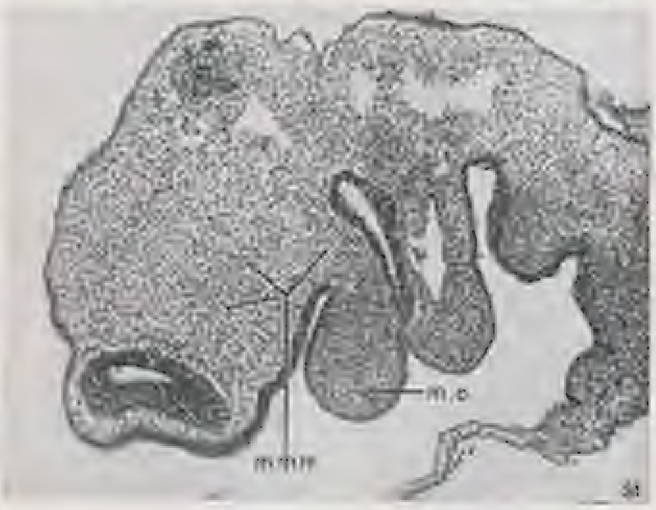

FIG. 26. Lateral view of a 29-somite embryo, approximately 26 days of age. Figures 27 to 31 are of parasagittal sections through the head of this embryo. No. 7724, × 17.

FIG. 27. Parasagittal section through part of the head of the embryo. A small head cavity is situated immediately above the internal carotid artery, near the junction of the left premandibular condensation with the transverse bridge of prechordal mesoderm. Section 2-3-11, × 105.

FIG. 28. Section 16 microns lateral to that in figure 27, showing the premandibular condensation. Section 2-3-13, × 105.

FIG. 29. Section lateral to that in figure 28, illustrating the maximum diameter of the premandibular condensation at this stage. Section 2-4-4, × 70.

FIG. 30. Section lateral to the premandibular condensation, which illustrates the maxillomandibular mesoderm at the upper end of the mandibular arch and maxillary process and caudal to the optic vesicle. Section 3-1-10, × 70.

FIG. 31. Adjacent section, lateral to that in figure 30, showing the extent of the maxillomandibular mesoderm. Section 3-1-11, × 70.

PLATE 8

FIG. 32. Transverse section through the head of a 28-somite embryo, approximately 26 days of age. One head cavity appears on the left side slightly dorsal and lateral to the internal carotid artery, and three, situated within the premandibular condensation of the right side, are arranged in a row roughly paralleling the floor and wall of the forebrain. No. 7999, section 2-1-12, × 70.

FIG. 33. The same section, at a higher magnification, illustrated in figure 32. No. 7999, section 2-1-12, × 140.

FIG. 34. Transverse section through the head of a 24-somite embryo, approximately 26 days of age. A small head cavity is present above the internal carotid artery on each side. No. 8505A, section 3-1-1, × 87.

FIG. 35. Parasagittal section through the head of an embryo of horizon xiv. From the premandibular condensation, an arm of mesoderm, the primordium of the superior rectus, has extended craniolaterally over the dorsomedial surface of the optic vesicle. No. 6500, section 2-6-4, × 42.

FIG. 36. Frontal section through the head of an embryo of horizon xiii. The lateral rectus condensation is situated medial to the Gasserian ganglion and caudodorsal to the premandibular condensation. Note the transverse bridge of prechordal mesoderm which connects the right and left premandibular condensations. No. 7618, section 3-2-3, × 42.

FIG. 37. Parasagittal section through the eye of an embryo of horizon xiii. The tapered medial end of the premandibular condensation is situated immediately above the internal carotid artery. No. 8239, section 3-2-6, × 70.

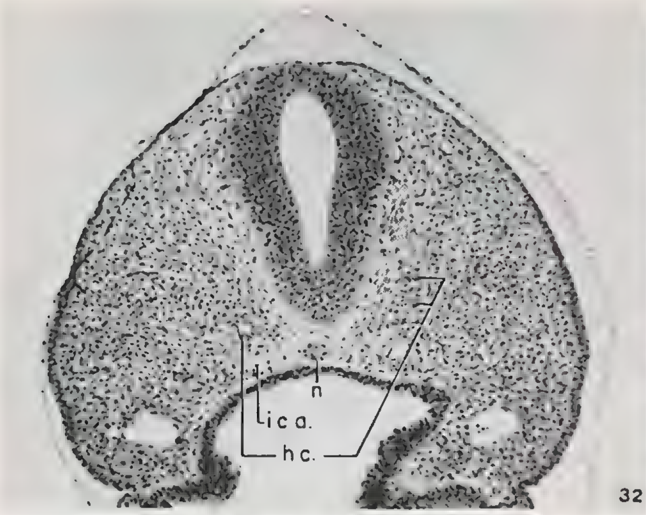

32

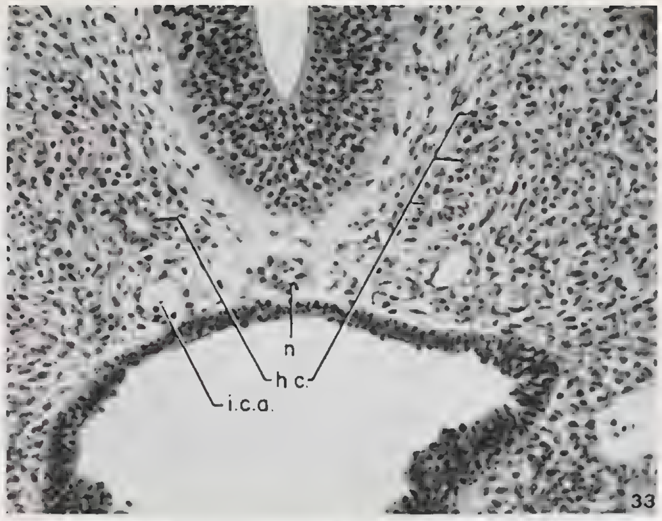

33

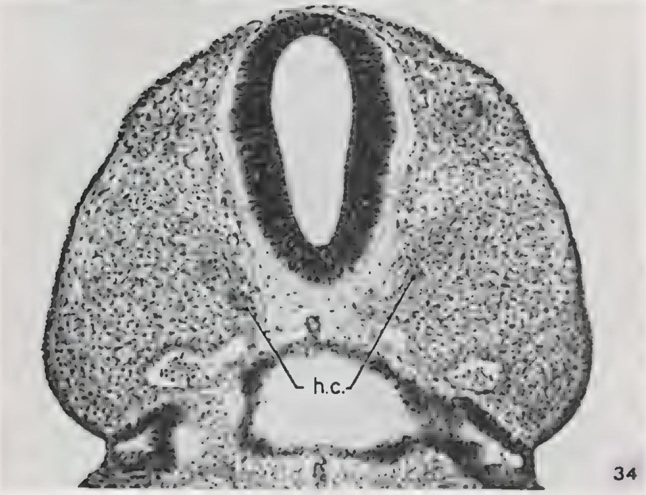

34

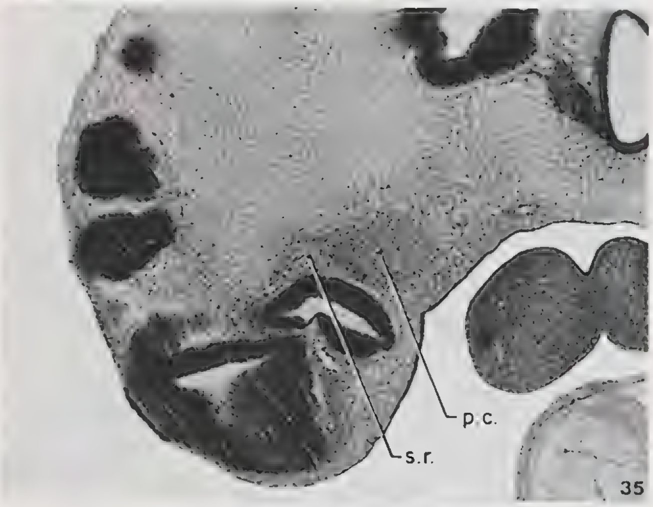

35

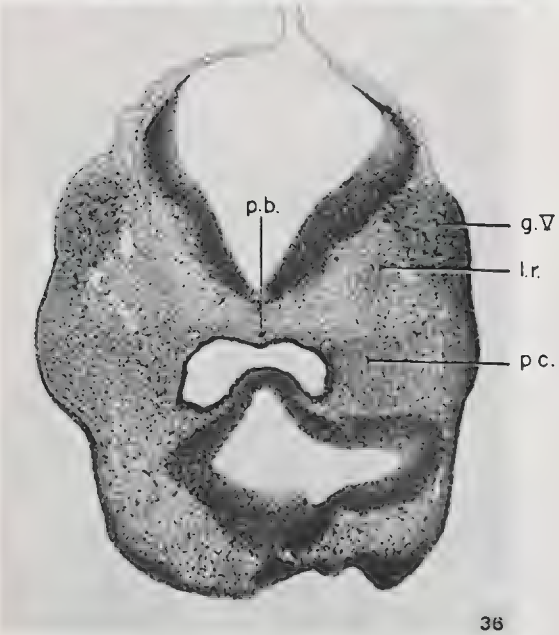

36

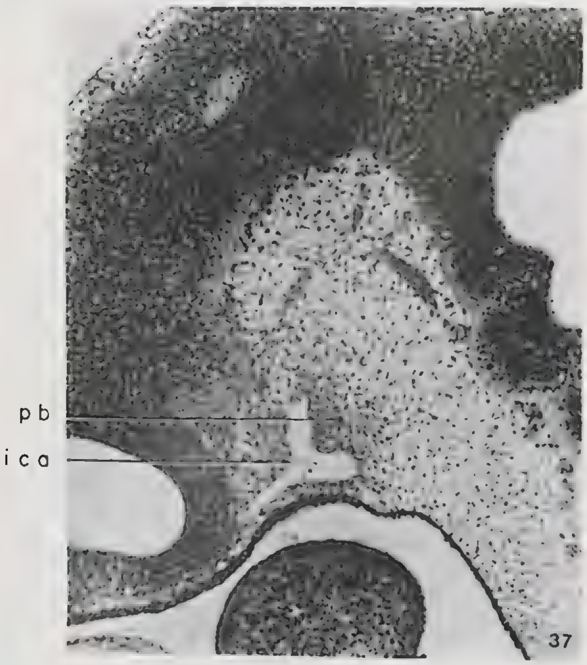

37

PLATE 9

FIG. 38. Parasagittal section through the head of an embryo of horizon xv. The condensation from which the proximal part of the lateral rectus will form is situated dorsal and caudal to the premandibular condensation which will give rise to the four oculomotor eye muscles. No. 4602, section 2-4-6, ×24.

FIG. 39. Parasagittal section 65 microns lateral to the one illustrated in figure 38. The lateral rectus and premandibular condensations at this level are in close apposition. No. 4602, section 2-4-1, ×24.

FIG. 40. Frontal section through the head of an embryo of horizon xv. The lateral rectus primordium extends laterally along the dorsocaudal face of the premandibular condensation to become continuous with the intermediate mass of the maxillomandibular mesoderm. No. 6506, section 9-1-5, ×38.

FIG. 41. Section some distance behind the one illustrated in figure 40. At this level the lateral rectus primordium is no longer in intimate contact with the premandibular condensation. No. 6506, section 9-4-4, ×38.

FIG. 42. Transverse section through the head of an embryo of horizon xv. The caudodorsal end of the lateral rectus primordium lies adjacent and medial to the vena capitis medialis. No. 3385, section 5-2-3, ×28.

FIG. 43. Transverse section some distance below that illustrated in figure 42. The lateral rectus and the superior rectus primordia have not quite reached their respective peripheral condensations. No. 3385, section 6-2-3, ×28.

FIG. 44. Transverse section some distance below that illustrated in figure 43. The caudal and medial sides of the premandibular condensation are characteristically enclosed at this level by branches of the vena orbitalis inferior. No. 3385, section 6-3-2, ×28.

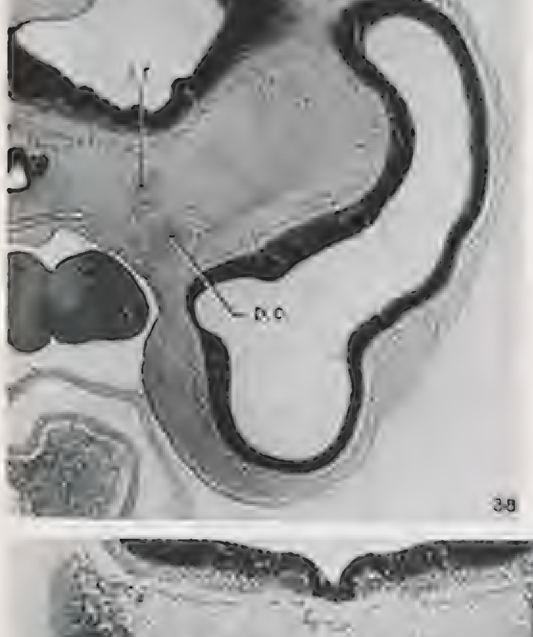

38

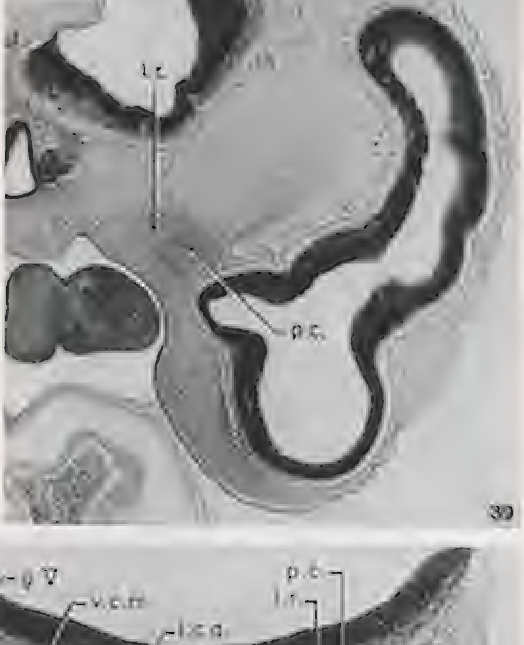

39

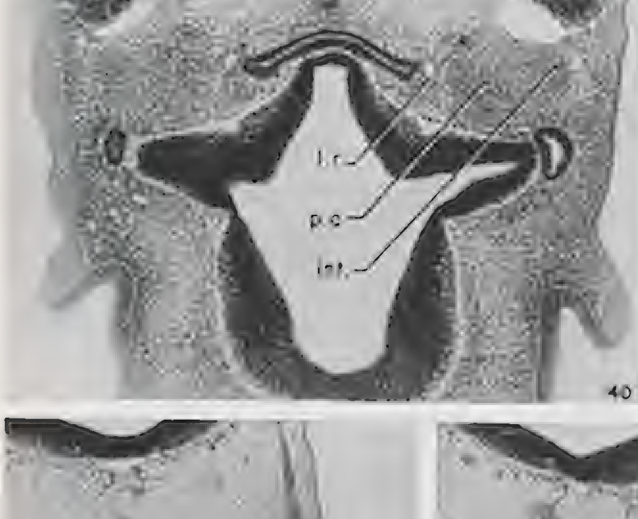

40

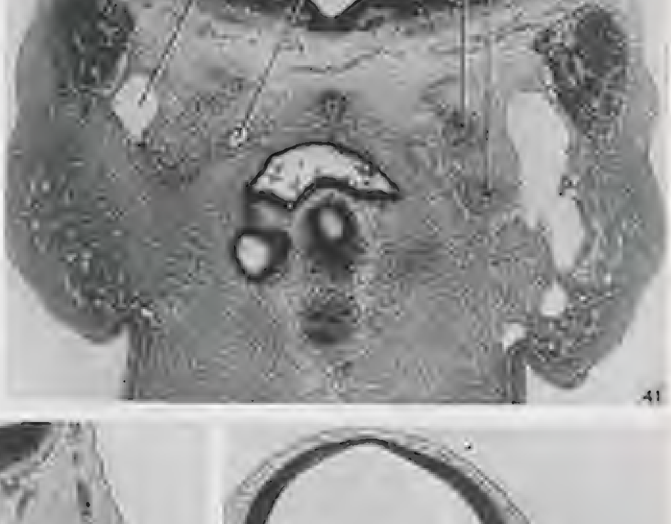

41

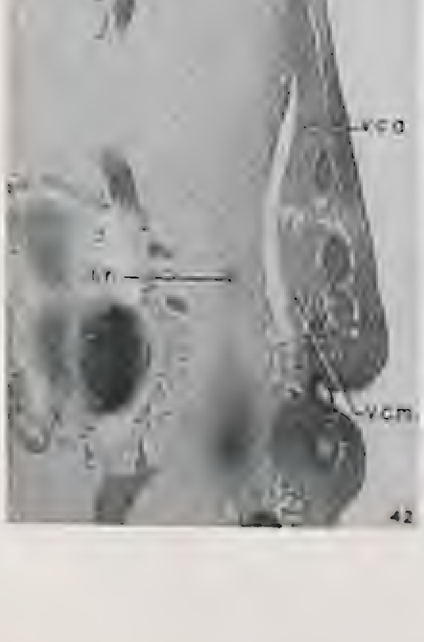

42

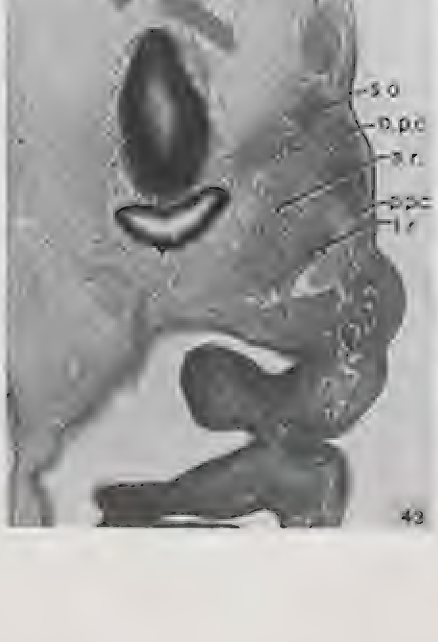

43

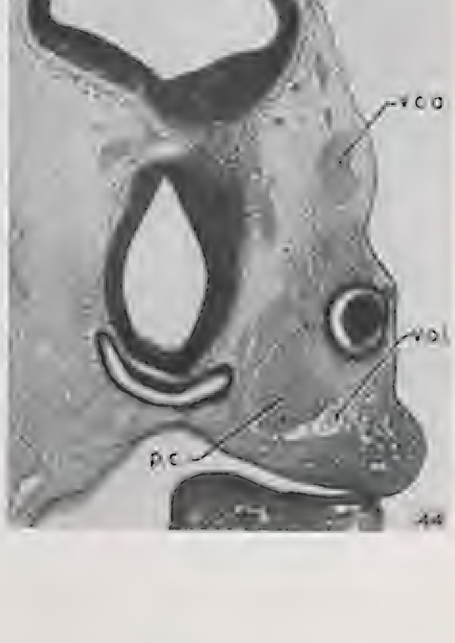

44

PLATE 10

FIG. 45. Frontal section, dorsal to the level of the eye, through the head of an embryo of horizon xvi. There is a common primordium at this stage for the inferior rectus and inferior oblique. No. 6507, section 8-2-7, ×24.

FIG. 46. Transverse section through the head of an embryo of horizon xvi. The denser condensation designated as the lateral rectus primordium forms the proximal part, whereas the less dense intermediate mass situated behind the eye contributes to the distal part, of the lateral rectus muscle. No. 6750, section 5-5-4, ×42.

Figures 47 to 50 are transverse sections, at four consecutive levels, through the head of an embryo of horizon xvi; figure 47 is most cranial. The relation of the lateral rectus primordium to the intermediate mass, the posterior peripheral condensation, and the premandibular condensation is illustrated.

FIG. 47. Caudodorsal end of the lateral rectus primordium, which is here penetrated by the abducens nerve. No. 6517, section 13-1-1, ×28.

FIG. 48. The dense lateral rectus condensation extends laterally in front of the fork in the vena capitis medialis and is continuous with the less dense intermediate mass of mesoderm situated medial and adjacent to the posterior peripheral condensation. No. 6517, section 13-1-6, ×28.

FIG. 49. Section adjacent to and below that illustrated in figure 48. Note the relation of the superior rectus primordium to the condensation which will form the proximal portion of the lateral rectus muscle. No. 6517, section 13-2-1, ×28.

FIG. 50. Section through the head some distance below that illustrated in figure 49. Cranial nerve III passes between the premandibular and lateral rectus condensations, and is a useful landmark at this level in delimiting the two condensations. No. 6517, section 13-3-1, ×28.

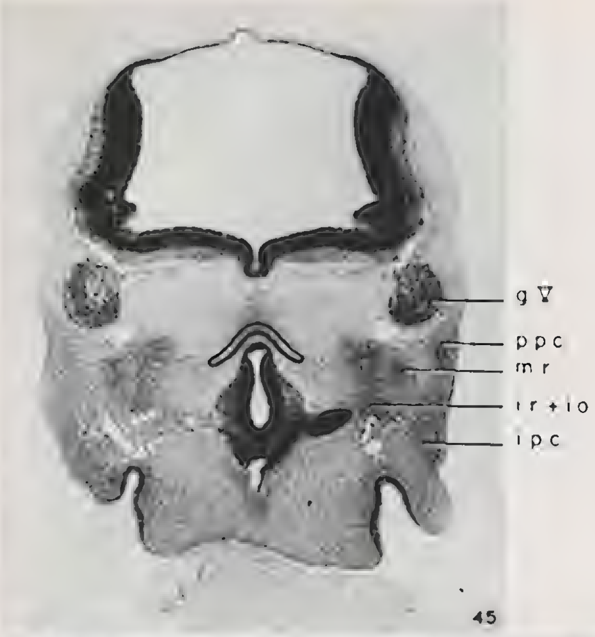

45

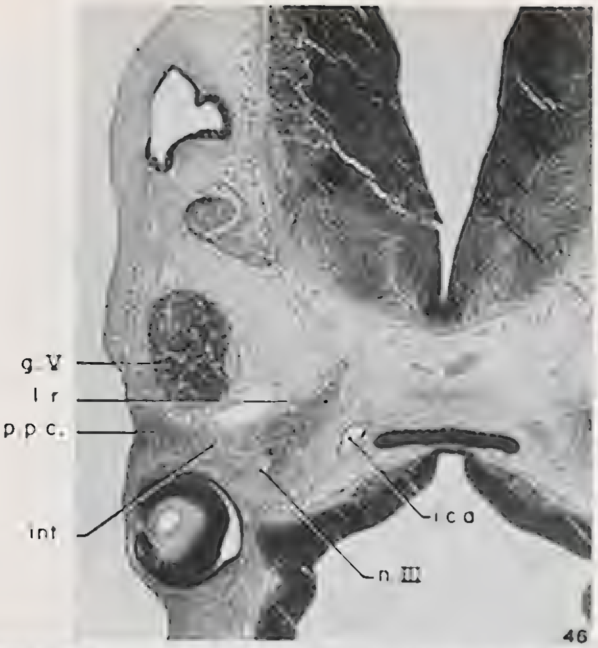

46

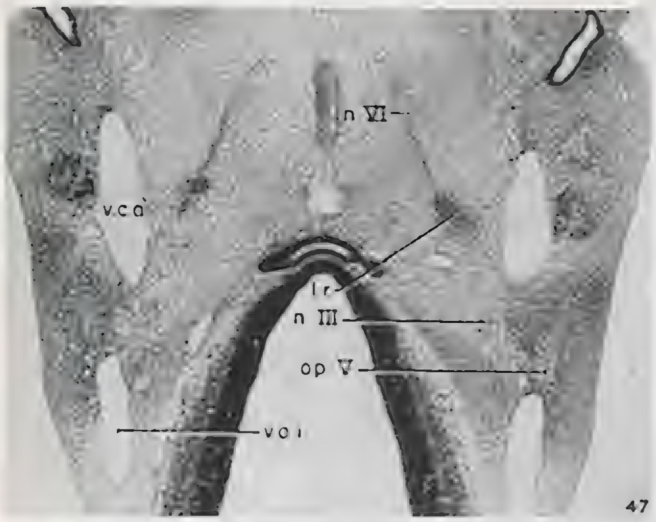

47

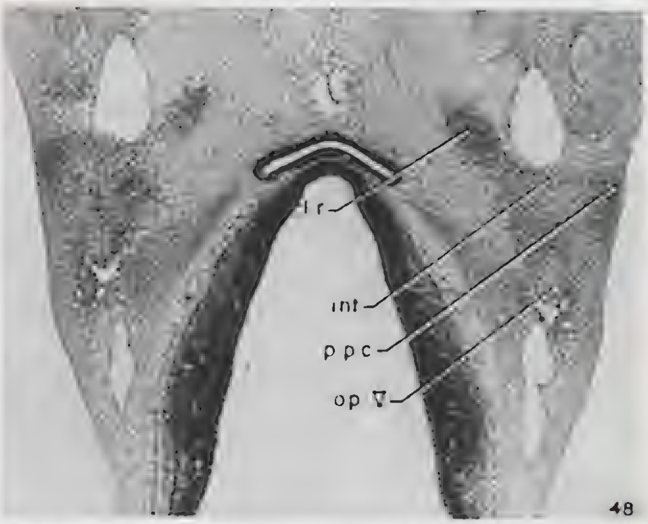

48

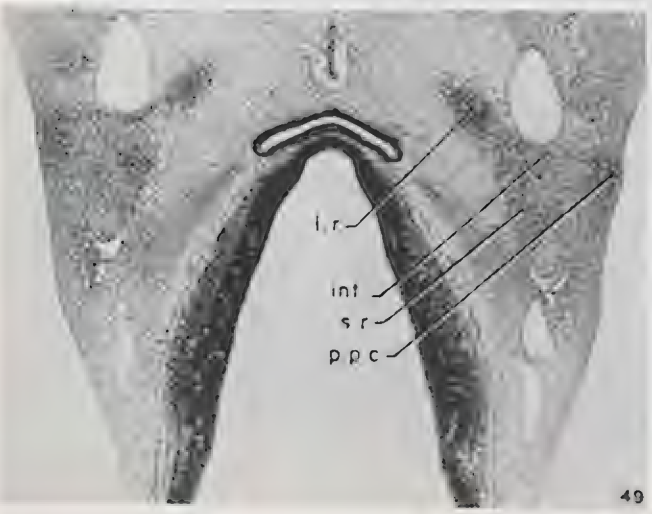

49

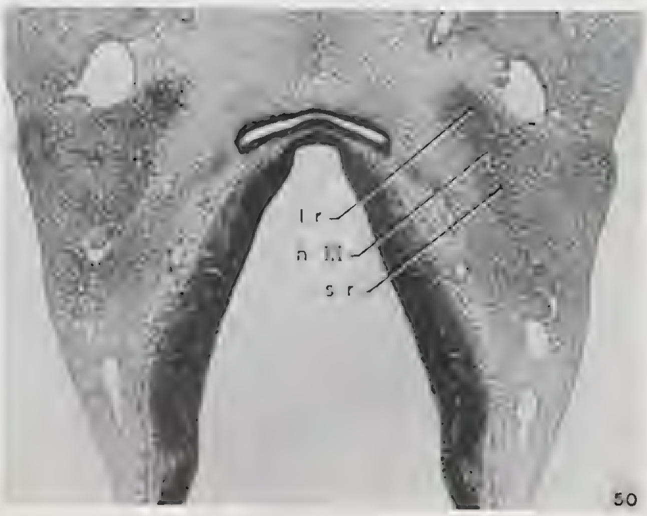

50

PLATE 11

FIG. 51. Parasagittal section through the head of an embryo of horizon xvi. At this level, the primordium of the superior oblique is situated adjacent and cranial to the superior peripheral condensation. No. 1197, section 7-2-2, ×28.

FIG. 52. Parasagittal section medial to that illustrated in figure 51. Three peripheral condensations are present at this level. No. 1197, section 7-3-2, ×28.

FIG. 53. Parasagittal section through the head of an embryo of horizon xvii. The four peripheral condensations, into which the four rectus muscles grow, are denser than in embryos of horizon xvi. No. 6519, section 8-1-1, ×28.

FIG. 54. Section medial to that illustrated in figure 53. Note the relation of the superior oblique primordium to the ophthalmic nerve and the superior peripheral condensation. No. 6519, section 8-2-4, ×28.

FIG. 55. Parasagittal section some distance medial to that illustrated in figure 54. Cranial nerve III passes between the proximal ends of the lateral and superior recti, and sends a branch ventrolaterally to supply the inferior rectus. No. 6519, section 12-1-4, ×28.

FIG. 56. Frontal section through the head of an embryo of horizon xvii. The inferior rectus condensation is continuous distally with the primordium of the inferior oblique. No. 6631, section 15-1-4, ×42.

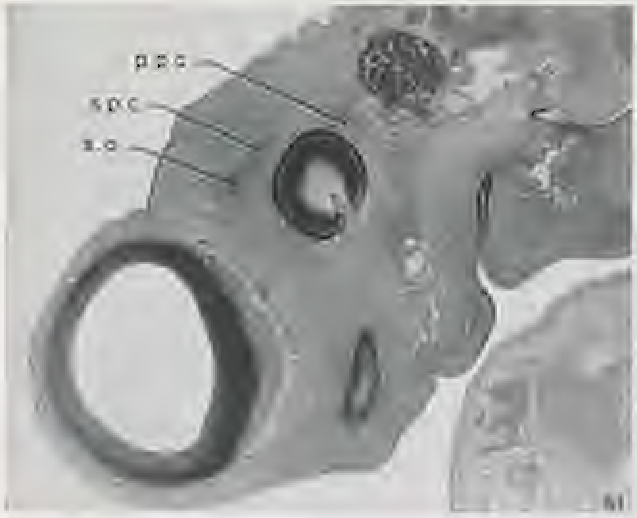
51

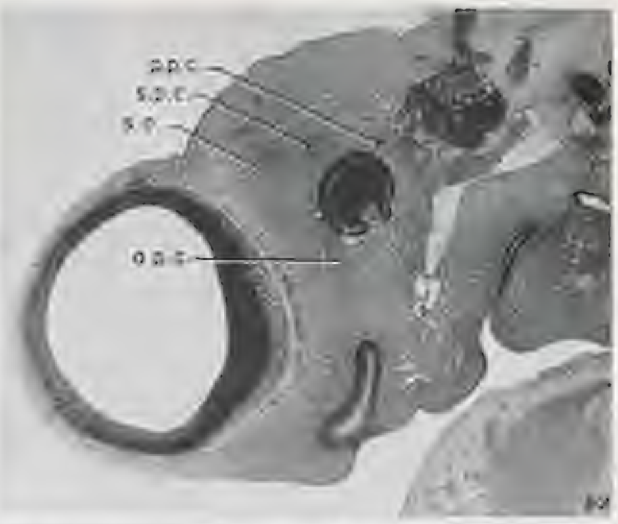
52

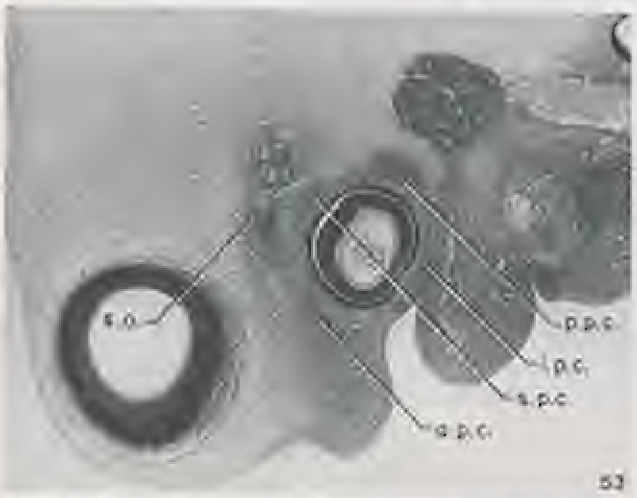
53

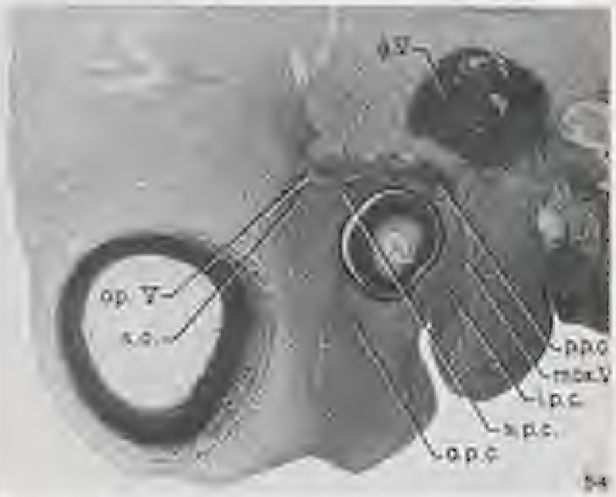
54

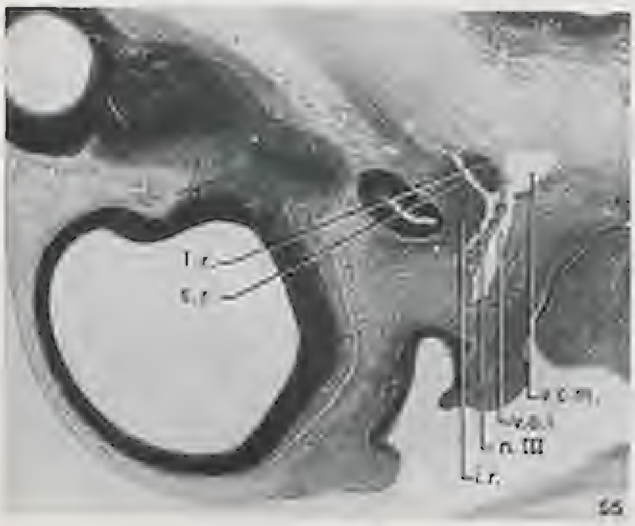
55

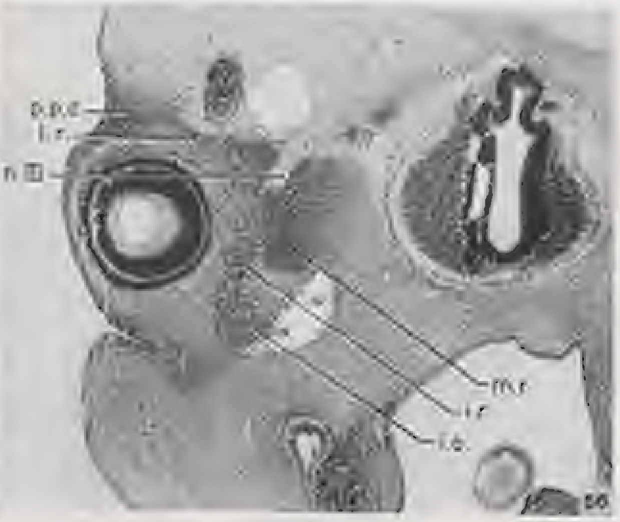
56

Plate 12

Figures 57 to 59 are transverse sections, at three consecutive levels, through the head of an embryo of horizon xvii; figure 57 is most cranial.

Fig. 57. Section through the lateral rectus and superior oblique primordia. No. 6258, section 11-2-2, ×28.

Fig. 58. Section passes through a plane about 60 microns above the eyeball. Note the location of cranial nerve III between the primordium of the lateral rectus and the superior rectus. The ophthalmic division of cranial nerve V divides at about this level into frontal and nasociliary branches. No. 6258, section 11-3-3, ×28.

Fig. 59. Section through the eye and four eye-muscle primordia. At this level the frontal branch of the ophthalmic nerve is intimately associated with the superior oblique primordium. No. 6258, section 12-1-5, ×28.

Figures 60 to 65 are frontal sections, at six consecutive levels, through the head of an embryo of horizon xviii; figure 60 is most ventral.

Fig. 60. Section through the superior oblique condensation near its insertion on the eyeball. No. 6522, section 25-1-4, ×28.

Fig. 61. Section through the superior oblique condensation proximal to that illustrated in figure 60. No. 6522, section 25-2-2, ×28.

Fig. 62. Section through the mid-part of the superior rectus and medial rectus primordia. No. 6522, section 27-2-2, ×28.

Fig. 63. Section through the eye at its greatest diameter. The relation of the superior rectus and medial rectus at this level to the optic stalk is illustrated. No. 6522, section 29-1-3, ×28.

Fig. 64. Section dorsal to the level of the optic stalk, illustrating the lateral rectus, which is now quite dense throughout its entire length. The lateral rectus is readily distinguished from the proximal ends of the oculomotor muscles, for cranial nerve III passes downward along its anterior surface. No. 6522, section 30-1-3, ×28.

Fig. 65. The primordium of the inferior oblique appears as a prominent condensation at the distal end of the inferior rectus. Subsequently, the connection between these two muscle primordia will become tenuous, and finally will disappear altogether. No. 6522, section 31-2-4, ×28.

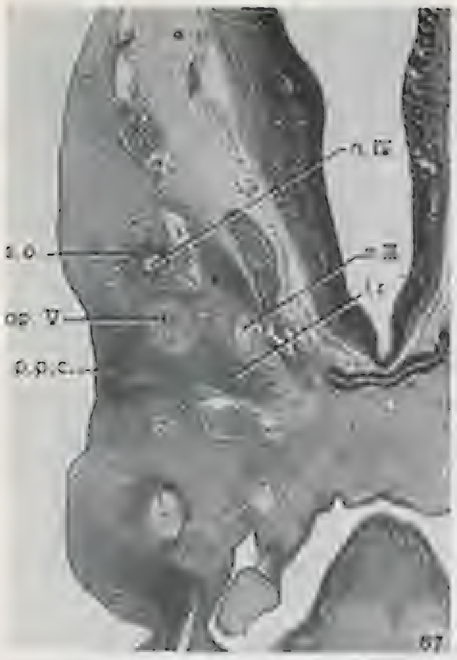
n.IV
s.o
n.III
op. V
i.r
p.p.c.
57

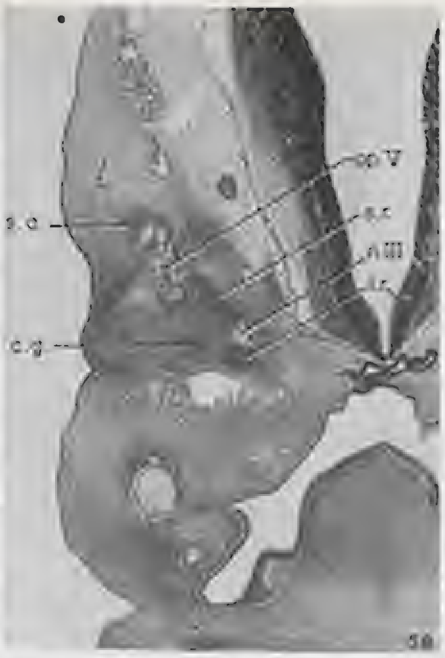
op.V
s.o
s.r
n.III
i.r
c.g
58

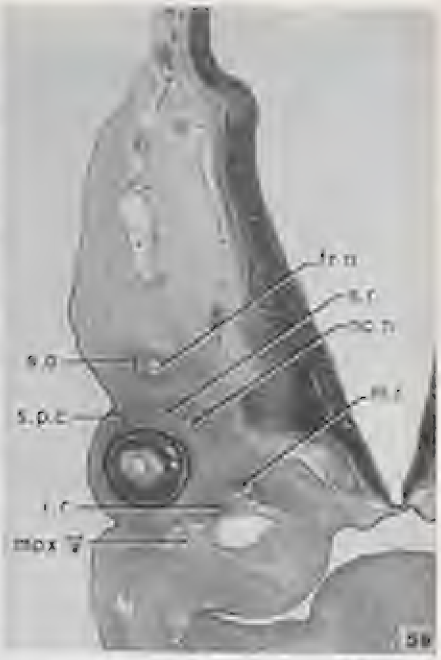
fr.n
s.r
oc.n
s.o
m.r
s.p.c
i.r
max V
59

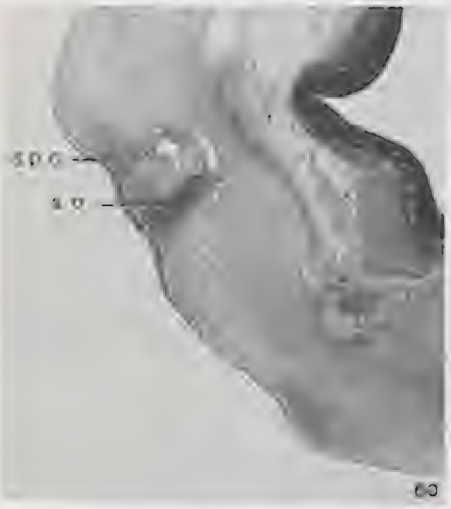
s.p.c
s.o
60

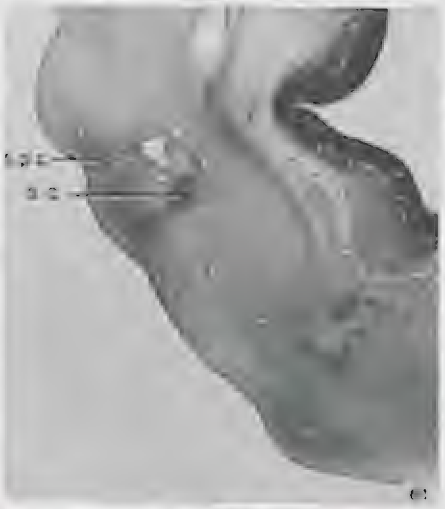
s.p.c
s.o
61

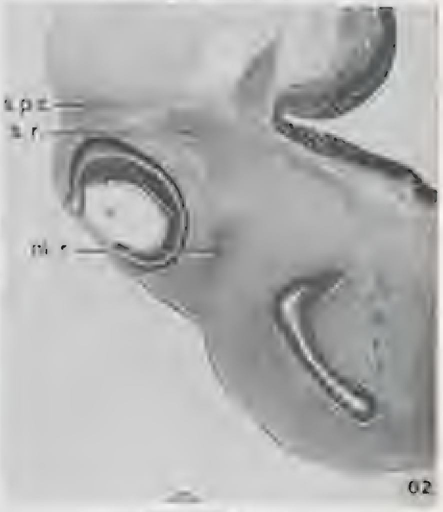
s.p.c
s.r
m.r
62

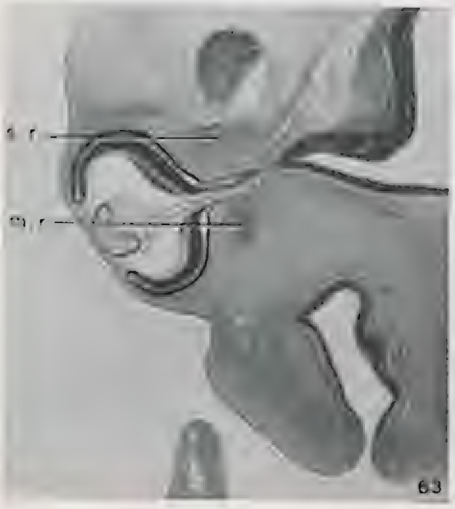
s.r
m.r
63

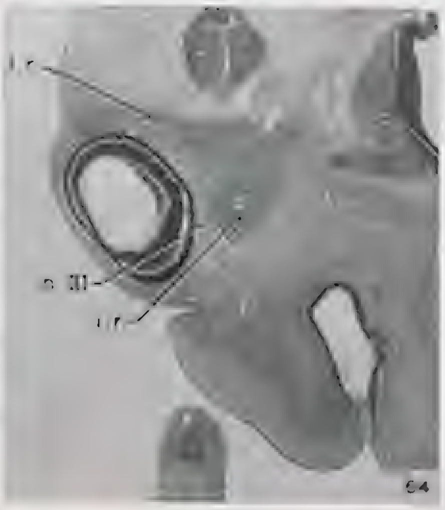
i.r
n. III
i.r
64

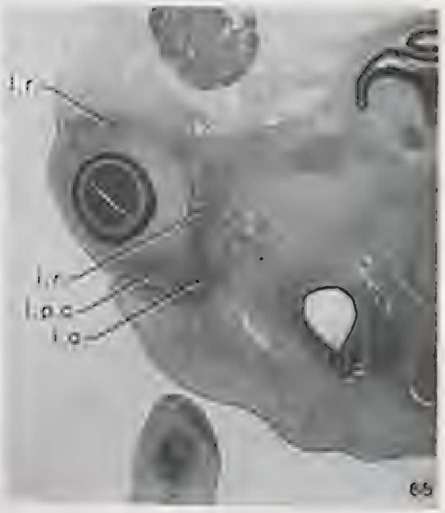
i.r
i.r
i.p.c
i.o
65

Plate 13

Fig. 66. Parasagittal section through the eye and Gasserian ganglion of an embryo of horizon xviii. At this level, cranial nerve IV sends a branch to the frontal division of the ophthalmic nerve, and then continues on to enter the superior oblique primordium. The proximal end of the superior rectus is characteristically wedged in between the frontal and nasociliary branches of the ophthalmic nerve. No. 6533, section 38-3-1, ×42.

Fig. 67. Parasagittal section through the optic stalk and Gasserian ganglion of an embryo of horizon xix. All the eye-muscle primordia are more dense and better defined than they were in horizon xviii. No. 1390, section 6-1-2, ×28.

Figures 68 to 70 are frontal sections through the head of an embryo of horizon xix. At this stage, the primordium of the inferior oblique has become more elongated, but is still attached to the distal end of the inferior rectus.

Fig. 68. Section through the inferior rectus, which is continuous with the club-shaped primordium of the inferior oblique. No. 5609, section 12-3-1, ×28.

Fig. 69. Section 50 microns caudal to the one illustrated in figure 68. At this level the long axis of the inferior oblique primordium is at almost a right angle to that of the inferior rectus, with which it still retains a tenuous connection. No. 5609, section 12-3-3, ×28.

Fig. 70. Section 50 microns caudal to that illustrated in figure 69. The inferior rectus extends outward to the inferior peripheral condensation, and the medial (origin) end of the inferior oblique has almost reached the orbital wall. No. 5609, section 12-3-5, ×28.

Fig. 71. Transverse section through the head of an embryo of horizon xxii. The peripheral condensations into which the four rectus muscles insert have spread over the optic vesicle to form part of the sclera. No. 8394, section 34-1-2, ×21.

Fig. 72. Transverse section through the head of an embryo of horizon xxiii. The levator palpebrae superioris has split off from the superior rectus, and extends as a thin sheet of muscle outward into the upper eyelid. Muscle fibers are present in all six eye muscles at this stage. No. 5154, section 53-1-3, ×21.

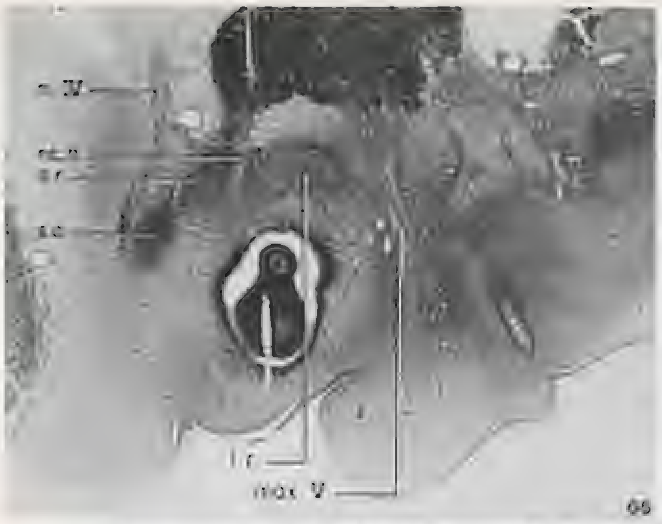

66

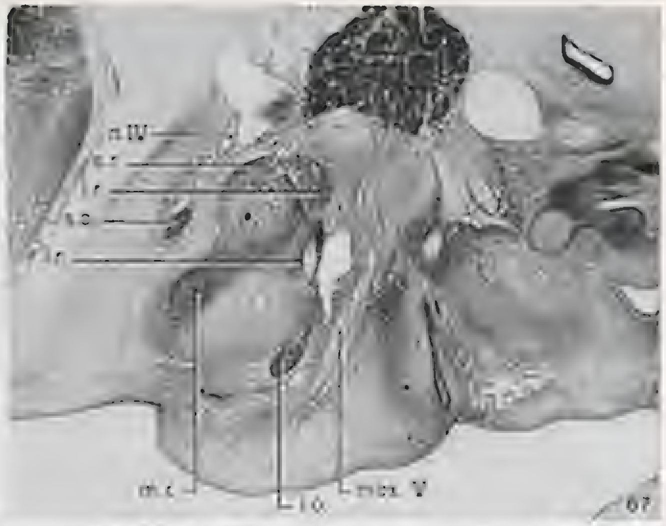

67

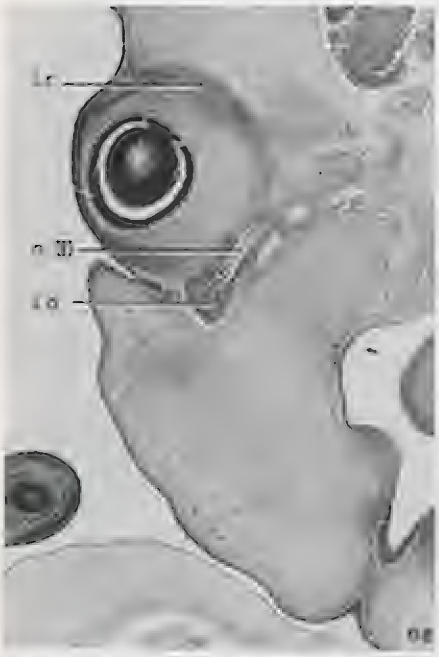

68

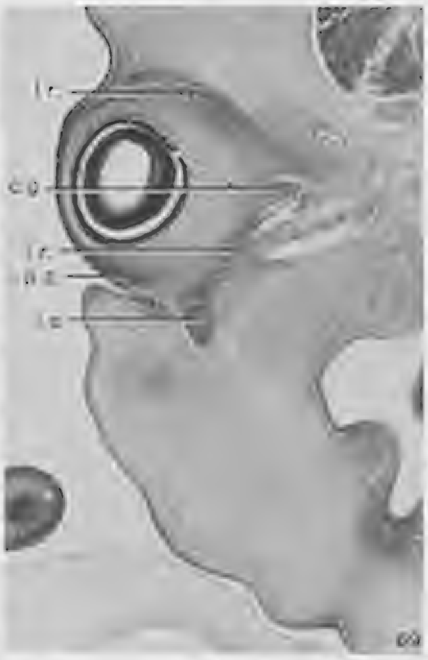

69

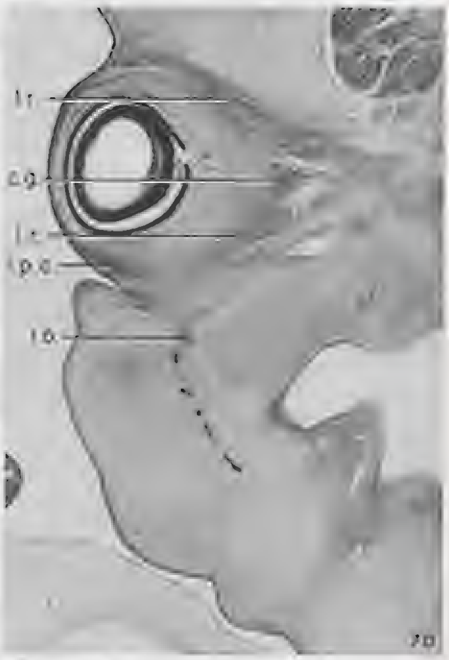

70

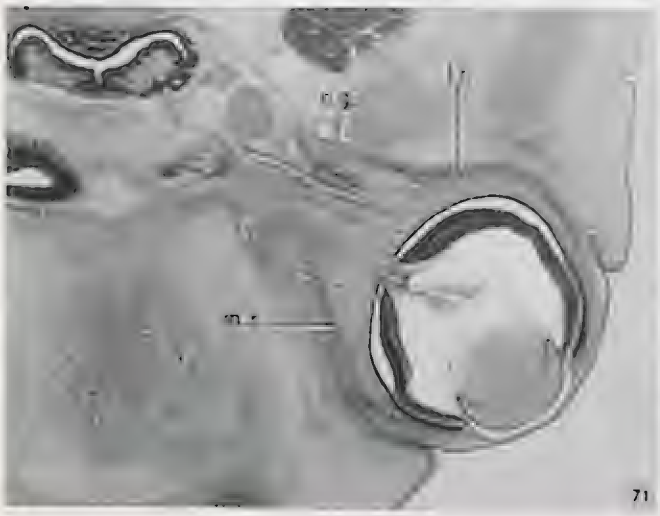

71

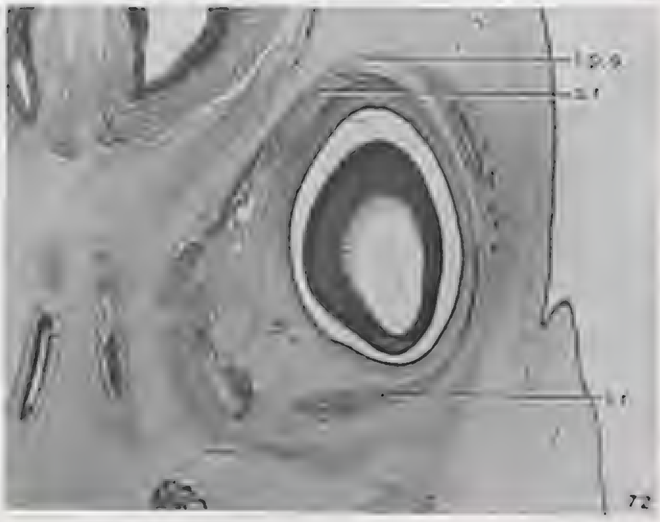

72

PLATE 14

Figures 73 to 79 illustrate stages in the development of the trochlea through which the tendon of insertion of the superior oblique muscle passes.

FIG. 73. Parasagittal section through the head of an embryo of horizon xx. The trochlea and enclosed superior oblique tendon are transected at this level. No. 431, section 16-1-2, ×28.

FIG. 74. Frontal section through the head of an embryo of horizon xx. The trochlea has not yet thickened appreciably. No. 4059, section 28-4-3, ×28.

FIG. 75. Transverse section through the head of an embryo of horizon xxii. This unusual section passes through almost the entire length of the superior oblique muscle. The inner wall of the trochlea is noticeably thicker than it was in embryos of horizon xx. The angle formed by the tendon of insertion with the main belly of the superior oblique muscle at the trochlea (trochlear angle) is approximately 95°. No. 8394, section 34-2-3, ×21.

FIG. 76. Transverse section through the head of an embryo approximately 9 weeks of age. The trochlea is now very thick, but as yet contains no fibrocartilage. No. 9226, section 71-1-4, ×17.

FIG. 77. Transverse section through the head of an embryo of horizon xxiii. The tendon of the superior oblique is sectioned longitudinally at the trochlea; the curve which it describes as it passes through the trochlea is clearly illustrated. The eye is now covered with a well defined sclera, into which all six eye muscles insert. No. 5154, section 57-2-1, ×21.

FIG. 78. Sagittal section through the head of an embryo approximately 9 weeks of age. The section cuts the belly of the superior oblique muscle longitudinally, and its tendon of insertion, as it passes through the trochlea, transversely. No. 5017, section 43-2, ×4.

FIG. 79. The superior oblique muscle, its tendon, and the trochlea, illustrated in figure 78, are here enlarged. The posterior side of the trochlea is noticeably thicker than it was in earlier horizons; the tendon of insertion of the superior oblique is now very dense and compact. No. 5017, section 43-2, ×17.

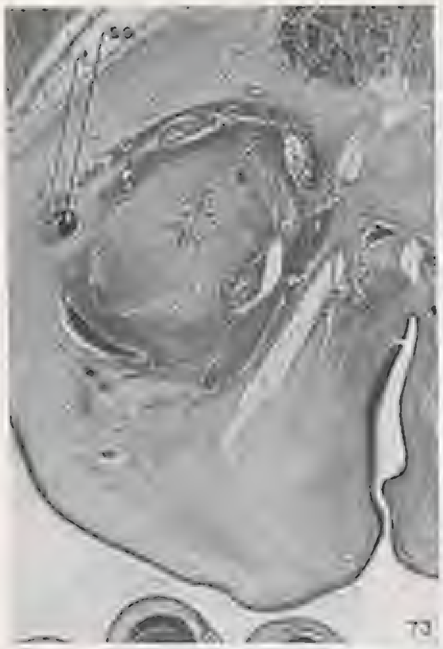

73

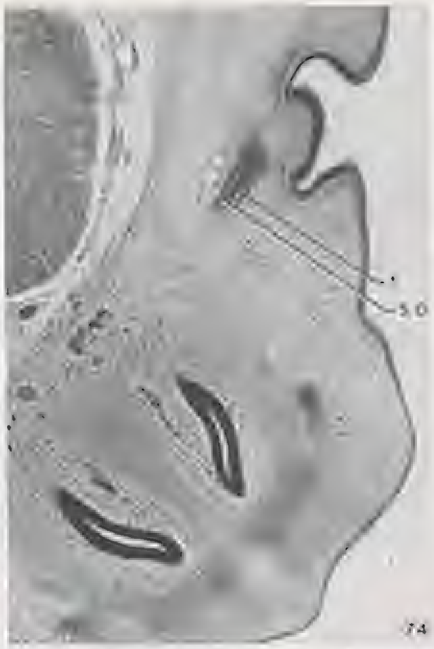

74

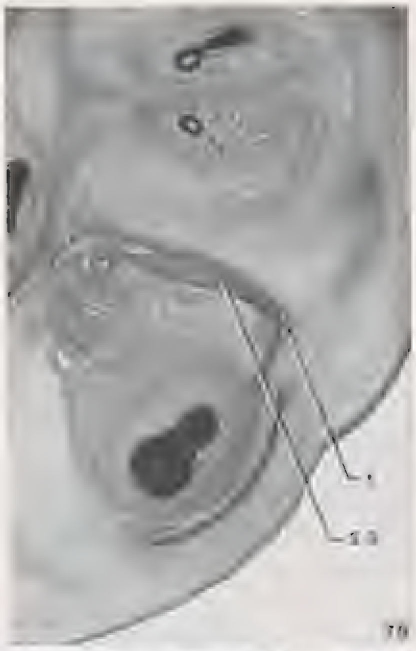

75

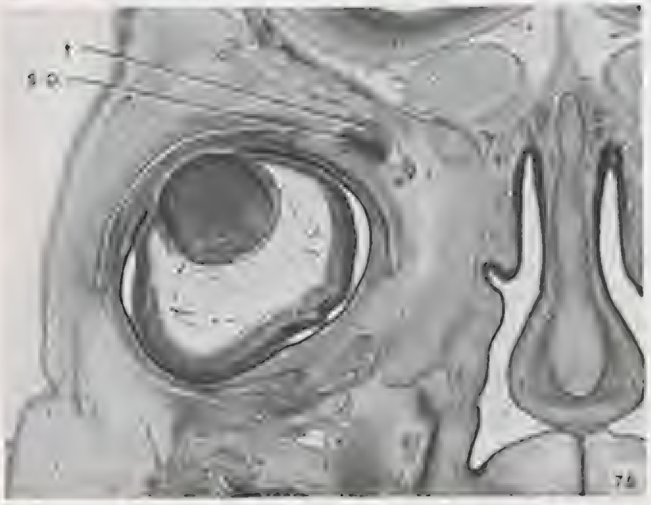

76

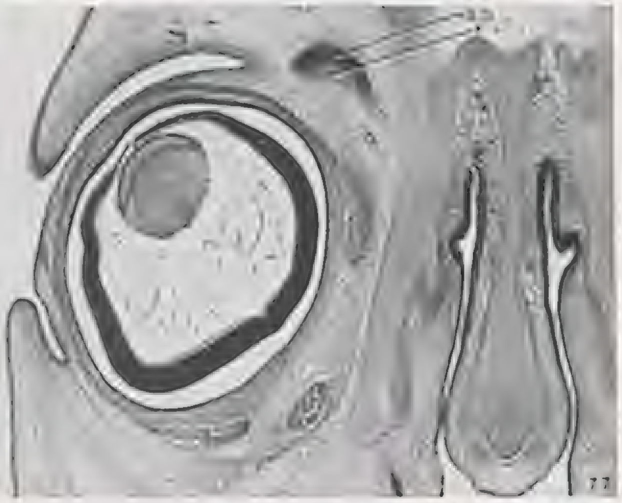

77

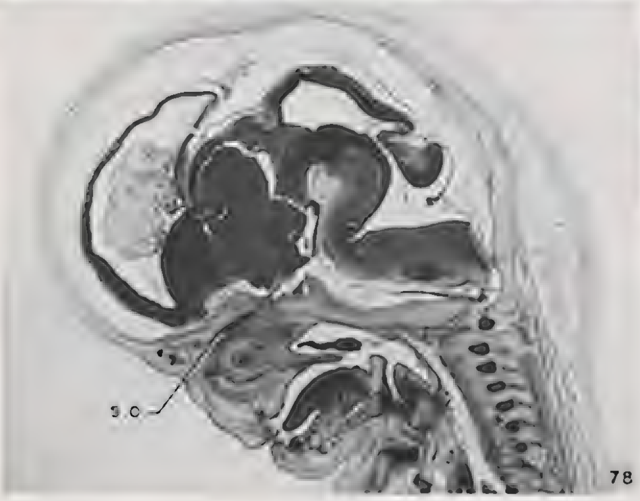

78

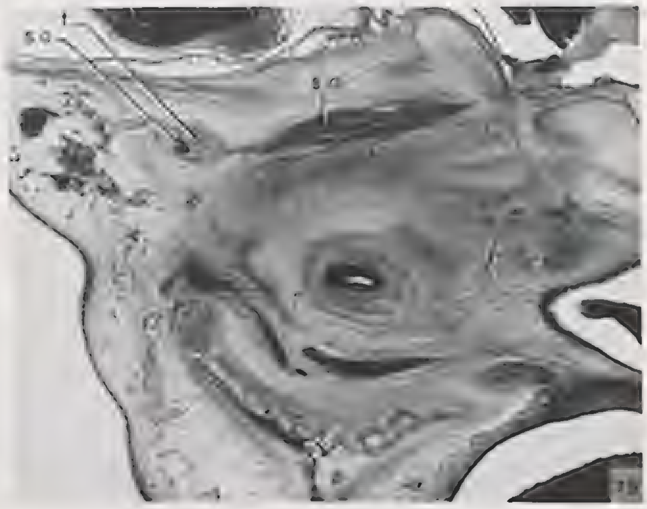

79

CONTRIBUTIONS TO EMBRYOLOGY, NO. 247

THE DEVELOPMENT OF THE CRANIAL VENOUS SYSTEM IN MAN, FROM THE VIEWPOINT OF COMPARATIVE ANATOMY

Dorcas H. Padget

Department of Embryology, Carnegie Institution of Washington, Baltimore;
Division of Neurological Surgery, University of Maryland
School of Medicine, Baltimore

With six plates (two colored) and eighteen text figures

CONTENTS

PAGE

Introduction 81

Embryonic Stages of Development 82
- Stage (1 and) 2. Embryos of Horizon XIV (5 to 8 mm.) 82
  - Primary Head-Sinus Continuous with Anterior Cardinal Vein 83
    - Tributaries of Anterior Cardinal System 83
- Stage 3. Embryos of Horizons XV, XVI (6 to 12 mm.) 86
  - Elaboration of Dural Channels Joining the Head-Sinus; Initial Pia-arachnoidal Tributaries 86
  - Primitive Internal Jugular Vein 88
- Stage 4. Embryos of Horizons XVII, XVIII (10 to 16 mm.) 89
  - Principles Governing the Formation of Veins Draining the Neural Tube 92
    - Relation of Pial Veins to the Arteries 93
- Stage 5. Embryos of Horizon XIX (16 to 21 mm.) 97
  - Involution of Primary Head-Sinus, Paralleling Formation of the Sigmoid Sinus 97
  - Primary Extracranial Veins 100
- Stage 6. Embryos of Horizons XX, XXI (18 to 26 mm.) 101
  - Pro-otic and Tentorial Sinuses 101
  - Asymmetry of Venous Channels, Notably in the Tentorial Plexus (Torcular) 104
  - Modification and Reduction of Pia-arachnoidal Veins 105
  - Emergence of External Jugular System; Facial Veins 107
- Stage 7. Threshold of Fetal Period (ca. 2½ mos. and 40 mm.) 109
  - Superior Sagittal Sinus and Primitive Galenic System 109
  - Inferior Petrosal and Cavernous Sinuses 112
  - Modifications of Intra- and Extra-cranial Channels 113
  - Veins of Orbit 114
  - Emissary Veins 116
  - Meningeal Drainage of Primary Membrane Bones; Independent Scalp Plexus 117
- Stage *7a*. Fetus at the Third Month (60 to 80 mm.) 120
  - Significance and Modifications of the Tentorial Sinus 120
  - Significance and Modifications of the Pro-otic Sinus and Its Tributaries 122
    - Superior Petrosal Sinus 122
    - Petrosquamosal Sinus, an Emissary of the Chondrocranial Spurious Jugular Foramen 123
    - Relation of Dural Meningeal Sinuses to the Arteries; Other Venous Channels Fundamentally Extrachondrocranial 126
  - Formation of the Basal Cerebral Vein 128
    - Variable Lateral Outlet of Basal Vein 132
  - Cerebellar Veins 132

Summary 134

Addendum 136

Literature Cited 137

List of Abbreviations in Figures 139

THE DEVELOPMENT OF THE CRANIAL VENOUS SYSTEM IN MAN, FROM THE VIEWPOINT OF COMPARATIVE ANATOMY[1]

INTRODUCTION

The present communication is the logical outcome of the author's companion study of the development of the cranial arteries in the human embryo (Padget, 1948, 1954). Following a pioneer report on the developing vasculature of the brain in man (Mall, 1904), there appeared the major contributions of Streeter (1915, 1918), which have been regarded as authoritative and are widely quoted. Streeter was chiefly concerned, however, with the dural sinuses as illustrative of fundamentals of the vascular apparatus dependent on changing factors in its environment (1918), and dealt only incidentally with the veins (and arteries) of the brain and extracranial parts. Although the present survey was begun to supplement Streeter's work, it became apparent that his interpretations regarding several important vessels could not be accepted. Near the close of the present author's study, attention was directed to a monograph on the development of the dural sinuses and vessels of the human brain by Markowski (1922), which work, essentially completed but delayed in publication, had been summarized earlier (1911). His detailed contribution was buried as a supplement to a relatively inaccessible journal and suffers in contrast to Streeter's exposition (1918) embellished with colored plates by James Didusch. Owing chiefly to the limitations of Markowski's illustrations (meager diagrams, 1911, plus photographs of sections and of models in color, 1922), his reports may not be fully understood except by one familiar with comparable embryos. With such material at hand, however, the author had come, independently, to similar conclusions regarding the identity of certain vessels. Furthermore, the points of agreement with Markowski coincided with some of the points of disagreement with Streeter. The present extended observations have shown in general that the developmental pattern, both phylogenetic and ontogenetic, of the whole cranial vasculature, especially of the venous part, must be visualized in order to prevent misconceptions regarding its subdivisions in embryonic or mature specimens.

The fact that there has long been wanting a comprehensive account of the veins of the head region is readily explained. Many vessels, together with the common variations of venous patterns, can be comprehended only from the comparative standpoint of their evolution in other vertebrates. Moreover, there is no overstatement in Mall's picturesque comment that the "history of the arteries is relatively simple when compared with the gyrations the veins undergo."

In respect to the arteries, the author was forearmed, from the literature and from personal observation, with a reasonably wide knowledge of the human adult configuration and its variations. For many reasons, similar knowledge of the venous system is less readily available. Routine removal of the brain from the skull tears the delicate veins that connect the pial and dural systems; careful removal to identify each connection is both difficult and time consuming. A number of the large but thin-walled veins are buried under the arteries in the great cerebral fissures, so that a considerable resection of brain tissue is necessary for their exposure. The blood, or even certain types of injection material (e.g. ink), may not always fill or be retained in all parts of a continuous channel, owing to uneven compression of the more deeply situated veins by the brain, before or after fixation. In either infant or adult, though for different reasons, a complete dissection of the dural channels at the base of the skull is difficult; the obstructing bone is densely adherent to the dura around the nerves and certain related vessels (Walker, 1933). To supplement observations on adult heads, a number of infants, in which the delicacy of the skull bones somewhat offsets the disadvantage of minute vessels, were dissected with the original intention of establishing a norm for the adult pattern. Although the present evidence is limited, it is apparent that at birth certain important venous channels differ from the adult configuration as generally described. Added to this unexpected finding were the differences in certain details found in embryos and fetuses of the same age group.

In spite of the confusion presented at the outset by all these factors, the constant comparison of embryonic, infant, and adult patterns, supplemented by what is known of other species, gradually clarified the picture, and what may be called, at least tentatively, a typical configuration in each case finally emerged. Attention is directed to a publication concerning obscure features of the adult pattern in man from the developmental point of view (Padget, 1956); this article includes a discussion of embryologic considerations regarding the origin of congenital arteriovenous aneurysms.

The final problem in the present study was the adequate pictorial presentation of the material within the limited number of figures. When preparing some of

---

[1] This work was primarily aided by grants made through Dr. George W. Corner by the Life Insurance Foundation, 1946–1950, and by a fellowship granted to the author by the Carnegie Institution of Washington, 1950–1953; it was completed in the Division of Neurological Surgery, University of Maryland School of Medicine, with aid from the Hoffberger Fund.

the illustrations, the author was faced with a choice between showing the complete or exact graphic reconstructions, which were too complicated to be readily understood, and risking errors of personal judgment by conversion to a semidiagrammatic picture. The resulting compromise makes no undue sacrifice to either clarity or accuracy.

Most of the material for this study was provided by the Carnegie Collection of Embryos, many being the same ones used in the earlier study of the arteries. From enlarged photographs of serial sections, graphic reconstructions were prepared in the three standard planes: lateral, horizontal, and coronal. Because of variations in details, it was necessary to compare the findings in more embryos of each stage than for the arteries, and more than 65 views of over 30 specimens were prepared. Dissections and sketches were made of 10 late fetal and newborn heads (3 were injected); a similar study of about 15 adult heads was possible through the courtesy of Dr. Allan L. Grafflin of the Johns Hopkins School of Medicine. Much appreciation is expressed to Dr. E. Carl Sensenig of the University of Alabama for helpful suggestions, and to Dr. George W. Smith and Mr. Carl W. Mueller, who facilitated study of their excellent corrosion preparations of the adult made in the department of Professor Eduard Uhlenhuth of the University of Maryland School of Medicine. (Unusually informative demonstrations of venous channels in several skulls were obtained by latex injections followed by digestion of the soft parts.) The essential comparative information, when not provided by the literature, was supplemented by study of several adult mammals, regarding which especial gratitude is expressed to the following: Dr. Karl R. Reinhard of the National Biological Institute, for the loan of many photographs of injected dog heads prior to his published report; Dr. David Bodian of the Department of Epidemiology, Johns Hopkins University, for specially prepared heads of the rhesus monkey; Dr. and Mrs. Frederic A. Gibbs of the University of Illinois College of Medicine, who sent a collection of their venous injections of the cat head. The author is particularly indebted to Dr. George W. Corner, who obtained the special grants for this study, and to Dr. George W. Bartelmez for his gracious help in review of the manuscript.

EMBRYONIC STAGES OF DEVELOPMENT

It was desirable to divide the complex process of venous differentiation in the head and neck into eight stages, including the postnatal pattern; the process can be summarized in eight illustrations to permit correlation with the arteries of this region.[2] Although arterial development falls naturally into this subdivision, based on essentially one specimen of a single age group, the prolonged emergence of definitive venous channels covers a considerably wider range of older embryos and must be more arbitrarily fitted into the classification. Actually, reduction to eight basic illustrations is feasible only for the lateral view (pl. 1); more figures are needed to show the most important changes in the vessels as viewed at the base of the brain and skull (pl. 2). The introductory text figures for each stage, showing its typical pattern in correlating lateral and basal views, in some instances are simplified composites of several embryos of the age group, necessitated by certain variations in detail. Furthermore, a designated venous stage sometimes covers two age groups, because the arteries resemble the adult conformation much earlier than do the veins, at about 40 and 80 mm., respectively; several important anastomoses typical of adult sinuses usually do not appear until after birth. Since the formation of venous channels depends upon the more precocious arteries, certain major arteries are shown in most of the text figures. As each important sinus or vein becomes definitive, its name, whether that of a temporary embryonic or a permanent adult vessel, is emphasized by italics. The Roman numerals refer to the developmental horizons (age groups) determined by Streeter (1942–1951) for the Carnegie Collection of Embryos that are less than 40 mm. in crown-rump length.

STAGE (1 AND)[2] 2. EMBRYOS OF HORIZON XIV
(5 TO 8 MM.)

The first stage fully described in the present series (fig. 2), and comparable to stage 2 of arterial development, consists of a relatively simple vascular plan. This plan, like that of earlier stages (fig. 1), is typical of vertebrate embryos: for instance, reptiles (Grosser and Brezina, 1895); birds, represented by the chick (Hughes, 1934, and others); and mammals like the bat (Grosser, 1901) and pig (Sabin, 1917). The head in stage 2 shows the three constant pharyngeal bars ("branchial" or "visceral arches"), namely the mandibular, hyoid, and glossopharyngeal, each with its contained cranial nerve. Subdivisions of the human neural tube at this stage indicate the five parts of the brain: the telencephalon and diencephalon (derived from the prosencephalon), the metencephalon or midbrain, the metencephalon and myelencephalon (derived from the rhombencephalon). Stage 2 is characterized by the indentation of the ectodermal lens vesicle within the optic cup. The internal carotid artery now supplies the fore parts of the brain by way of its cranial (anterior and middle cerebral) and caudal (posterior communicating) divisions, and the basilar artery is emerging by consolidation of bilateral neural arteries. The veins are relatively much less mature.

---

[2] It was not expedient in the present account to depict the exact venous pattern for vascular stage 1 (horizon xiii) as previously designated for the arteries. Its essentials, however, are present earlier, as described for horizon xii (fig. 1B). To avoid repetition, the reader is asked to assume henceforth that any undocumented reference to the arteries is to the author's 1948 monograph.

Primary Head-Sinus Continuous with Anterior Cardinal Vein

The head is drained by the anterior cardinal vein (future internal jugular vein), which meets the posterior cardinal vein from the body to form the common cardinal vein (duct of Cuvier), entering the sinus venosus of the primitive heart. Caudal to the 10th and 12th nerve roots, in embryos younger than stage 2, the anterior cardinal is continuous with a channel that lies not only medial to all the cranial nerve roots but, more importantly, directly upon the neural tube (fig. 1A). Although once considered part of the anterior cardinal vein, or called the "vena capitis medialis," this channel antedates the time of true circulation in the head. It is transitory, and is fundamentally the proliferative endothelial material from which both pial arteries and veins are soon derived. For these reasons it was renamed the *primordial hindbrain channel* ("primitive rhombencephalic vessel" of Sabin, 1917) by Streeter (1918).

By stage 2 (fig. 2), the medial primordial channel has disappeared, but has given origin to a definitive venous channel in a more lateral position. This channel is still medial to the 5th and 10th nerves, but is outside the 7th, 8th, and 9th nerves and the otocyst. It constitutes the first true drainage channel of the craniocervical region. Formerly called the "vena capitis lateralis," the new channel was renamed the "primitive head vein" by Evans (1912), and the "primary head-vein" by Sabin and by Streeter; in birds and mammals, it has also been called the "primary Stammvene" (van Gelderen, 1924; Hughes, 1934). These terms refer to the cranial part, as opposed to the future upper-cervical part, of the "anterior cardinal vein" designated by certain other writers.

The precise naming of embryonic vessels often presents a problem, not clearly resolved in this instance. The old designations, "medialis" and "lateralis," are often used for the most primitive head-veins of vertebrate embryos, but may be confusing unless it is realized that the later channel ("lateralis"), though lateral to the earlier channel ("medialis"), is not necessarily lateral to the nerve roots; for instance, "medialis" has been applied to the part of the secondary channel, i.e. "lateralis," which always lies medial to the 5th nerve root. Regarding the most recent terms noted above, which have the weight of distinguished authority, one must be careful to differentiate exactly in early embryos between the primordial hindbrain channel medial to all the nerve roots (horizon xi, fig. 1A), and the later "primary head-vein," which is medial to the 5th and 10th (horizons xii to xiv, figs. 1B, 2). Both have been observed simultaneously in the chick and pig injected *in vivo* (Sabin). The primordial channel can be identified by the fact that it lies directly upon the neural tube and is usually represented after horizon xii only by veins (and arteries) of the pial layer. In contrast, it is soon seen that the "primary head-vein," even when it remains medial to certain nerve roots, is dural in position. Since the present account emphasizes the distinction between vessels of the dural and pial layers, and since Streeter designated the dorsal tributaries of the "primary head-vein" as "dural" at this stage (see below), this vessel will henceforth be called the *primary head-sinus* (figs. 1B, 2).

Tributaries of anterior cardinal system. Only the major tributaries of the primary head-sinus are shown in the present illustrations. It must be understood that most of the neural tube is covered by a primitive capillary plexus (Padget, 1956, figs. 24, 27), as is well shown in the colored plates of Sabin and Streeter. This plexus drains laterally, at the dorsolateral aspect of the neural tube, into a more superficial venous plexus, which in turn drains into the head-sinus through three well defined stems in the future dural layer. Having a relatively constant relation to the nerve roots, these stems were called the "anterior, middle, and posterior cerebral veins" by Mall (1904), terms commonly used for other vertebrate embryos. The designation "vein," however, is misleading, for several reasons. The so-called "middle cerebral vein," for example, has nothing to do with the adult veins of the same name, which are derived later from the so-called "anterior cerebral vein" of this stage. In reference to the human embryo, Streeter grouped the superficial plexus drained by these "veins" of stages 1 and 2 into three parts, the *anterior, middle,* and *posterior dural plexuses.* The first part drains the forebrain and midbrain; the middle part, the future cerebellar region; and the last part comes from the medullar region near the 10th nerve root. For simplicity, the terminal "vein" draining each plexus may be called the *anterior, middle,* or *posterior dural stem,* and figures 1B and 2 show the levels relative to the nerve roots at which each joins the head-sinus. Since the three stems have important roles in the shaping of the adult dural sinuses and seem to be typical in the vertebrate line, their fate is of considerable interest phylogenetically.

At stage 2, only one noteworthy ventral tributary of the primary head-sinus appears. Typically, this vein is as prominent in young vertebrate embryos as the better-known dorsal tributaries just named, and ramifies extensively in the emerging maxillary process. It drains the ventrocaudal aspect of the optic vesicle at the lens pit through lateral tributaries, and the olfactory region, cranial and lateral to Rathke's pouch, through a medial vessel. The name *primitive maxillary vein* (cf. illustrations of chick and pig embryos in Sabin, 1917) is used

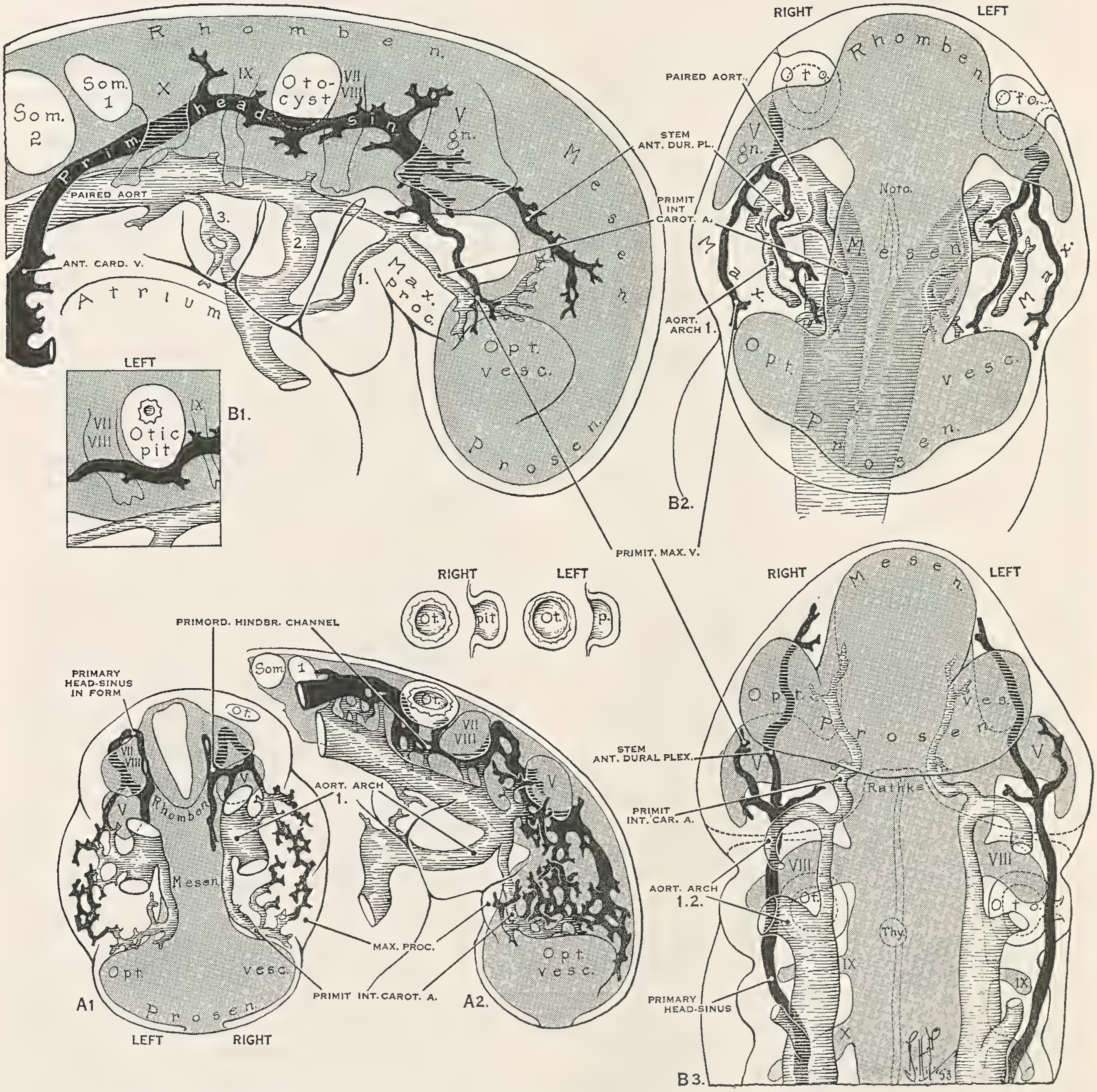

Fig. 1. Graphic reconstruction of two embryos of two stages earlier than those chiefly constituting the present series. A1, 2 (Carnegie no. 2053, 20 somites, xi) and B1, 2, 3 (no. 5923, 28 somites, xii) show the development of the primary head-sinus from the primordial hindbrain channel, and the emergence of the maxillary vein as drainage for the optic vesicle, supplied by the primitive internal carotid. Some asymmetry (see stage 6) appears as the result of moderately advanced development of certain right-sided structures: the maxillary process (A1, B2), degree of closure of the otic pit (A2, B1, 2), and the trigeminal ganglion (B2, 3).

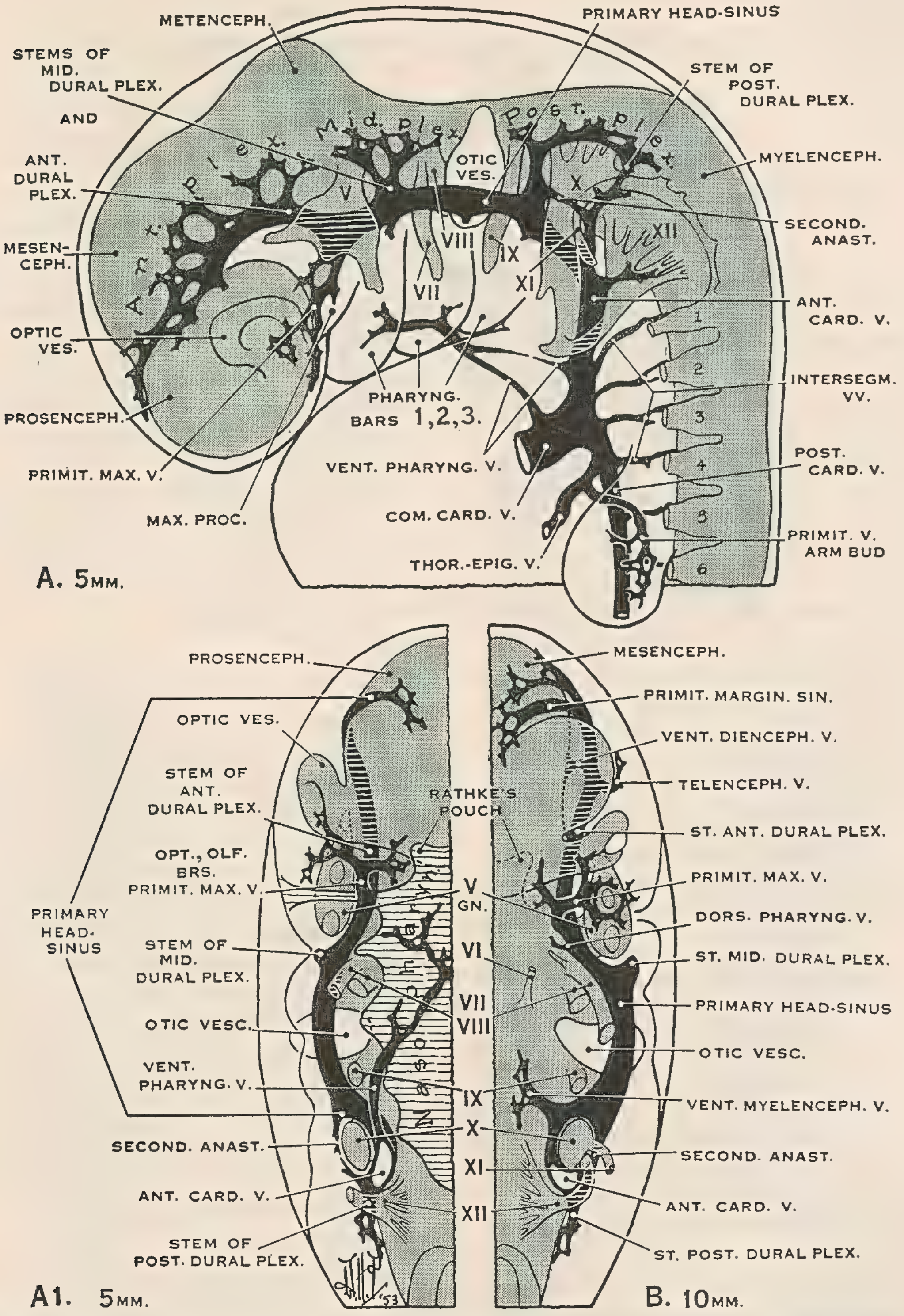

FIG. 2. Vascular stage 2 (which begins the present series) is typical of vertebrate embryos. The head-sinus, a lateral derivative of the primordial hindbrain channel (fig. 1), drains the brain through three stems consistent in their relation to the nerve roots. The optic vesicle is drained by the maxillary vein (cf. fig. 1), medial to the 5th nerve ganglion. A ventral pharyngeal vein primarily curves around the heart (fig. 1) to join the common cardinal, but soon migrates cranially upon the anterior cardinal vein (A). B shows the increased curvatures of the head-sinus and the definition of its initial pia-arachnoidal tributaries, coincident with expansion of the brain and otocyst in stage 3. (Crown-rump lengths in this and the other introductory illustrations of the typical pattern in each stage are approximate.)

here in preference to "infraorbital" or "ophthalmic" used by other writers, if they name it at all.

The primary significance of the maxillary vein is better understood by a glance at embryos younger than the stage under discussion. In embryo Carnegie no. 5923 of horizon xii (fig. 1B),[3] the primary head-sinus, recently derived from the primordial hindbrain channel, lies in its more primitive position medial to the 5th and 10th cranial nerve roots, and has just by-passed laterally the otic vesicle together with the acousticofacial and glossopharyngeal nerves, which border it. At this stage the head-sinus is formed by the junction of two vessels of about equal caliber: medially, the stem of the future anterior dural plexus; laterally, the maxillary vein, which originates from the top (superficial caudal margin) of the optic vesicle and courses through the bulging primitive maxillary process. The primary function of the maxillary vein, i.e. optic drainage (cf. injected chicks in Sabin's pl. 6; Hughes, 1934, pl. 4), is clear in embryos still younger that show the plexiform components of the vein (horizon xi; fig. 1A). In view of its conspicuous form in other vertebrate embryos illustrated in the literature, the maxillary vein is undoubtedly a morphological constant, the development of which, even before the three well known dorsal tributaries of the primary head-sinus, corresponds to the notably early formation of the optic vesicle. The history of the vein is of particular interest in man. Although its early role of draining the eye is soon supplemented by other vessels and is obscured by the addition of several larger tributaries from other regions, the stem of the maxillary vein finally becomes that of all the ophthalmic and orbital veins in the adult (stage 7).

The anterior cardinal vein, with which the primary head-sinus is directly continuous and which later constitutes the primitive internal jugular vein, is still medial to the 10th to 12th cranial nerves, instead of lateral as in the mature configuration. Furthermore, it must be emphasized that use of the adult designation does not imply the existence of an external jugular vein during early mammalian stages, or at any stage in many other vertebrates. Confusion has long existed regarding the developmental relation of the external and internal jugular systems, probably because the external system typically predominates over the internal in adult mammals except certain primates. Often called simply the "jugular" vein in reference to the adult of various species, the external jugular drains not only the face and extracranial parts, but also the intracranial sinuses through a temporal skull foramen (so-called "spurious jugular"; see stage 7*a*). In such cases the internal jugular vein, together with the "true" jugular foramen, is correspondingly small or essentially absent. Nevertheless, the internal jugular, representing the anterior cardinal, is the primary jugular vein of vertebrates. The external jugular vein is its secondary derivative, which does not become definitive in man until after horizon xx (ca. 20 mm.; stage 6); at the early human stage under consideration, it is represented only remotely by a *ventral pharyngeal vein* (fig. 2) draining the prominent mandibular and hyoid pharyngeal bars, from which the face and neck will be constituted. As indicated in figure 2, the pharyngeal vein primarily joins the common cardinal vein after coursing over the top of the heart, but its stem soon "migrates"[4] cranially to the anterior cardinal vein. At either position of exit, it is identified with the *linguofacial vein* (figs. 19–22, pl. 1), a "morphological constant" in vertebrates (F. T. Lewis, 1909). Although the vein is primarily a tributary of the internal jugular, it is eventually taken over, entirely or in part, by the exterior jugular vein at a much later stage; this secondary annexation occurs to the greatest extent in the many mammals in which the internal jugular dwindles in favor of the later external jugular (pl. 6).

STAGE 3. EMBRYOS OF HORIZONS XV, XVI (6 TO 12 MM.)

Externally, the most striking advance of stage 3 is the expansion of the frontal and maxillary regions relative to the mandibular and hyoid bars, together with the elongation of the limbs and the development of a definite hand plate. The optic stalk and cup, closed lens vesicle, and deep nasal pit characterize these embryos. The regularity in form of the pharyngeal bars has been changed by the marked growth of the maxillary process, the elevation of the auricular hillocks, and overgrowth of the third (glossopharyngeal) bar in the formation of the cervical sinus. Lateral evagination of the cerebral hemisphere has clearly differentiated the telencephalon from the diencephalon, and the growth of the cerebellar plate is beginning to produce the pontine flexure. Although most of the arteries of the brain are represented, including the recent basilar artery and the first stages in the formation of the vertebral artery, the adult venous pattern is not recognizable (fig. 3).

Elaboration of Dural Channels Joining the Head-Sinus; Initial Pia-arachnoidal Tributaries

The anterior dural plexus is now considerably elaborated, in keeping with the differentiation of the more cranial parts of the brain. Its foremost component is the *primitive marginal* sinus (Markowski's "marginal vein," see p. 104), which borders the craniodorsal margin of

---

[3] The head-vessels in this embryo as illustrated by Streeter (1942) are schematic for the purposes of his communication, and do not agree with the present figure.

[4] Streeter (1918, p. 26) fully described the way in which vessels are shifted in the primordial plexuses, and the initiating factors of such "migration of veins," "spontaneous" as opposed to "passive." A term he used for the former process, *anastomotic progression,* is particularly descriptive.

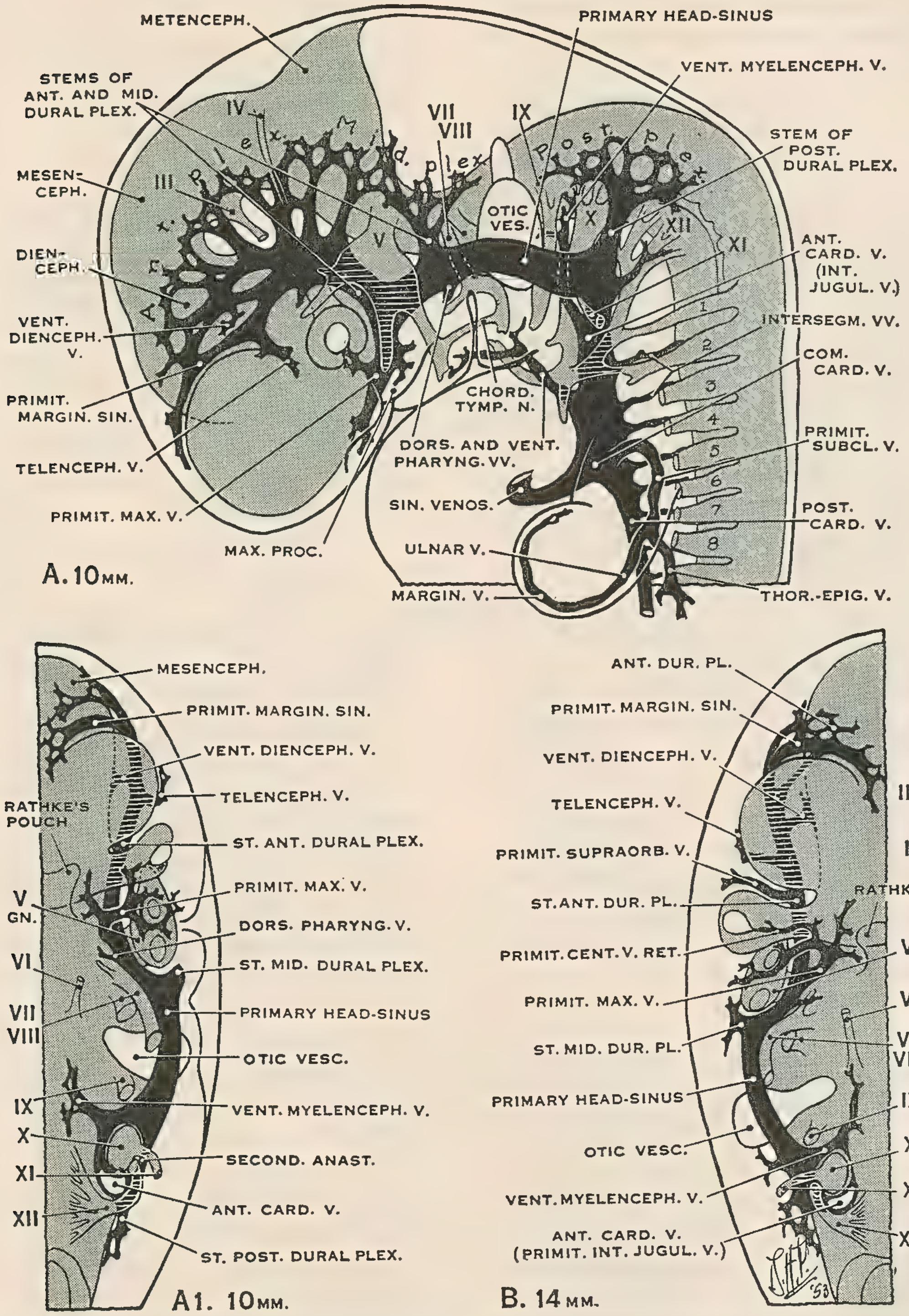

Fig. 3. Stage 3. With the development of the diencephalon, the anterior dural plexus is elaborated; its component marginal sinus encircles the telencephalon, expansion of which brings a diencephalic pia-arachnoidal vein into view (cf. A1 and B). A similar vein from the myelencephalon emerges (cf. A1 and B), as the head-sinus migrates lateral to the 10th nerve (A), thus defining the upper end of the primitive internal jugular (anterior cardinal) vein. From the choroid fissure a tributary (future central vein of retina) joins the prominent maxillary vein; the stump of a primitive supraorbital vein (A) is elongated in stage 4 (B).

the emerging cerebral hemisphere from the mid-line region, and includes elements of the future superior sagittal and transverse sinuses. Another component of the anterior dural plexus borders the caudoventral margin of the hemisphere, and may be called a telencephalic vein, because it drains the primordial striatal (nuclear) region; being dural, however, its stem represents the future tentorial sinus (pl. 1). A medial tributary of the anterior dural plexus traverses the primitive arachnoid layer. It is the stem of an initial pial vein, the *ventral diencephalic,* an augmented remnant of one of many vessels, short and laterally directed, that connected the pial and dural layers of earlier stages. The vein is now visible because the anterior dural plexus has become further removed from the neural tube owing to telencephalic expansion (see stage 4).

Although the middle dural plexus and its stem, draining the metencephalon, are larger and better defined, a more notable alteration in stage 3 concerns the stem of the posterior dural plexus at its junction with the head-sinus and the primitive internal jugular (anterior cardinal) vein. The head-sinus has moved laterally to the 10th nerve, a development foreshadowed by the venous ring around the nerve in stage 2 (fig. 2); this secondary anastomosis takes place dorsocranially to the distal fibers of the 11th nerve, leaving the 10th nerve to enter the primordium of the cervical muscles. As a result, the 11th nerve is deviated around the cranial border of the head-sinus before proceeding caudolaterally, and lies just above the entrance of the sinus into the primitive internal jugular vein (fig. 3). The lateral migration of the head-sinus is accompanied by a caudal migration of the posterior dural stem (cf. figs. 19, 20, pl. 1), which thus becomes directly continuous with the primitive jugular vein and will constitute the caudal end of the future sigmoid sinus.

After the permanent lateral position of the head-sinus is established, the more medial and cranial part of the venous ring around the 10th nerve, noted above, does not disappear. Since this part was derived earlier from the primordial hindbrain channel ("vena capitis medialis"), lying directly upon the brain wall, it is in position to receive a definitive *ventral myelencephalic vein,* more recently proliferated from the primordial channel (cf. fig. 3A1, B). The stem of this pia-arachnoidal vein, lying between the roots of the 9th and 10th nerves, is significant because it much later gives origin to the inferior petrosal sinus. The identical position, relative to these nerves, of the caudal end of the adult sinus, which is unusual in lying outside the skull (below the jugular foramen), is explained by its derivation from this primitive vein extending from the pial to the dural layer (see stage 7).

Primitive Internal Jugular Vein

The anterior cardinal vein may now properly be called the primitive internal jugular vein, since the apparent descent of the common cardinal vein to the level of the 7th or 8th cervical nerve is beginning to define the neck region (cf. figs. 19, 20, pl. 1). During this descent, the cranial end of the primitive jugular vein migrates from the medial to the lateral side of the 10th to 12th nerves. Such alterations are not foreordained by the adult configuration but are determined by adjacent structures. As Streeter (1918) wrote, embryonic channels should not be thought of as busily engaged in building mature vessels, but as carrying on their functional activity in the best manner possible for the moment with regard to the available space and the amount of work to be done.

A good example of the principle underlying the developmental alterations of embryonic vessels is the lateral migration of the internal jugular vein and the head-sinus. Sections of embryos of stage 2 show that the head-sinus, although appearing large in diameter in profile reconstruction (fig. 2A), is actually flattened into a crescent (fig. 4, insert) by the prominent inferior (nodosal) ganglion of the vagus around which it is detoured. By stage 3 (fig. 3A), the primitive internal jugular also appears to be subjected to mechanical compression in the wedge between two converging nerve roots. The separate roots of the 12th nerve unite, as they pass lateral to the primitive jugular vein, into a trunk which is closely applied to the lateral margin of the 10th nerve (at the caudal border of the nodosal ganglion), where these nerves are surrounded by a common fibrous sheath in the adult. Just cranial to this juxtaposition, in embryos of this period, a marked compression[5] of the jugular is effected by the 10th nerve in front and the 12th behind (fig. 4, insert). In one embryo of age group xvi (Carnegie no. 792), which is certainly atypical, if not abnormal, with reference to the head-veins, the 12th nerve is applied, not only to the lateral, but also to the caudal, border of the 10th nerve for a considerable distance; the primitive jugular vein, although conspicuous above and below, is not identified at all in this area. Subsequently, in stage 4, the confined position of the internal jugular vein will be overcome by its migration to the lateral side of the 12th nerve (fig. 5). The initial juxtaposition of the 10th and 12th nerves also appears to block the upward migration of the linguofacial vein on the jugular (fig. 3). Figure 4 shows a detail of some of the lateral anastomotic channels by way of which the jugular vein and its linguofacial tributary shift[4] into a less restricted position outside these nerves.

---

[5] Good sections of well preserved embryos show an amazing integrity of the vessel walls consisting of but a single endothelial layer; even in channels empty of primitive red cells, their original contour seems to be smoothly maintained by the mesenchymal strands, including the loose mesh of the primitive pia-arachnoid.

In the preceding stage 2, the arm bud is drained by a plexiform tributary of the *thoracoepigastric* (lateral thoracic) *vein,* which joins the posterior cardinal vein (fig. 2.) The arm in stage 3 is in a more cranial position, and the hand plate is drained by a vein along its superficial border, the so-called *marginal vein,* which joins the *primitive ulnar vein* (fig. 3). The common stem formed by the junction of the ulnar and lateral thoracic veins, having now moved cranially upon either the common or anterior cardinal (internal jugular) vein, may be called the *primitive subclavian vein.*

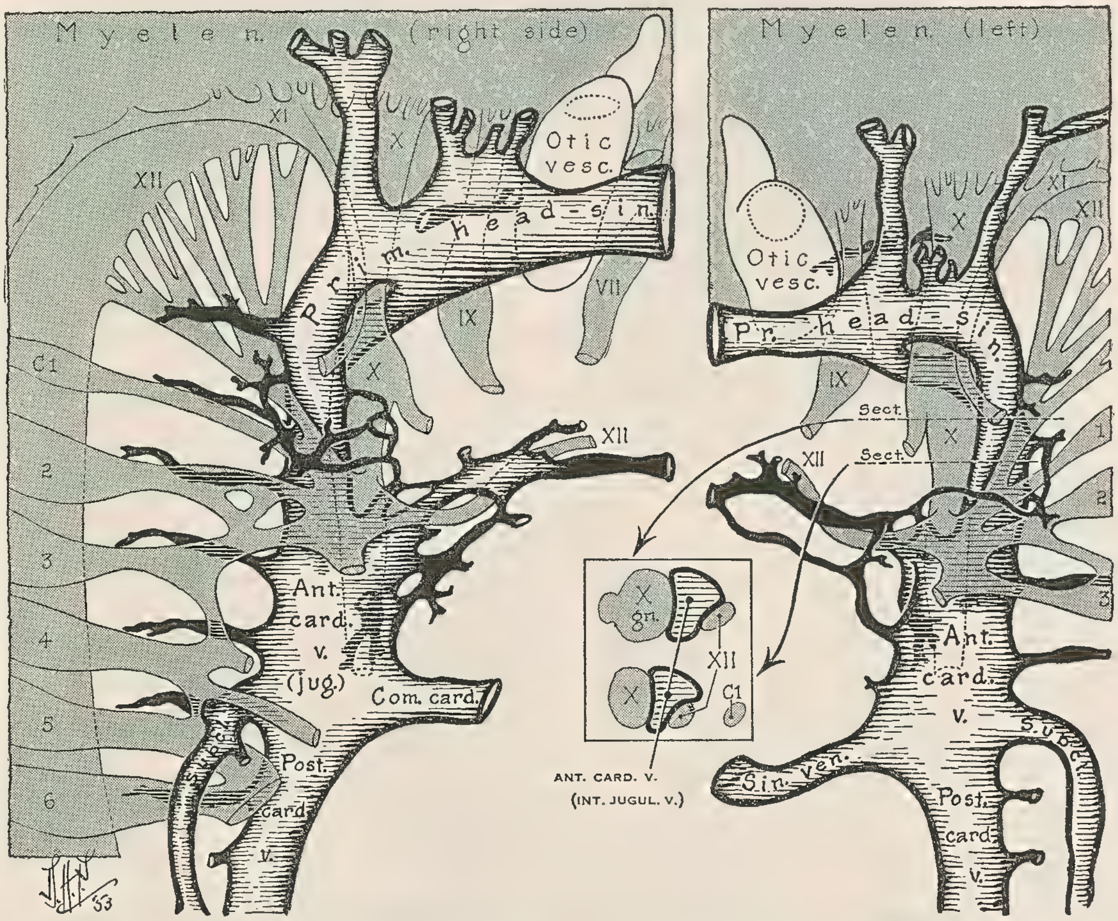

Fig. 4. Stage 3. Details of embryo Carnegie no. 3385, 8.3 mm., xv. Note the secondary anastomoses between vessels lateral to the nerve roots, by means of which the parent primitive internal jugular vein, compressed between nerves (insert), "migrates"[4] to its adult position. Similarly, the linguofacial vein, accompanying the 12th nerve, is migrating cranially on the jugular to become lateral to the nerve. The right otic vesicle is slightly more advanced than the left, which is still attached to the skin over a wider area; the right head-sinus is notably larger than the left.

Stage 4. Embryos of Horizons XVII, XVIII (10 to 16 mm.)

At stage 4, called the "postbranchial phase" because the row of pharyngeal bars homologous to the branchial arches of fishes no longer exists, the hyoid bar is more prominent than before, and the mandibular bar persists in its entirety as the lower jaw (fig. 5). This development is coincident with the formation of a definitive upper jaw by differentiation of the maxillary process, and includes growth of the lateral (nasal) rim of the nose, which places the primitive nostril (nasal pit) in a more medial position. Parts of the future external ear can be recognized in the hillocks surrounding the hyomandibular groove. A distinctive advance is the appearance of finger rays of the hand plate.

The more caudal parts of the chondrocranium outlining the base of the future skull are represented in horizon xviii by the basioccipital plate surrounding the notochord, by a dense area in the position of the sella, and by the bilateral otic capsules. The prominent condensation of mesenchyme called the membranous skull radiates dorsally from these primarily separate cartilages. It clearly defines the contiguous dural condensation, which contains the primary head-sinus with its three dorsal tributaries draining the three dural plexuses, as defined for stage 2. Particularly ventrally, the dural layer has become widely separated from the pial layer on the brain wall, in which lie the emerging pial veins and the defini-

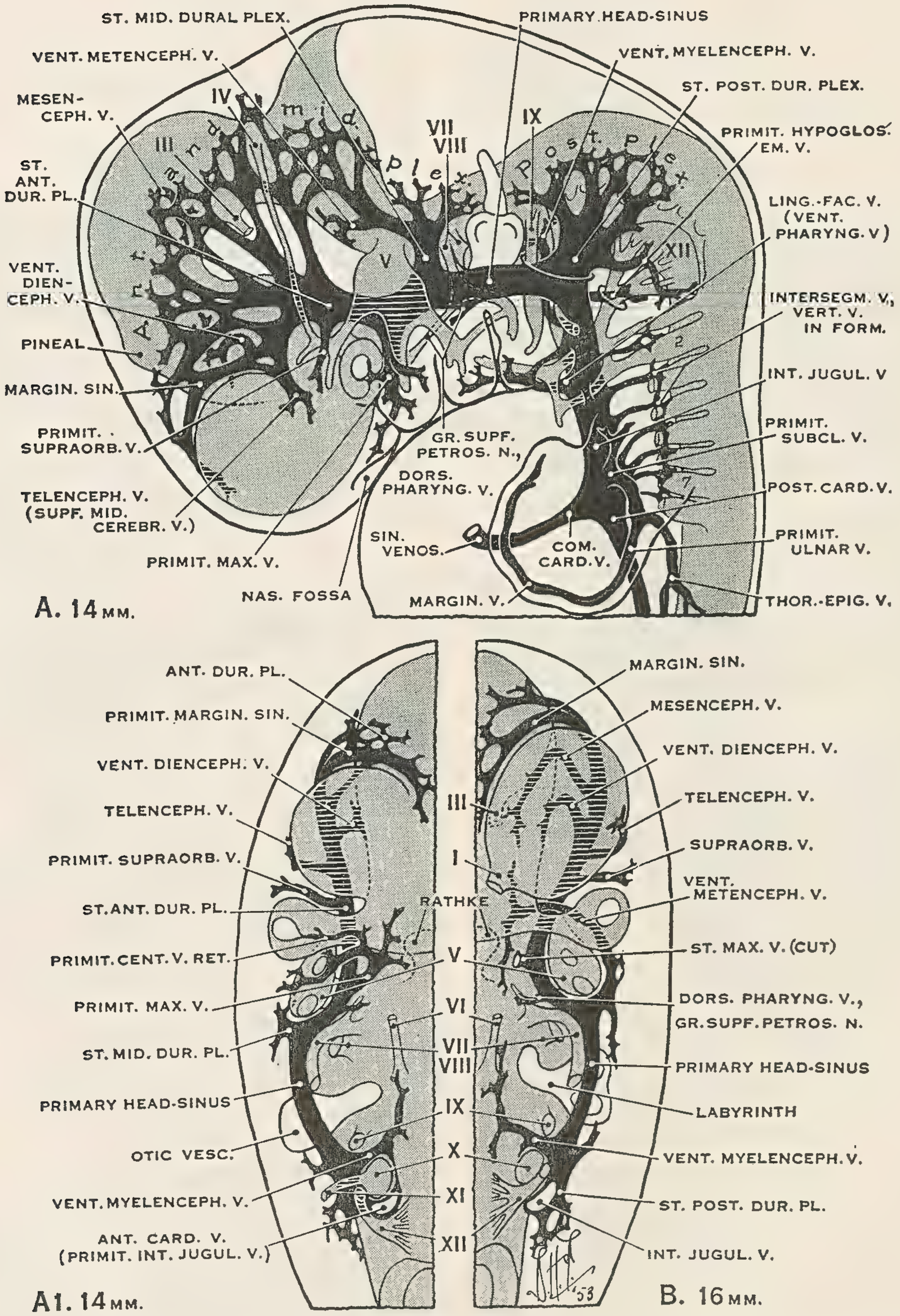

Fig. 5. Stage 4. Expansion of the future hemispheres of the brain clearly separates the dural and pial layers of venous channels. Consequently, the numerous anastomoses traversing the primitive pia-arachnoid begin to decrease, and can thus be identified; often at least one such transverse vein for each division of the brain is seen in older embryos of this stage (B; cf. fig. 6). Such pia-arachnoidal veins become connected by longitudinal anastomoses (B), succeeded by transverse anastomoses between them (cf. fig. 8B), thus initiating formation of the pial venous plexus and definitive veins.

tive arteries (fig. 6); the intervening space, a relatively wide layer of loose mesenchyme, is the primitive arachnoid.

Except for the clear demarcation of the three meningeal layers, stage 4 is not notable for definitive changes in dural channels (figs. 20, 21, pl. 1). The head-sinus, however, is paralleled dorsally by plexiform elements of a channel that will soon connect the anterior, middle, and posterior dural plexuses dorsal to the 5th nerve root and the otocyst (fig. 5A); its significance will be clear in the next stage.

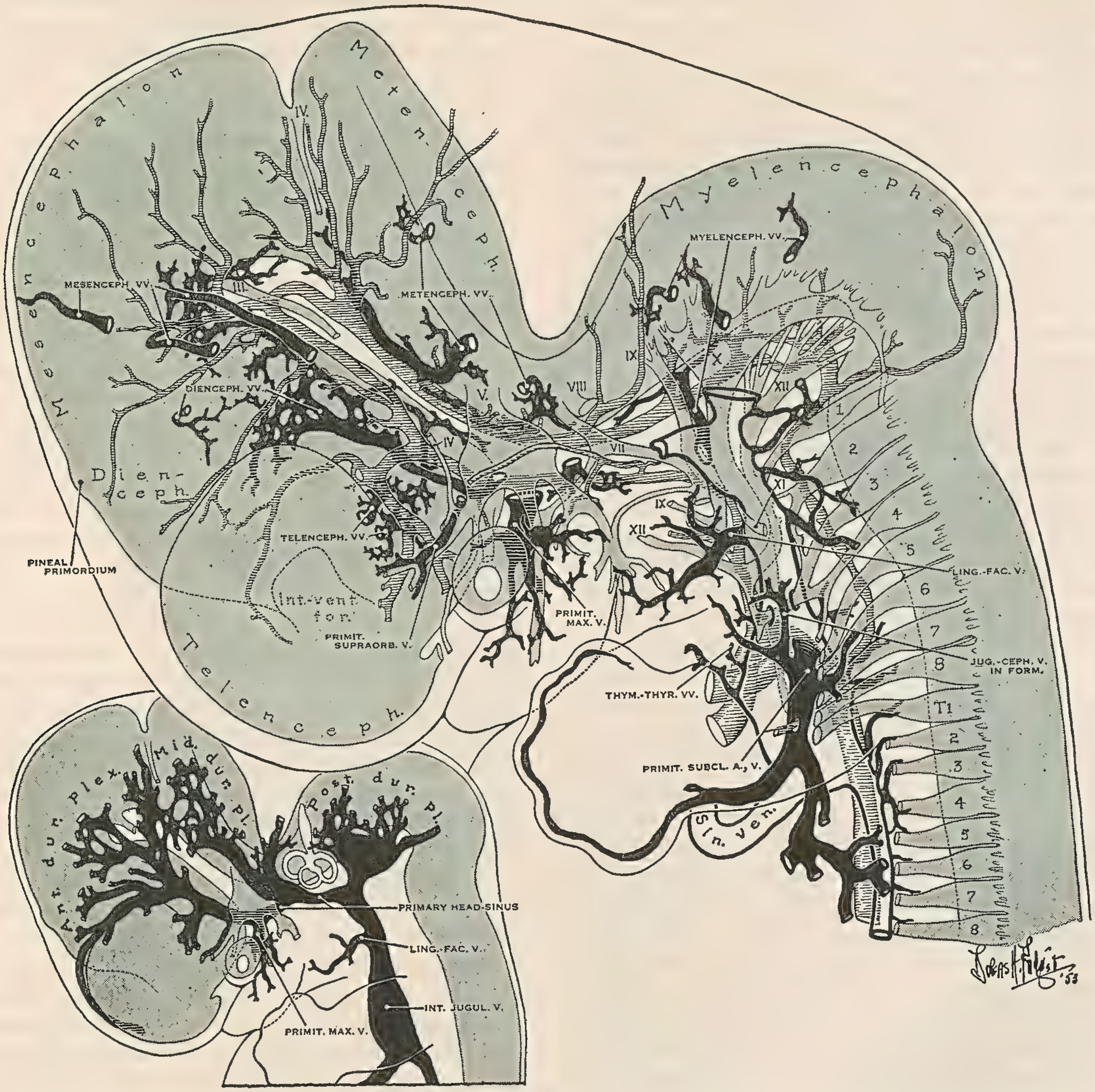

Fig. 6. Stage 4. Embryo Carnegie no. 492 (16.8 mm., late xviii, ink injection). The insert shows the largest extracranial veins and the major components of the primitive dural channels (cf. fig. 5), which are omitted in the main picture above to permit view of their tributaries. At least two laterally directed (transverse) veins of the pia-arachnoid, which are primary, leave each division of the primitive brain. Their most distal tributaries, in part joined by secondary pial anastomoses, pass subjacent to the definitive arteries (for identification of the arteries, cf. Padget, 1948, figs. 5*a*, 7*a*).

The only prominent ventral tributary of the head-sinus of earlier stages, namely the primitive maxillary vein, borders the primitive cartilaginous sella laterally. In keeping with the differentiation of the upper jaw, its tributaries are voluminous. They include a vein from the choroid fissure in the caudoventral aspect of the elongated optic stalk; hence, the future central vein of the retina is probably already represented (see stage 7). This vein, now subordinate, represents the optic drainage to which the primary maxillary vein of stages 1 and 2 was restricted, i.e. the exclusive drainage of the optic vesicle and, later, the lens region (figs. 1–3, 5). By stage 4, the maxillary vein receives a medial nasal tributary from the region of the olfactory pit and nerve, but it is the lateral tributaries that are most conspicuous; they ramify extensively in the regions lateral and caudal to the maxillary branch of the 5th nerve, i.e. the bulk of the upper jaw and the primordia of the pterygoid and temporal muscles (fig. 5).

Although drainage of the optic region before this stage has been exclusively through the voluminous primitive maxillary vein caudal and ventral to the eye, a smaller but well defined vein now comes from the superficial tissues cranial and dorsal to the eye. With the exception of its caudal end, this *primitive supraorbital vein,* coursing between the frontal nasociliary branches of the ophthalmic nerve, not only becomes the stem of the definitive vein, but will also constitute the major part of the adult so-called superior ophthalmic vein. The caudal end of the primitive vein entering the head-sinus or its anterior dural stem is temporary; it is dorsal and lateral to the junction of fibers between the 4th nerve and the ophthalmic division of the 5th (fig. 5A). Although this relationship remains constant for several stages, it will finally be changed during the emergence of the adult common stem of all ophthalmic and orbital veins in stage 7.

During stage 4, the definitive *internal jugular vein* completes its migration to the lateral side of the hypoglossal nerve trunk; embryos of horizons xvii and xviii show successive steps in this transposition, the nerve often passing through a hole in the vein (fig. 5). At the same time, the proximal (jugular) end of the linguofacial vein is freed from its previous confinement at the juxtaposition of the 10th and 12th nerves; by secondary anastomotic channels (fig. 4) this vein shifts to its permanent and less-fixed position, either lateral or just cranial to the 12th nerve, which swings medially to enter the tongue primordium. The descending branch of the hypoglossal nerve is now joined, as in the adult, by fibers of the 2d and 3d cervical nerves forming the cervical loop (ansa hypoglossi). These findings readily explain the adult variations in the relation of all these nerves to the jugular vein (see Grant, 1951, fig. 516), including reported occurrences of double internal jugular veins. The lateral migration of the jugular and its linguofacial tributary, the adult common facial vein, appears to be the result of its relative immobility in early stages, when it is compressed by the connections of the 10th and 12th nerves and sometimes by the upper cervical nerves.

Principles Governing the Formation of Veins Draining the Neural Tube

Stage 4 of the present series affords the first opportunity to see how the pia-arachnoidal veins are formed. Initially, the primitive capillary network on the surface of the neural tube is drained, by way of numerous and relatively short veins near its dorsolateral border, into the adjacent ramifications of the more or less continuous anterior, middle, and posterior dural plexuses. As the cerebral hemisphere and cerebellar primordium enlarge, and as the otocyst with its cartilaginous capsule expands, the head-sinus with its dorsal tributaries, the dural plexuses, are carried laterally, thus elongating their medial tributaries, the veins from the pial layer. Hence, a "cleavage of blood vessels" (Streeter, 1918) results in the sense that most of the numerous veins once connecting the primitive dural and pial layers are lost (Padget, 1956, figs. 1, 24, 27). The few elongated and augmented veins that remain, and are directed laterally (transversely) for some distance, can consequently be identified (fig. 7; see also p. 105). Definitive veins of the pial layer are formed by secondary anastomoses between the pial tributaries of the primary transverse veins coursing through the arachnoidal layer. The stems of two of the primary pia-arachnoidal veins were identifiable in stage 3, namely the ventral diencephalic and myelencephalic veins (fig. 3). The former is usually the more easily seen as it traverses the loose mesenchyme representing the arachnoid; it is well shown in a transverse head section of this stage by Markowski (1922, text fig. 2), who called it the "inferior" diencephalic vein. In some late embryos of stage 4, and more readily in stage 5, at least one pia-arachnoidal vein can usually be identified for each of the five regions of the primitive brain: the *telencephalic, mesencephalic,* and *metencephalic veins,* in addition to the veins from the diencephalon and myelencephalon, identified in stage 3 (figs. 3, 5, 6). Since these definitive veins emerge as augmented remnants in the reduction of many short pial-dural connections, variation in their position and number is inevitable.

An excellent embryo of horizon xviii (Carnegie no. 492, 16.8 mm.), which is injected with ink, shows fundamental details in the formation of the veins of the pia-arachnoid, as seen in figures 6, 7B, and 8B, lateral, coronal, and basal views, respectively. Together with an embryo somewhat younger (fig. 8A), this embryo reveals pertinent details most clearly in the basal view, including the basilar artery (fig. 8B2), description of which follows.

The actual or approaching anastomoses between the pial tributaries of the separate primary groups of pia-arachnoidal veins, named above (shown diagrammatically in fig. 5B), are seen particularly well in the reconstructions of embryo Carnegie no. 492 (figs. 6, 8B). Essentially, the secondary anastomoses are directed longitudinally and in line with each other, and thus parallel the basilar artery bilaterally. Secondary formation of such pial anastomoses furthers the reduction of the primary anastomoses, once multiple, between the pial and dural venous layers, a reduction that brings the regional pia-arachnoidal veins (telen- to myelen-cephalic) into view, subsequent to their elongation. In the present embryo, the transverse pia-arachnoidal veins have been reduced in most instances to two veins that are identifiable for each region of the brain.

Steps in the further reduction of the pia-arachnoidal veins, i.e. to essentially one regional vein in each instance, are particularly indicated in this embryo by the metencephalic group of veins, including their bilateral asymmetry (fig. 8B2). On each side, this group constitutes essentially two pia-arachnoidal veins, one in front of and one behind the 5th nerve root; their stems join chiefly the stem of the middle dural plexus on each side. On the left side of the embryo, the more cranial metencephalic vein is the favored of the two, being the larger; by way of the secondary longitudinal pial anastomosis noted above, it has annexed the pial tributary of the more caudal vein, the stem of which is about to disappear, leaving one *ventral metencephalic* vein, a significant vessel (see stage 7*a*). On the right side of the embryo, in contrast, the secondary longitudinal veins of the metencephalic pial layer drain more into the primary metencephalic vein caudal to the 5th nerve than into its cranial counterpart; they also join the head-sinus medial to the nerve. Such asymmetry shows how variations occur in the reduction of the pial-dural anastomoses, primarily numerous.

In certain areas of the hindbrain wall, further secondary pial anastomoses that are transverse, i.e. pass across the mid-line beneath the basilar artery (see below), have begun to connect the secondary longitudinal pial anastomoses formed earlier (fig. 8B2). In this way the venous net and the main pial veins of the cord, medulla, and pons are formed. The steps just outlined are similar for all the cerebral veins, including, in particular, the important basal cerebral vein. Components of this vein, which is not recognizable until stage 7*a*, involve secondary pial anastomoses cranially that are similar to those just described for the hindbrain region.

Another basal view of this embryo (fig. 8B1) includes the forebrain, internal carotid artery, and internal jugular vein. Pial tributaries of the mesencephalic veins are anastomosed with those of the diencephalic veins, two of which persist on each side (cf. figs. 6, 8). The ventral diencephalic vein, much better developed than it was in stage 3, lies on the primitive hypothalamus; it is dorsolateral and subjacent to the posterior communicating artery, in the position of the later basal cerebral vein, of which it is a component; it still empties, as earlier, into the head-sinus. Pial tributaries of the diencephalic veins are anastomosed with those of the *lateral telencephalic* (adult superficial middle cerebral) vein—the first stages in the formation of the *medial telencephalic* (deep middle cerebral) vein, which connects the adult basal and middle cerebral veins. On the right side of the embryo, the ventral diencephalic vein empties chiefly into the stem of the anterior dural plexus, a typical arrangement before stage 6 (figs. 21, 22, pl. 1).

Relation of pial veins to the arteries. The present study, based on many embryos of the previous report on the cerebral arteries, facilitated observations on the relation of veins and arteries to each other, a subject that apparently has received little if any comment in the literature, in reference to either embryo or adult. As for the adult brain, it is well known that the largest veins on its external surface are superficial to the arteries, and that arteries and veins in general do not accompany each other. Such large veins obviously are those immediately derived from the primitive dural plexus, specifically from channels in the inner dural layer that are the proximal ends of the primary veins traversing the arachnoidal layer (see below). A publication by Scharrer (1940) brought out an important principle regarding the extracerebral tributaries of the largest cerebral (terminal) veins just noted. His work includes beautiful photographs of the surface of the cerebral convolutions of the adult opossum and rhesus monkey, in which the arteries and veins were injected separately with different colors demonstrable in half-tone photography. These pictures show the pial arteries and veins to comprise two separate precapillary networks, one lying over the other (see also Padget, 1956, fig. 24). It can be seen (as Scharrer notes in the legend to his fig. 2) that the network of veins, including some veins of relatively large size, is not superficial to the arterial branches, as might be supposed, but rather lies between the arterial network and the brain wall.

The fact that pial veins typically lie medial to the pia-arachnoidal arteries is probably contrary to the general impression, as was exemplified indirectly by Scharrer's discussion. His injections (starch grains, which do not go beyond the capillaries) proved that arteries had been mistaken for veins, and vice versa, by Pfeifer (1928, 1930, detailed studies on the adult angioarchitecture of human and cat brains; see also Solnitzky's report on the monkey, 1940); Scharrer's finding confirmed Campbell (1938), who had made the same observations in regard to Pfeifer's reports. The author examined the cerebral convolutions of several human brains (newborn) with an excellent natural injection, which showed repeatedly the same relation of arteries to veins that was demonstrated by Scharrer for other mammals. Such evidence was supported by observations in all the embryos of the present series, beginning with the stage under discussion.

In reference to Scharrer's report, it is also interesting that, even before there is any difference in thickness of

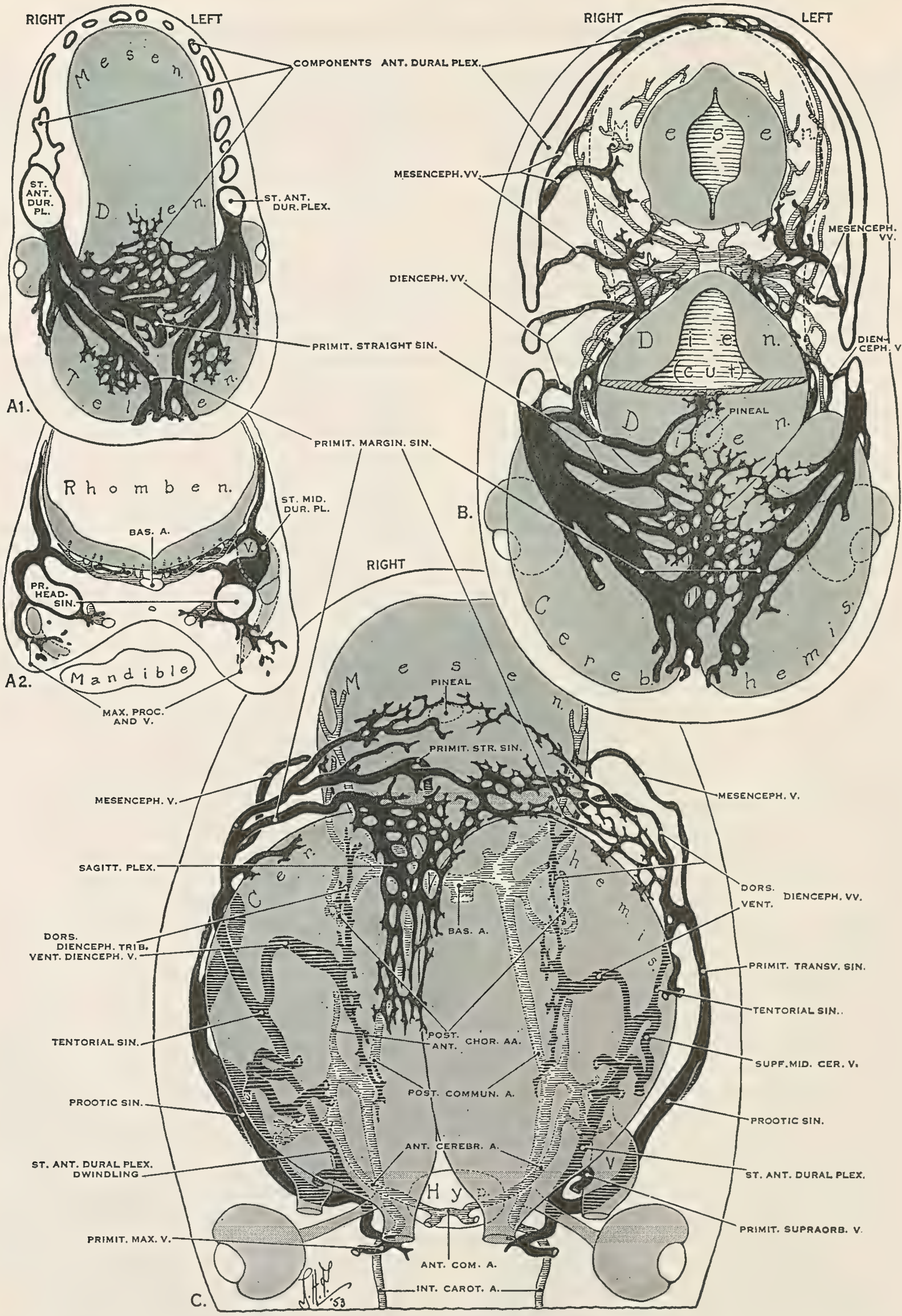

FIG. 7. Stages 3, 4, 6. Frontal views, reconstructed from coronal sections (same magnification): A1, 2, Carnegie no. 1121, 11.8 mm., xvi, stage 3; B, no. 492, 16.8 mm., xviii, stage 4; C, no. 966, 23 mm., xx, stage 6. The anterior dural plexus, from which the sagittal and straight sinuses are derived, drains to the right side predominantly, in all. In B and C the transverse pia-arachnoidal veins leave the brain wall subjacent to the arteries and cross them at a right angle. The greater depth of the mesenchyme on the right in A and B (see p. 105) is apparently not an artifact.

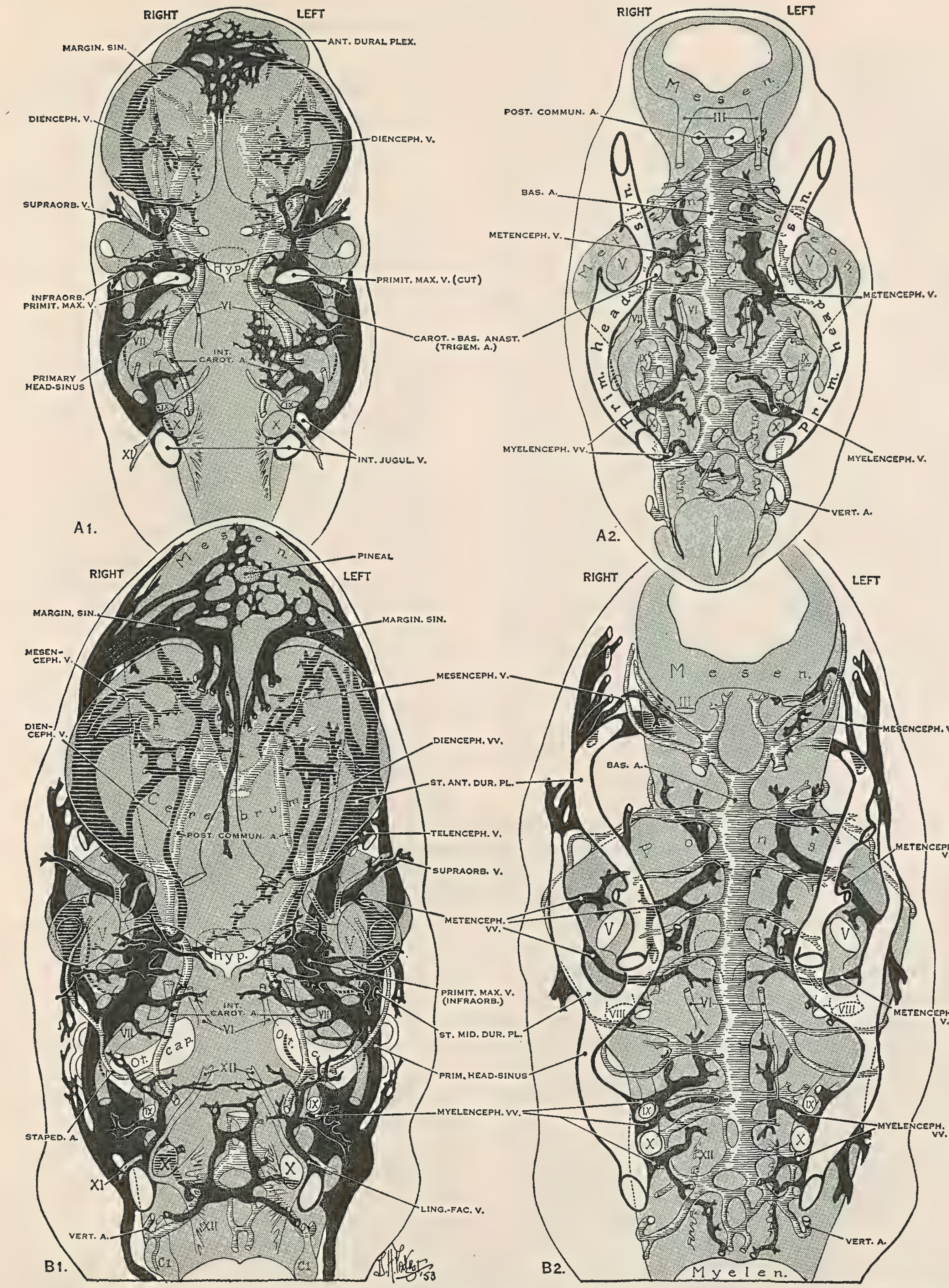

Fig. 8. Stage 4. Basal views of two embryos (A middle, B late stage 4) reconstructed from transverse sections (same magnification). In A2 (Carnegie no. 940, 14 mm., xvii) and B2 (no. 492, 16.8 mm., xviii), the fore part of the brain and certain venous channels are eliminated to show fundamentals of pial venous development. Note: the secondary anastomoses forming the pial venous net and veins, also their pattern and position in relation to the definitive arteries; the way in which the multiple stems of primary pia-arachnoidal (transverse) veins, here reduced to about two from each region of the brain (telen- to myelen-cephalon), can be further reduced to essentially one outlet from each region. This reduction is possible subsequent to the secondary pial anastomoses, longitudinal and later transverse, between the initial pial tributaries.

cerebral arterial and venous walls, certain morphologic differences between pial arteries and veins can, nevertheless, sometimes be seen in the human embryo of about horizon xx. As Scharrer noted in detail regarding adult intracerebral vessels, there are more arteries than veins, but veins have more tributaries than arteries have, and anastomose with each other less (Padget, 1956, fig. 24).

To return to stage 4, the embryo of figure 8B2 (xvii, 16.8 mm.), showing the base of the hindbrain, is to be compared with figure 8A2, which shows the same region in a younger specimen (xvii, Carnegie no. 940, 14 mm.). In both, the basilar artery is paralleled by the bilateral longitudinal veins that have just developed from pial anastomoses between the transverse myelencephalic, metencephalic, and mesencephalic pia-arachnoidal veins as described above. In embryos preceding stage 6, particularly those with a notable congestion of the vessels (e.g. Carnegie no. 940, which is atypical; fig. 8A; cf. Padget, 1948), it may be difficult to distinguish parts of certain cerebral arteries from veins: their walls as yet do not differ in thickness and consist of a single layer of endothelial cells; furthermore, such vessels are often in contact when crossing each other. In early stages, therefore, arteries and veins can be identified with certainty only by tracing each from beginning to end; in the present study both were reconstructed in every case. Knowledge of the principles of their interrelation facilitates the task of distinguishing between arteries and veins and should help to clarify the interpretation of vascular findings in other vertebrates (e.g. the chick, Feeney and Watterson, 1946).

One rule about primary vessels is that a vein and an artery cross each other approximately at right angles (figs. 6, 8B2; Padget, 1956, fig. 1). In this manner the bilateral longitudinal pial veins are crossed by the transverse branches of the basilar artery. Subsequently (horizon xviii and later), the secondary pial venules that cross the mid-line are perpendicular to the basilar artery (fig. 8B2). Another rule is that the pial veins lie between the arteries and the brain wall. Such basic relations of arteries to veins are also shown in a model by Markowski (1922, fig. 12, pl. 6), in which the bilateral longitudinal ("basal metencephalic") veins are overlain by the transverse branches of the basilar artery.

In other regions of the brain, during this and later stages, the same pattern of primitive veins, including their crossing the arteries at right angles, is observed. For instance, the pial tributaries of the diencephalic veins cross beneath the two choroid arteries, anterior and posterior; those of the mesencephalic veins cross beneath the mesencephalic arteries (figs. 6, 8, 11; Padget, 1956, figs. 24, 26). The only veins that are superficial to the arteries, as is shown by Markowski and the accompanying figures, are the terminal pia-arachnoidal veins (telen- to myelen-cephalic), which, now or earlier, pass laterally away from the neural tube. In most parts of the primitive brain, by late stage 4, these veins traverse a relatively wide layer of loose mesenchyme, the arachnoid, to enter the primitive sinuses in a layer of condensed mesenchyme, the dura. (These layers at the 40-mm. stage are not clearly demarcated by the arachnoid membrane and subdural space.) Hence, the largest veins on the surface of the adult brain belong more to the dural than to the pial layer, and are superficial to the arteries.

In consideration of the primary relations of vessels, confusion must be avoided regarding the relative position of the primary telencephalic veins and arteries as they appear in most of the reconstructions (figs. 6, 8, 11; pls. 4A2, 5C1). Though not so readily apparent, the situation is the same. The telencephalic vein drains the primordial striatal region in stages 3 and 4 (figs. 3, 6), by way of inconspicuous short remnants of primary pial-dural anastomoses. It never has the obviously transverse course of other pia-arachnoidal veins, e.g. the diencephalic, because of the lesser depth of the primitive arachnoidal mesenchyme over the cerebral hemisphere, the most superficial part of the brain. Furthermore, owing to early cerebral expansion in all directions, the elongating stem, or stems, of telencephalic veins are always in intimate contact with the dura. These veins are directly continuous with the tentorial sinus to be described below, and become the superficial group of middle cerebral veins. In contrast, the deep group of middle cerebral veins, to be enclosed within the late fetal Sylvian fissure, constitutes secondary pial anastomoses not clearly identifiable until stage 6 or later. They are the pial middle cerebral veins, which ramify beneath the proximal ends of the middle cerebral arteries and the brain in the anterior perforated area.

The largest cerebral veins on the surface of the postnatal brain, including not only the superficial middle cerebral veins but also the immediate tributaries of the superior sagittal and transverse sinuses, are well known to be superficial to the cerebral arteries. For the reasons noted above, these veins are often more or less intimately attached to the inner dural surface for some distance before they enter the sinus (Bailey, 1948). Only their more distal tributaries that form the smaller veins and the precapillary net on the surface of the convolutions lie beneath the arteries and their network of branches, as is shown for other adult mammals by Scharrer (1940; see fig. 24 in Padget, 1956). It is presumed that the relation of the pial arteries and veins just outlined is the same in all mammals, and probably in all vertebrates. The only direct evidence known to the author, however, is incidentally shown by Shindo (1915) for a mouse embryo; here the "collateral cerebral vein" (comparable to the ventral diencephalic or basal cerebral vein) lies next to the brain wall and is medial to two branches of the "cerebral carotid artery." It is interesting that the dural meningeal arteries and veins also have the same relation to each other in respect to the structure vascularized, the membrane bones (pp. 127, 135).

Speculation on the reasons for the primary relation between arteries and pia-arachnoidal veins is inevitable. The primitive pial veins undoubtedly represent endothelial material not utilized by the arteries, which are developed earlier than the veins from the primordial capillary net covering the neural tube (stage 2 and earlier; p. 83), inasmuch as the arteries are elevated from the primordial net as they become definitive. This sequence of development seems to explain the pattern of veins crossing beneath arteries at right angles, as is illustrated diagrammatically in another publication (Padget, 1956, fig. 27).

While the many primary pial-dural anastomoses are being reduced in number to result in definitive veins traversing the arachnoid layer, they appear to be "stretched," owing to the fact that the dural layer is continually being shifted laterally by the expanding brain and related structures. Since the main arteries of the cranial region are centrally located from the beginning, their branches are not subject to such "pull" between origin and destination. Although both arteries and veins of this region are little more than endothelial tubes before stage 7 (see below), the arteries are much better defined than the comparable veins; figures 6 and 8 show that many definitive branches of the internal carotid and basilar arteries have formed by stage 4, in contrast to the rudimentary (plexiform) venous configuration. The decrease in the number of primary transverse veins from pia to dura characteristic of venous development (Streeter, 1918; Padget, 1956, figs. 1, 26) initiates the formation of well defined pial anastomoses between the tributaries of those that remain. During the increasing separation of pial and dural layers, this secondary formation of pial veins might be facilitated because the primordial pial network is held in place on the neural tube, particularly before its penetration by blood vessels (under way in stage 2), by the relatively precocious arteries supplying an elevated, and thus overlying, arterial network.

It is impossible to consider the interrelation of the pial veins and arteries without speculation on the formation of congenital arteriovenous aneurysms of the brain (see discussion in Padget, 1956). In view of the actual close contact of certain primitive arteries and veins, with walls of endothelium only—not until stage 7 are the walls of cerebral arteries definitely thicker—such anomalies might be expected to occur more often. Is it possible, for instance, that the typical crossing of arteries and veins at a right angle is a factor in preventing anomalous connections as long as certain aspects of the blood flow in both are normal and the integrity of the thin walls is maintained? In the injected embryo of horizon xviii (Carnegie no. 492, fig. 8B1) described above, the right internal carotid artery is crossed by a component of the ventral diencephalic vein that is about to lose its connection with the head-sinus. This vein crosses the artery at a right angle in two directions—in fact, is closely wrapped around it.

Stage 5. Embryos of Horizon XIX (16 to 21 mm.)

At stage 5, development of the eye, nose, jaws, and ear has reached the point at which the human face is first recognizable (fig. 9). The cerebral hemisphere and cerebellar plate have expanded notably, and this growth, together with the enlargement and differentiation of the otic capsule, is responsible for conspicuous changes in the veins of the dural layer. The venous system, however, is far less advanced than the arteries of the brain, many of which are already definitive (cf. fig. 6).

The emerging pial veins with their arachnoidal stems, described for late embryos of stage 4, may be dismissed briefly since no fundamental changes are apparent. Some of them can more readily be identified, however, because their stems that pass laterally through the primitive arachnoid mesh toward the sinuses have elongated (fig. 9A1), owing to expansion of the cerebral hemisphere and, to a lesser extent, of the cerebellar plate (pl. 2). Such expansion increases the distance between the neural tube and the dural layer, particularly at the diencephalon and mesencephalon. At least five of these veins, one (or more) for each subdivision of the embryo brain, telencephalon to myelencephalon, can sometimes be identified at this time (fig. 9A), and are illustrated in an injected embryo of late stage 4 (fig. 6).

Involution of Primary Head-Sinus, Paralleling Formation of the Sigmoid Sinus

Elements of a new longitudinal channel, which connected the stems of the anterior, middle, and posterior dural plexuses dorsal to the nerve roots and otic capsule at stage 4 (fig. 5), are now definitely consolidated (figs. 22, 23, pl. 1). The conspicuous and continuous sinus thus formed is parallel and dorsal to the primary head-sinus, which is dwindling below the otic capsule and appears, in fact, to be compressed between it and the adjacent distal part of the 7th nerve. The new dorsal sinus is obviously being substituted for the more ventral head-sinus in the role of conveying blood from the brain into the internal jugular vein. The part of the secondary anastomotic channel between the middle and posterior dural plexuses, together with the main stem of the posterior dural plexus which it joins, remains virtually unchanged in later stages and constitutes the definitive

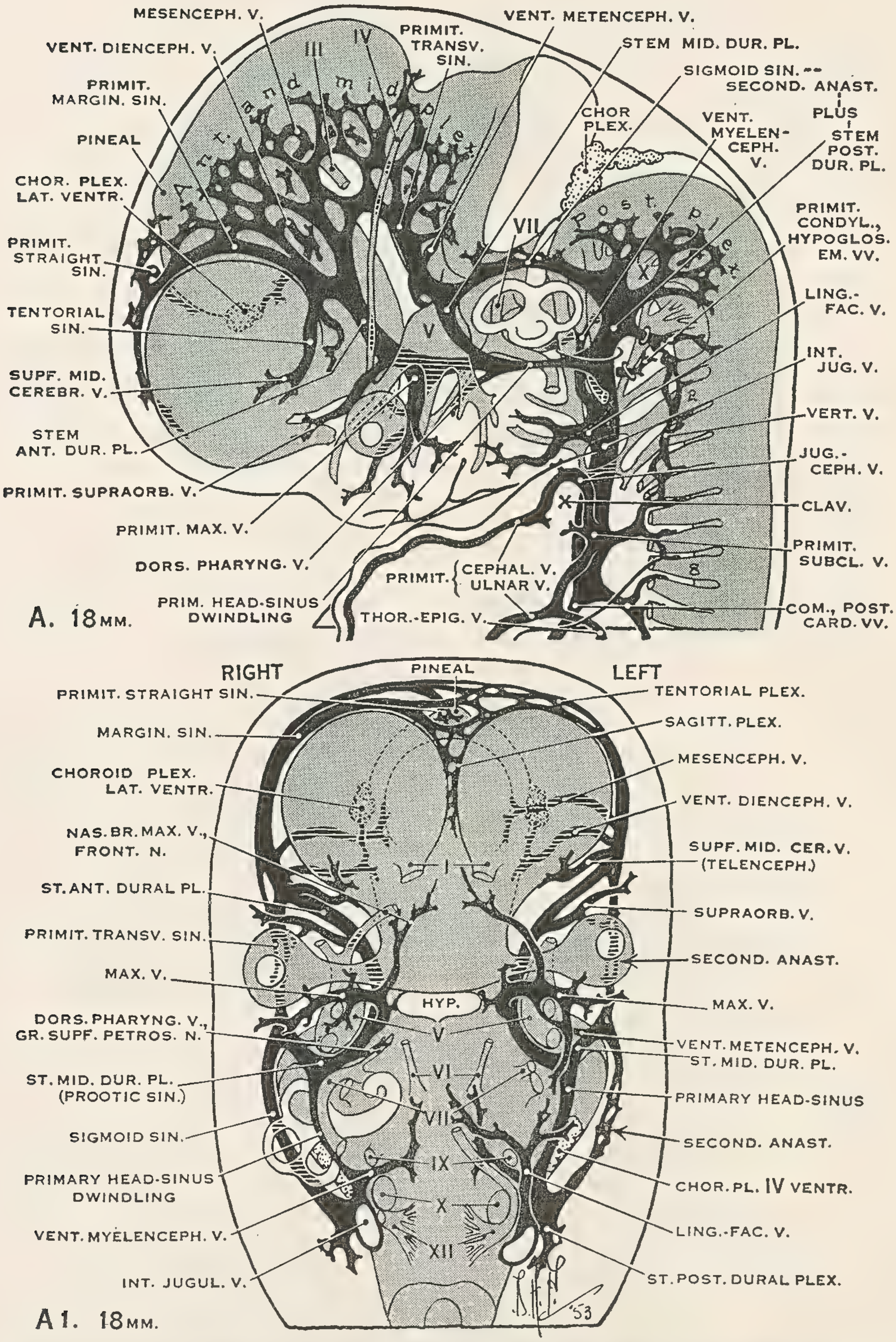

Fig. 9. Stage 5. The first definitive sinus, the sigmoid, is formed dorsal to the otocyst by an anastomosis between the middle and posterior dural plexuses (A). The head-sinus, thus replaced, has begun to dwindle (cf. two sides, A1). The voluminous maxillary vein, draining the orbital and nasal regions, soon anastomoses with the linguofacial (ventral pharyngeal) vein to form the anterior facial vein (shown on left side, A1). Note: the elongated stems of the pia-arachnoidal veins; the primary drainage of the lateral choroid plexus into the ventral diencephalic vein. The proximal end of the jugulocephalic tributary of the primitive subclavian vein, arching over the clavicle, becomes the stem of the future external jugular system.

sigmoid sinus.[6] It will be seen that the posterior dural plexus changes less in form and connections than do the anterior and middle dural plexuses. According to Streeter (1918), it merely becomes extended to constitute the adult occipital sinus. More specifically, however, the posterior dural plexus becomes the marginal sinus of the foramen magnum, at the margin of which it joins the sigmoid sinus. The occipital sinus is the variable augmentation of anastomoses between the remnants of the posterior and middle (tentorial) dural plexuses of late fetal stages (pl. 1).

The part of the new dorsal channel in front of the sigmoid sinus, between the stems of the anterior and middle dural plexuses, is the very primitive transverse sinus, now recognizable only in its connections, not in its position or direction. The cranial end of the channel near the mid-line is still plexiform, but its better-defined caudal end, joining the sigmoid, represents the most lateral part of the adult transverse sinus. It is seen (figs. 22, 23, pl. 1) that the new sigmoid sinus, curving dorsal to the otic capsule and replacing the dwindling primary head-sinus below, must result in a change of current from ventral to dorsal direction in the stem of the old middle dural plexus. As a result, this stem is sometimes smaller and less definite at stage 5 than previously (Streeter). The stem does not disappear, however, but is soon augmented into the conspicuous *pro-otic sinus,* the significance of which will be clear in later stages. Previously, the stem of the middle dural plexus (pro-otic sinus) drained the primitive cerebellar region ventrally into the temporary part of the head-sinus; henceforth, for several stages, but again temporarily, it will drain the forebrain and part of the midbrain dorsally into the sigmoid sinus.

Successive stages in the emerging sinuses, just described with reference to the lateral view of two embryos of two age groups (figs. 5, 9), can sometimes be seen by looking at the basal view, i.e. both sides, of one embryo (Carnegie no. 1390) of the present stage. Such difference is explained by the fact that the right side is typically a little more advanced than the left in respect to venous channels, a tendency observed both earlier and later (see stage 6). In figure 9A1, the primary head-sinus on the left at the present stage 5 is still large as compared to its dwindling counterpart below the otic capsule on the right, and the new dorsal channel (primitive sigmoid and transverse sinuses) is still plexiform as in stage 4. The caudal end of the primary head-sinus, the part that now accompanies the 7th nerve outside the otic cartilage, is soon reduced to a small remnant in man.

The dwindling of the human head-sinus ("vena capitis lateralis," p. 83) is in contrast to the condition in certain vertebrates, e.g. reptiles, in which it is permanently the chief drainage channel for the brain (Grosser and Brezina, 1895): maintaining its direct continuation with the (internal) "jugular"[7] vein, the head-sinus passes through a conspicuous foramen in the adult skull near the 5th nerve. This foramen is remotely represented in the human chondrocranium by the prominent ventral gap that is later ossified in membrane to form the middle fossa (fig. 18). In mammals, this remnant of the head-sinus has often been confused (Streeter, 1918; quoted, e.g. by van Gelderen, 1933) with the vein of the spurious jugular foramen, a vessel that is not associated, however, with the otic part of the 7th nerve (see stage 7*a*). In spite of the persistence of the head-sinus in reptiles, a secondary anastomosis between the stem of the middle dural plexus ("middle cerebral vein") and that of the posterior dural plexus ("posterior cerebral vein") does form; that is, the sigmoid sinus is represented as a small supplementary channel. The adult configuration is thus readily comparable to stage 4 of human development (fig. 5).

In birds, embryonic venous development at first parallels that of reptiles and mammals, but later deviates from both. The secondary anastomosis representing the sigmoid sinus is formed, but, as in reptiles, it soon anastomoses with that of the opposite side in the formation of the "mid-dorsal head sinus" (Hughes, 1934). Unlike the situation in reptiles, but resembling that of mammals, and for the same reason, there is an involution of the primary head-sinus. Its caudal end, the "primary Stammvene" of the chick (van Gelderen, 1924; Hughes), becomes crowded by the developing otic structures as in man. After being detoured dorsally, the primary trunk-vein is replaced, not by a dorsal and intracranial sigmoid sinus, but by a "secondary Stammvene" ventromedial to the extracranial parts of the 7th and 9th nerves. This anastomosis connects channels comparable to the ventral end of the extrachondrocranial middle dural stem (the pro-otic "middle cerebral vein") and the linguofacial tributary of the anterior cardinal (internal jugular) vein (cf. fig. 9). The secondary trunk-vein, like the primary one, is outside the avian skull, here receiving the prominent facial and orbital veins. It joins the primary (internal) jugular, which receives the vertebral and occipital veins, including an "external occipital" vein that emerges from the skull and is comparable to the mastoid emissary of mammalian development. Apparently, there is no definitive external jugular vein in either reptiles or birds, in contrast to the situation in mammals generally, wherein it becomes predominant (see below).

---

[6] Some writers apply the term "lateral sinus" to the combined *sigmoid* and *transverse* (BNA) sinuses of the adult; others apply it only to the latter; and still others include the sigmoid in the term "transverse sinus." It is not only expedient but also better from the developmental standpoint of all species to refer to each channel separately.

[7] The unqualified term "jugular" in the literature on both the embryo and the adult of various species has led to confusion, because it may refer to either jugular vein, the primary internal or the secondary external.

Primary Extracranial Veins

A noteworthy advance of stage 5 concerns the emergence of definitive extracranial veins. The region around the primitive orbit, now demarcated by the developing chondrocranium, is drained by two orbital veins, which have become almost equally prominent (fig. 9A): the most recent one is craniodorsal to the eye, the other caudoventral, and both now include ophthalmic tributaries. Earlier and later, however, these veins differ fundamentally. Naming them presents a problem, because of lack of precise terminology for the adult orbito-ophthalmic veins and because of their complicated development (see stage 7 and pl. 1).

In stage 3, the vein traversing the dorsal orbital region emerges dorsal to the primordial ophthalmic division of the 5th nerve, and is well developed by stage 4 (figs. 20, 21, pl. 1). By the present stage 5 (or 4; fig. 12), the distal end of the vein is associated with the supraorbital (and, soon, the frontal) branch of the ophthalmic nerve in the region supplied by the supraorbital division of the stapedial artery. An ophthalmic tributary, probably representing a primitive dorsal (superior) vorticose vein, joins the dorsal orbital vein. Except for its most proximal end (at the head-sinus), which is temporary, the present dorsal orbital vein constitutes the stem of the adult supraorbital vein from the earliest stages; in addition, however, its intraorbital part constitutes the most conspicuous adult vein among the superior ophthalmic group. In consideration of all the factors (see below), and granted that no simple name is adequate, the term *primitive supraorbital vein* is preferable to "ophthalmic" (e.g. Streeter, 1918) for this embryonic vein.

More appropriately than in the case of the supraorbital vein, the stem of the vein traversing the ventral orbital region, namely the primitive maxillary, has also been called the "ophthalmic" by various writers, including Markowski (1922) and Thyng (1914), in reference to an embryo of stage 5. The maxillary vein of the maxillary process has emerged before stage 2, in the role of exclusive ophthalmic drainage, i.e. of the optic cup (or vesicle) and stalk (see stage 2). In succeeding stages, however, its primary ophthalmic and later orbital tributaries become more and more disguised among the other voluminous and plexiform maxillary tributaries, particularly the components of the adult pterygoid plexus (see below and fig. 12); among them in stage 5 are included the primitive ventral (inferior) vorticose and ciliary veins, and also the future central vein of the retina, represented as early as stage 2. Another primitive ophthalmic remnant, which is anomalous postnatally (p. 116), often persists in embryonic stages; it extends from the cranial cavity in company with the optic nerve, by way of the optic foramen (fig. 14B3).

The primitive maxillary (infraorbital) vein reaches the height of its development in stage 5. Although it is the primary ophthalmic vein, as was noted above, it now shares drainage of the orbit and, to a lesser extent, of the eye with the augmented supraorbital vein. Its major territory has come to include the emerging nose and all of the expanded upper jaw (fig. 9). Figure 12 shows that its most medial tributaries are associated with the nasociliary branch of the ophthalmic nerve; the prominent lateral tributaries come from the primordia of the pterygoid and temporal muscles in close association with motor branches of the mandibular nerve. The maxillary vein, therefore, which was once confined to the maxillary process with the maxillary division of the 5th nerve, has begun to invade, cranially and caudally, the territory of the other two divisions of the 5th nerve (figs. 19–23, pl. 1). This development initiates the formation of the future anterior facial vein in stage 6. The lower jaw is still drained by the linguofacial vein, consisting of two main divisions. The medial tributary, as before, accompanies the 12th nerve to the base of the tongue, and the larger lateral tributary now drains structures associated with the mandibular division of the 5th nerve. Figure 9 shows that a plexiform anastomosis between lateral tributaries of the linguofacial and maxillary veins has already formed around the outer labial margin. Among the many plexiform and more medial tributaries of the maxillary vein, the adult pterygoid plexus is already represented.

Modifications in tributaries of the internal jugular vein are seen in figure 9. In the preceding stages, the only vein from the arm was caudal or ulnar in position; this primitive ulnar vein joined the *lateral thoracic* (thoracoepigastric) *vein* to form the primitive subclavian trunk. An inconspicuous cranial tributary of this trunk in stage 3 (fig. 5) has developed into a *primitive cephalic vein* following the radial border of the arm; this vessel is continuous with the ulnar vein by way of the marginal vein outlining the hand plate. The proximal end of the new cephalic vein is not that of the adult, however, but curves cranially around the superficial aspect of the clavicular primordium (fig. 9). This arched part of the vessel, which is the temporary proximal end of the cephalic vein, has been called the *jugulocephalic vein* (e.g. F. T. Lewis, 1909), a name appropriate for three reasons: it emphasizes the temporary cervical detour of the primitive cephalic vein, identifies the segment which usually disappears after the permanent infraclavicular relocation of the cephalic trunk, and suggests the imminent external jugular vein which will adopt the discarded postclavicular part of the cephalic vein as its terminal trunk.

The plexiform *vertebral vein* has now been formed comparably to its companion artery (Padget, 1954).[8] It is seen (figs. 19–22, pl. 1) that each cervical nerve is primarily accompanied by a cervical intersegmental vein (and artery), the most caudal veins joining the posterior cardinal vein. As elongation of the neck region separates the heart from the base of the cranium, the lower cervical nerve roots appear to rise to the level of the common cardinal vein. Consequently, the proximal ends of the lower cervical intersegmental veins, like those of the arteries, become grouped closely together in migrating cranially to and upon the anterior cardinal vein (fig. 9). Now a secondary longitudinal anastomosis between the primary transverse intersegmental veins has produced a primitive vertebral vein, and most of the jugular ends of the intersegmentals have dropped out. The vertebral vein remains plexiform around its companion artery and empties into the internal jugular or the primitive subclavian vein, before the formation of the left innominate vein in stage 6.

In the adult the caudal end of the vertebral vein passes through the transverse foramen of either the 6th or the 7th cervical vertebra, or it may be bifid, traversing both. Its cranial end, together with components of the deep cervical vein, joins one or more of the veins around the foramen magnum: specifically, the *primitive condylar* (condyloid) *emissary,* a tributary of the sigmoid sinus; or, particularly if the condylar is absent, the *primitive hypoglossal emissary,* which is a tributary of the primitive myelencephalic vein (future stem of the inferior petrosal sinus). These emissary veins, before the emergence of the external jugular system (stage 6), drain extracranial structures medially through their respective well defined foramina in the chondrocranium. Together with the *primitive mastoid emissary vein*—its foramen, sometimes formed at this stage, is characteristic of stage 6—these emissaries will finally constitute a source of voluminous collateral circulation between the sigmoid sinus and the external jugular system of the adult.

STAGE 6. EMBRYOS OF HORIZONS XX, XXI (18 TO 26 MM.)

At this significant stage in vertebrate embryology, the head has begun to lift off the chest, the expansion of cerebral hemispheres and cerebellar plate has brought the brain flexures to the height of their development, and the facial region is well defined (fig. 10). In the human embryo the fingers have appeared, and the arm is flexed at the wrist and elbow. Arterial development is particularly marked by the major components of the external carotid system, which emerged in stage 5. This system has annexed the three branches of the temporary stapedial artery (from the internal carotid), which are associated with the three divisions of the 5th nerve; in many mammals (e.g. the cat, Davis and Story, 1943), the external carotid takes over additional branches of the internal carotid, e.g. the ophthalmic, and finally becomes predominant to the primary carotid.

Similarly, the basic component of the external jugular system has now appeared—a system that will later annex most of the tributaries of the internal jugular vein, over which it is conspicuously predominant in many mammals. In man, although the tributaries of the primary head-sinus and, more variably, the primitive linguofacial (common facial) tributary of the internal jugular become anastomosed with the external jugular, they are only partly taken over by it. Apparently this stage is a crossroad in the development of craniocervical vessels, particularly the veins. From here on, in different species the growth of the brain relative to that of the face and neck determines which carotid and jugular systems, internal or external, will predominate in the adult; this concept is illustrated in plate 6.

Pro-otic and Tentorial Sinuses

Two major primary sinuses, prominent throughout fetal life, become clearly defined at this stage. Their history explains the fate of the typical primitive channels they represent, namely the stems of both the anterior and middle dural plexuses (stage 2). As was described in stage 5, the stem of the posterior dural plexus is stable in contrast to the two stems just named; it is merely augmented to form the caudal end of the sigmoid sinus.

The head-sinus, which the three dural stems originally joined, has essentially disappeared in stage 5 with the exception of its short segment (lateral wing of the future cavernous sinus) medial to the 5th nerve. A small remnant, however, accompanying the 7th nerve extracranially and immediately ventral to the otic capsule (fig. 10A), must be emphasized for these reasons: it is the only remains of the primary drainage vessel of the head region, typical of vertebrates, which is permanently retained in this capacity in the pattern of reptiles (see stage 5); it must not be identified, as has been done for stage 5 and later (p. 124), with the primitive temporal emissary vein of the foramen jugulare spurium, the augmented counterpart of which becomes the permanent major exit for intracranial blood in many mammals (pl. 6). Study of the developing vasculature of the ear region showed that the caudal remnant of the head-sinus in stage 5 is incorporated into the veins accompanying the superficial petrosal and the stylomastoid arteries,

---

[8] The earlier study (1948) was supplemented because the modern substitution of the preferable term *intersegmental* for "segmental," in reference to the arteries and veins passing between the embryonic somites, had resulted in much uncertainty about the identification of the vessels involved in the formation of the vertebral and subclavian arteries.

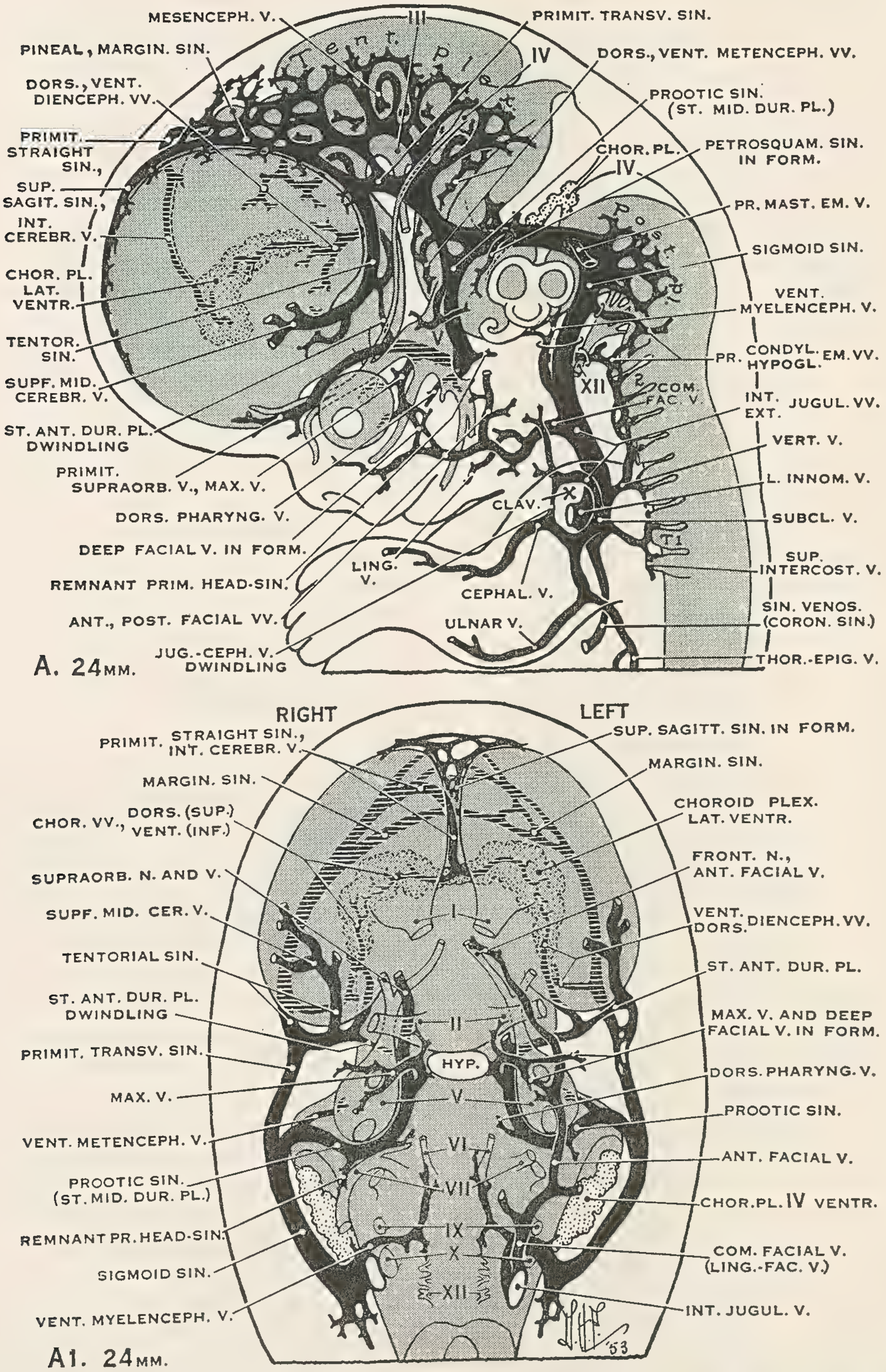

Fig. 10. Stage 6. The superficial middle cerebral veins, particularly on the right (A1), now drain dorsally through the tentorial sinus into a component of the future transverse sinus; as a result, the anterior dural stem is dwindling. With the disappearance of the caudal part of the head-sinus, the veins from the eye region drain dorsolaterally through the middle dural stem, now called the pro-otic sinus. Note (A1) that the primitive sagittal and straight sinuses both drain more to the right side. The new anterior facial vein (cf. A and left side A1) is annexing lateral tributaries of the maxillary vein, and is about to anastomose with a cranial (external jugular) tributary of the jugulocephalic vein.

which anastomose with each other in accompanying the intraosseous course of the 7th nerve (Padget, 1956).

In the augmented stem of the middle dural plexus, the blood flow has presumably undergone a reversal, from the former head-sinus, which was ventral, to the new sigmoid sinus, dorsally situated. The stem now constitutes the *pro-otic sinus*. Markowski (1911, 1922) called this prominent and constant dural channel the pro-otic "vein," but Mall (1904) and Streeter (1918) thought it to be the superior petrosal sinus. Granting that the present position of this channel bordering the craniodorsal aspect of the superior semicircular canal (fig. 10) does suggest the latter inference, such an error is explained by a prevalent lack of information regarding the two channels thus confused: the prominent remnant of the pro-otic sinus as usually found in the late fetus or infant, and the medial end of the adult superior petrosal sinus (the part connecting it to the cavernous sinus), which is both secondary and inconstant. Although the most caudodorsal (lateral) end of the pro-otic sinus is in the position of the adult superior petrosal sinus, which it later constitutes, its greater part has a different course. This course is more cranial than dorsal to the crest of the otic capsule, and is extracranial in reference to the chondrocranium. Furthermore, the pro-otic sinus leaves the cavernous sinus ventral and medial to the trigeminal ganglion at the origin of its mandibular division (pls. 1, 2). In contrast, the secondary medial end of the adult superior petrosal sinus, never in contact with the mandibular nerve, is usually formed dorsal and lateral to the 5th nerve root; the communication, moreover, between the superior petrosal and cavernous sinuses is a late secondary development (see stage *7a*), which often does not occur until after birth, if at all, and is absent in mammals generally. The significance of the pro-otic sinus will be clear in later stages when it gives origin to the middle meningeal sinuses (dural veins), elements of which can already be seen lateral to the trigeminal ganglion (fig. 10). The name *pro-otic,* as used hereafter, will include for simplicity the last remaining short segment of the primary head-sinus ("vena capita lateralis") of stages 1 and 2. From this segment, which has always been medial to the trigeminal ganglion, the cavernous sinus is derived during stage 7.

Comparison of figures 22 and 23 (pl. 1) shows that the pro-otic sinus, unlike the former middle dural stem it represents, does not chiefly concern drainage of the brain. Instead, it is the direct outlet for two extracranial veins, the supraorbital (superior ophthalmic) and the maxillary. The reason for this situation is that the once voluminous stem of the anterior dural plexus has dwindled to an insignificant channel or has disappeared. The blood from the fore parts of the head and brain, which heretofore drained ventrally through this stem into the head-sinus, now goes dorsally into the lateral segment of the primitive transverse sinus.

Concomitant with the definition of the pro-otic sinus, another important embryonic channel, to be called here the *tentorial sinus,*[9] becomes prominent. This sinus, represented earlier in the anterior dural plexus by a channel that drains telencephalic pial-dural tributaries, has become longer and more conspicuous (pl. 1). It borders the caudoventral aspect of the cerebral hemisphere, and receives not only the superficial and deep telencephalic (middle cerebral) veins but also the ventral diencephalic vein. The tentorial sinus of stage 6 (fig. 10) was called the "tentorial vein" by Markowski (1911, 1922) and the "inferior cerebral vein" by Streeter (1918). It must be emphasized, however, that the channel is dural, not pial, in position. Lying just superficially to the 3d and 4th nerves, it accompanies them for some distance through the primitive tentorium, which is now represented by a relatively wide wedge of condensed mesenchyme separating the cerebral hemisphere from the cerebellar plate. The phylogenetic significance of the tentorial sinus will be discussed in stage *7a,* after its subsequent elongation coincident with the expansion of the caudal part of the brain (cf. figs. 22, 23, pl. 1). For a long time, sometimes permanently, the sinus is the only drainage for the largest veins of the cerebrum; before the formation of the basal cerebral vein (stage *7a*), it also drains the diencephalon and the corpus striatal region.

The venous pattern of stage 6 (fig. 10) indicates the fate of the three prominent stems of the primitive dural plexuses, leading to the head-sinus, which were formed in stages 1 and 2 (before 8 mm.). The posterior stem (sigmoid sinus) is permanent, and the middle one (pro-otic sinus) often persists throughout fetal life, leaving definitive postnatal remnants. In contrast, the stem of the anterior dural plexus is temporary and is usually dwindling or absent at stage 6. Streeter thought, however, that the anterior dural stem represents the adult communication, as commonly described, between the middle cerebral (telencephalic) veins and the cavernous sinus (Streeter, 1918, fig. 27, pl. 5; p. 29). His interpretation again reflects a prevalent failure to appreciate certain details of human and comparative anatomy: the middle cerebral veins of many adult mammals drain exclusively to the junction of the sigmoid and transverse sinuses, or their counterparts, through a channel that represents the present tentorial sinus; a homologous retention of this arrangement is regularly found in the late human fetus or newborn and often in the adult (see stage *7a*).

---

[9] This must be distinguished from the postnatal tentorial sinus of Gibbs and Gibbs (1934), which drains cerebellar veins (see stage *7a,* p. 133).

Only in general may it be said that the "middle cerebral" veins of the early human embryo empty by way of the anterior dural stem into the "cavernous sinus," since this sinus will be derived in stage 7 from the primary head-sinus (pl. 2). This anterior stem later becomes anchored cranially by the sheath surrounding the juxtaposition of the 4th and 5th (ophthalmic) nerves (figs. 21–24, pl. 1). As such, it cannot represent the inconstant and secondary adult communication between the cavernous sinus and middle cerebral veins, which is lateral to the 4th nerve and borders the lesser sphenoid wing (fig. 39, pl. 2). Furthermore, at the present stage 6 the anterior dural stem usually has either dwindled considerably or has disappeared. The result is that the middle cerebral veins now drain dorsally, instead of ventrally, into the new primitive transverse sinus by way of the tentorial sinus.

The tentorial sinus must not be confused with the *tentorial plexus,* an appropriate name (Streeter) for the combined anterior and middle dural plexuses of preceding stages; from the former, the tentorial sinus was earlier derived (cf. figs. 20–23, pl. 1). Whereas the tentorial plexus is gradually reduced during caudal cerebral expansion and the elaboration of the major adult sinuses (pl. 1), and is finally represented by the adult torcular (confluence of sinuses), the tentorial sinus remains prominent throughout fetal life, and not infrequently later.

Coincidently with the loss of the stem of the anterior dural plexus and the compensatory development of the tentorial sinus emptying into the primitive transverse sinus, a second forebrain vessel belonging to the tentorial plexus has come into conspicuous view, namely the marginal sinus. This channel, bordering the dorsocaudal margin of the emerging cerebral hemisphere, was identified in stage 3 (cf. figs. 20–23, pl. 1), but now appears to be the direct continuation of the primitive transverse sinus to the mid-line (fig. 10). Although called for simplicity the medial component of the transverse sinus, the marginal sinus is not a stable vessel, as was fully discussed by Streeter (1918): for some time, as the hemisphere expands, it will be replaced by succeeding anastomoses with more caudal loops in the tentorial plexus. By stage 6 the marginal sinus ("anterior marginal vein" of Markowski, 1911, 1922) meets that of the other side in a plexiform anastomosis, named the *sagittal plexus* by Streeter, which lies between the cerebral hemispheres and constitutes the elements of the future superior sagittal sinus and its derivative, the inferior sagittal sinus. From now on, it will be simpler to refer to the more precocious and stable lateral part of the primitive transverse sinus and the shifting marginal sinus as one, namely the *primitive transverse sinus.*

Asymmetry of Venous Channels, Notably in the Tentorial Plexus (*Torcular*)

Consecutive stages (figs. 20–23, pl. 1) show that the anterior and middle dural plexuses become consolidated in the condensed mesenchyme representing the tentorium, and together constitute a *tentorial plexus* at stage 6. Typically, the tentorial plexus, which includes the sagittal plexus just noted, does not drain equally to the right and to the left sides. Instead, asymmetrical drainage is indicated by the relative size of the two transverse sinuses, specifically, of the marginal sinuses constituting their proximal (medial) ends: that on the left is often still notably plexiform, whereas that on the right is better defined and is the larger, because it receives most of the drainage of the primitive superior sagittal sinus (plexus)—a common adult pattern. A deep component of the sagittotentorial plexus is the future straight sinus, a continuation of the primitive internal cerebral vein, which is an irregular channel lying on the membranous roof of the diencephalon. This mid-line channel (fig. 10) drains the choroid plexus of both lateral ventricles at the interventricular foramina (of Monro) and, it should be noted particularly, also empties into the larger primitive transverse (marginal) sinus on the right. The configuration, in other words, is the opposite of that in a typical adult, in which predominant drainage of the straight sinus is to the left side. Streeter (1918) stated that the *primitive sagittal sinus,* derived from the sagittal plexus, drained more to the right side in 16 of 18 embryos from 17 to 80 mm. long. This configuration was noted by the author in most of these and in 9 other specimens within this range; furthermore, Streeter's observation of left-sided drainage could not be confirmed in the 2 specimens so designated. He noted that no explanation had been advanced for this interesting asymmetry.

According to the present study, it appears that the tendency toward venous asymmetry at the torcular, which is evident even earlier (stages 3, 4, fig. 7), depends upon the developmental alterations of the great veins leading to the heart, as summarized in plate 3. Initially, these veins are almost bilaterally symmetrical (pl. 3A). By stage 2 (5 to 8 mm.), although the right common cardinal vein still empties directly into the right atrial section of the heart, the left reaches it somewhat less directly by way of a channel caudal to the heart tube. At first, this embryonic sinus venosus (represented by the adult coronary sinus) is relatively wide and short. Owing to the differentiation of the heart, it is soon forced to elongate; while also becoming relatively reduced in size, it takes a marked curve from the front toward the back of the chest before entering the right atrium (pl. 3B). During and after stage 6 (horizons xx, xxi), the considerable subcardiac detour of the blood from the left side of the head can be counteracted to a variable extent by a secondary anastomosis—namely the formation of the *left innominate vein,* which connects the two internal jugulars (anterior cardinals) cranial to the heart (pl. 3E). Initial stages of this new channel are seen earlier, at stage 5 (horizon xix), as a plexus of small veins in the mid-line just cranial to the arch of the aorta (pl. 3D). These *thymicothyroid* veins, right and left, which drain the corresponding primordia, empty into the internal jugulars near the level of the subclavian veins. As was noted by Anikew (1909) and by Thyng (1914) in embryos of stage 6, one of these vessels enlarges to become the transverse left innominate vein, which receives the inferior thyroid veins in the adult.

The secondary left innominate may eventually permit almost as direct access to the heart for blood from the left side of the head as that from the right; this, however, is not typical of man. The ultimate difference, anatomically, of drainage on the two sides conceivably depends upon the variable length and direction of the secondary left innominate vein in the adult (see pl. 6; Padget, 1956, fig. 23).

It was not possible within the limits of the present study to explore the occurrence of venous asymmetry and possibly related factors in any orderly or conclusive way, and the observations below are merely for the record. The tendency of the veins, particularly near the top of the head, to drain more to the right than to the left side was most obvious and consistent at stage 6 in the present series. Whenever a difference was seen in either younger or older specimens, drainage to the right invariably predominated (figs. 7, 10B). Furthermore, it was noted that venous development tends to be a little more advanced on the right in embryos before horizon xxi, as shown in figures 1, 4, 7, 11, and 12.

Such observations raised the question whether there are any other dissimilarities on the two sides, especially in those embryos that definitely show the asymmetry in drainage. Essentially no disparity was detected in most cases, but, in a few, certain structures on the right side appeared to be somewhat more advanced than those on the left. Only particularly well preserved embryos, sectioned symmetrically and enlarged sufficiently in photographs for reconstruction, can demonstrate minor disparities, such as were detected in several younger embryos of this series. Here, the following factors provide a gross index to growth: (1) reduction of the opening of the otic pit to form the vesicle; (2) approximation of the optic vesicle to the skin stimulating the lens formation; (3) the relative size of these vesicles, of the nerve roots, and of the emerging maxillary process; and (4) the depth of the mesenchyme in general. In reference to such indices, the disparities found invariably suggested a certain lag of development on the left side, as shown in figures 1, 4, and 7.

Whether or not structural asymmetry is related to that of the veins noted above, including patterns which permit the anterior dural plexus to drain predominantly toward the right side (fig. 7), is problematical. No comparable discrepancy in the arteries happened to be observed in any embryo, although the arterial pattern frequently differs in detail on the two sides.

Modification and Reduction of Pia-arachnoidal Veins

The intracranial venous system of stage 6 shows relatively minor advances in the cerebral veins, of which the conspicuous and constant ventral diencephalic vein is the most noteworthy. Expansion of the brain and elaboration of the sinuses described above have brought about not only an elongation and a change in direction of this transverse pia-arachnoidal vein, but also an apparent change in its dural exit, now the tentorial sinus (figs. 10, 11). Fundamentally, however, the tentorial sinus is a part of the anterior dural plexus in which the diencephalic vein has terminated from its beginning in stage 2. As seen in the basal view of stage 6, the recent pattern has occurred only on the right side of the embryo, which is the more advanced from the venous standpoint (fig. 10A1). On the left, although the telencephalic veins now empty into the tentorial sinus, the ventral diencephalic vein empties, as more primitively, into the stem of the anterior dural plexus, which is still large compared with that on the right. On either side, the ventral diencephalic vein now drains not only the more ventral diencephalon but also the voluminous choroid plexus of the lateral ventricle. In fact, this ventral choroid drainage is primarily more marked than the dorsal route through the primitive internal cerebral vein (fig. 10), as discussed for stage 7.

The ventral diencephalic vein is often augmented at stage 6 by a *dorsal diencephalic vein* ("lateral diencephalic vein," Markowski, 1911, 1922) from the more caudal, dorsal, and lateral aspects of the primitive thalamus (fig. 11). Other findings include elaboration of the superficial lateral and deep medial telencephalic veins; there are often two (dorsal and ventral) mesencephalic and metencephalic veins. The stem of the mesencephalic vein (or veins), at its proximal junction with the tentorial plexus, usually disappears, as does that of the dorsal diencephalic at the transverse sinus after its tributaries are annexed by the ventral diencephalic vein, or vice versa. Similarly, the ventral metencephalic vein often annexes tributaries of the dorsal metencephalic, when present, to form one conspicuous stem (essentially the superior petrosal sinus of stage 7*a*), which empties into the pro-otic sinus at its junction with the sigmoid. The ventral diencephalic vein may remain prominent for some time, but finally (ca. 80 mm.) its stem of exit in the tentorial sinus is lost in most cases (pl. 5C).

As was discussed in stage 4, and by Streeter (1918), cranial venous development is characterized by a diminishing number of channels draining the pial venous system into the dural system (see Padget, 1956, figs. 1, 26). The reader must not be confused, therefore, by the fact that more of these transverse connecting veins are often

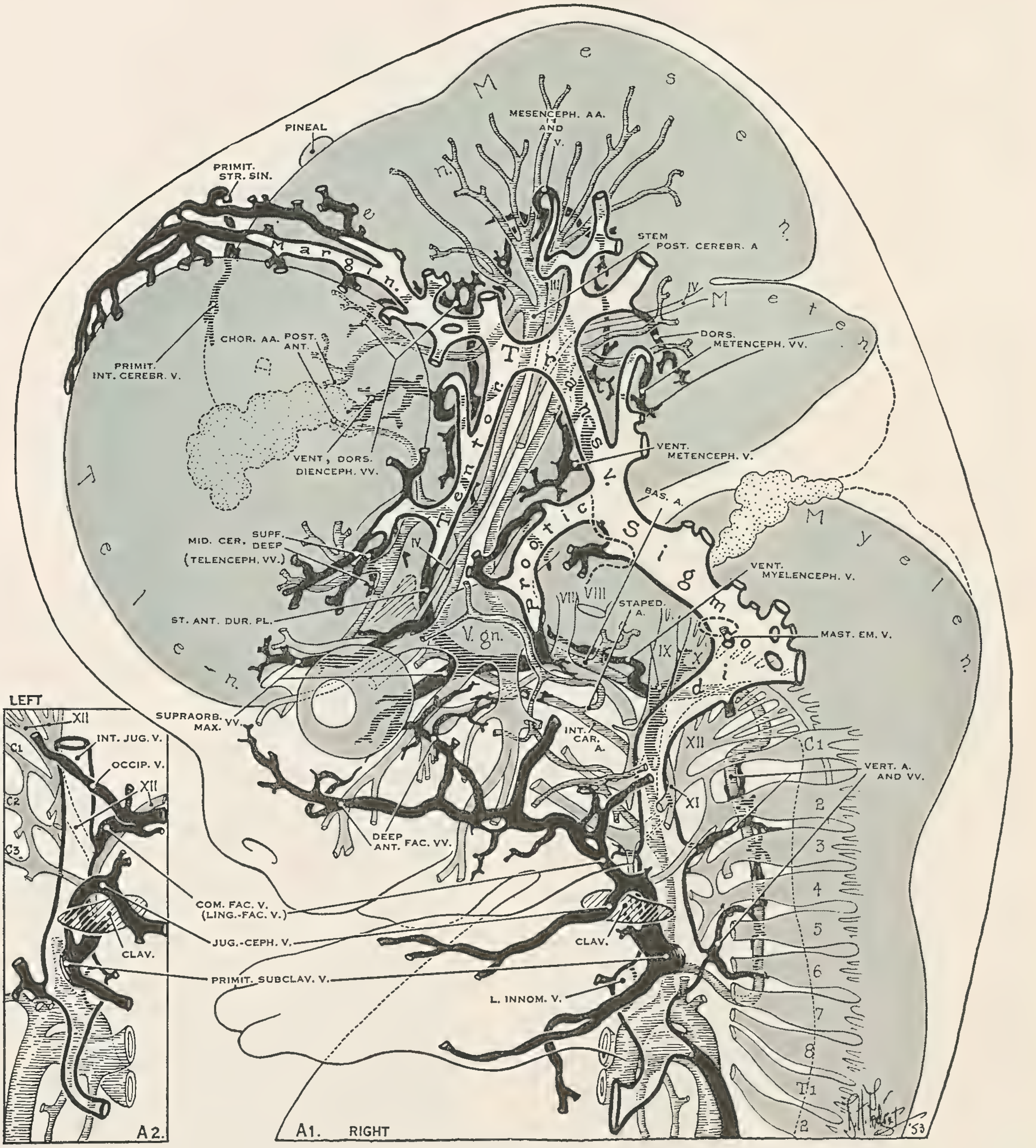

FIG. 11. Stage 6. Embryo Carnegie no. 966, 23 mm., xx, showing the typical relation of the primitive pial veins to the definitive branches of the internal carotid and basilar arteries. Two (or more) pia-arachnoidal veins from each region of the primitive brain are often identifiable. Their number becomes reduced as one of a pair annexes another, resulting in a single stem (cf. fig. 8), e.g. the ventral diencephalic vein, which joins the tentorial sinus. Note the different patterns on the two sides (reversed for comparison with other figures): the stem of the left common facial vein, as primarily, joins the internal jugular (insert); on the right, the stem has been annexed by the jugulocephalic vein, a component of the later external jugular vein.

readily visible at stage 6 (18 to 26 mm.) than previously. Such duplication of the regional veins (telen- to myelencephalic), even though not always identifiable in earlier stages, is not a secondary development in a strict sense, but rather represents the persistence of primary vessels, which are secondarily visible, but are eventually lost in most instances. Many pial-dural veins, relatively short and small, exist originally near the dorsomedial margins of the dural plexuses. These veins are reduced as the dural plexuses become smaller in elaboration of the sinuses, and as the dural layer becomes more and more separated from the pial layer. Those veins that remain are rendered more conspicuous as they become larger and longer in traversing the arachnoidal layer. Thus, although their number has been diminishing, it may appear to be maximum at the present stage. Hereafter, the stems of most of these veins will also drop out after secondary pial anastomoses between them have formed the definitive pial veins—a process coincident with the gradual reduction of the primitive tentorial and posterior dural plexuses, which constitute the adult torcular and the marginal sinus of the foramen magnum, respectively (figs. 23–26, pl. 1).

Emergence of External Jugular System; Facial Veins

By horizon xx the chondrocranium is prominent at the base of the brain (W. H. Lewis, 1920) and surrounds most of the cranial nerve roots; it is most advanced in the basioccipital and temporo-occipital regions, including the large otic capsule. Thus, the components of the intracranial venous system just described and the extracranial veins, which present notable changes in the developing face and neck, are readily distinguishable. Figures 21 to 23 (pl. 1) show that the new *anterior facial vein* has formed as follows: a prominent lateral tributary of the linguofacial vein has anastomosed at the outer labial angle with a posterolateral tributary of the maxillary vein, the stem of which is now considerably reduced in size. Caudal to the mandibular division of the 5th nerve, the anterior facial vein receives from the superficial temporal region a strong tributary representing the adult vein of the same name or, as it is sometimes called, the *posterior facial vein*. Hence, the embryonic linguofacial tributary of the internal jugular vein may now be called the definitive *common facial vein* (fig. 11). After anastomosis with the anterior facial vein, the lateral tributary of the dwindling maxillary vein constitutes the definitive *deep facial vein* (fig. 10). The cranial end of the anterior facial vein, which develops near the bridge of the nose in association with the frontal and nasociliary branches of the ophthalmic nerve (fig. 10A1), also anastomoses with the primitive supraorbital (superior ophthalmic) vein at the inner angle of the eye during this stage or the next (fig. 13). This emissary connection through the orbit between intracranial and extracranial veins is particularly significant in the adult configuration.

Figure 12 shows that the stem of the primitive maxillary vein, the lateral tributaries of which are being annexed by the new anterior facial vein, undergoes a marked reduction before stage 6 (figs. 20–23, pl. 1); its medial tributaries drain the optic nerve, nasal cavity, and pharyngeal roof. A remnant of one of its very primitive optic tributaries of stages 1 and 2 sometimes persists (cf. figs. 14B2, B3). In one injected embryo (Carnegie no. 460, xx, 21 mm.), this vessel ramifies intracranially around the cerebral end of the optic nerve before accompanying it through the optic foramen. It should be noted that the maxillary vein does not accompany the maxillary nerve through the foramen rotundum, now definitive in the primordial temporal wing of the chondrocranium (W. H. Lewis, 1920); instead, the vein is substantially medial to this cartilage, and borders the margin of the sella turcica at the site of the medial end of the future infraorbital fissure (cf. pl. 4A1).

As is generally known, and is well illustrated by F. T. Lewis (1909) and the Grant *Atlas* (1951), some, or most, of the adult tributaries of the common facial vein may empty into the external jugular vein, or sometimes into its anterior jugular tributary. The common facial (linguofacial) vein of the embryo, however, primarily joins the internal jugular (stages 2 to 6). Not until stage 6 (averaging 22 mm.) does the *external jugular vein* begin to emerge. Clearly, therefore, communications between the common facial and external jugular veins are secondary; they are present in stage 7, although variable (fig. 13).

Comparison of figures 22 and 23 (pl. 1) shows how the external jugular vein is formed. A small cranial tributary of the primitive cephalic vein in the arm at stage 6 (fig. 9) has grown larger in the differentiating tissues of the neck, and joins the jugulocephalic vein craniodorsal to the cartilaginous clavicle, which is now surrounded by a venous ring (fig. 10). The caudoclavicular part of this ring is a new anastomosis whereby the definitive *cephalic vein* overcomes its jugulocephalic detour and becomes directly continuous with the *subclavian vein,* now definitive. The old proximal end of the primitive cephalic vein, which is the craniodorsal part of the clavicular venous ring, may be recognized as the trunk of the adult external jugular vein. The part of the venous ring ventral and superficial to the clavicle, i.e. the jugulocephalic segment of the primitive cephalic vein (p. 100), often dwindles at stage 6 (fig. 10) and is usually lost.

Cases of atypical retention of the jugulocephalic vein in the adult are illustrated by F. T. Lewis (1909; see also fig. 1068 of the Toldt *Atlas,* 1941). Similarly, the adult cephalic vein may join either the external jugular vein or its *anterior jugular* tributary (sometimes definitive as

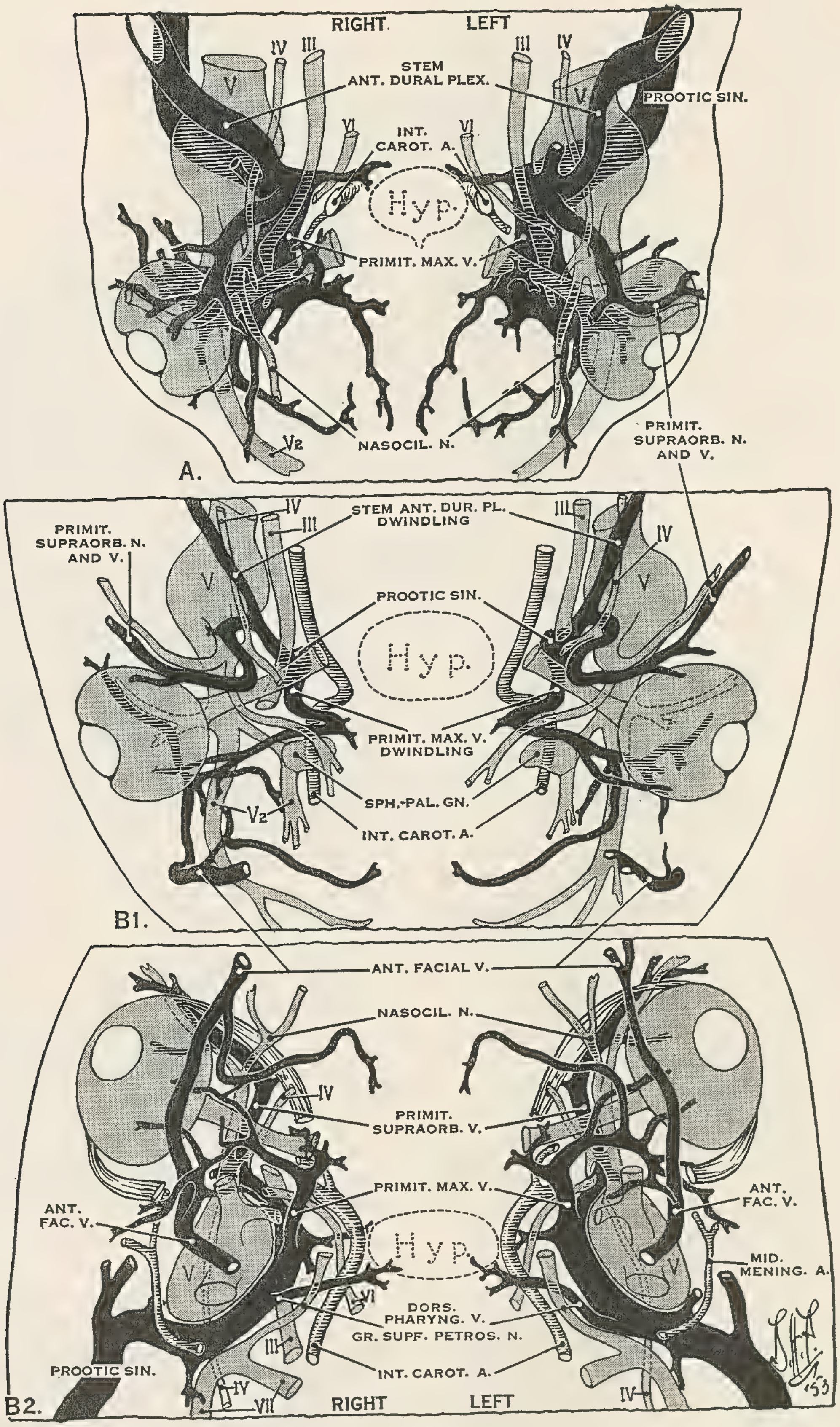

Fig. 12. Two embryos of late stage 4 and stage 6 (same magnification): A and B1, frontal views of coronal reconstructions of Carnegie no. 492, 16.8 mm., xviii, and no. 966, 23 mm., xx, respectively; B2 is a correlating basal view of no. 966. Note the voluminous maxillary vein (A), which includes infraorbital tributaries. By horizon xx (B1), the primitive supraorbital vein has become detoured dorsal to the juxtaposition of the 4th nerve with the ophthalmic nerve, established earlier (A); this indirect course precedes a secondary anastomosis whereby the stem of the maxillary vein will become that of all the adult orbital veins (cf. fig. 14). Owing to secondary annexation of its lateral tributaries by the new anterior facial vein, the stem of the maxillary vein dwindles (B), a development more advanced on the right side of this embryo.

a small vessel at the present stage) cranial to the clavicle. Remnants of the embryonic venous ring around the clavicle may also persist (F. T. Lewis), so that the adult subclavian is either double or passes between the clavicle and subclavius muscle. Plate 3E (coronal view of stage 6) shows bilateral asymmetry: on the left of the embryo, which is typically somewhat less advanced from the venous standpoint than the right side (see above), the stem of the external jugular, joining the supraclavicular (jugulocephalic) arch of the primitive cephalic vein, is ill defined and has no anastomosis with the common facial tributary of the internal jugular; on the right side, the external jugular stem not only is well developed but has annexed essentially all the tributaries of the common facial vein, the origin of which is represented by a small twig of the internal jugular (fig. 11A1). The secondary anastomosis between the external jugular and common facial veins, which is sometimes seen at this time and is regularly found in stage 7 (fig. 13), is commonly represented in the adult by a prominent channel; often called the posterior facial vein, the anastomosis is also designated as part of either the superficial temporal or the external jugular vein.

The considerable adult variety in detail of these veins, well illustrated in diagrams by F. T. Lewis (1909), can now be understood. Lewis emphasized that the linguofacial, later common facial, tributary of the internal jugular is a primary constant in mammals (and other vertebrates). In species except certain primates, it gives up most of its tributaries to the secondary external jugular coincident with a secondary retrogression of the internal jugular vein (pl. 6). In adult man, however, its derivatives, notably the anterior facial, lingual, superficial temporal, and internal maxillary veins, are commonly drained by both jugular systems, the external and internal.

Stage 7. Threshold of Fetal Period (ca. 2½ mos. and 40 mm.)

The change in designation from embryo to fetus, although somewhat arbitrary, is useful in denoting the acquisition of essentially all the characteristics recognizable in later life. By the 40-mm. stage, the cranial arteries that radiate from the completed circle of Willis are readily comparable to those of the adult. Whereas the pattern of these arteries, arising near the mid-line, will not be essentially changed by the great expansion of the cerebral and cerebellar hemispheres yet to come, that of the venous channels, except in the face and neck, awaits many major alterations before recognizable maturity (fig. 13).

Superior Sagittal Sinus and Primitive Galenic System

In previous stages, only one component of the adult sinuses has become definitive—the sigmoid. Although the whole length of the primitive transverse sinus is outlined in the tentorial plexus, its course is opposite to that of the adult (figs. 22–24, pl. 1). Its lateral end joining the sigmoid sinus is well defined, but its less-advanced medial segment, the marginal sinus, is still being transferred caudally; this process, called anastomotic progression (spontaneous migration),[4] is possible in the meshes of the tentorial dural plexus, or, more specifically, its cranial component near the mid-line, the sagittal plexus. This process initiates the formation of the *superior sagittal sinus,* described by Streeter (1918). As the cerebral hemispheres grow caudally and become approximated at the mid-line over a greater area, the marginal sinuses, which follow their dorsocaudal borders, join in a mid-line anastomosis. Like several other mid-line vessels derived from bilateral channels, notably the basilar artery, the superior sagittal sinus emerges by a combination of two processes: the unequal or alternate enlargement of the channel of one side with a dwindling of the opposing vessel; and, to a lesser extent perhaps (Streeter), a coalescence of the bilateral channels. As was discussed above, the sagittal sinus drains more into the right transverse sinus than into the left in all the embryos of this series (fig. 7), as it frequently does in the adult. Since its dural sheath is still histologically immature, the typical triangular shape of the adult sinus in cross section is not seen until much later. The sinus receives a number of ill-defined tributaries, remnants of the anterior dural plexus, on the dorsocaudal convexity of the hemisphere. Sometimes identifiable is the anastomosis between one or more of these primitive superior cerebral veins and the superficial middle cerebral (telencephalic) veins that represents the great anastomotic vein, or veins (of Trolard, 1868), commonly described for the adult. In contrast to their secondary pial tributaries, the stems of these major veins, immediately derived from the anterior dural plexus, are superficial to the arteries of the cerebral convexity (see stage 4).

Another differentiation of the mid-line sagittal plexus includes the first stages in the establishment of the Galenic system of intracerebral drainage. The *primitive straight sinus,* continuous with the *primitive great cerebral vein* (of Galen), leaves the membranous diencephalic roof near the pineal primordium (fig. 13). Like the primitive sagittal sinus, a plexus that drains predominantly to the right from its earliest stages, the channel representing the straight sinus also drains chiefly to the right side in the embryos of the present series. Although this configuration is compatible with the history of all the related channels until this time, the adult straight sinus is usually described as draining more to the left, i.e. to the side opposite that of maximum drainage of the superior sagittal sinus, as described in stage 6. An intermediate stage in the secondary transference of more drainage to the left side, which presumably occurs

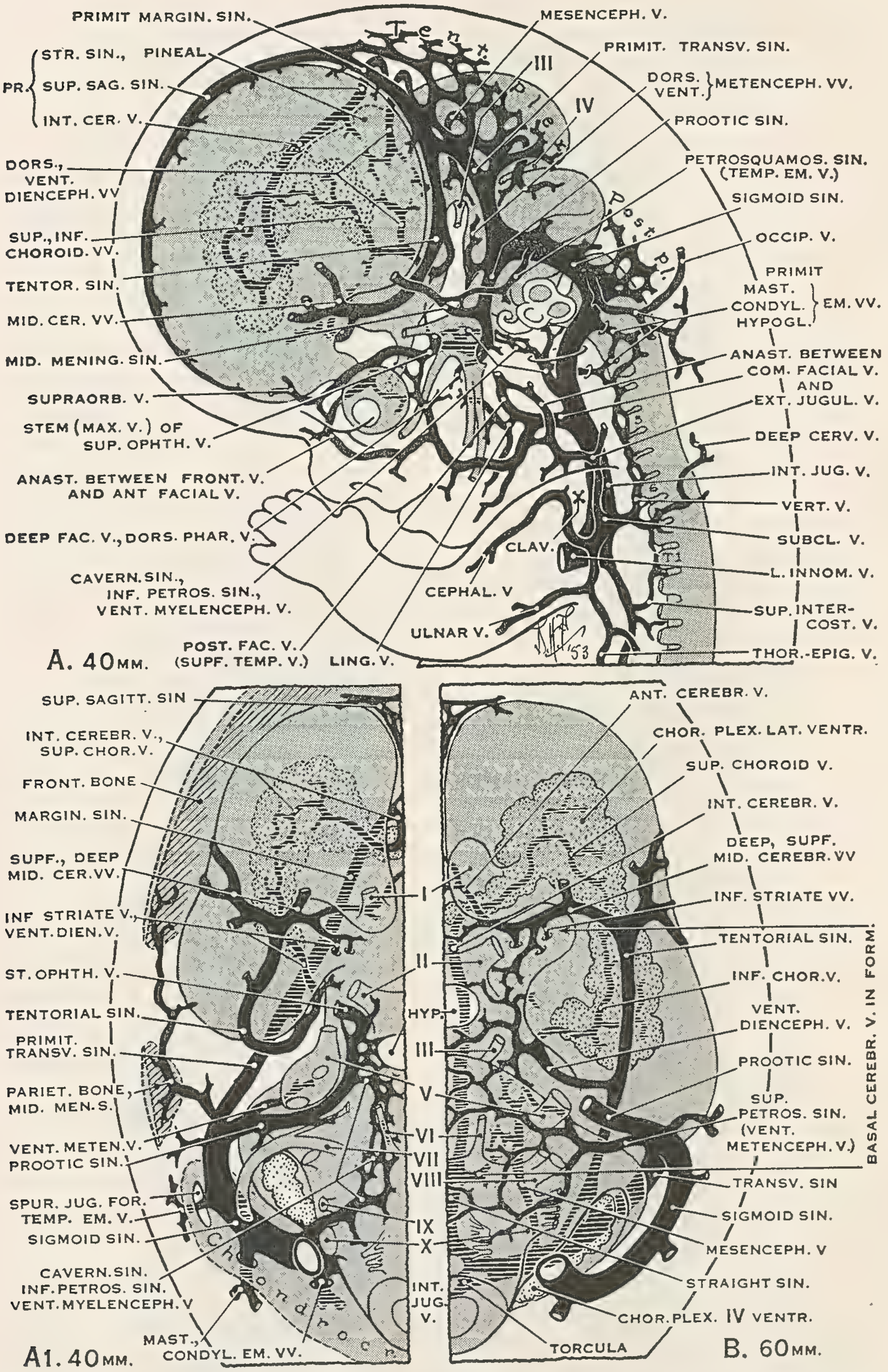

FIG. 13. Stage 7 (when the arteries resemble the adult configuration; cf. pl. 4A2). Although the ventral diencephalic vein continues to drain the lateral choroid plexus (A1, B), its dorsal drainage is established by way of the superior choroid vein, the only primary tributary of the primitive internal cerebral vein. The new cavernous and inferior petrosal sinuses are medial extensions of the pro-otic sinus and myelencephalic vein, respectively. The stem of the maxillary vein has become that of all the definitive orbito-ophthalmic veins. Anastomoses have occurred between components of the new external jugular vein and the primitive emissary veins. Note the elongation of the tentorial sinus (cf. A1 with B of stage *7a*) coincident with expansion of the hemisphere.

in many cases, is shown in Streeter's illustrations (1918, figs. 7–9) of the formation of the superior sagittal sinus; in the last stage pictured (a 54-mm. fetus), the primitive straight sinus has developed a relatively equal connection with each transverse sinus. It is here postulated (p. 104) that the early tendency of the mid-line venous channels which belong to the sagittal and tentorial plexuses to drain more toward the right side depends upon the temporary ventrocardiac detour, through the sinus venosus, of the blood in the left internal jugular vein in reaching the right cardiac atrium (pl. 3). The left innominate vein, formed in stage 6, reduces this detour to a variable extent in man and certain other mammals; it is a late development phylogenetically (McClure and Silvester, 1909).

The degree of persistent asymmetry of the sinuses at the torcular in the adult conceivably depends on that of the two innominate veins, since these develop differently: the vein on the left is a secondary anastomosis in its entirety; at first it is in transverse position and is relatively long, in contrast to the vein on the right, which is merely a segment of the primary anterior cardinal (internal jugular) vein (pl. 3), and hence is vertical. The relative length and direction of the two innominates, therefore, can vary considerably in the adult of different individuals and species; they are essentially symmetrical in mammalian types (McClure and Silvester). On evidence based in part on cases of persistent left superior vena cava (e.g. Halpert and Coman, 1930; Halpert, 1942), it is assumed that, the more nearly symmetrical the innominates become, the greater is the tendency toward equalization of drainage of the veins leading to the torcular (Padget, 1956, fig. 23). Since the developing straight sinus empties into the mid-line remnants of the tentorial plexus, i.e. the future torcular, it is in better position than the longer transverse sinuses, in the dwindling lateral parts of the tentorial plexus, to compensate for the primary inequality. Accordingly, a typical adult torcular in man appears to be one in which the superior sagittal sinus passes somewhat more to the right, and the straight sinus similarly to the left, with accessory channels, i.e. remnants of the tentorial plexus, on the contralateral sides.

At stage 7, the channel representing the combined primitive straight sinus and great cerebral vein of the adult is formed by the junction of a bilateral vein, the *primitive internal cerebral*. It must be understood that this vein, so named for convenience, is not definitive in the present series (under 80 mm.) in respect to either its adult position or its tributaries. Essentially, it is the continuation of a prominent *superior choroid vein* in the voluminous choroid plexus now almost filling the lateral ventricle, over which the hemisphere is a thin shell. Conversely, in the adult, the superior choroid vein is an inconspicuous tributary of the internal cerebral vein, formed by the junction of the septal vein (of the septum pellucidum) with the terminal (so-called thalamostriate) vein, which includes superior striate tributaries. Not until the formation of the corpus callosum and changes in the hippocampal complex at a stage beyond the present series is the internal cerebral vein enclosed within the brain, nor does it receive, with one exception, any intracerebral tributaries; they emerge later in response to the relatively great increase in the substance of the cerebral hemisphere.

The present drainage of the choroid plexus of the lateral (and third) ventricle into a superior choroid vein is secondary. At first, the choroid plexus, originating near the interventricular foramen (of Monro), is drained ventrally by way of an *inferior choroid vein,* a tributary of the prominent ventral diencephalic vein (figs. 9, 10). These veins will be incorporated into the later basal cerebral vein and its well defined inferior ventricular tributary (stage 7*a*). Apparently, the earlier inferior choroid vein is more or less annexed by the later superior choroid vein, while the internal cerebral tributaries are becoming predominant during cerebral expansion; anastomosis between the internal cerebral and basal cerebral veins by way of their choroid tributaries is frequent in the postnatal configuration.

Primitive patterns showing the Galenic system of intracranial drainage in stage 7 are well exemplified by an excellent embryo of 39 mm. with an unusually good natural injection (Carnegie no. 6203; photographs of the sections, ×25, facilitated graphic reconstructions, which unfortunately are among those that could not be included here). The corpus striatum, protruding into the ventrolateral aspect of the ventricular cavity, is drained ventrally, as primarily, by *inferior striate* tributaries of the anterior cerebral and deep middle cerebral veins, which are secondary pial derivatives of the primary superficial middle cerebral veins, shown in figures 33 and 34 (pl. 2). The thickened diencephalic wall, protruding into the narrowed third ventricle, is drained bilaterally by about six well defined tributaries of the dorsal diencephalic vein, sometimes annexed at stage 6 or 7 by the ventral diencephalic vein, definitive earlier (cf. figs. 10, 11).

The only exception in this embryo to the primary drainage of the basal nuclear masses ventrally into components of the future basal cerebral vein (stage 7*a*) is in the region of the interventricular foramen. It must be noted that the primitive internal cerebral vein is still extracerebral. Lying in dorsal contact with the epithelial diencephalic roof (future choroid membrane of the third ventricle), it is in contact with brain tissue, namely the diencephalon, only at the interventricular foramen. Here the vein receives one intracerebral tributary from the region of the anterior thalamic nucleus. This tributary, probably comparable to the adult "deep vein of the thalamus" (Browning, 1884) or to the "epithalamic vein" of Schlesinger (1939), but not of Bedford (1934*a, b,* in reference to the dog and rhesus monkey), may be called the *primitive deep thalamic vein.*

The single intracerebral (thalamic) tributary of the primitive internal cerebral vein, as it is found in the 39-mm. embryo identified above, is a clue to the way in which the conspicuous adult terminal vein is probably[10] formed at a later stage. At the interventricular foramen, this vein (unlabeled in fig. 13A), between its exit from the anterior thalamic region and its junction with the primitive internal cerebral (superior choroid) vein, lies for an appreciable distance in the pia-arachnoid still separating the primitive thalamus and corpus striatum. These two structures, primarily parts of the diencephalon and telencephalon, respectively, will become united by the increase of the internal capsule fibers which spread over the lateral surface of the thalamus as the lentiform nucleus extends caudally. Although it is well known that the adult internal cerebral vein, once extraventricular, is secondarily enclosed within the brain in a double fold of pia-arachnoid, an extraventricular derivation of the terminal vein is much less obvious in the adult, because it is covered by ventricular ependyma and its main stem also by the terminal stria (Spalteholz *Atlas,* 1937, fig. 720), which outlines the thalamostriate groove. In the 39-mm. embryo, a large venous plexus, bordering the internal cerebral veins on the epithelial diencephalic roof, lies adjacent to the hippocampus, which then extends caudally from the region of the interventricular foramen. This plexus anastomoses cranially with the stem of the thalamic vein, and caudally with the primitive internal cerebral. How it is possible for a derivative of this plexus to become enclosed in the floor of the lateral ventricle may be visualized in connection with embryonic stages in the secondary juxtaposition of the primitive thalamus and caudate nucleus, as illustrated by Hamilton, Boyd, and Mossman[11] (1952, fig. 326).

Sometime after the 80-mm. stage, the secondary terminal vein (not identified in the present series) receives the superior striate veins, which conceivably represent an annexation of certain inferior striate tributaries of the ventral diencephalic vein, well established at stage 7. Postnatally, there is some evidence (Padget, 1956) of a secondary anastomosis between the superior and inferior striate veins. In the 39-mm. embryo described above, one of several well defined ventral (inferior) striate veins is particularly long and prominent; it is also notable for its symmetrical configuration bilaterally. Its distal end coursing longitudinally through the primordial caudate just beneath its craniodorsal (intraventricular) surface is in the position, therefore, of the subependymal caudate tributaries of the adult terminal vein that receive the superior striate and other intraventricular veins. Such a vein could readily be involved in a later secondary anastomosis with the Galenic internal cerebral system, which is completed relatively late in cerebral venous development, paralleling cerebral dominance.

Inferior Petrosal and Cavernous Sinuses

The advanced growth of the chondrocranium and the beginning development of the frontal, parietal, and occipital components of the membranous skull at this stage (Macklin, 1921) lead to the emergence of the permanent derivatives of the pro-otic sinus. Its most lateral tributaries, associated with branches of the new middle meningeal artery, drain the primitive dura and adjacent bones, and are components, therefore, of the middle meningeal sinuses, to be discussed for stage 7*a* (figs. 13, 15; pl. 4). Of particular importance now are the new medial derivatives of the pro-otic sinus, the definitive inferior petrosal and cavernous sinuses, which appear simultaneously.

Although no well defined venous channel in the position of the *inferior petrosal sinus* is seen before the present stage 7, it is interesting that the adult trunk of the sinus, typically lying between the roots of the 9th and 10th nerves, appeared much earlier in stage 3. This trunk, which in all stages joins the internal jugular vein extracranially, represents the segment of the primary head-sinus that originally passed from the lateral aspect of the otocyst and the 9th nerve to the medial side of the 10th nerve during the transitory stage when the sinus lay between the 10th to 12th nerves and the brain (figs. 19, 20, pl. 1; figs. 27–30, pl. 2). After the head-sinus and the primitive internal jugular vein, continuous with it, are shifted outside the 10th nerve by way of secondary anastomoses (fig. 4), the former trunk of the sinus is retained as the stem of a transverse pia-arachnoidal vein from the medulla. Relatively early, this ventral myelencephalic vein, which drains the neural tube between the 6th and 10th nerves, also receives components of other adult veins, the hypoglossal emissary and the vein of the cochlear aqueduct. Just distal to these tributaries between 20 and 40 mm., the myelencephalic vein receives a dural plexiform collateral that extends ventrocranially in the angle of secondary junction between the well developed otic and basioccipital cartilages. Thus is clarified the trabecular conformation of the inferior petrosal sinus, now in definitive position, as shown in plate 4.

---

[10] A definitive conclusion could not be reached, because the meninges concerned had been distorted by technical procedures in the few early fetuses available for this study.

[11] Regarding their description, however, it was noted by Dr. George W. Bartelmez (personal communication) that what appears to be a "fusion" of the hemisphere and diencephalon is a thickening of the ventricular wall, at the dien-telencephalic sulcus, as the internal capsular fibers begin to pass through it. Hence, any enclosure of the terminal vein is not likely to occur within this sulcus. More probably, an extraventricular vein is enclosed within the choroid membrane of the third ventricle, in association with the development of the rhinencephalic complex, of which the terminal stria is a part. There is one other possibility. If it should be found that the veins of the ventricular walls (which include the transverse and longitudinal caudate veins of Schlesinger; see Padget, 1956, p. 315) result from secondary anastomoses between the primary veins stemming from the embryonic ependymal layer, the terminal vein itself conceivably may be formed in the same way. Furthermore, it may be that most of the proximal tributaries of the terminal vein (as precisely defined, only that part of the vein related to the terminal stria) that are prominent grossly in the ventricular walls result from a subependymal elongation of the primary embryonic veins as the cerebral hemisphere expands.

At the level of the 6th nerve root, which it surrounds, the emerging inferior petrosal sinus is continuous with another new plexiform channel medial to the trigeminal ganglion. Derived from the medial side of the pro-otic sinus, this plexus surrounds the carotid artery at the level of the hypophysis (fig. 15; pl. 4). For the first time, therefore, one may properly speak of a primitive *cavernous sinus,* although the part of the pro-otic sinus that is always medial to the 5th nerve ganglion, and is the sole remaining segment of the primary head-sinus of initial stages, has often been so designated (Streeter, 1918; and others). This conspicuous primary sinus is always notably lateral to the carotid artery and is smoothly outlined, however, and thus cannot represent the trabecular cavernous sinus through which the carotid and nerve roots pass in the adult—a singular anatomical configuration which can now be explained. The new cavernous and inferior petrosal sinuses, located medially and ventrally, will provide a more direct caudal exit (to the internal jugular vein) for the orbital venous blood than does the lateral, and soon devious, pro-otic sinus (cf. figs. 31–37, pl. 2). The *intercavernous sinuses* (forming the circular sinus) and the *basilar sinus* (*plexus*) of the adult are merely the mid-line plexiform extensions already beginning to anastomose the bilateral cavernous and inferior petrosal sinuses, respectively (pls. 3, 4).

Modifications of Intra- and Extra-cranial Channels

The alterations in the pia-arachnoidal veins resulting from cerebral growth, especially their trunks entering the dural sinuses, are notable in stage 7 (figs. 23, 24, pl. 1). The superficial middle cerebral veins, belonging more to the dural than to the pial layer, are particularly prominent. Their stem is joined in front of the optic nerves by a pial tributary from the mid-line, which is the primary component of the anterior cerebral and deep middle cerebral veins, and receives the inferior striate veins referred to above (fig. 13A1). All these cerebral veins, including the prominent ventral diencephalic vein with its strong inferior choroid tributary, are directly continuous with the tentorial sinus, which has been considerably elongated. Curved around the ventral margin of the future temporal lobe in following the course of the 3d and 4th nerves, the sinus is now unmistakably enclosed within the primitive tentorium. Through it the dorsal diencephalic and mesencephalic veins pass laterally to join components of the still immature medial end of the transverse sinus, after forming in each case a characteristic dorsal arch (figs. 11, 13). Their stems are often smaller at their entrance into the primitive dura surrounding the sinus, thus presaging their ultimate disappearance. Secondary anastomoses between some of the pial ramifications of these separate veins (see stage 4) foreshadow the emergence of the basal cerebral vein during stage 7*a*. It must be emphasized that, as before, all the veins of the brain empty directly into the sigmoid sinus. The cavernous sinus, just formed, plays no part in cerebral drainage; it is merely a secondary caudal outlet for the veins of the orbit, by way of the new inferior petrosal sinus.

The primitive venous communication between the tentorial sinus (draining the middle cerebral veins) and the pro-otic sinus (component of the cavernous sinus at this stage) is by way of the primary stem of the anterior dural plexus. This stem dwindled during stage 6 and is usually not found later (figs. 19–23, pl. 1). Its exceptional late retention, however, has led to errors of identification of important related vessels, as will be seen.

One 43-mm. embryo (Carnegie no. 886) of stage 7 is atypical in that the anterior dural stem has persisted as a small channel on the right side (pl. 4A2, unlabeled vessel connecting pro-otic and tentorial sinuses). Moreover, a large channel representing the same primary channel on the left side of this embryo still drains the middle cerebral veins, as originally, into the pro-otic sinus (see also Streeter, 1918, fig. 27, pl. 5); in keeping with this pattern, the tentorial sinus, which usually at this time connects these veins dorsally with the transverse sinus, is relatively small. The atypical configuration of this specimen, particularly on the left, is probably responsible in part for Streeter's (1918) impression that the termination of the middle cerebral veins in the cavernous sinus, although inconstant even in the adult, is an early primary connection. In his illustration of the same embryo, the prominent channel on the left labeled "cavernous sinus" is not medial but lateral to the trigeminal ganglion (not illustrated by Streeter, but see pl. 4A2). As such, it cannot represent the adult sinus. It does represent plexiform anastomoses sometimes occurring between the pro-otic sinus (middle dural stem) and the anterior dural stem, which lie upon the lateral surface of the ganglion.

Anastomoses similar to those just noted in stage 7 may occur in earlier stages, as shown by Mall (1904, fig. 13, pl. 3, in an embryo of horizon xviii), who erroneously thought[12] that they represented first stages in

---

[12] The material of the Carnegie Collection begun by Dr. Mall was itself in an embryonic stage in 1904 and thus was barely adequate for his brief but often-quoted report.

the formation of the primitive transverse sinus. He noted the fact that the cranial nerves, from the 5th to the 12th, very early "wander through" the "anterior cardinal vein" (head-sinus; see p. 83) during its transposition from their medial to lateral aspects, as described for the present stages 2 to 4. The 5th nerve ganglion alone is not extensively involved in this general migration, probably because it is a relatively large mass superficially situated, and because the head-sinus is anchored medially by its voluminous and constant maxillary tributary (pl. 1). At this level the head-sinus may share, however, in the tendency toward lateral migration, as witnessed by the small anastomoses just noted. The atypical dilatation of one of these vessels on the left side of the 43-mm. embryo is accompanied not only by a corresponding dwindling of the segment of the pro-otic sinus medial to the trigeminal ganglion, but also by the retention of the anterior dural stem; the 4th nerve, usually outside the stem, passes through it in this instance. This pattern results in drainage of the middle cerebral veins into the pro-otic sinus, and thus directly into the sigmoid, not the cavernous, sinus. Since the atypical channel is lateral to the trigeminal ganglion, drainage is essentially the same as in the typical pattern of middle cerebral veins that terminate in the tentorial sinus; both routes, leading into the transverse sinus, are lateral to the ganglion (pl. 4B).

In conclusion, the embryo described above is no exception to the typical history of the outlet of the superficial middle cerebral veins (pls. 1, 2): They first empty into the primary head-sinus (later pro-otic sinus), which is the lateral component of the future cavernous sinus. By the time the definitive cavernous sinus emerges, the primary communication, i.e. the anterior dural stem, has been lost. A similar communication, but in a notably different position, is finally regained in an indeterminate number of cases by a late secondary anastomosis, usually postnatal (fig. 18C, D).

The external jugular system, which emerged during stage 6, already resembles the adult conformation, far in advance of the intracranial venous channels (fig. 13), as can best be summarized by reference to the consecutive stages shown in plate 1. To be noted are the subclavian and external jugular veins with their major tributaries, including secondary anastomoses with ophthalmic and emissary veins. With growth of the lower jaw and the concomitant elevation of the external ear, the new external jugular has anastomosed with the definitive *superficial temporal vein,* continuous with the posterior facial tributary of the anterior facial vein. By way of this secondary anastomosis, the external jugular often becomes the chief drainage of the superficial vein and may even annex the primary common facial stem from the internal jugular (pl. 3E, F).

Veins of Orbit

A notable advance in the extracranial veins is the belated formation of the permanent stem of all the orbital veins, including the ophthalmic, of which the adult *superior ophthalmic* (so-called, BNA) is the major orbital component. In the outline below, it can be seen that these veins, briefly noted in stage 5, have a complicated development recalling that of the ophthalmic artery (fig. 14). Understanding of this development is further complicated by inexact terminology regarding the adult vessels.

Most of the dorsal orbital part of the primitive supraorbital vein, which emerged in stage 4 (fig. 5) and later also constitutes the chief superior ophthalmic (orbital) vein (pls. 1, 2), is permanent; its stem, however, is temporary. In stage 5 (or late stage 4) the course of this vein is still direct, but its proximal end at the head-sinus has become wedged against the dorsocaudal aspect of the tissue surrounding the juxtaposed 4th and 5th (ophthalmic) nerves, as shown in figures 9 and 12A. By stage 6 (figs. 10, 14A), shifting and unequal growth including the orbital structures have resulted in a circuitous course for the same vein. The course, best seen in a coronal view (fig. 12B1), is obviously the result of the anchoring of the vein by the approximation of the two nerves. Furthermore, a consideration of adult anatomy in this region shows that the primitive course, which is dorsal to all the orbital nerve roots and caudal to the juxtaposition of the 4th and 5th nerves within the region of the cavernous sinus, would be even more devious if it persisted after formation of the anterior clinoid process and lesser sphenoidal wing.

At the present 40-mm. stage, the devious primary trunk of the primitive supraorbital vein of earlier stages is replaced. Medial to the 4th and 5th (ophthalmic) nerves, a secondary anastomosis joins the supraorbital vein with the stem of the primary maxillary vein (fig. 14A, B1), which, by stage 6, has lost most of its tributaries to the anterior (and deep) facial vein (fig. 12). Since two vessels, previously continuous, i.e. the stems of the primitive supraorbital vein and of the anterior dural plexus (figs. 23, 24, pl. 1), have both disappeared, the stem of the old maxillary (infraorbital) vein has become the outlet of all the adult veins of the orbital region into the cavernous sinus. Some of the medial maxillary tributaries, which have always drained the caudoventral parts of the eye and orbit, are incorporated as the so-called *inferior ophthalmic* veins of the adult (see below).

With the definition of the permanent stem of all the orbital veins, it can be understood why the adult superior ophthalmic vein—since it is also the early primary stem of the supraorbital vein, it is the best developed and most constant vein of the orbit—typically does not join the cavernous sinus in the upper lateral extremity of the

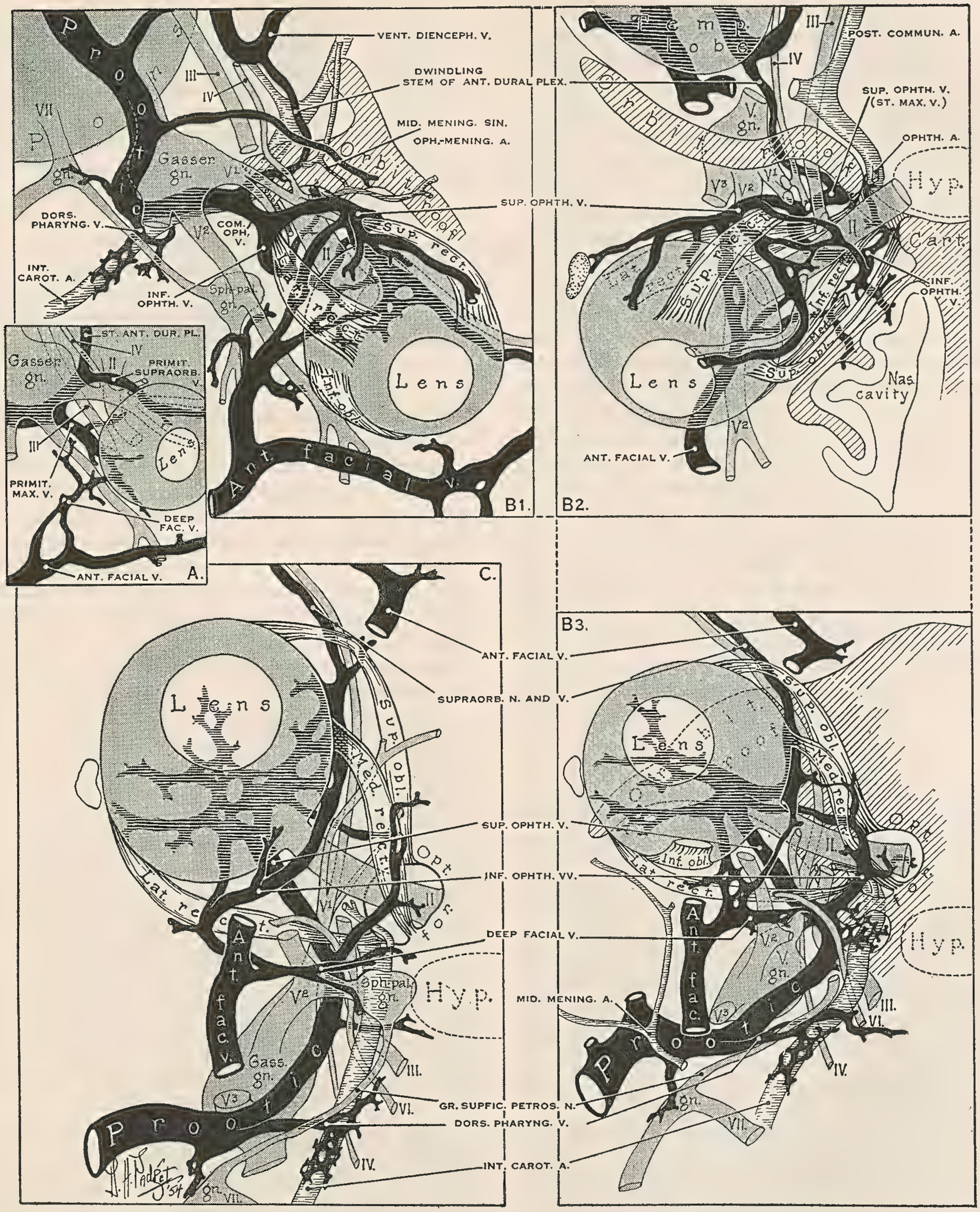

FIG. 14. Reconstruction of details around the right eye in three embryos of two stages (same magnification). A, lateral view of Carnegie no. 966, 23 mm., xx, stage 6; B1, 2, 3, no. 886, 40 mm., stage 7, viewed from the right, in front, and below, respectively; C, no. 6203, 39 mm., stage 7, viewed from below. At horizon xx (A) the orbital region is drained by two veins, one dorsal orbital and supraorbital, the other ventral orbital and infraorbital or maxillary. By 40 mm. (B1, 2, 3), the most proximal end of the primitive supraorbital vein, detoured by the junction of the 4th and ophthalmic nerves (A), has disappeared (B1); a new anastomosis joins it to the stem of the maxillary vein, which thereby becomes that of all the adult orbital and ophthalmic veins. The secondary anastomosis between the orbital and anterior facial veins is among the earliest of the emissary connections.

superior orbital fissure, although its course is dorsal and then lateral to the orbital structures, including the common tendinous ring (of Zinn). Instead, the end of the vein, a secondary anastomosis noted above, follows the outer edge of the orbital fissure to its lowest medial extremity, where it joins the cavernous sinus ventral to all orbital structures. Development shows that the adult outlet of the superior ophthalmic vein could more precisely be called the *common orbital* (orbito-ophthalmic) vein, comprising two main divisions, superior and inferior orbital, with respective ophthalmic tributaries. This common trunk is medial to the foramen rotundum, i.e. to the maxillary division of the 5th nerve, a structure that, even before stage 2, has marked the level of the maxillary vein, which the trunk represents (pls. 1, 2). The true inferior ophthalmic veins, contained within the cone of muscles, are, of course, augmented remnants of the maxillary vein. Outside the muscle cone, the inferior orbital veins, usually included in the adult group designated inferior "ophthalmic," are also primary maxillary remnants; they may include infraorbital, facial, ethmoid, and nasal tributaries. A very primitive ophthalmic tributary may persist (figs. 14B2, B3) as a vestige of the early stages when the maxillary vein was the only drainage of the optic stalk, vesicle, and cup (figs. 19–21, pl. 1): the dilated, tortuous remnant of this vein, emerging from the intracranial cavity by way of the optic foramen under the nerve (fig. 14B3), was seen by the author in an abnormal juvenile brain (congenital arteriovenous aneurysm; cited in Padget, 1956).

According to Mann (1950), no central retinal vein accompanying the hyaloid artery (later central artery of the retina) is seen until the third month. Its stem, however, appears to be represented very early (stages 1, 2) among the tributaries of the primitive maxillary vein that first ramify at the base of the optic vesicle (fig. 1) and later receive a vessel from the choroid fissure in the ventral part of the optic stalk (figs. 2, 3, 5). The adult retinal vein is said to join the cavernous sinus, and to have a communication with the superior ophthalmic vein (Wolff, 1954), or to be a tributary of either; such variation accords with the developments just described, but the vein is a primary tributary of the common orbital, i.e. the maxillary, vein. Similarly, reports that the adult stem of the inferior ophthalmic veins enters the cavernous sinus either alone or together with the superior ophthalmic vein are readily explained by the variable size and form of the adult cavernous sinus, which forms secondarily from a plexus, and by the position of the secondary anastomosis of stage 7 that joins the supraorbital (superior ophthalmic) vein to the stem of the primitive maxillary (infraorbital) vein. Since the resulting common orbital (ophthalmic) vein may be very short, the adult superior and inferior ophthalmic veins may appear to enter the sinus separately.

The intrinsic veins of the primitive embryonic eye, including the annular vessel of the pupil and the choriocapillary net on the optic cup (Mann), all drain primarily into the primitive maxillary (infraorbital) vein of stages 1 and 2 (under 8 mm.), which is before any supraorbital vein is present (figs. 1, 2). Voluminous orbital anastomoses often obscure specific vessels (fig. 14), but *primitive vorticose veins* could be identified in two embryos of late horizon xviii and xx (stages 4, 6, fig. 12B2): the craniodorsal tributary joins the primitive superior ophthalmic, and the caudoventral one joins the primitive maxillary vein ("inferior ophthalmic vein" of Mann, who pictures the latter veins diagrammatically between 13 and 18 mm.).

Emissary Veins

The emergence of the definitive emissary veins can be seen during stage 7. A frontal tributary of the primitive supraorbital vein anastomoses with the anterior facial vein at the inner angle of the eye, thus constituting the relatively constant *angular* (nasofrontal) vein (fig. 14); dorsal extensions in the scalp plexus (see below) of the superficial tributaries of the primitive supraorbital vein (figs. 22–24, pl. 1) form the definitive *frontal* and *supraorbital* veins. In various mammals below the primate level (Dennstedt, 1904; and others), such emissary communications incorporating the orbital veins develop to the extent that these veins drain more laterally into the external jugular system, by way of the facial vein, than medially into the atrophic internal jugular, by way of the cavernous sinus. In the human embryo of stage 6, an anastomosis between the primitive maxillary vein and the emerging anterior facial vein formed the deep facial vein (fig. 10). Since the stem of the old maxillary vein of stage 7 is now the permanent stem of all the orbital veins, as just described, the deep facial vein has become its tributary at the caudolateral margin of the orbit, and will pass through the adult inferior orbital fissure. Communicating with the *pterygoid plexus,* derived from the medial components of the voluminous maxillary vein of the early stages, the deep facial vein is the most proximal tributary of the adult stem of the common orbital vein (so-called superior ophthalmic stem) before its junction with the cavernous sinus.

With the formation of all essential elements of the external jugular system, of the dural sinuses, and of veins in the chondrocranial foramina in the present 40-mm. stage, the other emissary veins become definitive. It must be understood that the primitive emissaries of earlier stages (figs. 21–23, pl. 1), so called for convenience, drain extracranial structures medially into the primitive sinuses; the chondrocranium develops around their stems, thus forming the emissary foramina. Now that secondary anastomoses with the new tributaries of the external jugular vein are being formed, flow in the emissaries can be reversed peripherally.

As was noted above in the order of development of their foramina, the primitive hypoglossal emissary was the first to appear in stage 4 (fig. 5). It drains veins around the upper spinal cord medially into the ventral myelencephalic vein. This also constitutes a definitive emissary, namely the stem of the future inferior petrosal sinus, as soon as the jugular foramen is completed (late stage 4); it joins the internal jugular vein below its foramen. In stage 5 (fig. 9), the primitive condylar (condyloid) emissary drains the more superficial vessels around the upper spinal cord, which include components of the deep cervical and vertebral veins, into the sigmoid sinus at the level of the posterior dural plexus (adult marginal sinus of the foramen magnum). By stage 6 (fig. 10), the primitive mastoid emissary from the primordia of the occipital muscles drains into the sigmoid sinus just cranial to the conspicuous stem of the posterior dural plexus. These emissaries will constitute an important collateral between intracranial venous channels and veins around the vertebral column, by way of the external jugular system (Batson, 1940, and others). Whereas the recent anastomosis of the cavernous sinus with the anterior and deep facial veins, by way of the common stem of all orbital veins, represents an adult emissary, neither the orbital fissures, superior and inferior, nor the middle fossa are clearly demarcated in the fetal chondrocranium, or completed in bone until much later.

Formation of the cavernous sinus at stage 7 clarifies the origin of the remaining emissary commonly found at the base of the adult skull, the *sphenoid emissary* (of the foramen ovale). As early as stage 3 or 4 (figs. 3, 5), the dorsal pharyngeal vein, a tributary of the primary head-sinus, accompanies the great superficial petrosal nerve. When the head-sinus disappears ventrally to the labyrinth, the pharyngeal vein becomes a tributary of the pro-otic sinus (fig. 15A). By stage 7 it drains medially into the cavernous sinus, a medial derivative of the pro-otic sinus (fig. 15B, C). The vein becomes truly emissary when its lateral tributaries, already ramifying around the carotid artery as in the adult, anastomose with the deep facial tributaries of the primitive maxillary vein that comprise the adult pterygoid plexus.

Successive stages of the embryonic dorsal pharyngeal vein also clarify the origin of the inconstant and *accessory sphenoid emissary* (of the foramen of Vesalius; fig. 15). Though usually minute, this vessel is of interest because it explains the occurrence of its not-uncommon adult foramen, which lies just cranial and medial to the foramen ovale (Cunningham, 1951; Morris, 1953). Since neither of these sphenoid foramina occurs in embryonic cartilage—very little of the middle fossa is laid down in the fetal chondrocranium—nor is usually well defined by bone until after birth, it cannot be said which opening contains the embryonic pharyngeal vein. Obviously, however, the Vesalian emissary, when it occurs, is merely accessory to the relatively constant and more voluminous emissary vein (or venous plexus) of the foramen ovale. Both veins drain what is here designated the *lateral wing of the cavernous sinus,* a remnant of the pro-otic sinus; in the adult they also drain the ventral end of the middle meningeal sinus (fig. 18C, D).

By the present 40-mm. stage, the last opening has been formed in the caudal half of the fetal chondrocranium—the conspicuous *spurious jugular* ("capsuloparietal") *foramen,* of phylogenetic interest (see stage 7*a*). This foramen is unusual in the embryo in that it contains a vein relatively much smaller than the foraminal diameter (fig. 13A1). Plexiform anastomoses between this *primitive temporal emissary* (stem of petrosquamosal sinus; p. 123) and a deep tributary of the superficial temporal vein may be found at this time. The spurious jugular foramen must not be confused with the near-by mastoid ("capsulo-occipital") foramen, which earlier (stage 6) is formed around the relatively large and constant mastoid emissary vein. Although the *primitive petrosquamosal sinus* on the lateral aspect of the chondrocranium is not definitive until stage 7*a* (fig. 16), the anastomosis that it constitutes, between the primitive temporal emissary and a lateral tributary of the pro-otic sinus, is sometimes identified at stage 7 (fig. 13A; figs. 33, 36, pl. 2).

Meningeal Drainage of Primary Membrane Bones; Independent Scalp Plexus

A prominent tributary of the pro-otic sinus in stage 7 is the stem of irregular plexiform vessels representing the adult *middle meningeal sinuses* in the outer part of the dural layer. These extrachondrocranial vessels accompany the two primary branches of the adult dural artery of the same name (fig. 15C), which are best understood by reference to the developing skull, as fully described by Macklin (1921); his models (adapted for fig. 279 in Hamilton, Boyd, and Mossman, 1952) were made from the same 43-mm. embryo shown here (figs. 13, 15B; pl. 4A).

In two embryos of stage 7 (Carnegie no. 886, just noted, and no. 6203), the frontal meningeal (dural) artery supplies the frontal ossification center, which is the most advanced of the primitive membrane bones and overlaps about half of the cerebral hemisphere. The region of the primordial parietal and squamous temporal membrane bones (fig. 13A1) is supplied by a parietal meningeal (dural) artery, which already comprises two branches. These two primary dural arteries, frontal and parietal, of the present stage must not be confused with the two major branches of the parietal artery in the adult, i.e. the so-called "anterior" and "posterior" branches of

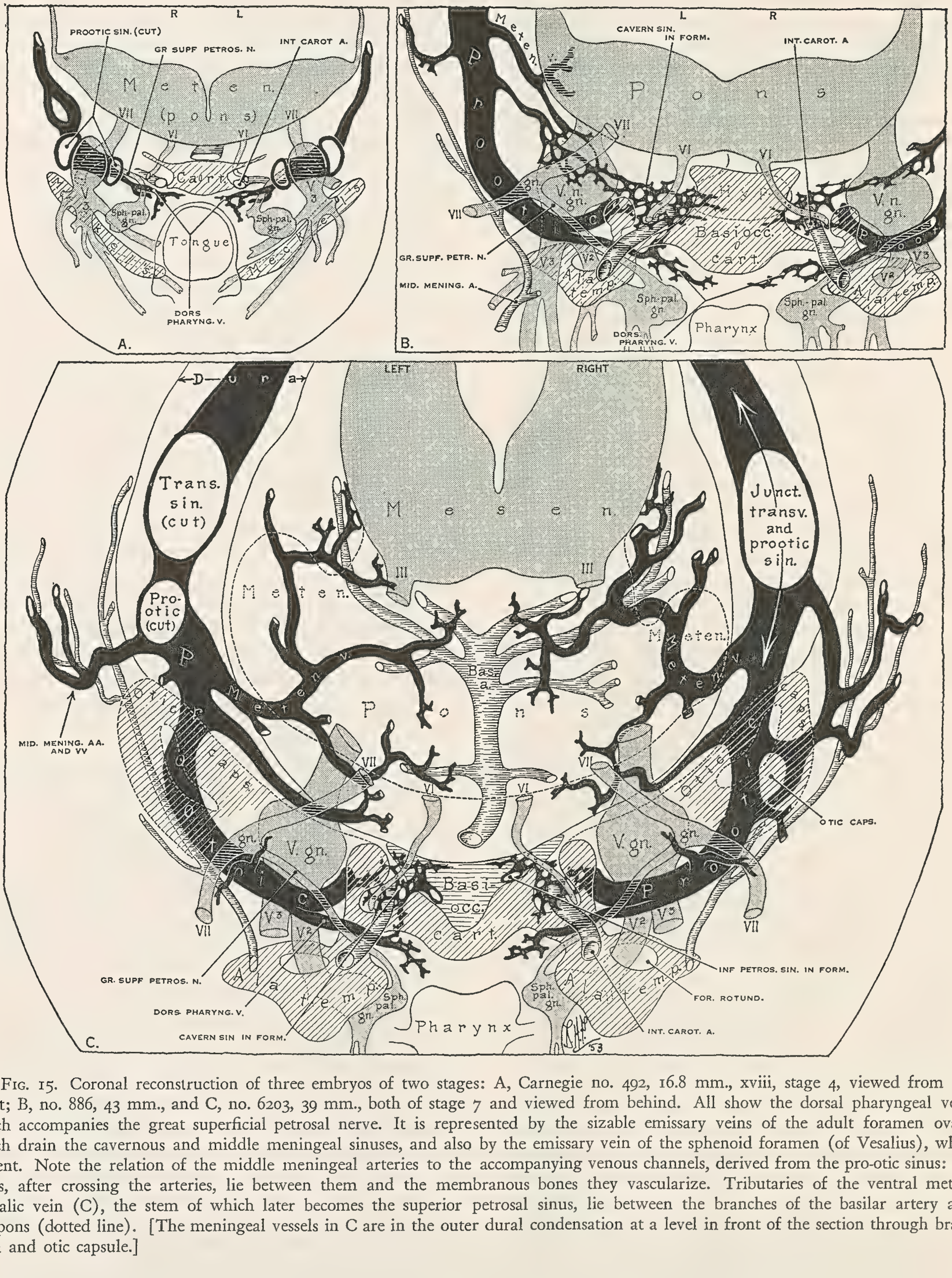

Fig. 15. Coronal reconstruction of three embryos of two stages: A, Carnegie no. 492, 16.8 mm., xviii, stage 4, viewed from the front; B, no. 886, 43 mm., and C, no. 6203, 39 mm., both of stage 7 and viewed from behind. All show the dorsal pharyngeal vein, which accompanies the great superficial petrosal nerve. It is represented by the sizable emissary veins of the adult foramen ovale, which drain the cavernous and middle meningeal sinuses, and also by the emissary vein of the sphenoid foramen (of Vesalius), when present. Note the relation of the middle meningeal arteries to the accompanying venous channels, derived from the pro-otic sinus: the veins, after crossing the arteries, lie between them and the membranous bones they vascularize. Tributaries of the ventral metencephalic vein (C), the stem of which later becomes the superior petrosal sinus, lie between the branches of the basilar artery and the pons (dotted line). [The meningeal vessels in C are in the outer dural condensation at a level in front of the section through brain stem and otic capsule.]

the middle meningeal artery vascularizing most of the adult cranial vault. As the embryonic growth of the parietal membrane bone overtakes that of the frontal bone, the frontal artery becomes subsidiary, and finally appears to be a branch either of the anteroparietal ("anterior") branch of the middle meningeal, or of its main stem.

The primary frontal dural artery, supplying the more lateral (greater) aspect of the frontal bone, has no specific name[13] in the adult; indeed, its proximal end in the middle fossa is often obscured in passing through a canal formation in the osseous thickening at the pterion. A medial branch of the frontal dural artery, namely the lacrimal or ophthalmomeningeal artery of potential importance, frequently passes through the superior orbital fissure, or a separate foramen, to anastomose with the lacrimal branch of the ophthalmic artery. Varying in size, this anastomosis represents the supraorbital branch of the temporary embryonic stapedial artery, which becomes the stem of the adult middle meningeal artery. Any venous channel accompanying the arterial anastomosis (fig. 18B–D) constitutes an *ophthalmomeningeal sinus* ("vein"; the origin of the name in the anatomical literature is not clear, but evidently it often refers erroneously to a remnant of the tentorial sinus; p. 122). The ophthalmomeningeal sinus may be continuous with the ventral end of the adult *sphenoparietal sinus,* a channel sometimes both meningeal and diploic, i.e. the sinus of Breschet (fig. 18D); it may, in general, be confluent with the stem of the *anteroparietal meningeal*[13] *sinus,* from which it is derived postnatally.

Veins in the dorsal scalp region are first clearly identified in the present 40-mm. stage. It must be emphasized that the membrane bones are primarily vascularized by the dural meningeal vessels just noted, not by scalp vessels (see below). Furthermore, apparently only one significant anastomosis develops between these intra- and extra-cranial systems of the skull vault, and it is often small and not constant. The fact that the *parietal emissary* (arterial or venous) was not identified except in the late fetal stages available for the present study does not mean that it never is formed between 40 and 80 mm., a stage that seems more likely. In any event, the parietal obviously is the last of the emissaries to be formed and, unlike the others near the skull base, apparently does not comprise a typical primary vessel.

In the gross specimen between 30 and 50 mm., the main stems of the superficial veins can often be seen through the transparent scalp region, namely the *frontal, superficial temporal, posterior auricular,* and *occipital veins;* the corresponding, but smaller, scalp arteries with their thicker walls can be identified in sections. This superficial cranial group, together with the dural meningeal arteries and veins, was graphically reconstructed in an excellent embryo (Carnegie no. 6203, 39 mm.; see p. 120): the occipital artery supplying the occipitocervical musculature is particularly conspicuous in length and gives off the so-called mastoid branch (latero-occipital meningeal artery,[13] the largest dural artery in the adult posterior fossa); as this artery enters the mastoid foramen, it lies upon the thin wall of the mastoid emissary vein, much larger in diameter (fig. 13), after bordering it outside the chondrocranium. Such configuration is notably in contrast with the pattern of arteries and veins of the endothelial tube stage, which do not accompany each other, but cross at a right angle (see stage 4). The parallel contiguity of certain vessels of stage 7 is significant in that the walls of even the smaller cranial arteries, at least, outside the brain, have become definitely thicker at 40 mm. than the walls of cranial venous channels, the diameter of which has become relatively much larger. Not until now do arteries and veins in certain areas accompany each other contiguously for the first time.

The superficial cranial vessels just named have developed in the meshes of a *scalp plexus,* the history of which has been considerably misinterpreted (see Padget, 1956). Erroneously, it is thought that the venous components of the scalp are primarily connected with those of the dura, and that the two layers are subsequently separated by the intervention of the membranous skull, leaving a number of emissary veins as remnants. Although Streeter's (1918) remarks about vascular "cleavage" have frequently been so misinterpreted, such secondary separation of vascular layers applies only to the dural and pial venous channels, as the result of expansion of the cerebral and cerebellar hemispheres and of the otic capsule (see stage 4). The arteries of the pia, dura, and integument are always separate systems.

Before stage 6, the thin scalp region covering the membranous skull is avascular. Between 20 and 40 mm., a scalp plexus, derived from the most superficial dorsocranial components of the emerging external carotid and jugular systems, specifically from the scalp vessels named above, advances dorsally from all sides up over the vault of the developing skull toward the region of the future parietal foramen. Initially, it seems, the scalp plexus does not vascularize the primitive membrane bones. In two embryos of about 40 mm. (identified below), the plexus is everywhere bounded medially by a conspicuous, though narrow, mesenchymal condensation, the primitive galea (aponeurotica), which, furthermore, is separated from the membranous skull by a considerable interval of loose avascular mesenchyme. As was described in detail by Finley (1922) and noted by Streeter (1918, 1951), the advancing margin of this superficial plexus is peculiarly well defined and is often conspicuous in the gross specimen. By 40 mm. it outlines a closing avascular area at the cranial vertex toward which all the meningeal and the superficial scalp vessels converge (graphically reconstructed in embryos Carnegie nos. 886, 6203). Presumably, later extension of the scalp plexus normally closes the primary vascular hiatus.

---

[13] The term *postero-* (or *latero-*) frontal would distinguish it from another adult meningeal artery—a branch of the ophthalmic artery, i.e. of its anterior ethmoid branch—which supplies the antero- (medio-) frontal dura and bone. Of the two major branches of the middle meningeal artery, primarily *antero-* and *postero-parietal,* the latter gives off the anastomotic branch passing through the parietal foramen (p. 120); an artery, albeit small, typically accompanies all emissary veins through their foramina.

The significance of the area of the terminal hiatus in the closing scalp plexus is genetically vestigial. It marks the area of the late fetal or postnatal parietal (so-called "sagittal") fontanel and its remnant, the parietal foramen, together with the relatively late and inconstant secondary anastomoses, namely arterial and venous emissaries that traverse these skull-hiatuses. This area in normal and abnormal cases, briefly discussed elsewhere (Padget, 1956), calls for study of more specimens, particularly between 40 mm. and term.

STAGE 7*a*. FETUS AT THE THIRD MONTH (60 TO 80 MM.)

Whereas the external appearance of the fetus, doubled in length between stage 7 and the end of stage 7*a* (fig. 16), the last of the present series, is not conspicuously altered, the expanding cerebral hemispheres grow caudally over the midbrain and the emerging cerebellar hemispheres (figs. 24, 25, pl. 1). This expansion, continuing throughout fetal life, together with the late ossification of the skull, necessarily delays the advent of certain channels. Nevertheless, the adult pattern of most venous sinuses and cerebral veins can be recognized by the end of this period. Notable changes, particularly seen in the basal views of the brain and skull (figs. 33–39, pl. 2), involve extension or modification of two channels that are prominent and primary, but are not always persistent, namely the tentorial and pro-otic sinuses, and their derivatives. For an understanding of these developments, frequent reference to other mammals is essential.

The *transverse sinus,* as distinguished from the sigmoid sinus, definitive in stage 5, is pushed into definitive position by cerebral expansion at about 80 mm. (pl. 5). Consequently, the tentorial plexus, which marks the junction of the transverse sinus with the superior sagittal and straight sinuses, is reduced in size to be recognizable as the adult torcular (confluence of sinuses). Comparison of figures 24 and 25 (pl. 1) shows that the marginal sinus, constituting the medial end of the primitive transverse sinus, has been shifted far caudally since the 40-mm. stage by the caudal growth of the cerebral hemisphere, the migration being accomplished by the successive use and discard of loops in the dwindling tentorial plexus (anastomotic progression).[4] The transverse sinus, having been swung caudally on the sigmoid sinus as on a hinge, has attained the approximate adult direction, which is opposite to that of earlier stages. This caudal swing is reminiscent of that of the posterior communicating artery between 18 and 40 mm., and it occurs for the same reason.

Significance and Modifications of the Tentorial Sinus

Another result of the notable expansion of the cerebral hemisphere between 40 and 80 mm. is a considerable elongation, under its temporo-occipital margin, of the tentorial sinus, which is still the sole drainage for the only definitive vessels now present on the surface of the hemisphere, the conspicuous middle cerebral group of arteries and veins.

It is now obvious that the tentorial sinus is the human counterpart of the mammalian "posterior rhinencephalic vein" described by Hofmann (1901), as indicated in plates 5 and 6. In many adult mammals (e.g. rabbit, pig, cat, and dog), this prominent vein follows the rhinal fissure; it collects veins from the region of the olfactory bulb, drains the middle cerebral veins, and empties into the transverse sinus near its junction with an inconspicuous channel comparable to the sigmoid sinus. In the horse, the rhinencephalic vein is represented by a dural channel for the greater part of its length (Hofmann's fig. 27), thus resembling the tentorial sinus during fetal stages in man. A comparable vessel, part vein and part sinus, follows the rhinal fissure of the rhesus monkey, according to the author's observations. After receiving the middle cerebral veins, which, it must be noted, have no primary connection with the cavernous sinus, the vessel passes caudolaterally under the temporal lobe into the lateral junction of sinuses, namely the transverse, sigmoid, and superior petrosal; the last-named sinus in man becomes definitive at this stage, as described below.

Between approximately 20 and 40 mm. in human development (figs. 23, 24, pl. 1), the tentorial sinus empties into the marginal sinus, i.e. the medial segment of the primitive transverse sinus, a route both short and direct. By 60 to 80 mm. (fig. 13; cf. A1, B), growth of the hemisphere, responsible for the caudal swing of the transverse sinus just noted, has also necessitated the marked elongation of the tentorial sinus emptying into it. Its caudal end, now attenuated and plexiform (pl. 4B), has begun a compensatory migration, by anastomotic progression,[4] caudally along the transverse sinus toward its junction with the sigmoid. Thus, the tentorial sinus attains the shortest route available through existing channels for drainage of the middle cerebral veins into the internal jugular vein (pl. 5); the configuration in stage 7*a* resembles that of the adult in other mammals (pl. 6).

The cranial end of the elongated tentorial sinus, which directly receives the superficial cerebral veins, is larger than its caudal end and is now curved ventrally, following the contour of the new middle cranial fossa (cf.

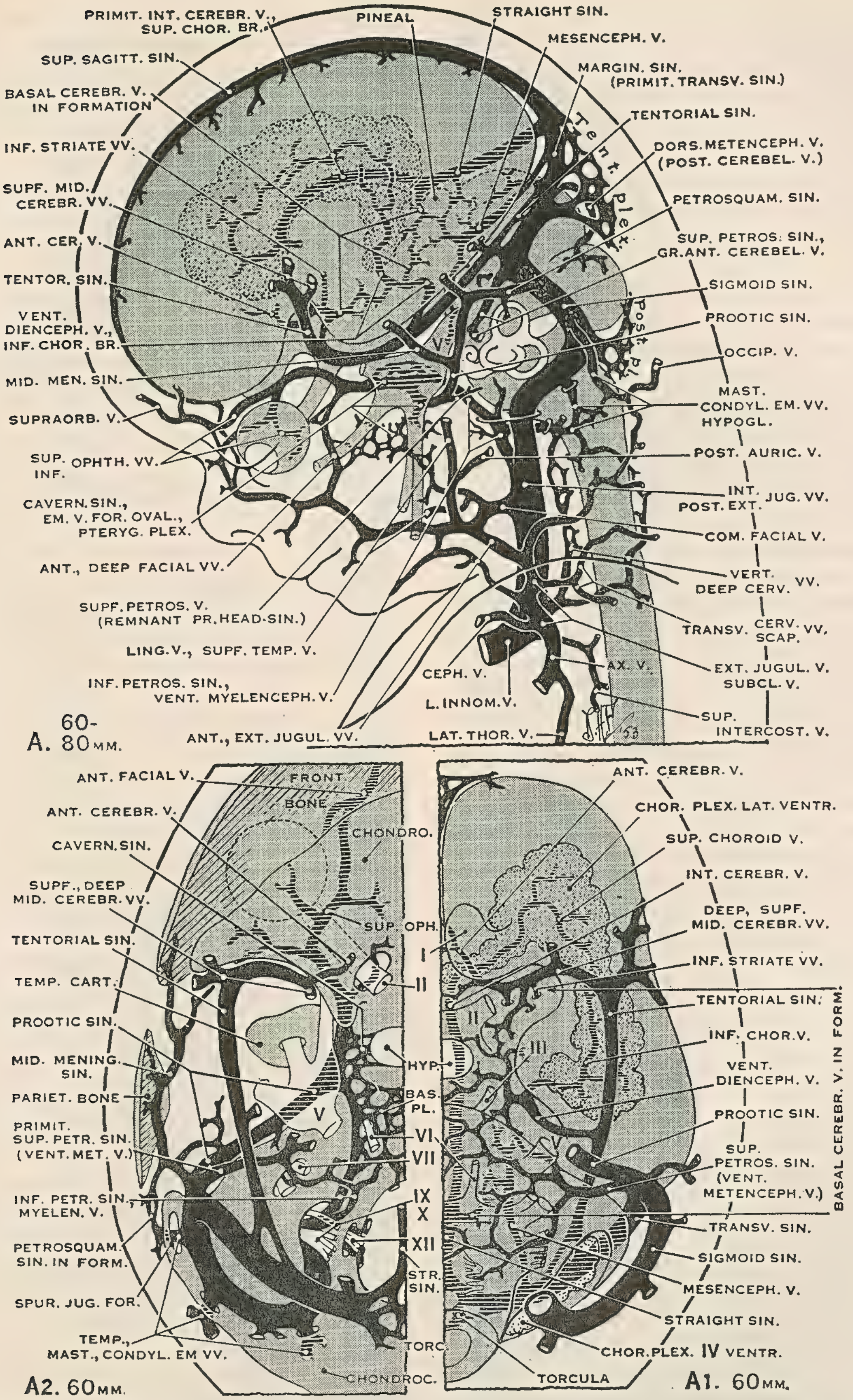

Fig. 16. Stage *7a*, in lateral (A) and basal views of the brain (A1) and chondrocranium (A2), when adult patterns become recognizable. The elongated tentorial sinus, draining the superficial cerebral veins, begins to migrate to the junction of the sigmoid sinus with the transverse sinus, which has been swung into definitive position. The superior petrosal sinus becomes definitive as the dural end of the metencephalic vein, which it represents, surmounts the expanding optic capsule. Tributaries of the pro-otic sinus drain the membrane bones. Note the spurious jugular foramen and its vein. The basal cerebral vein is formed by pial anastomoses between the primary transverse veins of the pia-arachnoid (A1).

pl. 5A, B). Specifically, the sinus often borders the edge of the cartilaginous lesser sphenoid wing (pl. 4B) in the position of the adult so-called sphenoparietal sinus (a term of dubious identity, which has obviously been applied in some instances to this part of the persistent fetal sinus, p. 119).

Considerable variation in the relations and position of the tentorial sinus has become apparent since its elongation. In this study, venous channels in all layers of the dural condensation of mesenchyme are called sinuses. Whereas the pro-otic sinus and its tributaries, e.g. the middle meningeal "veins" (usually so called; see below), belong to the outer dural layer, the tentorial sinus, directly continuous with the stem of superficial middle cerebral veins (pl. 1), belongs to its inner layer. The relatively late expansion of the temporal lobe and its fossa cranioventrally, while the cerebrum is expanding dorsally in all directions, not only elongates the tentorial channel; it also pulls the channel and the continuous arachnoidal stem of the veins diagonally for an increasing distance through the innermost and outermost layers, respectively, of the dense dural and loose arachnoidal mesenchyme. (No subdural space intervenes initially.) Hence, the transition between arachnoidal vein and dural sinus is a very gradual one, and varies considerably. All or part of the postnatal tentorial channel, therefore, may be either more or less deeply situated in the dura, or merely attached to it, in different individuals and mammalian species (Hofmann, 1901). When it is part "sinus" and part "vein," which is to say lying either in, on, or near the inner dural layer of the middle fossa, the tentorial channel resembles the dural end of other superficial cerebral veins as they approach the superior sagittal (and transverse) sinus (Bailey, 1948); their conformation is similarly explained.

Why the position of the tentorial sinus is not constant is now clear. It may be relatively lateral in the floor of the fetal middle fossa as seen in a 60-mm. specimen (fig. 18A), or medial near the edge of the tentorium as in one of 80 mm. (fig. 18B); either position occurs in newborn and adult heads (fig. 18C, D). The remnant of the sinus in postnatal stages has been designated in many ways, for example: erroneously it is called the "ophthalmomeningeal" or the "sphenoparietal" sinus (p. 119); a definitive term is *sphenotemporal sinus* (fig. 1189, Cunningham, *Textbook of Anatomy,* 1951). By way of the Sylvian vein, the channel obviously is the frequent adult termination into the transverse sinus, or secondarily into the superior petrosal, of the great anastomotic cerebral vein (of Trolard, 1868) according to this author's description (see also Bailey). Details of the pial tributaries of the tentorial sinus at stage 7*a* will be described below in connection with the formation of the basal cerebral vein.

Significance and Modifications of the Pro-otic Sinus and Its Tributaries

The modifications of the primary embryonic pro-otic sinus between 40 and 80 mm. depend more on the growth of the skull than on that of the brain (fig. 18A–D). A recent derivative, the inferior petrosal sinus, has become the caudal and intrachondrocranial outlet for the orbito-ophthalmic veins by way of the cavernous sinus, similarly derived in stage 7. This drainage, however, is still shared about equally with the extrachondrocranial pro-otic sinus, which leaves the cavernous sinus at the tip of the otic capsule and ventral to the trigeminal ganglion, as before, but has become deviated cranially and laterally by the expanded capsule, and borders its cranial aspect caudally to the junction of the transverse and sigmoid sinuses. The pro-otic sinus still receives the small remnant of the primary head-sinus, namely the definitive *superficial petrosal vein,* which accompanies the nerve of the same name by way of the facial hiatus of the otic capsule (pl. 4B). At its caudal end the pro-otic sinus has two conspicuous tributaries, which emerged at 40 mm., but are now recognizable as permanent adult channels: the medial tributary is the prominent old stem of the ventral metencephalic vein from the primitive cerebellum and pons, a stem that constitutes the new superior petrosal sinus (see below); the plexiform lateral tributaries, closely associated with branches of the middle meningeal artery (fig. 15B, C), are components of the primitive meningeal sinuses. In response to the emergence of the meningeal bones, particularly the frontal and parietal, the middle meningeal vessels develop extensive ramifications between 40 and 80 mm. (p. 126). The parietal bone superficially overlaps the parietal plate of the chondrocranium at the end of this period (pl. 4B; Hamilton, Boyd, and Mossman, 1952, fig. 380). The primary drainage of these bones in fetal stages is lateral into the pro-otic sinus, rather than ventral (through the foramen ovale) and dorsal (to the sagittal sinus lacunae) as in the adult.

Superior petrosal sinus. The dural channel that is augmented by stage 7*a* to constitute the superior petrosal sinus, the last of the major adult sinuses to become definitive in human development, has been present since stage 4. It is the dural end of the primary ventral metencephalic vein, typical of vertebrates (see below). Changes in the primitive brain and skull that bring the sinus into view can best be understood by referring to successive stages, particularly in the basal view (pls. 1, 2).

Between stages 5 and 7, the proximal end of the ventral metencephalic vein traverses the primitive tentorium, which is not shown in the accompanying illustrations. The embryonic origin of the tentorium, it must be understood, is the site of the future middle fossa: a condensation of mesenchyme, arising ventrally from the chondrocranial anterior clinoid process and temporal wing (ala temporalis, surrounding the foramen rotundum; pl. 4B), extends dorsally to the membranous skull vault, where it contains the tentorial plexus. As the result of its primary ventrodorsal direction, before the caudal expansion of the cerebral hemisphere, the primitive tentorium at first borders the cranioventral, rather than the dorsal, aspect of the otic capsule. Not until the tentorium has been swung caudally by cerebral expansion into more nearly transverse position at 80 mm., as was described above in reference to the tentorial sinus it contains, does the part of the tentorium containing the metencephalic channel come in contact with the dorsal crest of the expanded otic capsule.

During the time that cerebral expansion between 40 and 80 mm. carries the tentorium and its channels caudally (figs. 24, 25, pl. 1), otic expansion carries the pro-otic sinus cranially, thus separating the sinus from its tentorial tributary, the stem of the metencephalic vein (figs. 36, 37, pl. 2; fig. 18). The separation has been completed because the caudal end of the pro-otic sinus, as the result of a secondary anastomosis, now empties into the sigmoid by way of the petrosquamosal sinus, definitive in stage *7a* (see below). While being pushed forward by the otic capsule, the middle part of the pro-otic sinus dwindles; meanwhile the new cavernous and inferior petrosal sinuses, emerging in stage 7, annex the orbito-ophthalmic veins, of which the pro-otic sinus was formerly the exclusive drainage. Consequently, the tentorial end of the metencephalic vein, now the superior petrosal sinus, empties into the junction of the transverse and sigmoid sinuses. This secondary pattern of stage *7a,* typical of the adult, obscures the fundamental pattern of the metencephalic channel of stage 7 and earlier, i.e. its derivation from the pro-otic sinus (fig. 18A, B). Expansion of the otic capsule dorsally tends to bring it into contact with the primary metencephalic channel. Thus, the superior petrosal sinus is pushed into definitive position on the dorsal margin of the enlarging otic capsule (later petrosal bone) by two advances: otic expansion cranially and from below, and cerebral expansion caudally and from above, the latter being reflected in the caudal swing of the tentorium.

Although definitive in position by 80 mm., the fetal superior petrosal sinus, it must be noted, is still not that of the classic textbook picture: it has no well defined communication cranially with the cavernous sinus. The primary role of the sinus in all stages is drainage of the cerebellar and pontile regions, as is notably true of its counterpart in other mammals. The inference that the definitive position of the sinus is the result of the relatively great enlargement of the cerebral hemisphere, plus chondrocranial otic expansion, explains the absence of a definitive channel in mammals generally.

Apparently the significance of the superior petrosal sinus, belated in mammalian development, has not been understood. The channel has long been confused with the pro-otic sinus (e.g. Shindo, 1915; Streeter, 1918; van Gelderen, 1933), which is a prominent primary channel, i.e. the stem of the middle dural plexus typical of early vertebrate embryos. Essentially, the superior petrosal is its tributary. Inexact knowledge of the morphology and variations of the superior petrosal sinus in adult man—it is rarely as large as the inferior petrosal sinus, and its communication with the cavernous sinus is both secondary and inconstant—is probably chiefly responsible for many errors in its identification in other mammals.

The superior petrosal sinus has also been confused with the tentorial sinus: for instance, the channel so identified in the adult horse, cow, dog (Dennstedt, 1904, pls. 1–3), and rat (Greene, 1935, figs. 218, 219) does lie in the tentorium but is not contiguous to the petrosal bone. Since the channel originates in the anterior, not the posterior, cranial fossa, there draining the anterior and middle cerebral veins, it is the tentorial sinus, i.e. the dural end of the "posterior rhinencephalic vein" described above; its form and connections in these adult mammals resemble those in the human embryo at 60 to 80 mm. (fig. 16). Confusion regarding these vessels is a fundamental error, because the tentorial sinus drains the largest veins cranial to the tentorium, whereas the superior petrosal sinus drains the chief vein of the posterior fossa.

Not only does the definitive superior petrosal sinus appear late in human development; it is a new formation phylogenetically. The following examples of its counterpart in adult mammals recapitulate stages of its development in man: (1) in the bat (Grosser, 1901, fig. 36, pl. 20), the sinus is represented only by the dural end of the major metencephalic vein, i.e. the constant trigeminal vein (of Hofmann, 1901) characteristic of vertebrates; (2) in the horse and dog (Sisson, 1953), a homologous sinus, which, however, does not touch the petrosal crest, is the dural (tentorial) end of the major cerebellar vein, and enters the ventral (caudal) end of the transverse sinus, a pattern comparable to the 40-mm. stage in man; and (3) in the rhesus monkey, according to the author's studies, a definitive superior petrosal sinus is present, as the continuation of the great cerebellar vein, but it is relatively short, for the reason that it touches only the lateral part of the petrosal crest.

Fundamentally, in all species, the superior petrosal sinus is the major metencephalic vein of the posterior fossa, the proximal end of which becomes surrounded to a variable extent by dura, namely the tentorium, in so far as this is present. Application of the channel to the petrous crest apparently depends on the otic and cerebral expansion in certain primates. Furthermore, in contrast to the inferior petrosal, the superior petrosal sinus has no primary connection with the cavernous sinus. Any communication with a dural channel in the anterior fossa is a late development, perhaps belonging exclusively to man (the situation in most primates is unknown to the author). The primary cerebellar vein involved in the formation of the superior petrosal sinus, however, commonly does anastomose with a pial vein of the anterior fossa, as will be discussed below in reference to the basal cerebral vein.

Petrosquamosal sinus, an emissary of the chondrocranial spurious jugular foramen. Although the foregoing discussion shows why it can be said in general that the superior petrosal sinus is an elaboration of a metencephalic tributary of the pro-otic sinus (Markowski, 1911, 1922), close inspection of consecutive stages (pls. 1, 2) shows it to be the result of a rather complicated rearrangement of these channels. This complex includes the *petrosquamosal sinus,* which now constitutes, secondarily, the caudal end of the pro-otic sinus, leading into the sigmoid sinus. These alterations, dependent upon the developing skull, involve the interesting spurious jugular ("capsuloparietal") foramen of the chondrocranium, an opening definitive in stage 7.

Between 40 and 60 mm., a lateral (temporal emissary) tributary of the sigmoid sinus passes through the spurious jugular foramen and anastomoses, external to the temporoparietal lamina of cartilage, with a lateral (primitive dural meningeal) tributary of the pro-otic sinus (figs. 13A, 18A). This anastomosis is the primitive petrosquamosal sinus (stage 7). By 80 mm. (fig. 18B) the sinus is augmented to become the new caudal (sigmoid) end of the pro-otic sinus, the change being coincident with the utilization by the stem of the metencephalic vein of the old caudal (sigmoid) end of the pro-otic sinus in the formation of the definitive superior petrosal sinus. The petrosquamosal sinus, on the outer aspect of the chondrocranium, is now definitive in position, because it is being overlapped laterally by the emerging membranous skull (fig. 18B); thus it already suggests the subsequent intracranial and later diploic situation of the adult channel. A photomicrograph of a 69-mm. fetus (van Gelderen, 1924, fig. 65) shows well the fact that the "emissary of the capsuloparietal foramen" is medial to the bone after becoming lateral to the cartilage.

The junction of the transverse sinus with the sigmoid sinus, or with any less well developed channel comparable to it, a junction that includes the stem of the petrosquamosal (pro-otic) sinus, is a region of considerable significance in mammalian development. We have seen that, ever since its formation in stage 5, the cranial (dorsal) end of the sigmoid sinus has received, more or less directly, all the drainage from the brain and also that from the orbit and dura (figs. 22–25, pl. 1). By 80 mm., coincidentally with the migration of the tentorial sinus described above, the sigmoid receives cerebral drainage even more directly; it drains the posterior (cerebellar) fossa by way of the superior petrosal sinus.

In spite of the fact that ventral drainage into the primary internal jugular vein is predominant at all stages of human development, evidence exists, between 40 and 80 mm., of potential drainage laterally into the external jugular system: sometimes a deep tributary of the external jugular anastomoses with a lateral tributary of the petrosquamosal sinus, which is the embryonic temporal emissary; this route, only potential in man, is augmented in a typical mammal (see below and pl. 6). Although the petrosquamosal sinus has become continuous with the pro-otic sinus, it is still emissary in that it passes through the spurious jugular foramen (cf. fig. 18A, B). This lateral opening in the chondrocranium is at least as large as the true jugular foramen, i.e. the internal, and is much larger, therefore, than the vessel it usually contains in man. The opening is adjacent to the junction of the major fetal sinuses, the transverse and the sigmoid.

The relatively constant *spurious jugular foramen* in cartilage (see stage 7) must not be confused with the later *temporal foramen* in bone, rare in man, which nevertheless is related to it, and has often been called by the same name. That both foramina, particularly the osseous in the human adult, have elicited the interest of comparative anatomists for a hundred years is reflected by many names, e.g. the foramen of Verga, Rathke, Fischer, Krause, Luschka, and Flower. The spurious jugular foramen transmits, pre- and postnatally, the caudomedial end of the petrosquamosal sinus, the embryonic temporal emissary. The temporal foramen, when present in man—it is typically large in other adult mammals—represents late ossification around an inconstant lateral tributary of the craniolateral end of the petrosquamosal sinus.

The significance of the embryonic spurious jugular and the postnatal temporal foramina and the vessels concerned has often been misinterpreted. Because of its predominance in many mammals, often to the extent of virtual absence of the internal jugular vein (pl. 6), the external jugular was assumed to be the primary jugular of vertebrates (see stages 1, 2). On this erroneous premise, it was believed that a lateral route of intracranial drainage, by way of a petrosquamosal emissary of the temporal region, characterizes early fetal life in man. Furthermore, both foramina and their vessels have been confused, as by Streeter (1918), with the extrachondrocranial remnant of the primary head-sinus ("vena capitis lateralis"); this remnant is just superficial and ventral to the otic capsule during stages 5 to 7. In one 80-mm. embryo of stage 7*a,* plexiform remnants of the head-sinus still accompany the 7th nerve (pl. 5C1) on the lateral aspect of the otic capsule. Although persistence in adult man of a large remnant of the head-sinus traversing the petrous bone is probably rare (except in cases of abnormal venous dilatation), a small remnant is normally represented by the plexiform superficial petrosal and stylomastoid veins; they accompany arteries of the same name throughout the intraosseous course of the 7th nerve. Any remnant in association with this nerve would, of course, be caudal to the external acoustic meatus. In contrast, a position that varies but is cranial to the meatus, and sometimes also dorsal, is the rule for the osseous temporal foramen.

The mammalian temporal foramen, dependent not only on the volume of drainage it carries but also on the skull development of the region, varies considerably in size and exact location, examples of which follow. The conspicuous foramen typical of mammals except certain primates lies ventrolaterally between the external acoustic meatus and the posterior glenoid process; it is usually called the "postglenoid" foramen (Greene, 1935; Miller, 1948; Sisson, 1953). In the rhesus monkey, an inconspicuous foramen is more medially situated in the depths of the glenoid fossa; in accordance with the dural drainage conveyed, it was called the "posterior meningeal foramen" (Hartman and Straus, 1933). A small foramen that, nevertheless, is conspicuous, owing to its more dorsal position on the lateral wall of the skull at or near the root of the zygoma, has been seen in fetal monkeys and adult apes (Schultz, 1921, 1950, respectively), and is not uncommon in the human newborn (Limson, 1932). Anomalously, at any time after birth, a large foramen may be found in the human squamous temporal bone (Streit, 1903). In any of these positions in man, a small foramen (diameter about 1 mm.) for accessory drainage of tympanic or meningeal emissary veins may occur normally (p. 126); it is related developmentally to the lateral end of the so-called petrotympanic fissure (Glaserian; for precise naming of this fissure see later editions of the Cunningham *Textbook,* 1951).

The significance of the emissary temporal vein of the temporal ("spurious jugular") foramen in mammals was appreciated by Shindo (1915). He called it the cranial tributary ("vordere Ast") of the transverse sinus, as distinguished from the sigmoid sinus, established much earlier, which is its caudal tributary ("hintere Ast"). Shindo describes the predominance of one or the other route of intracranial drainage in a series of adult mammals, on the basis of several reports, particularly Dennstedt's (1904): for example, the anterior route into the external jugular system by way of the temporal foramen is well developed in the opossum, hedgehog, mole, bat, weasel, mouse, rabbit, cat, dog, cow, and horse. Although there was said to be no sigmoid sinus or internal jugular vein (small?) in one species of monkey (*Acrobatus pygmaeus*), the primary drainage through these channels does persist in the rhesus monkey (author's studies), to a variable degree. In the cat and pig, the anterior route was reported by Shindo to be undeveloped; Mivart (1895), however, found a posterior glenoid foramen "occasionally" in the adult cat skull. Among the excellent illustrations of rat anatomy by Greene (1935), the transverse sinus is shown leaving the cranium through the postglenoid foramen to join the internal maxillary vein (Greene, fig. 223).

Regarding comparative embryonic stages, the author has little information. The situation in the fetal pig, however, according to Mead (1909), resembles a comparable human stage: the spurious jugular ("capsuloparietal") foramen is notably larger than the vessel it contains, which represents the primitive petrosquamosal sinus of the human embryo at 40 mm. (fig. 16). The assumption is that a chondrocranial temporal emissary, which may or may not develop a sizable communication with the external jugular vein, is the rule in mammalian development. In any event, the basic pattern of representative adult mammals (cf. many illustrations of jugular veins by McClure and Silvester, 1909) is as follows: The temporal emissary ("vordere Ast") is considerably augmented to become the vein called "dorsal cerebral" (Sisson, 1953) or "superior cerebral" (Dennstedt, 1904); the vein is the direct continuation of the transverse sinus and empties into the largest vein of the neck, the "jugular." On the other hand, underdevelopment of a channel homologous to the human sigmoid sinus ("hintere Ast") of man is represented, respectively, by a small "ventral" or "inferior" cerebral vein that passes through the foramen lacerum in its part homologous to the internal jugular foramen. Whether or not this vein, together with the primary internal jugular, becomes notably atrophic, it may also enter, secondarily, the "jugular" vein, i.e. the secondary external jugular, which becomes dominant during the embryonic development of a typical mammal (pl. 6A).

The relatively constant spurious jugular foramen of the human chondrocranium, as first seen at 40 mm., was called the "capsuloparietal fissure" by Macklin (1914, 1921) because it occurs between two parts of the chondrocranium, the otic capsule and the parietal lamina. This name is in distinction to the equally constant "capsulo-occipital" (mastoid) foramen, similarly named and identified earlier in stage 6 (about 20 mm.; W. H. Lewis, 1920), which contains the primitive mastoid emissary vein. Lewis' figures show that the future spurious jugular foramen is indicated during horizon xx by a notch at the cranial end of the partly conjoined parietal lamina and otic capsule (cf. dotted lines, figs. 10A, 13A). By 80 mm., when the chondrocranium reaches its maximum development, both foramina are conspicuous: in reconstructions of 40- and 80-mm. skulls by Macklin and by Hertwig (1907), respectively, according to adaptations of their illustrations elsewhere (Hamilton, Boyd, and Mossman, 1952; Gray's *Anatomy,* 1954), the spurious jugular is the more dorsocranial of the two openings (unlabeled) dorsal to the otic capsule; the more ventrocaudal foramen is the mastoid (cf. fig. 16A, dotted lines; fig. 18A).

Both emissary openings also occur regularly in the chondrocranium of other mammals as illustrated by de Beer (1937; the spurious jugular and mastoid foramina are labeled "superior" and "inferior occipito-capsular fissures," respectively). The fact that the spurious jugular foramen is relatively large and irregular in outline in many species, including man, and is thus notably out of proportion to the size of its contained vein, as compared, for instance, with the mastoid emissary vein and foramen, is probably incidental but significant for the following reasons: the cartilaginous lamina that forms the craniodorsal border of the foramen varies considerably in size and shape in different species (and probably individuals); this lamina is consolidated much later than the otic capsule, to which it becomes partly joined by the parietocapsular commissure (so called in the human fetus)—a development which brings the irregular foramen (or fissure, often the more descriptive term) into existence. The spurious jugular is the most dorsally situated foramen, and the last to form, in the mammalian chondrocranium, which does not extend much above the base of the future adult skull, and varies most in its dorsal parts.

The early membranous bones of the skull in certain mammals are also shown by de Beer, including those adjacent to the spurious jugular foramen, namely the parietal and squamous temporal bones. Although none of these fetal skulls was sufficiently advanced to show ossification completely surrounding the foramen laterally, photographs of coronal sections of mammalian embryo-heads (in studies quoted by de Beer) show that conditions around the foramen resemble those in the human fetus, and subsequent development can readily be postulated. The temporal canal of mammals represents ossification around a channel comparable to the petrosquamosal sinus. Essentially, in all species this channel passes, at its medial end, through the spurious jugular foramen, typical in the cartilage, and, at its lateral end, through the temporal foramen, highly variable in the bone (cf. fig. 18B, C).

At the 80-mm. stage (fig. 18B) of human development, the definitive petrosquamosal sinus, i.e. the secondary channel that now receives the dorsal (caudal) end of the pro-otic sinus from which it was derived, lies between the chondrocranium and the primitive parietal and temporal bones. As ossification extends in later stages, the parietal lamina of cartilage in man is absorbed, to some extent, at least (Macklin, 1921). Consequently, the petrosquamosal sinus, in spite of lying on the outer aspect of the cartilage, comes to lie within the skull, since it is always medial to the membrane bones. Its position in all stages, cartilaginous and later osseous, is within a groove at the site of the adult petrosquamosal suture.

The fetal petrosquamosal sinus (fig. 18C) is homologous to the prominent "superior" or "dorsal cerebral vein" in the temporal groove or canal of typical mammals, as was noted above; by way of this sinus, the external jugular, which may become the only jugular vein, annexes most intracranial drainage from the primary internal jugular (pl. 6). The boundaries of the sinus vary in different species, but, to a greater or lesser extent, it is ultimately bridged over by bone. Such variable ossification also characterizes the occasional presence of the sinus in adult man. (See the Toldt *Atlas,* 1941, fig. 132; the osseous channel is part groove and part canal.) The petrosquamosal sinus frequently persists in the newborn, according to the author's studies: it may be partly covered internally by paper-thin cartilage, obviously representing the fetal capsuloparietal commissure (cartilage) noted above, outside of which the channel always lies; its caudal end at the sigmoid sinus sometimes traverses a cartilaginous foramen, the fetal spurious jugular; in the young adult an osseous foramen here may be the only remaining superficial evidence of the embryonic sinus.

In the typical adult, the petrosquamosal sinus, which is the relatively constant temporal emissary vein of the fetal chondrocranium, becomes part of the diploic system. The remnant of the sinus receives the posterior temporal diploic vein and also superior tympanic veins. The secondary and inconstant anastomosis between the fetal temporal emissary and the external jugular is represented by any adult anastomosis between a superior tympanic vein and an inferior tympanic tributary of the deep temporal vein; the inferior tympanic passes through the Glaserian fissure (p. 125) or a separate foramen lateral to it (identified in several skulls by the author). Any such anastomosis between inconspicuous tympanic veins is homologous to the major route of intracranial drainage into the external jugular, typical of many mammals (pl. 6).

Relation of dural meningeal sinuses to the arteries; other venous channels fundamentally extrachondrocranial. The ultimate diploic character of the pro-otic sinus in man is seen not only in its adult petrosquamosal derivative, just described, which may groove the inner table of the skull, but also in the conformation of its other important embryonic tributary, the stem of the *middle meningeal sinuses* accompanying the artery of the same name. Developing between 40 and 80 mm. (figs. 24, 25, pl. 1), these venous channels in the dura are the primary drainage of the membrane bones, and their primary relation to the middle meningeal arteries is of particular interest.

The primitive meningeal channels are also clarified by the situation in other mammals. For the adult bat, Grosser (1901, figs. 36, 37, pl. 20) described the counterpart of the petrosquamosal sinus as "diploic," a situation comparable to the temporal canal of other species. The transverse sinus terminates in two channels: a vessel representing the sigmoid sinus ("hintere Ast" of Shindo, 1915; see above); and a "diploic transverse sinus" (his "vordere Ast"), which passes cranially over the petrous bone, enters the conspicuous temporal foramen, and joins the external jugular, a vein notably larger than the internal jugular, as is typical of mammals in general. In two adult rhesus monkeys examined by the author, the petrosquamosal sinus is not enveloped medially by ossification, but occupies an intracranial sulcus, the "posterior meningeal groove" (p. 125; Hartman and Straus, 1933), which is directly continuous with the meningeal groove in the anterior part of the middle cranial fossa. Here it anastomoses with the external jugular system by way of a vein in a small temporal foramen.

The anatomy of the adult bat (Grosser) also illustrates the relation of the meningeal venous channels to the artery they accompany, a configuration comparable to that of the 40-mm. human embryo. The greater part of the embryonic stapedial artery constitutes the major meningeal (dural) artery, as in man, but even its stem from the internal carotid is permanent in the bat. Ventrally, this stem borders the lateral margin of the "transverse" (pro-otic) sinus. More dorsally, however, the relative position of artery to vein is reversed, so that the "meningeal ramus of the stapedial artery" is medial to the "diploic transverse sinus" (noted above), and partly enveloped by it.

The adult mammalian pattern just noted, which resembles that of the 40- to 80-mm. stages of human development (fig. 15C; cf. Grosser's text fig. 18), exemplifies the typical relation of primitive arteries and veins to each other, discussed for the pial vessels in stage 4 (see figs. 6, 7, 8, 11; pls. 4A2, 5C2). *In reference to the structure vascularized*—in the present instance, the membranous bone—arteries are superficial to veins, even though they are medial to the same veins in reference to the whole head. Their development explains the unusual conformation of the larger meningeal (dural) vessels in adult man. As the skull matures, i.e. as ossification occurs laterally around the dural vessels that vascularize it, a relatively large venous channel, consolidated from a previous plexus, often appears to be compressed lengthwise between the smaller artery it accompanies and the skull. The resulting partial obliteration of the long axis of the venous lumen, together with secondary venous anastomoses, gives the appearance of two veins bordering the meningeal artery, well illustrated for late fetal and adult stages by (Wood) Jones (1912). It should be noted that most arterial walls, external to the brain, at least, become definitely thicker than those of the veins by the 40-mm. stage, before which time arteries and veins do not accompany each other (cf. p. 119 and discussion in stage 4).

By stage *7a* it is clear that the pro-otic sinus, which has long been erroneously identified with either the superior petrosal or the tentorial sinus in several species including man (see above), is concerned with drainage not of the brain, but of its dural and osseous coverings. Although the primordial cartilage is not shown in the illustrations of earlier stages, it must be noted that the pro-otic sinus, which includes the stem of the middle dural plexus and a short segment of the primary head-sinus (so-called "vena capita lateralis"; see stages 1, 2), typically lies on the outer aspect of the chondrocranium. In illustrations of a mouse embryo by Shindo (1915; pls. 28, 29; text fig. 4), comparable to stage 5 (fig. 9), the counterpart of the pro-otic sinus (labeled "anastomosis between transverse sinus and vena capita lateralis") and its tributaries, the maxillary (infraorbital) and ophthalmic (supraorbital) veins, are also extracranial. The territory traversed by the pro-otic sinus, which is rostral to the otic capsule (later petrous bone), thus representing the middle cranial fossa and site of the adult foramina lacerum, ovale, and spinosum, remains permanently membranous in various mammals. In man, ossification here is late, often postnatal, and is superficial to the entire course of the pro-otic sinus, including its petrosquamosal component. The remnant of the sinus, therefore, in late fetal life is intracranial and finally becomes diploic in the adult (fig. 18).

There is evidence that the inferior petrosal sinus, together with the cavernous sinus, both derivatives of the pro-otic sinus (stage 7), is also an extracranial channel from the phylogenetic standpoint, and is secondarily enclosed within the skull of primates exemplified by man. We have already seen that both ends of the inferior petrosal in the human embryo are derived from extracranial channels: cranially, from the pro-otic sinus, and caudally, from the dural end of the ventral myelencephalic vein (of stage 2), which joins the internal jugular below its foramen (figs. 20–25, pl. 1). Although the main part of the inferior petrosal sinus develops intracranially, in reference to the cartilage, a similar anastomosis superficial to the bone constitutes the plexiform adult *petro-occipital vein;* this lies just outside the skull and borders the fissure of the same name, as was well demonstrated in two adult corrosion specimens (acknowledged in the Introduction). As opposed to the main part of the pro-otic sinus, its cranial end, which gives rise to the cavernous sinus, must be considered intracranial in human development, since it is dorsal (medial) to the narrow root of the sphenoid cartilage (ala temporalis, fig. 18A, B) attached to the sella; even this end of the primary sinus is undoubtedly extrachondrocranial in other mammals.

In the horse and cow, the region of the pro-otic sinus is neither ossified nor cartilaginous in the adult (Sisson, 1953). Dennstedt's plates 1 and 2 (1904) show a conspicuous "emissary vein," the counterpart of the pro-otic sinus, in a position just superficial to the skull; this vein anastomoses both the ophthalmic veins and the "veins of the subtemporal fossa" (maxillary vein) with the "superior cerebral vein" (comparable to the petrosquamosal sinus of man), which traverses the temporal (postglenoid) foramen. Moreover, the inferior petrosal sinus in the adult horse is also extracranial (Dennstedt's pl. 1 and text fig. 2). Whether this sinus, a secondary anastomosis, develops in the embryo horse on the inner or on the outer side of the chondrocranium is uncertain (see below). It unites channels, however, which are extracranial in all stages of man and are probably comparable, namely the pro-otic sinus (cranially) and the primary myelencephalic tributary of the internal jugular vein (caudally). Furthermore, the otic and basioccipital cartilages have fused by the 40-mm. stage (de Beer, 1937), so that the site of the sinus (also the site of the osseous petro-occipital fissure in man) in the equine chondrocranium resembles that in the human embryo of the same length (Macklin, 1914, 1921). Although de Beer's specimen may be atypical, apparently more fetal absorption of the secondary cartilage at the otic-basioccipital junction must occur in the horse than in man. In any event, this region is notably unossified in the adult equine skull, according to Sisson (1953, fig. 53), thus constituting a large "foramen lacerum" around the whole medial half of the petrous bone. As a result, the inferior petrosal sinus lies in dural membrane at the floor of the skull.

The apparent absorption of embryonic cartilage just noted is comparable to that presumed to take place elsewhere in the human fetus, for instance, in the chondrocranial capsuloparietal commissure medial to the petrosquamosal sinus (see above); here some variable absorption must occur coincidently with the ossification of the membrane bones (fig. 18) in order to result in the intracranial position of this sinus (sometimes in man and in certain primates, e.g. the rhesus monkey).

In summary, it is interesting that the embryonic prootic sinus—the primary stem of the middle dural plexus, not very aptly called the "middle cerebral vein" in vertebrate embryology—together with its tributaries seems to be transitional from the standpoint of both ontogeny and phylogeny: The sinus first drains the brain (metencephalon, stages 2 to 5), later the orbit (stages 6, 7), and finally the dura and bone (stage *7a;* see pls. 1, 2). Its medial and cranial end, relatively short, is intrachondrocranial, i.e. the part of the primary head-sinus between the narrow cartilaginous temporal wing, when present, and the trigeminal ganglion; its greater length is extrachondrocranial and extends laterally in bordering the otic capsule (fig. 2B). The sinus may ultimately be represented in mammals by venous channels lying on either the inner or the outer side of the mature skull, or both, or by those within its substance (diploic).

Formation of the Basal Cerebral Vein

It has been seen that the growth of the brain and primitive skull between stages 7 and *7a* has initiated significant alterations in the dural sinuses. These alterations, continued until birth and after, require adjustments of the cerebral and cerebellar veins and are responsible for a completely new channel, which has not been well understood, the important *basal* (*cerebral*)[14] vein (of Rosenthal) (figs. 16, 17, 18). Although this vein and many of its tributaries are noted briefly in most anatomical descriptions, one of the very few current illustrations is a diagram in Bailey (1948). In the adult the basal cerebral vein is often as large as the internal cerebral vein, which it joins (bilaterally) to form the great cerebral vein (of Galen). Unlike that of the primary Galenic veins, however, the formation of the basal vein is complicated, and certain aspects of the development of the primitive brain up to this time must be reviewed to understand why it comes into existence.

In spite of the conspicuous expansion of the primordial cerebral hemisphere by 80 mm., its bulk still consists chiefly of the lateral ventricle almost filled by the relatively huge choroid plexus (fig. 16). The dorsolateral brain wall is relatively little thicker than that of the 40-mm. embryo, and still comprises the three primary layers, ependymal, mantle, and marginal, of which the ependymal, where the cells of the future cortex are arising, appears to be the most active. Well injected specimens show the many notably straight veins (and arteries) that pass directly laterally from the ependymal layer to the external surface; these vessels are collected by the pial tributaries of the superficial middle cerebral veins and, to a considerably lesser extent, those draining into the primitive superior sagittal and transverse sinuses.

It is important to recall (see stage 7) that, in contrast with the adult brain, little if any part of the primitive brain of stage *7a,* including the corpus striatum protruding into the ventricle, is drained as yet into the conspicuous, but primitive, internal cerebral vein. The explanation is that this vein is primarily the continuation of the superior choroid vein and courses over the part of the diencephalon that is membranous (tela choroidea of the third ventricle). Accordingly, the internal cerebral vein touches brain tissue only at the interventricular foramen (of Monro). Here it receives one primitive intracerebral vein from the region of the anterior thalamus, as was noted for stage 7. The thickened thalamic wall, which has reduced the third ventricle to a narrow slit, is drained by tributaries of the primary ventral and dorsal diencephalic veins. The hypothalamic region is also drained by the ventral diencephalic vein, reinforced cranially by tributaries of the deep telencephalic vein (secondary pial derivative of the superficial middle cerebral veins), which is still the exclusive drainage of the corpus striatum. Until stage *7a,* all the veins draining the forebrain are still tributaries of the tentorial sinus emptying into the transverse sinus near its junction with the sigmoid sinus. This drainage route, however, is now remote, owing to cerebral expansion and the resulting caudal swing of the definitive transverse sinus, described above. A shorter route is about to be substituted, therefore, into the great cerebral vein by way of a new basal cerebral vein.

It is interesting that the internal cerebral tributary of the great cerebral vein—essentially a superior choroid vein, the first component of the adult Galenic system to appear, and the most constant and uncomplicated in form at all stages—does not fulfill its final role of draining parts of the internal brain until sometime after the separate components of the basal cerebral vein, a secondary Galenic tributary that develops in a complex way, have assumed this function.

To understand the emergence of the basal vein, it is useful to review fundamental principles of the formation of all pial

---

[14] The modifier *cerebral* (agreeing with Hofmann, 1901) is used here for emphasis. The term *basal* (BNA) is preferable to "basilar," because the vein is not comparable to the basilar artery and has no primary connection with the basilar dural plexus ventral to it.

veins discussed in stage 4, as supplemented by basic adult patterns in a series of vertebrates (well illustrated by Hofmann, 1901). The simplest pattern is seen on the spinal cord, where an intervertebral (intersegmental) collecting vein primarily accompanies each nerve root. Later, pial tributaries of these transverse veins are joined by secondary longitudinal anastomoses, and these, in turn, are irregularly joined in similar fashion across the mid-line; as a result, some of the transverse collecting veins accompanying the nerve roots from pia to dura drop out (see also Herren and Alexander, 1939). The anterior and posterior spinal veins, however variable in detail in different species, are formed in this way. At the medulla and pons, where the nerve roots are relatively closer to each other, the primary transverse pia-arachnoidal veins extending from the pia to the dura (originally numerous along the dorsolateral aspect of the neural tube) are typically reduced to three in the vertebrate series: a "hypoglossal," a "vagal," and a "trigeminal" (Hofmann). It was seen in stage 4 (fig. 8) that the ventral myelencephalic ("vagal") vein of the human embryo, anastomosed caudally with a spinal vein, makes another longitudinal anastomosis cranially on the medulla and pons with a pial tributary of the ventral metencephalic ("trigeminal") vein. The specialization of the fore parts of the neural tube obscures the basic pattern somewhat, but the veins at its base are formed in the same way. According to a succinct remark of Dr. Frederic A. Gibbs (personal communication) about his venous injections of the cat, "the cerebral venous drainage may be interpreted as a bulge in the cord drainage."

As illustrated by Hofmann, the "basal cerebral vein" of adult mammals is the cranial counterpart of the "basal vein of the medulla oblongata" on the hindbrain, with which it is usually more or less continuous. The caudal end of the basal cerebral vein is an anastomosis between a "lateral mesencephalic" tributary of the "trigeminal vein"—this is the largest and most constant of the three transverse pia-arachnoidal veins of the hindbrain—and the "superior mesencephalic" tributary of the great cerebral vein. The cranial end of the basal vein lies between the hypothalamic and temporal-lobe regions, where it receives telencephalic (anterior and deep middle cerebral) and diencephalic tributaries; it is usually not symmetrical in the mammals illustrated, and is not always continuous, being sometimes represented by more than one vein along its course.

Hofmann shows that the most primitive exit for the basal cerebral vein (his text figs. 1–6) is lateral, i.e. by way of the "trigeminal" vein, the stem of which is the mammalian counterpart of the human superior petrosal sinus draining the cerebellar region, as was described above. This finding again exemplifies the fact that, typically, in adult mammals, as in the human embryo, virtually all the veins of the brain are laterally drained into the junction of vessels representing the sigmoid and transverse sinuses (pl. 6). Medial drainage of the basal cerebral vein into the Galenic system, by way of a channel lying between the midbrain and thalamus, is secondary from the phylogenetic standpoint; this route is often predominant in certain primates typified by adult man (see below). According to Hofmann, the basal cerebral vein, as exemplified in the chick, rabbit, guinea pig, cat, dog, and horse, empties more laterally into the counterpart of the transverse sinus by way of the "trigeminal vein" than medially into the Galenic vein. In the rabbit, pig, cat (Hofmann), and dog (Bedford, 1934*a*), it has both lateral and medial communications with the transverse and straight sinuses, respectively, by way of the veins just mentioned. Bedford's studies (1934*b*) show the lateral route to be also frequent in the rhesus monkey. In a specimen dissected by the author, the basal cerebral vein on one side drained more laterally, that on the other side more medially—a "combination or transitional type," according to Bedford.

From the appearance of adult mammalian veins at the base of the brain as compared with those of the present fetal stage 7*a*, it is clear that the basal cerebral vein of all species emerges in essentially the same way. In the 60- to 80-mm. embryo, the course of the vein is well outlined by segments of a new longitudinal anastomosis connecting the pial ends of three or four of the primitive transverse (pia-arachnoidal) cerebral veins, as follows: (1) the telencephalic vein, near the junction of its deep middle cerebral and anterior cerebral tributaries; (2) the ventral diencephalic vein, draining the choroid plexus and the region of the descending horn of the lateral ventricle through a well defined tributary; (3) the dorsal diencephalic vein, which may be represented by a dorsal tributary of the ventral diencephalic vein; and (4) the dorsal diencephalic vein, anastomosing with one of several tributaries of the great cerebral vein in the region of the pineal primordium (fig. 16; cf. figs. 34, 35, pl. 2).

The primitive great cerebral vein is seen earlier in stage 7 (40 mm.) on the membranous roof of the third ventricle near the dorsolateral aspect of the thalamus (fig. 13); it drains a plexus extending cranially to the interventricular foramen, which communicates with the internal cerebral vein at its junction with the voluminous superior choroid vein and a small, deep thalamic tributary. As was noted above (stage 7), a component of this plexus undoubtedly represents the future terminal vein, the major tributary of the adult internal cerebral vein, which either supplements or annexes internal cerebral drainage from the primary pia-arachnoidal veins of the ventral surface of the brain; the vein ultimately becomes enclosed in the ventricular wall during the secondary embryonic juxtaposition of the thalamic and caudate nuclear regions, owing to development of the internal capsule.

The formation of the basal cerebral vein, like that of the terminal tributaries of the internal cerebral vein, is a result of the expansion of the cerebral hemisphere, particularly caudally. The vein compensates for the elongation not only of the tentorial sinus emptying into the transverse sinus but also of the primitive transverse diencephalic and mesencephalic veins, which are now stretched over the expanded temporo-occipital lobe in reaching these sinuses; these veins become attenuated near their entrance into the dura, where they will usually

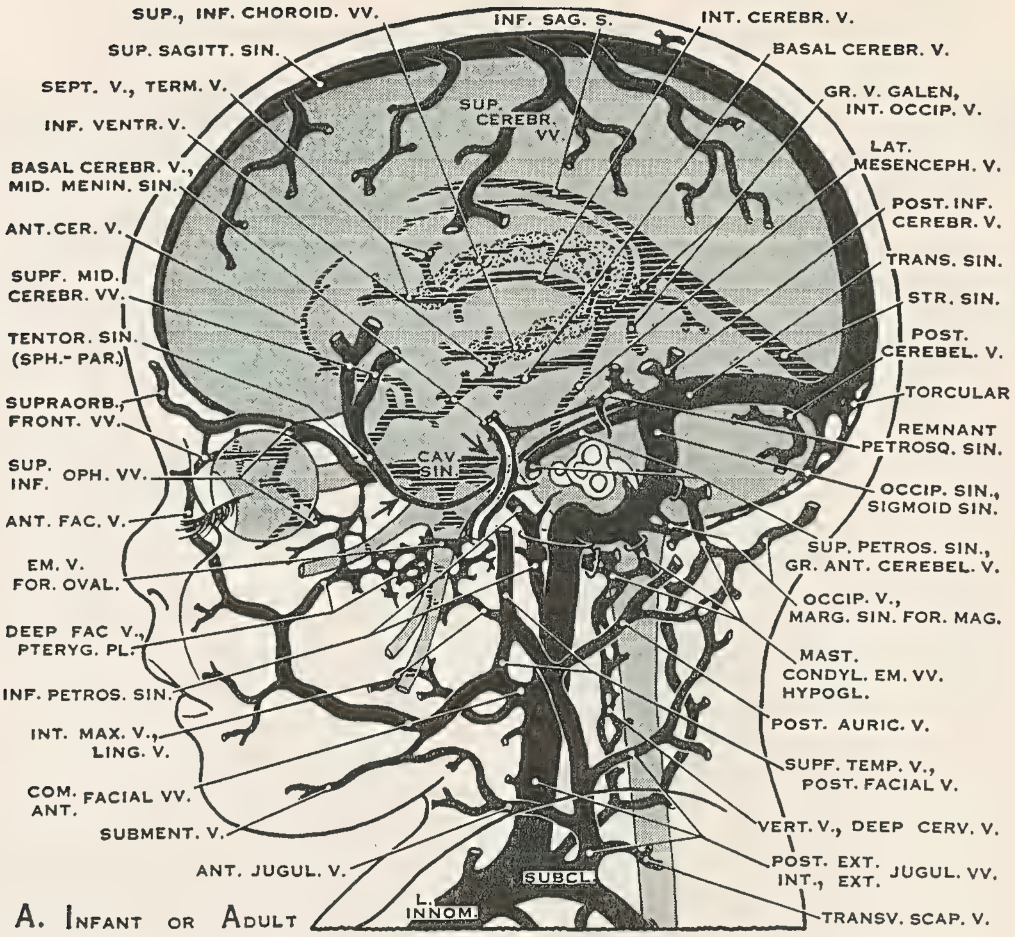

A. Infant or Adult

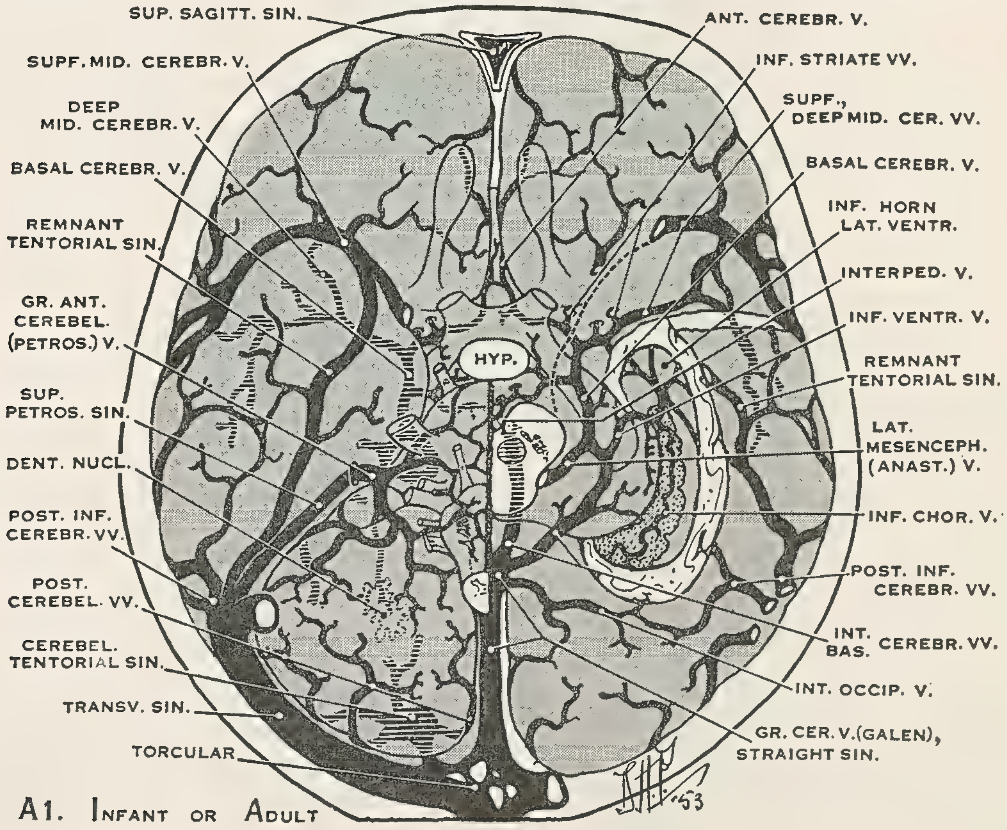

A1. Infant or Adult

Fig. 17. Adult patterns (in an infant head). Note particularly the following: (A) the conformation of the basal and internal cerebral veins, meeting (bilaterally) to form the great cerebral vein; remnants of the tentorial, pro-otic (dural meningeal), and petrosquamosal sinuses; the deep facial vein; the extracranial exit of the inferior petrosal sinus; the emissary veins; three primary veins draining the otic region (unlabeled); (B) the remnant of the tentorial sinus, sometimes constituting a superficial vein; the great anterior cerebellar vein; the tentorial lacuna that receives the posterior cerebellar veins. The tributaries of the basal vein, itself secondary and variable, are significant primary veins; its anastomosis with the great anterior cerebellar vein constitutes the lateral mesencephalic vein, potential drainage for both the basal and internal cerebral veins.

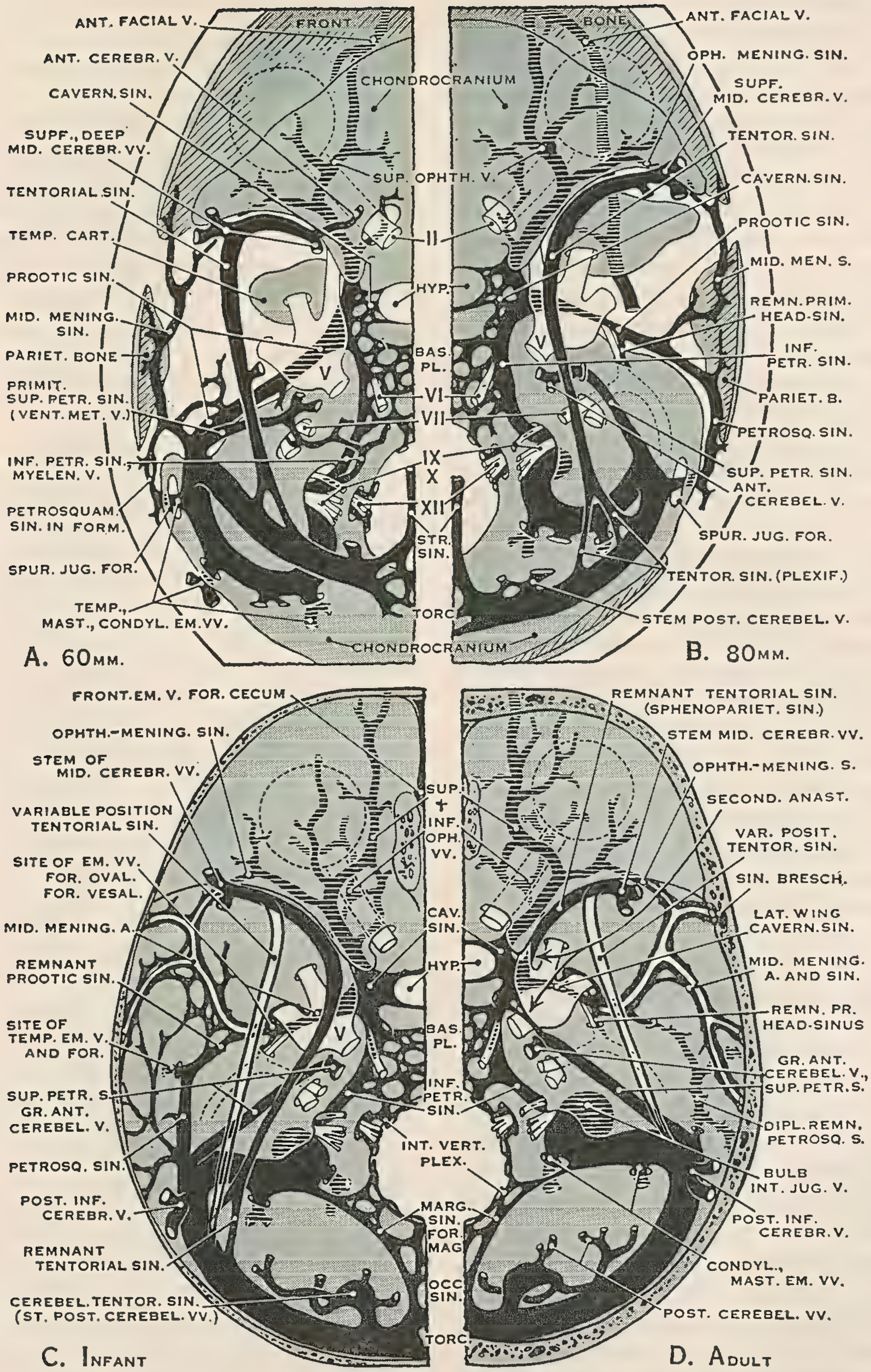

FIG. 18. Four stages in the vessels at the base of the chondrocranium (A, B) and the skull of the infant (C) and adult (D; C and D to be correlated with fig. 17). Expansion of the otic capsule between 60 and 80 mm. modifies several prominent channels: the pro-otic sinus dwindles and becomes continuous with the petrosquamosal sinus (comparable to the temporal emissary of mammals, generally); the dural end of the metencephalic (anterior cerebellar) vein (A) becomes the superior petrosal sinus (B). The position of the tentorial sinus varies in pre- and post-natal life (A–D). When it is situated medially (B, C), remnants of the sinus may secondarily connect the cavernous sinus cranially with the superficial middle cerebral veins, and caudally with the superior petrosal sinus (arrows, D).

be obliterated. When fully developed, the adult basal cerebral vein is often as large as the internal cerebral vein and may drain as much (if not more) territory. These veins, together with those of the opposite side, meet to form the great cerebral (Galenic) vein (fig. 17). The complicated formation of the basal vein from elements of widely separated embryonic veins explains its frequent existence in somewhat fragmentary form, as is well illustrated for other mammals by Hofmann (1901).

Variable lateral outlet of basal vein. The significance of an important adult modification affecting the caudal terminus of the basal cerebral vein in man, apparently unknown in general (see Padget, 1956), should be emphasized. According to the usual description, the vein empties medially into the internal (or great) cerebral vein. It may empty laterally, however, either in part or entirely, into the sigmoid sinus by way of the superior petrosal sinus, which represents the primary metencephalic vein.

The alternative or supplementary routes by which the basal vein empties either caudomedially or caudolaterally are better understood by reference to the development of comparable channels in other mammals, referred to above. Apparently lateral drainage of the basal vein is the more primitive type; it is cerebellar (infratentorial) with respect to the vessels involved, in contrast to medial drainage, which is cerebral (supratentorial). Drainage through the posterior fossa, frequently predominant in vertebrates, is by way of the "trigeminal vein," which is obviously a biological constant; the vein is homologous to the great anterior cerebellar vein (see below), including its outlet, the superior petrosal sinus of man, which is derived from the pro-otic sinus (stem of the middle dural plexus, typical of vertebrate embryos). The stem of the embryonic metencephalic (later trigeminal or anterior cerebellar) vein lies at the level of the 5th nerve root. A secondary anastomosis between one of its tributaries and the developing basal cerebral vein on the diencephalon must pass across the midbrain and thus incorporate part of the embryonic mesencephalic vein. The first stages in the longitudinal basal anastomoses between the primitive telencephalic, diencephalic, mesencephalic, and metencephalic veins were seen in several well injected embryos of the present series (figs. 6, 8, 11, 16; pl. 5C1).

A postnatal vein, often well defined in or near the lateral mesencephalic sulcus of the brain stem (fig. 17A1), results from the embryonic anastomoses forming the basal vein, and hence may be called the *lateral mesencephalic* (*anastomotic*) *vein.* Constituting an anastomosis between the great anterior cerebellar vein and the basal vein, near its junction with the internal cerebral vein, the mesencephalic vein was conspicuous in several newborn and adult brains dissected for the present study, and in one of two corrosion specimens (see Introduction). The only adequate illustration of an anatomical specimen known to the author, however, is by Hédon (1888, pl. 2). Hochstetter (1938) reported in detail on a human adult in whom the left basal cerebral vein emptied into the superior petrosal sinus, thus obviously representing a persistent and well developed lateral mesencephalic vein; on the right side, the basal cerebral joined the great cerebral vein, as is commonly described for adults—an example of Bedford's "combination type" (in the monkey), referred to above. Such exclusive or accessory lateral drainage of the basal cerebral vein, potentially important and including, of course, that of the internal cerebral vein, is undoubtedly more frequent than is generally realized.

Cerebellar Veins

Thus far, drainage of the cerebellum has been mentioned only incidentally. With regard to the veins of the cerebrum, it has been seen why those near its base are the first to develop. The often conspicuous, but highly variable, anastomoses in the adult between the superficial middle cerebral veins and the tributaries of the superior sagittal and transverse sinuses, namely the great anastomotic veins of Trolard and L'Abbé, are secondary; they are not identified until sometime after 80 mm., when the expanded dorsolateral cerebral wall, as contrasted to the more precocious medial parts comprising the basal nuclei, has begun to differentiate (between 3 and 6 months, according to Hédon; see his pl. 5). Similarly, very few of the larger adult cerebellar veins may be identified at the 60- to 80-mm. stage, because the adult hemispheres are still represented by the cerebellar plates only; these primordia have become fused cranially in the mid-line, but have not yet grown caudally to cover the membranes of the fourth ventricle (fig. 16A). The primary and most conspicuous vein of the cerebellum, therefore, is located at its base in the fore part of the posterior fossa. This is the ventral metencephalic vein, which emerged in stage 4 (fig. 8B) and has constantly provided drainage of the primitive pons and the cerebellar plate (pls. 1, 2). Although its proximal end becomes enclosed in the dura above the petrosal crest, to constitute the essential part of the definitive superior petrosal sinus, as was discussed above, the ventral metencephalic vein is clearly homologous to the relatively constant "trigeminal vein" of vertebrates (Hofmann, 1901); it has a comparable position and drainage.

The important primary cerebellar vein just noted has been given no specific anatomical name in the human adult. Its conspicuous trunk, entering the superior petrosal sinus, however (shown unlabeled in several textbook illustrations of actual specimens), is well known to neurosurgeons, and has been called the "petrosal" or "petrous" vein (Bailey, 1948); Hédon (1888, fig. 1, pl. 4) designated it the "vein of the pneumogastric lobule," in reference to an old name for the flocculus, near which its tributaries are consolidated into one or more main stems before they enter the superior petrosal sinus. The vein drains parts supplied by all three cerebellar arteries, particularly the anterior inferior, and also the territory of the internal auditory artery. As a primary vein constituting the predominant drainage of the metencephalon, it is comparable in the adult to the great cerebral vein, which secondarily develops intra- and extra-cerebral tributaries. The superior, inferior, lateral, and medial cerebellar tributaries of the metencephalic vein in the adult include drainage of the pons and medulla, and also the dentate nucleus (fig. 17B), as was noted by Bailey. In view of its importance, the name *great anterior cerebellar vein* is appropriate (fig. 16A1).

In the embryo of stage 4, the conspicuous ventral metencephalic ("trigeminal") vein anastomoses over the pons and medulla with the smaller ventral myelencephalic ("vagal") vein, from which the inferior petrosal sinus is derived (stage 7). Hence, the myelencephalic vein may become an *inferior medullary* tributary of this sinus; it is often annexed, however, by the predominant great cerebellar vein, which drains, therefore, all brain tissue of the posterior fossa except the most dorsal and caudal parts of the cerebellum, the last to develop. When present, the *median superior cerebellar* vein of the adult (designated and pictured by Hédon; also called the "superior vermian," Morris' *Textbook of Anatomy,* 1953) leaves the summit of the vermis to enter the great cerebral vein; it may ultimately be represented among the many tributaries of the great anterior cerebellar vein. At stage *7a,* its stem is sometimes seen among the plexiform channels in the region of the tentorial plexus, the future torcular (fig. 16A).

A relatively inconspicuous vein of the embryo is the dorsal metencephalic vein of stage *7a* (exaggerated in fig. 16A), first identified in late stage 4. This vessel is ultimately represented, however, by a prominent group of adult veins (including those exposed by the surgical suboccipital approach), which must be classified; to them, again, no precise anatomical name has been assigned. From the developmental standpoint, the cerebellar veins are essentially comprised of only two main groups, commonly joined by anastomoses. The more primitive group, developmentally and phylogenetically, constitutes the *anterior cerebellar* veins, which often terminate in the one conspicuous primary trunk just described, the essential component of the superior petrosal sinus (see above). In many cases, these veins drain all except the most caudal aspects of the cerebellar lobe. The *posterior cerebellar* group, which develops parallel with later cerebellar expansion, includes prominent superior and inferior tributaries, which were well illustrated for the adult by Hédon (1888, pl. 3). The interesting way in which they often enter the transverse sinus is clarified in the present study.

Primarily, the posterior cerebellar group of veins do not enter the transverse sinus as commonly portrayed, i.e. at various intervals between the superior sagittal and sigmoid sinuses. Instead, posterior cerebellar tributaries, superior, inferior, and lateral, meet in loops, either within the tentorium or densely attached to it, and join a lacuna-like intratentorial sinus; this in turn joins the transverse sinus through a more or less constricted (necklike) stem near the torcular (fig. 18C, D). The stem of the lacuna represents the tentorial end of the dorsal metencephalic vein of the present fetal stage (fig. 18B). In other words, the posterior cerebellar group of veins, like the anterior cerebellar, commonly enters the sinus by way of a single trunk, a primary vessel. This pattern, which must be frequent, has been well demonstrated bilaterally in adult specimens, including two corrosion preparations acknowledged in the Introduction. It is interesting that Gibbs and Gibbs (1934), in a dynamic study of the torcular region, incidentally pictured this tentorial lacuna: as a diverticulum of the transverse sinus, it was noted in 19 of their 25 corrosion preparations, bilateral in 17. The significance of the diverticulum was not relevant to their study, but they designated it the "tentorial sinus"; from the developmental point of view, it may more precisely be called the *cerebellar* tentorial sinus in distinction to the *cerebral* tentorial sinus,[15] described above, which is the primary drainage of the superficial middle cerebral veins. Although the caudal ends of these separate dural channels, various remnants of which are often found at birth and even later, may become essentially identical, one is primarily related to the cranial or cerebral layer of the tentorium, the other to its caudal or cerebellar side.

Whereas the cerebellar tentorial sinus superficially resembles a lateral lacuna of the superior sagittal sinus, the tributaries of each are primarily different: the cerebellar tentorial sinus receives essentially all the posterior cerebellar veins, but the cerebral dural lacunae are dilatations in adult life of the dorsal ends of the middle meningeal sinuses ("veins"; well illustrated in the Grant *Atlas,* 1951, fig. 479). Primarily, the parasagittal lacunae do not receive the superior cerebral veins, as was emphasized for the adult by Bailey (1948). Nevertheless, since both groups of dural channels are derived from the anterior dural plexus (see stages 1, 2), specifically, from its components in the outer and inner dural layers, respectively, communications between them may persist, particularly in pathologic vascular conditions.

---

[15] *Sphenotemporal sinus* is often definitive for its postnatal remnant (p. 122). It should be noted that the term "tentorial sinus" was formerly applied to the straight sinus (rectus).

SUMMARY

Full understanding of the complex pattern of veins in the region of the human head has been delayed because of inadequate knowledge of the basic plan. Particularly if complicated by variations, including arteriovenous anomalies, the plan is clear only when the stages of venous development in man are illuminated by comparison with embryonic and adult patterns in other vertebrates. Definitive venous channels emerge from the primitive vascular net later than do the arteries, which influence their development; furthermore, the complicated venous anastomoses are essential to facilitate a greater adjustment to the changing needs of their environment over a considerably longer period. The following outline of stages, which necessarily overlap, can be followed by reference to plates 1 and 2; these are comparable to plates similarly numbered in the arterial study (Padget, 1948), and are also accompanied by legends that summarize the sequence of events in man. (Vascular stage 1 is not represented in this pictorial summary of the veins; see p. 82.)

Stages 1 and 2 (fig. 19, pl. 1; fig. 27, pl. 2) of vascular development are similar in vertebrates. Characteristic features of the head are the pharyngeal bars, which are homologous to the gill-bearing arches of fishes and larval amphibians. In amniotes, the aortic arches in the first three bars contribute to the formation of the common and internal carotid arteries. Their dorsal branches supply a capillary plexus in the future pial layer, which drains through many short vessels, dorsolateral to the neural tube, into a superficial venous plexus of the future dural layer. By way of three relatively constant dural stems, anterior, middle, and posterior, this plexus drains ventrally into a primary head-sinus ("head-vein"), continuous with the anterior cardinal vein, which constitutes the primitive (*internal*) jugular vein. As the first two aortic arches are succeeded by a ventral pharyngeal artery (forerunner of the external carotid), the future facial region is drained by a corresponding vein, which becomes the typical linguofacial (common facial) tributary of the internal jugular vein. The optic vesicle is vascularized by prominent vessels in the emerging maxillary process, the spinal cord by intersegmental vessels, which are precursors of the vertebral system of arteries and veins (figs. 19–21, pl. 1).

During stages 3 and 4, the dural venous channels come to lie more laterally as the cerebral hemisphere and rhombic lip expand and the otic vesicle enlarges (figs. 27–30, pl. 2). As a result, the head-sinus and the primitive internal jugular—this vein, not the external jugular, is the primary neck vein of vertebrates—migrate laterally to certain cranial nerve roots except the trigeminal ganglion, medial to which the head-sinus appears to be anchored by its voluminous maxillary tributary (figs. 20, 21, pl. 1). With continuing separation of the dural and pial layers of venous channels, most of the numerous primary anastomoses between them drop out. The few remaining anastomoses enlarge and thus constitute the stems of the primary veins, which pass transversely through the pia-arachnoid (fig. 30, pl. 2). Sometimes, by late stage 4, at least one such vein for each of the five divisions of the brain can be identified (fig. 6). The pial veins develop as secondary anastomoses between the primary pia-arachnoidal veins; they probably represent an elaboration of channels in the parts of the primitive capillary mesh not used by the preceding arteries, which, in becoming definitive, are somewhat elevated from the neural tube. The intrinsic pial veins consequently pass under and at a right angle to the arteries; this fundamental pattern is particularly clear around the basilar artery and its branches (fig. 8).

At the end of stage 4 (fig. 21, pl. 1; figs. 29, 30, pl. 2), drainage of the mammalian head is comparable to that of adult reptiles. The brain is still drained through the primary head-sinus, which leaves the primitive skull between the medial side of the 5th nerve and the otic complex. In birds, the caudal end of the head-sinus, after becoming crowded dorsally by the hyoid pharyngeal pouch, is replaced by a secondary anastomosis between two vessels: one is comparable to the linguofacial vein; the other, to the ventral end of the middle dural stem, which constitutes the extrachondrocranial pro-otic sinus. In all stages of reptiles and birds, the head is drained by the primary internal jugular system representing the anterior cardinal vein. An external jugular vein apparently is not a typical development.

By stage 5 (fig. 22, pl. 1), which represents a fundamental pattern in mammals, the caudal end of the head-sinus, continuous with the internal jugular vein, has become crowded by otic development as in birds, but more laterally than dorsally. The head-sinus, therefore, is replaced by a secondary anastomosis that is intrachondrocranial, namely the sigmoid sinus, dorsal to the otic capsule. A similar anastomosis formed cranially is the very primitive transverse sinus, at first recognizable only through its connections. The facial region is drained cranially by the prominent ophthalmic and maxillary tributaries of the head-sinus, and caudally by the linguofacial tributary of the internal jugular.

Stage 6 (fig. 23, pl. 1) is particularly significant in mammalian development. It marks the emergence of the external jugular system, which succeeds the external carotid. Thereafter, the essential difference between the venous pattern of most macrosmatic mammals and of primates resembling man is that the secondary external jugular system annexes most components of the primary internal system in those species in which the brain becomes relatively less developed than the face and neck (pl. 6). At stage 6, however, all the brain except the medulla is drained into the junction of the sigmoid sinus (or its counterpart, underdeveloped in many mammals) with the primitive transverse sinus. Here, the cerebral veins empty by way of a conspicuous tentorial sinus (rhinencephalic vein typical of mammals), bordering the ventrocaudal aspect of the hemisphere. The primitive supraorbital and infraorbital (maxillary) veins also drain to this significant junction of channels by way of the extrachondrocranial pro-otic sinus.

By stage 6 (figs. 31, 32, pl. 2), venous asymmetry of mid-line channels has become conspicuous in human development, for which compensation is possible after the appearance of a new channel. When, as a result of cardiac development, the sinus venosus constitutes a substantial detour for flow from the left side of the head, both the primitive superior sagittal and straight sinuses in the embryo drain more to the right. In certain mammals, including man, an excessive detour to the heart is either more or less counteracted by the formation of the left innominate vein—a transverse anastomosis between the bilateral anterior cardinals (internal jugulars). If the secondary innominate later becomes essentially symmetrical with the primary right innominate vein (segment of the anterior cardinal), as does occur in many mammals (pl. 6A), a relative symmetry of the torcular pattern can result in the meshes of the tentorial plexus. Persistence of asymmetry of the innominate veins in anthropoid primates typified by man, however, is often reflected in persistent asymmetry of the sinuses at the torcular (pl. 6B).

In stage 7 (fig. 24, pl. 1), the secondary external jugular vein, just formed, begins to annex many tributaries of the primary internal jugular system, including the anterior facial (external maxillary) vein; this facial vein was formed in stage 6 by anastomosis of a tributary of the linguofacial vein with that of the maxillary vein, the stem of which has now become the outlet of all the veins in the orbit. The primitive emissary veins, which arose earlier to drain extracranial structures medially into the sinuses, become definitive by anastomosis with external jugular tributaries. The mastoid and temporal emissaries are particularly significant, and traverse foramina relatively constant in the mammalian chondrocranium (fig. 33, pl. 2). The mastoid vein, developed in response to the cervical musculature, thus may compensate for the small sigmoid sinus and internal jugular vein typical of adult mammals (pl. 6A). The embryonic temporal emissary (of the spurious jugular foramen in the chondrocranium) at first drains the region of the temporoparietal ossification centers medially into the sinuses; its stem later constitutes the fetal petrosquamosal sinus, which finally becomes diploic (tympanic) in man (fig. 24, pl. 1). The human pattern, however, is the exception in mammals. Generally, the petrosquamosal channel enlarges to become the chief drainage of the brain into the external jugular system, a secondary anastomotic development that is accompanied by secondary dwindling of the internal jugular vein. These contrasting patterns are shown diagrammatically (pl. 6).

The primary stems of the pia-arachnoidal veins draining the brain (stage 4) increase in length as the cerebral hemisphere expands before stage *7a*. Meanwhile the Galenic system of intracerebral drainage emerges as the result of accelerated growth of the basal nuclear masses and the choroid plexus almost filling the lateral ventricle, of which the bulk of the primitive cerebral hemisphere is constituted. The straight sinus, continuous with the great cerebral and internal cerebral veins, is primarily, however, the outlet of the superior choroid vein only (fig. 24, pl. 1); the terminal vein, and its intracerebral tributaries, are developed later, parallel with pallial expansion. In this and earlier stages, the choroid plexus, corpus striatum, and diencephalon are drained by primary pia-arachnoidal (telencephalic and diencephalic) veins, tributaries of the tentorial sinus that are incorporated into the later basal cerebral vein.

The extrachondrocranial pro-otic sinus (primary stem of the middle dural plexus) is the caudal outlet of the supraorbital and infraorbital veins until stage 7, when development of its secondary medial derivatives, the cavernous and inferior petrosal sinuses, substitutes an intracranial route in man. In other mammals, orbital drainage is chiefly annexed by the external jugular vein. While being pushed craniolaterally by the expanding otic capsule, the middle part of the pro-otic sinus dwindles in the human fetus (figs. 36, 37, pl. 2). Meanwhile, its lateral tributaries emerge to drain the frontal and subsequent parietal ossification centers; these centers are supplied by the middle meningeal artery, which annexes the stapedial branch of the internal carotid. The stem of the meningeal artery is just lateral to the pro-otic sinus, but the branches of the artery and tributaries of the sinus reverse this position: the venous channels, in other words, lie between the arteries and the primitive bones. As is clear in stage 4, the pia-arachnoidal veins, in approaching the sinuses, likewise change their position relative to the arteries. While they are both endothelial tubes, pial veins cross at right angles under the arteries, and consequently they do not parallel one another. When the arterial walls have notably thickened, the dural meningeal vessels, for instance, accompany each other. Similarly, the intimate relations in the cavernous sinus are not established until stage 7 (40 mm. in man).

The primitive membrane bones of stages 7 and *7a* (figs. 33–37, pl. 2) are not vascularized by the vessels of the scalp—a region initially avascular. Furthermore, the scalp plexus when it appears is not the result of a vascular cleavage, which occurs, it must be noted, only between layers of *venous* channels, specifically those of the dura and pia. Instead, the scalp plexus is separately derived from the external jugular and carotid systems during stage 6. Marked externally by a conspicuous margin, the plexus advances up over the vault on all sides, separated from the bones by a considerable interval of avascular tissue. The hiatus in the plexus closes sometime after the 40-mm. stage in the region of the future parietal foramen. Among the emissaries, which typically comprise primary vessels at the skull base, those of the parietal (and associated, but very rare, occipital) foramen appear to be unique. The entire complex, arterial and venous, seems to be a secondary anastomosis not incorporating primary vessels, and suggests genetically vestigial remnants of vascularity in the region of an ancestral pineal eye. This interesting region of the cranial vault, including the parietal ("sagittal") fontanel that ossifies to form the parietal foramen either before or after birth, calls for further study in reference to normal and abnormal morphology (Padget, 1956).

Stage 7*a* (fig. 25, pl. 1) is not represented in the previous account of the arteries (Padget, 1948), for they have already attained the essential adult configuration by 40 mm. (stage 7). Not until approximately 80 mm., when the venous pattern in the human embryo is comparable to that of the adult in other mammals, does the transverse sinus begin to assume its definitive position; its caudal swing on the sigmoid as the result of cerebral growth (figs. 22–25, pl. 1) resembles that of the posterior communicating artery. The expansion of the cerebral hemisphere and otic capsule by the 80-mm. stage is responsible for the definition of the last of the major adult sinuses to appear, the superior petrosal (figs. 36, 37, pl. 2). The direct contiguity of the sinus with the petrosal crest is peculiar to certain primates typified by man. Nevertheless, the stem of the great anterior cerebellar vein, of which the sinus constitutes essentially a dural envelopment, is the primary metencephalic (trigeminal) vein characteristic of representative vertebrates.

The most important vein at the base of the brain is not clearly defined until stage 7*a* (60 to 80 mm.) in man. The basal cerebral vein represents a channel, or fragments thereof, typical of adult mammals, which is derived from primary veins typical of vertebrates. These vessels include the primary drainage of the basal nuclear masses, in spite of the earlier appearance of the internal cerebral vein, which emerges as the outlet of the superior choroid vein only. The basal vein develops as a longitudinal pial anastomosis between primary pia-arachnoidal veins, i.e. the transverse telen-, dien-, mesen-, meten- (trigeminal), and myelen-cephalic (vagal) veins of stages 4 and 5. These primitive veins, particularly the first three, become the adult tributaries of the basal vein as shown in figure 35 (pl. 2). One of these tributaries, the lateral mesencephalic vein, is especially important. It may constitute part, or all, of the outlet of the basal cerebral (and/or internal cerebral) vein into the superior petrosal sinus by way of the great anterior cerebellar (metencephalic) vein. Such lateral drainage of the basal vein occurs often in many mammals (including certain primates), in which essentially all intracranial drainage converges to the junction of the transverse and sigmoid sinuses (pl. 6). This pattern typifies stages 6 and 7 in human development, and frequently persists, although the medial route into the great cerebral vein may usually be predominant in adult man.

Subsequent venous changes in human development depend chiefly upon the expansion of the cerebral and cerebellar hemispheres and the relatively late ossification of the skull. Since certain significant anastomoses in the dura often occur after birth, the typical configuration in the newborn differs from that in the adult[16] (figs. 38, 39, pl. 2). These contrasting patterns, together with an outline of other obscure features of the postnatal configuration, and including comments on the embryologic background of congenital arteriovenous anomalies, have been published elsewhere (Padget, 1956).

ADDENDUM

Since this paper was written, there has come to hand a monograph by Dr. Richard Lindenberg [1956: Die Gefässversorgung und ihre Bedeutung für Art und Ort von kreislaufbedingten Gewebsschäden und Gefässprozessen, *in* Lubarsch, Henke, and Rossle, Handbuch der speziellen pathologischen Anatomie und Histologie, vol. 13 (ed. W. Scholz), pt. 1B, chap. 2, pp. 1071–1164]. The section on anatomy is well illustrated by photographs of dissected specimens. Of these, his figure 28, a rare illustration of the basal cerebral vein, is directly comparable to the present figure 17A1; it includes the important potential anastomosis, the lateral mesencephalic vein (*v. sulci lateralis;* it is large in his fig. 18), together with two conspicuous tributaries draining the inferior ventricular horn and thalamus. By way of this vein, the more anterior group of cerebellar veins may sometimes drain the region of the dentate nucleus into the basal or great internal cerebral vein, as he notes; primary drainage of this region, however, is by way of the superior petrosal sinus. (Essentially, his *Vv. flocculares,* together with the *Vv. cerebellares rostrales, mediales,* and *laterales,* constitute the great anterior cerebellar system of the present account.)

---

[16] This evidence, though strong developmentally, is based on a small number of infant and adult heads (ca. 25; see Introduction). Owing to certain limitations of dissection, more corrosion specimens are particularly called for, especially of later fetal stages, although obtaining complete venous injections without extravasation is technically very difficult in postmortem material. Similarly, until more material has been collected, undue weight must not be given the author's observation (Padget, 1948, and earlier) that, typically, there is less relative difference in the size of the several arteries comprising the circle of Willis in infants than in adults; as stated in 1948, no essential difference in arterial patterns has been demonstrated, contrary to the situation regarding a number of dural venous channels.

Other observations of interest here (supplemented by personal communication) include the following.

1. The frontal emissary vein that traverses the region of the adult foramen cecum (Padget, 1956, p. 328) is identifiable with Zuckerkandl's vein of infancy (Lindenberg, pp. 1078, 1114), as it is called on the continent. This vein, apparently secondary in human development, passes through the skull at least prior to completed ossification. Its incidence, especially in juveniles, and whether its large size is abnormal or a normal variant are not apparent.

2. This ventral or orbital frontal emissary must be distinguished from a more dorsal *emissarium frontale* (Lindenberg's diagram after Clara, fig. 29), seen by Lindenberg in several specimens. Occasionally bilateral, but apparently not common, its foramen has been found just in front of the coronal suture near the mid-line. This perforating skull foramen, like the parietal (and rare occipital), is undoubtedly the remnant of one of the normal fontanels (Padget, 1956, p. 328); the vein is assumed to be a secondary anastomosis that forms sometime during fetal as opposed to embryonic life (pp. 119, 136).

3. The deep thalamic vein (Padget, 1956, p. 314), which Lindenberg refers to as the "Zentralvene der oralen Thalamushälfte" (his p. 1110; also fig. 64), is prominent and significant; in the very early fetal stages that conclude the present series, it is the only thalamic drainage into the internal cerebral vein.

4. A rich network of sinusoids is frequent in the tentorium, especially in juveniles, and represents remnants of the primary drainage of the embryonic cerebral and cerebellar hemispheres.

5. Lindenberg believes that there is strong evidence supporting, though not necessarily proving, the existence of the postnatal intracerebral anastomotic veins of Schlesinger (see Padget, 1956, p. 315). Certainly, most of the length of such veins would represent a persistence of embryonic conditions, in which all drainage of the ependymal region is directed laterally to the periphery. But how the veins concerned become anastomosed with the tributaries of the terminal vein, indeed, just how the stem of this vein beneath the stria terminalis, and possibly at first extracerebral, becomes enclosed within the ventricular wall (see footnote 11, p. 112), are interesting features of stages beyond the scope of this study that await clarification. Various details near the superior sagittal sinus and its lateral lacunae, which involve seemingly few and minor emissaries under normal conditions, also require exploration. It is to be hoped that future studies on the development (fetal and postnatal?) of the subarachnoid and subdural spaces, especially of the arachnoid granulations—and current observations (unpublished) show that macroscopic arachnoid villi are by no means limited to the region of the cranial vault—will answer these questions regarding venous development in later fetal stages.

LITERATURE CITED

Anikew, A. 1909. Zur Frage über die Entwickelung der Vena anonyma sinistra. Anat. Anz., vol. 34, pp. 24–29.

Bailey, P. 1948. Intracranial tumors. 2d ed. 478 pp. Baltimore.

Batson, O. V. 1940. The function of the vertebral veins and their role in the spread of metastases. Ann. Surg., vol. 112, pp. 138–149.

Bedford, T. H. B. 1934*a*. The great vein of Galen and the syndrome of increased intracranial pressure. Brain, vol. 57, pp. 1–24.

——— 1934*b*. The venous system of the velum interpositum of the rhesus monkey and the effect of experimental occlusion of the great vein of Galen. Brain, vol. 57, pp. 255–265.

Browning, W. 1884. The veins of the brain and its envelopes. Their anatomy and bearing on the intracranial circulation. 79 pp. Brooklyn.

Campbell, A. C. P. 1938. The vascular architecture of the cat's brain. A study by vital injection. *In* The circulation of the brain and spinal cord. A symposium on blood supply. Assoc. for Research in Nervous and Mental Disease Pub., chap. 3, vol. 18, pp. 69–93.

Cunningham, D. J. 1951. (Ed. J. C. Brash.) Textbook of anatomy. 9th ed. 1604 pp. London.

Davis, D. D., and H. E. Story. 1943. The carotid circulation in the domestic cat. Field Museum Nat. Hist., Zool. Series, no. 1, vol. 28, pp. 1–47.

de Beer, G. R. 1937. The development of the vertebrate skull. 552 pp. London.

Dennstedt, A. 1904. Die Sinus durae matris der Haussäugetiere. Anat. Hefte, vol. 25, pp. 1–96.

Evans, H. M. 1912. The development of the vascular system. *In* Keibel and Mall (eds.), Manual of human embryology, vol. 2, chap. 18, pp. 570–709. Philadelphia.

Feeney, J. F., Jr., and R. L. Watterson. 1946. The development of the vascular pattern within the walls of the central nervous system of the chick embryo. Jour. Morphol., vol. 78, pp. 231–303.

Finley, E. B. 1922. The development of the subcutaneous vascular plexus in the head of the human embryo. Carnegie Inst. Wash. Pub. 277, Contrib. to Embryol., vol. 14, pp. 155–161.

Gelderen, C. van. 1924. Die Morphologie der Sinus durae matris. Zweiter Teil. Die vergleichende Ontogenie der neurokraniellen Venen der Vögel und Säugetiere. Ztschr. f. Anat. u. Entwicklungsgesch., vol. 74, pp. 432–508.

——— 1933. Venensystem, mit einem Anhang über den Dotter- und Plazentarkreislauf. *In* Bolk, Göppert, Kallius, and Lubosch, Handbuch der vergleichenden Anatomie der Wirbeltiere, vol. 6, chap. 6, pp. 685–744.

Gibbs, E. L., and F. A. Gibbs. 1934. The cross section areas of the vessels that form the torcular and the manner in which flow is distributed to the right and to the left lateral sinus. Anat. Rec., vol. 59, pp. 419–425.

Grant, J. C. B. 1951. An atlas of anatomy by regions. 3d ed. 503 pp. Baltimore.

Gray, H. 1954. (Ed. C. M. Goss.) Anatomy of the human body. 26th ed. 1480 pp. Philadelphia.

Greene, E. C. 1935. Anatomy of the rat. 370 pp. Philadelphia.

Grosser, O. 1901. Zur Anatomie und Entwickelungsgeschichte des Gefässystemes der Chiropteren. Anat. Hefte, vol. 17, pp. 203–424.

——— and E. Brezina. 1895. Ueber die Entwicklung der Venen des Kopfes und Halses bei Reptilien. Morphol. Jahrb., vol. 23, pp. 289–325.

Halpert, B. 1942. Situs inversus of the superior vena cava. Arch. Pathol., vol. 33, pp. 75–77.

——— and F. D. Coman. 1930. Complete situs inversus of the vena cava superior. Amer. Jour. Pathol., vol. 6, pp. 191–198.

Hamilton, W. J., J. D. Boyd, and H. W. Mossman. 1952. Human embryology. 2d ed. 432 pp. Baltimore.

Hartman, C. G., and W. L. Straus, Jr. (eds.). 1933. The anatomy of the rhesus monkey. 383 pp. Baltimore.

Hédon, C. E. 1888. Étude anatomique sur la circulation veineuse de l'encéphale. Thesis. 96 pp. Bordeaux.

Herren, R. Y., and L. Alexander. 1939. Sulcal and intrinsic blood vessels of the human spinal cord. Arch. Neurol. and Psychiat., vol. 41, pp. 678–687.

Hertwig, O. 1907. *In* Kollmann, Handatlas der Entwicklungsgeschichte des Menschen, vol. 1, figs. 262–264. Jena.

Hochstetter, F. 1938. Ueber eine Varietät der Vena cerebralis basialis des Menschen nebst Bemerkungen über die Entwicklung bestimmter Hirnvenen. Ztschr. f. Anat. u. Entwicklungsgesch., vol. 108, pp. 311–336.

Hofmann, M. 1901. Zur vergleichenden Anatomie der Gehirn- und Rücken-marksvenen der Vertebraten. Ztschr. f. Morphol. u. Anthropol., vol. 3, pp. 239–299.

Hughes, A. F. W. 1934. On the development of the blood vessels in the head of the chick. Phil. Trans. Roy. Soc. London, B, vol. 224, pp. 75–130.

Jones, F. Wood. 1912. On the grooves upon the ossa parietalia commonly said to be caused by the arteria meningea media. Jour. Anat. and Physiol., vol. 46, pp. 228–238.

Lewis, F. T. 1909. On the cervical veins and lymphatics in four human embryos, with an interpretation of anomalies of the subclavian and jugular veins in the adult. Amer. Jour. Anat., vol. 9, pp. 33–42.

Lewis, W. H. 1920. The cartilaginous skull of a human embryo 21 millimeters in length. Carnegie Inst. Wash. Pub. 272, Contrib. to Embryol., vol. 9, pp. 299–324.

Limson, M. 1932. Observations on the bones of the skull in white and negro fetuses and infants. Carnegie Inst. Wash. Pub. 433, Contrib. to Embryol., vol. 23, pp. 205–222.

Macklin, C. C. 1914. I. The skull of a human fetus of 40 mm. Amer. Jour. Anat., vol. 16, pp. 317–385. II, pp. 387–426.

——— 1921. The skull of a human fetus of 43 millimeters greatest length. Carnegie Inst. Wash. Pub. 273, Contrib. to Embryol., vol. 10, pp. 59–103.

Mall, F. P. 1904. On the development of the blood-vessels of the brain in the human embryo. Amer. Jour. Anat., vol. 4, pp. 1–18.

Mann, I. 1950. The development of the human eye. 2d ed. 312 pp. New York.

Markowski, J. 1911. Ueber die Entwicklung der Sinus durae matris und der Hirnvenen bei menschlichen Embryonen von 15.5–49 mm. Scheitel-Steisslänge. Bull. de l'acad. sci. de Cracovie, B, sci. nat., pp. 590–611.

——— 1922. Entwicklung der Sinus durae matris und der Hirnvenen des Menschen. Bull. internat. de l'acad. polonaise sci. et lettres, B, sci. nat., Cracovie, pp. 1–269.

McClure, C. F. W., and C. F. Silvester. 1909. A comparative study of the lymphatico-venous communications in adult mammals. Anat. Rec., vol. 3, pp. 534–552.

Mead, C. S. 1909. The chondrocranium of an embryo pig, *Sus scrofa;* a contribution to the morphology of the mammalian skull. Amer. Jour. Anat., vol. 9, pp. 167–209.

Miller, M. E. 1948. Guide to the dissection of the dog. 2d ed. 427 pp. Ithaca.

Mivart, St. G. 1895. The cat. An introduction to the study of backboned animals, especially mammals. 557 pp. New York.

Morris, Henry. 1953. (Ed. J. P. Schaeffer.) Human anatomy. 11th ed. 1718 pp. New York.

Padget, D. H. 1948. The development of the cranial arteries in the human embryo. Carnegie Inst. Wash. Pub. 575, Contrib. to Embryol., vol. 32, pp. 205–261.

——— 1954. Designation of the embryonic intersegmental arteries in reference to the vertebral artery and subclavian stem. Anat. Rec., vol. 119, pp. 349–356.

——— 1956. The cranial venous system in man in reference to development, adult configuration, and relation to the arteries. Amer. Jour. Anat., vol. 98, pp. 307–356.

Pfeifer, R. A. 1928. Die Angioarchitektonik der Grosshirnrinde. 157 pp. Berlin.

——— 1930. Grundlegende Untersuchungen für die Angioarchitektonik des menschlichen Gehirns. 220 pp. Berlin.

Sabin, F. R. 1917. Origin and development of the primitive vessels of the chick and of the pig. Carnegie Inst. Wash. Pub. 226, Contrib. to Embryol., vol. 6, pp. 61–124.

Scharrer, E. 1940. Arteries and veins in the mammalian brain. Anat. Rec., vol. 78, pp. 173–196.

Schlesinger, B. 1939. The venous drainage of the brain, with special reference to the Galenic system. Brain, vol. 62, pp. 274–291.

Schultz, A. H. 1921. Fetuses of the Guiana howling monkey. Zoologica (New York Zool. Soc.), vol. 3, pp. 243–262.

——— 1950. *In* W. K. Gregory (ed.), The anatomy of the gorilla. Morphological observations on gorillas. The studies of Henry Cushier Raven, Part 5, pp. 227–251. New York.

Shindo, T. 1915. Ueber die Bedeutung des Sinus cavernosus der Säuger mit vergleichend-anatomischer Berücksichtigung anderer Kopfvenen. Anat. Hefte, vol. 52, pp. 319–495.

Sisson, S. 1953. The anatomy of the domestic animals. 4th ed., rev. by J. D. Grossman. 972 pp. Philadelphia.

Solnitzky, O. 1940. The angioarchitecture of the cerebral cortex of *Macacus rhesus.* Anat. Rec., vol. 76, Suppl. 2, pp. 52–53.

Spalteholz, W. 1943. Hand-atlas of human anatomy. 7th ed. in English (figures clearer in earlier editions). 902 pp. Philadelphia.

Streeter, G. L. 1915. The development of the venous sinuses of the dura mater in the human embryo. Amer. Jour. Anat., vol. 18, pp. 145–178.

——— 1918. The developmental alterations in the vascular system of the brain of the human embryo. Carnegie Inst. Wash. Pub. 271, Contrib. to Embryol., vol. 8, pp. 5–38.

——— 1942. Developmental horizons in human embryos. Carnegie Inst. Wash. Pub. 541, Contrib. to Embryol., vol. 30, pp. 211–245. For subsequent articles on the Horizon series, see *ibid.,* 557 (1945), 575 (1948), 583 (1949), and 592 (1951); the whole series was reproduced in Embryology Reprint Volume II, 1951.

Streit, H. 1903. Ueber otologisch wichtige Anomalien der Hirnsinus, über accessorische Sinus und bedeutendere Venenverbindungen. Arch. f. Ohrenheilk., vol. 58, pp. 161–167.

Thyng, F. W. 1914. The anatomy of a 17.8 mm. human embryo. Amer. Jour. Anat., vol. 17, pp. 31–112.

Toldt, C. 1941. An atlas of human anatomy for students and physicians. 2 vols. 2d ed. 957 pp. New York.

Trolard, P. 1868. Recherches sur l'anatomie du système veineux de l'encéphale et du crâne. Thesis. 32 pp. Paris.

Walker, A. E. 1933. The attachments of the dura mater over the base of the skull. Anat. Rec., vol. 55, pp. 291–295.

Wolff, E. 1954. The anatomy of the eye and orbit, including the central connections, development, and comparative anatomy of the visual apparatus. 4th ed. 491 pp. New York.

LIST OF ABBREVIATIONS IN FIGURES

a., *aa.*, artery, arteries
anast., anastomosis, anastomotic
ant., anterior
aort., aorta, aortic
arach., arachnoid
audit., auditory
auric., *aur.*, auricular
ax., axillary
b., bone
bas., basal, basilar
basiocc., basioccipital
br., *brs.*, branch, branches; brachial
br.-ceph., brachiocephalic
brach., brachial
branch., branchial
Bresch., Breschet
caps., capsule
card., cardinal
carot., carotid
carot.-bas., caroticobasilar
cart., cartilage
cavern., *cav.*, cavernous
cec., cecum
cent., central
cephal., *ceph.*, cephalic
cereb., *cer.*, cerebral
cerebel., cerebellar
cerv., cervical
ch., channel
chondrocr., chondrocranium
chor., choroid
chord., chorda (tympani)
clav., clavicle
clin., clinoid
com., common
commun., communicating
condyl., condylar or condyloid
coron., coronary
Cuv., Cuvier
definit., definitive
dent., dentate
dienceph., *dien.*, diencephalon, diencephalic
dipl., diploic
dors., dorsal
duct. ven., ductus venosus
dur., dural
em., emissary
ethm., ethmoid
ext., external
fac., facial
for., foramen
form., formation
front., frontal
gass., *gasser.*, Gasserian (trigeminal)
gn., ganglion
gr., great
hemis., hemisphere
h.-c. ch., hepatocardiac channel (of Streeter)
hindbr., hindbrain
hyp., hypophysis
hypoglos., *hypogl.*, hypoglossal
inf., inferior
innom., innominate
int., interval
int.-vent., interventricular
intercost., intercostal
interped., interpeduncular
intersegm., intersegmental
jugul., *jug.*, jugular
jug.-ceph., jugulocephalic
junct., junction
L., left
lab., labial
lat., lateral
lig., ligament
ling., lingual
ling.-fac., linguofacial
mag., *magn.*, magnum
mam., mammilary
margin., *marg.*, marginal (sinus; vein of hand plate)
mast., mastoid
max., maxillary
med., medial
mening., *menin.*, *men.*, meningeal
mesenceph., *mesen.*, mesencephalon, mesencephalic
metenceph., *meten.*, *met.*, metencephalon, metencephalic
mid., middle
myelenceph., *myelen.*, myelencephalon, myelencephalic
n., nerve
nas., nasal
nasocil., nasociliary
noto., notochord
nucl., nucleus
obl., oblique
occas., occasional
occip., *occ.*, occipital
olf., olfactory
ophth., *oph.*, ophthalmic
oph.-mening., ophthalmomeningeal
opt., optic
orbit., *orb.*, orbital, orbitalis
ot., *oto.*, otic (pit), otocyst
oval., ovale
pariet., parietal
petros., *petr.*, petrosal
petrosquam., *petrosq.*, petrosquamosal
pharyng., pharyngeal
plex., *pl.*, plexus
plexif., plexiform
posit., position
post., posterior

postglen., postglenoid
prim., *pr.*, primary
primit., primitive
primord., primordial
proc., process
proot., pro-otic (sinus)
prosenceph., *prosen.*, prosencephalon, prosencephalic
pteryg., pterygoid
R., right
rect., rectus (muscle)
remn., remnant
rhinenceph., rhinencephalic
rhomben., rhombencephalon
rotund., rotundum
s., *sin.*, sinus
sagitt., *sag.*, sagittal
scap., scapular
second., secondary
sect., section
sept., septal
sigm., sigmoid
sin. venos., sinus venosus
som., somite
sph.-pal., sphenopalatine
sphenopariet., sphenoparietal
spur., spurious
st., stem
stap., *staped.*, stapedial
str., straight
subclav., *subcl.*, subclavian
subment., submental
sup., superior
supf., superficial
supraorb., supraorbital
telenceph., *telen.*, telencephalon, telencephalic
temp., temporal, temporalis
tentor., *tent.*, tentorial
term., terminal
thor., thoracic
thor.-epig., thoracoepigastric
thym.-thyr., thymicothyroid
thyr., thyroid (primordium)
torc., torcular (Herophili; confluence sinuses)
transv., *trans.*, transverse (lateral)
trib., tributary
trigem., trigeminal
tymp., tympanic, tympani
uln., ulnar
umb., umbilical
v., *vv.*, vein, veins
v. c., vena cava
var., variable
venos., venosus
vent., ventral
ventr., ventricle, ventricular
vert., vertebral
ves., *vesc.*, vesicle
Vesal., Vesalius

PLATES

Plate 1

The development of cranial venous channels as related to the growth of their environment. The numbering of the vascular stages[2] facilitates correlation with the arteries (Padget, 1948, pls. 1, 2); Roman numerals denote the horizons (age groups) of Streeter (1942–1951); crown-rump lengths are approximate.

Fig. 19. Stage (1 and) 2, xiv, 5 to 8 mm. The walls of the neural tube, covered by a continuous plexus (not shown), drain dorsolaterally into a superficial (primitive dural) plexus, which empties through three (dural) stems into a head-sinus continuous with the anterior cardinal vein. The mandibular and hyoid pharyngeal bars are drained by a ventral pharyngeal vein; the emerging maxillary process, by a maxillary (infraorbital) vein.

Fig. 20. Stage 3, xvi, 8 to 11 mm. The head-sinus remains medial to the trigeminal ganglion, but is migrating lateral to cranial nerves 7 to 10. A remnant of the medial channel is part of a myelencephalic vein; this and a diencephalic vein are the first pia-arachnoidal veins. The ventral pharyngeal vein enters the primitive internal jugular at the junction of the 10th and 12th nerves. The maxillary vein drains both optic and olfactory regions. A marginal vein of the hand plate empties into the primitive subclavian vein.

Fig. 21. Stage 4, xvii, 11 to 14 mm. Having completed its migration lateral to the 12th nerve, in which the ventral pharyngeal vein shares, the anterior cardinal vein has the position of the adult internal jugular vein. The cervical intersegmental veins are uniting to form the vertebral vein. Each subdivision of the brain is drained laterally into the dural plexuses by at least one primitive pia-arachnoidal vein, as designated. Note the primitive supraorbital vein and its relation to the junction of the 4th and 5th nerves.

Fig. 22. Stage 5, xix, 17 to 20 mm. As the pharyngeal bars differentiate and their nerves develop, a channel between the middle and posterior dural plexuses forms the sigmoid sinus; accordingly, the head-sinus dwindles ventral to the labyrinth. Lateral tributaries of the maxillary and linguofacial veins drain the maxilla and mandible, respectively. Components of the anterior dural plexus, the marginal and tentorial sinuses, border the expanding hemisphere caudally. A jugulocephalic vein, derived from the primitive subclavian vein, arches over the primordial clavicle (*x*) and receives a vein from the radial border of the arm.

Fig. 23. Stage 6, xxi, 22 to 24 mm. The supraorbital vein no longer drains into the anterior dural stem, which has dwindled; it is continuous, by way of the head-sinus, with the pro-otic sinus (middle dural stem; note the reversal of its flow), which empties into the new sigmoid sinus (incorporating the posterior dural stem). After anastomosis of its lateral tributaries with the new anterior facial vein (lateral tributary of linguofacial vein), the stem of the maxillary vein is attenuated. A secondary left innominate vein unites the internal jugulars. An anastomosis involving the jugulocephalic vein forms the definitive subclavian vein, from which the external jugular vein arises. Cerebral growth has elongated the tentorial sinus draining the superficial middle cerebral veins. The shifting marginal sinus constitutes the medial end of the primitive transverse sinus. Drainage of the choroid plexus of the lateral ventricle is primarily by the ventral diencephalic vein, supplemented later by the primitive internal cerebral vein. Note the consolidation of the anterior and middle dural plexuses into a tentorial plexus (future torcular).

Fig. 24. Stage 7, 40 mm. Plexiform elements of the newly developing cavernous sinus are medial extensions of the pro-otic sinus. They are continuous with the new inferior petrosal sinus, a similar extension of the ventral myelencephalic vein, which joins the internal jugular below its foramen. The primary maxillary vein is no longer recognizable, because its trunk, after anastomosis with the supraorbital vein, has become the stem of all the veins of the orbit. A lateral tributary of the pro-otic sinus, which primarily receives the middle meningeal sinuses, anastomoses (through the spurious jugular foramen) with a primitive temporal emissary tributary of the sigmoid sinus to form the petrosquamosal sinus. An anastomosis between the external jugular and common facial veins constitutes the posterior facial vein. The primitive emissary veins near the skull base primarily drain medially into the sinuses; later they anastomose with the external jugular system.

Fig. 25. Stage 7*a*, 60 to 80 mm. Cerebral growth and expansion of the otic capsule are responsible for a new superior petrosal sinus, which is the dural (tentorial) end of the ventral metencephalic (great anterior cerebellar) vein. The primitive transverse sinus has been swung backward on the sigmoid sinus, and receives the elongated tentorial sinus continuous with the superficial middle cerebral veins. Being primarily the drainage of the superior choroid vein, the internal cerebral vein is still primitive; it receives only one intracerebral (anterior thalamic) tributary. The basal cerebral vein is formed by longitudinal pial anastomoses between several primitive veins: the telencephalic (deep middle or anterior cerebral), the ventral and dorsal diencephalic, the mesencephalic, and ventral metencephalic veins, and a caudal diencephalic tributary of the primitive internal cerebral vein; anastomosing the new basal vein with the ventral metencephalic (great anterior cerebellar) vein, the lateral mesencephalic vein is a potential lateral outlet of the basal (and internal) cerebral vein by way of the superior petrosal sinus. The pro-otic sinus is continuous with the definitive petrosquamosal sinus.

Fig. 26. Adult pattern (shown in an infant head). Between the fetus of the 3d month and term, secondary intracerebral tributaries of the internal cerebral vein supplement similar primary components of the basal cerebral vein, completed earlier; included are superior striate tributaries of the terminal vein, formed by extraventricular vessels that are secondarily enclosed in the floor of the ventricle. In the development of the superficial cerebral groups of veins, the superior and posteroinferior emerge considerably later than does the primary middle cerebral group. The petrosquamosal sinus and the tributaries of the pro-otic sinus primarily drain the dura and bone. They become diploic in adult life, when the middle meningeal sinuses drain secondarily through the foramen ovale and into the superior sagittal sinus. Remnants of the tentorial sinus, frequently persistent, may be involved in two late anastomoses (arrows) that unite the cavernous sinus cranially with the middle cerebral veins, and caudally with the superior petrosal sinus.

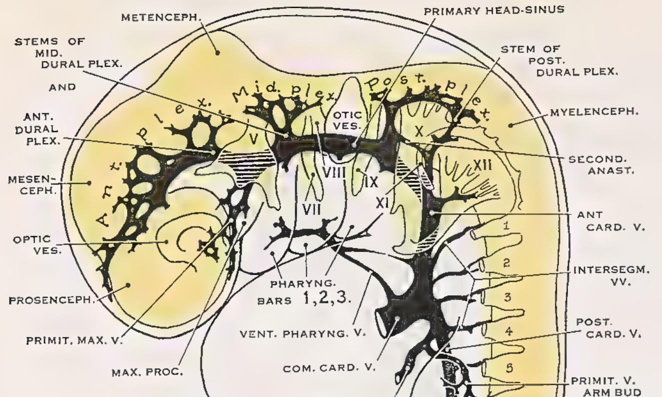

19. 5MM.

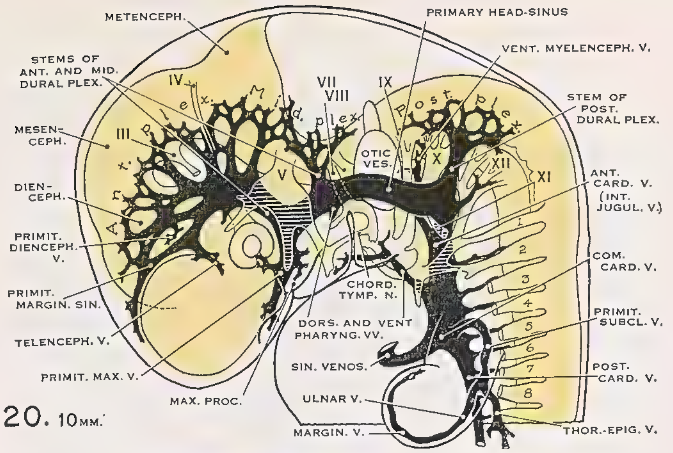

20. 10MM.

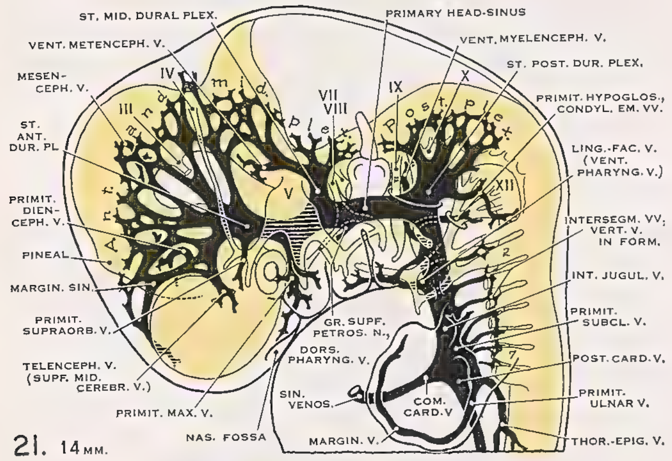

21. 14MM.

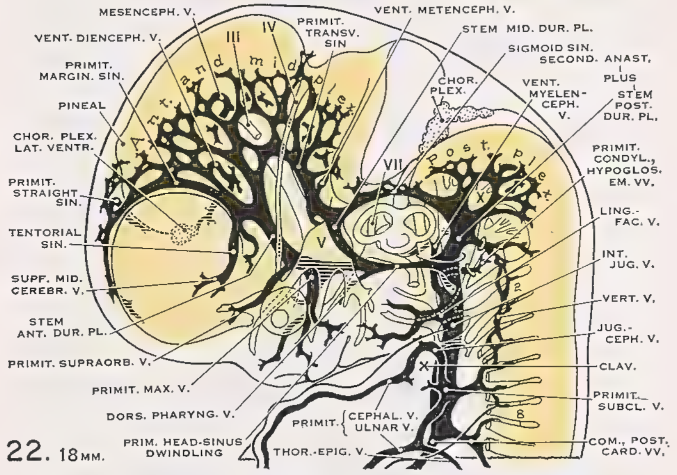

22. 18MM.

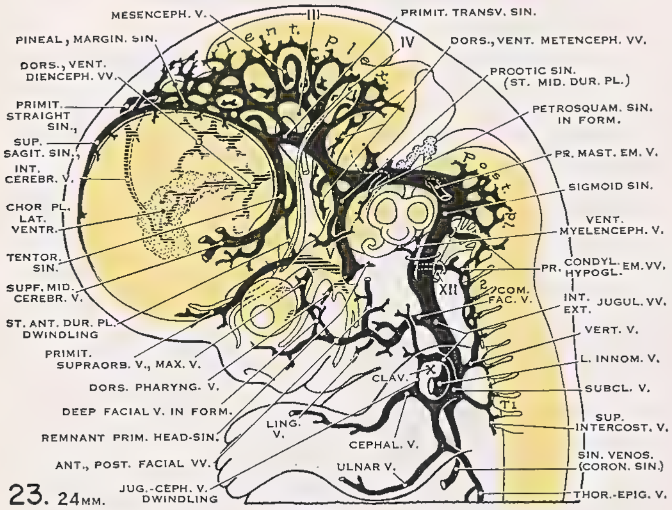

23. 24MM.

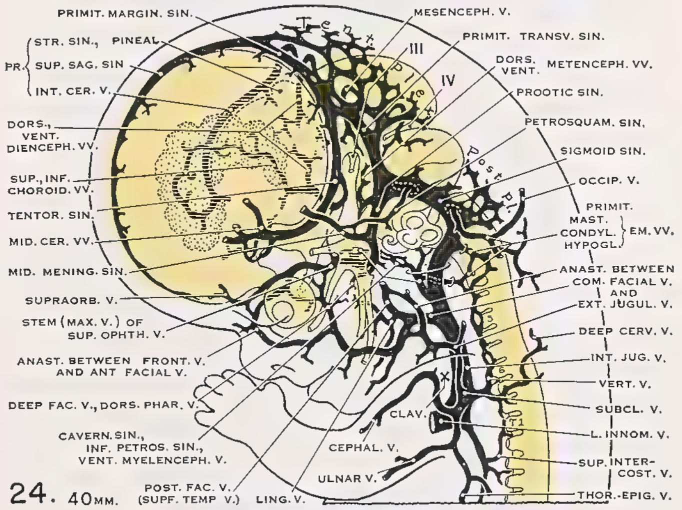

24. 40MM.

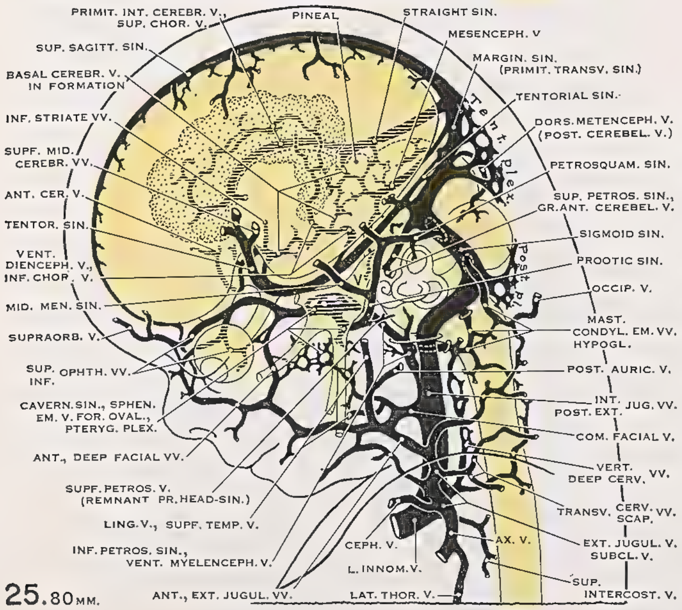

25. 80MM.

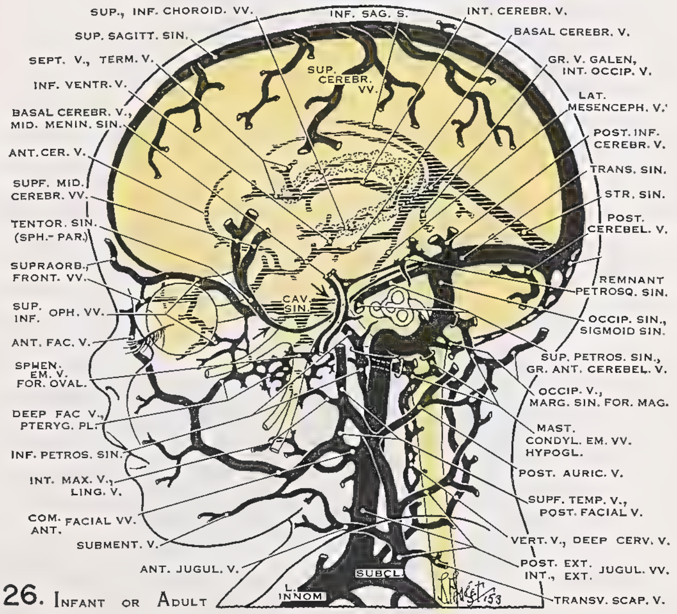

26. INFANT OR ADULT

These figures, to be correlated with those of plate 1, also show intermediate stages. Figures 27 to 35 are venous channels at the base of the brain as viewed from below.

FIG. 27. Stage (1 and) 2, xiv, 5 to 8 mm. The primary head-sinus is medial to the 5th and 10th nerves, but has migrated laterally to the 7th to 9th nerves and the otic vesicle. Its dorsal tributaries are the three dural stems of the superficial plexuses draining the neural tube dorsolaterally. Ventrally, a maxillary tributary drains the optic and olfactory regions. A ventral pharyngeal vein joins the anterior cardinal vein.

FIG. 28. Stage 3, xvi, 8 to 11 mm. With differentiation of the telencephalon and diencephalon, two veins draining these regions emerge; they join the anterior dural plexus, in the fore part of which is the primitive marginal sinus bordering the cerebral hemisphere. The head-sinus has begun to migrate laterally to the 10th nerve.

FIG. 29. Stage 4, xvii, 11 to 14 mm. Although the head-sinus is now essentially lateral to the 10th nerve, its former medial position is represented by the stem of a ventral myelencephalic vein. Voluminous tributaries of the maxillary vein include the primitive central vein of the retina. Note the primitive supraorbital vein.

FIG. 30. Stage 4, xviii, 14 to 16 mm. At least one vein identified from each subdivision of the primitive brain traverses the primitive arachnoid to join components of the dural plexuses. Longitudinal (and later transverse) anastomoses between the distal ends of these veins form the pial venous net and veins, which are subjacent to the arteries. A dorsal pharyngeal vein accompanies the great superficial petrosal nerve.

FIG. 31. A, B (in developmental sequence). Stage 5, xix, 17 to 20 mm. Note the venous asymmetry. On the embryo's left (A), the secondary anastomosis (between the middle and posterior dural stems) that forms the sigmoid sinus is less advanced than that on the right side (B); thus, the left head-sinus, which the new channel supersedes, has dwindled less than the right. Drainage from the mid-line, in the region of the superior sagittal and transverse sinuses, passes predominately to the right (B) by way of the marginal sinus. The primitive straight sinus also passes to the right. The ventral pharyngeal vein (shown on the left only) is now a definitive linguofacial vein; its lateral tributaries will anastomose with those of the maxillary vein.

FIG. 32. A, B (in developmental sequence). Stage 6, xxi, 22 to 24 mm. Asymmetry of drainage from mid-line channels is again evident, so that the lateral choroid plexus drains mostly to the right through the primitive straight sinus (B). The middle dural stem, now the pro-otic sinus, becomes the direct continuation of the primitive supraorbital vein. The anterior dural stem has dwindled, more on the right, resulting in dorsal drainage of the middle cerebral veins into the primitive transverse sinus. Anastomosis between the linguofacial and maxillary veins (shown on the left only) forms the anterior facial vein, which annexes lateral tributaries of the dwindling maxillary vein.

FIG. 33. Stage 7, 40 mm. Plexiform extensions of the pro-otic sinus and of the dural end of the myelencephalic vein, respectively, are the cavernous and inferior petrosal sinuses. The primary condyloid and mastoid emissary veins drain medially into the sigmoid sinus before their anastomosis with the external jugular system. The pro-otic sinus has two tributaries: the ventral metencephalic vein, to constitute the superior petrosal sinus; and the primitive middle meningeal sinus, draining the membrane bones. Including anterior and deep cerebral (pial) tributaries, the superficial middle cerebral veins are still directly continuous with the tentorial sinus, which is elongated by the expanding hemisphere, and joins the primitive transverse sinus.

FIG. 34. Stage 7*a*, 60 mm. A longitudinal anastomosis between the deep telen-, dien-, and mesen-cephalic veins constitutes the major part of the basal cerebral vein. A similar anastomosis between the diencephalic and metencephalic veins becomes a significant lateral mesencephalic vein. The stem of the ventral metencephalic (anterior cerebellar) vein becomes the superior petrosal sinus. Becoming plexiform and dwindling, the caudal end of the tentorial sinus is shifted toward the sigmoid sinus.

FIG. 35. The postnatal pattern. Parts of the left temporal lobe are cut away to show the basal cerebral vein. Note these tributaries: the variable anterior cerebral vein; the inferior striate veins; the interpeduncular vein from the posterior perforated area; the inferior ventricular vein with tributaries from the ventricular walls, including an inferior choroid vein; the lateral mesencephalic vein—an anastomosis with the great anterior cerebellar vein. The superficial middle cerebral veins drain through the remnant of the tentorial sinus (sometimes a superficial vein) or, secondarily, into the cavernous sinus. Note the internal occipital vein from the visual cortex, and the posterior cerebellar veins, emptying into a tentorial lacuna before reaching the transverse sinus.

Venous channels at the base of the chondrocranium (figs. 36, 37) and skull (figs. 38, 39) as viewed from above

FIG. 36. Stage 7*a*, 60 mm. The orbito-ophthalmic veins drain laterally through the primary pro-otic sinus, and medially through the cavernous and inferior petrosal sinuses, both secondary. The tentorial sinus, constituting the only drainage of the primitive middle cerebral veins, may follow the edge of the lesser sphenoid wing. Tributaries of the primitive superior petrosal sinus (end of the metencephalic vein) may annex those of the myelencephalic vein, whose stem is the caudal end of the inferior petrosal sinus. Between the primitive temporal emissary vein (of the spurious jugular foramen) and the dural meningeal tributary of the pro-otic sinus is the anastomosis constituting the petrosquamosal sinus.

FIG. 37. Stage 7*a*, 80 mm. The definitive superior petrosal sinus surmounts the enlarged otic capsule. Lying between this cartilage and the parietal (and temporal) bone, the petrosquamosal sinus becomes continuous with the pro-otic sinus, which is dwindling, since it is no longer the exclusive outlet of the orbito-ophthalmic veins. Although cranially anastomosed with the anterior facial vein, the orbital veins drain caudally into the new cavernous sinus continuous with the inferior petrosal sinus.

FIG. 38. Typical infant at birth. The cavernous and inferior petrosal sinuses, the new caudal outlet of the orbital veins, do not communicate with the middle cerebral veins, which drain, instead, through the tentorial sinus, which has a variable position. Veins of the posterior fossa, only, are drained by the superior petrosal sinus; it is not connected with the cavernous sinus. Since the middle meningeal sinuses are superficial to the artery, they look like two "veins" bordering it. The persistent petrosquamosal sinus may be connected with deep temporal veins by way of a temporal emissary vein. The marginal sinus of the foramen magnum is the remnant of the posterior dural plexus.

FIG. 39. Typical adult. Note the secondary anastomoses (arrows) between the cavernous sinus and (1) the tentorial sinus, which may lie in the position of the sphenoparietal sinus, and drains the superficial middle cerebral veins, and (2) the superior petrosal sinus, the dural continuation of the great anterior cerebellar vein; when the tentorial sinus is located more laterally, such anastomoses are less likely to occur. Extending below the mandibular nerve root, the typical lateral wing of the cavernous sinus is a remnant of the pro-otic sinus, continuous with the emissary veins of the foramen ovale. The ophthalmomeningeal sinus accompanies the artery of the same name, a primary anastomosis (variable) between the ophthalmic and middle meningeal arteries. Having become diploic, the petrosquamosal sinus receives superior tympanic veins. The head-sinus is represented by the superficial petrosal vein, which accompanies the nerve of the same name.

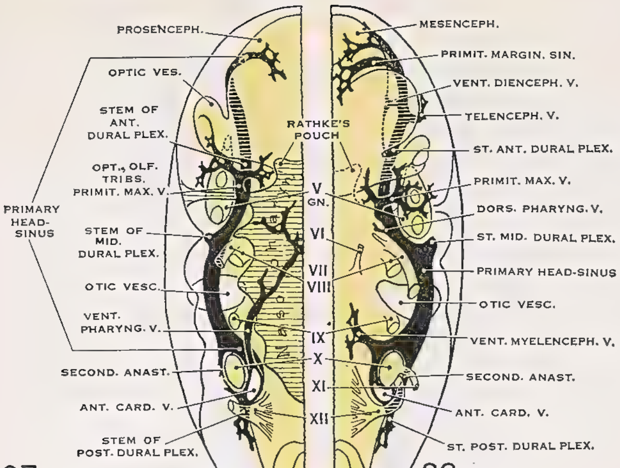

27. 5mm. 28. 10mm.

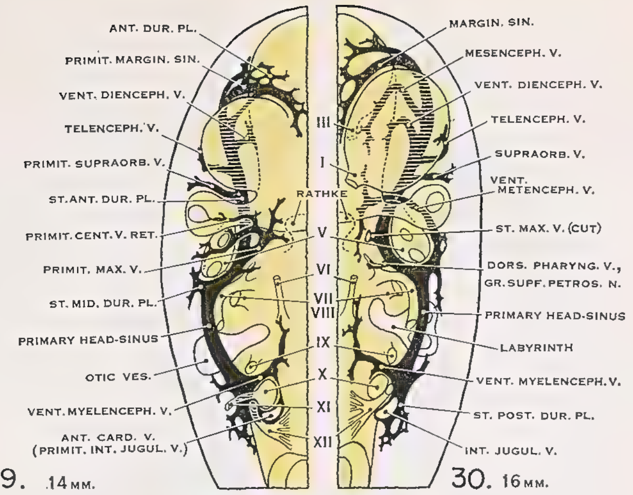

29. 14mm. 30. 16mm.

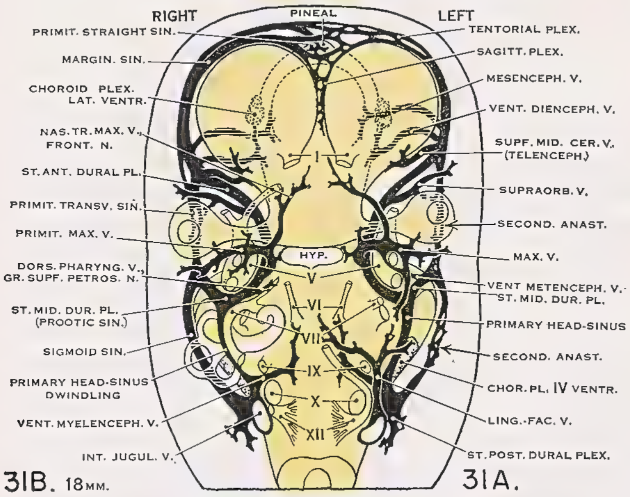

31B. 18mm. 31A.

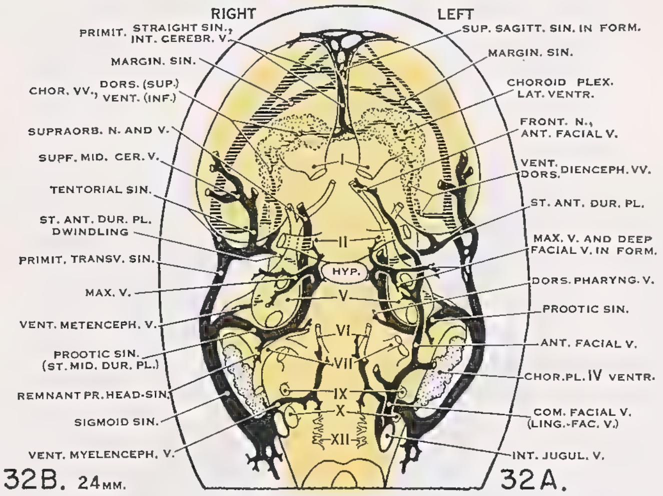
RIGHT
LEFT
PRIMIT. STRAIGHT SIN., INT. CEREBR. V.
MARGIN. SIN.
CHOR. VV., DORS. (SUP.) VENT. (INF.)
SUPRAORB. N. AND V.
SUPF. MID. CER. V.
TENTORIAL SIN.
ST. ANT. DUR. PL. DWINDLING
PRIMIT. TRANSV. SIN.
MAX. V.
VENT. METENCEPH. V.
PROOTIC SIN. (ST. MID. DUR. PL.)
REMNANT PR. HEAD-SIN.
SIGMOID SIN.
VENT. MYELENCEPH. V.
I
II
HYP.
V
VI
VII
IX
X
XII
SUP. SAGITT. SIN. IN FORM.
MARGIN. SIN.
CHOROID PLEX. LAT. VENTR.
FRONT. N., ANT. FACIAL V.
VENT. DORS. DIENCEPH. VV.
ST. ANT. DUR. PL.
MAX. V. AND DEEP FACIAL V. IN FORM.
DORS. PHARYNG. V.
PROOTIC SIN.
ANT. FACIAL V.
CHOR. PL. IV VENTR.
COM. FACIAL V. (LING.-FAC. V.)
INT. JUGUL. V.

32B. 24mm. 32A.

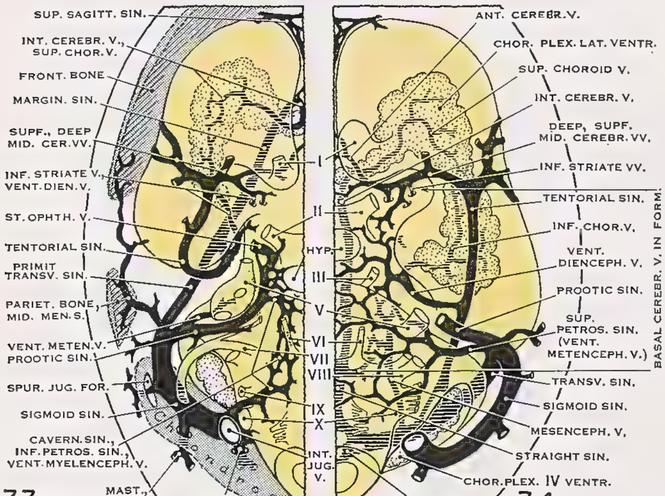

33. 40mm. 34. 60mm.

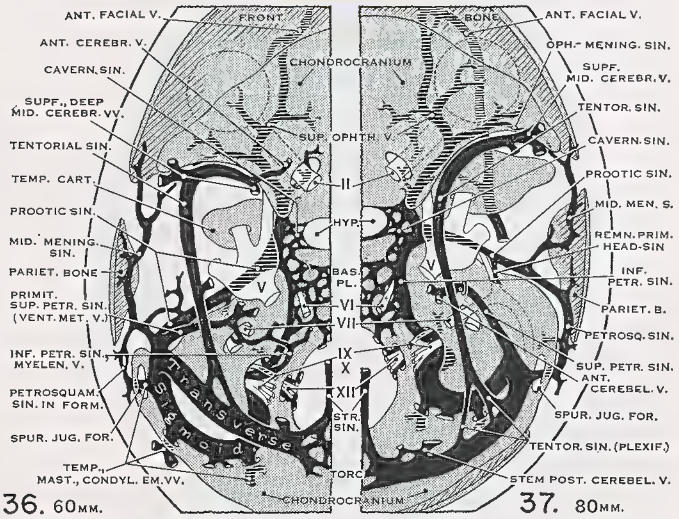

36. 60mm. 37. 80mm.

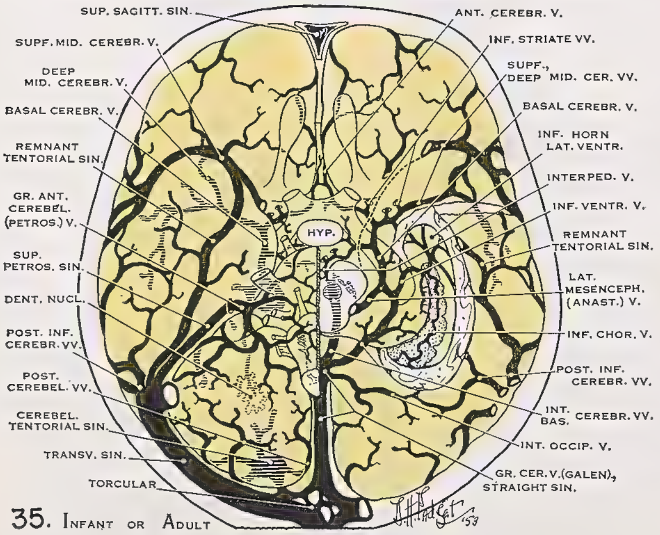

35. Infant or Adult

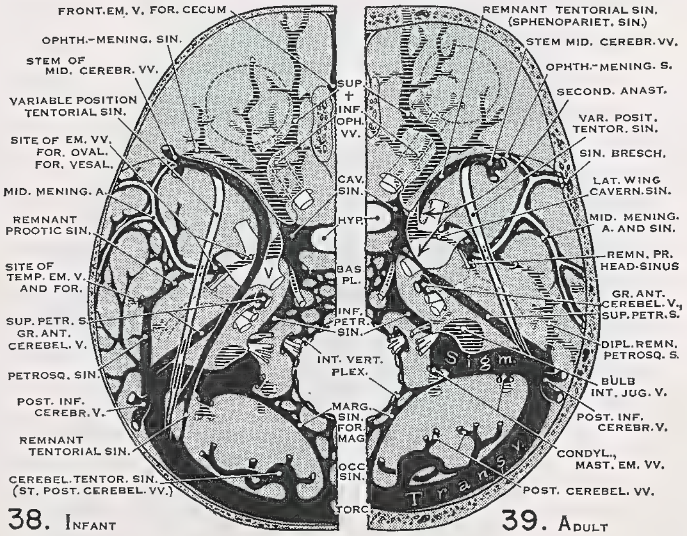

38. Infant 39. Adult

PLATE 3

Coronal reconstructions of six embryos of six stages viewed from in front: A, embryo Carnegie no. 2841, 5.3 mm., xiv, stage 2; B, no. 1121, 11.8 mm., xvi, stage 3; C, no. 1771, 12.5 mm., xvii, stage 4; D, no 492, 16.8 mm., xviii, borderline stages 4, 5; E, no. 966, 23 mm., xx, stage 6; F, no. 886, 43 mm., stage 7. A is twice the magnification of B, C, D, and E; F is one-fifth the magnification of A.

Note the secondary development of venous asymmetry above the heart. The cardiac sinus venosus, initially short and wide, shifts flow from the left side of the head into the right primitive atrium (A). By the next stage (B), this sinus is attenuated, curved, and elongated, thus constituting a substantial detour, reflected in the drainage of the primitive sagittal and straight sinuses to the right side predominantly. About horizon xx (D), a secondary plexus of thymicothyroid veins, surmounting the aortic arch, connects the bilateral internal jugulars (anterior cardinals). When a channel in this plexus is elaborated into the left innominate vein (E), the temporary detour is overcome, or lessened to an extent that varies, depending on the ultimate relative length and direction of the two innominates (F); in adult mammals generally, unlike man, typifying certain anthropoids, the secondary vein on the left becomes essentially symmetrical with the primary one on the right, which is merely a component of the anterior cardinal (internal jugular) vein (cf. pl. 6, inserts).

These figures also show certain stages in the development of the following vessels: the basilar sinus (D), medial anastomosing extensions of each inferior petrosal sinus (F), a plexiform derivative of the dural stem of the ventral myelencephalic vein (B–D); the intercavernous sinuses, similar extensions of each cavernous sinus, derived from the pro-otic sinus (F); the common facial vein [it is primarily an internal jugular tributary (E, left side of embryo) that represents the earlier linguofacial vein (B–D) and, before that, the ventral pharyngeal vein (A)], sometimes annexed by the external jugular vein (E, right side of embryo); the secondary anastomosis between the primitive subclavian and jugulocephalic veins (E) that defines the adult subclavian vein with its cephalic (and ulnar) tributary (F); the emergence of the external jugular vein (F) as a cranial extension of the jugulocephalic vein, which incorporates its proximal end (D, E).

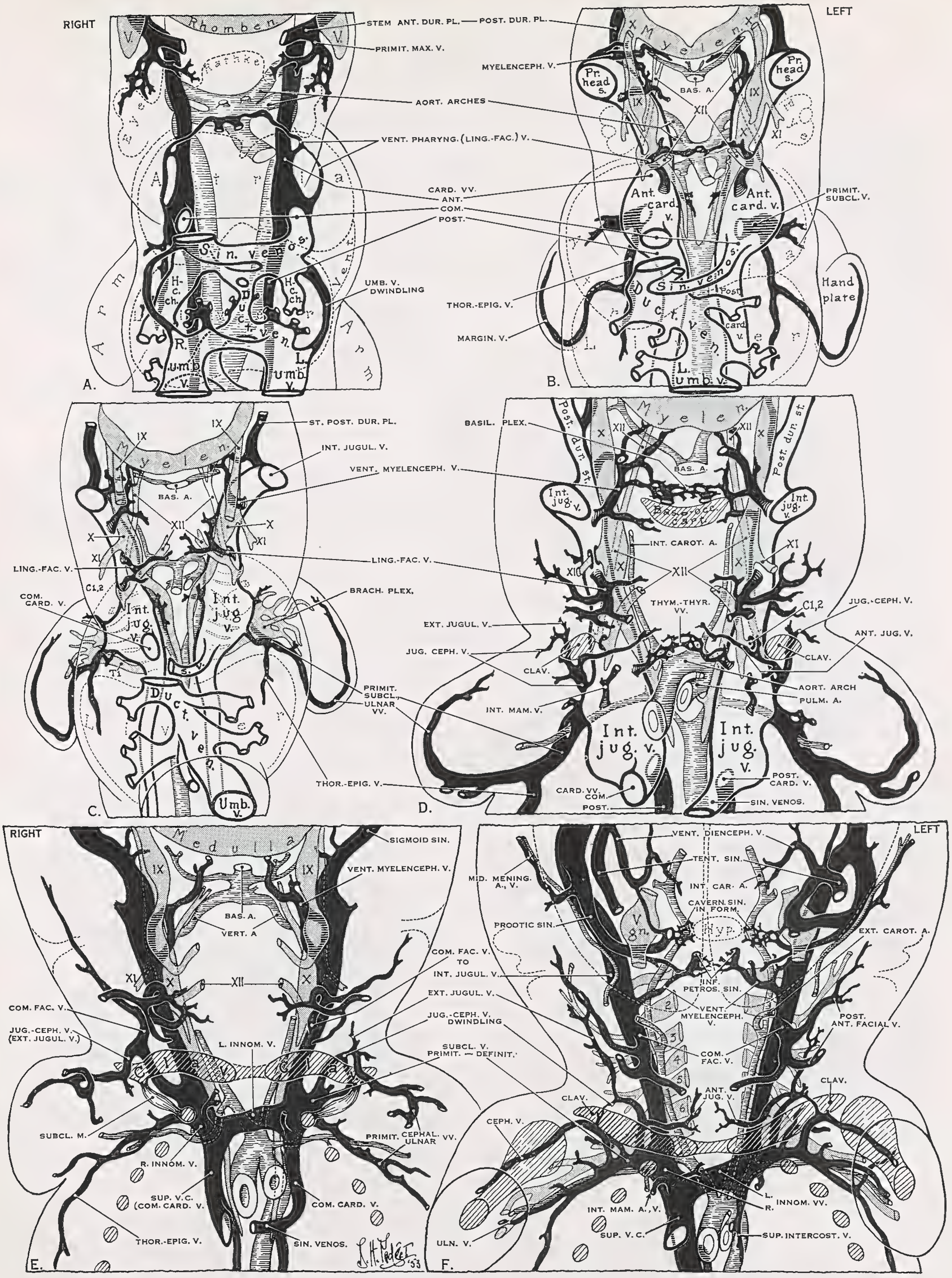
RIGHT
LEFT
Rhomben
Rathke
Eye
Arm
Atria
Sin. venos.
H. c. ch.
Duct. ven.
R. umb. v.
L. umb. v.
STEM ANT. DUR. PL.
POST. DUR. PL.
PRIMIT. MAX. V.
MYELENCEPH. V.
AORT. ARCHES
VENT. PHARYNG. (LING.-FAC.) V.
CARD. VV.
ANT.
COM.
POST.
UMB. V. DWINDLING
THOR.-EPIG. V.
MARGIN. V.
PRIMIT. SUBCL. V.
Myelen.
Pr. head s.
BAS. A.
IX
X
XI
XII
Ant. card. v.
Post. card. v.
Hand plate
A.
B.
ST. POST. DUR. PL.
INT. JUGUL. V.
VENT. MYELENCEPH. V.
LING.-FAC. V.
COM. CARD. V.
C1,2
Int. jug. v.
BRACH. PLEX.
PRIMIT. SUBCL. ULNAR VV.
Umb. v.
C.
BASIL. PLEX.
Post. dur. st.
Basi-occ. cart.
INT. CAROT. A.
THYM.-THYR. VV.
EXT. JUGUL. V.
JUG. CEPH. V.
JUG.-CEPH. V.
ANT. JUG. V.
CLAV.
AORT. ARCH
PULM. A.
INT. MAM. V.
CARD. VV. COM. POST.
POST. CARD. V.
SIN. VENOS.
D.
Medulla
SIGMOID SIN.
VERT. A
COM. FAC. V. TO INT. JUGUL. V.
COM. FAC. V.
JUG.-CEPH. V. (EXT. JUGUL. V.)
JUG.-CEPH. V. DWINDLING
L. INNOM. V.
SUBCL. V. PRIMIT. — DEFINIT.
SUBCL. M.
R. INNOM. V.
SUP. V.C. (COM. CARD. V.)
PRIMIT. CEPHAL. ULNAR VV.
COM. CARD. V.
THOR.-EPIG. V.
E.
D. H. Padget '53
VENT. DIENCEPH. V.
TENT. SIN.
MID. MENING. A., V.
INT. CAR. A.
CAVERN. SIN. IN FORM.
PROOTIC SIN.
V gn.
Hyp.
EXT. CAROT. A.
INF. PETROS. SIN.
VENT. MYELENCEPH. V.
POST. ANT. FACIAL V.
COM. FAC. V.
ANT. JUG. V.
CEPH. V.
L. R. INNOM. VV.
INT. MAM. A., V.
SUP. V.C.
SUP. INTERCOST. V.
ULN. V.
F.

PLATE 4

Graphic reconstructions of vessels related to the chondrocranium as viewed from above in two embryos of stages 7 and *7a:* A1, Carnegie no. 886, 40 mm., stage 7 (right side reversed); B, left side of no. 613, 80 mm., stage *7a;* A2, base of the brain of the younger embryo (no. 886; lesser magnification). The cavernous sinus constitutes medial and plexiform derivatives of the pro-otic sinus that surround the internal carotid artery (A1, B). The inferior petrosal sinus is a similar extension derived caudally from the dural end of the ventral myelencephalic vein. As the otic capsule expands, the pro-otic sinus (A) dwindles (B); its former exclusive drainage of the orbito-ophthalmic veins (A1) is being annexed by the new inferior petrosal sinus. Otic expansion also leads to the definitive appearance of the new superior petrosal sinus (B), which essentially constitutes the stem of the primary ventral metencephalic vein (A1). The formation of the petrosquamosal sinus begins with an anastomosis joining the primitive temporal emissary vein of the spurious jugular foramen (A1) with a tributary of the pro-otic sinus. By the time it becomes definitive in lying between the expanding parietal (and squamous temporal) bone and the otic capsule (B), the petrosquamosal sinus has annexed the caudal end of the pro-otic sinus. Note that the only part of the adult middle fossa represented in the chondrocranium is the temporal wing. Thus, the pro-otic sinus and its tributaries, including the middle meningeal sinus, are primarily extracranial. By the 80-mm. stage (B), the tentorium has been swung caudally and lies in approximate adult position. Within it, the elongated tentorial sinus still drains the prominent superficial cerebral veins (A2); its attenuated caudal end has begun to migrate along the transverse sinus toward the cranial end of the sigmoid sinus (B).

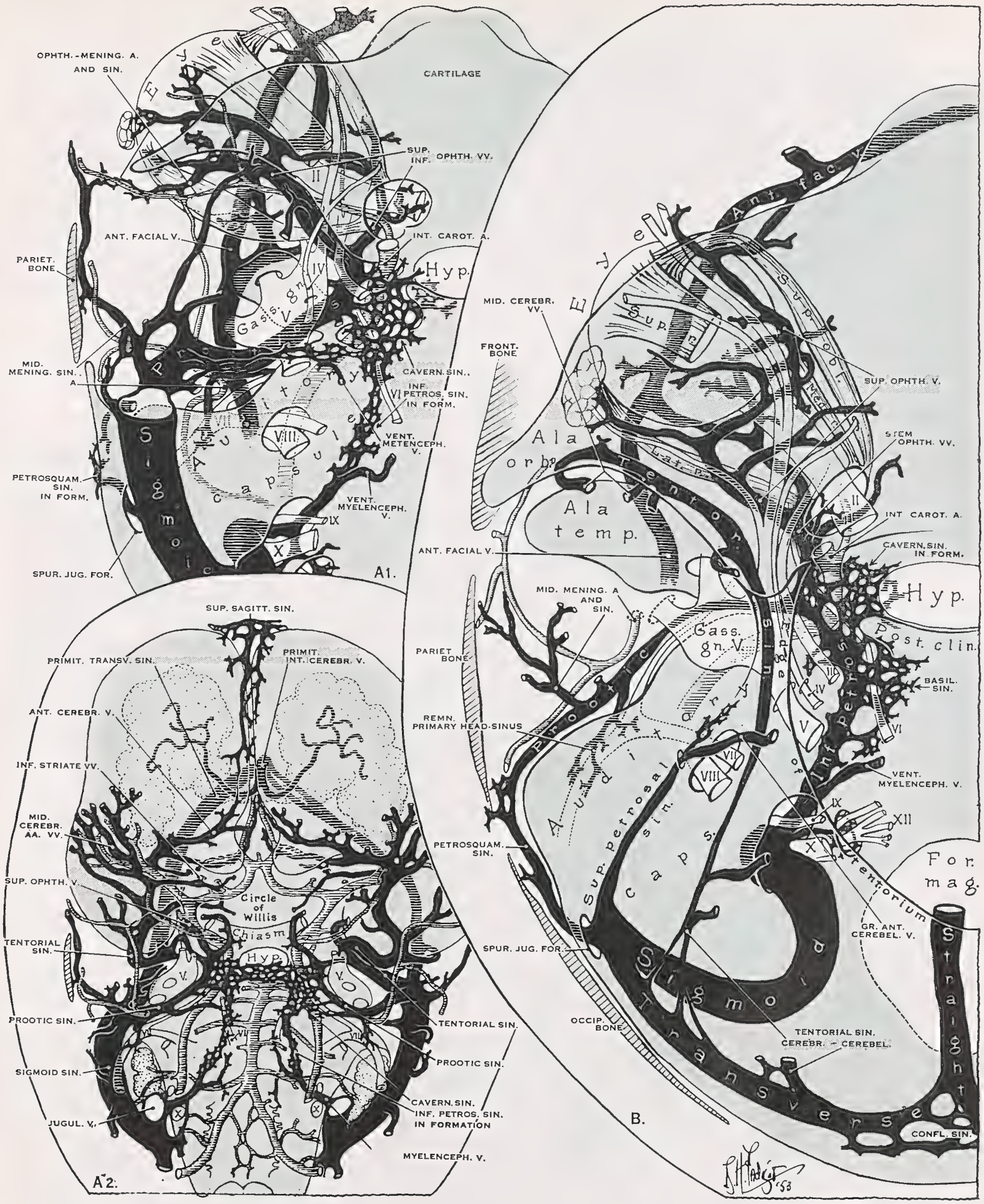
OPHTH.-MENING. A. AND SIN.
Eye
CARTILAGE
SUP. INF. OPHTH. VV.
II
III
IV
INT. CAROT. A.
Hyp.
ANT. FACIAL V.
PARIET. BONE
Gass. gn. V
MID. MENING. SIN.
A.
Prootic sin.
Auditory capsule
CAVERN. SIN.
INF. PETROS. SIN. IN FORM.
VI
VII
VIII
VENT. METENCEPH. V.
PETROSQUAM. SIN. IN FORM.
Sigmoid
VENT. MYELENCEPH. V.
IX
X
SPUR. JUG. FOR.
A1.
SUP. SAGITT. SIN.
PRIMIT. TRANSV. SIN.
PRIMIT. INT. CEREBR. V.
ANT. CEREBR. V.
INF. STRIATE VV.
MID. CEREBR. AA. VV.
SUP. OPHTH. V.
Circle of Willis
Chiasm
Hyp.
TENTORIAL SIN.
V.
PROOTIC SIN.
VII
SIGMOID SIN.
JUGUL. V.
X
TENTORIAL SIN.
PROOTIC SIN.
CAVERN. SIN.
INF. PETROS. SIN. IN FORMATION
MYELENCEPH. V.
A2.
MID. CEREBR. VV.
FRONT. BONE
Ala orb.
Ala temp.
Eye
Ant. fac. v.
Sup. obl.
Sup.
Med.
Lat. r.
SUP. OPHTH. V.
STEM OPHTH. VV.
Tentor.
II
INT. CAROT. A.
CAVERN. SIN. IN FORM.
Hyp.
ANT. FACIAL V.
MID. MENING. A AND SIN.
Gass. gn. V
Post. clin.
PARIET. BONE
Prootic
Tentor. sin.
Edge of
Inf. petros.
III
IV
V
BASIL. SIN.
VI
REMN. PRIMARY HEAD-SINUS
Auditory caps.
Sup. petrosal sin.
VII
VIII
VENT. MYELENCEPH. V.
IX
XII
X
PETROSQUAM. SIN.
For. mag.
tentorium
GR. ANT. CEREBEL. V.
SPUR. JUG. FOR.
Sigmoid
Straight
OCCIP. BONE
Transverse
TENTORIAL SIN. CEREBR. - CEREBEL.
CONFL. SIN.
B.
D.H. Padget '53

PLATE 5

Lateral reconstructions of three early fetuses to show the emergence of the postnatal configuration in stage *7a:* A, Carnegie no. 4193, 48.5 mm.; B, no. 234a, 80 mm., is more advanced than C1, no. 613, 80 mm. The primitive transverse sinus, bordering the margin of the expanding cerebral hemisphere, is pushed caudally into definitive position. Meanwhile, the tentorial sinus, previously elongated by cerebral expansion and initially joined to the torcular region (tentorial plexus, A), begins to migrate by anastomotic progression along the transverse sinus (B, C1). As the caudal end of the tentorial sinus thus dwindles and becomes plexiform, its once exclusive drainage of the superficial middle cerebral veins and their derivatives (A, B) is supplemented by the formation of a new basal cerebral vein (C1). This vein emerges as a longitudinal anastomosis between several of the primitive transverse veins, particularly the telen-, dien-, and mesen-cephalic (cf. fig. 16), whose stems subsequently dwindle; note such a remnant of the ventral diencephalic vein (C1). The lateral mesencephalic (anastomotic) vein, a similar anastomosis between the mesen- and meten-cephalic veins, connects the basal cerebral (and internal cerebral) vein with the great anterior cerebellar vein, the dural end of which becomes the superior petrosal sinus (C1). After the pro-otic sinus is annexed by the petrosquamosal sinus, its caudal end becomes that of the superior petrosal sinus (cf. A, B).

Insert C2 is a detail in the region of the left cavernous sinus (C1) viewed from the front. Note the dwindling pro-otic sinus, the medial end of which is typically retained as the lateral wing of the cavernous sinus, a lateral extension draining the emissary veins in the foramen ovale, which are initially represented by the dorsal pharyngeal vein (cf. fig. 15). The only cranial remnant of the primary head-sinus of early stages is the cranial end of the pro-otic sinus it constitutes, from which the cavernous sinus is derived; the only caudal remnant, small and plexiform, follows the 7th nerve (C1), and drains the middle ear region.

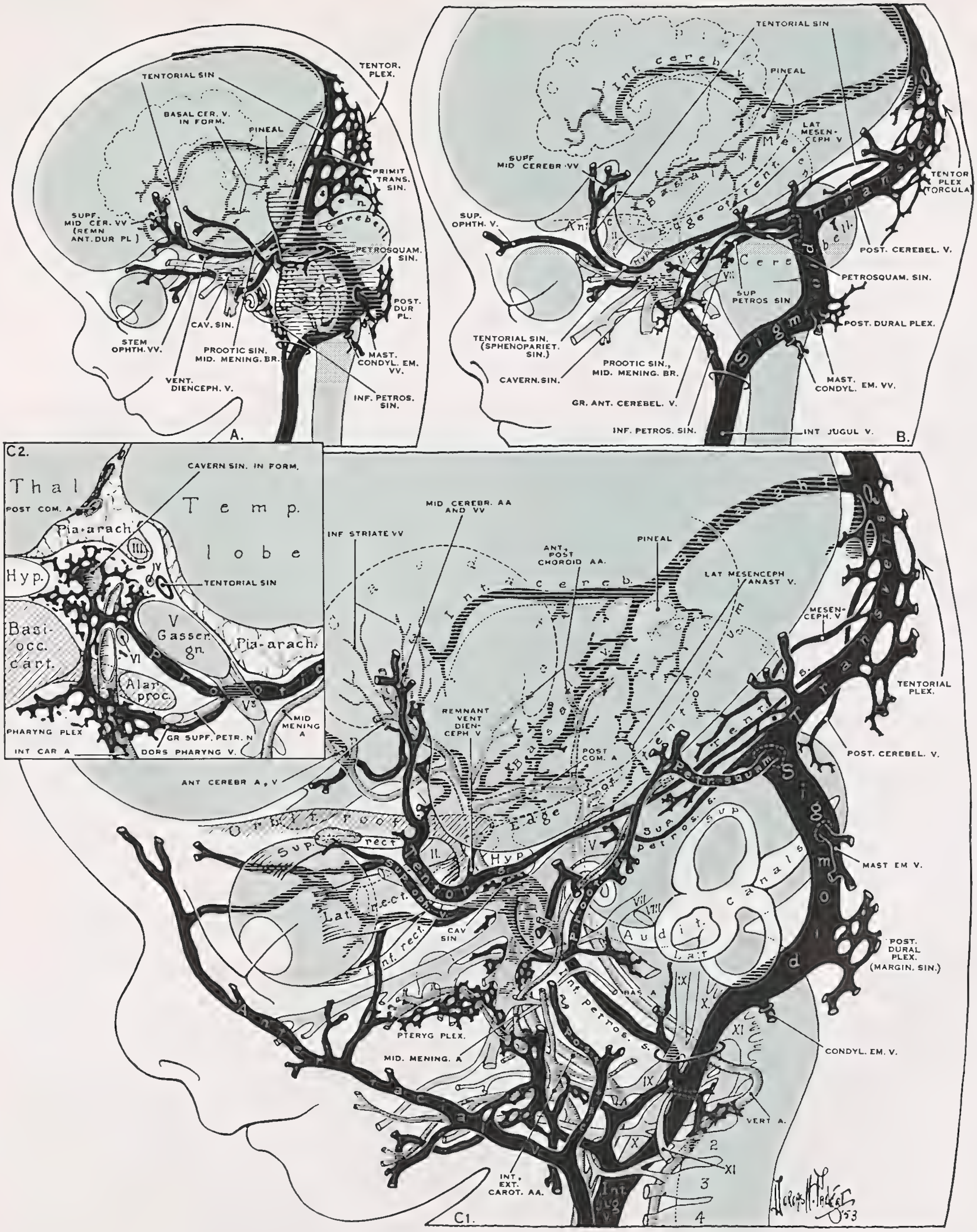
TENTORIAL SIN
TENTOR. PLEX.
BASAL CER. V. IN FORM.
PINEAL
PRIMIT. TRANS. SIN.
SUPF. MID CER. VV (REMN ANT. DUR PL.)
PETROSQUAM. SIN.
POST. DUR PL.
CAV. SIN.
STEM OPHTH. VV.
PROOTIC SIN. MID. MENING. BR.
MAST. CONDYL. EM. VV.
VENT. DIENCEPH. V.
INF. PETROS. SIN.
A.
TENTORIAL SIN
PINEAL
LAT MESENCEPH V
SUPF MID CEREBR VV
SUP. OPHTH. V.
TENTOR PLEX (TORCULA)
POST. CEREBEL. V.
PETROSQUAM. SIN.
SUP PETROS SIN
POST. DURAL PLEX.
TENTORIAL SIN. (SPHENOPARIET. SIN.)
CAVERN. SIN.
PROOTIC SIN., MID. MENING. BR.
MAST. CONDYL. EM. VV.
GR. ANT. CEREBEL. V.
INF. PETROS. SIN.
INT JUGUL V.
Transverse
Sigmoid
B.
C2.
CAVERN SIN. IN FORM.
Thal
Temp. lobe
POST COM. A
Pia-arach
Hyp.
TENTORIAL SIN
Basi-occ. cart.
V Gasser. gn.
Pia-arach.
Alar proc.
Prootic
PHARYNG PLEX
GR SUPF. PETR. N
MID MENING A
INT CAR A
DORS PHARYNG V.
MID CEREBR AA AND VV
INF STRIATE VV
ANT., POST CHOROID AA.
PINEAL
LAT MESENCEPH ANAST V.
MESENCEPH. V
TENTORIAL PLEX.
REMNANT VENT DIENCEPH V
POST COM. A
POST. CEREBEL. V.
ANT CEREBR A, V
Int. cereb.
Basal
Tentorius
Transverse
Sigmoid
Petrosquam
Sup. petros. s.
Orbit roof
Sup. rect.
Hyp
Lat. rect.
Inf. rect.
CAV SIN
Audit.
canals
MAST EM V.
POST. DURAL PLEX. (MARGIN. SIN.)
PTERYG PLEX.
MID. MENING. A
Int. petros. s.
BAS. A
CONDYL. EM. V.
Anter. facial
VERT A.
INT. EXT. CAROT. AA.
Int. jug. v.
C1.
Dorcas H. Padget '53

Plate 6

Basic patterns (semidiagrammatic) of the craniocervical venous channels in the adult of a typical mammal (A), and in the early human fetus (B), which emphasize the similar pattern of the vessels, but the significant differences in their size. (The common names for comparable vessels in each case are correspondingly placed and are underlined when the names differ.) In both types the embryonic head and neck are primarily drained by the internal jugular vein, which remains predominant in man, although certain tributaries are annexed to a variable extent by the secondary external jugular system. Conversely, owing to greater development of the face and neck relative to the brain in mammals except certain primates, the external jugular becomes predominant. It annexes most of the drainage of the internal jugular, which subsequently dwindles; note that compensation for such dwindling is available by way of a large mastoid emissary (A).

The cerebral and cerebellar veins in both types primarily converge to the junction of the transverse sinus with the sigmoid (B) or its small counterpart (A). In most mammals, essentially all intracranial drainage is received by the "dorsal cerebral vein," representing the human petrosquamosal sinus (common in the newborn), which leaves the skull through a temporal (postglenoid) foramen (4). Although a related, but not identical, spurious jugular foramen occurs regularly in the mammalian chondrocranium, a conspicuous temporal foramen in bone is anomalous in adult man. The common names of the other emissary foramina in each type are numbered as follows:

1. Anterior ethmoid foramen (A).
   Foramen cecum (B).
2. Orbital fissure (A).
   Superior and inferior orbital fissures (B).
3. Foramen ovale (A, B).
4. Temporal (postglenoid or spurious jugular) foramen (A, B).
5. Petrobasilar fissure (A).
   Jugular foramen (B).
6. Anterior condyloid foramen (A).
   Hypoglossal foramen (B).
7. Posterior condyloid foramen (A).
   Condyloid foramen (B).
8. Mastoid foramen (A, B).
9. Parietal foramen (A, B).

A persistent torcular asymmetry resulting in predominance of the right transverse sinus over the left is typical of embryonic life, and is common (ca. 50 per cent) postnatally, but apparently does not characterize other adult species. Such difference is explained by the contrasting patterns of the two innominate veins and their tributaries (cf. Padget, 1956, fig. 23). Although the left innominate in adult man is often relatively long and transverse (insert B)—a secondary anastomosis in contrast to that on the right, representing the anterior cardinal—the innominates are essentially symmetrical in a typical mammal (insert A). Anatomically, therefore, flow from each side of the head to the heart is about equally direct.

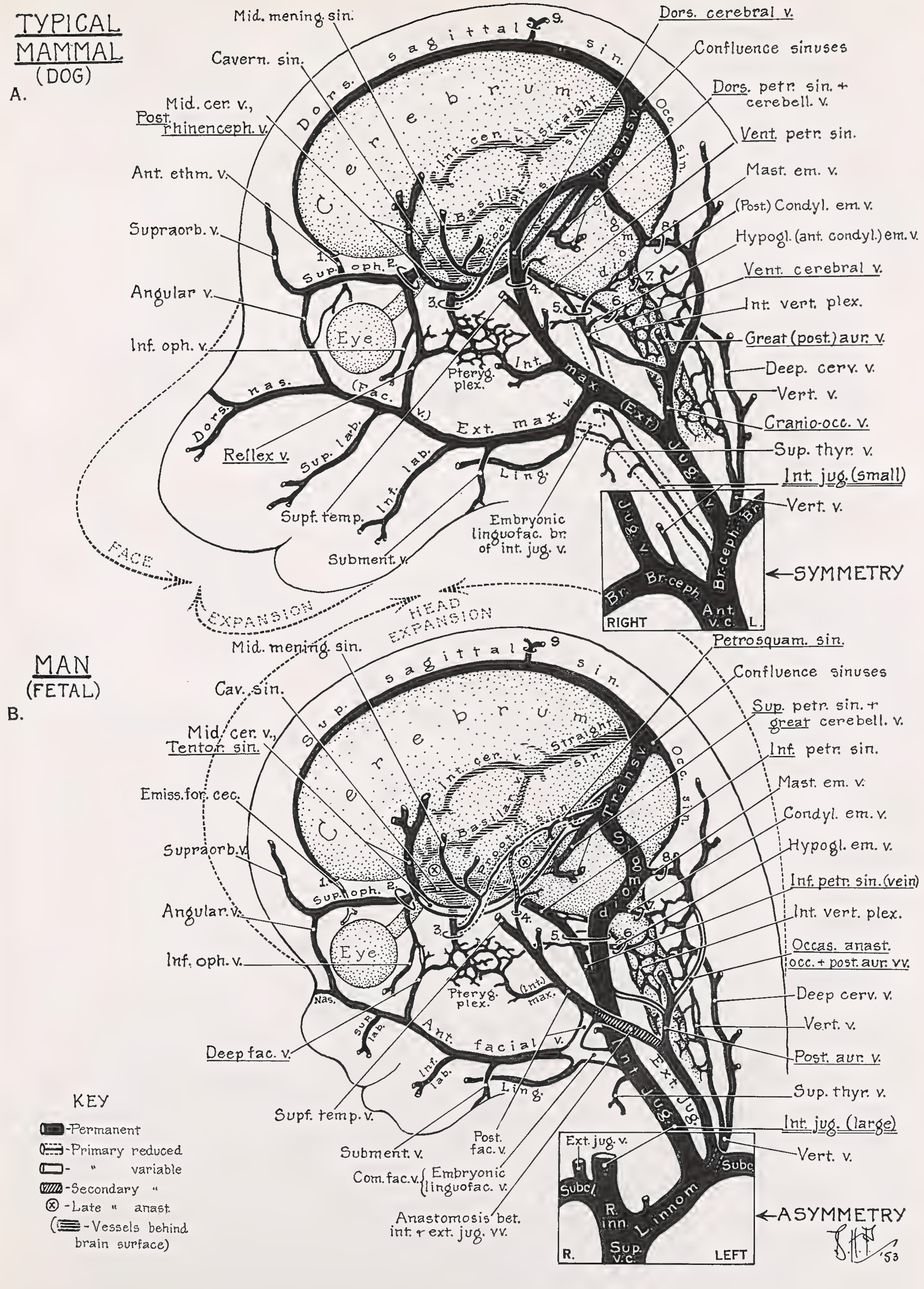
TYPICAL MAMMAL
(DOG)
A.
Mid. mening. sin.
Cavern. sin.
Mid. cer. v.,
Post. rhinenceph. v.
Ant. ethm. v.
Supraorb. v.
Angular v.
Inf. oph. v.
Reflex v.
Supf. temp.
Submenț. v.
Embryonic linguofac. br. of int. jug. v.
Dors. sagittal sin.
Cerebrum
Int. cer. v.
Straight sin.
Basilar sin.
Pr. oot. sin.
Transv.
Sigmoid
Occ. sin.
Sup. oph.
Eye
Pteryg. plex.
Int. max.
Ext. max. v.
(Ext.) Jug. v.
Dors. nas.
(Fac. v.)
Sup. lab.
Inf. lab.
Ling.
1.
2.
3.c
4.
5.
6.
7.
8.
9.
Dors. cerebral v.
Confluence sinuses
Dors. petr. sin. + cerebell. v.
Vent. petr. sin.
Mast. em. v.
(Post.) Condyl. em. v.
Hypogl. (ant. condyl.) em. v.
Vent. cerebral v.
Int. vert. plex.
Great (post.) aur. v.
Deep. cerv. v.
Vert. v.
Cranio-occ. v.
Sup. thyr. v.
Int. jug. (small)
Vert. v.
Jug. v.
Br. ceph.
Br.
Br. ceph.
Br.
Ant. v.c.
RIGHT
L.
←SYMMETRY
FACE EXPANSION
HEAD EXPANSION
MAN
(FETAL)
B.
Mid. mening. sin.
Cav. sin.
Mid. cer. v.,
Tentor. sin.
Emiss. for. cec.
Supraorb. v.
Angular. v.
Inf. oph. v.
Deep fac. v.
Supf. temp. v.
Sub. ment. v.
Com. fac. v.
Embryonic linguofac. v.
Post. fac. v.
Anastomosis bet. int. + ext. jug. vv.
Sup. sagittal sin.
Cerebrum
Int. cer. v.
Straight sin.
Basilar sin.
Pr. oot. sin.
Transv.
Sigmoid
Occ. sin.
Sup. oph.
Eye
Nas.
Sup. lab.
Inf. lab.
Pteryg. plex.
(Int.) max.
Ant. facial v.
Ling.
Int. Jug.
Ext. Jug.
1.
2.
3.c
4.
5.
6.
7.
8.
9
Petrosquam. sin.
Confluence sinuses
Sup. petr. sin. + great cerebell. v.
Inf. petr. sin.
Mast. em. v.
Condyl. em. v.
Hypogl. em. v.
Inf. petr. sin. (vein)
Int. vert. plex.
Occas. anast. occ. + post. aur. vv.
Deep cerv. v.
Vert. v.
Post. aur. v.
Sup. thyr. v.
Int. jug. (large)
Vert. v.
Ext. jug. v.
Subcl.
R. inn.
L. innom.
Subc.
Sup. v.c.
R.
LEFT
←ASYMMETRY
KEY
-Permanent
-Primary reduced
- " variable
-Secondary "
⊗ -Late " anast.
(-Vessels behind brain surface)
D.H.P. '53

CONTRIBUTIONS TO EMBRYOLOGY, NO. 248

THE DEVELOPMENT OF THE OCCIPITAL AND CERVICAL SEGMENTS AND THEIR ASSOCIATED STRUCTURES IN HUMAN EMBRYOS

E. Carl Sensenig

Department of Anatomy, University of Alabama Medical Center, Birmingham

With four plates

CONTENTS

PAGE
INTRODUCTION 143
IDENTIFICATION OF SEGMENTS 143
DESCRIPTION 144
  Period of Membrane Formation 144
    Stage I: Age Groups X, XI, and XII 144
    Stage II: Age Groups XIII and XIV 145
    Stage III: Age Groups XV and XVI 146
  Period of Cartilage Formation 147
    Stage IV: Age Groups XVII and XVIII 147
    Stage V: Age Groups XIX and XX 147
    Stage VI: Age Groups XXI, XXII, and XXIII 148
DISCUSSION 148
  Segmentation of the Occipital Region 148
  Proatlas, Atlas, and Axis 149
SUMMARY 149
LITERATURE CITED 149
ABBREVIATIONS USED IN PLATES 151

THE DEVELOPMENT OF THE OCCIPITAL AND CERVICAL SEGMENTS AND THEIR ASSOCIATED STRUCTURES IN HUMAN EMBRYOS[1]

INTRODUCTION

Interest in the segmentation of the skull was first developed by the school of "Natur-Philosophen" during the first quarter of the nineteenth century. These philosophers (Oken, 1811; Spix, 1815; Saint-Hilaire, 1818; Bojanus, 1819–1821; Goethe, 1820; Meckel, 1820; Carus, 1828) postulated that the skull is constructed from a series of bony rings, 3 to 7 in number, each of which represents a vertebra. Goethe is given credit for formulating this theory in 1790, even though he failed to publish it until 1820. These unsupported speculations were accepted by von Baer (1828), Reichert (1838), Rathke (1839), and, even as late as 1846, by Owen. It was Vogt (1842) who first questioned the Natural Philosophers; noting that the cranium consists of a chordal and prechordal portion, he pointed out that only that part of the skull which forms about the notochord can in any way be considered vertebral in origin. The hypothesis of a vertebral origin of the entire skull, however fanciful, served a useful purpose as the forerunner of more acceptable theories of the segmentation of the skull. As a result of the careful observations of the comparative anatomist Remak (1850–1855), and the comparative embryologists Gegenbaur (1872), Balfour (1876), and van Wijhe (1882), it was shown that at least the postotic portion of the cranium is developed from recognizably segmented primordia, namely the occipital somites. Subsequently, the occipital and cervical skeletal elements have received considerable attention from comparative embryologists, who have primarily studied the development of the occipito-atlanto-axial complex in an endeavor to clarify the details of the segmentation of the postotic skull.

Froriep (1886) initiated these studies in mammalian embryos with his extensive treatise on the development of the occipito-atlanto-axial segments in sheep embryos. Other investigations followed, including the analyses of Weiss (1901) on the albino rat, and of Bardeen (1908, 1910), Hayek (1923), and Reiter (1944) on man. General developmental studies of the mammalian spine, relevant to this study, are those of Dawes (1930), von Bochmann (1937), and Sensenig (1943) on rodent embryos, and those of Rosenberg (1876), Bardeen (1905, 1910), Ch. Müller (1906), Ask (1941), Reiter (1942), Wyburn (1944), and Sensenig (1949) on human embryos.

The present author, having at his disposal through the Department of Embryology of the Carnegie Institution of Washington much more extensive material than was available to previous investigators, undertook an intensive re-examination of the development of the postotic portion of the human cranium and of the upper cervical segments. For the study of the earlier stages up to 80-mm. crown-rump length, serially sectioned embryos of the Carnegie Collection were used. The author wishes to express his gratitude to the Carnegie Institution of Washington and to Dr. G. W. Corner, former Director of the Department of Embryology, for the privileges of the laboratory, and to Mr. Richard D. Grill for the photographs herein reproduced. For study of the later stages, from 80-mm. crown-rump length to full term, preserved fetuses received from the Carnegie Collection were prepared for microscopic study in the author's laboratory with the aid of a grant from the National Institutes of Health. Thanks are due Mrs. Helen B. Caldwell and Mrs. Georganne J. Holloway, research assistants, for the preparation of these older embryos.

IDENTIFICATION OF SEGMENTS

There are a number of methods for determining the segments involved in the formation of the occipital region. One may count the somites, the myotomes, the occipital ganglia, or the roots of the hypoglossal nerve. Unfortunately, none of these methods is dependable, so that the number of segments assigned to the occipital region varies considerably. As will be seen in the following list, the number ranges from 2 to 5 in man and 3 to 6 in other mammals.

In man:

2 segments	Johnson (1917)
2 to 3 segments	Bardeen and Lewis (1901)
3 segments	Mall (1891), Kollmann (1891), Ingalls (1907), Bardeen (1910), Davis (1923), Hayek (1923), Atwell (1930), West (1937)
3½ segments	Thompson (1907)
3 to 4 segments	Streeter (1904), Fischel (1929), Muggia (1931), Clara (1938)
4 segments	Beck (1896), Schmeidel (1932), Holmdahl (1934)

---

[1] This investigation was supported in part by a research grant (RG824) from the National Institutes of Health, of the National Institutes of Health, U. S. Public Health Service.

3 to 5 segments	Lewis (1910)
4½ segments	Wen (1928)
5 segments	Reiter (1944)

In other mammals the situation is much the same:

Mouse	5 segments, Dawes (1930), Sensenig (1943)
Rat	3 segments, Weiss (1901)
	4 segments, Butcher (1929)
Rabbit	4 segments, Chiarugi (1890), Hunter (1935)
Sheep	3 segments, Froriep (1883), Barge (1918)
	4 segments, Bonnet (1889)
Pig	5 to 6 segments, Prentiss (1910)
	3 segments, Kempermann (1929)
Cattle	3 segments, Froriep (1886)
Cat	5 segments, Martin (1891)

Arey (1938) points out the difficulties involved in counting the occipital somites. The variation in the size of the first somite and its rapid regression (it is small in embryos of 10 to 20 somites and has usually disappeared by the stage of 20 to 30 somites) make such a count uncertain. In descriptions of individual embryos, some authors (Gage, 1905; Thompson, 1907; Johnson, 1917; Davis, 1923; Wen, 1928; Atwell, 1930; West, 1937) have attempted to identify the first occipital somite when the presence or absence of this somite was questionable. Other authors (Low, 1908; Dandy, 1910; Bujard, 1915; Payne, 1925; Politzer, 1928, 1930; Corner, 1929; Heuser, 1930; West, 1930) have described the most cephalic somite observed in their respective specimens without trying to determine whether it was actually the first occipital somite.

There are similar difficulties in using the hypoglossal roots. Beck (1896), for example, in his series of human embryos, counted variously 12 to 16 rootlets which generally united to form 4 main trunks. Muggia (1931) stated that there is a progressive reduction in the number of main roots, there being 4 roots in embryos of less than 7 mm. and 3 in embryos of more than 7 mm.

The counting of myotomes is also hazardous, because the first myotome rapidly regresses and the second may be very small. Furthermore, if de Beer (1927) is correct, the first occipital segment never forms a myotome, and the rudimentary myotome appearing as the first may actually represent the second occipital segment.

The ganglia develop late in the somite stages, so that it is difficult to correlate their appearance with the somites and myotomes. Reiter (1944) confidently assigned 5 segments to the occipital region on the basis of a more careful examination of younger embryos than were studied by previous investigators. He made use of only 4 embryos of somite stages, however.

The present author has endeavored to secure greater certainty in this difficult task by combining the evidence from all available serial structures. The occipital segments were identified by counting somites, myotomes, ganglia, and hypoglossal nerve roots, and by determining the positions of the primitive hypoglossal and first cervical artery (Schmeidel, 1932; Padget, 1948). The rudimentary hypoglossal ganglia used by Reiter (1944) to determine the two most caudal occipital segments were not used, because their size is subject to wide variation and they have been considered to be associated with the accessory-vagal complex rather than with the hypoglossal nerve.

DESCRIPTION

Period of Membrane Formation

The descriptive materials will be presented in the same order as in an earlier paper (Sensenig, 1949) which gives a general description of the early development of the human vertebral column.

Stage I: age groups x, xi, and xii. In embryos of 10 somites or less (age group x), the neural tube is wide open in a 4-somite embryo, is beginning to close in its mid-portion in a 7-somite embryo, and is closed from the postotic region throughout the extent of the somites in a 10-somite embryo (fig. 1, pl. 1). In 10-somite embryos, cells indicating the trigeminal, acousticofacial, and occipitospinal neural crests are appearing. The notochord is a relatively broad, single-layered plate of cells, continuous laterally with the gut endoderm and forming the mid-dorsal roof of the archenteron. The dorsal surface of the notochordal plate lies in contact with the ventral surface of the neural tube. In a 10-somite embryo, the notochord is beginning to show a dorsal evagination (fig. 1, pl. 1).

The somites vary considerably in their development in the embryos of this age group. They exist very briefly as discrete structures, and shortly after their formation cells begin to migrate from them. These migrating sclerotomic cells are destined to give rise to the tissues that form the axial skeleton and the meninges. In a 4-somite embryo (Carnegie no. 3709), cell migration from the ventromesial surface of the somites has already begun. Active cell migration is present in the first two or three somites of the 7-somite Payne embryo (Carnegie no. 4216), and throughout all but the most caudal one or two somites in the 10-somite Corner embryo (Carnegie no. 5074, fig. 1, pl. 1). The first somite in the 4- and 7-somite embryos is as large as the succeeding somites, whereas in the 10-somite embryo the first somite is much smaller and shows far less differentiation than the second and following somites. In the younger embryos, a myocoel is only occasionally present, but in the older embryos of this group the majority of somites contain myocoels, except the first somite, which rarely develops a cavity. From the level of the otic plate to that of the first somite, the area between the neural tube and the surface ectoderm is filled with loosely dispersed mesenchymal cells.

In embryos of 13 to 20 somites (age group xi), the neural tube is closed throughout its extent except at its cephalic and caudal extremities. The development of the neural crests continues, and by the 20-somite stage the neural crests of the trigeminal, facial, glossopharyngeal, and vagus nerves are distinct; the crests of the occipitospinal nerves are beginning to be visible. The dorsal evagination of the notochord, first seen in 10-somite embryos, is present in all levels in a 13-somite embryo (Carnegie no. 6344), and the process of evagination is complete in the occipitocervical region of a 16-somite embryo (Carnegie no. 7611, figs. 2, 3, pl. 1). By the stage of 20 somites (Carnegie no. 2053), the notochord forms a tubular structure that remains in contact dorsally with the neural tube and ventrally with the gut.

In all embryos of age group xi the first somite is much smaller than the succeeding somites. In both a 19-somite embryo (Carnegie no. 6050, fig. 4, pl. 1) and a 20-somite embryo (Carnegie no. 2053), the first somite has almost completely disappeared. In all the somites in the region under investigation, a ventromesial migration of somitic (sclerotomic) cells is present (fig. 2, pl. 1), reaching as far as the lateral borders of the notochord; further migration is dependent upon an increase in the restricted space between the neural tube, the notochord, and the longitudinal vessels. The majority of the somites have a myocoel not continuous with the general coelomic cavity. The region between the otic plate and the first somite is filled with a dense cellular mesenchyme (fig. 3, pl. 1). There is no indication of segmentation in this head mesenchyme.

In embryos of 21 to 29 somites (age group xii), the neural crests show a rapid advance in development in the future cervical region. In a 22-somite embryo (Carnegie no. 4763), the crests are very small and indistinct; in 25-somite embryos (Carnegie nos. 6097, 7582), they have become well defined structures; by the end of this stage (Carnegie nos. 8942, 26-somite; 8941, 27- to 28-somite; 7999, 28-somite), they have increased considerably in size. The notochord now forms an elongated tube which in a mid-sagittal section shows an irregular outline, but there are no indications of segmental flexures. The notochordal cells are radially arranged with their nuclei located at the periphery. The notochord is now separated in both its cranial and cervical courses from the overlying neural tube. In its cranial part it remains in close contact with the underlying gut roof, whereas in the cervical region these structures are separated by a narrow interval (fig. 6, pl. 1). A lumen is occasionally observed within the notochord, but it extends only through a few sections.

In all segments, somitic cells are migrating into the space between the neural tube and the longitudinal vessels and are approaching close to the notochord. A few cells have entered the epichordal space (between notochord and neural tube), but only in the cervical region have cells entered the subchordal space (between notochord and gut). No mesodermal cells have oriented themselves about the notochord; a perichordal sheath is still absent. In all but the more cephalic somites, segmentation is clearly indicated by the intersegmental vessels (fig. 5, pl. 1). This segmentation extends only to the cephalic border of the last occipital somite. For the first time a sclerotomic fissure can be identified, subdividing each cervical somite into a cranial and caudal half (fig. 5, pl. 1). This fissure is also present in the most caudal occipital segment. The myotome, derived from the dorsolateral part of the somite, has flattened; its cells are becoming elongated, and indications of its future longitudinally striate condition are seen (figs. 5, 6, pl. 1). The first signs of vascularization of the tissues about the neural tube have appeared in the form of endothelial strands.

Stage II: age groups xiii and xiv. The second stage in the development of the occipitocervical region is characterized by a rapid proliferation and migration of sclerotomic cells, an increase in the size of the ganglia, and the formation of the occipitocervical nerves.

In the areas lateral to the neural tube, the spinal ganglia have increased in size so rapidly that they interrupt the continuity of the sclerotomic cells that have migrated dorsally about the neural tube (figs. 9–12, pl. 2). Froriep's ganglion, associated with the spinal accessory nerve, has attained its maximum development, and at its ventrocaudal extremity fuses with the ganglion of the first cervical nerve, which never attains the size of the remaining cervical ganglia. Early in this stage only the ventral nerve roots are present, but the dorsal roots soon appear and develop rapidly. The large ganglia are beginning to shift ventrally (figs. 10–12, pl. 2). Vascularization of the tissues, initiated in age group xii, advances rapidly, particularly about the periphery of the neural tube, and by the close of this stage endothelium-lined channels are present.

The myotomes have become transversely flattened and dorsoventrally elongated to form typical myotomic plates (fig. 7, pl. 2). In sagittal section these plates exhibit the striated condition indicated in earlier embryos (fig. 8, pl. 2), and now show well developed myosepta in addition. Three or four occipital myotomes can be identified in the occipital region, depending on the degree of regression of the most cephalic one. In figure 8, four myotomes are present in the occipital region, the first being very small, the second reduced in size, and the third and fourth equal in size to those of the succeeding cervical segment. At the point where the myotomic plate bulges inward, at the level of the notochord, is situated the area of rapid cell proliferation (figs. 10, 11, pl. 2).

For the first time the cell concentrations forming the vertebral rudiments are sufficiently cellular to be distinguishable from the less cellular areas adjacent to the neural tube. It is now possible, therefore, to define the vertebral rudiments and to identify the less cellular area about the neural tube as the meninx primitiva. The meninges, however, do not develop from the meninx primitiva, as the name implies, but predominantly from the inner surface of the skeleton-forming tissues of the vertebral rudiments (Sensenig, 1951).

The notochord is now well separated from the neural tube and also, except in the occipital region, from the gut (figs. 10–12, pl. 2). By the close of this stage, age group xiv, the segmental flexures of the notochord have developed, those in the cervical segments being more pronounced than those in the occipital region. In a transverse section passing between adjacent ganglia, a relatively large area exists between the myotomic plate and the periphery of the neural tube. Into this area sclerotomic cells have migrated to form the rudimentary neural processes. Sclerotomic cells have also orientated themselves about the notochord to form a perichordal sheath or tube (figs. 7, 10–12, pl. 2). The spinal nerves are situated in the cranial half of each sclerotome, whereas their greatly enlarged ganglia extend well beyond the limits of this sclerotome-half.

It should be noted at this point that a definitive vertebral segment is not equivalent to a primitive segment or somite. The rostrocaudal extent of each somite is defined by two adjacent intersegmental vessels. A somite is further subdivided into a cranial and a caudal sclerotome-half by the presence of a sclerotomic fissure, which may still be observed at this stage. The intersegmental vessels and sclerotomic fissures, however, indicate boundaries only; they are not delimiting structures, as cellular concentrations are everywhere continuous around and about them. A definitive vertebral segment is composed of the caudal sclerotome-half of one somitic segment together with the cranial sclerotome-half of the next succeeding segment. The occipital somites are concerned in the formation of the occipital bone. The atlas is formed from the caudal sclerotome-half of the first primitive cervical segment and the cranial sclerotome-half of the following segment. Consequently, the cranial sclerotome-half of the first cervical segment, which contains the first cervical nerve, is left as a half segment. The further development of this half segment, the derivative of which has been called the proatlas, will be considered later.

In sagittal sections (fig. 9, pl. 2), segmentation is clearly indicated by the intersegmental vessels. Here the primitive hypoglossal and first cervical arteries define the boundaries of the most caudal occipital segment, which shows a concentration of cells equal to that of the following cervical segments. No segmentation is present rostral to the primitive hypoglossal artery, and there is a great decrease in cell concentration. Only in the area about the notochord, in the cervical segments, may differentiation of tissue be observed, other than a strong concentration of cells at the mid-point of each segment with a looser area at the cranial and caudal extremities of the segment, i.e. adjacent to the intersegmental vessels. In this medial concentration the perichordal disk may now be distinguished (fig. 11, pl. 2) in the dense caudal sclerotome-half. Rostral to the perichordal disk is an epichordal strand of cells (fig. 10, pl. 2), and caudal to it, a hypochordal strand of cells (fig. 12, pl. 2). In the cranial sclerotome-half the medial concentration is loosely cellular, forming the primary centrum. A very short rib rudiment is present in the most caudal occipital segment and in the atlantal segment. Elsewhere in the cervical region the rib rudiment is typical in form.

Stage III: age groups xv and xvi. In the third stage the membranous occipitocervical segments attain their greatest development before the appearance of cartilage. The proliferation of cells in the sclerotome has greatly decreased. A distinct differentiation of the sclerotome tissue is now visible, and the vertebral rudiments can be identified.

The spinal ganglia are losing their dorsal continuity, and occupy a smaller area in each segment. They are still broad, however, and take up much of the area lateral to the neural tube (fig. 14, pl. 3). The dorsal nerve roots are well developed, and the ganglia have continued their migration ventrally (fig. 17, pl. 3). Froriep's ganglia and the ganglia of the first cervical nerve are reduced in size (fig. 14, pl. 3). The hypoglossal nerve is formed by a number of roots that converge into four trunks (fig. 15, pl. 3). The more caudal of these roots may have ganglion cells associated with them; these cells are continuous with the reduced first cervical ganglia.

The myotomes are well developed in the cervical region (fig. 13, pl. 3), lying, in their greater part, lateral to the loose-celled concentrations of the cranial sclerotome-half, between two adjacent densely cellular neural arch rudiments (fig. 13, pl. 3). The last occipital myotome is as well developed as the succeeding cervical myotomes. Rostrally, three greatly reduced myotomes are occasionally present. Thus, in some of the embryos of this stage, four occipital myotomes can still be identified.

Each sclerotome is divided into a loosely cellular cranial sclerotome-half situated caudal to an intersegmental vessel, and a densely cellular caudal sclerotome-half cranial to the adjacent intersegmental vessel (figs. 14, 15, pl. 3). The first cervical segment, bounded rostrally by the first cervical segmental artery (which indicates the boundary between the definitive skull and vertebral column), contains in its cranial sclerotome-half a ganglion of reduced size. The dense caudal sclerotome-half of this segment enters into the formation of the first definitive vertebra or atlas. This first cranial sclerotome-half, lying between the future atlas and occipital bone, is the proatlas.

The neural arches, dense concentrations of cells, are formed predominantly in the caudal sclerotome-half; at their bases they are continuous with the medial vertebral rudiments located ventral to the neural tube and surrounding the notochord (figs. 16, 17, pl. 3). In the occipital region, a neural process develops only in the most caudal segment (fig. 14, pl. 3). In the cervical region, the cell population of these medial rudiments is not uniform throughout, being less dense in a large part of the cranial sclerotome-half and more dense in most of the caudal sclerotome-half (fig. 17, pl. 3). The cranial sclerotome-half of the last occipital segment has few cells, whereas the more rostral unsegmented part has a much greater density throughout. In the cervical region, the loose-celled areas form the primitive centrum; the dense-celled areas form the perichordal disk from which the intervertebral disks and the rostral and caudal ends of the definitive centrum are derived later.

Period of Cartilage Formation

Stage IV: age groups xvii and xviii. The inner wall of the vertebral canal is distinct ventrally and ventrolaterally, and can be distinguished dorsally and dorsolaterally from the underlying meninx primitiva (figs. 19, 20, pl. 4), which progressively becomes more definite. The first cervical ganglion, smaller than the succeeding cervical ganglia, is still associated with Froriep's ganglion, now greatly reduced in size (fig. 22, pl. 4). All ganglia have migrated farther ventrally, and their ventral parts now lie ventral to the anterior surface of the neural tube (fig. 18, pl. 3; figs. 19, 20, pl. 4). Filaments of the hypoglossal nerve are combined into three rootlets, of which the most rostral is by far the smallest; occasionally a fourth rootlet may still be seen on one side. As the nerve pierces the rudiment of the occipital bone, the rootlets unite into two large roots.

Chondrification is now appearing in the basioccipital bone and in the bodies of the vertebrae (fig. 21, pl. 4). There is no indication of cartilage in the occipital arch. The hypoglossal nerve pierces a chondrified area. The dorsal extremities of the occipital and vertebral arches are connected dorsally above the brain stem and spinal cord by the membrana reuniens dorsalis (figs. 19, 20, pl. 4). This membrane appears only as a condensation of mesenchyme, with no indication of lamination. The arch of the atlas shows early chondrification in the pedicles (fig. 19, pl. 4). Its body shows distinct chondrified areas ventral to the notochord, these being separated by a membranous strip in the mid-line (fig. 19, pl. 4). A lesser amount of chondrification is present in the suprachordal areas (fig. 19, pl. 4) and in the body of the axis and succeeding cervical vertebrae, but a greater degree of chondrification exists in the suprachordal region (fig. 20, pl. 4). The odontoid process is entirely membranous. Slight mesenchymal condensations extending laterally from the tip of the odontoid indicate the extent of the future alar ligaments. There is no indication of a separation of the odontoid rudiment from the body of the atlas. The apical ligament is not yet formed; there is still no indication of the occipitoatlantal joint or other joints of the cervical spine. The transverse process is well developed and chondrified, whereas the rib process shows no chondrification and is not as thick as the transverse process.

In age group xvii, as the somites disappear, the rudiments of the axial musculature can be separated from those of the vertebrae (fig. 18, pl. 3; figs. 19, 20, pl. 4). These rudimentary muscle masses divide into two groups: one group lying lateral to the transverse processes and rudimentary laminae—the future postvertebral musculature; and the other group lying ventromedial to the pedicle—the future prevertebral musculature. In age group xviii, the postaxial muscle masses have become laminated into three zones.

Stage V: age groups xix and xx. In both age groups xix and xx, the rootlets of the hypoglossal nerve unite to form two distinct roots which pass through the basioccipital rudiment. The reduction in size and the ventral displacement of the first cervical ganglion continue, so that in age group xx it is lying close to the intervertebral foramen. The other cervical ganglia also have migrated further ventrally but are still intradural.

These age groups are characterized by an advance in the chondrification of the vertebral rudiments. The basioccipital bone is now heavily chondrified. The arch of the atlas is still short, and chondrification extends to the tip of this short rudiment. In the earlier age groups the odontoid process is not separate from the atlas, but with the increased chondrification seen in age group xx it is separated from the atlantal arch by a membranous area. The ventral arch of the atlas, the subchordal strand or hypochordal *Spange,* has become chondrified, and is separable from the odontoid. In both age groups the transverse process of the atlas is chondrified, but the rib rudiment still remains a slender membranous strand.

In the axis, chondrification occurs throughout the body and arches; the rib rudiment is better developed than in the atlas, and is beginning to become chondrified. In the cervical vertebrae, 3 through 7, chondrification is under way throughout the arches, bodies, and rib rudiments.

The arches, however, are longer, extending farther dorsally than those of the atlas and axis.

The suboccipital muscles can now be identified as well as the other muscles of the postaxial and preaxial groups. For the first time the atlanto-occipital and atlantoaxial arch articulations are indicated by the presence of a membranous strip at the site of each of these future joint cavities.

Stage VI: age groups xxi, xxii, and xxiii. The state of development of the hypoglossal nerve is similar to that of previous age groups, its rootlets uniting to form two separate roots, which may traverse the occipital rudiment separately or together.

The cervical ganglia in general continue their ventral migration (fig. 24, pl. 4), so that by age group xxiii they have reached their position in the intervertebral foramen; all of them are now extradural, except the first, which is still intradural. The reduction in size of the first cervical ganglion differs in the various embryos.

Age groups xxi, xxii, and xxiii are characterized by continued chondrification, resulting in a more distinct definition of the vertebral elements. By the end of the embryonic period (age group xxiii), the dorsal arches of all cervical vertebrae have extended farther dorsally. This cartilage does not form endochondrally within a mesenchymal precartilage, but by proliferation of cells from the tip of the cartilaginous arch rudiment (fig. 23, pl. 4). The arch rudiments of the axis and successive cervical vertebrae now extend above the dorsal level of the spinal cord and are beginning to bend medially. Their tips curve laterally, indicating their future bifid condition. The odontoid process is everywhere chondrified except for its tip, and is clearly differentiated from the chondrified ventral atlantal arch. The rib rudiment of the atlas shows a different degree of development in each embryo. In some it is represented by a very poorly developed, narrow membranous rudiment; in others it is well developed and cartilaginous. In the other cervical vertebrae the rib rudiments are well developed and chondrified.

DISCUSSION

Segmentation of the Occipital Region

From the foregoing description, it is evident that the most cephalic somite is the first to develop, and that development of the somites continues in the caudal direction only. This finding is in agreement with Arey's (1938) careful study of the first somite and with the conclusions of Reiter (1944). No support has been obtained for Ludwig's (1928) arbitrary identification of the single pair of somites in his embryo as occipitocervical, or for the conclusion of Sternberg (1927), who, in disagreement with Dandy (1910), considers the poorly developed first somite in the Dandy embryo to have developed after the following somites. It is also impossible to give credence to Broman's (1911) assertion that the earliest somite arises at the upper border of the neck, and that, during the fourth week, three somites arise cephalic to this original somite. By the fourth week, human embryos are, in fact, passing out of the somite stage.

The regressive condition of the first somite is clearly indicated in the 19-somite embryo (fig. 4, pl. 1). On the basis of myotome counts in a 29-somite embryo (fig. 5, pl. 1), the first cervical artery defines the caudal boundary of the last occipital segment. In an adjacent section the primitive hypoglossal artery forms the cephalic boundary of this segment. Rostral to the hypoglossal artery, three distinct myotomes are present, the most rostral of which closely approaches the vagus ganglion. Between this ganglion and the first myotome is a small mass of tissue which is difficult to identify but may represent a very rudimentary myotome. Four occipital myotomes (fig. 8, pl. 2) can be identified in a 4-mm. embryo, the first being very small, the second slightly larger, and the third and fourth normal in size. As seen in figure 9 (pl. 2), the primitive hypoglossal and the first cervical arteries clearly delimit the most caudal occipital segment. Rostral to the primitive hypoglossal artery, at least eight rootlets of the hypoglossal nerve can be identified. These unite into no less than three main roots and indicate three segments. In the embryos studied, the filaments of the hypoglossal nerve were usually united into three to five roots, and in only two embryos were five roots observed. It should be mentioned that the most rostral hypoglossal fibers are very small and can easily be overlooked. These findings agree in part with Streeter's (1904) count of three or four roots, and are in complete agreement with the statements of Beck (1896), Muggia (1931), and Schmeidel (1932), all of whom demonstrate the presence of four roots.

The observations do not definitely support Reiter's (1944) findings of five segments. In Reiter's favor, however, it should be recalled that indications of a fifth segment were found in the present investigation, as mentioned above. Reiter's first occipital somite, moreover, does not form a myotome; this statement agrees with de Beer's (1937) description of a fifth somite which forms no myomere and ultimately disappears. De Beer believes that nine segments participate in the formation of the skull. Of these, somites 6 through 9 are occipital, somite 5 becomes rudimentary, and the first four are involved in the formation of the preotic cranium. This fifth somite may represent Reiter's first occipital segment; such an interpretation would support his thesis that there are five segments in the occipital region.

All the information assembled in this study, therefore, supports a minimum of four segments in the occipital region, with the possible existence of a fifth rudimentary segment.

Proatlas, Atlas, and Axis

Remak's (1850–1855) theory of the rearrangement of the vertebral column, which is accepted here, asserts that a definitive vertebra develops from the caudal sclerotome-half of one segment and the cranial sclerotome-half of the next succeeding segment (for a discussion of Remak's theory, see Sensenig, 1949). Thus, a vertebra is an intersegmental structure. The short intervertebral muscles, derived in a strictly segmental fashion from the primitive segments, secure attachment to two vertebrae and are enabled to act upon the vertebral column.

By this arrangement of the sclerotomes, the first cervical cranial sclerotome-half, represented by the first cervical spinal ganglion and nerve, remains as a half segment between the occipital and atlantal rudiments. The derivative of this cranial sclerotome-half was termed proatlas by Albrecht (1880), and has received special attention in the investigations of Froriep (1886), Weiss (1901), Barge (1918), Hayek (1923, 1927), and Reiter (1944); the two authors last named dealt with human embryos. It is generally accepted by these investigators, as well as by Dawes (1930), Gadow (1933), and Sensenig (1943), that the primitive centrum developing within this half segment forms the tip of the odontoid process of the axis. The fate of the arch rudiment, however, is not so well established, and apparently varies in the different forms. In species other than man, the proatlantal arch rudiment fuses either with the atlantal arch (Barge, 1918; Hayek, 1923; Sensenig, 1943) or with the occipital bone (Froriep, 1883). Hayek (1927) and Ingelmark (1947) doubt that in human embryos this rudiment is incorporated into the atlantal arch, and the present author supports Hayek's (1927) observation that it assists in the formation of the occipital condyles. It also assists in the formation of the alar ligaments as well as of the other ligaments of the occipitoatlantal joint.

The dorsal arch of the atlas follows the same sequence of development as the other cervical vertebrae except that its ultimate closure is slightly later. In contrast, the ventral atlantal arch, represented in the earlier stages by a densely cellular but relatively slender membranous band, chondrifies late and gradually separates from the primitive centrum, which becomes incorporated into the dens epistrophei. The atlantal rib rudiment is extremely variable in its development, and is often incomplete.

The axis develops like the typical cervical vertebrae except that its body is not separated from that of the atlas and proatlas. Its odontoid process consists, then, of two and one-half segments in which all early indication of segmentation is lost. No traces of intervertebral disks are observed within the odontoid; therefore, the first of these disks to develop is the one lying between the axis and the third cervical vertebra.

SUMMARY

In this paper are presented the early stages in the development of the occipitocervical segments as observed in a closely graded series of human embryos. This study includes the development of intersegmental vessels, somites, myotomes, occipitocervical ganglia, and roots of the hypoglossal nerve, as well as the occipital bone and cervical vertebrae.

1. The most cephalic somite is the first to develop, and development of somites occurs in a caudal direction only.
2. Four occipital myotomes are identified; the first is very small, and the second not as large as the succeeding ones.
3. Rootlets of the hypoglossal nerve are usually united into three to five roots; in only two embryos were five roots observed.
4. The occipital bone is formed from at least four somites, with some indication that a fifth may be involved.
5. A definitive vertebra develops from the caudal sclerotome-half of one segment and the cranial sclerotome-half of the next succeeding segment. By this arrangement the first cervical cranial sclerotome-half remains as a half segment between the occipital and atlantal rudiments, i.e. the proatlas.
6. This proatlantal primitive centrum forms the tip of the odontoid process; its arch rudiment assists in the formation of the occipital condyles.
7. The vertebral arch of the atlas separates from its respective primitive centrum, which forms part of the odontoid process. The atlantal rib rudiment is variable in degree of development and often incomplete.
8. The axis forms from the second definitive vertebral segment; its odontoid process represents the primitive centra of the atlas and the proatlantal half segment.

LITERATURE CITED

Albrecht, P. 1880. Ueber den Proatlas, einen zwischen dem Occipitale und dem Atlas der amnioten Wirbelthiere gelegenen Wirbel, und den Nervus Spinalis I.s. pro-atlanticus. Zool. Anz., vol. 3, pp. 450–456.

Arey, L. B. 1938. The history of the first somite in human embryos. Carnegie Inst. Wash. Pub. 496, Contrib. to Embryol., vol. 27, pp. 233–269.

Ask, O. 1941. Studien über die embryologische Entwicklung des menschlichen Rückgrats und seines Inhaltes unter normalen Verhältnissen und bei gewissen Formen von Spina bifida. Uppsala Läkarefören. Förhandl., vol. 46, pp. 243–348.

Atwell, W. J. 1930. A human embryo with seventeen pairs of somites. Carnegie Inst. Wash. Pub. 407, Contrib. to Embryol., vol. 21, pp. 1–24.

Baer, K. E. von. 1828. Ueber Entwicklungsgeschichte der Thiere. Beobachtung und Reflexion. Part 1. 271 pp. Königsberg.

Balfour, F. M. 1876. The development of elasmobranch fishes. Jour. Anat. and Physiol., vol. 10, pp. 672–688.

Bardeen, C. R. 1905. The development of the thoracic vertebrae in man. Amer. Jour. Anat., vol. 4, pp. 163–174.

——— 1908. Early development of the cervical vertebrae and the base of the occipital bone in man. Amer. Jour. Anat., vol. 8, pp. 181–186.

——— 1910. Development of the skeleton and of the connective tissues. *In* Keibel and Mall (eds.), Manual of human embryology, vol. 1, chap. 11, pp. 292–453. Philadelphia.

——— and W. H. Lewis. 1901. The development of the limbs, body-wall and back in man. Amer. Jour. Anat., vol. 1, pp. 1–35.

Barge, J. A. J. 1918. Die Entwickelung der Cranio-Vertebralgrenze beim Schaf. Anat. Hefte, vol. 55, pp. 415–442.

Beck, Wilhelm. 1896. Ueber den Austritt des N. hypoglossus und N. cervicalis primus aus dem Centralorgan beim Menschen und in der Reihe der Säugetiere unter besonderer Berücksichtigung der dorsalen Wurzeln. Anat. Hefte, vol. 6, pp. 249–346.

Bochmann, G. von. 1937. Die Entwicklung der Säugetierwirbel der hinteren Körperregionen. Morphol. Jahrb., vol. 79, pp. 1–53.

Bojanus, L. H. 1819–1821. Anatome testudinis Europeae, indagavit, depinxit, commentatus est. 178 pp. Wilnae.

Bonnet, R. 1889. Beiträge zur Embryologie der Wiederkäuer, gewonnen am Schafei. 2. Vom Auftreten der ersten Ursegmente bis zur Bildung der Extremitätenstummeln. Arch. f. Anat. u. Physiol., Anat. Abt., pp. 1–106.

Broman, I. 1911. Normale und abnorme Entwicklung des Menschen. 808 pp. Wiesbaden.

Bujard, E. 1915. Description d'un embryon humain (Eternod-Delaf), de 20 somites, avec flexion dorsale. Internat. Monatsschr. f. Anat. u. Physiol., vol. 31, pp. 238–266.

Butcher, E. O. 1929. The development of the somites in the white rat (*Mus norvegicus albinus*) and the fate of the myotomes, neural tube, and gut in the tail. Amer. Jour. Anat., vol. 44, pp. 381–439.

Carus, K. G. 1828. Von den Ur-Theilen der Knochen- und Schalengerüstes. 186 pp. Leipzig.

Chiarugi, G. 1890. Le développement des nerfs vague, accessoire, hypoglosse et premiers cervicaux chez les sauropsides et chez les mammifères. Arch. ital. biol., vol. 13, pp. 309–341, 423–443.

Clara, M. 1938. Entwicklungsgeschichte des Menschen. Hochschulwissen in Einzeldarstellungen. 479 pp. Leipzig.

Corner, G. W. 1929. A well-preserved human embryo of 10 somites. Carnegie Inst. Wash. Pub. 394, Contrib. to Embryol., vol. 20, pp. 81–102.

Dandy, W. E. 1910. A human embryo with seven pairs of somites, measuring about 2 mm. in length. Amer. Jour. Anat., vol. 10, pp. 85–108.

Davis, C. L. 1923. Description of a human embryo having twenty paired somites. Carnegie Inst. Wash. Pub. 332, Contrib. to Embryol., vol. 15, pp. 1–51.

Dawes, B. 1930. The development of the vertebral column in mammals as illustrated by its development in *Mus musculus*. Phil. Trans. Roy. Soc. London, B, vol. 218, pp. 115–170.

de Beer, G. R. 1927. The early development of the chondrocranium of *Salmo fario*. Quart. Jour. Microsc. Sci., vol. 71, pp. 259–312.

——— 1937. The development of the vertebrate skull. 552 pp. Oxford.

Fischel, A. 1929. Lehrbuch der Entwicklung des Menschen. 822 pp. Berlin.

Froriep, A. 1883. Zur Entwickelungsgeschichte der Wirbelsäule, insbesondere des Atlas und Epistropheus und der Occipitalregion. I. Beobachtung an Hühnerembryonen. Arch. f. Anat. u. Physiol., Anat. Abt., pp. 177–234.

——— 1886. Zur Entwickelungsgeschichte der Wirbelsäule, insbesondere des Atlas und Epistropheus und der Occipitalregion. II. Beobachtung an Säugethierembryonen. Arch. f. Anat. u. Physiol., Anat. Abt., pp. 69–149.

Gadow, H. F. 1933. The evolution of the vertebral column: a contribution to the study of vertebrate phylogeny. 356 pp. London.

Gage, S. P. 1905. A three weeks' human embryo, with especial reference to the brain and the nephric system. Amer. Jour. Anat., vol. 4, pp. 409–443.

Gegenbaur, C. 1872. Das Kopfskelett der Selachier; ein Beitrag zur Erkenntniss der Genese des Kopfskelettes der Wirbelthiere, vol. 6. 316 pp. Leipzig.

Goethe, J. W. 1820. Zur Naturwissenschaft überhaupt, besonders zur Morphologie, vol. 1, p. 250.

Hayek, H. von. 1923. Ueber den Proatlas und über die Entwicklung der Kopfgelenke beim Menschen und bei einigen Säugetieren. Sitzungsb. d. Akad. d. Wissensch., Wien, vol. 130, p. 25 (Abt. 3).

——— 1927. Untersuchungen über Epistropheus, Atlas und Hinterhauptsbein. Morphol. Jahrb., vol. 58, pp. 269–347.

Heuser, C. H. 1930. A human embryo with 14 pairs of somites. Carnegie Inst. Wash. Pub. 414, Contrib. to Embryol., vol. 22, pp. 135–154.

Holmdahl, D. E. 1934. Neuralleiste und Ganglienleiste beim Menschen. Ztschr. f. mikrosk.-anat. Forsch., vol. 36, pp. 137–178.

Hunter, R. M. 1935. The development of the anterior postotic somites in the rabbit. Jour. Morphol., vol. 57, pp. 501–531.

Ingalls, N. W. 1907. Beschreibung eines menschlichen Embryos von 4.9 mm. Arch. f. mikrosk. Anat., vol. 70, pp. 506–576.

Ingelmark, B. E. 1947. Ueber das craniovertebrale Grenzgebiet beim Menschen. Acta Anat. (suppl. 6), vol. 4, pp. 1–116.

Johnson, F. P. 1917. A human embryo of twenty-four pairs of somites. Carnegie Inst. Wash. Pub. 226, Contrib. to Embryol., vol. 6, pp. 125–168.

Kempermann, C. Th. 1929. Ein Beitrag zum Problem der Regionenbildung der Wirbelsäule. Morphol. Jahrb., vol. 60, pp. 560–612.

Kollmann, J. 1891. Die Rumpfsegmente menschlicher Embryonen von 13 bis 35 Urwirbeln. Arch. f. Anat. u. Physiol., Anat. Abt., pp. 39–88.

Lewis, W. H. 1910. The development of the muscular system. *In* Keibel and Mall (eds.), Manual of human embryology, vol. 1, chap. 12, pp. 454–522. Philadelphia.

Low, A. 1908. Description of a human embryo of 13–14 mesodermic somites. Jour. Anat. and Physiol., vol. 42, pp. 237–251.

Ludwig, E. 1928. Ueber einen operativ gewonnenen menschlichen Embryo mit einen Ursegmente. Morphol. Jahrb., vol. 59, pp. 41–104.

Mall, F. P. 1891. A human embryo twenty-six days old. Jour. Morphol., vol. 5, pp. 459–480.

Martin, P. 1891. Die Entwickelung des neunten bis zwölften Kopfnerven bei der Katze. Anat. Anz., vol. 6, pp. 228–232.

Meckel, J. F. 1820. Handbuch der menschlichen Anatomie. 4 vols. Halle and Berlin.

Muggia, G. 1931. Evoluzione dei segmenti mesodermici occipitali negli embrioni umani. Monit. zool. ital., vol. 42, pp. 275–284.

Müller, Ch. 1906. Zur Entwicklung des menschlichen Brustkorbes. Morphol. Jahrb., vol. 35, pp. 591–696.

Oken, L. 1811. Lehrbuch der Naturphilosophie. 3 vols. Jena.

Owen, Sir Richard. 1846. Lectures on the comparative anatomy and physiology of the vertebrate animals. (Delivered at the Royal College of Surgeons of England.) Hunterian lectures, vol. 2. 308 pp. London.

Padget, D. H. 1948. The development of the cranial arteries in the human embryo. Carnegie Inst. Wash. Pub. 575, Contrib. to Embryol., vol. 32, pp. 205–261.

Payne, F. 1925. General description of a 7-somite human embryo. Carnegie Inst. Wash. Pub. 361, Contrib. to Embryol., vol. 16, pp. 115–124.

Politzer, G. 1928. Ueber einen menschlichen Embryo mit 18 Ursegmentpaaren. Ztschr. f. Anat. u. Entwicklungsgesch., vol. 87, pp. 674–727.

——— 1930. Ueber einen menschlichen Embryo mit sieben Urwirbelpaaren. Ztschr. f. Anat. u. Entwicklungsgesch., vol. 93, pp. 386–428.

Prentiss, C. W. 1910. The development of the hypoglossal ganglia of pig embryos. Jour. Comp. Neurol. and Psychol., vol. 20, pp. 265–282.

Rathke, H. 1839. Ueber die Entwickelung des Schädels der Wirbelthiere. Vierter Bericht über das naturwissenschaftliche Seminar zu Königsberg. 31 pp.

Reichert, K. B. 1838. Vergleichende Entwickelungsgeschichte des Kopfes der nackten Amphibien nebst den Bildungsgesetzen des Wirbelthierkopfes im allgemeinen und seinen hauptsächlichsten Variationen durch die einzelnen Wirbelthier-Klassen. xxi + 275 pp. Königsberg.

Reiter, A. 1942. Die Frühentwicklung der menschlichen Wirbelsäule. I. Mitteilung. Die Frühentwicklung der Brustwirbelsäule. Ztschr. f. Anat. u. Entwicklungsgesch., vol. 112, pp. 185–220.

——— 1944. Die Frühentwicklung der menschlichen Wirbelsäule. II. Mitteilung. Die Entwicklung der Occipitalsegmente und der Halswirbelsäule. Ztschr. f. Anat. u. Entwicklungsgesch., vol. 113, pp. 66–104.

Remak, R. 1850–1855. Untersuchungen über die Entwickelung der Wirbelthiere. 194 pp. Berlin.

Rosenberg, E. 1876. Ueber die Entwickelung der Wirbelsäule und das Centrale Carpi des Menschen. Morphol. Jahrb., vol. 1, pp. 83–199.

Saint-Hilaire, G. 1818. Philosophie anatomique. 1. Des organes respiratoires sous le rapport de la détermination et de l'identité de leurs pièces osseuses. 517 pp. Paris.

Schmeidel, G. 1932. Die Entwicklung der Arteria vertebralis des Menschen. Morphol. Jahrb., vol. 71, pp. 315–435.

Sensenig, E. C. 1943. The origin of the vertebral column in the deer-mouse, *Peromyscus maniculatus rufinus.* Anat. Rec., vol. 86, pp. 123–141.

——— 1949. The early development of the human vertebral column. Carnegie Inst. Wash. Pub. 583, Contrib. to Embryol., vol. 33, pp. 21–41.

——— 1951. The early development of the meninges of the spinal cord in human embryos. Carnegie Inst. Wash. Pub. 592, Contrib. to Embryol., vol. 34, pp. 145–157.

Spix, J. B. von. 1815. Cephalogenesis sive capitis ossei structura, formatio et significatio, per omnes animalium classes, familias, genera ac aetates digesta, legesque simul psychologiae, cranioscopiae ac physiognomiae inde derivatae. 72 pp. Monachii.

Sternberg, H. 1927. Beschreibung eines menschlichen Embryos mit vier Ursegmentpaaren, nebst Bemerkungen über die Anlage und früheste Entwicklung einiger Organe beim Menschen. Ztschr. f. Anat. u. Entwicklungsgesch., vol. 82, pp. 142–240.

Streeter, G. L. 1904. The development of the cranial and spinal nerves in the occipital region of the human embryo. Amer. Jour. Anat., vol. 4, pp. 83–116.

Thompson, P. 1907. Description of a human embryo of twenty-three paired somites. Jour. Anat. and Physiol., vol. 41, pp. 159–171.

Vogt, K. 1842. Untersuchungen über die Entwicklungsgeschichte der Geburtshilfkröte (*Alytes obstetricans*). 134 pp. Solothurn.

Weiss, A. 1901. Die Entwickelung der Wirbelsäule der weissen Ratte, besonders der vordersten Halswirbel. Ztschr. f. wissensch. Zoöl., vol. 69, pp. 492–533.

Wen, I. C. 1928. The anatomy of human embryos with 17 to 23 pairs of somites. Jour. Comp. Neurol., vol. 45, pp. 301–376.

West, C. M. 1930. Description of a human embryo of eight somites. Carnegie Inst. Wash. Pub. 407, Contrib. to Embryol., vol. 21, pp. 25–35.

——— 1937. Human embryo of 25 somites. Jour. Anat., vol. 71, pp. 169–200.

Wijhe, J. W. van. 1882. Ueber die Mesodermsegmente und die Entwickelung der Nerven des Selachierkopfes. 50 pp. Amsterdam.

Wyburn, G. M. 1944. Observations on the development of the human vertebral column. Jour. Anat., vol. 78, pp. 94–102.

ABBREVIATIONS USED IN PLATES

a. v. a., atlas ventral arch
b. o., basioccipital rudiment
c. a. 1., first cervical artery
c. m. 1., first cervical myotome
e. s., epichordal strand
g. c. 1., first cervical ganglion
g. c. 2., second cervical ganglion
g. Fr., Froriep's ganglion
h. s., hypochordal strand
i. v., intersegmental vessel
m., myotome
m. r. d., membrana reuniens dorsalis
m. p., myotomic plate
m. pr., meninx primitiva
n. p., neural process
n. p. c. 1., neural arch atlas
n. p. c. 2., neural arch axis
n. p. o., occipital neural process
n. s. a., spinal accessory nerve
o. a., odontoid, atlantal portion
o. m. 1., first occipital myotome
o. s. 1., first occipital somite
p. a. m., primitiva axial muscles
p. c., primary centrum
p. d., perichordal disk
p. h. a., primitiva hypoglossal artery
p. s., perichordal sheath
r. h., rootlets of hypoglossal nerve
s. f., sclerotomic fissure

PLATE 1

FIG. 1. Transverse section through cervical somite of embryo no. 5074, 10-somite Corner embryo, age group x, thickness of section 10 microns. × 200. Paired somites with myocoel, ventromesial migration of sclerotomic tissue, and continuity of notochord and gut.

FIG. 2. Transverse section of no. 7611, 16 somites, xi, 8 microns. × 100. Paired somites, myocoels, ventromesial migration of sclerotomic tissue, and dorsal evagination of notochord from gut.

FIG. 3. Transverse section of occipital region of no. 7611, 16 somites, xi, 8 microns. × 200. Nonsegmented densely cellular mesenchyme situated between otic plate and first somite and notochord shows a tubular structure.

FIG. 4. Frontal section of no. 6050, 19 somites, xi, 10 microns. × 100. Shows regressive condition of first somite.

FIG. 5. Sagittal section of cervical region of no. 7724, 29 somites, xii, 8 microns. × 100. Intersegmental vessels, indication of sclerotomic fissures, and myotomes with remnants of myocoels.

FIG. 6. Transverse section of cervical region of no. 6097, 25 somites, xii, 10 microns. × 100. Separation of notochord from neural tube and gut, sclerotomic cells surrounding notochord, and myotomic plates.

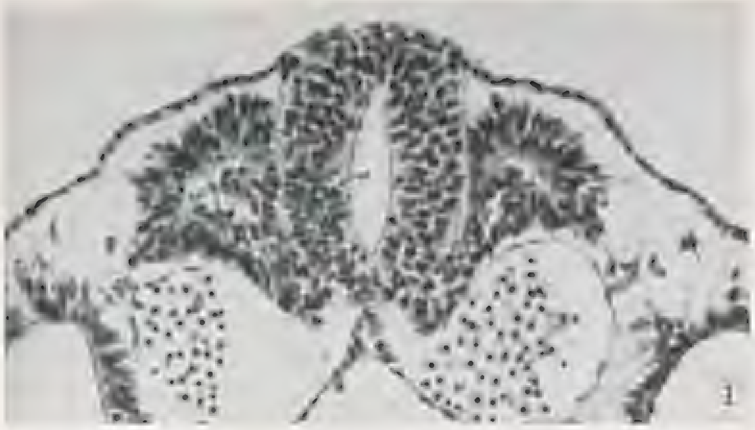

1

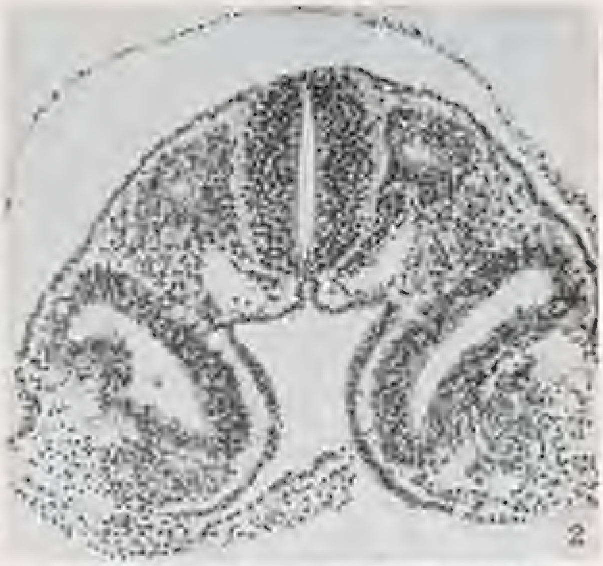

2

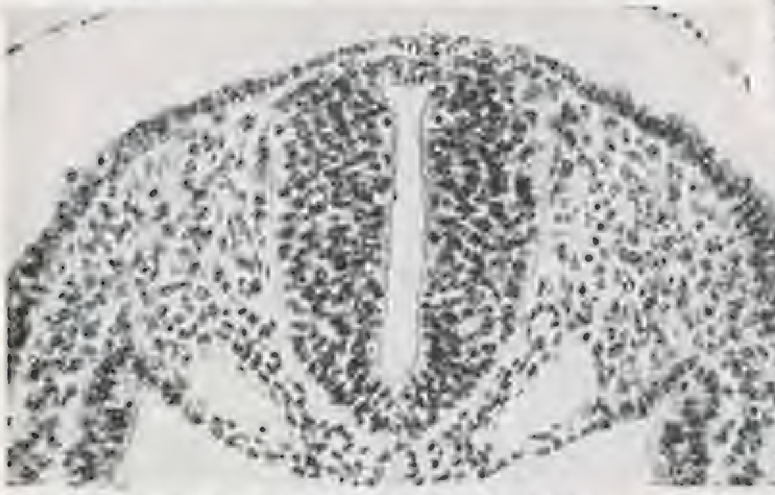

3

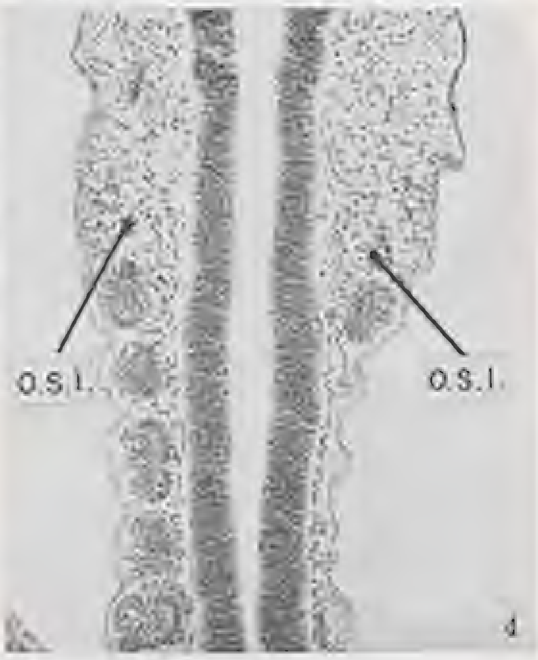

4

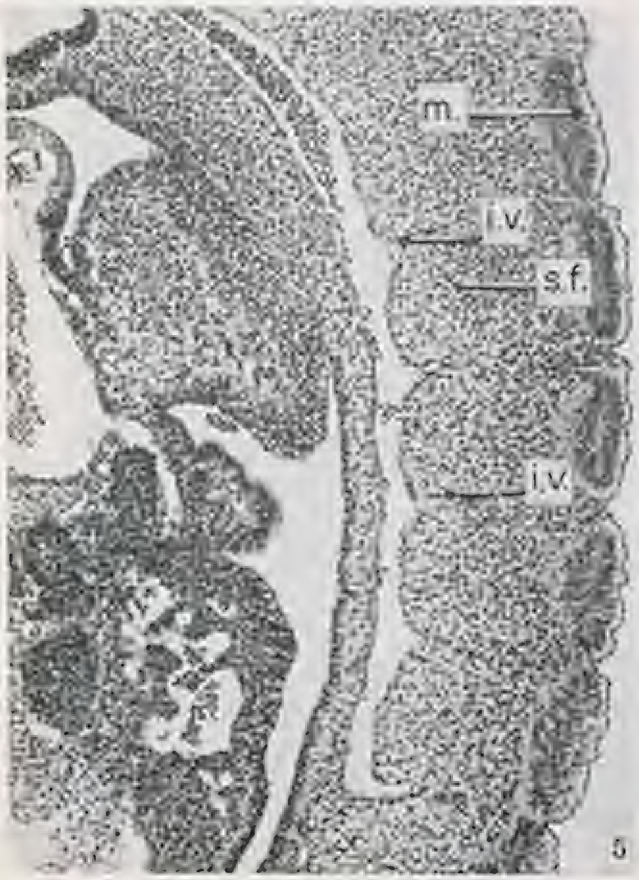

5

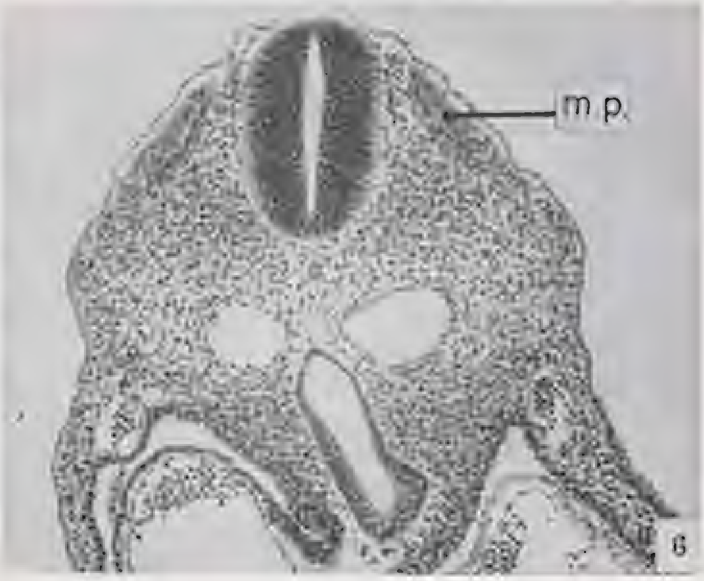

6

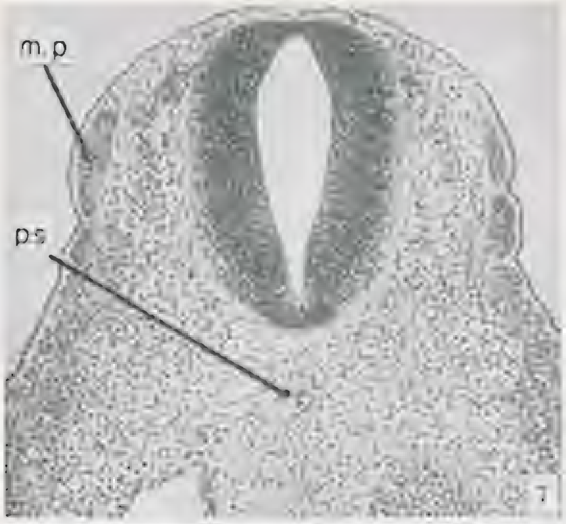

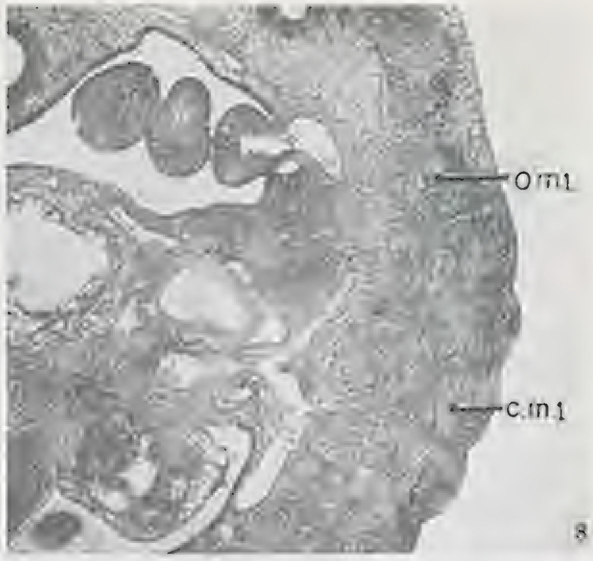

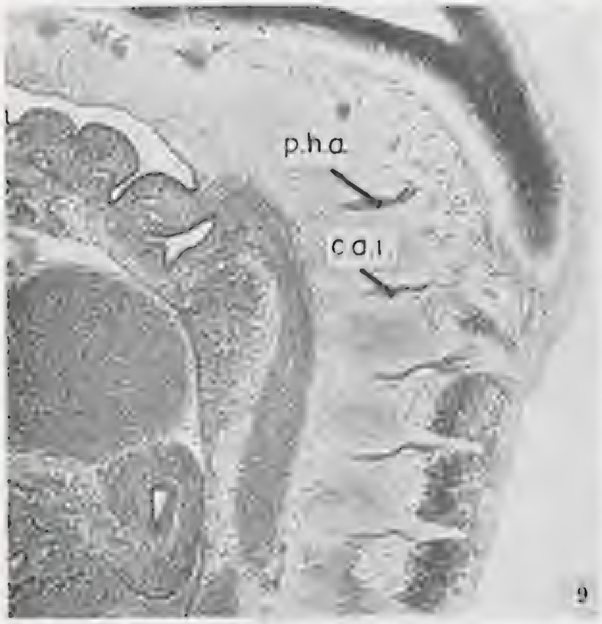

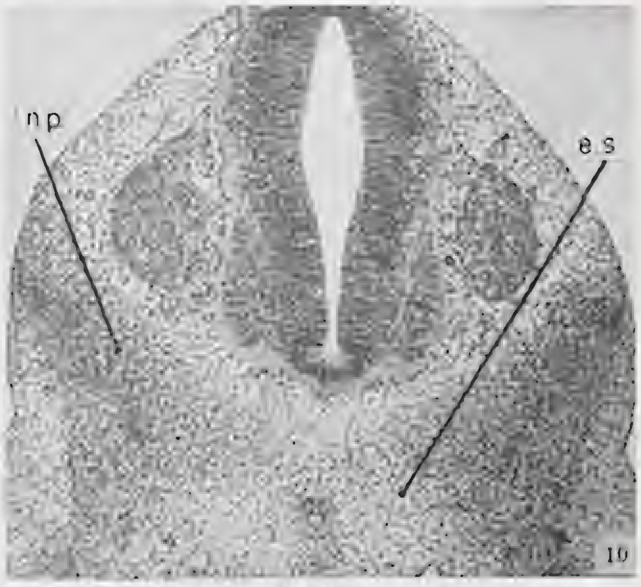

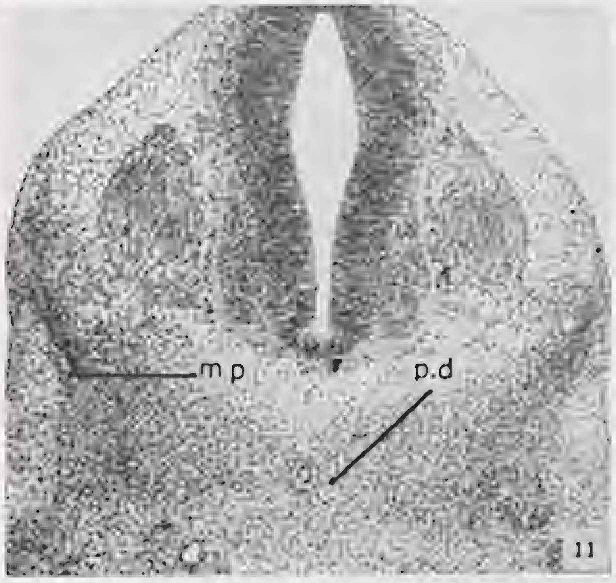

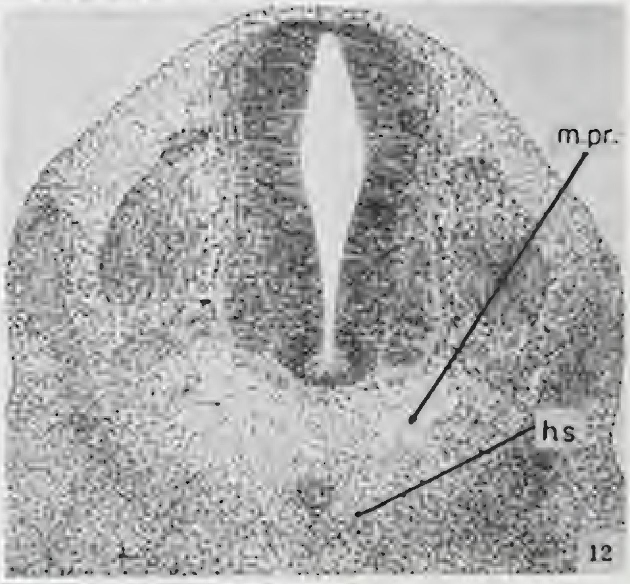

Fig. 7. Transverse section of cervical region of embryo no. 8066, 5.6 mm., age group xii, thickness of section 8 microns. ×80. Continued separation of notochord from neural tube and gut, myotomic plates, and orientation of sclerotomic cells around notochord forming perichordal sheath.

Fig. 8. Sagittal section of occipitocervical region of no. 8239, 4.3 mm., xiii, 8 microns. ×36. Shows 4 occipital myotomes, the first being very small.

Fig. 9. Sagittal section of occipitocervical region of no. 6739, 8 mm., xiv, 20 microns. ×36. Note intersegmental vessels with primitive hypoglossal artery and first cervical artery bounding the most caudal occipital segment.

Figs. 10–12. Transverse section of cervical region of no. 7829, 7 mm., xiv, 8 microns. ×68. Notochord with perichordal sheath, inward bulge of myotomic plate, neural processes, large ganglia, and meninx primitiva. Epichordal strand of cells (fig. 10), perichordal disk (fig. 11), and hypochordal strand of cells (fig. 12).

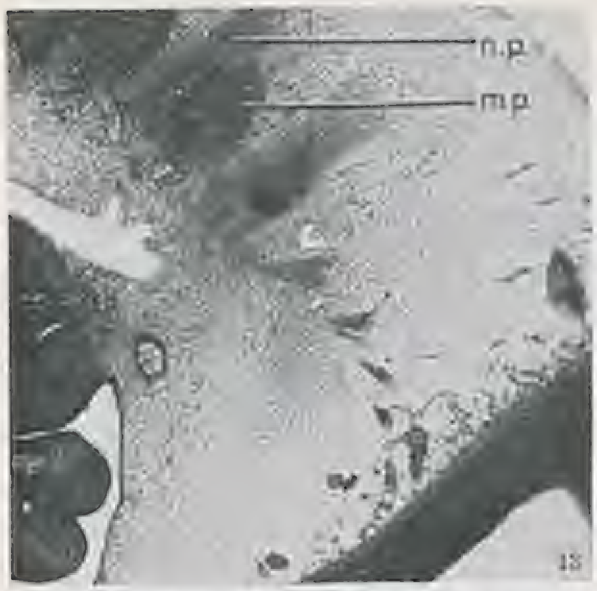

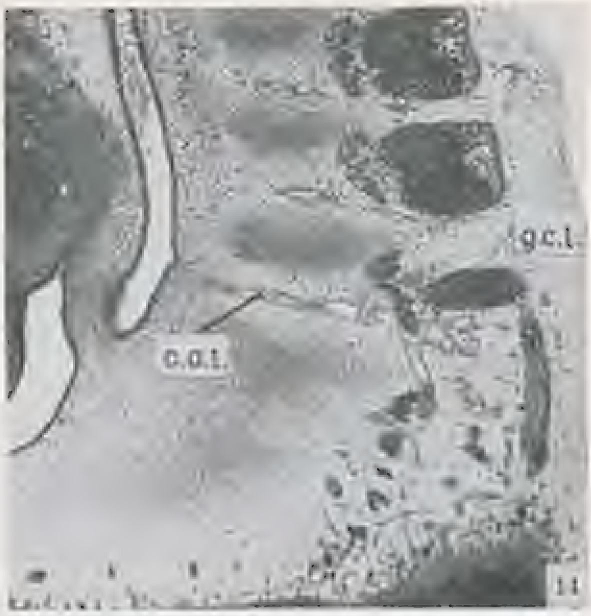

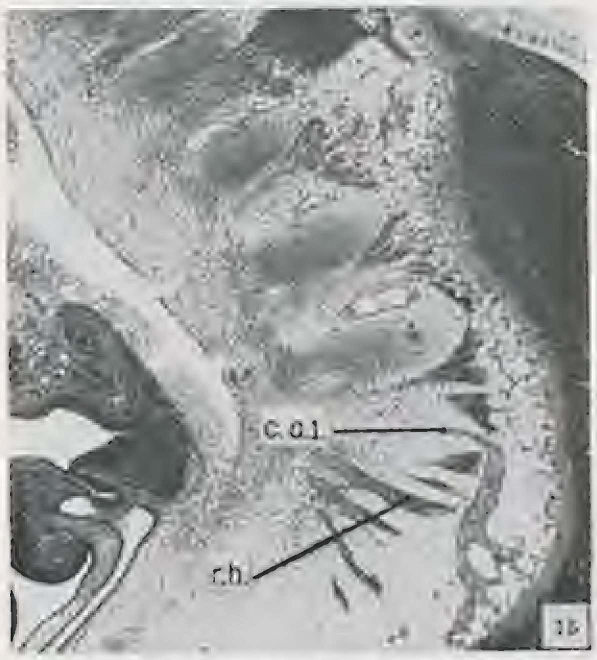

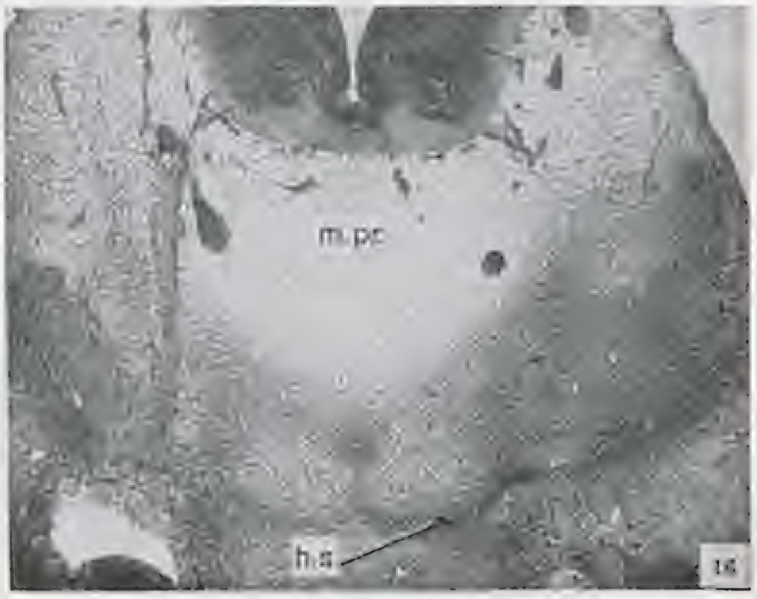

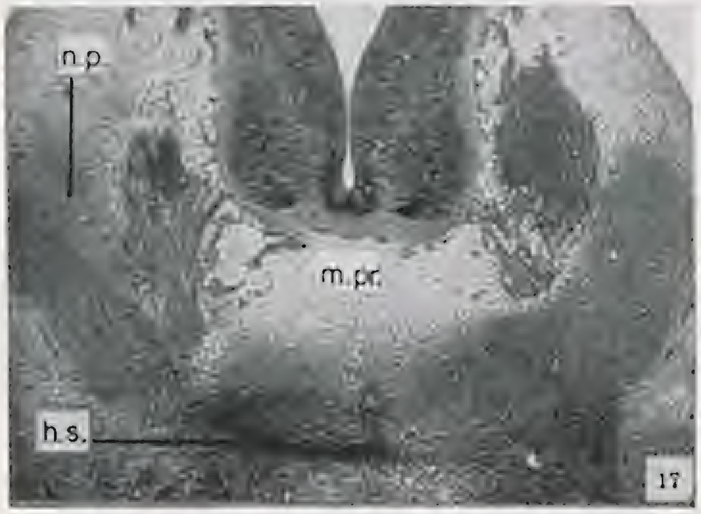

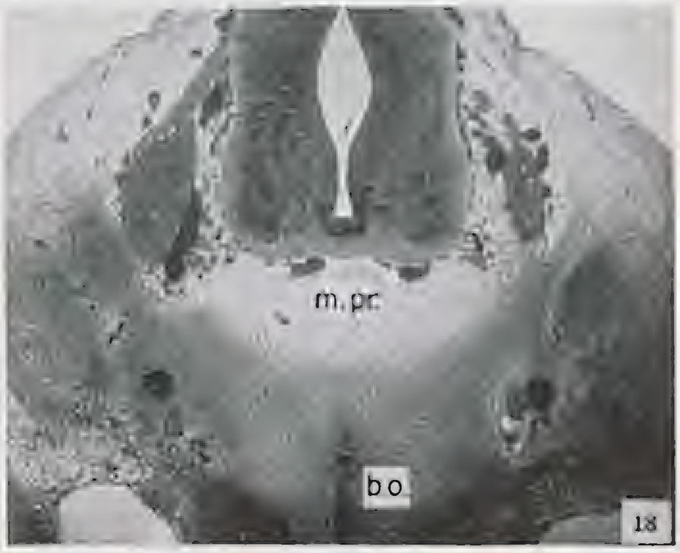

FIGS. 13–15. Sagittal sections of occipitocervical region of embryo no. 8966, 7.1 mm., age group xv, thickness of section 10 microns. ×48. Myotome, neural-arch rudiments, and rootlets of the hypoglossal nerve (fig. 13); large typical spinal ganglion, reduced first cervical ganglion and Froriep's ganglion, intersegmental vessels, loosely cellular cranial sclerotome-halves, and densely cellular caudal sclerotome-halves (fig. 14); intersegmental vessels and rootlets of the hypoglossal nerve (fig. 15).

FIGS. 16, 17. Frontal sections of upper cervical region of no. 8112, 10.9 mm., xvi, 8 microns. ×48. Note medial vertebral rudiments surrounding the notochord with subchordal strand and lateral vertebral arch rudiments.

FIG. 18. Transverse section of occipital and upper cervical region of no. 8101, 13 mm., xvii, 10 microns. ×36. Meninx primitiva, ventral displacement of spinal ganglia, and rudiments of basioccipital bone and atlas.

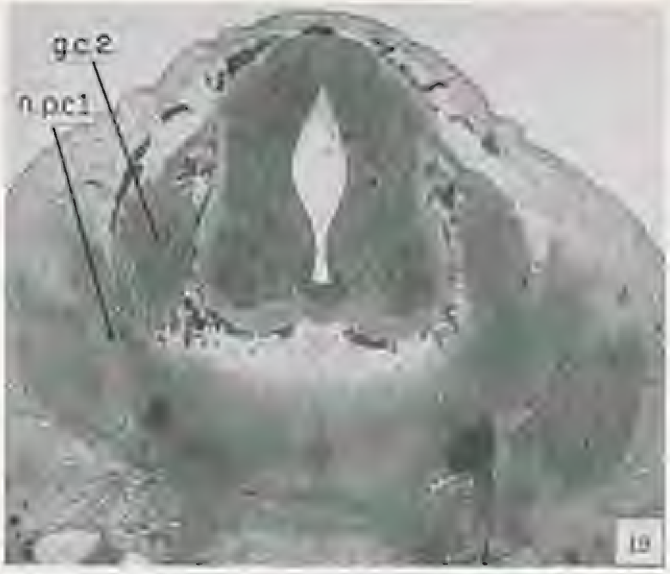

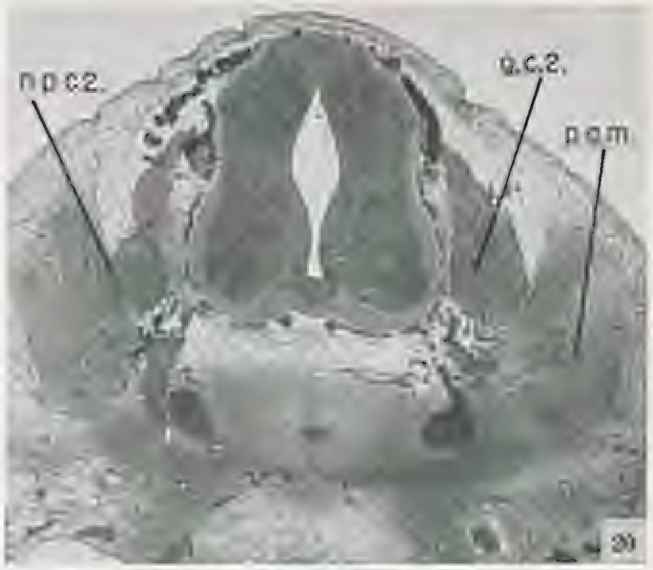

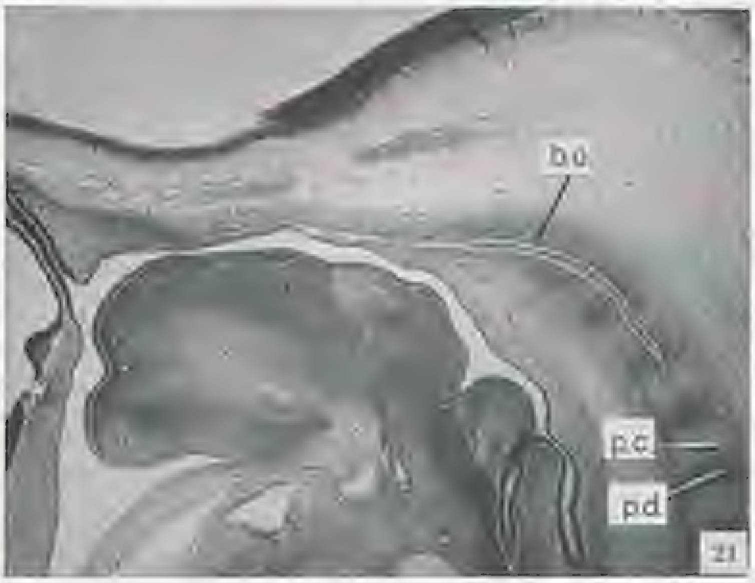

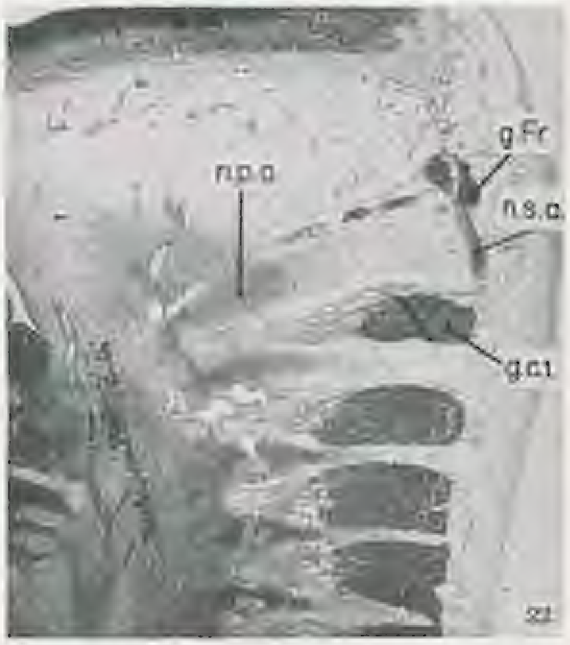

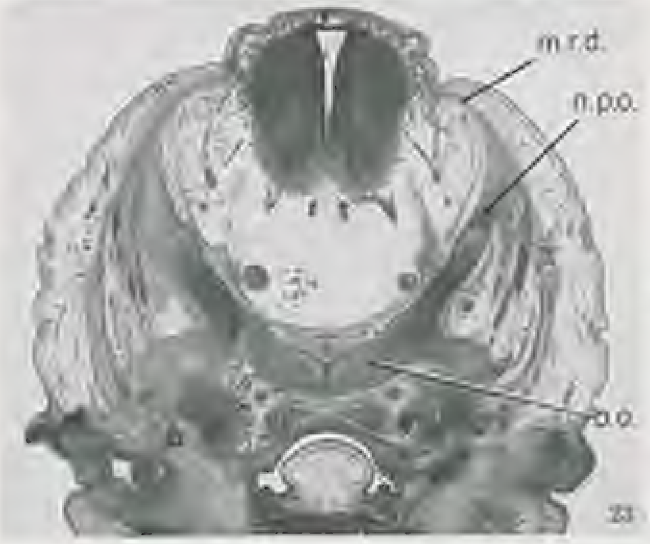

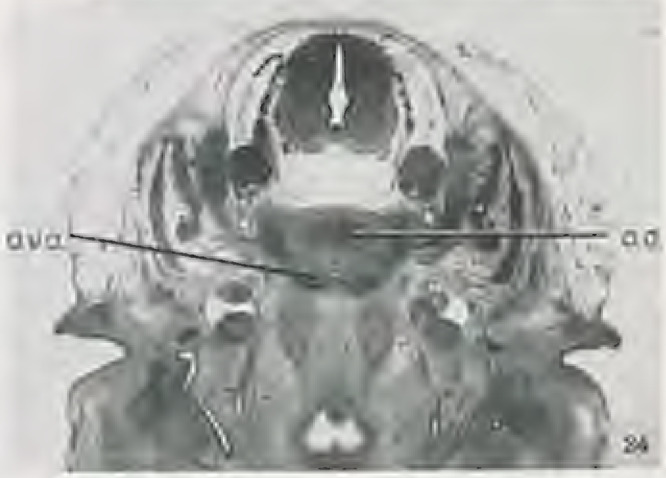

Figs. 19, 20. Transverse sections through cervical region of embryo no. 8101, 13 mm., age group xvii, thickness of section 10 microns. ×36. Meninx primitiva, membrana reuniens dorsalis, ventral migration of ganglia, rudimentary axial muscle masses. Arch of atlas, areas of chondrification of atlantal body (fig. 19). Arch and chondrified body of atlas (fig. 20).

Figs. 21, 22. Sagittal sections of no. 6519, 10.8 mm., xvii, 8 microns. ×32. Occipital and upper cervical notochord, intervertebral disks, and chondrified bodies of cervical vertebrae (fig. 21); cervical ganglia, the first small, Froriep's greatly reduced; arch rudiments of cervical and most caudal occipital segments (fig. 22).

Fig. 23. Transverse section through occipitocervical region of no. 7254, 22.5 mm., xxi, 20 microns. ×12. Chondrified basioccipital, tip of odontoid, cell proliferation from tip of occipital arch rudiment, and membrana reuniens dorsalis.

Fig. 24. Transverse section through first cervical segment of no. 7274, 18 mm., xx, 10 microns. ×12. Ventral migration of second cervical ganglion, separation of odontoid from ventral atlantal arch, and further subdivision of axial musculature.

CONTRIBUTIONS TO EMBRYOLOGY, NO. 249

THE FORM AND THE FUNCTIONS OF THE UTERINE BLOOD VESSELS IN THE RHESUS MONKEY

George W. Bartelmez

Department of Embryology, Carnegie Institution of Washington, Baltimore,
and Department of Anatomy, The University of Chicago, Chicago

With fifteen plates

CONTENTS

PAGE

Introduction 155

Endometrial Zones 156

Material and Methods 157

Protocols 157

- Transition from Menstruation to Repair 157
- Transition from Repair to Follicular Phase 158
- Early Follicular Phase 159
- Late Follicular Phase 159
- Phase of Ovulation 161
- Early Progravid (Preimplantation) Phase 161
- Early Progravid Endometrium Associated with a Recent Corpus Aberrans 163
- Progravid Phase 163
- Transitions from Progravid to Ischemic Phase 166
- Ischemic Phase 167
- Ovulatory Menstruation 167
- Anovulatory Menstruation 170

Discussion 172

- Endometrial Arteries 172
  - Factors That Influence the Form of Type I Arteries 173
  - Constrictions 175
- Capillary Beds 176
- Venous System 177
- Adaptive Significance of Certain Unique Features of the Uterine Vascular System 178

Summary 179

Literature Cited 180

THE FORM AND THE FUNCTIONS OF THE UTERINE BLOOD VESSELS IN THE RHESUS MONKEY[1]

INTRODUCTION

Cyclic changes in the vasculature might have been inferred from the observations of Hitschmann and Adler (1908) on the stroma of the endometrium. The reasons why no such study was made for 18 years are apparent in the pioneer work of Freund (1904), which indicated the difficulties of obtaining a series of normal human uteri available for injection and of injecting the endometrium. Only 2 of his 23 cases can be regarded as normal, and current dogmas led him to brand one of these as "prematurely senile." To obtain a satisfactory injection, he found it necessary to wait for 1 to 4 days after death or removal at operation; by that time the endometrium is well-nigh worthless histologically. The seriation of the uteri for cyclic changes, however, demands good fixation. The first study of cyclic changes in the vasculature of the endometrium was that of Saito (1926). His paper is written in Japanese, and has only a brief German summary. The review in *Berichte der Gynäkologie* is likewise brief. His photomicrographs from thin sections show only capillary beds and premenstrual congestion. Diagrams of the "proliferative" and the "secretory" phases show the closer capillary mesh superficially and a wider capillary mesh in the "spongiosa" as compared to the "basalis"; they indicate little understanding of cyclic change in arterial or venous patterns.

The basis for thorough anatomical and physiological studies of the menstrual cycle was laid by Corner (1923), when he introduced the rhesus monkey into the field and demonstrated its fundamental similarity to the human cycle. An abundance of normal, perfectly preserved, and expendable material was made available; the ovarian and uterine cycles could be accurately correlated; the age of corpora lutea could be determined; and adequately controlled physiological experiments with hormones could be performed. With this background, significant studies on the vascular changes during the cycle could be made.

The first of these was Daron's (1932, 1936). He introduced a vascular injection technique that came closer to revealing physiological states than any standard method. He injected intravenously into the lightly anaesthetized animal a nonirritating colloidal solution which produced no clotting. The pelvic organs were rapidly frozen while the blood was circulating. He was able to demonstrate a condition unique among mucous membranes, namely a superficial zone in corpus and fundus supplied exclusively by a distinct system of arteries. Radial arteries pass from the stratum vasculare, often with few branches, to the endometrium, where they become coiled (Daron, type I). Usually they have only terminal branches. Shortly before and during menstruation, he found constrictions in the myometrial components (radial arteries) that produced an ischemia in the superficial zone. He pointed out the significance of the ischemic injury for the understanding of menstrual sloughing. These conditions explain the superficial loss in menstruation which could not be accounted for by the general contraction of the myometrium to which Westman (1932) ascribed the menstrual ischemia. Myometrial contractions powerful enough to occlude vessels as large as radial arteries have been found by Caldeyro-Barcia y Alvarez (1953) only in cases of severe eclampsia. Daron concluded that, after the initial arterial hemorrhage, the menstrual blood comes from superficial veins torn during sloughing. In 1937 he briefly summarized his observations on the venous network and noted the presence of "venous lakes."

In this field, all observations on dead material must be controlled by the detailed and extensive observations of Markee (1940, 1950*a*) on living endometrial transplants. His findings are invoked on many of the following pages to justify inferences from material prepared for histological study. He has recently summarized his work on ocular transplants in rhesus monkeys and discussed its implications (1950*b*). His observations on the blood flow and the behavior of the coiled arteries provide direct evidence of the immediate cause of menstrual extravasation and sloughing. Milder but fundamentally similar changes occur in the sexual skin of rhesus (Collings, 1926). The cyclic changes in the vasculature of the human bulbar conjunctiva are similar and suggest that the reactions are systemic (Landesman *et al.*, 1953). Abnormal exacerbations appear in vicarious menstruation.

Hasner (1946) has provided the only description of the human uterine vasculature based on an adequate series of normal uteri, well injected and prepared, and studied judiciously, not simply for the purpose of substantiating an hypothesis. He obtained uteri and ovaries from 100 necropsies, 37 of which came from suicides and were presumably normal. The ovaries were sliced grossly; the corpora lutea were not studied histologically. He had, in addition, 50 curettings adequately preserved for detailed histological study. He concludes that the form of the coiled arteries in the "first proliferation phase" is influenced both by the extent of tissue loss during the preceding menstruation and by their subse-

---

[1] Aided by a grant from The Dr. Wallace C. and Clara A. Abbott Memorial Fund of the University of Chicago.

quent growth. The thickening of the stroma outstrips the increase in length of the arteries, which have thin walls. There is one coiled artery per square millimeter. In the "secondary proliferation phase," they grow in length and diameter, their branches reach the surface, and the coils are well separated from one another. In the next phase they may become complex deep in the "functional" zone, and the adventitia of the adjacent coils fuses. Branches may extend parallel to the surface. With the development of edema in the "secondary secretory phase," the dense stroma of the arterial columns loosens, and the vessels appear stretched. Some are contracted before menstrual desquamation. During the flow the coiling decreases in the intact area. In the phase of regeneration the arteries are coiled at the surface, and have many lateral branches. The basal capillary net is irregular in form and is supplied by coiled arteries, basal arteries, and rami of myometrial arteries. In the primary proliferation phase the superficial capillaries are parallel to the surface, and the glandular and interstitial nets develop gradually.

In addition, Hasner made hysteroscopic observations on two normal young women, one on day 21, the other on day 24. He noted a bluish tinge of the endometrium, which he associated with dilated capillaries, and a reduced rate of blood flow.

Markee (1940) had observed that in ovulatory cycles the transplants became paler in his "2d growth phase." He was able subsequently (1950*a*) to determine by stroboscopic illumination the rate of blood flow in long capillaries (of "zone II") through which a single row of blood corpuscles was passing. The observations were made on ocular transplants in 5 rhesus monkeys during ovulatory cycles. The rate of movement on days 5 to 7 of the cycle increased from a mean of 388 microns per second to 443 microns on days 11 to 15. There was a drop on day 16 ranging from 401 to 430 microns (mean, 422). This finding of a regression at about the time of ovulation is of particular interest in connection with his observation that the transplants may shrink at this time (see p. 161). The range in rate of flow on days 17 to 25 was from 398 to 440 microns. On day 26 the average reading was 378 microns, and it remained in this vicinity from the 4th to the 2d *premenstrual* day; then stasis supervened. Taken in conjunction with the various experiments he had made with ovarian hormones on spayed monkeys, this finding indicates a fall of available hormones as the cause of the ischemic phase, which in turn is the essential prelude to menstruation.

Phelps (1946) has studied the effects of ovarian hormones on ocular transplants of endometrium in spayed rhesus monkeys. *In vivo* observations and subsequently prepared sections demonstrated the prime importance of stromal ground substance in changing the volume of the transplants. In 1947 she pointed out the cumulative effects of several courses of hormone injections on the vasculature and on the duration of bleeding in such transplants.

Kaiser (1947) discusses the coiled arteries of primates on the basis of the literature and observations on a few thin sections. He points out that Daron's finding of simply "coiled" arteries in anovulatory menstruation proves that coiling is not necessarily involved in menstrual degeneration. He also finds (1947) no coiled arteries in new world monkeys, which probably menstruate, and correlates the scanty discharge with the simple form of the arteries. It must be remembered in this connection that the menstrual discharge in anovulatory menstruation of rhesus monkeys cannot be routinely distinguished from that of ovulatory menstruation (Hartman, 1932).

Ramsey (1949), in her studies on the development of placental vessels in rhesus monkeys, describes the afferent coiled arteries in early stages and their subsequent uncoiling associated with the stretching of the decidua basalis. She concludes that the coiling is an adaptation for the form changes of the uterus during pregnancy.

Reynolds (1949) reviewed and evaluated the extensive literature on the structure and functions of the uterine vasculature and its relations to the menstrual cycle. Schlegel (1945 and 1946), Dalgaard (1946), and Okkels (1950) concluded that there are arteriovenous anastomoses in the endometrium. Their failure to offer any valid evidence for this hypothesis is pointed out by Bartelmez (1956).

ENDOMETRIAL ZONES

The horizontal zoning proposed by Bartelmez *et al.* (1951) for convenience in description is based on differences in the reactions of the stroma and glands at different levels in the rhesus monkey.

Zone I consists of the surface epithelium and a narrow band of stroma that is reorganized postmenstrually and at first resembles granulation tissue. During the follicular phase it remains avascular. In the course of the progravid phase it is vascularized and can usually be recognized by its loose structure. In early pregnancy it becomes highly edematous, especially at the margins of the placental sites.

Zone II has more interglandular stroma than glands, and there are striking changes in the ground substance and reticulum of the stroma during the cycle. In the corpus the glands tend to be perpendicular to the surface. The gland cells in zones II and III respond promptly to hormonal stimuli. In *Homo,* predecidual cells usually develop in this zone premenstrually.

Zone III is distinguished by the crowded glands, irregular in form and sometimes branched. When secretion accumulates in the glands, the stroma is reduced to thin septa. Zones II and III together constitute the "functionalis" of Schröder.

Zone IV has a denser stroma (except during repair); its connective-tissue fibers are coarser than in zones II and III; mitoses in the glands become abundant later in the follicular phase and persist into the progravid phase. Sometimes the gland cells respond to the corpus luteum hormones, but more tardily than do those in zones II and III. In the follicular phase they are actively secreting. When new glands are formed, they arise in this zone (O'Leary, 1929).

MATERIAL AND METHODS

In order to study the vessels of the uterus as a whole and to obtain three-dimensional views of capillary beds as well as arteries and veins, I. Rossman and the author made postvital injections of the pelves of a series of rhesus monkeys in 1938 to 1940. The systematic study of the material was interrupted by war and other duties. Various stages in the cycle were obtained by recording changes in the color of the sex skin with the aid of a hemoglobinometer chart, by doing rectal palpations (Hartman, 1930), and occasionally checking with laparotomies. The 25 normal adult animals selected for description can be grouped as follows:

Repair	1
Follicular phase	4
Ovulation	2
Progravid phase	7
Ischemic phase	4
Ovulatory menstruation	3
Anovulatory menstruation	4

In 4 of these animals the endometrium presents features of two phases.

If the cyclic changes in the vasculature are to be understood, it is essential that the material be well fixed so that the vessels can be studied histologically. The details of the histologic study and comparisons with human material are reserved for a future publication. The difficulty of obtaining satisfactory injections of the endometrium immediately after death was overcome by the use of vasodilators. With the exception of 2 uteri prepared by the method of Daron (1936), the procedure was as follows (see Rossman and Bartelmez, 1957): After being anaesthetized with nembutal, the animal was killed with illuminating gas containing CO. The abdominal aorta was immediately cannulated, and the pelvic organs were perfused with a minimum of warm 1 per cent aqueous $NaNO_2$ to which a trace of histamine had been added. Raising and lowering the perfusion bottle gave rhythmic fluctuations in pressure from 60 to 110 mm. Hg. A colored gelatin injection mass was then introduced. The most satisfactory injection mass proved to be 1 part of india ink to 9 parts of 1 per cent gelatin. When the uterus appeared well injected, a suspension of deeply stained starch grains was substituted. The starch grains averaged 10 microns in diameter and rarely passed beyond the arterioles (see p. 166). After chilling, the uterus was opened, and a wedge of the wall was removed for cytological study. The rest was sectioned serially at about 500 microns with an occasional section between 50 and 300 microns.

Preparations of this sort cannot be interpreted by a superficial examination under low powers of the microscope. The details in a well injected specimen cannot be fully appreciated until they have been projected and drawn. This makes it necessary to dissect out individual vessels optically, following their branches with high powers of the microscope.

The author is indebted to Dr. I. Rossman and Dr. David Clark and to Miss C. M. Bensley for invaluable expert help in the preparation of this material. Discussions with Dr. G. W. Corner during the past six years have been stimulating and helpful.

PROTOCOLS

Transition from Menstruation to Repair

B329. The material was obtained on day 5[2] of an April cycle before the flow had ceased. The 24-day March cycle had been anovulatory. In February, sex skin color and rectal palpation had indicated ovulation on the left, and this was confirmed by the finding of the corresponding corpus luteum. Previous ovulations are indicated by two older corpora lutea in each ovary.

The endometrium measures up to 1.9 mm. Figure 58 (pl. 14) presents a typical field. Most of the surface is denuded. The glands are sinuous, with low, slim cells. In the superficial disorganized zone, which comprises about 15 per cent of the endometrium, the stroma is exceedingly dense (420 stroma cells plus 24 erythrocytes and 8 wandering cells per 100 square microns). Relatively few of these cells appear to be degenerating. It is significant that zone II can be recognized promptly after rehydration of the mucous membrane begins. Zone II has an average of 200 cells. The uterine lumen is dilated with the discharge. These conditions are features of menstruation. Features of the phase of repair are: the sheets of epithelium that spread out from the gland mouths; the actively secreting glands that have a few mitoses in zone II; the looser stroma of zone IV compared with earlier stages (200 stroma cells plus 4 mononuclear granule cells per unit area). The vasculature also shows transitional conditions.

---

[2] The misreading of the original notes is responsible for the statement as to the last menstruation of this case in Bartelmez, Corner, and Hartman, 1951, p. 131.

Arteries. Figure 1 (pl. 1) shows a coiled artery with terminal branches that extend into the disorganized zone (indicated by fine stipple). Since such rami are characteristic of zone II in other phases of the cycle, they provide evidence that all of zone II had not been shed. The main stem and the superficial branches appear compressed. Evidence that this is an indication of the preceding involution is summarized on page 174. Extravasation of ink (indicated by small rings), as at the right, is rare. Many arterioles are dilated, however, although the pressure did not exceed 91 mm. Hg. In some arterioles, starch grains entered as far as the disorganized zone. In this zone the terminal arterioles reach a diameter of 42 microns, and, close to the necrobiotic end, they may have two or three ranks of muscle cells. The elastic tissue has dispersed or disappeared superficially, and, in the disorganized zone, the muscle cells are vacuolated. These conditions are typical of menstruation. In figure 1 (pl. 1), the ramus at the left had retained some capillary connections, and the circulation through them may have been restored, although in this spot the surface is still denuded. Many arteries that extend through the endometrium are not coiled but merely sinuous, as in figure 2 (pl. 1). It would seem that they had undergone extensive involution during the preceding anovulatory cycle. Most radial arteries are dilated, and at the endomyometrial junction the injection of the endometrial arteries is complete so that they could be counted.

Capillaries. Despite the excellent arterial injection, the capillary beds appear incomplete. Figure 8 (pl. 2) presents a capillary bed taken just below the dense pycnotic zone in an area where the surface epithelium had been restored. It shows wide capillaries (solid black) supplied by a terminal arteriole. The ends of at least 10 of the capillaries are not cut off but are blind ends lying within the 480-micron section, indicating that the rest of the vessel was still collapsed or had perhaps degenerated. The venous net, however, seems to be complete. Some arterial capillaries are long; others promptly join venous capillaries which form a close network. Many of these capillaries were omitted from the drawing for the sake of clarity. Even the wider ones are simple endothelial tubes without an adventitial sheath. There is no reticular framework in this zone.

Veins. Venules form an all-pervading irregular network that is more or less dilated as in other late menstrual stages. Bits of it are shown in figures 1 and 2 (pl. 1). Dilated veins or sinuses may extend through most of the thickness of the endometrium (fig. 3, pl. 1). The emissaries to the myometrium are usually slim, even when they drain sinuses. The veins of the inner half of the myometrium are inconspicuous.

Transition from Repair to Follicular Phase

B334. The specimen was obtained on day 8 of a May cycle, 5 days after the end of external bleeding. The preceding cycle had been anovulatory; ovulation had occurred in February and March, as indicated by palpation and corpora lutea. The largest follicles in the ovaries measure 2 mm.

The endometrium is low (1.2 to 2.3 mm. in corpus); other features of repair are dense superficial stroma, with red blood corpuscles scattered about in it, and minute aggregations of mononuclear leucocytes. There are small avascular areas at the surface, 14 to 70 microns thick, where the stroma is loosening. These herald the typical zone I of the follicular phase (see Bartelmez *et al.*, 1951, p. 109). In zone II the stroma has loosened (average 136 plus 8 wandering cells per 100 square microns). The surface epithelium is continuous; the glands of the corpus are sinuous with narrow lumina, but cells are actively secreting. Mitoses in the superficial epithelia average 2.1 per cent. These features and the observed brightening of the sex skin indicate the beginning of a typical follicular phase.

Arteries. Type I arteries are, for the most part, simple in form, as is usual after an anovulatory cycle (figs. 4*d*, 5*c*, pl. 1). There are only 6 in the entire uterus as contorted as that in figure 5*a* (pl. 1), which resembles the one in Daron's (1936) figure 1 from a specimen of the repair phase. The type I vessels basally have the general structure of other small arteries, but many continue into zone II as straight tubes with a thin media of loosely arranged cells. The injection mass herniated the endothelium between the loose elements of the media; this occurred only in specimens from the follicular phase. The vessel appears to be stretched and the media loosened as zone II thickens with the accumulation of stromal ground substance. This apical segment has numerous lateral branches and supplies the superficial ¼ to ½ of the endometrium (fig. 4, pl. 1). The type II arteries vary in length, but promptly break up into tufts of precapillary arterioles (fig. 5*b*, pl. 1).

Capillaries. Zone I is thin, and the capillary net of zone II may extend to within 14 microns of the surface epithelium (figs. 4, 5*a*, *c*, pl. 1). In some areas this net reaches a width of 77 microns. It is dilated in a band 5 to 13 microns wide. Figure 43 (pl. 11) shows the rich blood supply of the endometrium, compared with which the myometrium is sparsely vascularized.

Veins. The endometrium, except for the avascular zone I, is pervaded by a coarse meshwork of venules, the tributaries of the larger ones usually entering at acute angles. Rarely, a straight, narrow venule passes through zone II with few or no tributaries. Such vessels become abundant later in the follicular phase (fig. 17, pl. 3). Sinuses are largely confined to zone IV. There are some dilated veins that spread, spiderlike, through zones II, III, and IV. The dilated sinuous radial veins are shown in figure 4 (pl. 1). The vascular bed is fully injected in this endometrium; in the survey of the entire uterus nothing was found that resembles an arteriovenous anastomosis. The emissaries to the myometrium are broad, and may drain into larger branched vessels that are spread out parallel to the endomyometrial junction.

Early Follicular Phase

B302. On day 15 of the January cycle there was a 3-mm. Graafian follicle in early atresia; no others were larger than 1 mm. The preceding (December) cycle had been anovulatory; the corpus luteum of the November cycle was in one ovary, a still older one in the other.

The endometrium is typical of the early follicular phase. It is from 1.7 to 2.8 mm. thick, with straight, slim glands except in zone IV, where they are characteristically irregular and dilated. In all zones the epithelial cells show evidences of secretory activity. Zones I and II are thicker than in the preceding specimen primarily as a result of the accumulation of tissue fluid. Mitoses in surface epithelium reach 2.2 per cent; in zone II glands, 3.8 per cent; in zone IV glands, 0.4 per cent. In a survey of 2 sections with oil-immersion lens, 2 stroma cell mitoses were found and 2 in capillary endothelium. Stroma cells in zone II range from 76 to 123 per 100 square microns. They have not begun to hypertrophy as they do in the late follicular phase. Reticulum in zone II is delicate and hazy except around glands and blood vessels.

Arteries. Type I arteries are more loosely coiled in zone IV than in B334, and they have come to be farther apart (see p. 176). Figure 7 (pl. 1) shows a typical large artery. A single apical ramus extends to the superficial capillary net, giving off 7 branches to zones II and III. This ramus is only slightly sinuous; in 11 arteries of the corpus it is more sinuous, and in 3 there is a loop in zone II, as in figure 18 (pl. 4). These features indicate that the coils and irregularities of the arteries of postmenstrual stages are straightened out as the stromal ground substance accumulates (see p. 174). In the superficial moiety of zone II, these rami have the incomplete media described above. Many type I arteries are no more sinuous than the one in figure 15 (pl. 3). The major branches have a spread of 0.4 to 0.8 mm. The numerous type II arteries are likewise variable in form. They have outer diameters of 25 microns or less at the junction. Some promptly break up into precapillary arterioles, which occasionally turn back into the myometrium. They may have a series of lateral branches, or they may terminate in a tuft of capillaries (fig. 11, pl. 2). Some, like that at the right in figure 6 (pl. 1), pass through most of zone IV before branching, and may reach zone III. The radial arteries, which give rise to one or more basals, usually have myometrial branches as well. No constriction was observed in any radial or coiled artery.

Capillaries. The superficial capillary net marks the boundary of the avascular zone I. It is from 60 to 75 microns wide. Where the apical rami of the coiled arteries are dilated, the arterial capillaries are also dilated up to 12 microns (fig. 37*b*, pl. 9). The character of the net can be readily depicted only in surface views (fig. 9, pl. 2), since the meshes are spread out parallel to the surface. Frequently, the arterial are superficial to the venous capillaries. Some extend parallel to the surface for relatively long distances (arrow at left in fig. 37*b*, pl. 9). In zones II and III, the anastomoses between capillaries are less frequent; after one or two dichotomous branchings, they usually pass to venous capillaries (fig. 10, pl. 2) which gradually become wider as they approach the venules. A series of arterial capillaries in zone II can be followed for distances of 220 to 300 microns. In zones II, III, and IV, characteristic nets of capillaries are spread out between two or more venules (fig. 12, pl. 2). The mesh is coarser than that of the typical capillary bed. Arterial capillaries can only occasionally be found supplying such nets, which may serve to slow down the flow of blood through the mucosa. In zone IV, the basal arteries supply a continuous capillary net (fig. 11, pl. 2). The meshes are smaller here than superficially.

Veins. Veins are far more abundant than arteries, and they form a network topographically unrelated to the arteries. Two types of venules drain the superficial capillary net. Most of them join the irregular network that pervades the entire endometrium (left edge of fig. 7, pl. 1). Less common in this specimen are radially directed venules that pass straight and with few tributaries to large veins or sinuses in zones III or IV. In the following specimen, these radial veins of the endometrium are prominent (fig. 17, pl. 3). Sinuses are small in comparison with the preceding specimens, and are usually in zone IV. The emissaries to the myometrium are wide and numerous (fig. 7, pl. 1). The veins of the myometrium anastomose as irregularly as in the endometrium. Thus, the entire uterine wall has a venous system in the form of a continuous network without valves at any level. This condition explains why an injection mass introduced by way of the uterine arteries may fill the uterine veins if the injected mass passes through any one capillary bed within the uterus. Many small arteries may remain uninjected in these instances (see p. 166, end).

Late Follicular Phase

B338. This uterus is associated with a normal 6-mm. Graafian follicle (1st maturation division) obtained on day 12 of the February cycle. The December and January cycles had involved ovulation. The endometrium reaches 4 mm. with a loose stroma, zones II and III comprising ⅝ of the thickness. The avascular zone I varies from 22 to 90 microns. The cells of the superficial stroma are characteristically enlarged. The glands are straight and slim except in zone IV, where they are dilated, branched, and contorted. All gland cells not actually dividing are secreting.

Arteries. Figure 18 (pl. 4) shows two adjacent arteries coiled in zone IV; in zone III the coils are looser; the apical ramus in zone II extends to the superficial capillary net. Lateral branches are rare in zone IV; there may be many in zones II and III (fig. 14, pl. 3), or the branching may be confined to zone II (at right in fig. 18, pl. 4). As compared with figures 1 and 5*a* (pl. 1), it would appear that the apical segment had been uncoiled and lengthened as the endometrium thickened. The arterial loops in zone II (fig. 18, pl. 4) are survivals, accordingly, of the superficial coils seen in repair stages. As in the two preceding specimens, the endothelium of the apical ramus was herniated out between the surrounding cells, and, as the vessel is followed toward the surface, the media becomes more and more disorganized. There is no evidence whatever of growth in these vessels commensurate with the progressive thickening of zone II during this phase. In the present specimen no mitoses could be found in any blood vessel, although epithelial mitoses average 8.3 per cent, and dividing stroma cells are not rare. The vessels are obviously stretched as well as straightened out.

The vessels in figure 14 (pl. 3) show variation in the branching of the large type I arteries. That at the left has a branch in zone IV, many in zones II and III, and it also supplies the superficial net. That at the right is the most contorted vessel in this specimen, but it has no long apical ramus. This may have been so greatly injured by the preceding menstrual ischemia that it degenerated to the level of zone III. Basally, the distance between the large coiled arteries averages 0.62 mm. (see table 1, p. 176). Type II arteries vary widely in size and distribution. Many, like the one between the large vessels in figure 18 (pl. 4), are simply rami of myometrial arterioles or small branches of radial arteries. These promptly break up into capillaries. Others extend farther into zone IV (fig. 16, pl. 3), and some reach zone III (fig. 15, pl. 3).

Capillaries. The avascular stroma of zone I separates the surface epithelium from the superficial capillary net. This net is dilated over most of the corpus and fundus, as in other late follicular endometria. It manifests the superficial hyperemia discovered by Markee (1929, 1940) at estrus. The dilatation is not uniform, and it is absent in small areas both laterally and in the thick median prospective placental sites. This variability indicates individuality in the behavior of the coiled arteries, for where they are dilated superficially the capillaries are also wide (fig. 14, pl. 3). Here, as in the preceding specimen, the arterial capillaries are superficial to the venous. An occasional sprout extends into the stroma of zone I.

Deeper in zone II, the arterial capillaries rarely form nets. Figure 13 (pl. 2) shows the vascular bed at this level. The precapillary arteriole in the figure is the apical ramus of a coiled artery; its lumen is 12 microns in diameter. Its branches arise approximately at right angles and promptly become capillaries, as can often be seen where they are near or cut off at the surface of the section. They may be as long as 180 microns before branching, and they usually divide dichotomously before reaching the wider venous capillaries. Venous capillary nets are present, as in figure 12 (pl. 2). The capillaries of zone II are farther apart than earlier, as might be expected since the stromal ground substance has increased, and there is no evidence of capillary proliferation. Figures 15 and 16 (pl. 3) show capillary beds in zone IV, where networks are the rule.

Veins. Figure 17 (pl. 3) shows the veins and larger venules in an area of a single 300-micron section. The irregular network extends throughout the endometrium, the diameters of the vessels varying as much as their branching. The radial endometrial veins have become more prominent than earlier in this phase, and extend straight, with few or no tributaries, from the superficial net to large veins or sinuses in zone IV. They are usually narrow and uniform in diameter (at right, fig. 17, pl. 3). The sinuses are transient enlargements in the venous system of the endometrium (Markee, 1940). Some can always be found in zone IV (see p. 178).

B327. The specimen was obtained on day 11 of an April cycle. On day 8, both ovaries were described as "small" when palpated; on day 10, the right was definitely enlarged, and on the following day the animal was prepared in the usual manner. A follicle about 6 mm. in diameter was found on the right. As the uterus and adnexa were being removed, the follicle ruptured; no ovum was recovered from the washings of the pelvic cavity. The wall of the follicle is histologically normal.

The endometrium agrees in most respects with the other two associated with mature Graafian follicles (Bartelmez *et al.*, 1951). It reaches 5.1 mm. in thickness. The glands are straight in zone II, with narrow lumen; in zones III and IV, they are contorted, the lumen dilated, as is typical of this phase. Gland cells at all levels are secreting. Zone I is well defined, avascular, and lacking reticulum except for the basement membranes of the epithelia. Some red blood corpuscles are scattered about superficially, and the characteristic large stroma cells of this period are common in zones I and II. Zone II comprises about 50 per cent of the endometrium. It differs from the others in that epithelial mitoses average only 3.3 per cent.

Vasculature. The coiled arteries confirm the findings in the preceding specimen in all significant details. The coiled segment of the larger arteries usually extends farther toward zone II. The superficial capillaries are dilated in only a few areas, but, in other respects, the capillary beds and veins resemble those of the preceding specimen.

Phase of Ovulation

B323. After a 26-day cycle, the ovary was found enlarged on day 9. The follicle ruptured between 5 P.M. on day 10 and 8:45 A.M. on day 11. Perfusion was done 5 hours later, and a normal egg was washed from the tube. The endometrium differs greatly from preovulatory stages and also from some others associated with tubal eggs (Bartelmez *et al.,* 1951). There are, however, two others obtained a few hours after ovulation that present similar pictures. These three are, obviously, examples of mid-cycle regression observed in certain cycles by Markee (1940). The mucosa is thin (3 mm. or less); the glands are sinuous or irregular; the stroma is dense, up to 144 cells per 100 square microns.

Arteries. The form of the large type I arteries suggests a recent reduction in the thickness of the endometrium. The vessel in figure 19 (pl. 4) appears compressed, its coils flattened, and the apical ramus contorted, in comparison with the vessels in figure 18 (pl. 4; see figs. 46, 47, pl. 11). The frequency of the constrictions in radial arteries is significant. They resemble the "constriction cones" found by Daron (1936) in early menstruation. In 26 vessels the constricted segment is included within a single section so that it can be readily measured, and the continuity of the radial and coiled arteries can also be demonstrated. The photomicrograph reproduced in figure 47 (pl. 11) shows a constriction 265 microns long. The lumen narrows abruptly from 25 to 4 microns and then to 2 microns. The nature of the constriction is shown by the differences in the diameter of the vessel as a whole. In the constricted segments the diameter (including only the media) is 75 microns; elsewhere it is 110 microns or more. It would appear, then, that the constrictions are due to localized elongations of the vessels which involve a narrowing of the lumen. They are identical with the constrictions during menstruation. This is very different from the passive collapsing of the thin-walled veins by myometrial contractions; the veins are flattened into the form of ribbons.

Capillaries. The capillary beds also give evidence of a sudden collapse of the superficial endometrium after the disappearance of fluid from the stroma. A comparison of figures 23*a, c,* and *d* (pl. 6) with figures 9 and 13 (pl. 2) and 24 and 25 (pl. 6) shows a narrowing and distortion of the form of the meshes in zone II. Sprouts projecting into zone I are more common than in the preceding specimen.

Veins. Radial veins passing through to zone IV are common. In areas where the mucosa is thin, they are sinuous rather than straight, as they are in other phases. Their form can be interpreted as a result of rapid involution (see p. 169). Usually the veins end in sinuses that form an almost continuous chain in zone IV. Their emissaries to the myometrium are narrow, as a rule, but some are large vessels that have few tributaries and can be followed to the stratum vasculare. The carmine in the injection mass diffused out from the larger veins of the corpus and fundus, although there is no such diffusion in the myometrium or in the mucosa of the isthmus or the cervix. The diffusion must, accordingly, be ascribed to the altered permeability of these particular vessels and not to the unduly high degree of dispersion of carmine in the injection mass. Diffusion of carmine occurred in only one other specimen—an early stage of menstruation (see B313, pp. 169–170).

B319. This uterus was obtained 21 hours after a large follicle had been palpated. The follicle presents the earliest postovulatory stage seen by Corner (1945). A histologically normal egg was washed from the tube. As in the preceding specimen, the endometrium is thin, the stroma dense in zone II. The glands are sinuous with narrow lumina and tall, often pseudostratified, epithelium. There are epithelial mitoses at all levels (see Bartelmez *et al.,* 1951). The tube was removed under evipal-ether, and the animal was killed with illuminating gas before the injection was begun. Although the arteries of the stratum vasculare are greatly dilated, injection mass entered very few radial arteries, and the endometrium remained uninjected except for a few simple type I arteries. This situation was due either to the insults of surgery or to the omission of the preliminary $NaNO_2$-histamine perfusion, or both, at a time when the radial arteries are more or less constricted and perhaps highly irritable. The uterus was prepared for cytologic study and very little of it cut into thick sections. In these, typical constrictions could be recognized in three radial arteries, in confirmation of the conditions in B323.

Early Progravid (Preimplantation) Phase

B309. This uterus was injected on day 17 of a February–March cycle. The recent corpus luteum was diagnosed as 6 to 7 days old by G. W. Corner. Three old corpora lutea were present, probably from the December, January, and February cycles. The endometrium is typical of the preimplantation stage. It is 4.9 mm. thick at the middle of the prospective placental site. The glands have begun to accumulate secretion that is richer in glycogen than it was in the follicular phase. The gland cells are pseudostratified, and the large basal vacuoles that arise as the intracellular glycogen is plasmolyzed during fixation are more common than in the follicular phase. In the surface epithelium and in the glands of zone IV, 1 per cent of the cells are dividing; in zones II and III, only 0.3 per cent (Bensley, 1951). Zone I is being vascularized, but very few capillaries have reached the surface epithelium. Zone II now comprises 53 per cent of the thickness, and its stroma is loose, for the most part, except about the coiled arteries; the vascular fields are accordingly prominent.

Arteries. Figure 48 (pl. 12) is a photograph from a 480-micron section taken near the mid-line of the corpus. The coiled segments of the large arteries had extended well into zone II. Vessels as contorted as the one in figure 21 (pl. 5) are found in certain other uteri that have histories of several recent ovulatory cycles. It would appear that, in these specimens, the arteries grow longer during successive progravid phases, and in zone IV there is but little intervening regression. Cumulative growth would also account for the unusually thick endometria sometimes seen at the end of the cycle (see Bartelmez *et al.,* 1951, p. 124). Five apical rami spread out toward the surface in all directions (fig. 21, pl. 5). These vessels, which are structurally arterioles, are not as sinuous as in B323 (fig. 19, pl. 4). By comparison, they appear to have unfolded as zone II thickened. Their spread varies from 1 to 2.2 mm.; since they appear similar in sagittal and transverse sections, they are probably radially symmetrical. Usually each artery and its branches occupy a definite territory. Artery *d* in figure 48 (pl. 12) has two rami that turn toward a neighbor and ramify among its branches. These vessels are accordingly not intolerant toward their kind, as developing nerve fibers are. The media can be recognized in some apical rami to within 100 microns of the surface, but sometimes the cells are irregularly disposed and may be vacuolated. In these rami the differentiation that was begun in the follicular phase has not yet been completed. There are 19 arteries as large and contorted as the artery in figure 21 (pl. 5); all but 2 of them are in the corpus. They are growing at this time, as is indicated by the presence of 14 dividing cells in 7 successive 8-micron sections of one vessel. This fact is significant, since no stroma cell mitoses were found, and the mitoses in the glands of zone II have fallen off materially in comparison with those of the late follicular phase (Bensley, 1951).

A projection reconstruction on the horizontal plane was made from the sagittal series of the dorsal wall. It shows 62 type I arteries in the corpus, 26 in the fundus. Most of the larger vessels are in the paramedian region of the corpus, where the endometrium is thickest (see p. 173). The branches spread over 1.12 sq. mm. on the average. The 43 arteries smaller than the one in figure 21 (pl. 5) vary greatly. They are less contorted, and so the arterial fields are narrower. Where dorsal and ventral walls of the endometrium join, that is, at the lateral limbus and in the depths of the fundus, the arteries are usually as simple as those in figure 30 (pl. 7); some are merely sinuous. They ramify at the surface, however, and also resemble other type I arteries in that they seldom have branches in zone IV.

Capillaries. The dilatation of the superficial capillary net, characteristic of the late follicular phase, has practically disappeared. The stroma of zone I is in the process of being vascularized, so that the avascular border is narrower than in the ovulation phase, 6 microns, on the average, as compared to 21 microns (the greater width of this zone in figures 23*a, b,* plate 6, is due to the tangential plane of section). In B309, the number of capillary sprouts projecting into zone I has increased, and a few have reached the basement membrane of the surface epithelium. The invaders are arterial capillaries, which continue to spread superficial to the venous net. The meshes are elongated in the transverse plane, and sometimes a long capillary courses parallel to the surface. Such capillaries are not in close contact with the epithelium as in the late progravid phase (cf. figs. 24, 27, pl. 6). Below the superficial net, the zone II capillaries are supplied by precapillary branches of type I arteries; from them, capillaries arise both laterally and terminally. They branch dichotomously, and pursue a sinuous course (fig. 25, pl. 6). The capillary beds in zone II are looser than in earlier phases, as if they had been spread out by the development of edema fluid (cf. fig. 10, pl. 2; figs. 23*c,* 25, pl. 6). The capillaries usually dilate toward the venous end. Rarely, a precapillary arteriole supplies a net of venous capillaries such as that in figure 12 (pl. 2). Capillaries are spread irregularly through the stroma, and there is no indication that the glands are closely invested by a capillary bed; the occasional approximation of a capillary to the glandular epithelium appears to be coincidental.

Veins. The network is the prominent feature of the venous system in this specimen. The straight radial veins of the previous phases do not reach zone IV, and usually join the network at the middle of zone II. There is an occasional small sinus at this level, as at the right in figure 22 (pl. 5). Irregularity is the outstanding feature of the net. The individual venules vary in length and become wider or narrower, irrespective of tributaries or anastomoses, which are likely to occur at acute angles. The sinuous arterioles, on the other hand, have a series of lateral branches that arise approximately at right angles. Venules vastly outnumber arterioles, and their delicate walls suggest that they are not merely conduits but are concerned in fluid exchange.

B326. The animal died during an exploratory laparotomy under nembutal, 35 days after the last menstrual period in January. After vasodilation, india ink was injected *per aortam,* carmine gelatin *per venam cavam.* There had been a 20-day postmenstrual period of ovarian quiescence followed by the development of brilliant sex skin color and enlargement of the right ovary. At autopsy, only one corpus luteum was found, which was diagnosed as 5 to 8 days old by G. W. Corner. Ovulation accordingly occurred 6 to 9 days after the enlargement of the ovary was diagnosed.

The endometrium has reached a thickness of 5.0 mm. in one area. Much of the corpus is only 2.8 mm. thick. The glands are abundant in some areas, sparse in others. They are sinuous, dilated in zones II and III, narrow in zone IV. Abrupt transitions from the slim pseudostratified gland cells of the early progravid phase to the short broad cells of the later phase give a "sawtooth" appearance (Bartelmez *et al.,* 1951). Mitoses are present in 0.85 per cent of all epithelial cells. The stroma is loose, with abundant metachromatically staining ground substance in zones I, II, and III.

Arteries. Figure 20 (pl. 4) shows as contorted an artery as any in this endometrium. It might well have developed in the course of a week from one like that at the left in figure 18 (pl. 4) if the apical segment had continued to grow faster than the mucosa thickened. The greatest superficial spread of the branches of a coiled artery noted is 1.6 mm. The main trunk resembles Daron's (1936) figure 4 from the early progravid phase. The majority of the type I arteries are no more contorted than the transitional arteries of figure 30 (pl. 7). The history of this case provides an explanation of the difference between it and B309 (see p. 174). Precapillary arterioles have differentiated to within 0.2 mm. (rarely 0.1 mm.) of the surface. This condition represents progress over B309. Mitoses in their walls show that they were still growing. The prolonged anaesthesia may account for their narrow lumina, for Markee (1940) observed a blanching of the endometrium under these conditions.

Capillaries. The only difference from B309 as far as the capillary beds are concerned is that zone I is more completely vascularized, and capillaries in contact with the surface epithelium have become common.

Veins. The general pattern of the veins is like that of figure 22 (pl. 5) in that the network is the dominating feature. The superficial veins and venules are more dilated, presumably as a result of the direct injection *via vena cava* after the capillaries had been filled *via aorta.*

EARLY PROGRAVID ENDOMETRIUM ASSOCIATED WITH A RECENT CORPUS ABERRANS

B307. The animal was sacrificed on day 26 of a February cycle. She had been received on November 30 with an infected skin wound, and did not menstruate in December. The right ovary had a corpus aberrans (Corner, 1942; Corner *et al.,* 1936) and two old corpora lutea; none was found on the left.

The endometrium has a maximum thickness of 4.9 mm.; the glands are sinuous with a somewhat dilated lumen. The surface epithelium is low (21 microns) with the nuclei in two ranks, so that there is no peripheral border of cytoplasm. In zones II and III, the glandular epithelium is typically early progravid: 28 to 34 microns in height and pseudostratified with large basal glycogen artifacts. In zone IV, it reaches 50 microns, and 1 per cent of the cells are in mitosis. The stroma of zones I and II is of the variable type with from 97 to 143 cells per 100 square microns. There are a few mitoses. The reticulum at this level stains feebly, a definitely aberrant finding for this phase. Zone II involves 40 to 60 per cent of the thickness. Sclerotic arteries and hemophages in the inner myometrium indicate a recent pregnancy.

Arteries. The large coiled arteries are more contorted in zone II than the artery in figure 21 (pl. 5), as may be seen in figure 49 (pl. 12). As in B309, there are usually two or more superficial rami. In B307 they have differentiated closer to the surface. They resemble Daron's figure 5 except that, in B307, zone II is edematous and the apical rami are sinuous. Arterioles up to 57 microns in diameter occur 200 microns below the surface, and there are precapillary arterioles in zone I. The distance between the larger coiled arteries of the prospective placental sites is less than in the more edematous B309 (see p. 176). These features seem to indicate the onset of involution. No constrictions were found in radial arteries.

Capillaries. The pattern of the capillary beds of zones II and III is only occasionally shown. Usually there is so little prussian blue in them that they fade out, in the necessarily thick sections, as they are followed out from the arterioles. Where the capillary beds are complete, they resemble figures 24 and 25 (pl. 6).

Veins. The irregularity of the network is more striking in this specimen than in figure 22 (pl. 5). Numerous anastomoses and tributaries almost completely replace the through routes represented by the radial veins. In the dorsal wall at the inferior end of the corpus, close-meshed networks of venules in zones II and III were injected. Sinuses are more common in the ventral than in the dorsal wall. Long chains of them extend longitudinally through zone IV; their emissaries to the myometrium may be broad or slim. There are a few sinuses in zones II and III (fig. 49, pl. 12). Two spiderlike sinuses, such as are seen during menstruation, were noted spreading through zones II, III, and IV.

PROGRAVID PHASE

B324. This uterus was obtained on day 23 of a February cycle. The four preceding cycles had been ovulatory (Rossman, 1942). In February the sex skin color did not rise until day 13, and it fell again on day 18. The structure of the corpus luteum indicates ovulation between days 14 and 16.

The endometrium is somewhat more advanced than in B326. The maximum thickness is 5 mm. The surface epithelium is tall and pseudostratified. The glands are sinuous, and most have a wide lumen in zone II. The cells are 24 to 33 microns high and 4.2 microns wide, with nuclei in a single rank. A few narrow glands have a single rank of tall cells 3.5 microns wide. The shorter, broader cells of the dilated glands suggest that the accumulation of secretion in the gland lumen is at least a factor in changing the form of the cells. The basal glycogen artifacts of the early progravid phase are present in the great majority of gland cells; on the other hand, no mitoses were found, even in zone IV. Zone I is well defined by edema, and is fully vascularized. There are patches of dense stroma in zone II, as in certain other early progravid specimens.

The animal had been under nembutal for 1 hour when illuminating gas was administered for 20 minutes instead of the usual 5 minutes. Perfusion with $NaNO_2$ and histamine preceded the injection. Various extravasations of starch and the entrance of starch into capillaries can be ascribed to the slow CO poisoning, since these conditions were not observed in other specimens of this phase. However, the constricted superficial arterioles described below can hardly be explained on this basis.

Arteries. The more complex of the type I vessels resemble figure 20 (pl. 4) basally, although they are more contorted in zone II (see p. 163). The apical rami are extremely small with narrow lumina. They come within 350 microns of the surface epithelium. One 28-micron vessel has a lumen of 10.5 microns. Starch entered only an occasional endometrial artery. At the center of the corpus is an area where zones I and II remained entirely uninjected. Here the lumina of the arterioles are virtual, although the injection is good in the basal half of the endometrium (see B332, pp. 171 and 175).

Capillaries. The effect of long exposure to CO is seen in widely dilated superficial capillaries that may reach a diameter of 14 microns or more. One capillary in contact with the surface epithelium measures 10.7 microns where a solitary starch grain lodged in it; at the ends, it tapers off to 3.6 microns. Starch had passed from the capillaries into some of the superficial venules. A careful search through this series brought to light only capillary communications between arteries and veins. The superficial capillary beds are like those in figure 27*a* (pl. 6).

Veins. The venous pattern resembles that of figure 22 (pl. 5) in that the network is more prominent than the radial venules. Aside from an occasional small sinus in zone III, the sinuses are near the junction with the myometrium. The emissaries to the myometrium are inconspicuous.

B239. Ovulation was diagnosed by palpation between days 12 and 13 of a March cycle. On day 23, an intravenous injection of HgS was made according to Daron's method (1936). The uterus was opened in the plane of the broad ligaments and sectioned serially, mostly at 400 microns. After all sections had been studied and drawn, one of them was embedded in celloidin-paraffin and sectioned serially at 6 microns.

The endometrium is typically progravid (see fig. 50, pl. 12, and its legend). It is thickest at the middle of the dorsal wall, where it reaches 8.7 mm. In zone II, the glands are straight with rather wide lumina; in zones III and IV, they are branched and contorted. Local dilatations occur at all levels. The gland cells are intermediate between early and late progravid types. Pseudostratified epithelia with basal glycogen artifacts are characters of the early progravid phase. Where the nuclei are in a single rank, the late type is present. Mitoses are almost completely absent in all tissues, as in B324, and zone II, with 33 cells per 100 square microns, comprises 61 per cent of the mucosa. These features are typical of the late progravid phase.

Arteries. The intravital injection makes this specimen a control for those prepared postvitally as far as the form and diameter of the vessels are concerned. The wider, closely coiled segment of the larger arteries extends as far as zone II (cf. fig. 50, pl. 12). The spread of the coils, i.e. the width of the arterial fields, is less than in figures 20 (pl. 4) or 21 (pl. 5), and the apical rami are slimmer. The diameter of the larger coiled arteries reaches 118 microns with a lumen of 68 microns.

The complete series makes this case available for the study of the number and distribution of the arteries. The largest are obviously in the middle half of the prospective placental sites in both dorsal and ventral walls, as in B309. The average width of the 22 largest arterial fields, i.e. the maximal extent of the coils, in the dorsal wall is 385 microns (range, 275 to 518 microns); of 32 in the ventral wall, it is 359 microns (range, 235 to 552 microns). In the fundus, the average extent of the vessels in the dorsal and ventral walls is 203 and 147 microns, respectively. There are, in addition, 10 small coiled arteries laterally in the dorsal wall, which average 173 microns, and 22 ventrally, averaging 194 microns. The distance between adjacent arteries at the level of the endomyometrial junction gives an indication of the spread of these vessels. The average distance dorsally is 1.0 mm., 0.74 mm. ventrally. For the larger paramedian vessels, the value dorsally is 1.21 mm., 1.0 mm. ventrally. It appears, then, that in the dorsal wall, which is ⅓ thicker, the vessels cover more territory; in the ventral wall they are smaller and more numerous (see p. 173).

The apical rami are sinuous, and precapillary arterioles 20 microns in diameter with a 10-micron lumen extend to within 160 microns of the surface epithelium.

Capillaries. In these intravital injections, the capillaries cannot be followed for more than a few microns from terminal arterioles and venules, since not enough HgS is present to show microscopically, nor is there a continuous file of red blood corpuscles to reveal them.

Veins. The veins are admirably visualized. Outstanding features are the radial veins that occasionally extend, without a tributary, from the superficial net to a sinus in zone III. Usually they are narrow (enlarging from 18 to 22.5 microns), but they may reach 53 microns before emptying into a sinus. They seldom have more than three tributaries in zone II. The network of veins, which dominates figure 22 (pl. 5), is less conspicuous. This intravitally injected specimen is particularly useful in showing that the sinuses are not veins artificially enlarged by postvital manipulations. They are local dilatations of the venous system, although, as Markee showed, they come and go. They are common in zones III and IV, extending parallel to the surface. One of them extends vertically from the middle of zone II through to zone IV. They are rare in zone II. Many of the zone IV sinuses have broad emissaries to myometrial veins; some of them are narrow at the junction before they open into large myometrial veins. These may pass to the stratum vasculare with but few tributaries.

B325. Only one cycle, 27 days in length, was observed between the receipt of this animal, at the end of December, and the injection, which was done on day 21 of the February cycle. The corpus luteum corresponds to the 10- to 11-day stage of Corner (1945). No other corpora lutea were noted. After vasodilation, carmine gelatin was injected *per aortam,* prussian blue *per venam cavam,* and india ink intramyometrially.

The endometrium is typical of this phase, corresponding in all respects to early implantation stages (Bartelmez *et al.,* 1951). Unlike the three following specimens, it shows no indications of regression. It reaches a maximum of 7.0 mm. with dilated and sacculated glands in zone III, some of which have the same form in zone IV, a condition sometimes seen also in pregnancy. Zone I, recognized by greater edema, averages 168 microns in thickness; the surface epithelium is low. Zone II comprises 60 per cent of the thickness, and has a loose stroma, in which the arterial fields stand out sharply, since the stroma surrounding them is dense. Mitoses are very rare in any tissue.

Arteries. The form of the arteries is unusually variable; in all of them the vascular fields are narrow. Figure 31 (pl. 7) and figure 51*b* (pl. 12) show one of the most complex. It is loosely coiled in zone IV, most contorted in zone III, and sinuous in the superficial half of zone II. At the level of the arrow, the main trunk divides dichotomously, and a lateral branch arises. The branches in zones III and IV are unusual in this as in other progravid endometria. The two terminal rami reach to within 100 microns of the surface, where they are precapillary arterioles with outer diameters of 14 to 17 microns. Their presence so close to the surface is distinctive of this phase of the cycle. Figure 51*c* (pl. 12) shows one of the simple type I arteries. Such vessels predominate in the fundus and in the band of corpus that borders on the isthmus. The distance between coiled arteries ranges from 1.2 to 2.2 mm. (average, 1.4 mm.) in the corpus, 1.1 mm. in the fundus (table 1, p. 176).

Capillaries. Zone I is completely vascularized, and long capillaries are closely applied to the basement membrane of the surface epithelium. Figure 26*a* (pl. 6) shows the meshwork to be looser than in earlier phases, which would indicate either that new capillaries are not formed later in the progravid phase, or that they do not keep pace with the development of edema at this level. The same is true also deeper in zone II, where the dilating glands appear to spread out the capillary mesh (fig. 26*b,* pl. 6). In the thin septa between the crowded glands of zones III and IV, the capillaries appear to be shorter and closer together.

Veins. Straight, radially directed veins are common as in B239, and they may extend through zone II to zone III. Unlike the vein shown at the left in figure 31 (pl. 7), they usually have tributaries in zone II. They differ from the radial veins of the follicular phase that pass directly to zone IV (fig. 17, pl. 3). In addition, the all-pervading venous network is present, as usual. The groups of venous capillaries joining venules are also common. Sinuses are uncommon except in zone IV, where they may occur in long chains extending sagittally. Only two sinuses were found in zone II. Emissaries to the myometrium are slim or flattened, and consequently inconspicuous.

After the blood vessels had been injected and the uterus chilled to stiffen the gelatin, ink was injected into the myometrium with a hypodermic needle in the hope of demonstrating lymphatics. Many myometrial veins and some endometrial veins were filled with ink. They were recognized as such by following them to carmine-filled veins. No vessels in the endometrium were found that could be identified as lymphatics.

B330. This uterus was obtained on day 27 of an April cycle. Inadequate fixation of the corpus luteum precludes conclusive determination of age; it was mature or in early regression. There is another (old) corpus luteum in this ovary, two fairly recent and three old corpora in the other. The number of primordial follicles is so much smaller than usual as to indicate a rather old animal.

The endometrium, 6.3 mm. or less in thickness, shows no signs of regression and presents several features of the early progravid phase. The surface epithelium is tall and pseudostratified with 1 per cent mitoses. The lumen of the sinuous glands is only moderately distended; the epithelium is pseudostratified or of the sawtoothed type (Bartelmez *et al.,* 1951). The characteristic early basal glycogen artifacts are present in zones II and III, and 0.85 per cent of the cells at this level were dividing. There is a well defined zone I, 20 to 100 microns thick, which was only beginning to be vascularized. Zone II comprises half of the mucosa.

Arteries. The larger type I arteries are the most contorted in the present series (fig. 32, pl. 7; fig. 55, pl. 13). They resemble Daron's (1936) figure 5 except that the most contorted segment is in zones III and IV. At the endomyometrial junction the large arteries are on the average 1.1 mm. apart. The coiled apical ramus is a late progravid feature, as is the differentiation of precapillary arterioles to within 70 microns of the surface epithelium. As usual, there are also simply coiled and even sinuous type I arteries, and transitions from these to basal arteries which may branch through some or all levels of zone IV. No constriction was found in any radial artery.

Capillaries. Where zone I is thickest, it does not seem to have been invaded by any capillaries. Elsewhere, the avascular zone varies according to the extent to which loops or blind sprouts have grown into it. The superficial network is narrower (fig. 29, pl. 6) than it is nearer zone III. Figure 29 (pl. 6) shows the complex pattern of the capillary bed at this level. The finding of an occasional starch grain in capillaries led to an intensive study of the capillary beds. Twelve fields, which looked, under low magnification, as if arteriovenous anastomoses might be present, were drawn in full detail and checked under the oil-immersion lens. In every instance, it was obvious that only typical capillary beds separated arteries and veins.

Veins. The general orientation of the venous net is radial: radial veins are common in zone II, a few pass through to zone IV, as in the follicular phase, and the meshes of the network are elongated in the same direction. Most radial veins have tributaries and end in sinuses in zone III. The large spiderlike sinuses are present, as in B332 (fig. 62, pl. 15), and there are chains of sinuses in zone IV extending in the sagittal plane. Some emissaries to the myometrium are broad, others narrow, and occasionally a sinus has several minute emissaries to a myometrial vein.

Transitions from Progravid to Ischemic Phase

B316. This specimen was obtained on day 29 of a February cycle. Previous cycles recorded were 37, 27, 28, and 26 days; the preceding (January) cycle had probably been ovulatory. The sex skin brightened on day 8 of the following cycle, and the right ovary enlarged. Laparotomy on day 28 showed a large corpus luteum on the right, and the injection was done on the following day. Whether the operation contributed to the degeneration present in the corpus luteum cannot be said.

The endometrium shows evidences of regression. It had reached 6.8 mm. on the ventral wall, 4.6 mm. on the dorsal. The surface is pitted with deep, wide gland mouths; the surface epithelium is tall and pseudostratified (24 to 32 microns tall). The glands are wide, crowded, and sinuous in zone II, sacculated in zones III and IV, their cells of the low, wide progravid type even in some glands adjoining the muscle. No mitoses were found. Zone II comprises only 45 per cent of the thickness of the mucosa, and has numerous dense areas; the average number of stroma cells per 100 square microns is 144; this figure is definitely greater than in the late progravid stages. The intense staining of the ground substance of zone I also indicates a loss of water. There are neither collapsed glands nor infiltration (fig. 52, pl. 12). The arteries, however, present indications of regression.

Arteries. The most contorted arteries resemble the artery in figure 32 (pl. 7). The apical rami appear compressed as they might be if there had been a reduction in the thickness of zone II. The proximity of the coiled arteries to one another also gives evidence of a reduction in the volume of the mucosa. The distance between them at the endomyometrial junction is materially less than in B325; it ranges from 0.45 to 0.7 mm., the average, 0.6 mm. Precapillary arterioles are closer to the surface than in earlier phases. One vessel 32 microns below the epithelium has an outer diameter of 17 microns, a lumen of 7 microns. The arterial constrictions one would expect at the beginning of regression can be found, but they are not common. It is significant, however, that the starch, which fills most myometrial arteries, reached very few type I endometrial arteries.

Capillaries. The capillaries applied to the surface epithelium are well shown in this specimen; they may reach 300 microns in length. The network is loose at this level (figs. 27*a, b,* pl. 6). Although illuminating gas, chloral hydrate, and sodium nitrite were used, there are circumscribed areas of corpus endometrium in which arteries and capillary beds remained uninjected. This condition obtains also in other specimens in which there were many constricted radial arteries, such as the ovulation stage B323 and the early menstruating stages B317, B314, and B313. The deeper capillary beds are loosely spread out in the narrow septa between the crowded glands.

Veins. In most areas the veins are well injected, even where no mass entered the arteries and capillaries. Since the entire vasculature of the myometrium is injected, the endometrial veins were presumably filled by retrograde flow from it. Such flow is demonstrated, as in B325, by the partial filling of endometrial veins with ink from myometrial veins that had been filled by hypodermic needle injection from the broad ligament. In this uterus, as in B325, there are straight radial veins that reach zone III, sometimes without tributaries. They are straight, despite the evidence of regression of the endometrium indicated by the sinuous glands and contorted apical rami of the coiled arteries. Apparently the veins adjust to gradual changes in thickness of the endometrium (see p. 177) as also during menstruation. This is in harmony with the relatively rapid changes observed by Markee (1940) in the sinuses. The sinuses here are almost entirely in zone IV, or at its boundary with zone III. Emissaries are slim, in general, and empty into a network of venules in the inner zone of the myometrium.

B318. This specimen was obtained in February, 42 days after the last menstrual period. The three previous cycles had been 23, 22, and 22 days in length. An enlargement of the right ovary was noted on day 8 of the January cycle. The expected period did not appear, and on day 26 the same ovary was again enlarged. Palpation indicated ovulation between days 29 and 30, and 11 to 12 days later a mature corpus luteum with degenerating cells was found on the right (Rossman and Bartelmez, 1946). Beside it is a corpus aberrans of about 8 weeks.

The endometrium reaches 5.0 mm. in thickness; half of it is zone II. The surface epithelium is pseudostratified, but only 16 to 22 microns in height. The glands are straight or sinuous, crowded in zone IV. Many are widely dilated, especially in zone III; their cells are of the low, broad, late progravid type. Such cells are present even in some glands of zone IV where the epithelium is, for the most part, tall and pseudostratified, and mitoses reach 0.5 per cent. The stroma of zone II is dense as compared with the late progravid specimens. The average is 129 cells per 100 square microns, with areas ranging from 119 to 169 cells. In view of the findings in the corpus luteum, this points to the onset of regression, as do the arterial constrictions and the thick myometrium (table 1, p. 176).

Arteries. Few endometrial arteries were injected. The form of type I is, in general, simpler than in any of the other progravid endometria; none are more coiled than the artery in figure 20 (pl. 4), and many are sinuous, like the arteries of figure 30 (pl. 7). In thin sections the arterial fields are inconspicuous, because the stroma about the coils is loose. The typical coarse collagenic fibers are present, however. In zone III, where the coiling is the greatest, the fields do not exceed 166 microns in diameter. The distance between them averages 0.77 mm. (see p. 176). One of the largest has a diameter of 62 microns at the endomyometrial junction, with a lumen of 21.4 microns, which narrows to 7.3 microns in the radial artery. Constrictions occlude some type I arteries in zone IV. Starch entered very few radial arteries of the corpus and the fundus, and the numerous constrictions are doubtless responsible for the irregular distribution of injected areas. Other myometrial arteries and those of the stratum vasculare were dilated by injection mass, as in B319 (p. 161). The apical rami are unusually narrow, and precapillary arterioles, which can be followed close to the surface, often have only a virtual lumen (see p. 164).

Capillaries. The superficial net is better injected than the others. Zone I has been as completely vascularized as it is in figures 27*a* and *b* (pl. 6), and the mesh is similarly wide. The capillary beds of the myometrium are well injected, especially between the stratum vasculare and the peritoneum.

Veins. Straight radial veins may extend to zone III without tributaries, and the usual venous network is present, but so many veins remained uninjected that the picture is incomplete. Sinuses are present in zones III and IV; their emissaries may be broad or narrow.

Ischemic Phase

B115. This endometrium has been described and illustrated by Daron (1936) and Bartelmez *et al.* (1951). It was obtained on day 30 of the November–December cycle and injected intravitally with colloidal HgS. Corner found early regression in the corpus luteum. The irregularly wrinkled form of the glands in contrast to the widely dilated glands of the late progravid phase, the denser stroma, and the narrower zone II, which comprises but 43 per cent of the thickness of the mucosa, all indicate the onset of collapse. Daron's (1936) figure 5 of a typical large coiled artery shows extreme contortion superficially, such as Markee (1940) observed in progress during regression. This contortion and the crowding of the arteries, separated by 0.46 mm. on the average, are in harmony with the interpretation of the early ischemic phase. The apical ramus in Daron's figure extends to within 0.5 mm. of the surface. Precapillary arterioles are present in zone I, which is still somewhat edematous near the mid-line of the corpus, that is, in the midst of the prospective placental site. Long capillaries are closely applied to the surface epithelium, as in figures 27*a* and *b* (pl. 6).

Ovulatory Menstruation

B317. This uterus came from an animal on day 1 after a 51-day ovulatory cycle in December–January. It was obtained early enough in the menstrual phase so that there are still areas that have all the features of the ischemic phase. The largest of these areas is a band 7 to 8 mm. wide at the inferior end of the corpus where the glands and vessels slope toward the fundus.

Ischemic area. The endometrium varies from 3.2 to 4.7 mm. The surface is intact, and no vessels have ruptured (see Bartelmez, 1956, fig. 1). The glands are crowded and deeply wrinkled, which condition can be correlated with the broad progravid gland cells. In zone II, the lumina are narrow, gradually widening basally. Evidences of secretory activity are present everywhere, including zone IV, the cells having responded, though tardily, to hormonal stimuli. There is no visible ground substance in the stroma, which is infiltrated with lymphocytes. The number of cells per 100 square microns reaches 200 plus 40 wandering cells in zone II, which is narrower than in the progravid phase, constituting 40 per cent of the thickness.

Arteries. Figure 33 (pl. 8) presents a typical coiled artery of this area. The arterial fields are narrow, for they occupy the interglandular septa, which presumably shrank during involution. The arteries and their branches out to the precapillary arterioles are filled with the injection mass. Nearer the isthmus, the arteries become smaller and sinuous. The constriction near the endomyometrial junction in figure 33 (pl. 8) is short and not as slim as that of a neighbor, the lumen of which narrows from 10 to 5 microns and then to 1.5 microns.

Capillaries. The capillary beds are fairly well injected. The superficial net differs from that of the late progravid phase in three respects: The long capillaries applied to the surface epithelium are no longer visible. They appear to have been collapsed except for minute spurs projecting from the superficial loops (arrow in fig. 35*a*, pl. 9), which are separated by a zone of dense stroma from the surface epithelium. As might be expected from the presence of constrictions in the coiled arteries, the precapillary arterioles and adjoining capillaries are narrow. On the other hand, the venous capillaries and venules are wide, so that under low magnification they dominate the picture. This is Markee's (1940) premenstrual venous congestion. Finally, the capillary meshes are narrower than in the progravid phase, owing, it would seem, to the disappearance of edema fluid (cf. figs. 26*a*, *b*, pl. 6; fig. 35*a*, pl. 9). Deeper in the mucous membrane, the capillary beds are like those of the bleeding areas (figs. 35*c*, *d*, *e*, pl. 9).

Veins. The dilated venules near the surface are characteristic of the venous congestion. The one shown in figure 33 (pl. 8) is exceptionally long. Such vessels are almost always flattened, no wider than capillaries when viewed on edge. The deeper veins are inconspicuous (fig. 33, pl. 8). There is an occasional radial vein that passes to zone IV without tributaries. These are not wide but straight, and may represent recently developed highways through the venous net. Sinuses are practically absent, and the emissaries to the myometrium are very slim.

Menstruating areas. Where the surface is still intact, the mucosa reaches 5.0 mm., and the hemorrhagic zone constitutes 18 to 38 per cent of the total thickness (see also fig. 34, pl. 8). The fissures, which initiate sloughing, are present in several spots, and their depth shows the extent of the slough (fig. 53, pl. 13). There is no evidence of any subsequent massive loss of tissue (Markee, 1940), so that a part of zone II persists throughout menstruation, gradually shrinking and dedifferentiating. In the hemorrhagic zone, little can be recognized except blood and the more or less necrobiotic ends of the arteries, which are often dilated with packed red blood corpuscles. Although bleeding arteries are to be expected at so early a stage in menstruation, the carmine gelatin was extravasated from arterioles in only one small area.

A comparison of figures 33 and 34 (pl. 8) shows the increased contortion of the coiled arteries deeper in zone II, and indicates continued involution. There are no starch grains in the coiled arteries or in the corresponding radial arteries, owing, no doubt, to their constrictions. Carmine gelatin did enter all type I arteries, so that the number in the series could be counted (see p. 173). Among 165, there were 51 in which the plane of section was favorable for establishing the connection with the radial arteries and which had constrictions included within single sections. At the constrictions the lumina range from 2.2 to 10 microns; the adjoining segments are at least 10 times wider. Most constrictions are short, unlike the long "contraction cones" observed by Daron (1932) in uteri frozen rapidly while the blood was circulating. The difference is due, in part, to the use of vasodilators in the postvital injections. Further evidence that the constrictions were not produced by myometrial contractions is their presence at different levels in neighboring vessels (Bartelmez, 1956).

The transitional arteries are more or less coiled; the type II arteries are usually sinuous, but some are straight.

Capillaries. In some areas, precapillary arterioles and capillary beds close to the hemorrhagic zone are well injected (fig. 35*c*, pl. 9). Where they stretched out in the slim septa of interglandular stroma, the network can be visualized only on the surface of a tangentially cut gland, as in figure 35*c* (pl. 9), where the meshes are actually narrower than the figure indicates, since some vessels were omitted for the sake of clarity and the section is only half as thick as those from which figures 35*a* and *b* (pl. 9) were taken. Capillary loops are sometimes enclosed within a wrinkle of a collapsed gland, but there is no evidence of the widespread association of epithelium and capillary, such as characterizes the surface epithelium of the progravid phase (figs. 27*a*, *b*, pl. 6).

Veins. Only the venous net is usually present, but radial veins extending to zone III may occur in denuded areas and are sometimes more prominent than the venous network. They are straight, although other structures are distorted by the thinning of the endometrium.

The veins, in general, are wider than in the ischemic area. Some venules can be followed into the hemorrhagic zone, the end surrounded by extravasated injection mass. In denuded areas they open to the surface.

B314. The specimen was obtained on April 7, 47 days after the last menstrual period. During the last cycle, palpations and the color of the sex skin indicated a long postmenstrual period of ovarian quiescence and a 5- to 6-day premenstrual ischemic phase (Rossman and Bartelmez, 1946, case 1). Beside the recent corpus luteum, there is an old corpus aberrans (Rossman, 1942).

It would be difficult to find two endometria in the same stage of the cycle that differ more in appearance than B314 and B317. On the basis of the endometrium alone, B314 would be diagnosed as "anovulatory menstruation." However, the corpora lutea in the two cases are essentially similar—"early menstrual degeneration" (G. W. Corner). The long ischemic phase in B314 would explain the extensive involution of the endometrium. It is 2.5 mm. thick in the fundus, where menstrual changes are least advanced, and the surface epithelium is intact; the glands are wider, and about the ostium tubae there is no extravasation. In the corpus the surface is denuded, and the thickness is 2.2 mm. or less. Some slough is still *in situ* at the inferior end of the corpus. Despite the thinning-out of the mucosa as a whole, the glands are, in general, perpendicular to the surface, and sinuous, with narrow lumina that widen in zone IV. The greater thickness of the mucosa where the glands are dilated indicates that the extrusion of secretion and the reduction in volume of the gland cells are involved in the involution. The latter explains the absence of wrinkling in the glands (fig. 54, pl. 13). The stroma of zone II is typically dense, with 264 stroma cells plus 30 wandering cells per 100 square microns. Denuded areas have a superficial hemorrhagic zone with pycnotic nuclei. The wider spacing of the glands identifies zone II, which constitutes from 20 to 30 per cent of the thickness.

Arteries. The arteries give evidence of a general reduction in the volume of the endometrium in areas where there has been little loss of tissue. The presence of the characteristic apical branches of type I arteries shows that only part of zone II had been sloughed. They are contorted or sinuous not only superficially but in all zones (fig. 54, pl. 13). The crowding of the type I arteries also provides evidence of involution. The distance between them in 37 measurements ranges from 0.33 to 0.42 mm., with an average of 0.38 mm. There is the usual variability in the form of type I arteries. They may be as simple as that in figure 38 (pl. 10). All are sealed at the surface, so that there was no escape of injection mass. In an area of the corpus, none of it reached the endometrial arteries of either uterine wall, owing to the constriction of a major ramus of the uterine artery in the stratum vasculare. The myometrial arteries are, accordingly, narrow in this area. Elsewhere, there are the typical local constrictions of the radial arteries. Some are over 1 mm. in length with a starch grain or two trapped in them.

Capillaries. Throughout zone II there are some injected capillary beds, even close to the pycnotic zone. This finding is significant in view of Markee's (1940) observation that the superficial circulation is promptly restored after the ends of the type I arteries are sealed following the initial hemorrhage. As a rule, however, but few capillary branches of terminal arterioles are injected, so that the capillary beds are not complete. The condensation of the interglandular septa in zones III and IV makes the analysis of capillary beds difficult in the necessarily thick sections. Figure 36 (pl. 9) shows the narrow mesh of a spot in zone III.

Veins. The prominence of the veins, like various other features, contrasts with the preceding specimen. All the veins seem to have been injected. At the center of the corpus, there is an area where radial veins extend to zone III with few tributaries. They are sometimes dilated. Since all their afferent superficial net was sloughed, they offer good illustrations of retrograde injection. The caliber of the veins that constitute the venous net is extremely variable (fig. 38, pl. 10). The sinuses, in general, are flattened, as in B317. They occur chiefly at the junctions of the zones, although there are a few in zone II. All the emissaries to the myometrium are slim.

B313. In this specimen, a flow began either on April 2 or probably on April 3, 31 (or 30) days after the previous period. The February cycle was a 35-day one; that in January was 23 days. The diagnosis of the age of the luteum is "degeneration as of the 2d day" (G. W. Corner). Sclerotic arteries and hemophages mark former placental sites.

The uterine lumen was dilated with the discharge. The endometrium ranges from 1.8 mm. in denuded areas to 3.0 mm. where the slough is still *in situ.* The surface is, for the most part, denuded. The hemorrhagic zone varies from 9 to 23 per cent of the thickness. As in the preceding specimen, the glands are sinuous, their cells highly involuted. The wider interglandular spaces indicate zone II, which, with the hemorrhagic zone, comprises about half of the mucosa. The stroma of the hemorrhagic zone reaches 250 cells per 100 square microns, and deeper in zone II there are as many as 190. In corpus and fundus the injected carmine diffused from the vessels into the superficial ⅓ of the endometrium. Since this type of diffusion did not occur in other regions, it may be an indication of vascular injury in regions where gland and stroma cells as well as vessel walls appear normal histologically. It is interesting that the only other endometrium in which our colloidal carmine diffused from blood vessels was also one with many constricted radial arteries (see B323, p. 161).

Arteries. Figure 39*b* (pl. 10) presents a characteristic coiled artery. The presence of terminal rami identifies zone II, and the compressed appearance of the coils documents the extreme reduction at this level. The stretching of the mucous membrane involved in the dilatation of the lumen presumably contributes to this as, indeed, to the thinning of the entire mucosa. The arteries of this uterus stand out especially clearly, for starch grains entered most of them. All the radial arteries that could be followed to coiled arteries have constrictions. The proximity of the constriction to a well dilated vein demonstrates its independence of a possible local contraction in the myometrium, such as would assuredly have compressed the thin-walled vein. Constrictions at different levels in adjacent arteries (Bartelmez, 1956) also show the individuality of the arterial reactions. This specimen is favorable for measurements of the media of the arteries. The measurements of a typical radial artery are as follows: the outer diameter of the media is 48 microns where the lumen is 26 microns, and 30 microns where the lumen is 2.9 microns. We are dealing, then, with a local elongation of the vessel, not with a thickening of the entire vessel wall.

The distance between adjacent type I arteries averages 0.5 mm., with a range of 0.3 to 0.6 mm. This is somewhat greater than in B314, where the stroma is denser. Another factor may be involved, viz. the stretching of the endometrium, for the uterine lumen is dilated with accumulated menstrual discharge (see p. 171, end). Transitional and type II arteries are illustrated in figure 39*a* (pl. 10). The latter are sinuous or directed obliquely, an indication of involution in zone IV.

Capillaries. In the myometrium the capillary beds are well injected, but they usually appear fragmentary in the endometrium, partly because of the shrinkage of the dilute gelatin of the transparent carmine injection mass. It often becomes so tenuous that it cannot be followed in the capillaries through the thick sections. Where the capillaries can be followed, the mesh resembles that in figures 35*c* to *e* (pl. 9). In zone IV it is wider than it is more superficially.

Veins. The injection of the veins is uniformly good (fig. 39*b*, pl. 10). The carmine gelatin was extravasated from many of them into the hemorrhagic zone and often into the uterine lumen. The larger endometrial veins are usually flattened. No starch grain was found in any vein or sinus. Most sinuses are in zone IV; with their long, dilated tributaries, they often dominate the field (fig. 61, pl. 15). Emissaries to the myometrium are common; some are wide channels, others are slim vessels, sometimes grouped.

Anovulatory Menstruation

B312. This fully mature animal was killed on April 29 at the onset of menstruation, following an anovulatory cycle. Blood was not visible externally, but was found microscopically in the lavage. Recorded cycles between October and April were 23, 24, 22, 27, 42, 37, and 23 days in length. There was an old corpus aberrans on the right, two "objects" on the left, probably very old corpora lutea.

There are several stages in the process of menstruation in the corpus, as is usually found to be the case in early stages of menstruation when entire uteri are surveyed. In this specimen, six distinct areas can be recognized in the sagittal series. The band of obliquely directed glands adjoining the isthmus has an intact epithelium and no extravasated blood. It is 1.3 mm. thick, and the capillary beds are well injected. Adjacent to it is an area measuring 1.9 mm. where the surface is also intact, but the superficial ¼ is hemorrhagic and disorganized. A narrow band where sloughing had occurred separates it from another intact area 2.3 mm. thick. Near the mid-line, this band has blood extravasated in the superficial ⅓, but laterally bleeding had not yet begun. Between it and the fundus is another denuded spot; the fundus has surface epithelium except for small defects here and there. The hemorrhagic zone is 92 microns wide. The glands are sinuous or straight, their cells low and narrow. The stroma is typically dense throughout. The circumscribed bleeding areas resemble those described by Jones and Brewer (1939) in human deciduae verae associated with ectopic pregnancies.

Arteries. The type I arteries are narrow and simple in form; few are as contorted as the artery at the right in figure 40 (pl. 10*a*). The superficial rami of many were injected even in areas where sloughing had occurred. Arterioles extend to within 150 microns of the surface, and precapillary arterioles can be recognized in the hemorrhagic zone. No starch grains were extravasated. The vessel at the left in figure 40 (pl. 10*a*) is of the transitional type, and its sinuous form indicates that there had been little or no involution in zone IV. Constrictions may occur in zone IV and are present in many radial arteries, but the plane of section is seldom favorable for demonstrating their connection with type I arteries. Starch grains and prussian blue were found in a greatly dilated vessel near the stratum vasculare. Under low powers, it appeared to be a vein with a lumen 150 microns wide and media 25 microns thick. It connected not with any veins but with one of the large arteries of the stratum vasculare. Some starch entered all the arteries, and so they contrast strongly with the prussian blue-filled veins. This specimen would accordingly have been in a favorable stage for the demonstration of arteriovenous anastomoses, if there had been any to demonstrate.

Capillaries. There are injected fragments of capillary beds in all zones, but few are complete. The diameter of the capillaries is 4 microns or less. In other phases of the cycle, the endometrium is clearly differentiated from the myometrium by its richer capillary beds. The lack of such differentiation in this specimen, and in some other menstruating ones, indicates the enfeebled endometrial circulation. Long capillaries can be found, especially near, but not at, the surface. One extended parallel to the surface for 287 microns in an area with intact epithelium.

Veins. Figure 40 (pl. 10*a*) gives an indication of the irregular dilated venous net, which is the dominating feature of the corpus. In the fundus, radially directed veins are more common. The prussian blue, which was extravasated onto the surface, came almost entirely from veins, although at so early a stage of menstruation one would expect to find many bleeding arteries. The sinuses, with rare exceptions, are in zone IV (fig. 40, pl. 10*a*). The emissaries to the myometrium are usually minute; few are as wide as the one shown in the figure.

B332. The specimen was obtained on the 2d day of bleeding in April. The preceding March–April cycle was 22 days in length, and anovulatory. The March and February cycles of 24 and 26 days' duration, respectively, had been ovulatory, as indicated by the corresponding corpora lutea.

The endometrium of the dorsal wall measures 2.4 mm.; of the ventral wall, 2.9 mm. The distribution of the glands, the greater activity of the gland cells in zones II and III where, in addition, the reticulum is fragmented or absent, and the coarse connective-tissue fibers of zone IV clearly define the zones. On the dorsal wall the original surface epithelium is still present in spots, and the disorganized zone involves up to 12 per cent of the thickness. The gland cells of zone II are low and narrow. In a count of 1725 cells, there were 0.8 per cent mitoses, all in early prophase, with intact nuclear membranes. Zone II comprises about 46 per cent and zone IV about 45 per cent of the mucosa. In zone II, the cell population reaches 214 cells per 100 square microns; in zone IV, it is 143 cells. No stroma cell mitoses were found.

Arteries. Figure 41*b* (pl. 10*a*) shows a coiled artery typical of the corpus. The dilated, tortuous segment extends into zone II, occasionally to within 0.46 mm. of the surface. Some of these type I arteries have branches in zone IV. Terminal rami are well injected only in the fundus and near the isthmus where little or no tissue had been lost; elsewhere, their lumina are virtual. Although injection mass reached but few superficial rami of the corpus, constrictions in radial arteries are rare (fig. 56, pl. 14). When present, they are close to the stratum vasculare. There was, however, no extravasation of ink, since most superficial branches of the type I arteries are constricted (see p. 175, end).

The dorsal and ventral walls differ in thickness and also in the distance between the type I arteries. In the thicker dorsal wall the range is 0.52 to 0.66 mm., with an average of 0.6; in the ventral wall, which may have been thinner because it was more distended, the range is 0.51 to 0.79, the average 0.65 mm. (see table 1, p. 176).

The vessel at the left in figure 41*b* (pl. 10*a*) is probably a small type I artery, and so may be that in figure 41*a* also. In the fundus no arteries are more contorted than these two. The radial artery in figure 41*c* (pl. 10*a*) with its tuft of myometrial and basal arteries is of an unusual type.

Capillaries. In the fundus, where the surface is still intact, the injection is complete. In most of the corpus the capillary beds, like the arterioles, remained uninjected. Near the isthmus, where there has been little loss except for the surface epithelium, capillary beds also are more complete. Figure 37*a* (pl. 9) shows a tangential section of such a field. The capillaries are spread out among the loose coils of an artery in zone II. An arteriole (solid black) breaks up into capillaries. Like the venous capillaries below, they appear stretched in the sagittal plane. Figure 60 (pl. 14) is from zone IV of the same area; the network here is largely in a single optical plane so that it could be photographed. In both fields the mesh is of the narrow menstrual type.

Veins. The network of veins is injected throughout the endometrium. The vein at the left in figure 41*a* (pl. 10) corresponds to the radial veins of other phases. Great sinuses in the corpus are outstanding features; some may be spread through the entire thickness of the mucosa (fig. 62, pl. 15). There are also long chains of sinuses in zone IV, which extend in the sagittal plane. In the fundus, where the vascular bed is completely injected, only one such sinus was found. Many venules reach the disorganized zone, and injection mass was extravasated from them and onto the surface. Emissaries to the myometrium are common. They may be large vessels that can be followed to the stratum vasculare, or they may be slim; sometimes a group of them drains a sinus.

B331. Day 4 of menstruation. The specimen was obtained in April after a 50-day anovulatory cycle in which the flow had continued for 8 days. Each ovary contained a single old corpus luteum. When the animal was killed, the bleeding had become microscopic. The average duration of the flow in the four preceding cycles was 6 days. The endometrium shows no signs of the phase of repair.

The lumen of the uterus was dilated with the discharge. The denuded mucosa measures 1 mm. or less. The endomyometrial boundary is very irregular, owing to interdigitation. The glands are sparse, straight, or slightly sinuous with low slim cells. The disorganized zone comprises 5 per cent of the endometrium and has 263 stroma cells per 100 square microns; about 1 per cent of them are obviously degenerating. Those bordering the uterine lumen appear normal. There is no sign of resurfacing. In a survey of 2070 gland cells in five sections, only two early prophases were found. None were seen in either stroma or blood vessels. There is little extravasated blood, and wandering cells are uncommon. In zone IV, the average number of stroma cells is 116 per unit area.

Arteries. Practically all the type I arteries are as simple as those in figure 42*a* and *b* (pl. 10). A little injection mass was extravasated into the disorganized zone in some instances, that is, the ends were sealed in most of them. Occasionally there is an artery with branches to all levels of the endometrium. No constrictions were found in them or in the radial arteries (fig. 57, pl. 14).

Capillaries. The well injected capillary beds suggest the resumption of the circulation, and many capillaries have extravasated injection mass into the superficial zone. The fact that the capillary mesh is much coarser than in early menstruation (see fig. 42*a*, pl. 10, at right) may be due to the collapse of some, or it may be that not all capillaries survive the menstrual ischemia; the absence of gaps in the network indicates that incomplete filling is not the cause.

Veins. The dilated veins are as striking a feature as in the preceding endometrium. As in other phases, they may be found at all levels. Unique are the dilated veins that may extend for several millimeters parallel to the surface in the superficial ¼ of the endometrium; some are large enough to be called sinuses. They are probably not artifacts of the injection technique, for they occur in some uninjected material of late menstrual stages.

B335. Day 6 of menstruation. This animal was nursing when received in March. In April there was a 6-day flow, and 35 days later another flow appeared. When killed 6 days later, it still had some blood in the vagina. The right ovary had only the corpus luteum of the recent pregnancy; only one very old corpus luteum was present on the left.

The uterine lumen is widely dilated, the mucosa 1 mm. or less in thickness. The ends of glands project from the denuded surface. In a few minute areas, cells about 7 microns tall extend out over the surface from gland mouths. The glands are straight or sinuous, sometimes dilated with secretion. Their cells are low and slim. In the disorganized zone, 276 normal stroma cells, 52 cells with wrinkled, pycnotic nuclei, and 24 red blood corpuscles were counted in 100 square microns. Nearer the myometrium there were 132 normal and 9 pycnotic cells. No mitoses were found in stroma cells; a few early prophases, in the glands.

Arteries. The injection is very uneven. The arterial trunks of the stratum vasculare are dilated, but starch entered only a few radial arteries. Many are narrow through the myometrium. Very few radial and coiled arteries are dilated with the injection mass. The latter are mostly simply coiled, but a few are as contorted as the one in figure 1 (pl. 1). Only an occasional type II artery was injected.

Capillaries. The only capillary beds injected are in the fundus, where they extend to the disorganized zone. The mesh is irregular and narrow.

Veins. The venous pattern cannot be made out, as only the great sinuses can be followed. Most of them are near the endomyometrial junction; none were found near the surface. Some large emissaries can be followed to the stratum vasculare.

DISCUSSION

Endometrial Arteries

Types. The two types of endometrial arteries recognized by Daron (1936) are distinguished fundamentally by the capillary beds they supply. The superficial ¼ to ⅓ is supplied only by his *type I,* the "coiled" artery. The rest of the mucous membrane is supplied by: (1) branches of type I when present, (2) small "basal" arteries (*type II*), and (3) vessels transitional between these two. Markee (1940) originally called attention to transitions of this sort. When an entire uterus is surveyed, it is obvious that the type I arteries vary greatly in form and size (pls. 1, 4, 5, 7, 8, and 10). They may be elaborately or simply coiled, or merely sinuous. Sometimes the lumen is exceptionally wide or the coiling is more complex or looser; that is, the "arterial fields" are wider. When neighboring vessels in the paramedian corpus (prospective placental sites) exhibit such differences in form and size (figs. 48*a, b,* and 51*b, c,* pl. 12), it is apparent that individual vessels have varied in their response to the hormonal stimuli. Some arteries respond sooner than others to such changes (Markee, 1940, and observations on the ischemic phase, pp. 166–167). They account for the different stages of menstruation in different regions of the same uterus, such as have been described both in *Homo* and in rhesus (see Bartelmez, 1933, p. 146).[3] Some vessels resemble in form the simpler type I arteries, but do not reach the surface (fig. 6*a*, pl. 1). Others confined to zone IV are intermediate between these and the small type II arteries (figs. 4*a*, 7, pl. 1; figs. 15, 16, pl. 3). It is possible, in other words, to find a series of transitions between types I and II. This variability must be taken into account in any significant discussion of endometrial arteries. It necessarily involves surveys of serial sections through prospective placental sites at least.

---

[3] Such differential responses to hormones are obvious in different regions of the endometrium. The potential placental sites show greater changes than the limbus between dorsal and ventral walls ("lateral angles of uterine cavity" and "depths of fundus"). These regions and also the transitional band between isthmus and corpus are tardy in reacting to hormonal stimuli. The gland cells of zone IV respond late or not at all to the secretory stimuli of the progravid phase (Bartelmez *et al.*, 1951). The latter differences may be due to the rate at which the blood flows through this zone since the vascular rhythm is absent.

The transitions between types I and II arteries vary greatly in form and in the extent to which they supply the same deep capillary beds as the type I ("coiled") arteries. An endometrial zone supplied exclusively by a type I artery is usually so severely injured by the ischemia that results from the premenstrual constriction that it is sloughed during menstruation. A zone supplied by both a type I and a transitional artery which does not constrict will not be seriously injured and will not be shed. Differences in the relations of these arteries would account for the variations in the width of the slough in various areas of an endometrium and in different endometria. If, furthermore, the entire capillary bed supplied by a type I artery were to suffer extravasation, that part which also receives blood from the transitional vessel might not be shed. This is suggested by the frequent occurrence of extravasated blood superficially at the end of menstruation and during repair. Such red blood corpuscles are usually crenated or distorted, and they are covered by the epithelium as it migrates from the gland mouths.

Endometrial arteries exhibit two types of branching: apical elm-tree-like branching and diffuse bushlike branching. Type I usually has a terminal crown of branches, few or none arising from the trunk (fig. 1, pl. 1; figs. 18, 20, pl. 4). The trunk may divide abruptly into several large rami, as in figure 21 (pl. 5). Rarely, there are two major trunks, as at the right in figure 49 (pl. 12). On the other hand, some, especially in the follicular phase, have branches at all levels (fig. 14, pl. 3). This is the usual form of type II and of transitional arteries (*b* in figs. 4, 5, pl. 1; figs. 15, 16, pl. 3). Tufted endings, as *b* in figure 6 (pl. 1), are not rare. Figure 41*c* (pl. 10*a*) shows a myometrial artery of this type.

Number of endometrial arteries. Whenever starch entered all arteries, the number of these vessels can be readily determined by counting them at the endomyometrial junction. In 200- to 500-micron sections cut perpendicular to the surface, there is little likelihood of duplication. The number of type I vessels is necessarily underestimated unless they are all followed to the surface in projection reconstructions. Some preliminary counts indicate that more than 2000 arteries of all types enter the corpus-fundus area. In an early progravid specimen injected intravitally (B239, p. 164), the type I arteries were counted in projection drawings of every section of a complete series through the corpus-fundus, as follows:

	Dorsal wall	Ventral wall	Total type I
Large type I	63	58	214
Small type I	38	55	

In a similar specimen injected postvitally, a projection reconstruction of one wall showed most of the larger vessels near the mid-line of the prospective placental site (see B309, p. 162). In a third progravid specimen (B307, p. 163), the coiled arteries in both walls were counted, and 315 were found; of these, 198 could be readily traced to the surface. A reconstruction will doubtless increase the number.

Factors That Influence the Form of Type I Arteries

Cyclic changes. During the repair and follicular phases, the coiled segments of the type I arteries that were at the surface or near it during menstruation are found to be progressively farther removed from it. This shift was supposed by Bohnen (1927) to be due to the growth of new tissue at the surface, as Schröder had concluded and indicated by his term "proliferative phase." As a matter of fact, mitoses are rare or absent in the stroma at this time, nor can they be found in the walls of blood vessels. Even in the epithelia they do not become abundant until late in the follicular phase, by which time the coiled segment is usually in the basal ¼ of the endometrium (fig. 7, pl. 1; fig. 14, pl. 3). Schröder (1914 and subsequently) and his followers have paid little or no attention to the stroma, although Hitschmann and Adler (1908) had described and figured cyclic changes in it. Later, Bartelmez (1931, 1933) and Phelps (1946, 1947) emphasized its importance for the understanding of cyclic changes. The outstanding feature of the phase of repair is not cell division but the development of ground substance in the stroma.

The return of an active circulation toward the end of menstruation is indicated by the condition of the radial arteries. In figure 56 (pl. 14), some are dilated. In figures 57 (pl. 14) and 43 (pl. 11), they are all prominent and dilated. As the moiety of zone II, which persisted throughout menstruation, becomes thicker, the superficial ends of the arteries are passively uncoiled (compare fig. 1 with fig. 5*a*, pl. 1; fig. 18, pl. 4; Daron, 1936, fig. 2).

The dedifferentiation of the arterial walls, which began at the end of the menstrual period, continues, and the reorganization of zones I and II also plays a part (Bartelmez *et al.,* 1951). These changes are obviously greater after ovulatory than after anovulatory menstruation. With the rapid expansion of zone II during the follicular phase, the apical rami of type I arteries are stretched (fig. 7, pl. 1; fig. 18, pl. 4), so that the media becomes reduced to a single rank of more or less discontinuous cells. It is not until just before ovulation that mitoses can readily be found in type I arteries. The fact that the injection was complete in all specimens from the follicular phase both in the myometrium and in the endometrium indicates an especially active circulation. This is well shown in figure 45 (pl. 11) from the end of the phase.

Figure 46 (pl. 11) shows the narrow radial arteries and the poorly injected inner myometrium in a specimen from the phase of ovulation. In many cycles, Markee (1940) observed a mid-cycle cessation of growth, and, sometimes, there was a brief regression in the transplants. B323, obtained a few hours after ovulation, shows various evidences of such regression (see p. 161): the endometrium is definitely thinner than in the preovulatory cases; the glands are sinuous, and the coils of the type I arteries appear compressed (fig. 19, pl. 4).

During the progravid phase, the apical rami are more sinuous in some specimens than in others (fig. 20, pl. 4; fig. 21, pl. 5; fig. 31, pl. 7). A preceding postovulatory regression may play a role in this variation, for the rate at which the ground substance accumulated in zones I and II would determine the extent of the uncoiling from a condition like that in figure 19 (pl. 4). Attention may be called, in this connection, to the group of 6 early progravid endometria described by Bartelmez *et al.* (1951, p. 115, and table 4*a*), in which the stroma of zone II is dense as compared to that in 17 others of the same phase. The dense group may have been emerging from the postovulatory regression.

In any event, arterial growth is a feature of the progravid phase (see p. 162). The rate of growth compared with the expansion of the stroma determines the extent of coiling superficially. Thus, the apical rami are more sinuous in B309 (fig. 21, pl. 5) than in B326 (fig. 20, pl. 4), also an early progravid specimen. In B239, progravid growth throughout the endometrium seems to have been rapid, for the endometrium reached 8.5 mm. in thickness. Here the apical rami are more contorted than in any other progravid specimen (arrow in fig. 50, pl. 12). There is further growth of the type I arteries during pregnancy (Ramsey, 1949). On the other hand, in the late progravid and highly edematous B325 (p. 165), the increase in length of the arteries was but little greater than the expansion of zones I and II (fig. 31, pl. 7).

In the progravid phase the radial arteries are not prominent, as may be seen in figure 51 (pl. 12). This figure also shows the change that has occurred in the thickness of the endometrium compared with the myometrium (see table 1, p. 176). At the onset of regression, it becomes difficult to inject the inner myometrium and the endometrium (see p. 166). The uterus is still large; the myometrium is thin (fig. 52, pl. 12). The sinuous glands and narrower lumina, in comparison with figure 51 (pl. 12), indicate involution in zone II. Endometrial involution continues before and after extravasation as the myometrium thickens (table 1). The coiling of the type I arteries increases rapidly, as Markee (1940) was able to observe directly in his transplants (figs. 33, 34, pl. 8; fig. 39*b*, pl. 10; Daron, 1936, fig. 5). When sloughing ensues, the contorted ends of the arteries that survive sloughing are at the surface (fig. 59, pl. 14), and they may even project beyond it when the surrounding stroma is dispersed. During menstruation, the superficial ends show degenerative changes, and their component cells, like all other endometrial cells, are materially reduced in size. As a result, the coiling is found to be looser, especially superficially. Hartman's (1932) observations on the contraction of the myometrium at this time are visualized in figures 54 and 55 (pl. 13). During repair, the involution of the type I arteries continues. As the circulation is restored, and the stroma begins to "loosen" with the reappearance of ground substance, the endometrium thickens, and the uncoiling of the arteries proceeds more rapidly. These changes are more obvious after ovulatory menstruation; in the anovulatory type, the tissue loss may be minimal, and there may be little more than rehydration of the superficial tissues. This was Gebhart's idea of menstruation.

Effect of preceding cycles on the form of type I arteries. When the larger type I arteries in different endometria from the same phase of the cycle are compared, striking differences may be encountered. They naturally become most obvious in the later phases of the cycle. Figures 21 (pl. 5) and 48 (pl. 12) show characteristic large arteries of the early progravid B309. They are similar in B307 (fig. 49, pl. 12). In B239 (fig. 50, pl. 12), the apical rami are more contorted, but the arterial fields are narrower; i.e., the diameter of the coils is less. Fundamentally, however, the arteries are similar in all three. B326 also presents a typical early progravid endometrium, but the arteries are simple in comparison. The artery in figure 20 (pl. 4) is as complex as any of them; most are but little more coiled than the transitional arteries of figure 30 (pl. 7). The history of B326 is as follows: The animal was received in December. The 25-day January cycle was anovulatory and complicated by a 2 weeks' diarrhea. In February, there was a 20-day postmenstrual period of ovarian quiescence followed by an abrupt rise in the color of the sex skin. Ovulation probably occurred on day 27 of the cycle. The only corpus luteum on the right was that of the current cycle. In the other ovary, the only "object" seen was an ancient corpus luteum. In B309, on the other hand, the ovarian findings indicate ovulation in the three preceding cycles. Similar conditions probably obtained in B307, B330, and B316, although the histologic data on the ovaries are not so complete. It would appear, then, that in these three, as in B309, the growth of the arteries had been cumulative during the previous ovulatory cycles. In B326, on the other hand, it would seem that there had been progressive regression in the arteries during the period of ovarian inactivity, and that some type I arteries had attained the form shown in figure 20 (pl. 4) in the course of the final cycle. That such rapid growth may occur in a single cycle was demonstrated by Hartman (1944).

The events in preceding cycles, however, do not tell the whole story. In B324 (see p. 164), the type I arteries are no more complex than in B326, at least as far as the basal coils are concerned, yet the ovaries contain a series of corpora lutea corresponding to the four preceding cycles, as was determined by Rossman (1942, fig. 1) in his detailed study. The antithesis of this is no. 115 of Daron's series (1936, fig. 5), which comes from the beginning of the ischemic phase. This endometrium has the most highly contorted type I arteries in his series. Yet it was obtained at the end of the 1st cycle following a 6-months' amenorrhea. It would seem more probable that this vessel had grown rapidly during the final October–November cycle than that it had remained highly contorted during the period of ovarian inactivity characteristic of the summer months.

When regression is in full swing at the end of the ischemic phase and during menstruation, the coiling is increased. The collapse of a vessel like that in figure 34 (pl. 8) from day 1 into one like that in figure 39*b* (pl. 10) obtained on day 2 (or 3) can readily be accounted for by the involution that Markee (1940) observed continuing during menstruation. The presence of slough *in situ* in some areas of the 2- to 3-day specimen shows that only part of zone II had been lost; the major apical rami indicate that the entire stem of the vessel is intact; we are dealing with more than the basal part of the vessel. The sinuous type I arteries of anovulatory cycles necessarily show less coiling during menstruation, even though the degree of involution may be as great as after ovulatory cycles (fig. 40, pl. 10*a*). In anovulatory menstruation, both complex and simply coiled arteries may be present in the same endometrium (figs. 1, 2, 5*a, c,* pl. 1). The contorted vessels (see also fig. 41*b,* pl. 10*a*) had probably developed during previous ovulatory cycles and had not regressed subsequently.

Constrictions

Daron's (1932, 1936) observations on constrictions in radial arteries were made upon thick sections of material obtained under exceptionally favorable conditions for the study of vascular reactions (p. 155). The only uteri in which he found many constrictions were from early stages of menstruation; they were present in all 4 cases that had been preceded by ovulatory cycles, and in 2 of the 3 cases of anovulatory menstruation. He describes the radial arteries as tapering toward the endometrium in the absence of branching (hence "constriction cones"). The constrictions are usually long, extending in one specimen from the stratum vasculare to the endometrium. The constricted lumen is 7 microns or less in diameter and enlarges abruptly at the junction with the mucosa. In our postvital injections after vasodilation, the constrictions are short, as a rule, and there may be two or three in a single vessel. Since starch grains often passed through the constrictions, it would seem that the cones of Daron had been dilated while the injection was in progress and that segments of them reappeared in the interim between injection and the arrival of the fixing agent. It is of interest, in this connection, that during menstruation Hasner (1946) found constrictions in human uterine arteries that had probably not been reached by the fixative until days after removal of the uterus.

In a thick section of Daron's no. 115, which he kindly lent the author, the following measurements of a radial artery were made with the X60 immersion lens:

	Lumen (microns)	Diameter, including media (microns)
At origin from stratum vasculare....	23	173
Near constriction	25	75
Constricted segment	7.5	37
	6.5	21
At endomyometrial junction........	15	50

In the material injected postvitally after vasodilation, the lumen is 3 to 10 times greater on either side of the constrictions, and the diameter, including the media, is always less in the constricted segment (see pp. 161, 170, and fig. 19, pl. 4). It appears, then, that local elongations of the vessels narrow the lumen. Markee's (1940) observations of constrictions in transplants consisting of endometrium only show that the coiled arteries of the endometrium are as sensitive to hormonal changes as the radial arteries. This is corroborated by observations on specimens from the ischemic phase.

In the ischemic phase, constrictions in radial arteries are not so common as during menstruation. Daron (1936) states that in his no. 115 they are rarely narrower than the endometrial arteries. As was noted above, some typical constrictions can be found in this specimen. A striking feature of this uterus is the complete capillary injection of the peritoneal ¼ to ⅓ of the myometrium, whereas less HgS reached the endometrium, generally, and few capillaries can be recognized (Bartelmez *et al.,* 1951). In his no. 123, which is on the verge of menstruation, Daron finds the caliber of the type I arteries extremely variable, and many are dilated superficially. The radial arteries are not described. In both our postvitally injected uteri from the early ischemic phase, the injections are incomplete. In B316 (see p. 166 and fig. 52, pl. 12), the injection is very uneven. The myometrium is well injected on the whole, and, in some endometrial areas, arteries, veins, and capillaries are well filled (figs. 27*a, b,* 28, pl. 6). Elsewhere, constrictions in radial arteries and in type I vessels prevented the entrance even of carmine gelatin into any endometrial vessels. In addition, the apical rami of many coiled arteries remained narrow and empty when the rest of the vessel was filled with the injection mass. In B318 (see p. 167), many radial arteries, especially those supplying the prospective placental sites, were so highly constricted that even the carmine gelatin did not enter them. The usual injection procedure including vasodilators had been followed; the arteries of the stratum vasculare are dilated, and the myometrium between it and the peritoneal surface is well injected, as in Daron's no. 115. In the ischemic areas of B317 (see p. 168), constrictions are common in the radial arteries, but the type I arteries, veins, and capillary beds are fairly well injected. The significance of this behavior of the vessels that supply the superficial capillary net is considered on page 178.

Spacing of coiled arteries. When the distance between the coiled arteries of an endometrium is estimated in a series of thick sections, it appears that the various specimens from a particular phase of the cycle are similar and that the distance varies with the phase of the cycle. Such measurements are comparable, since all the specimens were similarly prepared. When the cyclic changes in this distance are compared with the stroma-cell density in zone II, it is evident that, the denser the stroma, the closer the arteries are to one another; in other words, the distance varies directly with the amount of ground substance in the stroma. This finding is to be expected if the number of coiled arteries does not change in the course of a cycle. There is no evidence of such a change in number. The average values of a number of specimens from the present series are given in table 1.

TABLE 1

SPACING OF TYPE I ARTERIES IN RELATION TO PHASE OF CYCLE AND UTERUS AS A WHOLE

Number of specimen	Phase of cycle	Average distance between arteries (mm.)	Number of stroma cells per 100 square microns in zone II	Ratio * $\frac{\text{endometrium}}{\text{myometrium}}$
B334	Repair-follicular	0.45	136 8 wandering cells	0.38
B338	Late follicular	0.62	30–61	0.83
B319	Ovulation	0.53	113–154	0.72
B309	Early progravid	1.08	68–126	1.13
B325	Late progravid	1.4	68–99	2.33
B316	Transition to ischemic	0.6	124–155	2.5
B318	Early ischemic	0.7	119–169	0.73
B317	Early menstrual (ovulatory)	0.54	200 67 wandering cells	1.09
B314	Day 1 ovulatory menstruation	0.38	264 30 wandering cells	0.45
B335	Day 5 anovulatory menstruation	0.23	226 8 wandering cells	0.3
B329	Menstrual-repair	0.55	187–420 4 wandering cells	0.35

* The thickness of the endometrium in any phase of the cycle is subject to great variation. In some individuals, the uterus as a whole is larger than in others. This variable feature can be compensated for by using the $\frac{\text{endometrial}}{\text{myometrial}}$ ratio. The measurements for this ratio were made on thick sections near the center of the corpus, where the cyclic fluctuations in thickness are maximal. They are illustrated on plates 11 to 15.

With the postmenstrual loosening of the stroma in the phase of repair, the arteries are farther apart than during menstruation, and the spreading continues during the follicular phase. In a specimen taken immediately after ovulation, they are slightly closer together. During the progravid phase, when the corpus uteri enlarges (Hartman, 1932) the arteries are separated, each supplying a broader territory. At this time, mitoses in them, especially in the walls of the terminal rami of type I arteries, reach the maximum. The endomyometrial ratio shows that, as the uterus enlarges, the myometrium thins out and the endometrium thickens. With the shrinkage of the endometrium in the ischemic phase, the arteries are brought closer together; this mutual approach continues through the phase of menstruation, at least until the uterus becomes dilated with the accumulated menstrual discharge.

CAPILLARY BEDS

Superficial net. The superficial net is a distinctive feature of the endometrium, and is presumably of physiological importance. Like the rest of the superficial capillary bed, it is supplied entirely by type I arteries, and its blood flow changes with the varying responses of these vessels and the radial arteries to hormonal stimuli. Since it is a continuous network, there is the possibility of some collateral circulation when any one artery constricts. That is to say, the potential capillary bed of a type I artery is greater than the spread of its apical rami. Thus, Markee (1948) found the surface area supplied by type I arteries *in vivo* ranging from 4 to 7 sq. mm. According to the measurements on thick mounted sections described on page 157, the greatest spread of the apical rami of a type I artery covers a circular area of 3.65 sq. mm. This figure is for the progravid phase; at other times the area is smaller.

The superficial net exhibits cyclic changes. It takes form during the phase of repair as the avascular stroma of zone I begins to thicken. In the specimen illustrated in figure 4 (pl. 1), it varies from 54 to 77 microns in width. The form of the network can be best appreciated in sections cut tangential to the surface, as in figure 9 (pl. 2) taken from an endometrium of the follicular phase. The arterial capillaries are superficial to the venous capillaries, which unite to form the radial veins. When these are numerous, a more rapid flow of blood can be envisaged. At the end of the follicular phase, the superficial capillary net is dilated, 92 to 115 microns in thickness, and accordingly more prominent than at any other time (fig. 45, pl. 11; fig. 14, pl. 3).

In a specimen obtained immediately after ovulation, the mesh is more irregular and narrower (see tangential sections in fig. 23*a,* pl. 6)—one of several indications of regression (see p. 161). During the progravid phase, zone I is vascularized and becomes edematous; the superficial net reaches a width of 200 microns, and its meshes become wider (figs. 24, 26*a*, pl. 6). In the ischemic phase there is no change before the superficial zones begin to shrink (figs. 27*a, b,* pl. 6). The intimate relation of the capillaries to the surface epithelium is manifest everywhere in this endometrium (see p. 166). In the ischemic areas of B317 (day 1, obviously just before extravasation), there are no longer any capillaries in contact with the epithelium; stumps on some that are injected suggest capillary collapse (arrow in fig. 35*a,* pl. 9). In this area the net is 15 microns in width. The venules are dilated. The meshes are narrow, as can be seen by comparison with figure 37*b* (pl. 9). The net is completely lost in the slough during ovulatory menstruation. To judge from conditions in B329 (fig. 8, pl. 2), it is reorganized after anovulatory cycles, although sometimes but little tissue has been shed.

Deep capillary beds. The capillary beds in the deeper reaches of zone II and zone III present very different pictures. The capillaries tend to divide dichotomously, like the precapillary arterioles, and often extend as stems with few branches for 300 microns or more. Where they are close to the upper surface of the section, they can be identified as capillaries under oil-immersion objectives. Anastomoses occur, but are uncommon (fig. 10, pl. 2). Figure 13 (pl. 2) presents a typical field in B338 (late follicular phase), which was completely injected throughout the uterus. Here the capillaries are well separated from one another in harmony with the loose structure of the stroma (see p. 160). In the area illustrated, all capillaries connect directly with venules. In zones II and III, venous capillary nets often extend between neighboring venules, as in figure 12 (pl. 2) and figures 25 (lower right) and 28 (pl. 6). These vessels are capillaries in structure and dimensions; usually no arterial connections can be established. Such venous nets may serve to retard the flow of blood through the endometrium, thus facilitating diffusion.

Zone IV. In this zone the network predominates so that adjacent arteries supply the same capillary bed (fig. 11, pl. 2), as is the case in the superficial net. Small type II arteries (Daron, 1936) supply the zone for the most part, but lateral branches of both type I and transitional arteries may ramify throughout zone IV (fig. 4*d,* pl. 1; at left in fig. 14, pl. 3). The network is not different during the progravid phase, but contributions from type I arteries are rare (fig. 32, pl. 7). During menstruation the mesh may be wider (fig. 35*e*, pl. 9), probably because of the collapse of some capillaries.

Venous System

The pattern of the veins is so irregular that few generalizations are possible. In the endometrium the pervading network is so close meshed that the number of veins appearing in a section is greater than the number of arteries. There is no relation between the tree- or shrub-like arterial pattern and the venous network. The variations in the caliber of the veins is extreme, and it probably fluctuates from time to time, as Markee (1940) observed in the case of the sinuses in his transplants. In a specimen injected intravitally and frozen rapidly, there are veins in the middle of zone II, 70 microns in diameter, one of which receives tributaries of 3.6, 18, and 37 microns. The variations in caliber of individual veins are more extreme in the postvitally injected material (fig. 22, pl. 5).

As long as the superficial capillary bed is intact, the venous capillaries unite to form a series of veins that extend for greater or lesser distances to deeper levels. These radial veins of the endometrium tend to be uniform in diameter and have few or no tributaries. They obviously provide for the rapid drainage of the superficial bed. In the follicular phase many of the radial veins are long and straight, extending as far as zone IV (arrow in fig. 17, pl. 3). In zone II, they often appear as if they had been stretched as the zone thickened. The meshes of the venous network are likewise elongated radially at this time. Shortly after ovulation (B323) some reach zone IV, as in the follicular phase. Where the endometrium is thin, they are bowed (fig. 19, pl. 4). Rapid involution seems to have occurred here, and the veins did not retract. In menstruating endometria like B314 and B317, on the other hand, where involution was more gradual, they are usually straight. In the four early progravid endometria, the radial venules join the network at the middle of zone II (fig. 22, pl. 5). The network is, consequently, the dominant feature of the venous pattern.

In the thick, edematous mucosa of B239 (see p. 164), the radial vessels are more prominent, occasionally extending to zone III without tributaries. They are usually narrow, enlarging from 18 to 22.5 microns where they reach the sinus. These measurements are significant, since the uterus was injected intravitally. The late progravid B325 (see p. 165) presents a similar picture. In the aberrant B330 (p. 166), there are radial veins that, as in the follicular phase, reach zone IV directly. The early ischemic cases (p. 167) resemble B325 in that there are long radial venules. In B115 (p. 167), Daron (1936) noted a superficial venous congestion, which Markee

(1940) saw developing in some premenstrual cases but not in others. In the ischemic areas of B317 (p. 168), there are also superficial veins that course parallel to the surface. Vessels such as those in figure 33 (pl. 8) are like irregularly twisted ribbons, appearing broad only where the flat surface is in the plane of section. In this area, radial veins may also reach zone III. The fact that they are straight, despite the evidences of compression manifest in stroma, glands, and arteries, would indicate that they maintain their course by shortening as the endometrium becomes thinner. A few observations on the form of the endothelial cells suggest this explanation. In any event, this is another example of the passive adaptation of the vasculature to stromal changes.

In the menstruating areas of B317, there is little evidence of through routes. Almost all veins are collapsed; since most of them are viewed obliquely, the size of the lumen is exaggerated in a projection such as figure 34 (pl. 8). The slim, irregular venules of zone IV are not represented in the figure. Figures 39*a* and *b* (pl. 10) show the character of the network in a somewhat later stage of menstruation. Here, too, the great majority of veins are collapsed, both in endometrium and myometrium. On the other hand, sinuses, as in figure 62 (pl. 15), have become common. In the specimen from day 2 of anovulatory menstruation (see p. 171), where the myometrium is well injected and many radial arteries are dilated, the larger endometrial veins are likewise dilated (figs. 41*a, b,* pl. 10; fig. 62, pl. 15). This condition continues later in menstruation (fig. 42*b,* pl. 10; fig. 1, pl. 1) and even into the phase of repair (figs. 4, 5*a,* pl. 1).

Enlarged veins or sinuses are present in all phases of the cycle. Markee (1940) found that they appear, enlarge, and soon disappear. In postvitally injected material, they may be somewhat isolated from one another, or a chain of them may extend half the length of the corpus. In the follicular phase they are predominantly in various levels of zone IV (fig. 7, pl. 1; fig. 17, pl. 3). Rarely, in various phases, large veins with many tributaries converge on a deep sinus (cf. fig. 62, pl. 15). Unlike the radial veins, which primarily drain the superficial net, these are through drainage routes within the network (fig. 41*a,* pl. 10; fig. 3, pl. 1). In the early follicular phase, the sinuses are well filled, and the emissaries to myometrial veins are prominent. In B338, taken from the end of the follicular phase, some sinuses and their emissaries are flattened; others are dilated. In a survey of this specimen, 56 sinuses were counted in zone IV, 5 in zone III, and 20 deep in zone II. In the progravid and ischemic phases most of them are also in zone IV. The emissaries are slim and uncommon, especially in the ischemic phase. In the ischemic areas of B317 (day 1), all veins are narrow or completely collapsed, as might be expected, from the greatly reduced blood flow and contracted myometrium (fig. 33, pl. 8). Plate 15 shows the prominence of the larger veins later in menstruation. In figure 61, most veins are flattened, but there are some with their emissaries open. In the specimen of anovulatory menstruation shown in figure 62, the circulation had been re-established, except superficially, and the veins, in general, were dilated. Large sinuses near the junction and wide emissaries characterize later menstruation.

Adaptive Significance of Certain Unique Features of the Uterine Vascular System

The earlier interpretations of the menstrual cycle were based on human material, and the point of view of the gynecologist has dominated most clinical discussions of it. No distinctive changes in an organ of reproduction, however, can be interpreted except in the light of their possible role in the initiation and maintenance of pregnancy. The recent advances in knowledge of the early stages of primate development provide a basis for profitable speculations as to the raison d'être of various features of the menstrual cycle. The primate endometrium is unique among mucous membranes in having a superficial zone supplied exclusively by a set of arteries that exhibit distinctive cyclic changes in behavior and form.

Certain hormonal reactions of these arteries appear to facilitate implantation of the ovum. These (type I) arteries of the endometrium grow rapidly under the influence of the corpus luteum, and their coiling may be the chief factor in the progressive retardation of the superficial capillary flow, which was demonstrated by Markee (1950*a*). This retardation results in an edema which is greatest near the mid-line of the corpus, just below the surface epithelium. It provides a medium favorable for the spread of the invading trophoblast. The accumulated edema fluid spreads out the meshes of the characteristic superficial network of capillaries (figs. 26*a,* 27, pl. 6). This action, together with the slowing of the blood flow, reduces the chances of an extravasation from capillaries eroded by the trophoblast such as might otherwise be great enough to wash away the newly implanted ovum. It must be remembered that at this time the human ovum is less than half a millimeter in diameter, and in the rhesus monkey it is not much larger.

The stasis of the ischemic phase has been interpreted as a means of weakening maternal tissues so that they become pabulum for the trophoblast, which is rapidly expanding at this period. The stasis is due to constrictions in type I arteries, and is followed by a brief extravasation of blood. Such an extravasation occurs in human pregnancies at about the time of the expected but lapsed menstruation (Brewer, 1937). It is more extensive in the rhesus monkey (Hartman, 1929). The individuality in the reactions of the type I and radial arteries (p. 175) is manifested by the restriction of extravasation to the arteries at the implantation site. The bleeding at the time of implantation leads to the interpretation of *menstrual* bleeding as a reaction of all the type I arteries, exacerbated, in the absence of pregnancy, by the greater fall in available ovarian hormones (see Bartelmez, Corner, and Hartman, 1951).

In her detailed studies on the development of the placental circulation of primates, Ramsey (1949 and subsequently) has demonstrated growth and increased coiling in endometrial and myometrial arteries during the earlier stages of pregnancy. With the great expansion of the uterus during and after conversion (Reynolds, 1954), the coils are gradually paid out. Ramsey has accordingly interpreted this coiling as an adaptation for the increase in the volume of the pregnant uterus.

SUMMARY

The endometrium is unique in having a special system of arteries that supplies its superficial ⅓. These arteries are confined to corpus and fundus. Radial arteries arise from the stratum vasculare and continue in the endometrium as type I ("coiled") arteries. This system of arteries is highly sensitive to changes in available ovarian hormones. Their responses vary individually in growth (fig. 51*b, c,* pl. 12), in threshold, and according to the region of the uterus in which they are located (see p. 172; fig. 55, pl. 13, where smaller type I arteries are present in lateral limbus at right). This variation is in harmony with differences in the hormonal reactions of various regions and zones of the endometrium, which may, in turn, be due to differences in the rate of blood flow. The largest type I arteries are in the paramedian region of the corpus where implantation usually occurs. There are many transitions between the type I and type II arteries of Daron, and sometimes part of the deeper capillary bed of a type I artery is also supplied by a transitional vessel. Differences in the extent of the overlap account for variability in the width of the zone shed during menstruation (see p. 172).

The most superficial capillary bed is a network ranging in width from 50 microns at the beginning of the follicular phase (fig. 4, pl. 1) to 200 microns at the end of the progravid phase (fig. 24, pl. 6). Since apical rami of type I arteries supply this continuous net, the surface area that each artery can supply is greater than the spread of the arterial tree (see p. 176). The overlap of potential capillary beds thus provides for collateral circulation at this level.

Toward the end of the follicular phase the apical rami of type I arteries and their capillary beds are dilated; the blood flows more rapidly than at any other time (Markee, 1948), and "through routes" develop in the venous network (fig. 17, pl. 3). These radial endometrial veins extend at this time with few or no tributaries from the superficial net to sinuses in zone IV, which have wide emissaries to myometrial veins.

In two specimens obtained shortly after ovulation, constrictions are present in radial arteries (fig. 19, pl. 4; figs. 46, 47, pl. 11). The endometria are thin; the type I arteries appear compressed. This finding can be correlated with the endometrial regression observed in 40 per cent of the specimens at about the time of ovulation (Markee, 1940).

In the early progravid phase, mitoses are numerous in type I arteries, which grow faster than the endometrium thickens. Rate of blood flow is gradually reduced (Markee, 1948). Through routes to myometrial veins become inconspicuous. Edema develops progressively. Zone I, avascular in the follicular phase, is invaded by arterial capillaries (compare fig. 23*a* with fig. 24, pl. 6). By the end of the phase, the capillaries come into intimate contact with the surface epithelium and zone I becomes loose; its capillary mesh is wide (figs. 26*a,* 27*a, b,* pl. 6). Throughout the progravid phase the myometrium relaxes as the endometrium thickens and the uterus as a whole enlarges (Hartman, 1932; compare fig. 45, pl. 11, with fig. 52, pl. 12). All these phenomena are distinctive of the period of implantation of the ovum.

During the ischemic phase, constrictions in radial arteries gradually become widespread, and complete injections of endometrium are practically impossible to obtain. The constrictions are due to local elongations of the arteries, and may result in complete occlusion of the lumen. Sometimes only the apical rami of type I arteries are constricted, a condition seen also in menstruation (see p. 171). The veins may be congested or slim and almost empty. Eventually there is a marked thinning out of endometrium with thickening of myometrium (compare figs. 54, 55, pl. 13). The superficial ends of the arteries become more contorted as involution progresses during menstruation (figs. 33, 34, pl. 8; fig. 39*b,* pl. 10). Capillary meshes become narrower or remain uninjected (compare figs. 35*a–e* with fig. 37*b,* pl. 9).

Before the end of external menstrual bleeding, superficial endometrial capillaries can be injected in part.

Involution and shedding of part of zone II during ovulatory menstruation bring the coils of type I arteries to the surface (fig. 59, pl. 14). The presence of apical rami at the end of menstruation indicates the survival of part of zone II (fig. 1, pl. 1).

During repair, two factors are involved in the uncoiling and elongation of the superficial ends of the type I arteries: development of ground substance in the surrounding stroma, and regression of the arterial walls. The uncoiling in zone II is sometimes not complete at the end of the follicular phase (fig. 18, pl. 4).

As zone II thickens during the follicular phase, the apical rami of type I arteries are stretched. Mitoses in their walls are uncommon until after the corpus luteum has become active. By the end of the progravid phase, precapillary arterioles have extended into zone I.

Endometrial arteries of types I and II (Daron, 1936) are characteristic of corpus and fundus. Transitions between them can be found (fig. 16, pl. 3). Type II arteries outnumber type I by about 10 to 1 (see p. 173). Endometrial arteries, in general, exhibit two kinds of branching: treelike, with an apical crown or tuft of branches, and diffuse bushlike branching (see p. 159).

The form of type I arteries is influenced by four factors:

1. Changes in the stromal ground substance, especially in zone II. In the repair and follicular phases, they are uncoiled and stretched; sometimes in the ovulation phase, and always during menstruation, the coils appear compressed by endometrial involution (compare figs. 18, 19, pl. 4; fig. 31, pl. 7; fig. 39*b*, pl. 10). These are passive adjustments to the immediate environment.
2. Intrinsic growth by mitosis in the progravid phase.
3. Cumulative increase in complexity, which may but does not necessarily occur in the course of a series of ovulatory cycles (see p. 174).
4. Extent of menstrual and postmenstrual regression. In anovulatory menstruation, they may be simple (fig. 40, pl. 10*a*) or contorted (fig. 41*b*, pl. 10*a*).

As the endometrium increases in volume, the larger (type I) arteries are separated from one another; as it decreases, they come closer together. There is no evidence for a material change in their number in the course of a menstrual cycle.

Aside from the restoration of relatively slight losses during menstruation, there is but little growth in capillaries. The mesh of the capillary beds widens or contracts as the stroma becomes looser or denser (pls. 2, 6, 9). The wide mesh at the end of menstruation indicates collapsed capillaries.

Endometrial veins are thin walled. In all phases of the cycle, they form a close-meshed network pervading the endometrium. In zones II, III, and IV, nets of wide capillaries are often spread out between venules. Since arterial afferents to such nets can only occasionally be found, they may be a mechanism for retarding blood flow (see fig. 12, pl. 2; fig. 28, pl. 6).

Elongation of the meshes of the venous net and radial veins passing directly from the surface to zone IV characterizes the follicular phase (fig. 7, pl. 1; fig. 17, pl. 3). In the progravid phase, the intricate network is the dominant feature of the venous system as the radial veins enter the network at the middle of zone II (fig. 22, pl. 5). The irregularly anastomosing endometrial veins are not spatially related to the dichotomously branching arterial tree.

Superficially dilated veins are present only in menstruating endometria.

The network of endometrial and myometrial veins is continuous. Since there are no valves within the uterus, arterial injection masses introduced postvitally can spread from any injected capillary bed retrograde through the entire venous system even when the arterial injection is incomplete.

No arteriovenous anastomoses were found in any specimen. Had any been present, they could hardly have been overlooked in the thick serial sections of these doubly, and usually completely, injected preparations.

Certain vascular changes characteristic of the menstrual cycle can be correlated with events in early pregnancy and interpreted as adaptations for insemination and the implantation of the ovum (see p. 178).

LITERATURE CITED

Bartelmez, G. W. 1931. The human uterine mucous membrane during menstruation. Amer. Jour. Obstet. and Gynecol., vol. 21, pp. 623–643.

——— 1933. Histological studies on the menstruating mucous membrane of the human uterus. Carnegie Inst. Wash. Pub. 443, Contrib. to Embryol., vol. 24, pp. 141–186.

——— 1956. Premenstrual and menstrual ischemia and the myth of endometrial arteriovenous anastomoses. Amer. Jour. Anat., vol. 98, pp. 69–95.

——— G. W. Corner, and C. G. Hartman. 1951. Cyclic changes in the endometrium of the rhesus monkey (*Macaca mulatta*). Carnegie Inst. Wash. Pub. 592, Contrib. to Embryol., vol. 34, pp. 99–144.

Bensley, Caroline M. 1951. Cyclic fluctuations in the rate of epithelial mitosis in the endometrium of the rhesus monkey. Carnegie Inst. Wash. Pub. 592, Contrib. to Embryol., vol. 34, pp. 87–98.

Bohnen, P. 1927. Wie weit wird das Endometrium bei der Menstruation abgestossen? Arch. f. Gynäkol., vol. 129, pp. 459–472.

Brewer, J. I. 1937. A normal human ovum in a stage preceding the primitive streak. (The Edwards-Jones-Brewer ovum.) Amer. Jour. Anat., vol. 61, pp. 429–481.

Caldeyro-Barcia, R., and H. Alvarez. 1953. Nuevos hechos sobre la fisiologia, fisiopatologia y farmacologia del utero humano. Ann. Facultad de Medicina de Montevideo, vol. 38, pp. 383–400.

Collings, M. R. 1926. A study of the cutaneous reddening and swelling about the genitalia of the monkey, *Macacus rhesus*. Anat. Rec., vol. 33, pp. 271–287.

Corner, G. W. 1923. Ovulation and menstruation in *Macacus rhesus*. Carnegie Inst. Wash. Pub. 332, Contrib. to Embryol., vol. 15, pp. 73–101.

——— 1942. The fate of the corpora lutea and the nature of the corpora aberrantia in the rhesus monkey. Carnegie Inst. Wash. Pub. 541, Contrib. to Embryol., vol. 30, pp. 85–96.

——— 1945. Development, organization, and breakdown of the corpus luteum in the rhesus monkey. Carnegie Inst. Wash. Pub. 557, Contrib. to Embryol., vol. 31, pp. 117–146.

——— G. W. Bartelmez, and C. G. Hartman. 1936. On normal and aberrant corpora lutea of the rhesus monkey. Amer. Jour. Anat., vol. 59, pp. 433–457.

Dalgaard, J. B. 1946. The blood vessels of the human endometrium. Acta Obstet. et Gynecol. Scandinav., vol. 26, pp. 342–378.

Daron, G. H. 1932. The arterial pattern of the tunica mucosa of the *Macacus rhesus* uterus. Anat. Rec., vol. 52, suppl., p. 9.

——— 1936. The arterial pattern of the tunica mucosa of the uterus in *Macacus rhesus.* Amer. Jour. Anat., vol. 58, pp. 349–419.

——— 1937. The veins of the endometrium (*Macacus rhesus*) as a source of the menstrual blood. Anat. Rec., vol. 67, suppl., p. 13.

Freund, R. 1904. Zur Lehre von den Blutgefässen der normalen und kranken Gebärmutter. 86 pp. Jena.

Hartman, C. G. 1929. Uterine bleeding as an early sign of pregnancy in the monkey, etc. Bull. Johns Hopkins Hosp., vol. 44, pp. 155–164.

——— 1930. Bimanual rectal palpation as applied to the female rhesus monkey. Anat. Rec., vol. 45, p. 263.

——— 1932. Studies in the reproduction of the monkey *Macacus* (*Pithecus*) *rhesus,* with special reference to menstruation and pregnancy. Carnegie Inst. Wash. Pub. 433, Contrib. to Embryol., vol. 23, pp. 1–161.

——— 1944. Regeneration of the monkey uterus after surgical removal of the endometrium and accidental endometriosis. West. Jour. Surg. Obstet. and Gynecol., vol. 52, pp. 87–102.

Hasner, E. 1946. Endometriets vasculaere Cyklus. En anatomisk-histofysiologisk Undersøgelse. Thesis, University of Copenhagen. 143 pp. Copenhagen, Berlingske Bogtrykkeri.

Hitschmann, F., and L. Adler. 1908. Der Bau der Uterusschleimhaut des geschlechtsreifen Weibes mit besonderer Berücksichtigung der Menstruation. Monatschr. f. Geburtsh. u. Gynäkol., vol. 27, pp. 1–82.

Jones, H. O., and J. I. Brewer. 1939. The arterial phenomena associated with uterine bleeding in tubal pregnancy. Amer. Jour. Obstet. and Gynecol., vol. 38, pp. 839–861.

Kaiser, I. H. 1947. Absence of coiled arterioles in the endometrium of menstruating New World monkeys. Anat. Rec., vol. 99, pp. 353–367.

——— 1948. Newer concepts of menstruation. Amer. Jour. Obstet. and Gynecol., vol. 56, pp. 1037–1047.

Landesman, R., R. G. Douglas, G. Dreishpoon, and E. Holze. 1953. The vascular bed of the bulbar conjunctiva in the normal menstrual cycle. Amer. Jour. Obstet. and Gynecol., vol. 66, pp. 988–996.

Markee, J. E. 1929. Rhythmic variations in the vascularity of the uterus of the guinea-pig during the estrus cycle. Amer. Jour. Obstet. and Gynecol., vol. 17, pp. 205–208.

——— 1940. Menstruation in intraocular endometrial transplants in the rhesus monkey. Carnegie Inst. Wash. Pub. 518, Contrib. to Embryol., vol. 28, pp. 219–308.

——— 1948. Morphological basis for menstrual bleeding: relation of regression to initiation of bleeding. Bull. N. Y. Acad. Med., vol. 24, pp. 253–268.

——— 1950*a*. The relation of blood flow to endometrial growth and the inception of menstruation. *In* E. T. Engle (ed.), Menstruation and its disorders: Proceedings of the conference held under the auspices of the National Committee on Maternal Health, pp. 165–185. Springfield, Illinois.

——— 1950*b*. The morphological and endocrine basis for menstrual bleeding. Progress in Gynecol., vol. 2, pp. 63–74.

Okkels, H. 1950. The histophysiology of the human endometrium in menstruation. *In* E. T. Engle (ed.), Menstruation and its disorders: Proceedings of the conference held under the auspices of the National Committee on Maternal Health, pp. 139–163. Springfield, Illinois.

O'Leary, J. L. 1929. Form changes in the human uterine gland during the menstrual cycle and early pregnancy. Amer. Jour. Anat., vol. 43, pp. 289–346.

Phelps, D. H. 1946. Endometrial vascular reactions and the mechanism of nidation. Amer. Jour. Anat., vol. 79, pp. 167–197.

——— 1947. The factor of previous treatment in experimental menstruation. Jour. Clin. Endocrinol., vol. 7, pp. 611–623.

Ramsey, E. M. 1949. The vascular pattern of the endometrium of the pregnant rhesus monkey (*Macaca mulatta*). Carnegie Inst. Wash. Pub. 583, Contrib. to Embryol., vol. 33, pp. 113–147.

——— 1955. Vascular patterns in the endometrium and the placenta. Angiology, vol. 6, pp. 321–338.

Reynolds, S. R. M. 1949. Physiology of the uterus. 2d ed. 611 pp. New York.

——— 1954. Hemodynamic characteristics of the fetal circulation. Amer. Jour. Obstet. and Gynecol., vol. 68, pp. 69–80.

Rossman, I. 1941. Cyclic changes in the endometrial lipins of the rhesus monkey. Amer. Jour. Anat., vol. 69, pp. 187–227.

——— 1942. On the lipin and pigment in the corpus luteum of the rhesus monkey. Carnegie Inst. Wash. Pub. 541, Contrib. to Embryol., vol. 30, pp. 97–109.

——— and G. W. Bartelmez. 1946. Delayed ovulation, a significant factor in the variability of the menstrual cycle. Amer. Jour. Obstet. and Gynecol., vol. 52, pp. 28–33.

——— ——— 1957. The injection of the blood vascular system of the uterus. Anat. Rec. (in press).

Saito, O. 1926. Beiträge zum Studium der Uterusgefässe. Okayama I-gakkai Zasshi, no. 435, pp. 431–471. (In Japanese.)

Schlegel, J. U. 1945–1946. Arteriovenous anastomoses in the endometrium in man. Acta Anat., Basel, vol. 1, pp. 284–325.

Schröder, R. 1914. Ueber das Verhalten der Uterusschleimhaut um die Zeit der Menstruation. Monatschr. f. Geburtsh. u. Gynäkol., vol. 39, pp. 3–21.

——— 1915. Anatomische Studien zur normalen und pathologischen Physiologie des Menstruationszyklus. Arch. f. Gynäkol., vol. 104, pp. 27–102.

——— 1930. Weibliche Genitalorgane. *In* Möllendorff, Handb. d. mikr. Anat. des Menschen, vol. 7, pt. 1, pp. 329–556. Berlin.

Westman, A. 1932. Studien über den Sexualzyklus bei Makakus-Rhesus Affen, nebst einigen Bemerkungen über den menstruellen Blutungsmechanismus. Acta Obstet. et Gynecol. Scandinav., vol. 12, pp. 282–328.

The illustrations on plates 1 to 10 were drawn by the author with camera lucida or Edinger projection apparatus, at magnifications ranging from 50 to 250 diameters. They were checked, and details added, by the use of the 4.0-mm. Zeiss apochromat or the X60 ultraopaque immersion lens of Leitz. The areas selected are representative; the form and relations of the vessels are shown as projected on a plane surface, which involves certain distortions, but fundamental relations are not altered. Nothing was added, but most neighboring vessels and glands that would obscure the picture were omitted. That is to say, particular vessels or vascular beds have been dissected out optically from the sections, which range in thickness from 100 to 500 microns. Representative vessels in critical stages were drawn before any interpretations of cyclic changes in the vascular system were attempted. They are not diagrams elucidating hypotheses. In some instances, parts of vessels in adjacent serial sections were combined in a single drawing. To avoid the use of color, certain conventions are employed to differentiate kinds of vessels, epithelia, boundaries, etc.

Arteries and arterial capillaries	solid black
Veins	hatched
Other capillaries	single or double contoured
Extravasations	small rings
Disorganized zone (fig. 3)	fine stipple
Myometrium	coarse stipple
Endomyometrial junction	broken line
Denuded surface	dotted line

Roman numerals are placed at the middle of the respective endometrial zones (p. 156).

Many of the original drawings were copied by J. F. Didusch and drawn for reproduction as line cuts. After his death, figures 3, 6, 9, 12, 22, 23–29, 31, 34, 35*a*, *b*, 36, and 37*a* were similarly prepared by Mrs. Ranice W. Davis. The photomicrographs (pls. 11–15) are the work of Richard D. Grill.

Plate I

Projections of vessels from endometria of repair and early follicular phases. Reduced in reproduction to 40 diameters.

Fig. 1. Transition from menstruation to repair (p. 158). Day 5 in April (following anovulatory cycle). Type I artery is as contorted as any in this specimen, and appears compressed (see p. 174). Apical rami confirm persistence of part of zone II (see p. 169). Small type II artery below at right. Projection reconstruction from two sections, each 500 microns thick. B329, transverse sections 43, 44.

Fig. 2. From same uterus as figure 1. Two type I arteries representing usual form in this mucosa. Artery between them resembles type II in form but has branches in zone II. Veins form irregular network. Restored epithelium (arrow) 6 microns in height. B329, transverse sections 37, 38, each 480 microns.

Fig. 3. From same uterus as figure 1. A characteristically dilated venule with its tributaries. Superficial venule parallel to surface is a typical menstrual feature. Venules were still bleeding in this specimen. B329, transverse section 36, 480 microns.

Fig. 4. Transition from repair to follicular phase. Preceding cycle anovulatory. Day 8 of May cycle, 5th after end of bleeding (see p. 158; fig. 43, pl. 11). Complete vascular bed from dorsal wall near mid-line. *a* is transitional between type I and II arteries since it reaches zone III. *b* is a typical type II. *c* becomes an endothelial tube beyond level of arrow. It supplies superficial capillary bed, which defines border of avascular stroma of zone I. Most type I arteries resemble *d* and figure 5*c*. Venous system predominantly a network. Venule draining superficial net enters sinus which spreads through zones III and IV. B334, sagittal section 6, 250 microns.

Fig. 5. From same uterus as figure 4. Each of these vessels is complete within a single section. *a*, unusually contorted artery. Dilated apical ramus reaches superficial capillary net. It has no definite media in zone II, and branches are usually capillaries. Radial vein accompanies it. Sagittal section 3, 500 microns. *b*, artery from lateral limbus, simple as any basal artery but reaches zone III. Transverse section 13, 300 microns. *c*, most common form of type I in this mucosa, taken from corpus near mid-line. Apical ramus is an endothelial tube 7.5 microns in diameter. Capillary net in zone IV. Transverse section 18, 300 microns.

Fig. 6. From early follicular phase. Day 15, preceding (December) cycle anovulatory (see p. 159; fig. 44, pl. 11). Transitional artery is as contorted as any, but supplies only zones III and IV. Complete capillary bed indicated by arrow. Only endothelium above level of the asterisk. Type II artery at left (*b*), like many in other phases, terminates in tuft of capillaries. B302, transverse section 29b, 250 microns.

Fig. 7. From same uterus as figure 6. Larger artery coiled in zone IV, sinuous in zone III. Apical segment dedifferentiated and superficially dilated. Capillary bed indicated by arrow. Smaller artery reaches zone III. Radial veins that drain superficial capillary bed are uniform in diameter in zones II and III and have few tributaries or anastomoses. Venous net at left. B302, transverse section 31a, 480 microns.

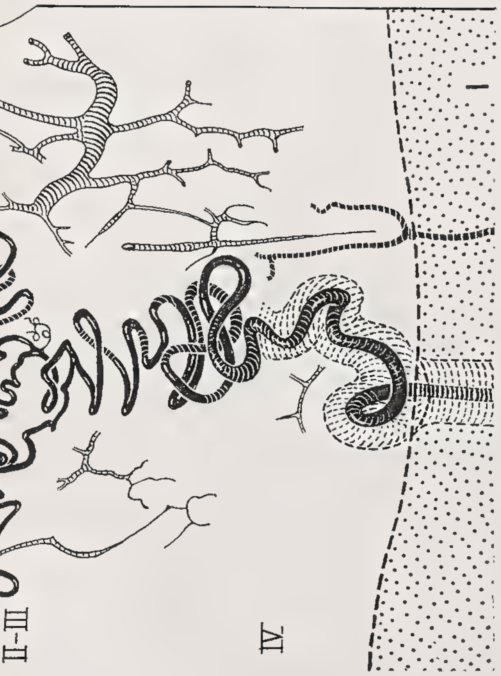

1

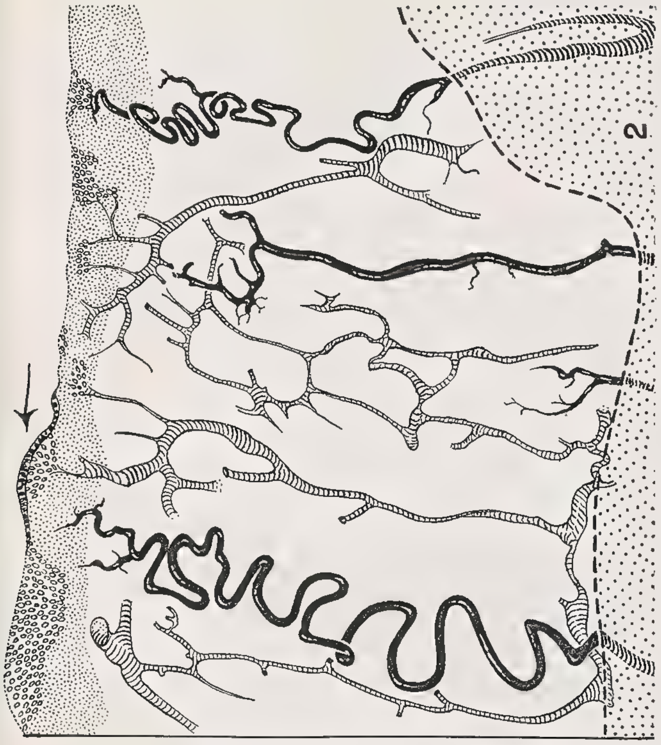

2

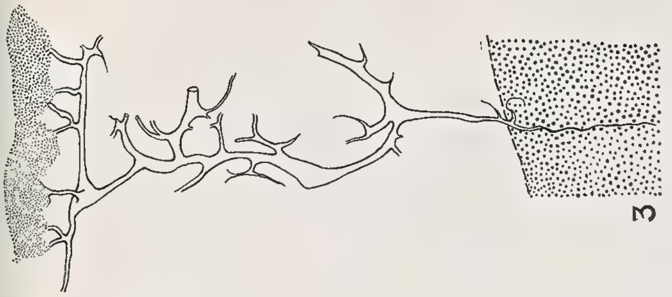

3

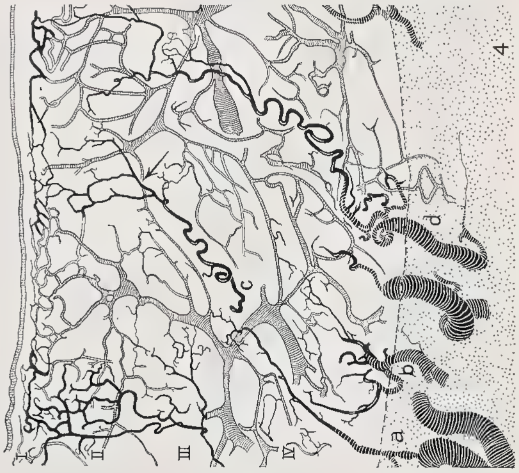

4

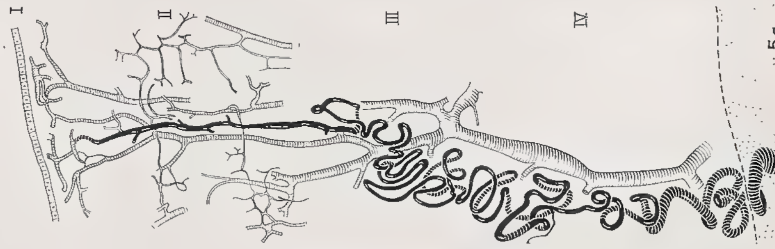

5a

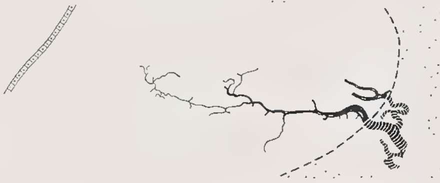

5b

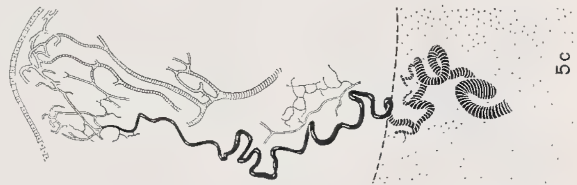

5c

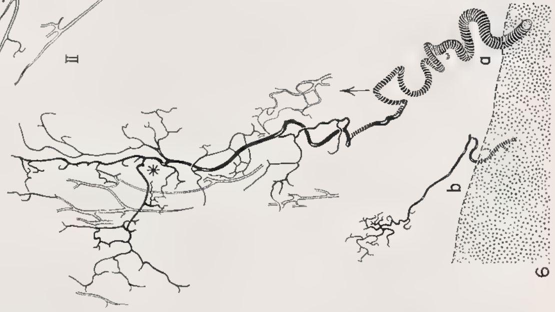

6

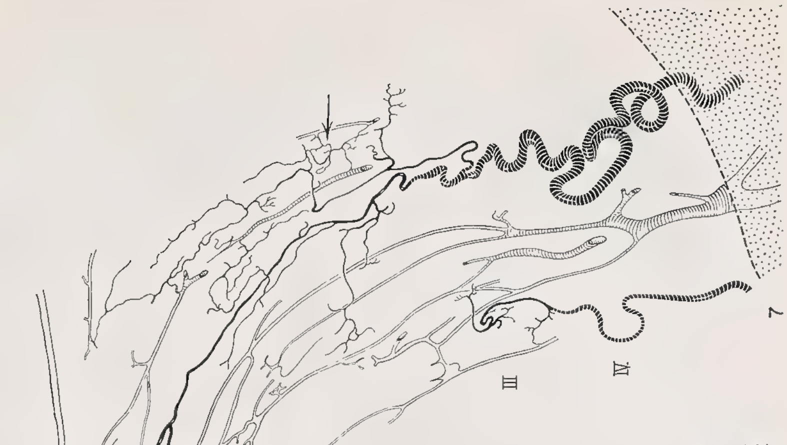

7

PLATE 2

Camera lucida drawings of vascular beds from repair and follicular phases. Zeiss 4.0-mm. apochromat. Checked with Leitz X60 ultraopaque immersion lens. Reduced in reproduction to 125 diameters.

FIG. 8. From surface of same endometrium as figures 1 to 3 (early repair). The predominance of venules (double contoured) is obvious. Tuft of capillaries arises from terminal arteriole (solid black); latter is cut off near its superficial end; extravasated injection mass (stippled). B329, transverse section 31, 480 microns.

FIG. 9. From same endometrium as figures 6 and 7 (early follicular phase). Section tangential to surface, showing superficial capillary net spread out beneath avascular zone I. Capillaries dilated, reaching 12 microns in diameter; arterial capillaries (solid black) superficial to the venous (hatched). B302, transverse section 15b, 480 microns.

FIG. 10. From same uterus as figure 9. Capillary bed deep in zone II. A precapillary arteriole (lumen, 4.8 microns) at arrow with its capillaries and the venules with which they connect. Arteriole and its capillaries (solid black); venous capillaries, often wider (double contoured); venules (hatched). B302, transverse section 33b, 480 microns.

FIG. 11. From same uterus as figure 9. Capillary net in zone IV supplied by two precapillary arterioles and drained by a venule (hatched); arterioles (solid black); capillaries (double contoured). Arrows indicate short capillaries. B302, zone IV, transverse section 19b, 480 microns.

FIG. 12. From same uterus as figure 9. Zone II, corpus. Coarse net of venous capillaries spread between three venules. Such nets can also be found in zones III and IV. B302, transverse section 29b, 250 microns.

FIG. 13. Endometrium associated with mature ovarian follicle (see pl. 3). Characteristic vascular bed in zone II of corpus. Apical ramus of type I artery (black) with lumen 12 microns in diameter at this level. Precapillary arterioles arise at approximately right angles and promptly divide into capillaries, identifiable as such wherever close to surface of section. Part of radial vein at right. B338, transverse section 10, 300 microns.

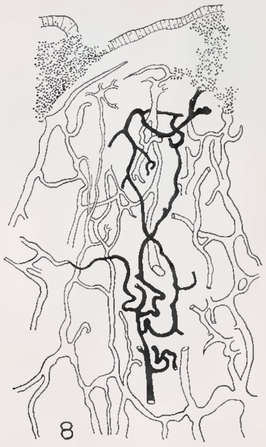
8

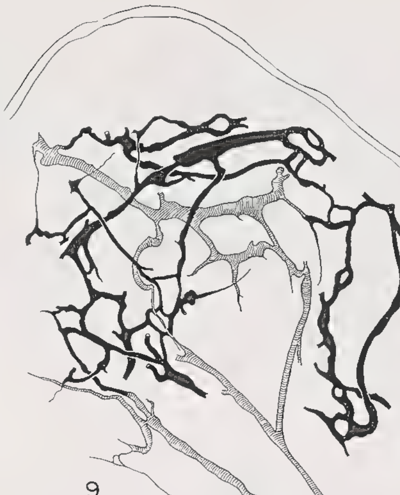
9

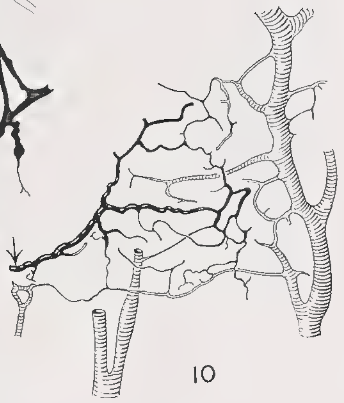
10

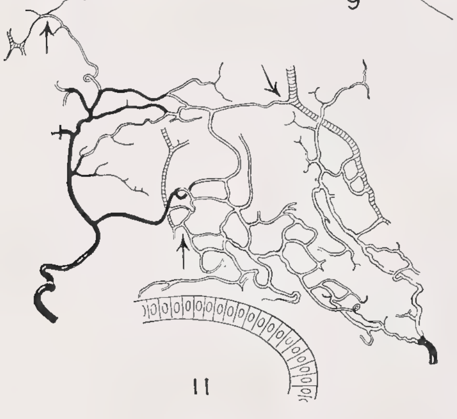
11

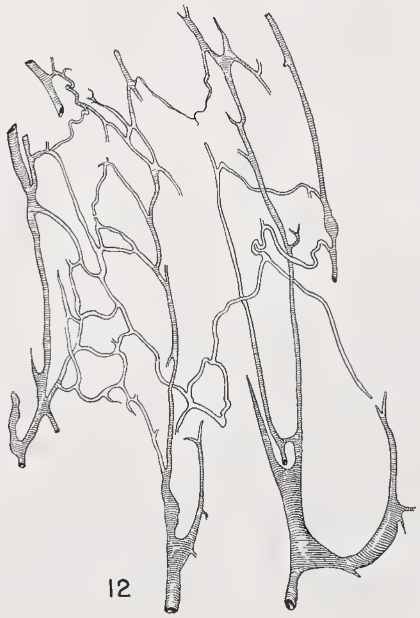
12

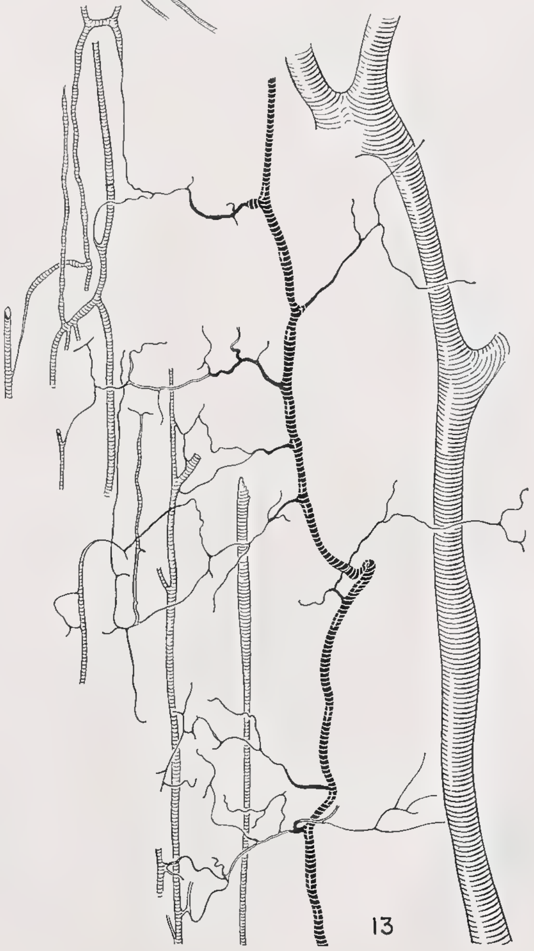
13

Plate 3

Late follicular phase

B338. Uterus associated with a 6-mm. mature Graafian follicle on day 12 of February cycle (see p. 160; fig. 45, pl. 11). Vascular beds in corpus of ventral wall near mid-line. ×40.

Fig. 14. Coiled segment of artery at left is in zone IV; one branch arises at this level. Branches of long apical ramus supply zones II and III, and one branch reaches superficial capillary net. Dilatation of this ramus due partly to absence of a continuous tunica media. Artery supplied area in plane of section of more than 1.45 mm. in zone II. Loose capillary bed with long capillaries in zone II contrasts with closer meshes in zone IV, as shown in figures 15 and 16. Artery at right is more contorted than any other in this mucosa; it lacks an apical ramus. Dilated radial veins are not rare; they suggest rapid drainage. Transverse section 1, 500 microns.

Fig. 15. Large vessel (from lateral limbus) is sinuous but supplied superficial zones as well as zone IV, extending to within 320 microns of surface. Below, branches of small myometrial arteries supply zone IV. Arrow indicates small basal artery. Transverse section 5, 200 microns.

Fig. 16. Large and small type II arteries supplying same capillary bed. Larger reaches all levels of zone IV. Large radial artery at left has small branch to base of zone IV. Transverse section 2, 400 microns.

Fig. 17. Typical pattern of veins, drawn from a single 300-micron section. At right, slim radial vein, uniform in diameter, extends from superficial capillary bed to sinus in zone IV. At arrow, a similar vessel, dilated as far as sinus between zones III and IV, also drains the diffuse venous network. Sinus at endomyometrial junction has slim emissaries to myometrium; in other sections, they are wider. Transverse section 9, 480 microns.

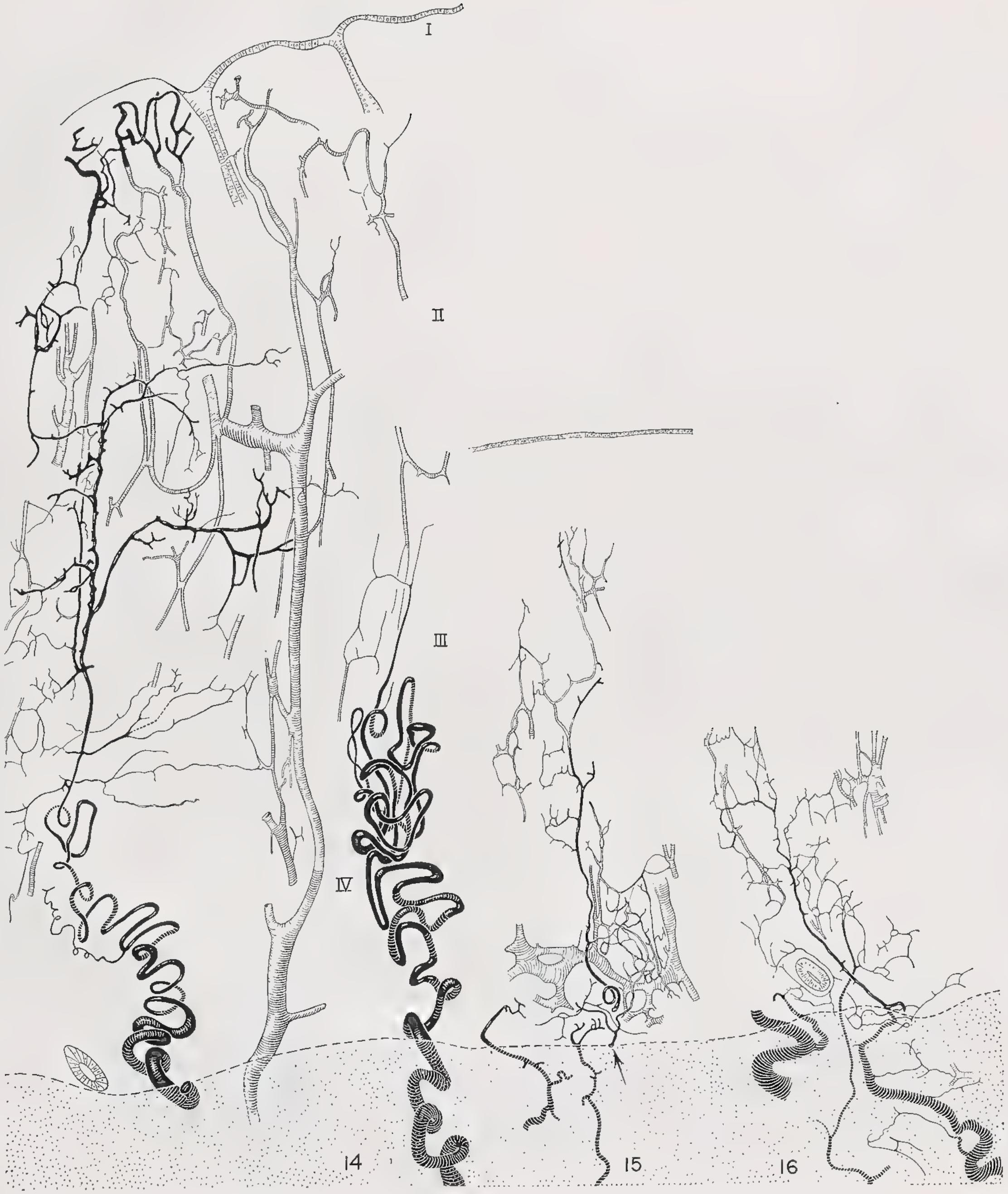

14

15

16

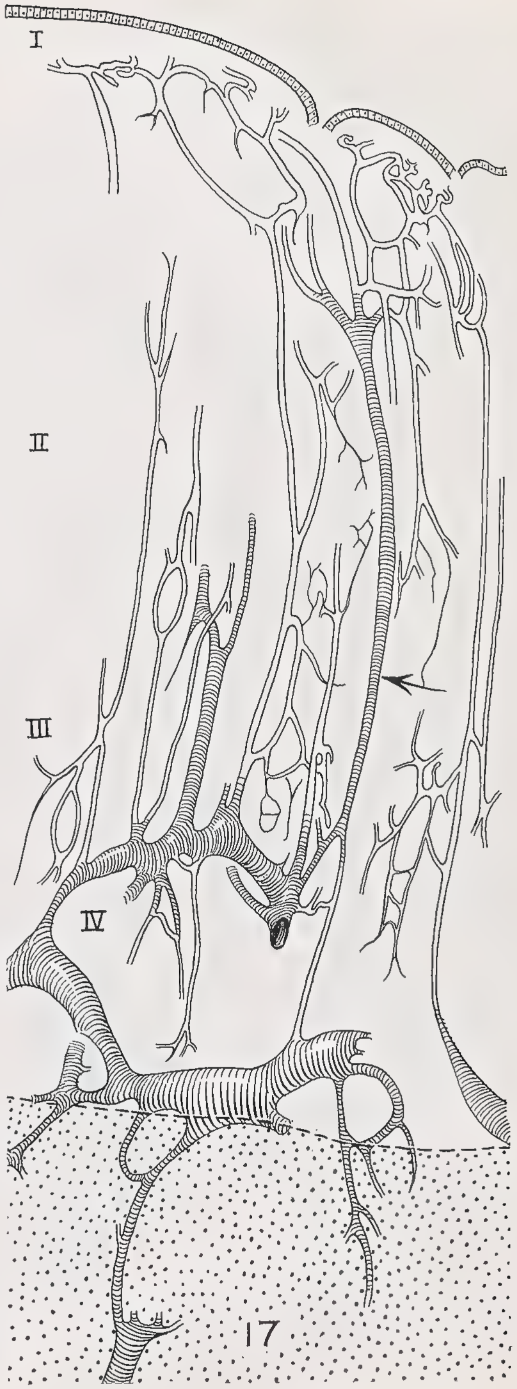

17

PLATE 4

FROM FOLLICULAR, OVULATION, AND EARLY PROGRAVID PHASES

Reduced in reproduction to 40 diameters

FIG. 18. From same uterus as figures 14 to 17 (pl. 3). Two adjacent type I arteries supply same part of dilated superficial net. The arteries have loops in zone II, which presumably persisted from previous cycle. Artery at left has branches throughout zones II and III; the other has only superficial branches. The large descending arterial capillary at upper right is unusual. Two minute type II arteries supply zone IV only. Dilated vein at center drains into a basal sinus at lower right. From a paramedian 400-micron section of corpus. B338, sagittal section 2.

FIG. 19. From a uterus obtained less than 15 hours after ovulation on day 11 (see p. 161). Typical large type I artery (see fig. 46, pl. 11). Endometrium is thin; artery and its branches appear compressed in zones II and III. Dense stroma and curved radial vein also indicate the rapid postovulatory involution. Constrictions in this and many other radial arteries. (See fig. 47, pl. 11.) Media of radial artery indicated. B323, sagittal section 12, 480 microns.

FIG. 20. From an endometrium associated with a corpus luteum of about 7 days, obtained 35 days after the last menstrual period (see p. 163). This simply coiled type of artery is characteristic of many other progravid endometria, both pregnant and nonpregnant (see fig. 31, pl. 7). In this specimen many type I arteries are simpler (see fig. 30, pl. 7). Compared with figure 18, it appears that the apical ramus had grown faster than zone II thickened. A postovulatory regression may also have been involved. The most contorted segment of the artery is in zones III and IV. Most of the artery is in a single 480-micron section; details were added from neighboring sections. Anastomoses dominate the venous pattern, as in figure 22 (pl. 5). B326, sagittal sections 11 to 13.

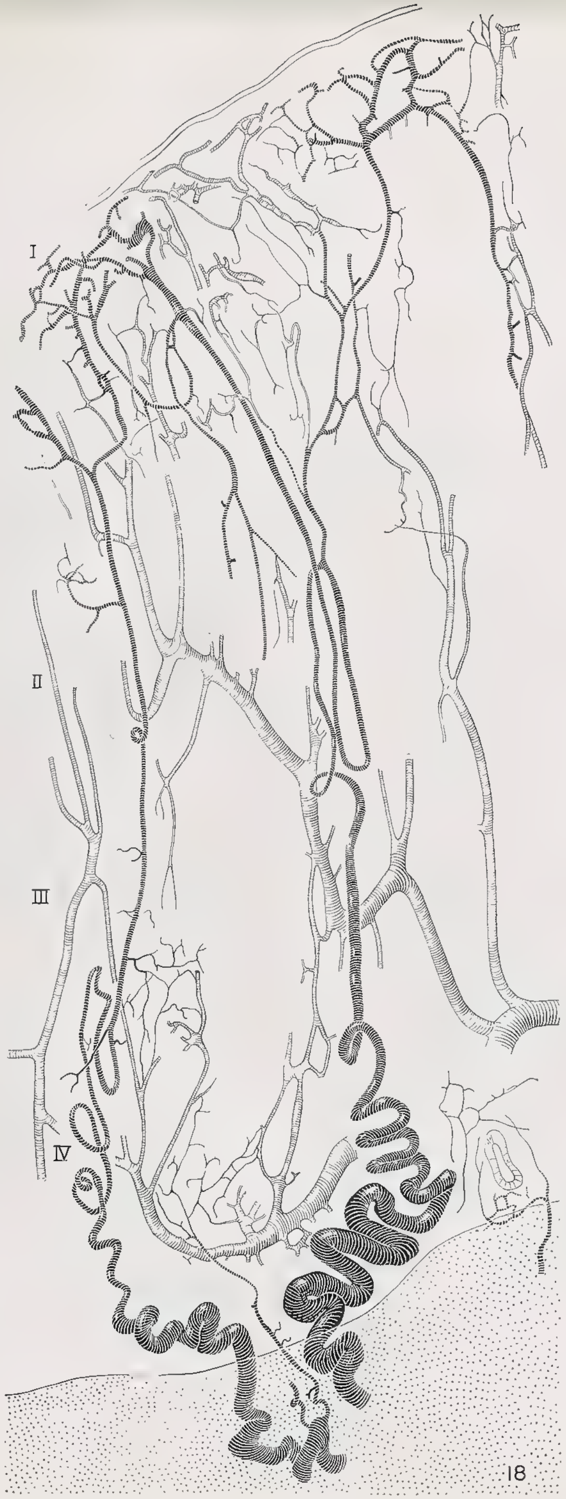

18

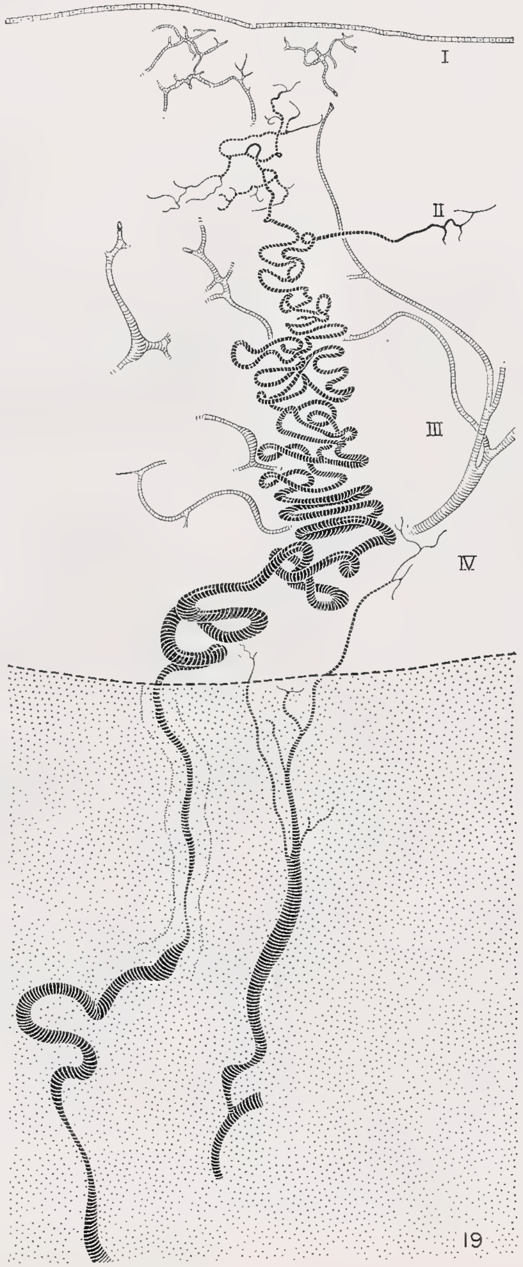

19

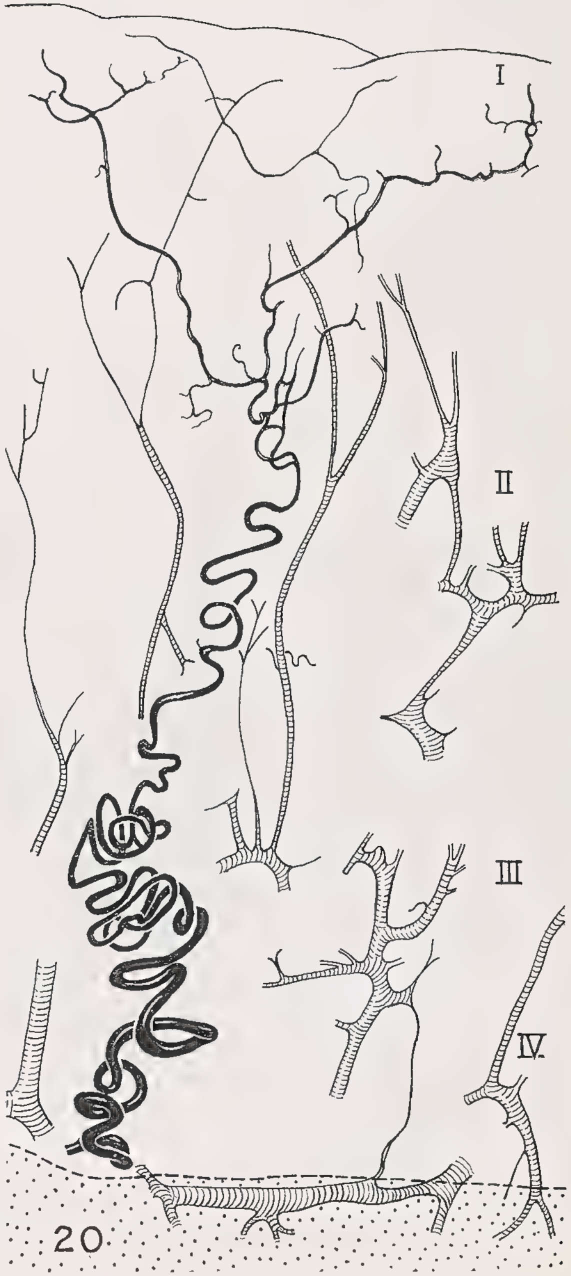

20

Plate 5

Early progravid phase

B309. Endometrium associated with 6- to 7-day corpus luteum obtained on day 17 of cycle in March (see p. 162; fig. 48, pl. 12). Vessels from a sagittal section 480 microns thick. × 37.5.

Fig. 21. Typical large type I artery from paramedian area of corpus. Closely coiled segment in zones III and IV gives rise in zone II to five apical rami, which supply this zone and superficial capillary net. Such terminal branching corresponds to the "tufting" in small arteries (see fig. 6, pl. 1). Transitional arteries on either side of it. A myometrial artery has two branches to basal zone IV. Sagittal section 22 (some additions from section 23).

Fig. 22. Venous system of area between *c* and *d* in figure 48 (pl. 12). Network predominates over radial veins, which join diffuse network at middle of zone II. Irregular diameter and numerous irregular anastomoses distinguish venules from the slim sinuous arterioles with dichotomous or lateral branching. Sagittal section 22 only.

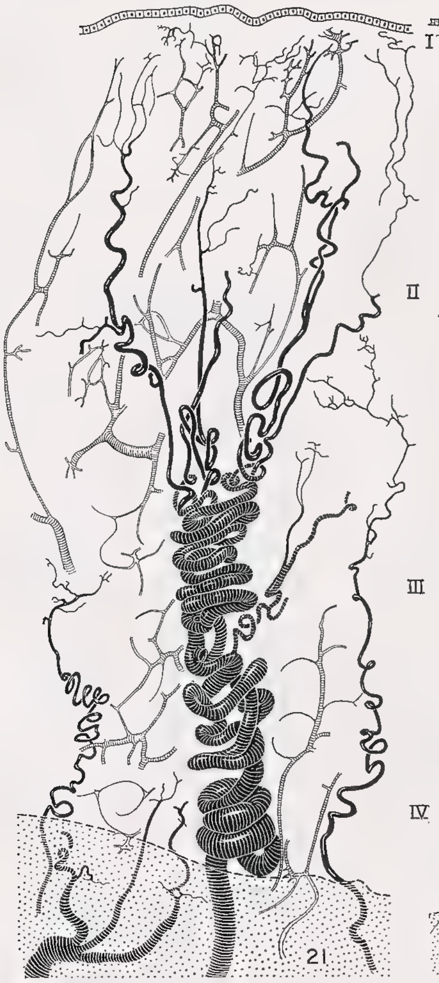

21

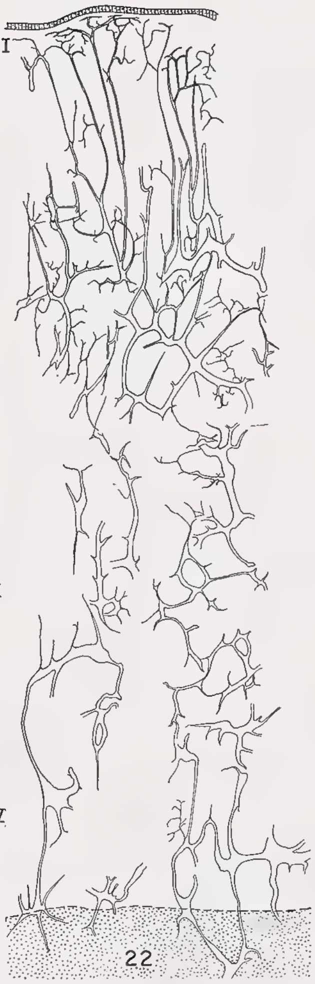

22

Plate 6

Capillary beds from ovulation and progravid phases

Camera lucida drawings reduced in reproduction to 125 diameters (see pl. 2).

Fig. 23. From an involuted endometrium obtained shortly after ovulation on day 11 (see fig. 19, pl. 4; fig. 46, pl. 11). B323.

a. Tangential section of superficial capillary bed adjoining mouth of gland. Some capillaries were probably artificially dilated by the injection. Compare size and form of meshwork with figures 24, 26*a*, and 27. At lower right, a network of venous capillaries joins a venule. From two sections, each 100 microns. Sagittal sections 3, 4.

b. Surface adjacent to *a.* Precapillary arteriole at left. Sagittal section 7, 100 microns.

c. Capillaries in dense area of zone II. Their irregular form probably due to collapse from loss of stromal ground substance (cf. fig. 25). Transverse section 15, 480 microns.

d. Capillary bed in zone II spread out parallel to surface, suggesting compression as endometrium became thinner (cf. figs. 25 and 26*b* from thicker sections). Sagittal section 9, 100 microns.

Fig. 24. From early progravid endometrium, day 17 (see p. 162; pl. 5). Terminal branching of apical ramus of coiled artery; its cut end (lower right) measures 35.8 microns with 17.8-micron lumen. Precapillary arterioles (solid black) branch dichotomously and have a lumen of 6 microns or less. Both arterial and venous capillaries form nets (latter cross hatched, like venules). Vascularization of zone I is under way. B309, sagittal section 22, 480 microns.

Fig. 25. From zone II of the same endometrium as figure 24. At left, precapillary arteriole (solid black) supplying capillary net. At lower right, network of capillaries spread out between two venules. Such venous nets are common in endometrium (see fig. 12, pl. 2; fig. 28). B309, sagittal section 30, 480 microns.

Fig. 26. From a late progravid endometrium obtained on day 21 of cycle. B325 (see p. 165; fig. 31, pl. 7).

a. Subepithelial net showing size of meshes, from section cut tangential to surface. Precapillary arteriole (left) differentiated as such to within 88 microns of surface. Sagittal section 23, 200 microns.

b. Capillaries spread out over dilated gland (epithelium outlined) in zone II. Capillaries are longer and have fewer anastomoses than in superficial bed (fig. 26*a*). Lumen of arteriole at right is 5 microns in diameter. Sagittal section 15, 200 microns.

Fig. 27. From an early ischemic endometrium associated with some regression in corpus luteum, obtained on day 29. B316 (see fig. 52, pl. 12).

a, b. Superficial capillary beds from zone I of corpus. Long capillaries applied to epithelium are characteristic of this, as well as late progravid, phase, and are probably adaptations for epithelial proliferation, which develops at this time after implantation or trauma. Arterial capillaries superficial to venous. Meshes appear spread out by edema. Transverse sections 14, 16, 480 microns.

Fig. 28. From same endometrium as figure 27. Capillary net spread out between two venules. No afferent arteriole found. 480-micron section. B316, sagittal section 13.

Fig. 29. From a progravid endometrium obtained on day 27 (see p. 166; fig. 32, pl. 7; fig. 55, pl. 13). Dense capillary bed throughout endometrium is correlated with unusually rich vascularity and extremely contorted coiled arteries. Section oblique to surface. Avascular zone I is a feature of follicular phase. It has been vascularized in all other progravid specimens (cf. figs. 24, 26*a*, 27). B330, sagittal section 20, 480 microns.

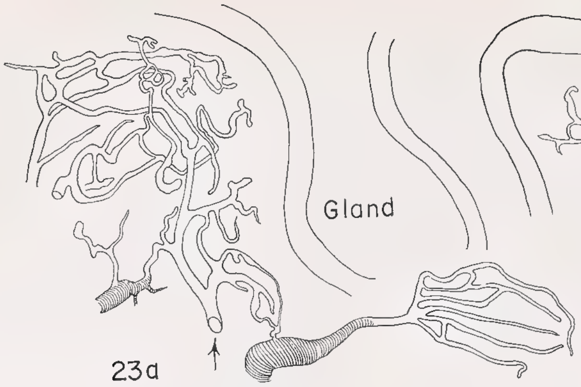

23a

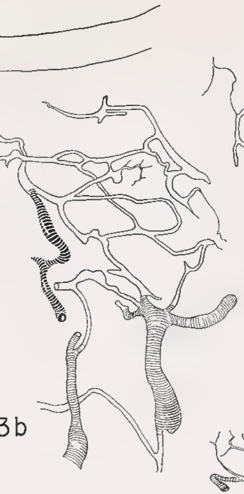

23b

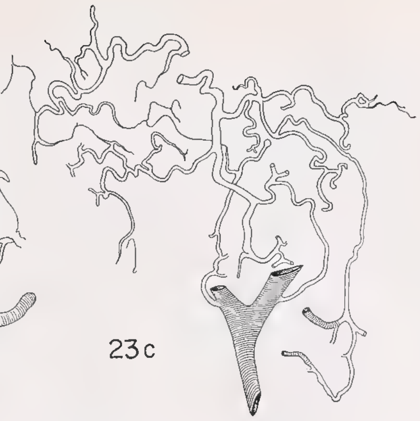

23c

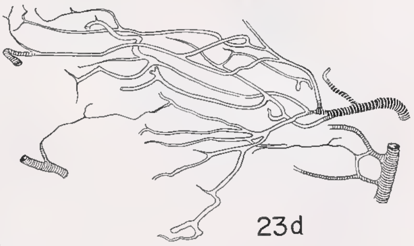

23d

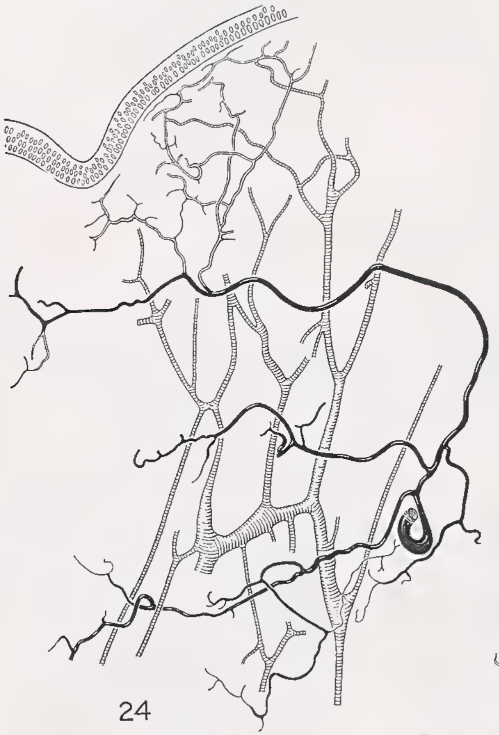

24

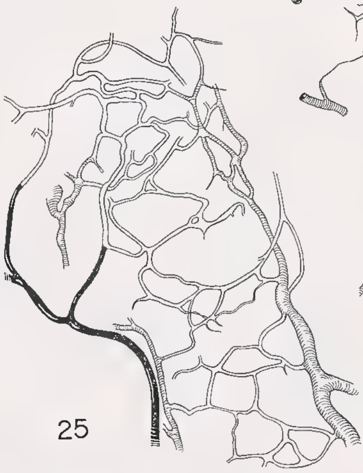

25

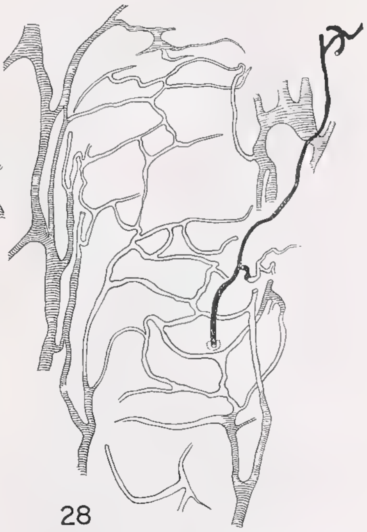

28

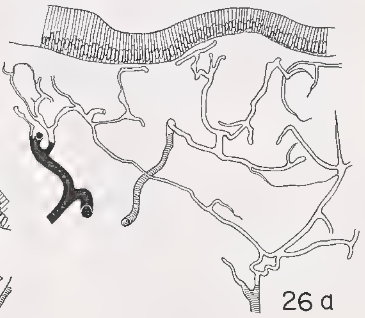

26a

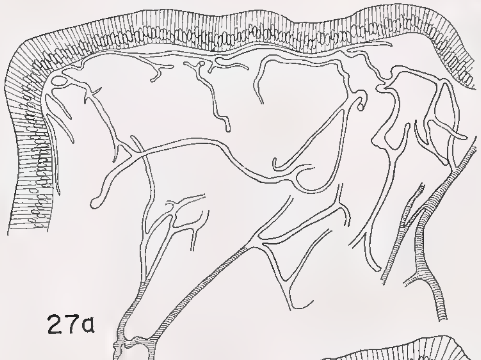

27a

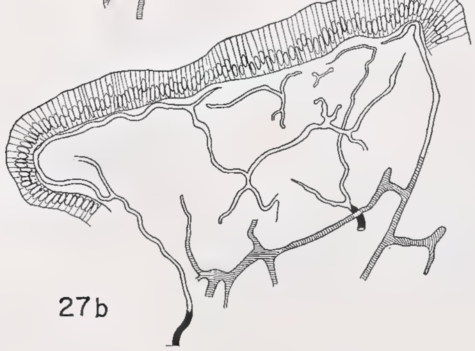

27b

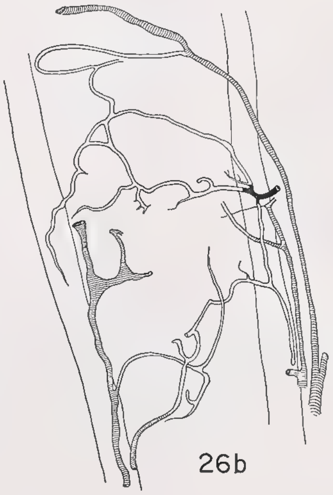

26b

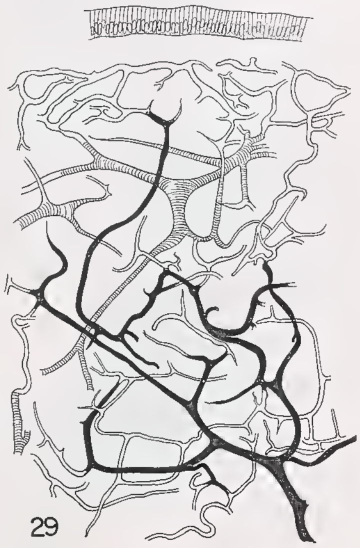

29

PLATE 7

VESSELS FROM THREE PROGRAVID UTERI

Reduced in reproduction to 40 diameters

FIG. 30. From same uterus as figure 20 (pl. 4), in which the artery is as contorted as any in this specimen. Endometrium is 3.4 mm. thick. Most type I arteries in this specimen are no more contorted than these transitional arteries. B326, free-hand section, ca. 1 mm. thick.

FIG. 31. From uterus associated with 10- to 11-day corpus luteum obtained on day 21 of a February cycle (see p. 165). As contorted an artery as is usually seen in late progravid phase of menstrual cycle and in implantation stages of pregnancy. Two or more long apical rami are not uncommon; arrow indicates level of branching (cf. fig. 21, pl. 5). Basal branch in zone IV is rare in this phase. This vessel and neighboring arteries are shown in figure 51 (pl. 12). Projection reconstruction from three serial sections of corpus. B325, sagittal sections 25–27, each 200 microns.

FIG. 32. From uterus associated with mature corpus luteum obtained on day 27 of April cycle. It shows various features of follicular phase (see p. 166 and fig. 29, pl. 6). No other endometrium in present series has more elaborately coiled arteries than this (see fig. 55, pl. 13). Profuse branching in all zones and rich capillary net show unusual growth of vascular system (see fig. 29, pl. 6). In this area, veins form network; elsewhere, radial veins are common. B330, sagittal section 18, 480 microns.

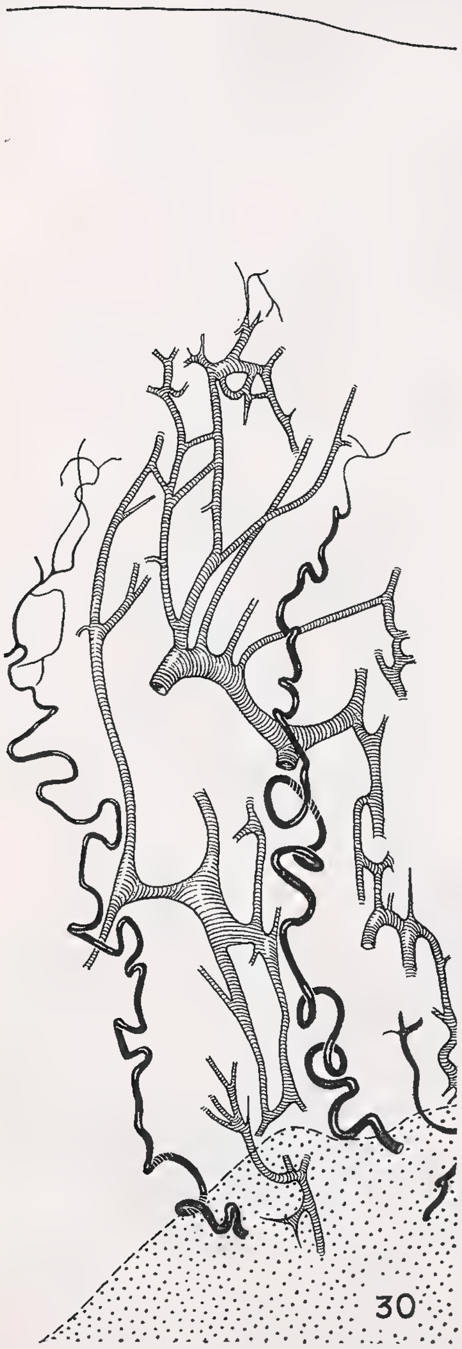

30

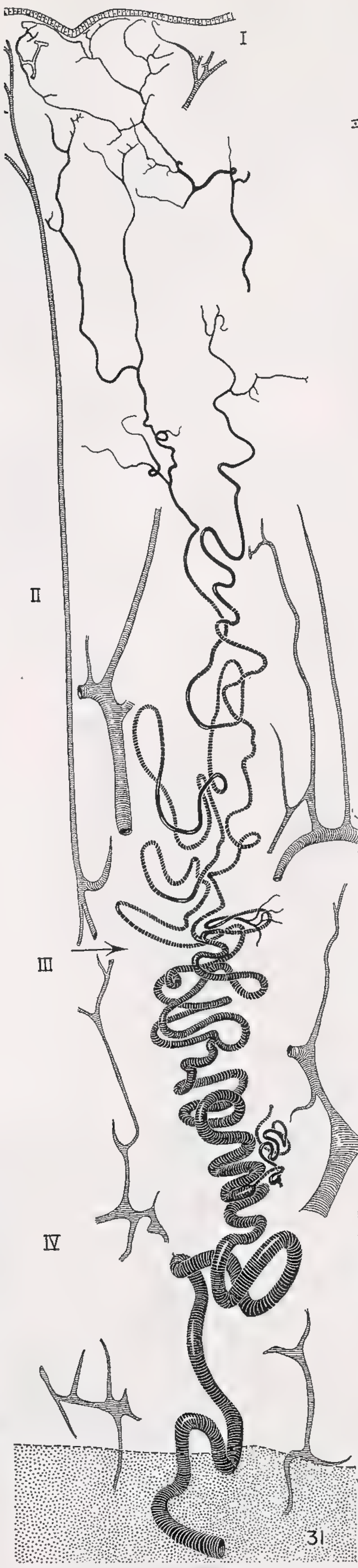

31

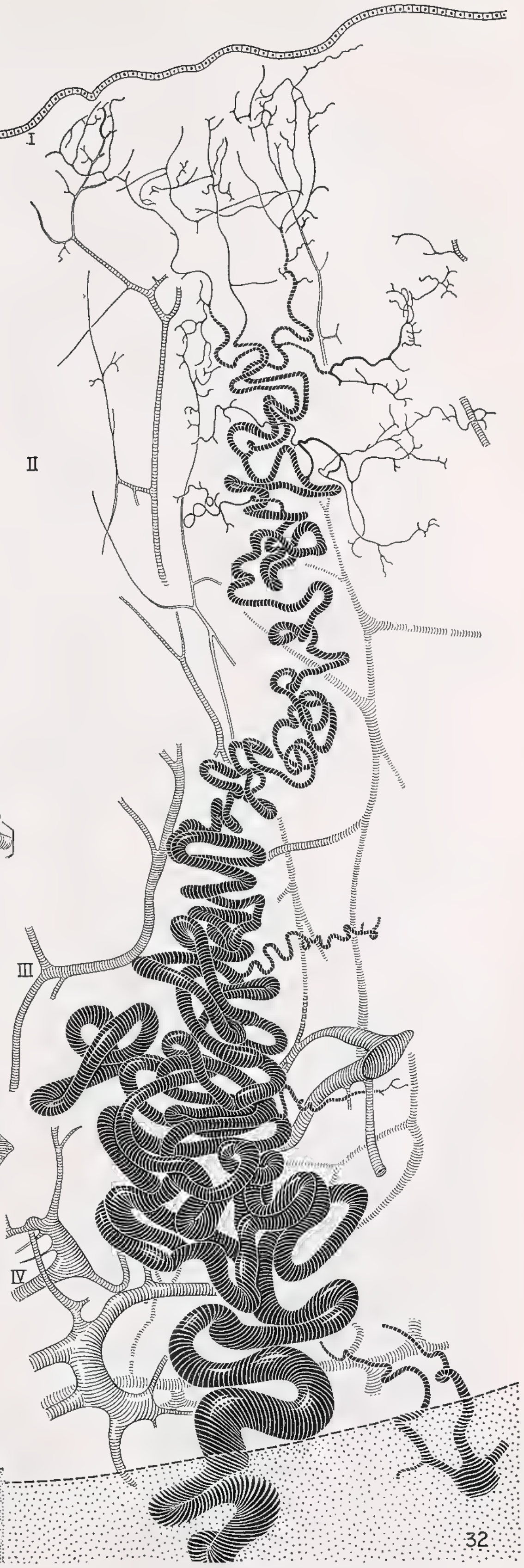

32

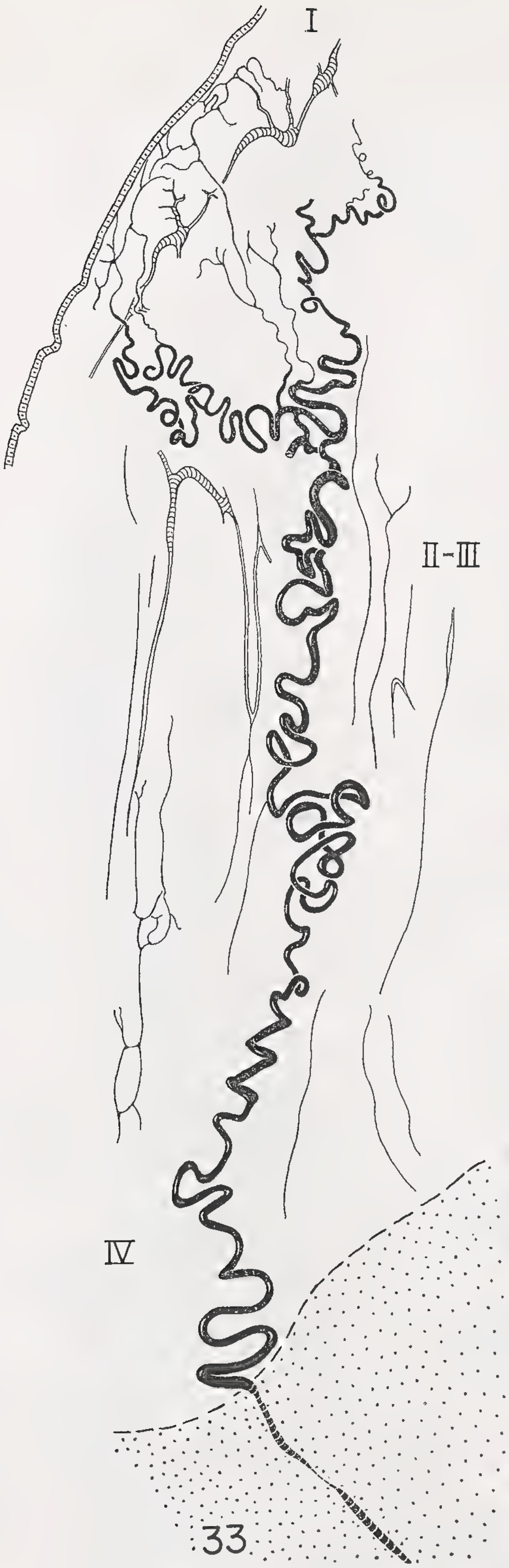

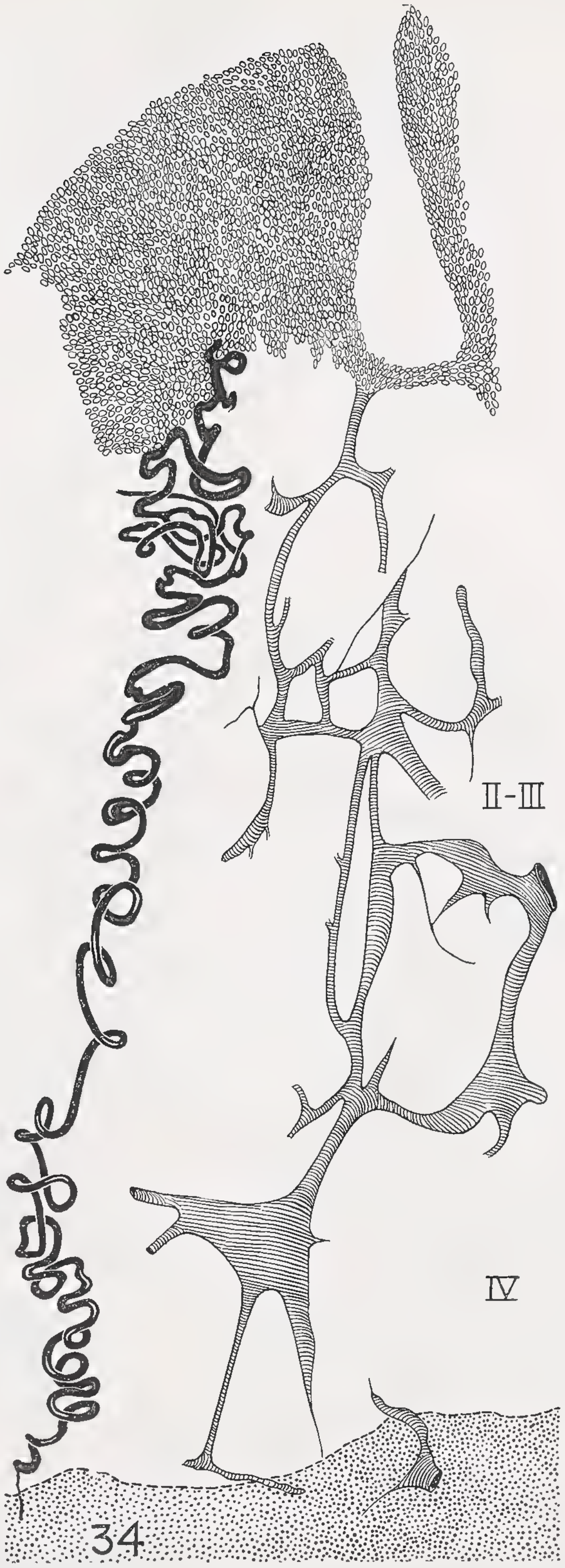

From a uterus with both ischemic and menstruating areas, obtained shortly after onset of flow. Reduced in reproduction to 40 diameters. B317 (see p. 168).

Fig. 33. Ischemic area from inferior border of corpus. Type I artery simply coiled in zone IV, contorted in zones II and III, which indicates greater involution superficially. Venous capillaries are narrow, veins slim. Superficial venules resemble twisted ribbons. Projection reconstruction from two sections, with additions from two others, each 200 microns. Sagittal sections 5–8, each 200 microns.

Fig. 34. Menstruating area from corpus where only surface epithelium had been shed. Apical rami of type I artery are necrobiotic in hemorrhagic zone, which is indicated by small circles. End of vessel sealed. Superficial contorted segment compared with figure 33 indicates continued involution of mucosa during menstruation (see fig. 53, pl. 13). Fissure at upper right indicates extent of slough. Projection reconstruction from two sections. Sagittal sections 12, 13, each 480 microns.

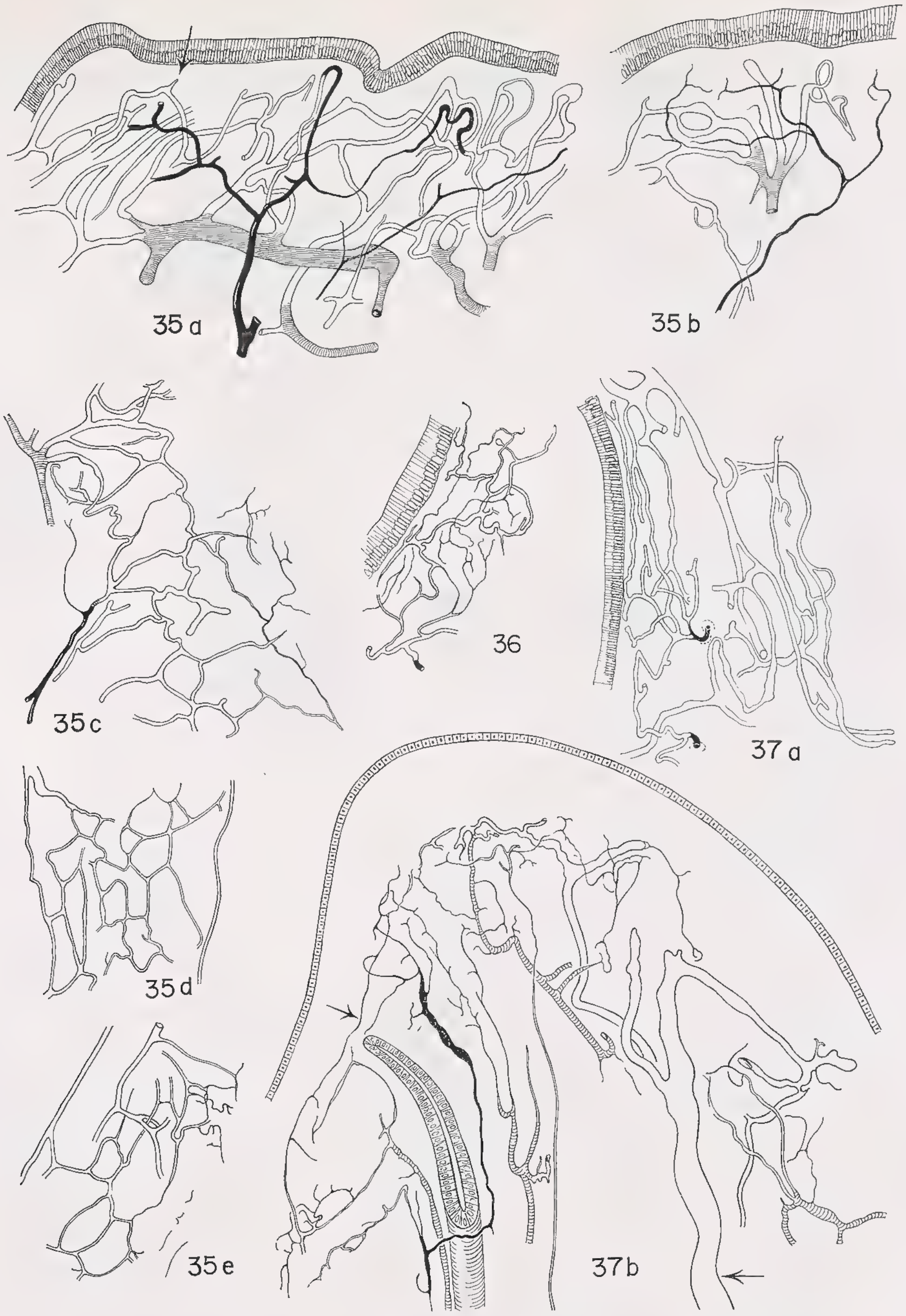

Capillary beds from three endometria from days 1 and 2 of menstruation, compared with one from follicular phase. Precapillary arterioles solid black, except fig. 37*b*. Reduced in reproduction to 125 diameters. Camera lucida drawings (see pl. 1).

Figs. 35*a, b*. From the surface of ischemic area shown in figure 33 (pl. 8). *a*. Long subepithelial capillaries of progravid phase are not visible. Stump at arrow may indicate collapsed capillary. Venous capillaries wider than arterial. Edge of gland mouth at upper left. B317, sagittal section 3, 200 microns. *b*. From area adjoining figure 35*a*. Precapillary arteriole has lumen of 3.5 microns. Venous capillaries dilated. Sagittal section 8, 200 microns.

Figs. 35*c–e*. From menstruating areas of same endometrium. *c*. Capillary mesh in zone II. Wide mesh due to incomplete injection (capillaries collapsed?). Transverse section C9, 200 microns. *d*. Capillary net in zone III. Transverse section B6, 480 microns. *e*. Capillary net in zone IV. Transverse section B7, 480 microns.

Fig. 36. From same endometrium as figure 38 (pl. 10). Capillary bed in zone III showing narrow mesh, threadlike and sinuous capillaries typical of early menstruation. At left, epithelium of gland. B314, sagittal section 10, 480 microns.

Fig. 37*a*. From 2d day of anovulatory menstruation (see fig. 41, pl. 10). Capillaries in zone II spread out among coils of an artery, which are omitted. The approximation of capillaries to gland epithelium seems to be incidental. B332, sagittal section 10, 200 microns.

Fig. 37*b*. From early follicular phase (day 15). Superficial capillary net in tangential section. Arrow at right indicates dilated apical ramus of type I artery. No media can be recognized in zone II under oil-immersion lens (see p. 159). Arrow at left indicates long capillary of superficial net. Afferent capillary at left (solid black) had a short dilated segment. Superficial capillaries it supplies are not dilated. No sheath of capillaries about gland at left. B302, transverse section 15a, 50 microns.

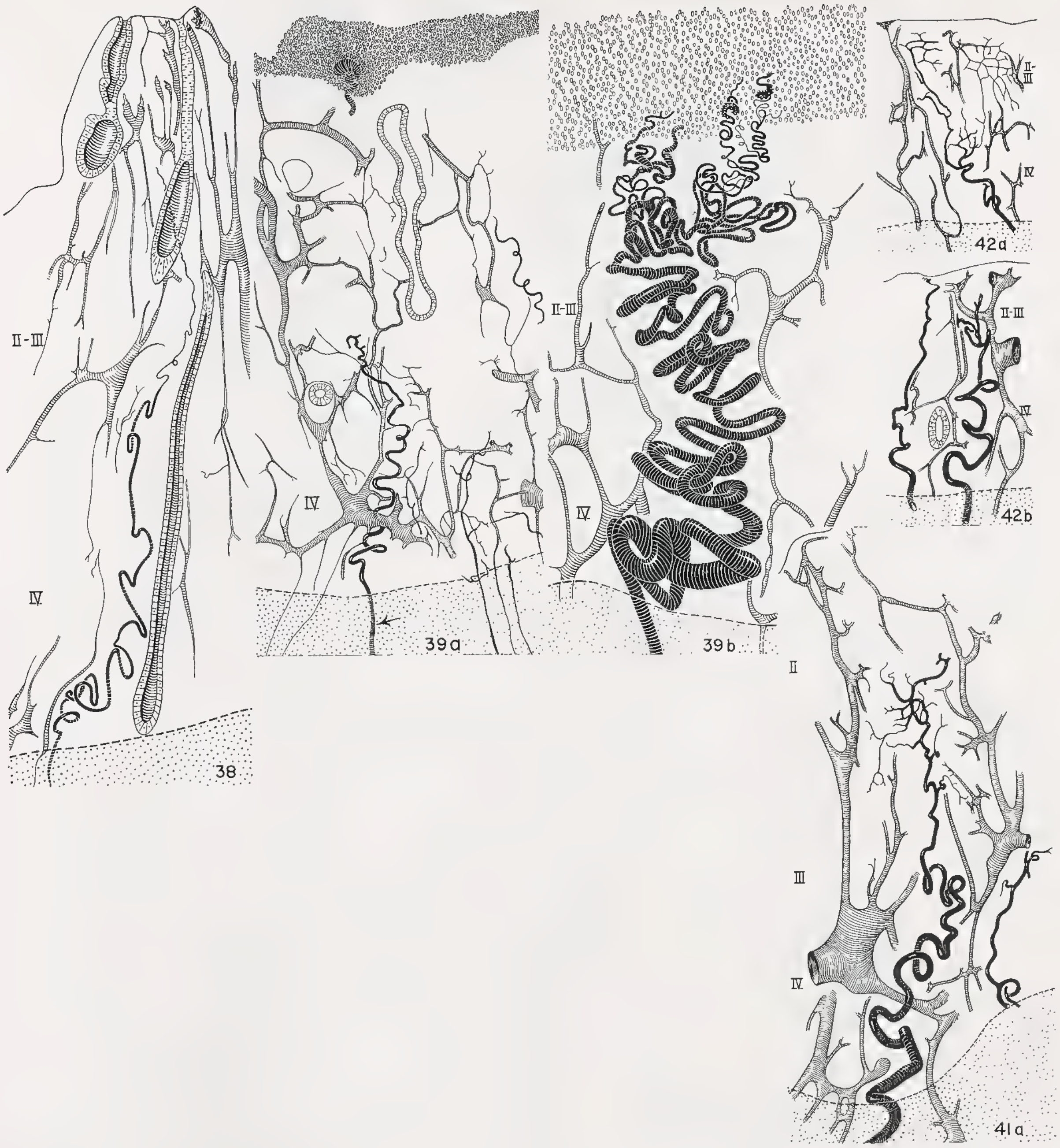

Vessels in menstruating uteri, ×40

Fig. 38. From a uterus obtained on day 1 of ovulatory menstruation after long ischemic phase showing advanced involution (see p. 169). Type I artery of corpus is simply coiled, like many in this specimen. Constriction is close to endomyometrial junction. See figure 54 (pl. 13) for a more contorted artery. Glands simple in form with involuted epithelium. B314, transverse section 24, 480 microns.

Fig. 39. From a uterus removed on day 2 (or 3?) of ovulatory menstruation (see pp. 169–170; fig. 61, pl. 15). B313.

a. Transitional artery, three type II arteries (solid black), venous net, and basal sinus present in a 200-micron section. Parts of two glands included. Transverse section 26, 200 microns.

b. Large type I artery appears compressed. Presence of apical rami indicates that part of zone II persisted after sloughing. Constriction in radial artery is below level of drawing. Transverse sections 15, 16, each 480 microns thick.

Fig. 40. From a uterus obtained on day 1, following anovulatory cycle in April (see p. 170). Corpus where only surface epithelium was lost. No type I arteries are more contorted than that at right. Terminal rami, structurally precapillary arterioles, close to surface. Veins dilated; network predominates. Injection mass usually extravasated from venules, rarely from arterioles. Most sinuses in zone IV. Projection reconstruction from three sections aggregating 700 microns. B312, sagittal sections 28–30.

Fig. 41. From a uterus obtained on day 2 following an anovulatory cycle in April (see p. 171; fig. 56, pl. 14; fig. 62, pl. 15).

a. Simply coiled type I and type II arteries. At left, a sinus in

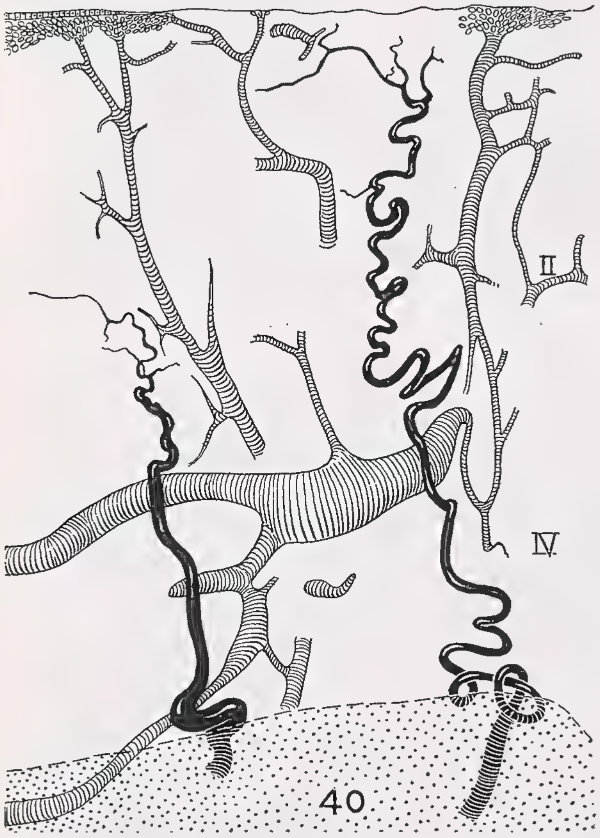

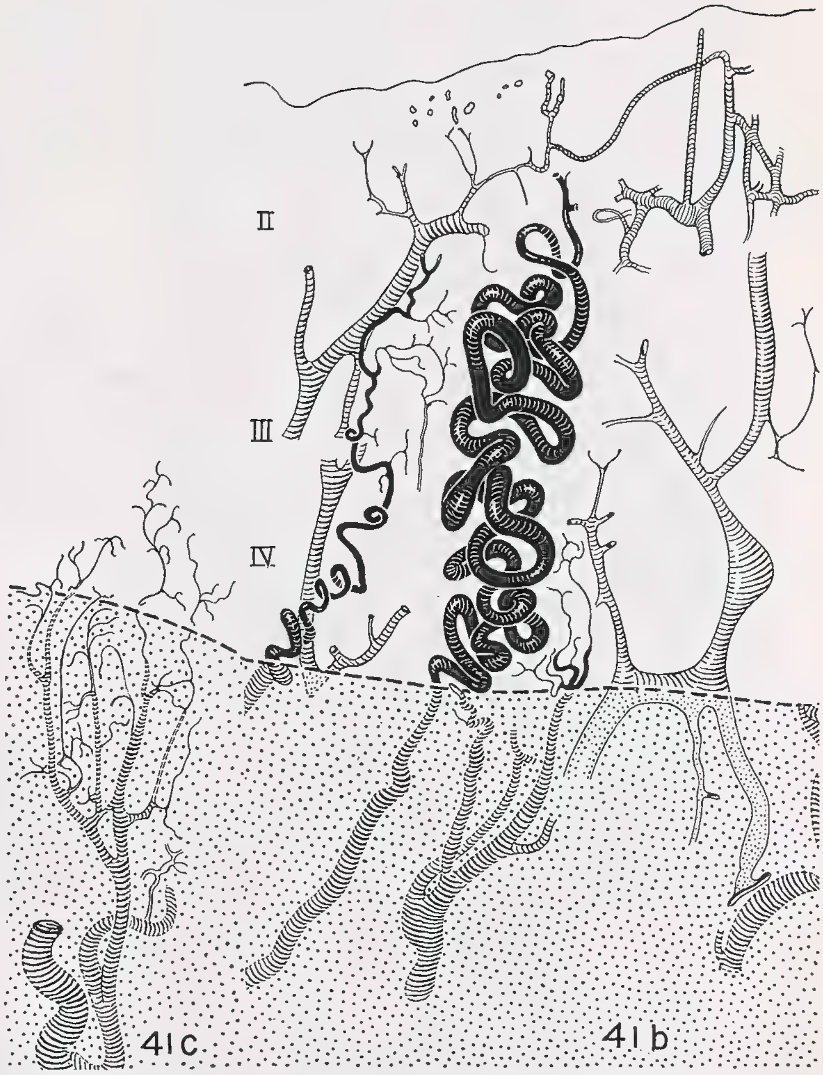

zone IV with direct drainage from surface, and large emissary to myometrium. B332, sagittal section 10, 200 microns.

b. Contorted artery typical of corpus with small, simply coiled type I artery at left. Radial arteries dilated in this area. Veins dilated, and myometrial emissaries broad. B332, sagittal section 8, 500 microns.

c. A tufted myometrial artery with endometrial twigs. B332, sagittal section 8, 500 microns.

Fig. 42. Day 4 of anovulatory menstruation in April (see p. 172; fig. 58, pl. 14). *a,* area of dorsal wall, showing simply coiled type I arteries. Artery at left supplies all levels of endometrium. The capillaries it supplies are wide; the mesh is coarse (see p. 158). *b,* from ventral wall; artery at right as contorted as any. Dilated sinuses and tributaries, as at right, are common. B331, transverse section 33, 200 microns.

Plates 11 to 15 present photographs of thick sections from near the center of the corpus, magnified 15 times with a 32-mm. anastigmat (except for figure 47). Arrows indicate endomyometrial junction.

Plate 11

Fig. 43. Phase of repair, day 8 of cycle. Injection complete. Endometrium 1.2 to 1.9 mm., myometrium 3.9 to 4.3 mm. thick. Note dilated radial arteries extending from stratum vasculare to junction. For details of endometrial vessels, see figures 4 and 5 (pl. 1). B334, transverse section, dorsal wall, 300 microns.

Fig. 44. Early follicular phase, day 15. Injection complete. Endometrium 1.7 to 2.5 mm., myometrium 3.0 to 3.3 mm. For endometrial vessels, see figures 6 and 7 (pl. 1). B302, transverse section, 480 microns.

Fig. 45. Uterus associated with mature Graafian follicle, day 12. Endometrium 3.3 to 4.0 mm., myometrium 4.0 to 4.2 mm. Injection complete. Note dilated radial arteries, superficial capillary net, and type I arteries coiled in zone IV (see fig. 18, pl. 4). B338, sagittal section, 400 microns.

Fig. 46. Phase of ovulation, day 11. Incomplete injection due to many constricted radial arteries. Endometrium 2.1 to 3.0 mm., myometrium 5.0 to 5.4 mm. Note contorted type I arteries (see fig. 19, pl. 4) and poor injection of inner myometrium. B323, sagittal section, 480 microns.

Fig. 47. From same uterus as figure 46. Basal moiety of type I artery with constriction in its associated radial artery (see p. 161 for measurements). Dilated transitional artery at lower left. Segments of radial artery that are out of focus have been strengthened. Arrow at endomyometrial junction. Transverse section, 480 microns enlarged to 70 diameters.

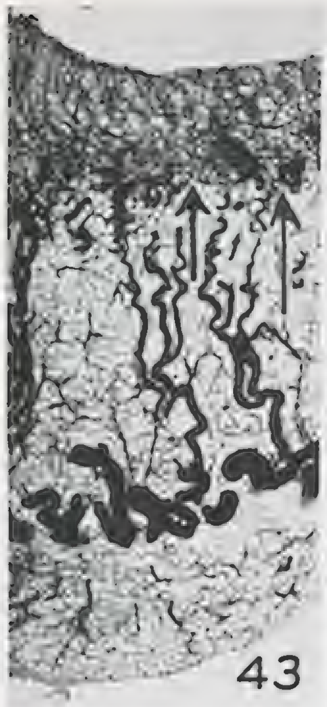

43

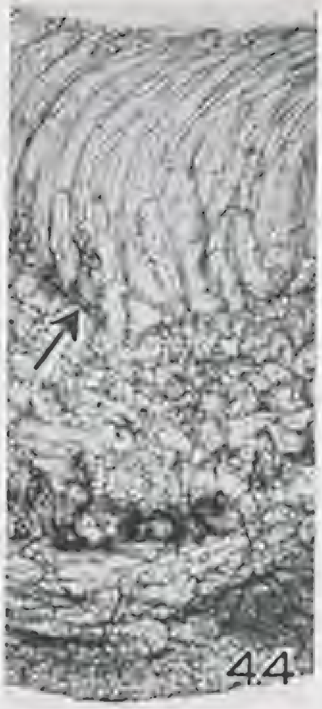

44

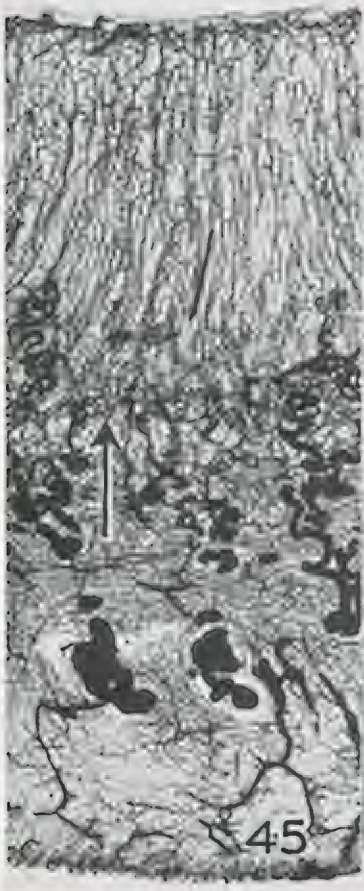

45

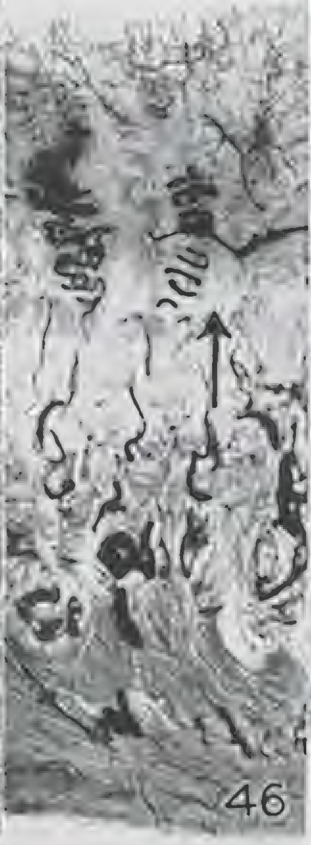

46

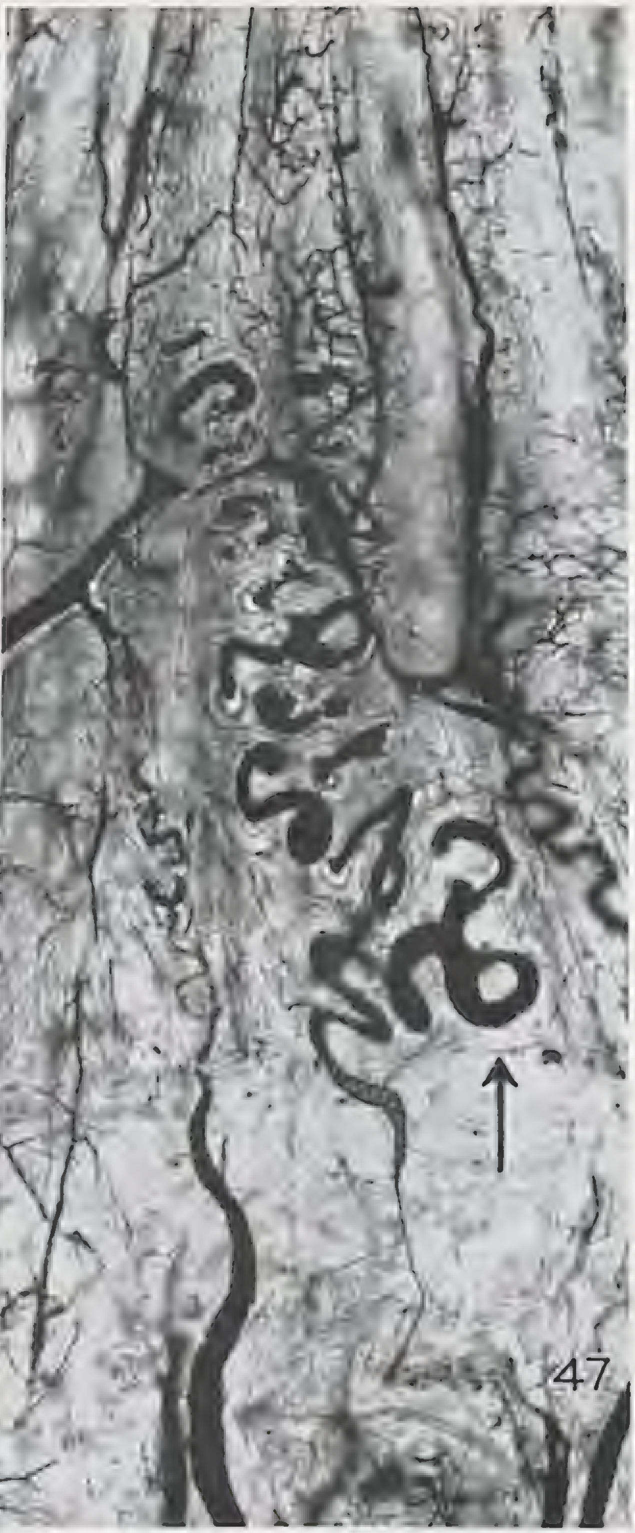

47

Plate 12

Photographs of sections as in plate 11, ×15

Fig. 48. Early progravid phase, day 17 (see p. 162). Injection complete, no constrictions in radial or endometrial arteries. *a* is large type I artery shown in figure 21 (pl. 5). *b* is small artery of same type. Apical rami of *c* and *d* ramify in same area of zone II. Endometrium 4.9 mm., myometrium 4.2 mm. B309, sagittal section, 480 microns.

Fig. 49. Uterus associated with corpus aberrans, day 26. Endometrium 4.1 to 4.9 mm., myometrium 3.5 to 4.1 mm. Some regression in fairly typical early progravid endometrium. Note contorted arteries in zone II and sinus at base of this zone. B307, sagittal section, 480 microns.

Fig. 50. Uterus associated with mature corpus luteum, day 23. Endometrium (mid-line dorsal wall) 8.5 mm., myometrium 3.3 mm. *Intra vitam* injection of HgS; arteries, veins, and capillaries of zone I visualized; elsewhere capillaries cannot be followed. Type I arteries not so greatly contorted as in figure 48; arterial fields narrower. Arrow indicates a sinuous apical ramus. B239, transverse section, 400 microns.

Fig. 51. Late progravid phase, day 21; corpus luteum 10 to 11 days old. Endometrium 7.0 mm., myometrium 3.0 mm. Injection complete. Large artery (*b*) is reconstructed in figure 31 (pl. 7). Sinuous transitional artery at *a*. Coiled vessel (*c*) is small type I artery. B325, sagittal section 26, 200 microns.

Fig. 52. Early ischemic phase, day 29. Endometrium 4.6 to 6.8 mm., myometrium 2.4 mm. Note collapsed form and narrow lumina of glands in zone II. Sinus at left between zones II and III. Injection variable in endometrium owing to constrictions in some radial arteries. B316, transverse section 21, 200 microns.

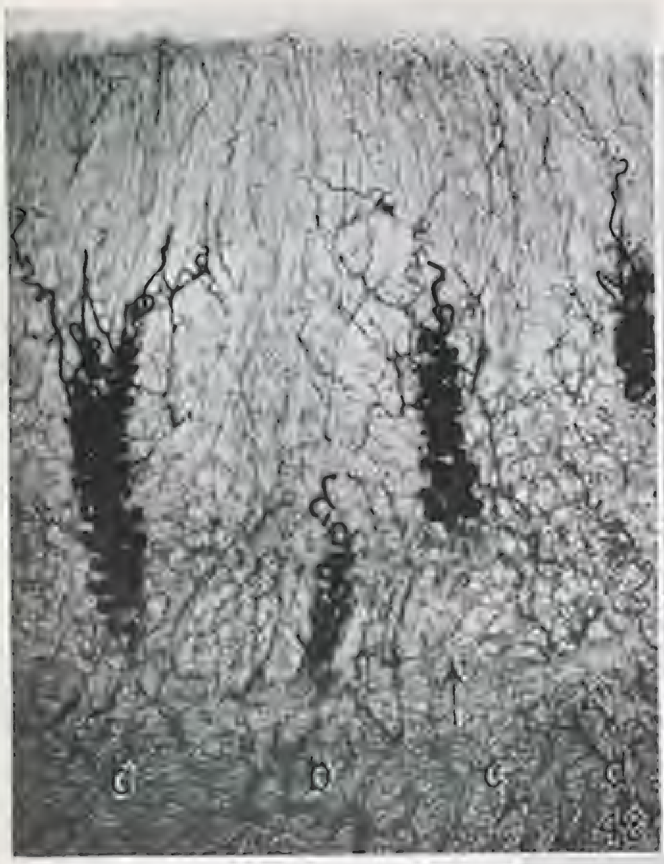

48

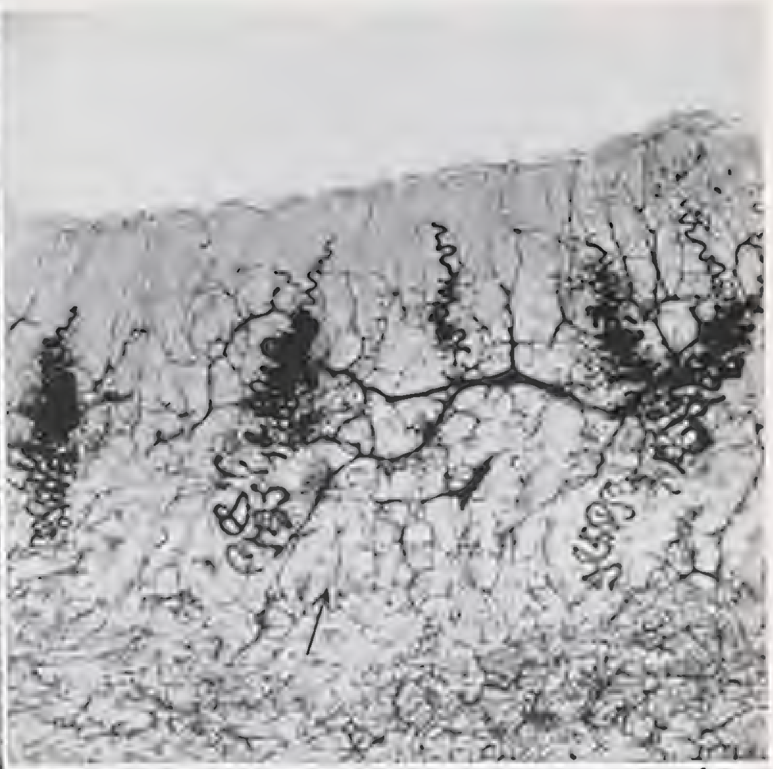
49

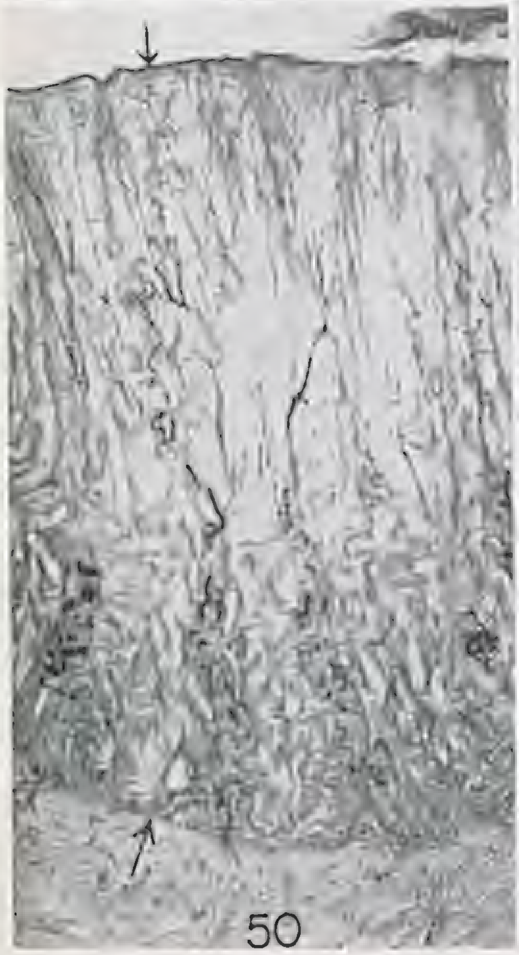
50

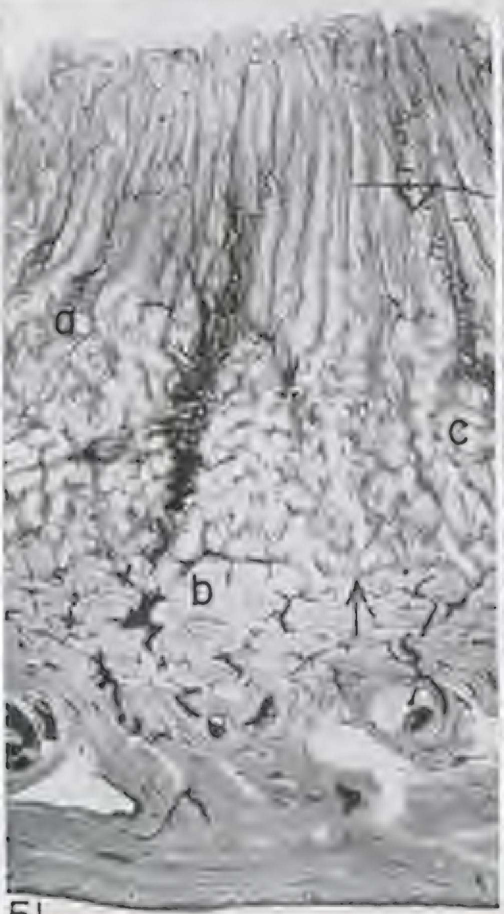

51

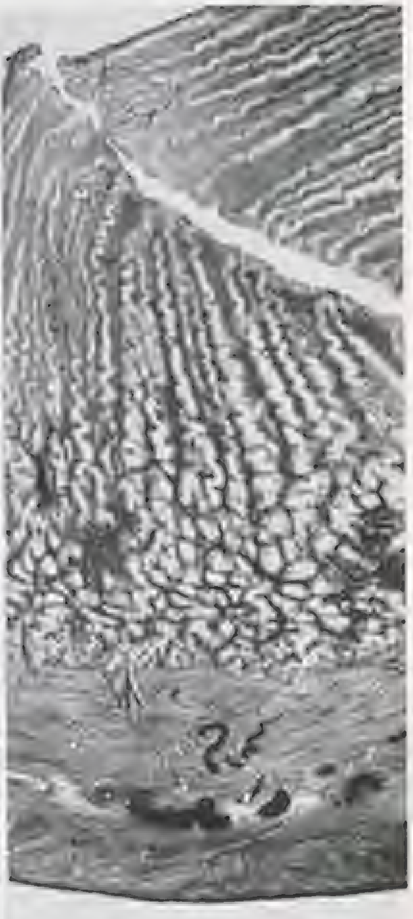
52

PLATE 13

PHOTOGRAPHS OF SECTIONS AS IN PLATE 11, ×15

FIG. 53. Early ovulatory menstruation (see p. 168). Injection complete in some menstruating areas. Endometrium 3.3 mm. (excluding slough), myometrium 3.8 mm. Left of middle is superficial segment of large artery reconstructed in figure 34 (pl. 8). Small type I arteries on either side of it. Note fissures at right that soon undermine the slough (Markee, 1940). B317, sagittal section A12, 480 microns.

FIG. 54. Day 1 of ovulatory menstruation (see p. 169). Endometrium 1.8 to 2.5 mm., myometrium 4.2 mm. Thicker myometrium indicates contraction characteristic of menstruation (cf. fig. 52, pl. 12). Type I artery as contorted as any in this specimen. Coils out of focus have been strengthened. Venous sinus in zone II near fissure. B314, transverse section 28, 480 microns.

FIG. 55. Early regressive phase, day 30. Injection complete. Contortion of type I arteries (see fig. 32, pl. 7) and crowding indicate regression in endometrium, which has some features of early progravid phase (see p. 166). Lateral limbus at right; note smaller size of coiled arteries. Endometrium 6.3 mm., myometrium 2.3 mm. B330, sagittal section 19, 500 microns.

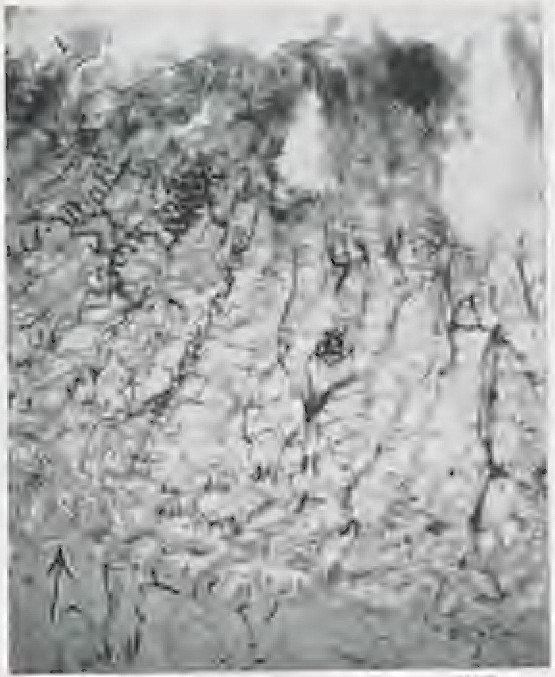

53

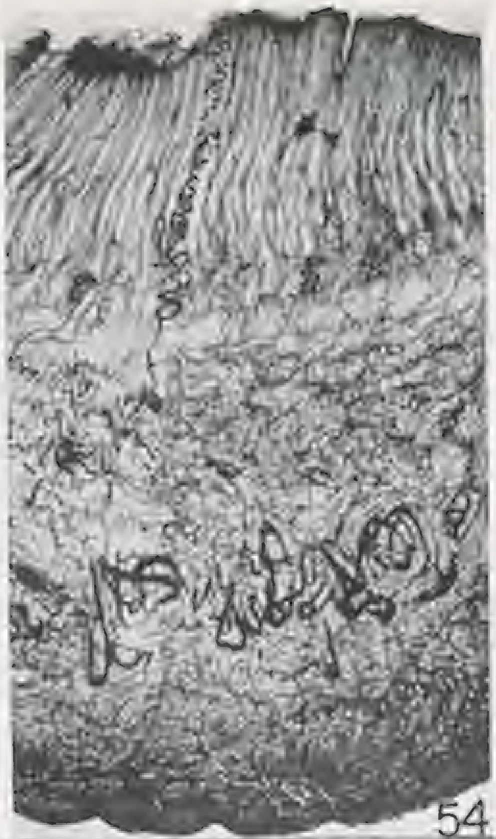

54

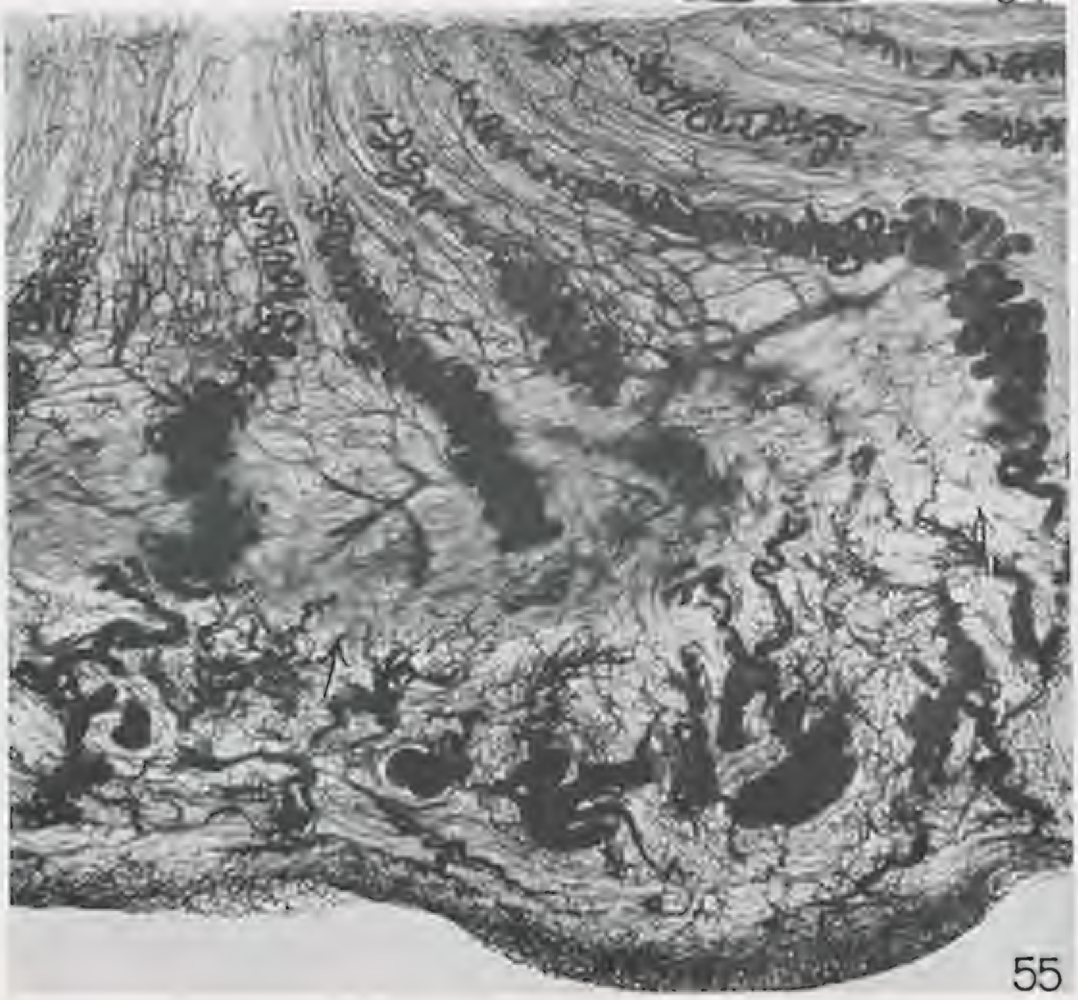

55

Plate 14

MENSTRUATING UTERI. PHOTOGRAPHS OF SECTIONS AS IN PLATE 11

Magnified 15 times (except figure 60)

FIG. 56. Day 2, anovulatory menstruation. Injection complete except for superficial ¼ of corpus endometrium, where only veins are filled. Superficial rami of type I arteries constricted; relatively few constrictions in radial arteries. Artery at left is simply coiled compared to that in figure 41*b* (pl. 10*a*). Endometrium 2.4 mm., myometrium 4.4 mm. B332, transverse section 21, dorsal wall, 500 microns.

FIG. 57. Day 4, anovulatory menstruation. Injection complete. Endometrium 1.0 mm. or less, myometrium 3.0 mm. (see fig. 42, pl. 10). Note dilated radial arteries. Uterus dilated with discharge. B331, transverse section 27, 500 microns.

FIG. 58. Day 5, anovulatory menstruation with beginning of repair. Endometrium 1.9 mm., myometrium 4.1 mm. Lateral limbus at right. Arterial injection complete; capillaries fragmentary except in zone II (see figs. 1, 2, pl. 1). Connective tissue of myometrium edematous, although minimal saline solution preceded injection of ink. B329, transverse section, 8 microns.

FIG. 59. Early day 1 of ovulatory menstruation. Crowding and contortion of type I arteries is corollary of involution of stroma. Lateral limbus at left. B127 (see Bartelmez *et al.,* 1951), 12-micron section.

FIG. 60. Photomicrograph from the same uterus as figure 56. Capillary bed in vicinity of gland in zone II. Despite the involution of the stroma, capillaries are not in contact with the glandular epithelium (*gl*). Vessels out of focus have been strengthened. B332, sagittal section, 200 microns. × 100.

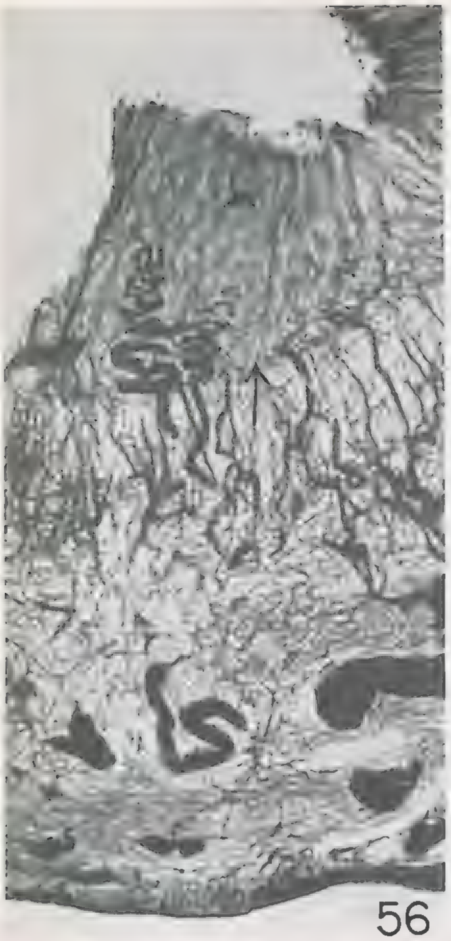

56

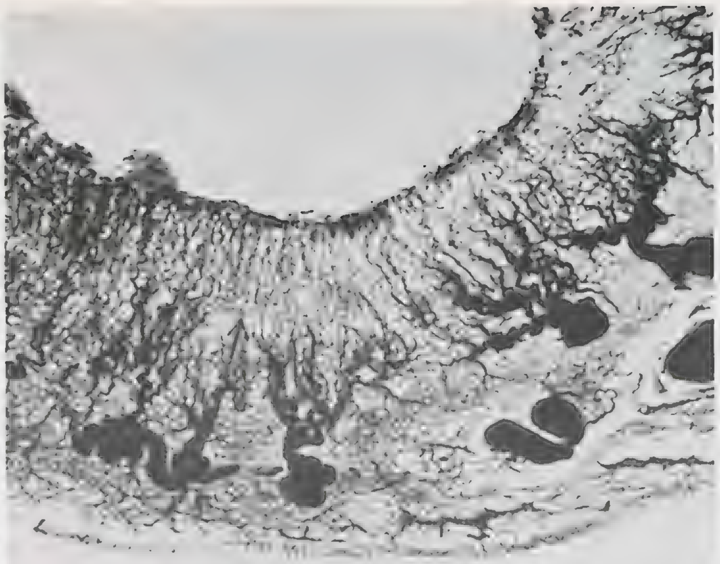

57

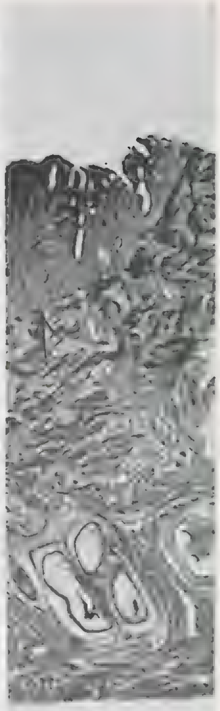

58

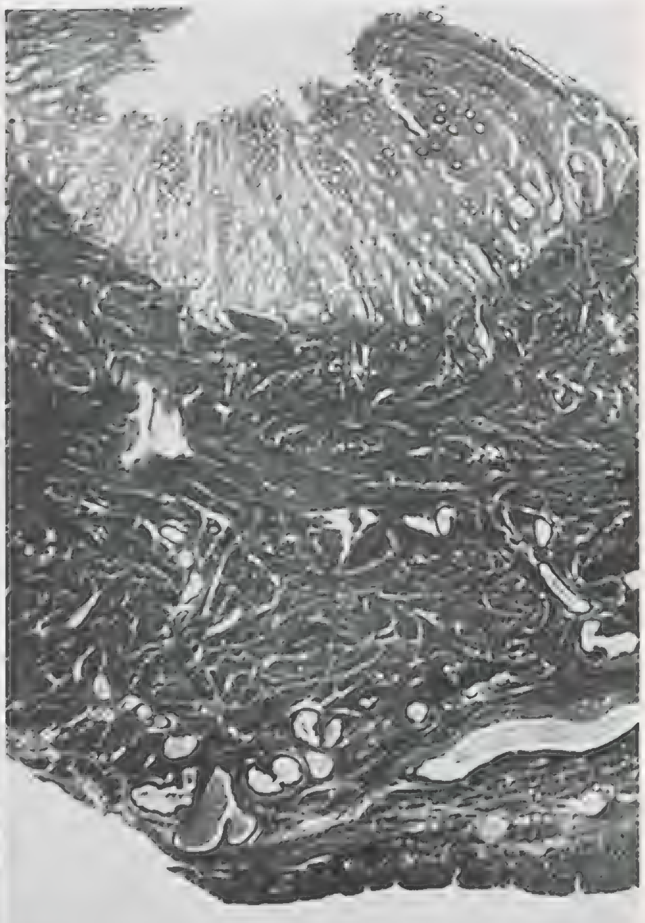

59

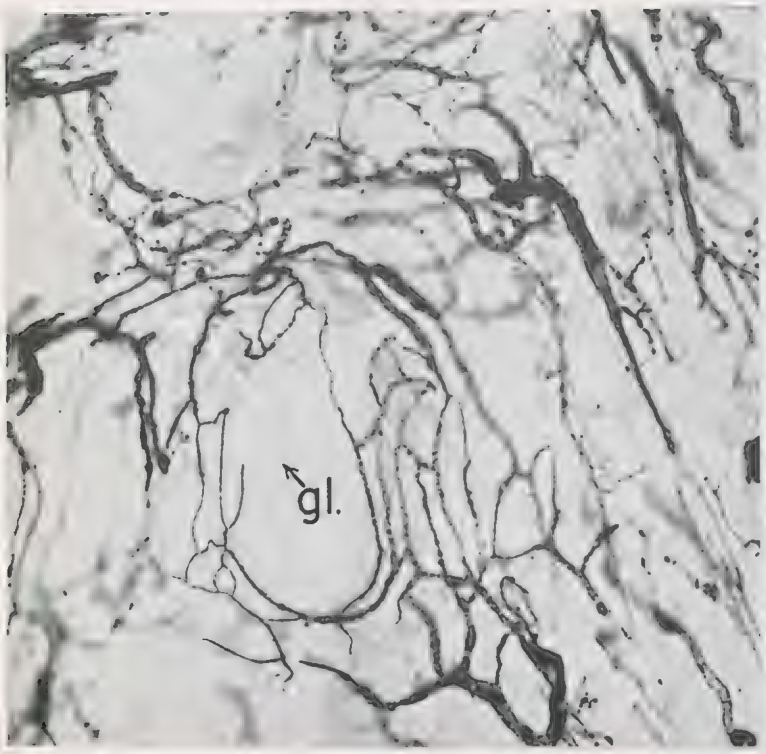

60

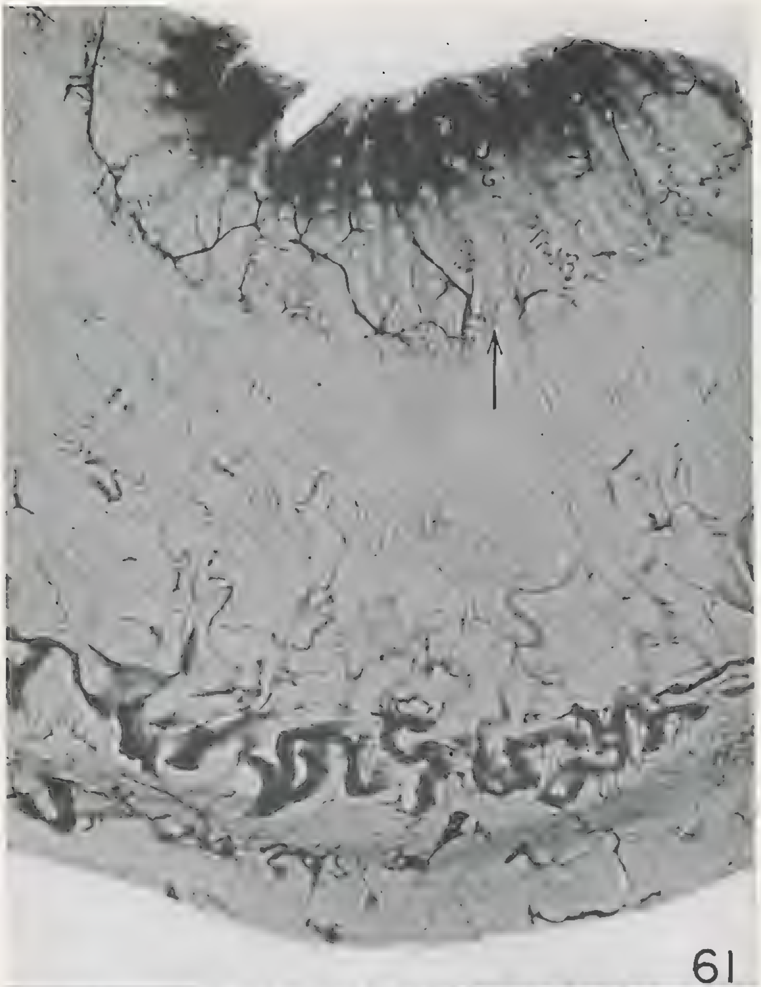

61

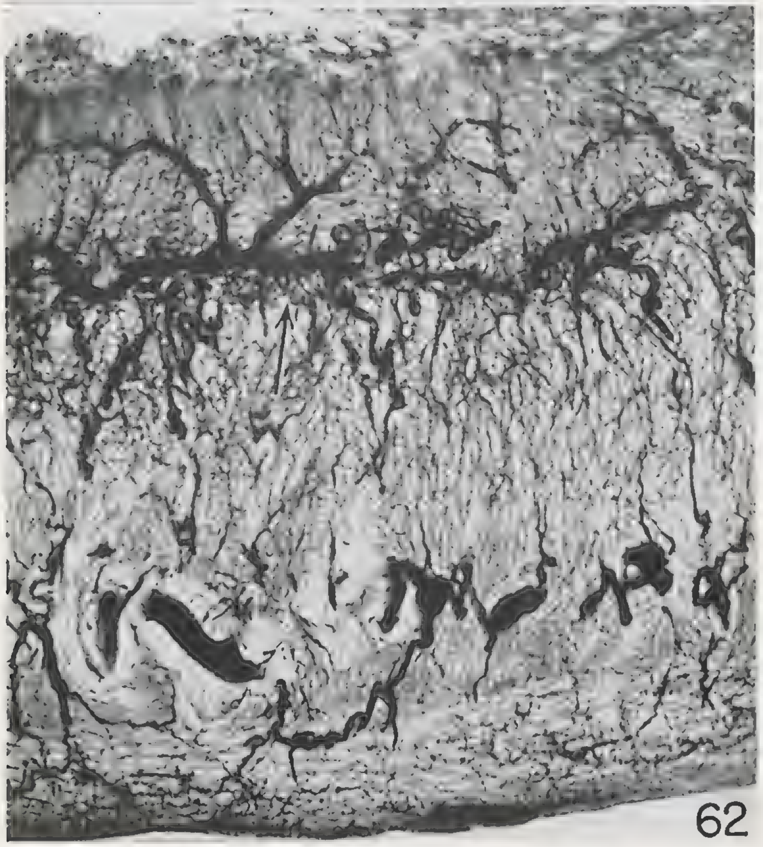

62

PHOTOGRAPHS OF THICK SECTIONS, × 15

FIG. 61. Day 2, ovulatory menstruation. Injected carmine diffused into superficial zone of endometrium (dark) in corpus and fundus but in no other areas of uterus. Through routes in venous network empty into sinuses at junction. Radial arteries usually constricted in this specimen (note poorly injected inner myometrium) (see p. 169). Endometrium 2.5 mm., myometrium 5 mm. B313, transverse section, 480 microns.

FIG. 62. From the 2-day specimen shown in figure 56 (pl. 14). Endometrium 2.4 mm., myometrium 4.4 mm. Veins, which are more dilated during menstruation than at other times, predominate in this area. The great sinus at the junction of endo- and myo-metrium extends longitudinally through the corpus and receives radiating tributaries from zone II. Note complete injection of myometrium. B332, sagittal section 11, 500 microns.

CONTRIBUTIONS TO EMBRYOLOGY, NO. 250

CHONDRIFICATION IN THE HANDS AND FEET OF STAGED HUMAN EMBRYOS

RONAN O'RAHILLY, D. J. GRAY, AND ERNEST GARDNER

Departments of Anatomy, Wayne State University College of Medicine, Detroit, Michigan, and Stanford University School of Medicine, Stanford, California

With one plate

CONTENTS

PAGE

Introduction 185

Materials and Methods 186

Observations 186

- Upper Limb 186
  - Horizon XV (6.0 to 11.0 mm.) 186
  - Horizon XVI (7.0 to 12.2 mm.) 186
  - Horizon XVII (8.6 to 14.5 mm.) 186
  - Horizon XVIII (11.7 to 18.0 mm.) 186
  - Horizon XIX (15.5 to 21.0 mm.) 187
  - Horizon XX (18.5 to 25.0 mm.) 187
  - Horizon XXI (19.0 to 26.4 mm.) 187
  - Horizon XXII (23.0 to 27.5 mm.) 187
  - Horizon XXIII (23.0 to 32.2 mm.) 187
- Lower Limb 187
  - Horizon XV (6.0 to 11.0 mm.) 187
  - Horizon XVI (7.0 to 12.2 mm.) 187
  - Horizon XVII (8.6 to 14.5 mm.) 187
  - Horizon XVIII (11.7 to 18.0 mm.) 188
  - Horizon XIX (15.5 to 21.0 mm.) 188
  - Horizon XX (18.5 to 25.0 mm.) 188
  - Horizon XXI (19.0 to 26.4 mm.) 188
  - Horizon XXII (23.0 to 27.5 mm.) 188
  - Horizon XXIII (23.0 to 32.2 mm.) 189

Discussion 189

- Hand 189
- Foot 190

Summary 191

Literature Cited 191

CHONDRIFICATION IN THE HANDS AND FEET OF STAGED HUMAN EMBRYOS[1]

INTRODUCTION

The prenatal development of the skeleton of human limbs has been studied by many investigators. Reports based on their studies have related mainly to ossification, however, as in the recent papers by Noback and Robertson (1951) and O'Rahilly and Meyer (1957). Comparable attention has not been given to the earlier development of the skeletal elements, particularly to those of the hands and feet. Apart from Senior's (1929) abstract, no adequate account has been published of the onset and sequence of chondrification in a large series of hands and feet.

Investigators generally agree that chondrification begins in the metacarpals before it begins in the carpals, and that the lunate and pisiform are the last of the carpals to begin to chondrify (Henke and Reyher, 1874; Rosenberg, 1876; Leboucq, 1884; Gräfenberg, 1905; Martin, 1929). A few authors have reported that they could distinguish carpal elements in the blastemal stage (Lewis, 1902; Schmidt-Ehrenberg, 1942; Haines, 1947). Chondrification begins in the proximal phalanges, and extends progressively to the most distal members (Henke and Reyher, 1874; Hagen, 1900; Lewis, 1902; Gräfenberg, 1905; Hesser, 1926). In a 27-mm. embryo, Schulin (1879) found that all the skeletal elements of the hand were chondrified except the sesamoids.

It is also generally agreed that the digits of the foot, like those of the hand, chondrify in a proximodistal sequence (Henke and Reyher, 1874; Schulin, 1879; Schomburg, 1900; Bardeen and Lewis, 1901; Leboucq, 1904; Bardeen, 1905; Martin, 1929; Trolle, 1948). Several authors have reported chondrification in the foot beginning in embryos of about 14 to 21 mm. in length (Henke and Reyher, 1874; Baur, 1886; Bardeen and Lewis, 1901; Bardeen, 1905; Martin, 1929; Hintzsche, 1930; Haines, 1947; Trolle, 1948), but none of these writers has given information regarding the sequence of chondrification in the tarsus. Leboucq (1886) stated that he found the tarsal elements differentiated in a 12-mm. embryo, but it is not clear from his account whether he intended to use "differentiated" as synonymous with "chondrified."

Senior (1929) was the first to report a precise sequence in chondrification in both hand and foot. In an abstract based on a study of 77 embryos, ranging from 12.5 to 24.8 mm. crown-rump length, he reported that with few exceptions the hands and feet fit into one of the stages listed in tables 1 and 2, respectively. Senior pointed out that "chondrification, being cumulative, affords an excellent guide to the relative stage of development of embryonic limbs while the increase in the number of centers lasts." Streeter (1929) considered using the order of chondrification established by Senior as an aid in staging human embryos. Unfortunately, however, Senior did not publish a complete account of his findings, and attempts to locate his original data have been unsuccessful.

TABLE 1

SENIOR'S STAGES OF CHONDRIFICATION IN THE HAND

(Numerals refer to digits)

Stage	
1	Hamate, capitate, metacarpals 2 to 4
2	Metacarpal 5
3	Trapezoid
4	Proximal phalanges 2 to 4
5	Triquetrum, trapezium, metacarpal 1, proximal phalanx 5
6	Scaphoid, centrale
7	Proximal phalanx 1
8	Lunate
9	Middle phalanges 2 to 4
10	Middle phalanx 5
11	Pisiform
12	Distal phalanx 1
13	Distal phalanges 2 to 4
14	Distal phalanx 5

TABLE 2

SENIOR'S STAGES OF CHONDRIFICATION IN THE FOOT

(Numerals refer to digits)

Stage	
1	Metatarsals 2 to 4
2	Cuboid, metatarsal 5
3	Calcaneus, talus, lateral cuneiform
4	Intermediate cuneiform
5	Medial cuneiform, metatarsal 1
6	Navicular
7	Proximal phalanges 2 to 4
8	Proximal phalanx 5
9	Proximal phalanx 1
10	Middle phalanges 2 to 4
11	Middle phalanx 5
12	Distal phalanx 1
13	Distal phalanges 2 to 4
14	Distal phalanx 5

Correlation of Senior's stages of chondrification in both hand and foot with Streeter's (1942, 1945, 1948, 1949, 1951) developmental horizons seems desirable. For this purpose, a study was made of embryos in the collection of the Department of Embryology, Carnegie Institution of Washington. The writers are indebted to Dr. George W. Corner, former Director, for the opportunity to undertake this work.

---

[1] This investigation was supported by research grants A-550 (C2) and A-532 (C7) from the National Institute of Arthritis and Metabolic Diseases, of the National Institutes of Health, U. S. Public Health Service.

MATERIALS AND METHODS

Serial sections of the limbs of 103 staged human embryos, belonging to horizons xv to xxiii inclusive and ranging from approximately 6½ to 30 mm. in length, were studied. In the case of the upper limb, 102 sectioned embryos were examined; lower limbs of 101 embryos were analyzed.

Since special staining techniques for cartilage matrix had not been used in the preparation of the embryos, it was necessary to establish arbitrary histological criteria for the onset of chondrification. In this study, a blastemal condensation of a skeletal element consists of closely packed cells having indistinct boundaries. When the separation of nuclei in a localized part of a condensation results in a lighter appearance, matrix is presumed to have been deposited in this area, and chondrification is said to have begun.

In the carpals and tarsals, chondrification usually begins near the center, and a more or less rounded chondrified area surrounded by blastemal tissue is formed. This area then spreads until it reaches the periphery of the blastemal condensation, at which time a perichondrium may be said to exist. Further growth depends on the multiplication of perichondral as well as of cartilage cells, and on the formation of matrix. Chondrification is basically similar in long bones. In the metacarpals and metatarsals, as in other long bones, Streeter's (1949) five phases in the growth of cartilage can be recognized.

The term "hand" as used throughout this paper includes the carpus, metacarpus, and phalanges. The terminology employed is the *Nomina anatomica emendata* of 1955, translated into English where appropriate.

OBSERVATIONS

UPPER LIMB

Horizon xv (6.0 to 11.0 mm.). Five embryos examined: Carnegie nos. 2, 721, 6504, 6506, 8997.

A central, mesenchymal condensation for muscle and bone in the proximal part of the limbs was present in two specimens and absent in three. The central part of this condensation was avascular. A photomicrograph illustrating a section of the upper limb at this stage was reproduced by Streeter (1949, fig. 8, pl. 1). An ectodermal ridge, first visible in the previous horizon, was also found at this stage (O'Rahilly, Gardner, and Gray, 1956).

Horizon xvi (7.0 to 12.2 mm.). Ten embryos examined: Carnegie nos. 163, 617, 6507, 6509, 6510, 6512, 6517, 7115, 8112, 8773.

The humerus, radius, and ulna could be distinguished as mesenchymal condensations in most of these embryos. Early chondrification of the humerus was noted in one. The appearance of the humerus during early chondrification is shown in a photomicrograph by Streeter (1949, fig. 9, pl. 1).

Horizon xvii (8.6 to 14.5 mm.). Twenty-one embryos examined: Carnegie nos. 353 (1), 559, 623, 940 (1), 1771, 5642 (1), 5893 (1), 6258, 6519, 6520 (1?), 6521, 6631 (1), 6742, 6758, 8101, 8118, 8253, 8789 (1), 8969, 8998, 9100. (Figures in parentheses in lists of embryos examined in this and subsequent horizons are Senior's stages of chondrification for the hands.)

The humerus and radius were chondrifying in almost all these embryos. Although the ulna was chondrifying in many of them, chondrification was entirely absent in two embryos and doubtful in two others. The radius and ulna were short and widely separated in embryos in which they were chondrifying (fig. 1). Their distal parts, still composed of condensed mesenchyme, were continuous with a common skeletal blastemal mass from which digital prolongations extended (fig. 1). The blastemal condensation of the thumb was very short or absent; that of the fifth digit was short.

Chondrification had not yet begun in the hands of approximately two-thirds of the embryos. In the remaining third, it was beginning in the 3d and 4th metacarpals (fig. 1); the hands of these embryos, therefore, are in early Senior's stage 1, a stage in which Senior included chondrification of the 2d metacarpal and the hamate and capitate. Aside from three embryos in which chondrification had possibly begun in the hamate and capitate, none was found in the carpus. The ectodermal ridge, present since horizon xiv, disappeared during horizon xvii.

Horizon xviii (11.7 to 18.0 mm.). Seventeen embryos examined: Carnegie nos. 106 (1), 109 (1), 144 (6), 175 (2–3), 492 (2), 4430 (5), 6522 (4–5), 6524 (4), 6525 (4), 6527 (4), 6528 (2), 6533 (4), 7707 (2), 8097 (1), 8172 (4), 8355 (1), 9247 (3).

The radius and ulna were widely separated from each other, their distal parts still composed of condensed mesenchyme. In the embryos in which the carpus was still mainly blastemal, localized variations in density were noticed, but individual carpal elements were not identified on the basis of these differences. In the embryos in which several carpal elements had begun to chondrify, however, mesenchymal condensations of the remaining carpal elements were usually distinguishable. Nonsegmented mesenchymal condensations extended distally from the common carpal blastema into the digits in which chondrification had not yet begun.

On the basis of chondrification in the hand, most embryos ranged from an early Senior's stage 1 to stage 4, although two were found to be in stage 5 and one in stage 6. Four specimens were classified as early stage 1 because, although they included chondrification in the 3d and 4th metacarpals, one or more of the other elements (2d metacarpal, capitate, hamate) assigned by Senior to this period had not yet begun to chondrify. In the specimen most advanced in chondrification (Senior's stage 6), the following elements were chondrifying: all carpals except the lunate and pisiform, all five metacarpals, and the proximal phalanges of the 2d to 5th fingers. Figure 2 illustrates chondrification at Senior's stage 5 in a hand of an embryo not included in the seventeen listed above.

Horizon xix (15.5 to 21.0 mm.). Twelve embryos examined: Carnegie nos. 17 (11), 43 (7), 409 (9), 432 (7), 576 (8), 1324 (7–8), 1390 (8–9), 2114 (6), 4405 (7), 5609 (9?), 6150 (9–10?), 8965 (7–9).

Streeter's cartilage phases 1 to 3 were present in the radius and ulna. The styloid processes of both these elements were chondrifying in some specimens, were mesenchymal in others, and were not recognizable in still others. When the styloid process of the ulna was observed, it was very closely related to the triquetrum.

Although a few of the embryos in this age group exhibited chondrification ranging from Senior's stages 6 to 11, the chondrification of most members of the group could be classified in stages 7 to 9. (By stage 11, all skeletal elements except the distal phalanges have started to chondrify; the centrale is chondrified by stage 6.)

The chondrific centers in the capitate and hamate were larger than those in the other carpals, whereas relatively small areas of the trapezium and trapezoid were chondrified. No close correlation was noted between Streeter's point scores for the entire embryo and Senior's stages of chondrification for the hand, except that the two embryos most advanced in development had the higher Senior stages.

Horizon xx (18.5 to 25.0 mm.). Eleven embryos examined: Carnegie nos. 431 (12), 460 (10–11), 462 (11), 966 (10), 4148 (9–10), 5537 (10), 6202 (11), 6426 (11), 7274 (9), 7906 (9?), 8157 (12).

The humerus, radius, and ulna of some specimens contained phase 4 cartilage. The styloid processes of the radius and ulna were mesenchymal in some embryos, whereas they had begun to chondrify in others. The styloid process of the ulna was closely related to the triquetrum in all embryos of this age group. In three specimens, the styloid process of the 3d metacarpal was identified, and in one it had begun to chondrify. Chondrification in the hands ranged from Senior's stages 9 to 12. (By stage 12, all skeletal elements except the distal phalanges of the 2d to 5th digits are chondrifying.) The lunate was consistently less advanced in chondrification than the other carpal elements.

Horizon xxi (19.0 to 26.4 mm.). Fourteen embryos examined: Carnegie nos. 22 (13–14), 455 (14), 903C (14), 1008 (14), 1358F (14), 2937 (14), 4090 (13–14), 4960 (14), 5596 (14), 6531 (12–14), 7254 (11), 7392 (14), 7864 (13), 8553 (14).

The humerus had a primary bone collar in at least three specimens, the radius in one. Phase 3 cartilage was generally present in the metacarpals and proximal phalanges. The styloid process of the ulna was hook-shaped and chondrified in most specimens. The hook of the hamate appeared as a cellular condensation. Chondrification in the hands ranged from Senior's stages 11 to 14, the majority of hands belonging in stage 14. Only one specimen was at stage 11. (All skeletal elements of the hand have begun to chondrify by stage 14.) The lunate and pisiform were less advanced in chondrification than the other carpal elements. The centrale had begun to fuse with the scaphoid in some specimens.

Horizon xxii (23.0 to 27.5 mm.). Five embryos examined: Carnegie nos. 1458, 3681, 4339, 4638, 8394.

The humerus of all specimens, and the radius and ulna of most, had a bone collar. By horizon xxii, all skeletal elements were chondrifying. Of the distal phalanges, the 1st was generally the most advanced in chondrification. As in the previous horizon, the centrale had begun to fuse with the scaphoid in some specimens.

Horizon xxiii (23.0 to 32.2 mm.). Seven embryos examined: Carnegie nos. 75, 86, 1945, 2561, 4525, 5621A, 7425.

The bone collars of the humerus, radius, and ulna were thicker than in the previous horizon. Calcification had begun in the cartilage matrix, but no cellular, vascular invasion of the bone collar was observed, except in one specimen in which periosteal buds were beginning to enter the humerus and radius bilaterally. Although cellular condensations of sesamoids were noted in embryos sectioned so as to show these areas favorably, no chondrification was seen in them. The centrale was partly fused with the scaphoid in all specimens.

Lower Limb

Horizon xv (6.0 to 11.0 mm.). Six embryos examined: Carnegie nos. 2, 721, 6504, 6506, 8997, 9140.

The mesenchyme of the lower limbs was of uniform density in four embryos. In two other specimens, however, a denser arrangement of the nuclei in the central and proximal parts of the limbs suggested an early blastemal condensation for skeleton and muscles. An ectodermal ridge was present for the first time in the lower limb at this stage (O'Rahilly, Gardner, and Gray, 1956).

Horizon xvi (7.0 to 12.2 mm.). Ten embryos examined: Carnegie nos. 163, 617, 6507, 6509, 6510, 6512, 6517, 7115, 8112, 8773.

A blastemal condensation, avascular in its central part, was present proximally in at least four of these specimens.

Horizon xvii (8.6 to 14.5 mm.). Twenty-one embryos examined: Carnegie nos. 353, 559, 623, 940, 1771, 5642, 5893, 6258, 6519, 6520, 6521, 6631, 6742, 6758, 8101, 8118, 8253, 8789, 8969, 8998, 9100.

In the least-advanced limbs at this stage, no blastemal condensation was observed. In the most-advanced limbs, the entire femur was chondrifying. Centers of chondrification were present in the tibia of some specimens, in the fibula of only two. A common cellular condensation for the tarsus was noted, as well as condensations for the 2d, 3d, 4th, and, occasionally, 5th toes.

Horizon xviii (11.7 to 18.0 mm.). Seventeen embryos examined: Carnegie nos. 106, 109, 144 (3), 175, 492 (2), 4430 (2), 6522 (1–2), 6524, 6525, 6527, 6528 (1?), 6533 (1?), 7707, 8097, 8172, 8355, 9247. (Figures in parentheses in lists of embryos examined in this and subsequent horizons are Senior's stages of chondrification for the feet.)

Chondrification in the tibia extended about halfway to the region of the ankle and included very early Streeter's phase 3 cartilage. The chondrified part of the fibula was very short, and less advanced than that of the tibia. In the majority of embryos, no chondrification was present in the foot. Separate digital prolongations extended distally from the common cellular condensation of the tarsus. A prolongation of the big toe was absent in some specimens and very short in others.

In the minority, the chondrification of the feet of specimens ranged from 1 to 3 of Senior's stages. (By stage 3, chondrification is present in the cuboid, calcaneus, talus, lateral cuneiform, and 2d to 5th metatarsals.) Blastemal condensations extended distally from the cartilage of the metatarsals and, in the 1st digit, distally from the tarsal condensation. The ectodermal ridge, present since horizon xv, disappeared during horizon xviii. Figures 3 and 4 illustrate chondrification in an early Senior's stage 1 in feet from an embryo not included in the seventeen listed above.

Horizon xix (15.5 to 21.0 mm.). Eleven embryos examined: Carnegie nos. 17 (9), 43 (4 and navicular), 409 (4), 432 (4), 576 (4–5 and navicular), 1324 (6), 1390 (4 and navicular), 4405 (3), 5609 (4–5), 6150 (6), 8965 (3).

The tibia and fibula were still blastemal in their distal parts. Chondrification in the fibula was less advanced than it was in the tibia. Chondrification in the feet ranged from Senior's stages 3 to 6, except one specimen at stage 9. (By stage 6, all tarsals and metatarsals have begun to chondrify.) The specimen assigned to Senior's stage 9 on the basis of chondrification in the feet had the maximal Streeter's point score for horizon xix and an unusually high Senior stage in the hand. In three specimens assigned to stage 4, the navicular was also beginning to chondrify. According to Senior, the navicular (stage 6) usually chondrifies after the medial cuneiform and 1st metatarsal (stage 5). The center of chondrification in the cuboid was relatively large and well advanced, whereas the centers in the talus and calcaneus were relatively small. A cellular condensation of the tuber calcanei appeared in this horizon.

Horizon xx (18.5 to 25.0 mm.). Eleven embryos examined: Carnegie nos. 431 (9), 460 (9), 462 (9), 966 (9), 4148 (4 and navicular), 5537 (7), 6202 (8), 6426 (7–8), 7274 (6), 7906 (7), 8157 (9).

The lower ends of the tibia and fibula still consisted of condensed mesenchyme and were closely related to each other. Streeter's phase 4 cartilage was present in the tibia but not in the fibula.

Chondrification in the feet ranged from Senior's stages 6 to 9, except one specimen assigned to stage 4, even though it included chondrification in the navicular. Only one specimen fell into stage 6, whereas about half of the specimens were at stage 9. (By stage 9, all the tarsals, metatarsals, and proximal phalanges have begun to chondrify.)

The centers of chondrification in the cuboid and lateral cuneiform were relatively larger than those in the talus and calcaneus. The cartilage was less advanced in the navicular and medial cuneiform than in other tarsal elements. In the cellular condensations that extended distally from the chondrifying proximal phalanges, there was no segmentation into middle and distal phalanges. Figure 5 illustrates chondrification in digits at Senior's stage 7 in a foot from an embryo not included in the eleven listed.

Horizon xxi (19.0 to 26.4 mm.). Thirteen embryos examined: Carnegie nos. 22 (10), 455 (11–12), 903C (12), 1008 (12), 1358F (12), 2937 (12), 4090 (10–12), 4960 (10), 5596 (12), 7254 (9), 7392 (9–10), 7864 (9), 8553 (10).

No bone collars were found in the long bones, although osteoblasts were observed in the perichondrium of the femur and tibia of some embryos. Streeter's phase 4 cartilage was noted in the tibia of all embryos and in the fibula of some. The patella was beginning to chondrify in some embryos.

Chondrification in the feet ranged from Senior's stages 9 to 12; about half were at stage 12. (By stage 12, all skeletal elements of the foot are chondrifying except the distal phalanges of the 2d to 5th toes.) The tuber calcanei was beginning to chondrify in some embryos. A cellular condensation of the sustentaculum talare was identifiable in at least one specimen, and a condensation of the tuberosity of the 5th metatarsal in another. Streeter's early phase 3 cartilage was present in the metatarsals and proximal phalanges.

Horizon xxii (23.0 to 27.5 mm.). Five embryos examined: Carnegie nos. 1458 (12), 3681 (12), 4339 (12), 4638 (12), 8394 (12).

A bone collar encircled the shafts of the femur and tibia of most specimens. The fibula contained phase 4 cartilage but lacked a bone collar. The patella was chondrifying in all embryos. All the feet were assigned to Senior's stage 12. The distal phalanges were present as mesenchymal condensations. The fibula and calcaneus were still closely related to each other.

Horizon xxiii (23.0 to 32.2 mm.). Seven embryos examined: Carnegie nos. 75 (14), 86 (14), 1945 (13), 2561 (12), 4525 (14), 5621A (13), 7425 (13–14).

A definite bone collar did not yet surround the fibula, but a layer of matrix was barely visible in the fibula of one specimen. The bone collar of the tibia of another specimen was being eroded by periosteal buds. The fibula was still closely related to the calcaneus, but usually separated from it by a small part of the talus.

The feet of all embryos were in Senior's stages 13 and 14 except one in Senior's stage 12. (By stage 14, all the skeletal elements of the foot have begun to chondrify.) No distinction was made between stages 13 and 14 in embryos in which the 2d and 3d phalanges of the 5th digit were present as a single cartilage. Such a specimen was present in the series upon which this report is based.

DISCUSSION

HAND

Although a skeletomuscular condensation was sometimes present in the upper limbs by horizon xv, the humerus, radius, and ulna could not be distinguished as separate blastemal condensations until horizon xvi. Chondrification of these elements began during horizons xvi and xvii, whereas that in the hand, sometimes beginning in horizon xvii, was more commonly under way by horizon xviii.

The sequence of chondrification in the hand agrees with that reported by Senior (1929); all elements except sesamoids were chondrifying by horizon xxi. Thus, chondrification begins in the various elements of the hand during approximately the 6th ovulation week, in embryos ranging from about 11 to 24 mm. in length.

Senior reported that, in his first stage, the hamate, capitate, and metacarpals 2 to 4 chondrify "almost simultaneously." Data from the present study indicate a slight difference in sequence within this first stage, metacarpals 3 and 4 chondrifying first. Senior found no significant deviations from the general sequence for the hand; this conclusion is corroborated in the present investigation. Table 3 lists the horizons that correspond to Senior's stages of chondrification in the hand.

The centrale, which begins to chondrify at stage 6 (horizons xviii and xix), started to fuse with the scaphoid in some specimens at horizons xxi and xxii, and was partly fused with the scaphoid in all specimens examined in horizon xxiii.

The carpus is first apparent as a common blastemal mass from which digital prolongations extend. Just before chondrification of a carpal element begins, the blastema in that area sometimes becomes more densely cellular. According to Haines (1947), in a 13-mm. embryo each carpal element is "represented not by a chondrified centre in the interior of the continuous blastema, but by a separate condensation of the blastema itself, separated from the neighbouring elements by intervening sheets of rarefied tissue. By 14 mm. the carpal . . . elements are chondrified. . . ." The planes of section of the embryos in the present series were generally unfavorable for distinguishing the individual carpal elements during the blastemal stage. When some of the elements had begun to chondrify, however, the adjacent blastemal condensations were more readily identifiable. For example, after the triquetrum had begun to chondrify, the mesenchymal condensation for the pisiform could be more easily delimited.

Nothing in the hand or foot was found that suggested the temporary appearance of structures characteristic of lower vertebrates, such as a prepollex or a postminimus.

TABLE 3

Horizons in which a given Senior's stage of chondrification in the hand has been found

Senior's stage	Horizons
0	xvii
1	xvii–xviii
2	xviii
3	xviii
4	xviii
5	xviii
6	xviii–xix
7	xix
8	xix
9	xix–xx
10	xix–xx
11	xix–xxi
12	xx–xxi
13	xxi
14	xxi on

The findings reported by Schmidt-Ehrenberg (1942) in the single human embryo (15 mm.) that she examined are not confirmed.

Some upper limbs studied by Bardeen and Lewis (1901), and by Lewis (1902), were included in the present series. Lewis, who examined embryo no. 43 (horizon xix), stated that all proximal phalanges were chondrifying, except that of the thumb; this finding would place the hand in Senior's stage 6. The present writers, however, found chondrification beginning in the proximal phalanx of the thumb also (Senior's stage 7). From studies of embryo no. 22 (horizon xxi), Bardeen and Lewis, and Lewis, concluded that of the distal phalanges only the thumb was chondrifying (Senior's stage 12). The present authors found chondrification in the distal phalanges of the 2d to 4th digits also, but were uncertain about that of the 5th finger (Senior's stages 13 to 14). It should be kept in mind that Bardeen and Lewis may have used different criteria for the onset of chondrification from those employed in the current study.

Foot

A skeletomuscular condensation is ordinarily not present in the lower limb until horizon xvi, and even then not in all specimens. The femur, tibia, and fibula could not be distinguished as separate blastemal condensations until horizon xvii. Chondrification in these elements begins during horizons xvii and xviii, whereas that in the foot, occasionally noted in horizon xvii, is commonly initiated in horizons xviii to xix.

The sequence of chondrification in the foot confirms that reported by Senior, with few variations; all elements except sesamoids were usually chondrifying by horizon xxiii. Thus, chondrification begins in the various elements of the foot between approximately 5½ and 7 ovulation weeks, in embryos ranging from about 13 to 30 mm. in length.

No clear-cut distinction was found between Senior's stages 1 and 2. Although the navicular usually does not chondrify until stage 6, in several specimens its chondrification preceded that of the medial cuneiform and 1st metatarsal (stage 5); these feet were assigned to stage 4 plus navicular. Such deviations were minor in the light of the over-all regularity in the sequence of chondrification in both hand and foot.

The foot lags behind the hand in development, and, in any given embryo up to horizon xxii, usually 5 to 12 fewer chondrifying centers are found in the foot than in the hand (table 5). Table 4 lists the horizons that correspond to Senior's stages of chondrification in the foot.

Streeter found the degree of development of the humerus to be a valuable aid in staging embryos. The development of other skeletal structures of the limbs likewise follows a definite pattern, and information about them should serve as a further aid in staging embryos. Streeter (1929) had already expressed the hope that the sequence of chondrification worked out by Senior might serve this purpose. Such information about skeletal elements in both upper and lower limbs is summarized in table 6. Table 7 is a more detailed summary of the process of chondrification in the hand and foot.

The tarsus first appears as a common blastemal mass from which digital prolongations extend. As in the hand, it was noted that sometimes the blastema in the area of a tarsal element became more densely cellular just before chondrification began. Haines (1947) reported that in an embryo of 13 mm. each tarsal element was represented by a separate condensation of the blastema, and that by 14 mm. the tarsal elements were chondrified. The planes of section of the embryos in the pres-

TABLE 4

HORIZONS IN WHICH A GIVEN SENIOR'S STAGE OF CHONDRIFICATION IN THE FOOT HAS BEEN FOUND

Senior's stage	Horizons
0	xviii
1	xviii
2	xviii
3	xviii–xix
4	xix–xx
5	xix–xx
6	xix–xx
7	xix–xx
8	xix–xx
9	xix–xxi
10	xxi
11	xxi
12	xxi–xxiii
13	xxiii
14	xxiii on

TABLE 5

THE RANGE OF SENIOR'S STAGES OF THE FOOT USUALLY FOUND FOR A GIVEN SENIOR'S STAGE OF THE HAND UP TO HORIZON XXII

Senior stages of hand	Senior stages of foot
1	0
2	0–2
3	
4	
5	1–3
6	3
7	3–6
8	
9	
10	4–9
11	7–9
12	9
13	9–12
14	

Note: In terms of the total number of chondrifying centers present, the foot has usually 5 to 12 centers less than the hand in any given embryo up to horizon xxii.

TABLE 6

HORIZONS IN WHICH FIRST APPEARANCE OF SKELETAL LIMB ELEMENTS IS USUALLY FOUND

	Condensed mesenchyme	Cartilage	Bone
Humerus	xvi	xvi–xvii	xxi–xxii
Radius	xvi	xvii	xxi–xxiii
Ulna	xvi	xvii–xviii	xxii–xxiii
Hand	xvii	xvii–xxi	In fetus * and after birth
Femur	xvii	xvii–xviii	xxii–xxiii
Patella	xx	xxi	After birth
Tibia	xvii	xvii–xviii	xxii–xxiii
Fibula	xvii	xvii–xviii	In fetus
Foot	xvii–xviii	xviii–xxiii or later	In fetus and after birth

* Intramembranous ossification at the tips of the distal phalanges of the hand may begin in horizon xxiii.

ent series were generally unfavorable for distinguishing the individual tarsal elements during the blastemal phase.

Many investigators have claimed that, during the ontogeny of the limbs, temporary structures of phylogenetic significance are found. In the case of the human foot, some have reported that structures characteristic of lower vertebrates, such as a prehallux, are present during development (Schmidt-Ehrenberg, 1942; Trolle, 1948). The present writers have found nothing to substantiate such claims.

TABLE 7

Horizons in which first appearance of chondrification in skeletal elements of hand and foot is usually found

	Horizons
Carpus except pisiform	xviii–xix
Pisiform	xix–xxi
Metacarpus	xvii–xviii
Proximal phalanges	xviii–xix
Middle phalanges	xix–xx
Distal phalanges	xx–xxi
Tarsus	xviii–xix
Metatarsus	xviii–xix
Proximal phalanges	xx
Middle phalanges	xxi
Distal phalanges	xxi–xxiii

Some lower limbs studied by Bardeen and Lewis (1901), and by Bardeen (1905), were included in the present series. Bardeen and Lewis examined embryo no. 22 (horizon xxi), and stated that all bones of the leg were in the form of cartilage except "that the terminal phalanges of the 3 outer toes have not yet appeared." Bardeen, however, reported that embryo no. 22 was similar to embryo no. 17 (horizon xix), in which only the middle phalanx of the 2d digit was chondrifying. His illustration supports this statement; the feet would thus be assigned to Senior's stages 9 to 10. The present authors found the feet of embryo no. 22 to be in stage 10. Bardeen's findings would place embryo no. 17 in stages 9 to 10 also. The present authors found the feet of this embryo to be in stage 9.

Comparisons based on the investigations of chondrification by Senior and the present authors, and the studies of ossification by Francis and Werle (1939) and Noback and Robertson (1951), indicate that the sequence of chondrification in the hand and foot differs from that of ossification. In the carpus, for example, the hamate and capitate are the first to chondrify and to ossify, but the sequences differ in the other carpal elements. In the tarsus, the cuboid is the first element to chondrify, but the calcaneus and talus are the first to ossify. Of the metacarpals and metatarsals, the 2d to 4th begin to chondrify before the 5th, and the 5th before the 1st. The order is usually the same in diaphyseal ossification. The phalanges of both hand and foot begin to chondrify in proximodistal sequence, whereas the order is distal, proximal, and middle in diaphyseal ossification. Chondrification is present in the carpus before the tarsus; the converse is true of ossification.

SUMMARY

1. Serial sections of the limbs of 103 human embryos, ranging from horizons xv to xxiii inclusive, were examined.
2. The skeleton of the hand was blastemal by horizon xvii, and the various elements began to chondrify between horizons xvii and xxi, i.e. approximately during the 6th ovulation week.
3. The skeleton of the foot was blastemal by horizons xvii to xviii, and the various elements began to chondrify between horizons xviii and xxiii, or later, i.e. from approximately 5½ to 7 ovulation weeks.
4. Chondrification of the various elements of the hand and foot occurred in a definite sequence; Senior's 14 stages were confirmed.
5. Senior's stages of chondrification in the hand and foot were correlated with Streeter's developmental horizons.

LITERATURE CITED

Bardeen, C. R. 1905. Studies of the development of the human skeleton. Amer. Jour. Anat., vol. 4, pp. 265–302.

——— and W. H. Lewis. 1901. The development of the limbs, body-wall and back in man. Amer. Jour. Anat., vol. 1, pp. 1–36.

Baur, G. 1886. Bemerkungen über den "Astragalus" und das "Intermedium tarsi" der Säugethiere. Morphol. Jahrb., vol. 11, pp. 468–483.

Francis, C. C., and P. P. Werle. 1939. The appearance of centers of ossification from birth to 5 years. Amer. Jour. Phys. Anthropol., vol. 24, pp. 273–299.

Gräfenberg, E. 1905. Die Entwickelung der Knochen, Muskeln und Nerven der Hand und der für die Bewegungen der Hand bestimmten Muskeln des Unterarms. Anat. Hefte, vol. 30, pp. 1–154.

Hagen, W. 1900. Die Bildung des Knorpelskeletts beim menschlichen Embryo. Arch. f. Anat. u. Physiol., Anat. Abt., pp. 1–40.

Haines, R. W. 1947. The development of joints. Jour. Anat., vol. 81, pp. 33–55.

Henke, W., and C. Reyher. 1874. Studien über die Entwickelung der Extremitäten des Menschen, insbesondere der Gelenkflächen. Sitzungsb. d. k. Akad. d. Wissensch., Math.-nat., vol. 70, pp. 217–273.

Hesser, C. 1926. Beitrag zur Kenntnis der Gelenkentwicklung beim Menschen. Morphol. Jahrb., vol. 55, pp. 489–567.

Hintzsche, E. 1930. Beitrag zur Entwicklung des menschlichen Fersenbeines. Ztschr. f. mikrosk.-anat. Forsch., vol. 21, pp. 531–551.

Leboucq, H. 1884. Recherches sur la morphologie du carpe chez les mammifères. Arch. de Biol., vol. 5, pp. 35–102.

——— 1886. Sur la morphologie du carpe et du tarse. Anat. Anz., vol. 1, pp. 17–21.

——— 1904. Recherches sur le développement des phalanges terminales des doigts chez l'homme et les mammifères. Ann. soc. méd. de Gand, vol. 84, pp. 227–242.

Lewis, W. H. 1902. The development of the arm in man. Amer. Jour. Anat., vol. 1, pp. 145–184.

Martin, P. 1929. Contribution à l'étude des articulation des membres chez l'embryon humain. Thése. 56 pp. Université de Lausanne.

Noback, C. R., and G. G. Robertson. 1951. Sequences of appearance of ossification centers in the human skeleton during the first 5 prenatal months. Amer. Jour. Anat., vol. 89, pp. 1–28.

O'Rahilly, R., E. Gardner, and D. J. Gray. 1956. The ectodermal thickening and ridge in the limbs of staged human embryos. Jour. Embryol. and Exper. Morphol., vol. 4, pp. 254–264.

——— and D. B. Meyer. 1956. Roentgenographic investigation of the human skeleton during early fetal life. Amer. Jour. Roentgenol., vol. 76, pp. 455–468.

Rosenberg, E. 1876. Ueber die Entwickelung der Wirbelsäule und das Centrale carpi des Menschen. Morphol. Jahrb., vol. 1, pp. 83–197.

Schmidt-Ehrenberg, E. C. 1942. Die Embryogenese des Extremitätenskelettes der Säugetiere. Ein Beitrag zur Frage der Entwicklung der Tetrapodengliedmassen. Inauguraldissertation. 131 pp. Genève.

Schomburg, H. 1900. Untersuchung der Entwicklung der Muskeln und Knochen des menschlichen Fusses an Serienschnitten und Rekonstruktionen und unter Zuhülfenahme makroskopischer Präparation. Dissertation. 61 pp. Göttingen.

Schulin, K. 1879. Ueber die Entwickelung und weitere Ausbildung der Gelenke des menschlichen Körpers. Arch. f. Anat. u. Physiol., Anat. Abt., pp. 240–274.

Senior, H. D. 1929. The chondrification of the human hand and foot skeleton. Anat. Rec., Abstracts, vol. 42, p. 35.

Streeter, G. L. 1929. Chondrification of the hand and foot. Carnegie Inst. Wash. Year Book No. 28, p. 8.

——— 1942. Developmental horizons in human embryos. Description of age group xi, 13 to 20 somites, and age group xii, 21 to 29 somites. Carnegie Inst. Wash. Pub. 541, Contrib. to Embryol., vol. 30, pp. 211–245.

——— 1945. Developmental horizons in human embryos. Description of age group xiii, embryos about 4 or 5 millimeters long, and age group xiv, period of indentation of the lens vesicle. Carnegie Inst. Wash. Pub. 557, Contrib. to Embryol., vol. 31, pp. 27–63.

——— 1948. Developmental horizons in human embryos. Description of age groups xv, xvi, xvii, and xviii, being the third issue of a survey of the Carnegie Collection. Carnegie Inst. Wash. Pub. 575, Contrib. to Embryol., vol. 32, pp. 133–203.

——— 1949. Developmental horizons in human embryos (fourth issue). A review of the histogenesis of cartilage and bone. Carnegie Inst. Wash. Pub. 583, Contrib. to Embryol., vol. 33, pp. 149–167.

——— 1951. Developmental horizons in human embryos. Description of age groups xix, xx, xxi, xxii, and xxiii, being the fifth issue of a survey of the Carnegie Collection. (Prepared for publication by C. H. Heuser and G. W. Corner.) Carnegie Inst. Wash. Pub. 592, Contrib. to Embryol., vol. 34, pp. 165–196.

Trolle, D. 1948. Accessory bones of the human foot; a radiological, histo-embryological, comparative-anatomical, and genetic study. Translated by E. Aagesen. 272 pp. Copenhagen.

Plate 1

Fig. 1. Frontal section of hand of embryo, Carnegie no. 8789, 11.7 mm., horizon xvii. ×56. Senior's stage 1. Blastemal condensations of digits 2 to 5. Radius and ulna are chondrifying. Carpus is blastemal, except very early chondrification in metacarpals 3 and 4, barely suggested in this figure by lighter-staining areas (arrows).

Fig. 2. Frontal section of left hand of embryo, Wayne University no. 15, not included in text because the embryo has not been assigned to a Streeter horizon. ×75. Senior's stage 5. Metacarpals 3 to 5 in the upper part of the figure. Hamate indicated by arrow; capitate and trapezoid to its left; triquetrum just below at its right. Radius and ulna in lower part of figure.

Fig. 3. Sagittal section of right foot of embryo, Wayne University no. 15. ×75. Senior's stage 1 (early). Early chondrification in metatarsal 4 (arrow). A blastemal condensation for the cuboid is visible as a more darkly stained region just below the metatarsal.

Fig. 4. Horizontal section of left foot of embryo, Wayne University no. 15. ×75. Senior's stage 1 (early). Condensations of metatarsals 2 to 4 in upper part of figure (arrow indicates metatarsal 3). Lighter staining, as compared with tarsus (more darkly stained region just below metatarsals), suggests beginning chondrification.

Fig. 5. Horizontal section of left foot of embryo, Wayne University no. 17-2, not included in text because the embryo has not been assigned to a Streeter horizon. ×75. Senior's stage 7. Chondrification in metatarsals 2 to 4. Section includes proximal phalanges 3 and 4. Arrows indicate metatarsal 3 and proximal phalanx 3. Part of marginal vein is present above.

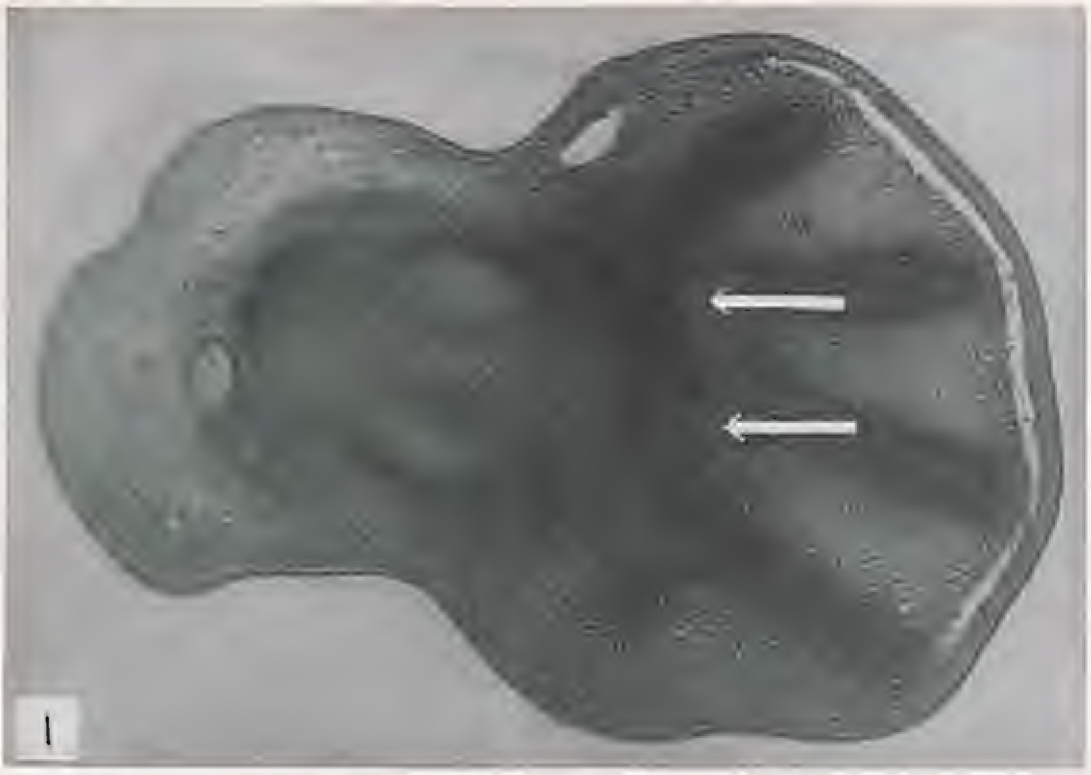

1

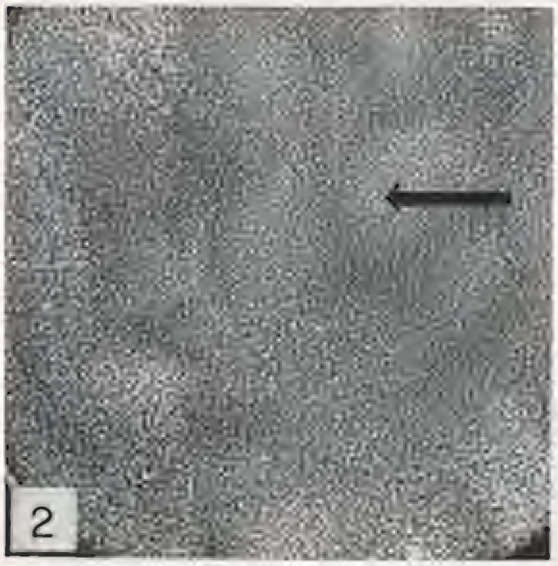

2

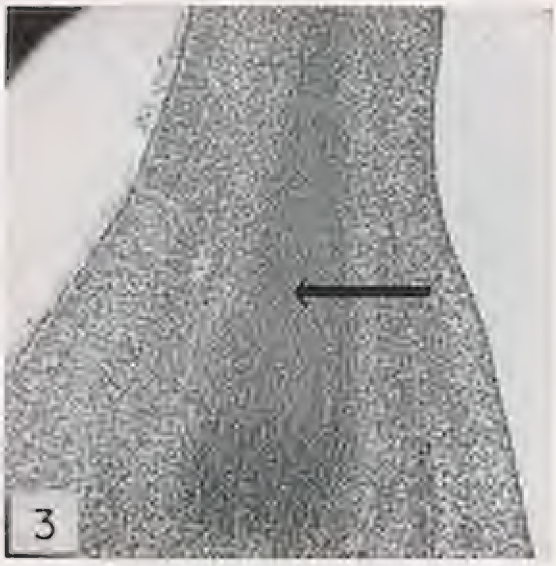

3

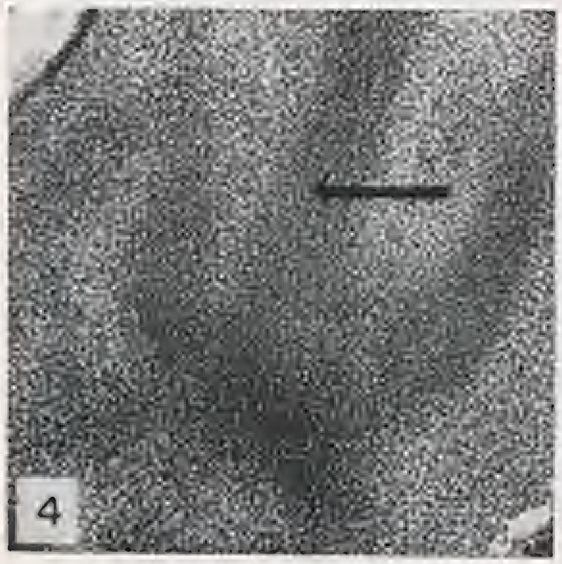

4

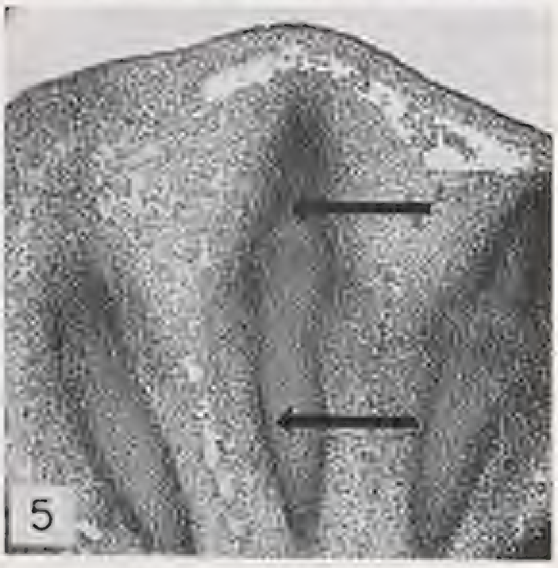

5

CONTRIBUTIONS TO EMBRYOLOGY, NO. 251

THE DEVELOPMENT OF THE ADRENAL GLAND IN MAN, WITH SPECIAL REFERENCE TO ORIGIN AND ULTIMATE LOCATION OF CELL TYPES AND EVIDENCE IN FAVOR OF THE "CELL MIGRATION" THEORY

Roy E. Crowder

Medical Department of the United States Navy, Naval Hospital,
Camp Lejeune, North Carolina

With eight plates and seven text figures

CONTENTS

PAGE

INTRODUCTION 195

DEFINITIONS 195

MATERIALS AND METHODS 196

DEVELOPMENT OF THE ADRENAL CORTEX 197

DEVELOPMENT OF THE ADRENAL MEDULLA 202

DEVELOPMENT OF BLOOD SUPPLY OF THE ADRENAL 203

DISCUSSION 204

- Adrenal Cortex 205
- Adrenal Medulla 206
- Blood Supply 207

SUMMARY AND CONCLUSIONS 208

ACKNOWLEDGMENTS 209

LITERATURE CITED 209

THE DEVELOPMENT OF THE ADRENAL GLAND IN MAN, WITH SPECIAL REFERENCE TO ORIGIN AND ULTIMATE LOCATION OF CELL TYPES AND EVIDENCE IN FAVOR OF THE "CELL MIGRATION" THEORY[1]

INTRODUCTION

A voluminous literature has accumulated on the development of the adrenal gland. In 1902, Josef Wiesel apologized for adding one more article. Others, including the present author, have not been so restrained.

In a study of the sources of certain of the adrenal hormones, a review of the literature on the embryology and histology of the gland was undertaken. In spite of the number of articles published on the subject, including extensive reviews (Parkes, 1945; Lanman, 1953), there was no consecutive life history of the source and ultimate distribution of the various cell types found in the gland, and, therefore, it was not possible to associate the synthesis of the adrenal hormones with specific cell types.

The wealth of closely seriated, well preserved, and adequately stained material available in the Carnegie Embryological Collection, in Baltimore, Maryland, made a complete histologic and embryologic study possible. The study was begun with the idea of determining the types of cells in the adrenal cortex. It was soon found that, to do this adequately, the whole embryologic history must be reviewed. The results of this undertaking are set forth herein. It is hoped not only that they will assist in an understanding of the sequence of events in the histogenesis of the adrenal cortex and clarify a few of the points of controversy, but also that the descriptions of cell types in the cortex may be of value in determining the oligoplasia or hyperplasia of certain of these cell types in relation to many clinical entities.

DEFINITIONS

The following terms are defined to clarify the presentation:

Fetal cortex: The fetal adrenal cortex is composed of the same cell types as the adrenal cortex of the adult human, but the proportions and arrangements differ.

Medullary cells: The cells of neural origin which take up a location in the central portion of the gland during development. The process of localization begins in the embryonic period and continues until childhood.

Cell types: Cell types in the cortex are differentiated by the structure of their nuclei; they are numbered according to the order of their appearance in the primordium, as C-I (fig. 38, pl. 8), C-II (fig. 39, pl. 8), and C-III (fig. 40, pl. 8). As will be made clear, three distinct cell types may be recognized in the development of the medulla; these cells, designated M-I, M-II, and M-III, are described beginning on page 202.

Celomic epithelial cells: The cells of the adrenal cortex which have their origin in the celomic epithelium. They are of two types: Type C-I (fig. 38, pl. 8), the first cells to enter the primordium, are large polyhedral cells, each of which contains a large round nucleus with little chromatin, a large round nucleolus, and a spherical, refractile inclusion. In a later stage, type C-III cells (fig. 40, pl. 8) begin to emerge from the celomic epithelium, together with type C-I. Type C-III cells are smaller than type C-I, and each contains a smaller round nucleus which stains more deeply with hematoxylin. In the nucleus, there is a large amount of chromatin, which tends to aggregate into four to five major clumps and one or two globules or vacuoles.

Cells of mesonephric origin: These cells arise from Bowman's capsule of the mesonephros. They are designated as type C-II cells (fig. 39, pl. 8), and are first seen streaming from the glomerular capsule across the ventral portion of the early primordium (figs. 14, 15, pl. 2). The type C-II cells and their successors form most of the adrenal capsule, and, during horizon xxiii, are diverted inward by the arteriolar capillaries. Thereafter, they are found in the cords of cells within the cortex. Their nucleus is round, and stains a little more deeply than does that of type C-I. The chromatin is distributed in fine strands in a spider-like manner just beneath the nuclear membranes, the nucleolus corresponding to the body of the spider. The center of the nucleus is occupied by one or more large globules or vacuoles.

Immigration and migration: The passage of cells from one region to another; the addition of cells by movement from an adjacent region. Ameboid movement is not implied.

Invasion: The entrance of cells after destruction or disruption of pre-existing tissue, and the assumption of position without reference to former relations.

Staging of embryos: The dating of the embryos follows the horizons described and graphed by Streeter (1951). This method of seriation affords a much better concept of the progress of development than does measurement of the length. Frequently, the organogenesis of the adrenal gland was found to be in a much further advanced stage in an embryo with a shorter crown-rump length than in a longer one, particularly in the earlier stages when the dorsal curvature varies so remarkably among embryos in the same horizon. This finding speaks well for the method, since Streeter did not use the adrenal among his criteria for staging. The age in weeks is the estimated conception age. To obtain menstrual age, two weeks must be added. There are enough stages to provide a consecutive account of the organogenesis of the adrenal.

---

[1] The ideas herein expressed are those of the author and do not reflect those of the United States Navy.

MATERIALS AND METHODS

The following embryos of the Carnegie Collection were selected for the study of the embryonic and early fetal development of the adrenal gland.

Serial no.	Crown-rump length (mm.)	Plane of section	Histologic condition	Stain
		Horizon XIII		
836	4.0	Trans.	Exc.	Al. coch.
7433	5.2	Frontal	Exc.	H.-E.
8066	5.3	Trans.	Exc.	H.-E.
8119	5.3	Trans.	Exc.	H.-E.
		Horizon XIV		
3805	5.9	Trans.	Exc.	H.-E.
6502	6.7	Trans.	Exc.	H.-E.
7324	6.6	Trans.	Good	H.-E.
7829	7.0	Trans.	Exc.	H.-E.
7870	7.2	Trans.	Exc.	H.-E.
8314	8.2	Trans.	Exc.	Azan
		Horizon XV		
2	7.0	Trans.	Good	Al. carm.
721	9.0	Trans.	Exc.	H.-E.
3385	8.3	Trans.	Exc.	H.-E. or G.
3441	8.0	Sag.	Exc.	Al. coch.
3512	8.5	Trans.	Exc.	Al. coch.
6504	7.5	Sag.	Exc.	Al. coch.
6508	7.3	Trans.	Good	Al. coch.
6595	8.0	Sag.	Good	H.-E.
7199	8.4	Frontal	Good	Al. coch. phloxine
7364	9.5	Frontal	Poor	H.-E.
8929	6.3	Frontal	Exc.	Azan
8997	9.0	Trans.	Exc.	Azan
9140	7.0	Trans.	Exc.	Azan
		Horizon XVI		
792	8.0	Trans.	Good	Al. coch.
6511	8.1	Sag.	Good	Al. coch. iron H.
6512	7.0	Trans.	Exc.	Al. coch.
6517	10.5	Trans.	Exc.	Al. coch.
7115	9.7	Frontal	Exc.	H. and phloxine
7804	9.5	Trans.	Good	H.-E.
7897	12.2	Trans.	Good	H.-E.
8773	11.0	Frontal	Exc.	Azan
		Horizon XVII		
940	14.0	Trans.	Good	H.-E. or G.
5893	13.2	Trans.	Good	Al. coch.
6258	14.0	Trans.	Good	H.-E.
6519	10.8	Sag.	Exc.	Al. coch.
6520	14.2	Trans.	Exc.	Al. coch.
6742	11.0	Trans.	Good	H.-phloxine
6758	12.8	Trans.	Good	H.-phloxine
8101	13.0	Trans.	Exc.	H.-E.
8118	12.6	Frontal	Exc.	H.-E.
8789	11.7	Sag.	Exc.	Azan
8998	11.0	Frontal	Exc.	Azan
		Horizon XVIII		
492	16.8	Frontal	Exc.	Al. coch.
1909	14.6	Frontal	Good	Al. coch. or G.
4430	14.0	Trans.	Exc.	Al. coch. or G.
6524	11.7	Trans.	Exc.	Al. coch.
6525	13.8	Sag.	Exc.	Al. coch.
6527	14.4	Trans.	Exc.	Al. coch.
6528	13.4	Frontal	Exc.	Al. coch.
7707	14.5	Trans.	Exc.	H.-E. phloxine
8172	16.5	Trans.	Exc.	H.-E.
8812	12.2	Trans.	Exc.	H.-E.
9247	15.0	Sag.	Exc.	Azan
		Horizon XIX		
4405	15.5	Trans.	Good	Coch. Mallory
4501	18.0	Trans.	Exc.	Coch. or G.
5609	18.0	Frontal	Exc.	Al. coch.
6150	17.0	Trans.	Good	H.-E.
6824	18.5	Sag.	Good	H.-E.
8092	16.3	Trans.	Exc.	H.-E. phloxine
9113	18.5	Trans.	Exc.	Azan
		Horizon XX		
966	23.0	Frontal	Exc.	Al. coch.
5537	22.0	Trans.	Exc.	Al. coch.
6202	21.0	Sag.	Exc.	H.-E.
7274	18.3	Trans.	Exc.	H.-E. phloxine
7906	19.5	Frontal	Exc.	H.-E.
8226	18.0	Sag.	Exc.	Azan
		Horizon XXI		
5596	21.5	Sag.	Good	H.-E.
7254	22.5	Trans.	Exc.	H.-E.
7392	22.7	Trans.	Exc.	H.-E.
7864	24.0	Frontal	Exc.	H.-E.
8553	22.0	Trans.	Exc.	H.-E.
		Horizon XXII		
1458	27.5	Sag.	Exc.	H.-E. or G.
4304	25.0	Trans.	Good	H.-E.
4638	23.4	Trans.	Exc.	Al. coch.
6701	24.0	Frontal	Poor	H.-E.
6832	25.8	Frontal	Exc.	H.-E.
8394	25.3	Trans.	Exc.	H.-E.
		Horizon XXIII		
4205	29.5	Trans.	Good	Al. coch.
4289	32.2	Trans.	Good	Al. coch.
4570	30.7	Trans.	Exc.	H.-E.
5422	27.0	Sag.	Good	H.-E.
5621A	27.5	Trans.	Good	H.-E.
6573	31.5	Trans.	Good	H.-E.
6719	30.1	Trans.	Good	Chrom. alum hem.
7425	27.0	Frontal	Exc.	Chrom. alum hem.
9226	30.1	Trans.	Exc.	Azan

Serial no.	Crown-rump length (mm.)	Plane of section	Histologic condition	Stain
Fetal				
3105......	34.0	Trans.	Good Broken sections	Chrom. alum hem.
5762......	34.0	Trans.	Good	H.-E.
4415......	37.0	Trans.	Poor	H.-E.
6658......	40.0	Trans.	Exc.	H.-E.
301......	44.0	Trans.	Poor	H.-E.
6694......	44.0	Trans.	Exc.	H.-E.
84......	54.0	Trans.	Fair	H.-E.
172......	80.0	Trans.	Good	H.-E.

In addition to the materials listed, a number of glands from late embryos and fetuses (100-mm. crown-rump length upwards) and newborn children, through the first month of postnatal life, were collected by the author, fixed in Bouin's fluid, and stained by various means, including hematoxylin and eosin, Mallory-azan, and chrome alum hematoxylin counterstained with phloxine or Mallory trichrome in which the aniline blue was replaced with light green SF, C. I. No. 670. Portions of some of the glands were fixed in Bouin's and then placed in a saturated solution of potassium dichromate at 37° C. for 72 hours, after fixation, to preserve the lipids, according to the method suggested by Thomas (1948) for spheroid bodies in nerve cells. Frozen sections were prepared and stained for lipids with Sudan III, as were some of the post-chromated sections.

Adrenals of children and adults were selected from the pathology collections in the United States Naval Hospitals in St. Albans, New York, and Camp Lejeune, North Carolina. All were fixed in neutral formalin and stained with hematoxylin and eosin or hematoxylin and phloxine.

Adrenal glands in the macaque embryos in the Carnegie Collection were examined, as were glands from adult cats, hamsters, and guinea pigs, to see whether cell types in the human were species specific.

DEVELOPMENT OF THE ADRENAL CORTEX

The adrenal primordium is first recognizable in embryos early in horizon xv (fig. 1; fig. 8, pl. 1). A change in the characteristics of the cells of the celomic epithelium over the area between the gastric mesentery and the lateral extremity of the mesonephros can be seen late in horizon xiv, but not until horizon xv is a new type of cell (type C-I) found in the mesenchyme dorsal to the epithelium in this region. It can be traced by continuity of cords from the celomic epithelium (fig. 10, pl. 1). The portion of the celomic epithelium medial to the mesonephros produces cells destined for the adrenal cortex, whereas the region ventral to the mesonephros produces cells destined for the gonad. In the earliest stages, cells from the two areas are morphologically similar.

Mitotic figures are seen in profusion in the celomic epithelium, and cells in various stages of differentiation are present immediately dorsal to it. The orientation of the mitoses is such that one daughter cell is seen in the developing primordium while the other remains in the epithelium. It is suggested that, in this manner, as cells are formed, the epithelium moves ventrally, leaving columns of cells in the primordium (figs. 9, 10, pl. 1).

In the epithelium, the cells, which are cuboidal to low columnar, are crowded together. The chromatin of the nuclei is fairly dense, and there is little cytoplasm. As the cells move into the adrenal (and the gonadal) area, they increase in size and assume the form of large polyhedral epithelioid elements with light-colored, eosinophilic cytoplasm. The nucleus also enlarges; it becomes spheroidal, with a relatively small amount of chromatin loosely arranged in fine strands and small knots. The nucleolus is somewhat eccentrically placed, and the center of the nucleus is occupied by a large spherical refractile body which displaces about one-tenth of the nuclear volume (fig. 10, pl. 1; fig. 38, pl. 8).

In horizon xv, a change appears in the characteristics of the cells in the medial wall of the capsule of the mesonephric glomerulus (fig. 2; fig. 11, pl. 1; fig. 12, pl. 2). Until this time, the cells of Bowman's capsule are large and squamous, having biconvex nuclei. As the new cells (type C-II; fig. 23, pl. 4) are produced, they are columnar, with their long axes at right angles to the capsular surface. In figure 13 (pl. 2), some of these cells have already migrated into the adrenal primordium. During horizon xvi, there is an enormous immigration of cells originally derived from Bowman's capsule. For the most part, they leave the medial surface of the glomerular capsule and pass medially just beneath the celomic epithelium as a layer four or five cells deep (fig. 3; figs. 14, 15, pl. 2). Toward the dorsal portion of the medial surface of the actively proliferating Bowman's capsule, near the hilum of the glomerulus, are located cells which send their progeny into the dorsolateral part of the primordium. At first, these cells are comparatively few, but they form a nidus which sends forth a great shower of cells to the adrenal and the gonad in horizon xviii (figs. 22, 23, pl. 4).

The cytoplasm of these type C-II cells is inconspicuous in horizon xvi. The nuclei, however, are distinctive, for they are long ellipsoids. The chromatin is scanty and is distributed in very fine strands that weave a coarse, netlike pattern beneath and close to the nuclear membrane. Where the strands intersect, there are small knots. A few of the strands touch the nucleolus, which is an irregular, small, flat mass lying in contact with the nuclear membrane, usually near the middle of the long axis. The nucleus is translucent. Its center is occupied by one or two ellipsoid globules or vacuoles. Figure 39 (pl. 8) shows a type C-II cell in the cortical cords of an embryo in horizon xxiii.

In horizon xvi, also, the first evidence of a change in the cell types in the celomic epithelium is seen. Cell type C-I is still present and continues to multiply in the celomic epithelium, together with another cell type having a smaller, darker nucleus, type C-III of the adrenal cortex (fig. 40, pl. 8). The cells emerge and enter the gland primordium in columns in juxtaposition to, but discrete from, the type C-I cell columns. The difference between the two types can be seen clearly after they enter the primordium. The new cell is smaller; its nucleus is three-fifths to three-fourths the size of the nucleus of type C-I. The chromatin appears clotted. There are four to five fairly large clumps of deeply staining basophilic material connected by ragged strands. The nucleolus is erratically placed and rarely central. As a rule, two or more small globules or vacuoles can be made out in the center of the nucleus. The cytoplasm is more basophilic than in types C-I or C-II.

From the first appearance of the primordium until well into horizon xviii, mitotic figures are seen in the central portion of the gland. Most of these mitoses are in blood cells, others in the capillary endothelium, but some are in cells of types C-I or C-III. As far as can be seen, type C-II cells do not enter the body of the gland until horizon xxiii.

In horizon xvi, nerve tissue in and around the sympathetic ganglion begins to grow and extend, passing ventrally between the gland and the aorta along the caudal third to half of the gland. Cells of neural origin have already begun to migrate into the gland, disrupting its more or less homogeneous pattern (fig. 3). The neural elements tend to pass between the cells of the primordium, separating them into islands rather than destroying them (fig. 4; fig. 15, pl. 2).

During horizon xvii, the first neural migration is at its height. This period is marked by the development of the great para-aortic complex of nervous tissue that eventually forms the abdominal plexuses. The growth is extensive; most of the tissues in the path of the invading nerves are penetrated. In the adrenal area, nerve fibers, accompanied by large "paraganglion" (type M-III, to be discussed later) cells, pass into the cortical primordium (fig. 15, pl. 2). As a result, by the end of the horizon, the cortical cells are divided into clusters or islands in the dorsal part of the gland. The structure of the ventrolateral portion of the gland, however, is not disturbed by the invading nerves. In this area, the cells streaming medially from Bowman's capsule appear to act as a barrier to further progress of the nerves (fig. 18, pl. 3). The line of demarcation is striking. The celomic epithelium, which is still actively proliferating, and the layer of mesonephric cells are left undisturbed. This is the stage in which Keene and Hewer (1927) postulated a "permanent cortex" (figs. 17, 18, pl. 3). As will be seen in this horizon and in horizons xviii and xix, the pause is merely a temporary interruption in the migration of cells from the celomic epithelium directly into the primordium in certain areas.

The caudal end is the first portion of the cortex disturbed by the neural migration. All levels have been involved by the end of horizon xvii. The neural elements increase the volume of the primordium in the human embryo, so that a cross section late in horizon xvii is more than 2½ times the area at a similar level at the end of the previous horizon. Throughout the remainder of the fetal period, the cortical cells increase in number at a steady and rapid rate, whereas the neural elements have periods of relative quiescence and periods of rapid growth. During the growth periods, the relation of the cortical cells to the nerve cells may be altered by the relative volume of the two elements (figs. 6, 7; figs. 16, 17, pl. 3; fig. 28, pl. 5). The nerve fibers and neuroblasts are not seen in the body of the gland until horizon xxiii, except in those areas where they are entering the gland or where they are destined to become definitive nerves. From evidence found in later stages, it appears that the distinctive cells (M-III) destined for the medulla are derived from the large cells that accompany the sympathetic nerves during the primary immigration in horizons

---

Figures 1 to 5, drawn to the same scale, × 100, illustrate the relative size of the adrenal in horizons xiv to xvii, compared with surrounding structures. Figures 6 and 7 represent the disruption of the cortex by the neural elements in horizon xxiii.

Fig. 1. Earliest evidence of adrenal primordium and change in character of cells in celomic epithelium over adrenal and gonadal areas.

Fig. 2. Genital and adrenal ridges are formed, with adrenal groove separating them. The two groups of cells in the medial wall of Bowman's capsule have differentiated preliminary to migration shown in figure 3. Active proliferation in the sympathetic ganglion is beginning.

Fig. 3. Active migration of cells from Bowman's capsule. Beginning invasion of primordium by sympathetic neural elements.

Fig. 4. Massive growth of sympathetic elements. So-called "permanent" cortex. Cell types C-I, C-II, C-III are present in it.

Fig. 5. Height of sympathetic invasion. Cortex pattern is disrupted by sympathetic elements. Rim of cortex is still intact along the celomic border. Cells from Bowman's capsule and celomic epithelium are still being added to the primordium. Islands of cortical cells are scattered among the neural elements.

Fig. 6. Conditions near the caudal pole of the adrenal at the beginning of the second impetus to growth of sympathetic nerve elements. Much of the cortex is displaced. No capsule is yet formed in this area.

Fig. 7. Condition of the gland when proliferation of sympathetic neural elements is most active. The cortical cords are pushed aside to make room for the nerves and chromaffin elements. The retiform pattern of the sympathetic is well illustrated.

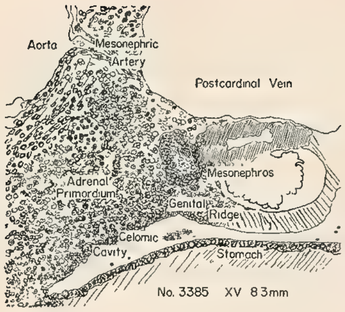

FIG. 1

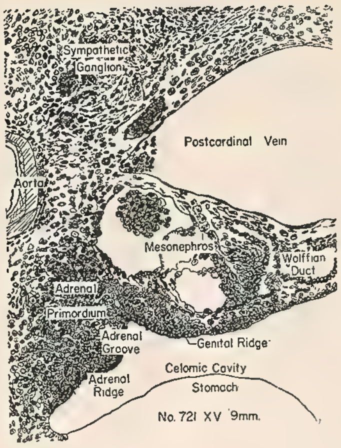

FIG. 2

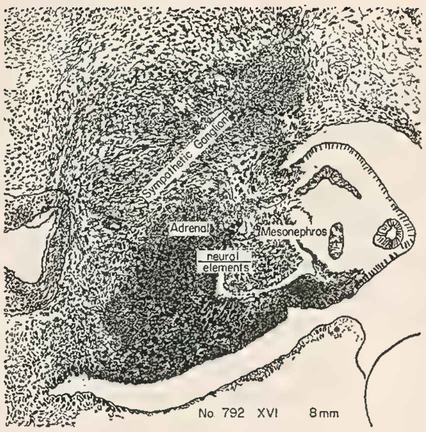

FIG. 3

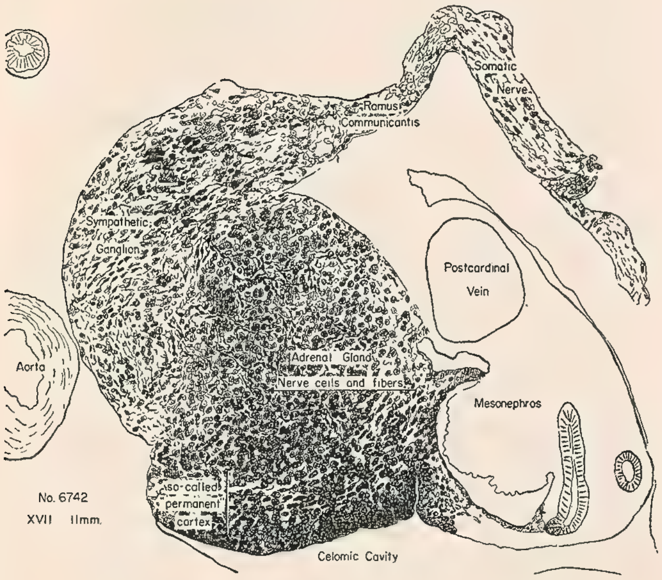

FIG. 4

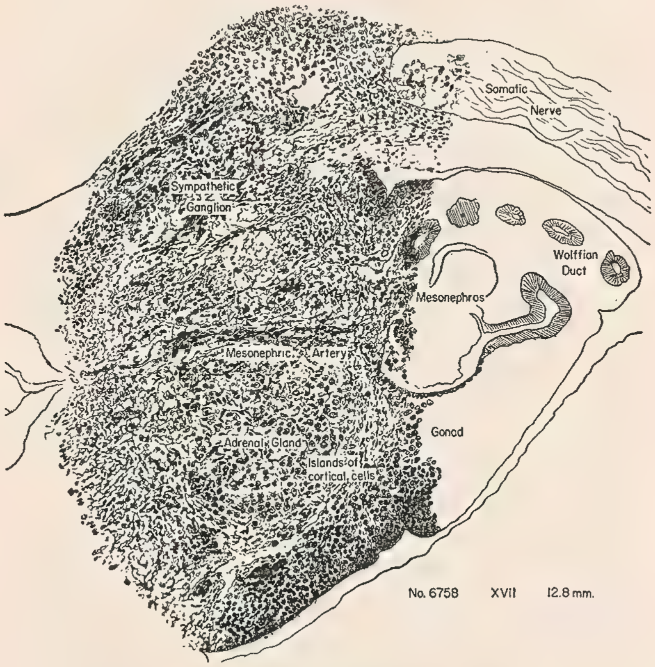

FIG. 5

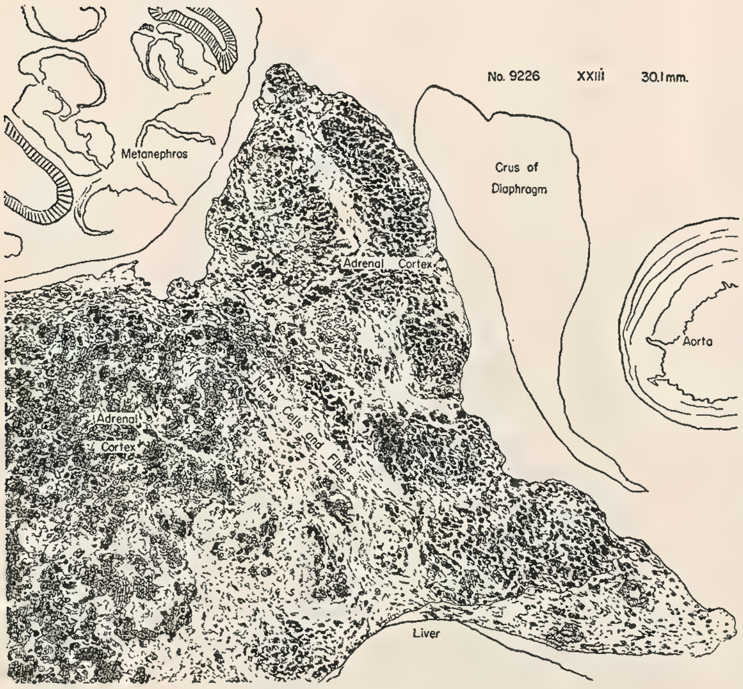

FIG. 6

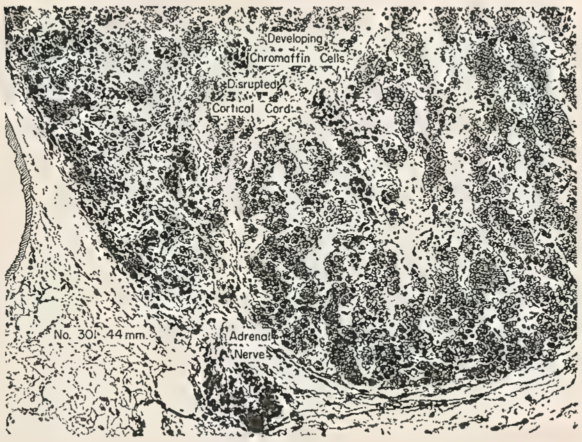

FIG. 7

xvi and xvii (see "Development of the Adrenal Medulla," below).

From horizon xix until horizon xxii, and particularly during xxiii, the character of the cytoplasm of the cortical cells differs only slightly in the peripheral and central zones of the gland. The cells are more densely packed in the outer zone of the gland, where there are fewer capillaries than in the center. Cells similar in all respects to types C-I and C-III, formerly found in the celomic epithelium, are closely packed just central to the capsule, which is composed of type C-II cells. More centrally, they are expanded into the three cortical cell types and are grouped into cords of varying thickness by the sinusoids (fig. 25, pl. 5). The cord formation started in horizon xviii with the beginning growth of the sinusoids. At first, there are only a few thick cords near the center of the gland. As the sinusoids increase in number and ramify toward the periphery of the gland, the thickness of the cords is reduced; i.e., the number of cell columns per cord diminishes. The gland continues to expand peripherally, and the type C-I and type C-III cells are found in the cords, supported by the endothelium of the sinusoids.

The characteristics of the cells of the adrenal groove do not seem to differ at any time during its existence from the cells in other parts of the celomic epithelium which pass into the adrenals and gonads (fig. 22, pl. 4).

The type C-II cells from the nidus (figs. 22, 23, pl. 4) are identical with those that came from Bowman's capsule during horizons xvi and xvii, described above. During horizon xix, these cells come to lie on the surface of the gland on all sides, forming the capsule of the gland. Where its surface is in contact with the celomic cavity, the capsule assumes a position in direct contact with the peritoneum, either by migrating there or as a result of migration of the epithelial cells inward, leaving the mesonephric cells to take their place. The former seems more likely, since many groups of cells of types C-I and C-III are found outside the capsule as accessory adrenals. Also, in figure 23 (pl. 4), the cells from the nidus are seen to be migrating between the cells in the celomic epithelium.

By horizon xx, the layer of cells of type C-II is found around the periphery of the gland as a loosely organized capsule (fig. 25, pl. 5). During horizons xxi and xxii (fig. 26, pl. 5), the capsule becomes better organized and is covered with a layer of fibrous tissue, and arteries appear over the surface. The celomic surface is now covered by peritoneum. With further development of the fetus and growth in the perirenal area, the gland soon becomes completely separated from the peritoneum.

During horizon xviii, the cortical elements are restored to order (fig. 24, pl. 5), and the succession of events proceeds. The reorganization of the gland is brought about early in the horizon by a rapid migration of cells from the celomic epithelium and multiplication of the cells in the islands and around the periphery of the gland. Since most mitoses are at or near the surface, the gland grows centrifugally; i.e., as cells form they remain in place, enlarging and differentiating, and new ones are added at the surface. The gland is not yet separated from the celomic epithelium except caudally. In the caudal region, it expands retroperitoneally on the left late in horizon xvii; on the right, it expands dorsal to the liver. Cells continue to proliferate from the celomic epithelium until, in horizon xix, the gland is separated from it by the spreading type C-II cells.

The separation begins in horizon xviii. When the nidus formed by cells from the dorsal portion of the mesonephric glomerular capsule during horizon xvi and early xvii (fig. 22, pl. 4) springs into activity, the cells from this source spread around the periphery of the gland, some dorsally but most ventrally. Those passing ventrally are split by the prominent adrenal groove, part going to the adrenal and part to the gonad.

In horizon xxiii, the capsule, which is now completely formed, is penetrated in many areas by arterial capillaries which join the sinusoids. Where they enter, the capsule appears to be invaginated, so that the surface of an enlarged model of the gland would have a cobblestone appearance (fig. 27, pl. 5).

The glomerular zone is now formed (fig. 27, pl. 5). It is composed of nests of types C-I and C-III cells, similar in all respects to their ancestors in the celomic epithelium during the embryonic period, held in place by the canopies of capsular (type C-II) cells between the penetrating arterial capillaries. The cells of types C-I and C-III in the glomeruli are closely packed, with little cytoplasm and with compact nuclei. The number of each cell type varies widely from one glomerulus to another, the distribution apparently depending on the random location of the two types in the periphery of the gland when the glomeruli were formed in horizon xxiii. The nuclei of the C-II type cells in the capsule, which changed from plump, translucent ellipsoids to compact spindle shape during horizon xxi, resemble nuclei of fibrous connective tissue. If embryos of the transitional period had not been available, the identity of these cells would have been lost.

As new cells of types C-I and C-III are formed in the glomeruli, they migrate, or are forced by the *vis a tergo* of multiplying cells, toward the center of the gland in cords between the capillary tributaries of the sinusoids. During the exit from the glomerulus, they are joined by the type C-II cells from the capsule, which are maturing and moving from the surface toward the center of the gland on the surface of the cords and along the arterial capillaries and sinusoids (fig. 27, pl. 5; fig. 36, pl. 8). All three types of cortical cells are now found in the cell cords in a more or less random pattern. Where the cords are straight enough, however, it is possible to see each type of cell in a chainlike arrangement side by side with one or both other types of cells. By the time the fetus is 40 mm. in crown-rump length, the cells of type C-II are as numerous as those of the other types and are found in proportionate numbers in relation to them and well down the length of the cords.

At about 35-mm. crown-rump length, the cytoplasm of all cells in the central region of the gland becomes finely granular and markedly eosinophilic, and some of the cells near the large venous channels in the center seem to be vacuolated.

Between horizon xx and 50-mm. crown-rump length, the gland develops a pyramidal form with an overhanging lip on the medioanterior border because of the adjustment to the enlarging metanephros posterolaterally. During the next 10 to 15 mm. of growth, the adrenal vein and its three tributaries are formed (see "Development of Blood Supply of the Adrenal"). At the same time, the cords of cells from the periphery of the gland appear to disintegrate in the central portion (figs. 32–34, pl. 7). After this disintegration, the walls of the gland begin to collapse around the veins. The collapse is not complete, however, since the cells in the glomerular zone are still multiplying rapidly and going into the cords. The growth is about the same on all sides; therefore, the cords from the periphery to the three tributary veins are approximately equal in length. The gland then assumes a trilobate form, with a vein as the axis of each arm. Under normal conditions, there is little folding of the capsule during fetal life such as is found after the first postnatal month. The rapid replacement of the cells in the cords during fetal life keeps the gland plump and the capsule relatively smooth.

When the cells emerge from the glomerular zone into the cords, and the cytoplasm expands, they assume polyhedral shapes, owing to their compaction. In the peripheral portion of the fasciculoreticular zone, there are six to twelve or even more cells in a cross section of a cord. The cytoplasm has a lightly homogeneous basophilic appearance.

As the cells progress farther toward the center of the gland, the cytoplasm of some cells, without reference to type, becomes acidophilic and then granular. Inclusions in the cytoplasm of most of the cells will now stain with Sudan III. Next, each such cell swells to two to three times its previous size, rounds out, and crowds its neighbors. The nucleus, in the meantime, also enlarges; the globules within it increase in size and break up into numerous smaller ones. Finally, the parts of the nucleoplasm appear to undergo autolysis, and the nuclear membrane gives way, spilling its contents into the cytoplasm. The cell in turn collapses and disintegrates, and the intracellular material disappears. The surrounding cells close in and fill the space, narrowing the cord by that much, so that the volume of all of the cords is constantly being reduced. Many of the cells retain their homogeneous appearance well down the cord, but the vast majority disintegrate, as described above.

It is not in one cell, in a cord, or at any one level that the process goes on, but in many cells at all levels of the cords at the same time. Thus, in the central part of the gland there is considerable variation in the appearance of the cords. In the fetal gland, the whole of the central part of the gland has a light, mottled appearance because of the contrast between the "light" cells, which are actively maturing and disintegrating, and the "dark" cells, which have not yet begun to disintegrate.

Many of the cells in the adult gland approach the center of the gland in cords one or two cells thick. The support for these cords is slight, either from neighboring cords or from the sinusoid walls. The cords become erratic in their direction, and form a much more reticular pattern here than farther toward the periphery. Any one or all cell types may be found in these attenuated cords.

The presence of fascicular and reticular zones, per se, during fetal life, is not a normal condition. The one exception is at the 50- to 60-mm. stage, just previous to the degeneration of the central portion of the gland during the formation of the central veins, when there may be an ill-defined fascicular zone. After 75 mm., the growth of the gland is very rapid in a limited space, and the cords take an erratic course and have a reticular appearance regardless of the plane in which the gland is sectioned. The rapid destruction of cells in the cortex, as described above, leaves few cords intact to reach the veins, and, furthermore, since the medulla, with its interstices between the groups of chromaffin cells, has not yet been formed, there is no place for the residual cords to grow to form a reticular zone. For these reasons, the whole central portion of the gland can be designated the fasciculoreticular zone. It is this portion of the fetal gland that is now, by general usage, called the *fetal cortex*. Because it degenerates beginning immediately after birth and is eventually replaced by the fascicular and reticular zones and the medulla, the term is acceptable, particularly because of its long usage in the literature, provided that it is understood that the "fetal cortex" is composed of cells derived from the same sources as the "permanent cortex."

Beginning a few hours after birth, degenerative changes and marked hyperemia are present in the fasciculoreticular zone. By the end of a week or 10 days, there is almost complete disorganization of the cortical elements central to a relatively wide band of basophilic cells, which includes the capsule and glomerular zone. The gland has shrunk in size to compensate for its loss of substance. By 4 to 6 weeks, the shrinking is almost completed.

The components of the chromaffin system, which had been distributed throughout the fasciculoreticular zone in a retiform manner during fetal life, have become concentrated about the central veins; they will be described under "Development of the Adrenal Medulla."

The histologic description of the postnatal degeneration of the fasciculoreticular zone was presented by Kern (1911), and has been confirmed by the author. Morphologic and volumetric changes have been elucidated by Lewis and Pappenheimer (1916), Scammon (1925–1926), Keene and Hewer (1927), Benner (1940), and Hunter (1954).

The fascicular and reticular zones of the postnatal gland develop from cells in the capsule and glomerular zone during the regenerative period. When the fascicular zone is formed, not all the cells in its cords disintegrate during their passage from the glomerular zone; attenuated cords one to two cells thick continue on into the interstices between the nests of chromaffin cells around the veins. These attenuated cords form the reticular zone. Surrounding the medulla there is an area in which the cords become tortuous, and the intervening spaces are filled with large blood sinuses. The reticular zone becomes a constant, although a rather poorly organized, feature of the adrenal during the second year of life, and assumes its permanent characteristics by the end of the twelfth year.

In the adult gland, the cells of the fascicular zone and the peripheral part of the reticular zone degenerate by swelling and disintegration. A few of the cells in the cords in the terminal portion of the reticular zone may also degenerate. In general, the cells in the reticular zone have a homogeneous or finely granular cytoplasm similar to that of the cells in the outermost fascicular zone. They may even have a hyalinized appearance. In older individuals, some of the cells near the veins contain brown pigment, the nature of which has not been established to the author's satisfaction. The usual fate of the cells in the adult reticular zone is a characteristic shrinking of the cell, pycnosis of the nucleus, and phagocytosis of the remains. Except as stated above, these conditions are not found in a normal fetal gland.

DEVELOPMENT OF THE ADRENAL MEDULLA

The development of the adrenal medulla has been the subject of much controversy since the beginning of the century. Wiesel (1902) and Zuckerkandl (1912) have given the classic descriptions. The findings of the present study are consistent with the descriptions by those authors, but a few additional observations may be helpful for a further understanding of the developmental process.

During horizon xiv, the paravertebral sympathetic ganglia begin to increase in size as a result of cell division and the addition of nerve fibers from the rami communicantes. At this stage, there are three types of cells in the ganglia, as differentiated by the character of the nuclei. One type of cell, M-I, is small, with a small, round, compact nucleus, and tends to be located at the periphery of the ganglion. In a second type of cell, M-II, which is not illustrated, the nucleus is larger, and the chromatin is decidedly basophilic and coarsely clumped. A few of these cells have a teardrop nucleus and may have developing axonal processes. A third type of cell, M-III (*E*, fig. 37, pl. 8), has a large ellipsoid nucleus. The chromatin is scanty, and is evenly distributed in fine particles. The nucleoplasm has a pale lilac tint when stained with Mallory-azan, a characteristic of these cells until they mature into chromaffin cells. They are the "sympathetic formative cells" of Wiesel (1902), the "parasympathetic cells" of Zuckerkandl (1912).

During horizons xv and early xvi, all types of cells increase in number. Mitoses are present in the ganglia, markedly increasing in horizon xvi. Late in horizon xvi, nerve fibers begin to appear ventrally and laterally from the ganglia, accompanied by the M-I and M-III cells. The M-I cells are arranged around the nerve fibers; the M-III are sparsely scattered among the fibers. The M-II cells remain in the ganglia and become the sympathetic ganglion cells. The nuclei of the M-I cells change their shape from spherical to compact ellipsoid when they leave the ganglia.

During horizons xv through xviii, the adrenal primordium is a cigar-shaped structure extending from the 6th thoracic to the 1st lumbar segment, lateral to the aorta and mesogastrium. The bundles of nerve fibers and cells, which pass laterally, enter the adrenal primordium as finger-like processes and pass between the future cortical cells, splitting them into islands (figs. 3–5; fig. 15, pl. 2; figs. 16–18, pl. 3). The nerves leaving the ganglia tend to pass caudally and ventrally before branching laterally into the adrenal primordium. As a result, relatively few processes enter the cephalic pole of the primordium; a larger number enter the caudal pole, owing to the presence of the 11th and 12th ganglionic nerve fibers. Most of the nerve fibers and their accompanying cells, from ganglia 6 to 10, take a ventrocaudal course along the lateral side of the aorta, between it and the adrenal primordium, and eventually become the splanchnic nerves. The splanchnic nerves, combined with the fibers from the 11th and 12th ganglia, form a relatively huge mass in the caudal end of the adrenal primordium.

By the end of horizon xvii, the neural tissue has invaded the gland in such quantity that the volume of the adrenal primordium has been greatly increased. In the caudal half of the gland, the cross-sectional area is more than twice that in the previous horizon (figs. 16, 17, pl. 3; also p. 198), whereas the cephalic end is only slightly enlarged. The whole plexiform complex is derived from the 6th to the 12th thoracic and usually the 1st lumbar paravertebral sympathetic ganglia. Included in it are the primordia of the celiac, the superior mesenteric, and the renal plexuses, as well as the adrenal medulla.

There is a quiescent period during horizons xviii through xxii in which the increase in cells and nerve fibers is limited principally to the definitive nerves. Between the aorta and the adrenal, the splanchnic nerves are beginning to take form.

During horizon xxiii and continuing through embryos of 50- to 60-mm. crown-rump length, there is a very rapid multiplication of the M-III cells that accompanied the nerve fibers during the initial neural growth in horizons xvi and xvii. These paraganglion cells, as they are called in the literature, are scattered like seeds along the course of the nerve tracts. At first, and continuing until about 80-mm. crown-rump length, they multiply as embryonic cells, but, from 30-mm. crown-rump length until birth, at least, there are always some that are differentiating into chromaffin cells (fig. 37, pl. 8). This transformation is found in all parts of nerve plexuses derived from the primary neural invasion, which began in horizon xvi.

Within the confines of the capsule of the adrenal, terminal nerve fibers have not been seen to penetrate or extend through it, once the capsule has been formed. Primary nerve tracts entering the gland, before encapsulation, particularly in the hilar area (fig. 28, pl. 5), as well as a few other isolated areas scattered over the surface of the gland (fig. 29, pl. 6), maintain their place of entry indefinitely.

In the adrenal, the pattern of distribution of the sympathetic nerves, with the accompanying paraganglion cells, is established by the end of horizon xvii. It consists of a plexus of nerves similar in all respects to the periaortic plexuses. Its extent is, as was stated above, circumscribed by the adrenal capsule. When the rapid multiplication of the paraganglion cells begins in horizon xxiii, the few cells which migrated into the area originally act as nidi from which islands of these cells develop. They are scattered throughout the cortex, without definite organization. During the fetal period, the distribution of the neural and chromaffin elements is in all respects similar to the adult condition in birds (as described by Hartman and Brownell, 1949). They are not oriented with reference to the central veins during the fetal period (fig. 35, pl. 7).

The maturation of the paraganglion cells into chromaffin cells begins in horizon xxiii (fig. 37, pl. 8) and continues into the neonatal period.

The degeneration of the central portion of the gland during the first postnatal month of life, so beautifully described by Kern (1911), results in the loss of support for the plexus of nerves which has, up to now, been held in place by the reticulum and cords of the cortex. With this support gone, the neural elements migrate to the nearest stable structure—the central veins—where they remain.

DEVELOPMENT OF BLOOD SUPPLY OF THE ADRENAL

Throughout the late somite stages and through the first half of horizon xvi, a small branch of the postcardinal vein runs in a cephalocaudal direction through the region where the adrenal will develop. It is this vein that Velican (1950) states will become the central vein of the adrenal. He says, also, that the adrenal primordium forms about it as a muff. Carnegie embryo no. 8066, section 9-2-3, horizon xiii, 5.3 mm. (not illustrated), exemplifies the condition of which he speaks. However, under higher magnification, these cells are seen to be no different from those entering the mesenchyme from the celomic epithelium in general. They do not have the characteristics of the cells found in the celomic epithelium between the mesogastrium and the lateral border of the mesonephros during horizon xiv and in the primordium thereafter (fig. 1; fig. 8, pl. 1). They may appear massed here because of the mechanical impediment offered by the vein.

This vessel and its branches drain the area until cells from the first celomic invasion become differentiated in the region. The vein loses its identity by the middle of horizon xvi. From then until horizon xviii, the venous drainage of the developing gland is by way of segmental veins paired with the mesonephric arteries. During late horizon xiv, and horizons xv, xvi, and early xvii, the blood enters the gland at the dorsolateral corner from a branch of each mesonephric artery, which breaks up into a globular arborization of capillaries. The capillaries pass between the cords of cells and collect to form a vein for each body segment, which begins near the ventromedial border of the primordium. These veins pass laterally and dorsally, receiving the bulk of the blood from the adrenal primordium through a few larger capillaries, and enter the postcardinal vein together with the veins from the mesonephros and genital ridge. These veins are the forerunners of the subcardinal-postcardinal anastomosis. The condition is well illustrated in Carnegie embryo no. 8101, slides 25 and 26, horizon xvii (not illustrated).

After the invasion of the neural elements, this vascular arrangement is disorganized, and in late horizon xvii and early xviii a new method of supply and drainage is initiated. At this time the central portion of the gland is made up of capillary blood sinuses and cords of the cells that formerly occupied the area. Nerve cells M-I and M-III are irregularly dispersed among the cortical cells and along the walls of the blood sinuses (figs. 3–5). The vascular channels anastomose freely, and soon become the sinusoids of the fetal cortex.

During horizon xviii (11 to 14.5 mm.; Carnegie embryos nos. 6524, 6527, 7707), by proliferation of the cortical cells in the central area and by a rapid accretion from the celomic epithelium and the mesonephric cell nidus, the cortex recovers from the effects of the neural invasion. Reticular cords of cells separated by the sinusoids have formed in the central portion of the gland.

Carnegie embryo no. 7707 (not illustrated) shows the two methods of drainage at this stage; i.e., in each segment blood flows both into the postcardinal veins and into the subcardinals. By comparison with previous horizons, it will be noted in figure 21 (pl. 4) that the subcardinal vein has grown to approximately the size of the postcardinal vein, which, in relation to the other structures, is now smaller. These efferent veins are the beginning of the adrenal veins in the adult. They empty into those portions of the subcardinal veins that will become the inferior vena cava on the right and the adrenal vein on the left. As the gland grows, the vein of exit is located more laterally (compare fig. 24, pl. 5; fig. 31, pl. 7). The blood supply to the sinusoids is still from branches of the mesonephric arteries; the venous return, however, is tending to the now burgeoning subcardinal veins. At first, there are numerous efferent veins, remnants of the postcardinal-subcardinal anastomosis, emptying into the subcardinal veins. The number is rapidly reduced so that by the end of horizon xxiii there are only two or three at the most, but usually only one vein of exit (fig. 31, pl. 7).

By the time this has happened, large central sinuses form an irregular confluence into the vein of exit. A central vein, such as exists in the mammals usually studied, is not found in the human gland, which is trilobate. There are really three central veins and one vein of exit: the adrenal vein. In an embryo of 37 mm. (Carnegie no. 4415, 106-1-3; fig. 31, pl. 7), the number of sinuses has been reduced to three main sinuses, one of which runs from posterolaterally, a second from the cephalic pole, and the third from the caudomedial pole. They coalesce into the large vein of exit. These sinuses are only irregular channels until the definitive arrangement has been accomplished as seen in embryo no. 84, 51-2-1, 54 mm. (fig. 32, pl. 7).

The adrenal veins empty into the hepatic portion of the developing vena cava on the right side, as encountered in embryo no. 8553, 83-4-5, horizon xxi (not illustrated); they enter at a much higher level than that described and diagrammed by McClure and Butler (1925). It is the more cephalic branches that are retained by both glands.

In horizon xviii, during the reconstitution of the cortex and the beginning formation of the permanent blood supply and drainage, several of the former mesonephric arteries metamorphose into permanent form. Among them are the adrenal, the diaphragmatic, the renal, and the gonadal arteries. Branches from any or all of these arteries may be retained. Since the gland is growing principally from the ventral surface at this time, the mesonephric arteries are pushed dorsally. The branches that formerly supplied the gland still function, supplying blood principally from the dorsolateral surface. Gradually, as the major portion of the blood is drawn off from many of the arteries to supply other organs and structures, one vessel gains ascendancy and becomes the adrenal artery while branches of the others remain in an auxiliary role.

This condition prevails in horizon xix. During the next three horizons, the capillaries begin to spread over the surface of the gland, sending branches through the capsule. In horizon xxiii, there is a rapid growth of the arterial vessels and their connections with the sinusoids beneath the capsule, producing a picture like the one shown in figure 27 (pl. 5). A retiform plexus of arterial vessels is formed in and superficial to the capsule of the gland. A few of these vessels eventually differentiate into arteries, but most of them remain capillaries or arterioles as growth and development progress. Whether or not there are arteries passing through the substance of the cortex to anastomose directly with the central veins could not be determined from available material.

This account presents the general relation of the arterial supply, sinusoid circulation, and venous return throughout life, with minor variations due to changes in configuration.

DISCUSSION

Before discussing some of the controversial points in the development of the human adrenal gland, a short résumé of the findings during the present investigation is in order.

The earliest evidence of the adrenal primordium is found in horizon xv, when type C-I cells enter the mesenchyme between the aorta and the mesonephros from the level of the 6th to the 12th thoracic segments. During horizon xvi, type C-II cells enter the ventral surface of the primordium from the capsule of the mesonephric glomeruli. A nidus of these cells is formed in the primordium just ventral to each segmental mesonephric artery, from which type C-II cells migrate into the adrenal periphery during horizon xviii to become the capsule in horizon xxii. In horizon xvi, cell type C-III makes its appearance in the primordium by migrating from the celomic epithelium together with type C-I cells.

The dorsal portion of the whole primordium is disorganized in horizon xvii by the invasion of sympathetic nerves and the "parasympathetic" cells of Zuckerkandl (1912), while the band of C-II cells and the celomic epithelium remain intact.

During horizon xviii, the gland becomes reorganized. The C-I and C-III type cells continue to enter the primordium as before; some of these cells situated in the periphery of the primordium begin to multiply, as is evidenced by mitotic figures. The disruption by the sympathetic elements in the previous horizon (xvii) causes a change in the blood supply and drainage in the central portion of the gland. Sinusoids have begun to form and divide the primordium into thick cords. Type C-II cells from the actively proliferating nidus spread around the periphery of the primordium. In horizon xix, the C-II cells move to the peritoneal surface, and migration of C-I and C-III cells from the celomic epithelium ceases. By horizon xxii, the type C-II cells have changed to resemble fibrocytes.

During horizon xxiii, the pattern of the arterial blood supply is established; the glomerular zone containing types C-I and C-III cells is formed, and type C-II cells enter the cortical cords, for the first time, along with the other two types. From this stage on, the changes in the gland are mostly morphological. The source and distribution of the three cell types remain essentially the same throughout life.

Adrenal Cortex

Early in this century, anatomists (Wiesel, 1902; Soulié, 1903; Poll, 1906) described the origin, mode of formation, and perpetuation of the adrenal cortex. Kern (1911) adequately considered the postnatal involution. Soulié (1903) is responsible for the concept of the cortex developing from little buds of celomic epithelium, which resulted from a similar condition found in his researches on lower vertebrates and transferred to higher classes, and which still persists in the literature (Felix, 1912; Jordan and Kindred, 1948). From his descriptions, he also may have mistaken the primary tubule formation in the gonad in the human as the source of the epithelioid cells in the adrenal. It is now generally agreed that no buds are found in mammalian primordia (Keene and Hewer, 1927; Uotila, 1940).

The cellular composition of the fetal cortex is the same as that of the postnatal or permanent cortex. Having served its function, the fetal cortex degenerates after birth and is replaced by the adult type of cortex, which derives its cells from the glomerular zone and the capsule in the same manner as did the fasciculoreticular zone in the fetus. Until recently, there has not been sufficient evidence concerning the chemistry of the fetal cortex to warrant discussion of its possible functions. After this paper had been outlined, Benirschke, Bloch, and Hertig (1956) and Bloch, Benirschke, and Rosemberg (1956) published a substantial body of evidence which indicates that the early fetal adrenal cortex synthesizes primarily weak androgenic steroids and a sodium-retaining factor similar to aldosterone. C_{19} steroid synthesis is considered to occur in the fetal zone with decreasing activity as fetal age advances; according to these authors, C_{21} steroidogenesis is performed by the definitive cortex. They advance the hypothesis that the fetal and reticular zones are sites of adrenal androgen production, whereas the fascicular and glomerular zones, respectively, are the sites of glucocorticoid and mineralocorticoid synthesis. By evidence deduced in the present investigation, the "fetal cortex" is composed of cells originating in the glomerular zone and capsule. No reference is made by these authors to cell types in which lipids are demonstrated. The location and time of appearance of the demonstrable steroids are possibly dependent upon the functional activity of the gland initiated by the pituitary or hypothalamus.

The term "fetal cortex" was introduced into the literature by Keene and Hewer (1927) as descriptive of a structure formed by cells from the celomic epithelium before the stage corresponding to Streeter's horizon xvii (1951). According to them, the "fetal cortex" is segregated from the celomic epithelium by a band of connective-tissue cells, and from then on is self-perpetuating. Politzer (1938) and Uotila (1940) express the same opinion. Figure 17 (pl. 3) illustrates the condition described by all these authors. In most areas in embryo no. 6758, from which the illustration was taken, as well as other embryos in horizons xvii and xviii, the continuity between the celomic epithelium and the central portion of the gland is retained.

Keene and Hewer (1927), on the basis of four embryos, of 5, 10, 12, and 18 mm., respectively, in the period of the primordium development, postulated a fetal cortex and a true cortex. The 5-mm. embryo showed no adrenal primordium. The 10-mm. embryo was "unfortunately cut obliquely," so that the relations were distorted. Their description is accurate for this stage. In the 12-mm. embryo, "the cells of the celomic epithelium immediately on either side of the root of the mesentery are no longer columnar and are proliferating, forming a cap of cells 3 or 4 layers thick over the developing gland (better seen in an 18-mm. embryo); some of these cells tend to push posterolaterally between the mesonephros and the suprarenal mass." This is a fairly accurate description of embryo no. 6742, 11 mm., as shown in figure 4; figure 3, however, shows that the apparent layers of cells posterior to the celomic epithelium are derived from Bowman's capsule.

Uotila (1940) followed the lead of Keene and Hewer, utilizing a larger number of embryos. His statement that the gland is separated from the celomic epithelium *at both poles* in embryos between 9 and 10 mm. in length is confirmed. Sagittal sections, however, show three-fourths to two-thirds of the length of the gland to be in contact with and receiving cells from the celomic epithelium until the embryo has attained a length of 19 to 20 mm. Uotila also says, "In an embryo of 9.4 mm. a thin layer of mesenchymal cells definitely intervenes between the glandular epithelium and the mesothelium [celomic epithelium], so that separation of the gland has been completed."

In horizon xviii, after reorganization of the cortex of the gland, following its disruption by the sympathetic nerves, cell cords from the celomic epithelium continue to enter the gland. The cords contain both C-I and C-III types of cells, just as they did previous to the neural invasion. It is only in horizon xix, when the C-II cells move to the surface of the gland, that cells cease to enter the gland from the celomic epithelium. Figures 11 to 25 (pls. 1–5) and figure 36 (pl. 8) illustrate the life history of the type C-II cells from their first differentiation in Bowman's capsule through their transformation into cells resembling fibroblasts in the capsule and final conversion to cells in the cords of the cortex. During all this time, the nuclei have the characteristics of that in figure 39 (pl. 8), even though the shape varies, except in the capsule, after horizon xx when they are very compact. During horizon xviii, when the migration of type C-II cells from the nidus is at its height, some of the cells enter the primordium of the gonad. These are the cells of which Gillman (1948) speaks as "an accretion from the mesonephric mesenchyme" that helps form the interstitial cells of the testes. The three types of cells illustrated in figures 38 to 40 (pl. 8) are to be found in the cortex at all times after horizon xxiii in all fetal and postnatal glands. The types are not species specific.

The development of the adrenal is a continuing process from the first differentiation of cells in the celomic epithelium until the adult gland is formed. No interruption of the continuity could be found in the material studied; only hyperplasia and rapid disintegration make the central part of the fetal gland appear different.

For many years, it was thought that the regressive changes in the early postnatal period were limited to primates. Deane (1955) observed in the guinea pig a 25 per cent decline in volume immediately after birth. A similar decline has been found in the hamster (Crowder, unpublished). Development of the adult type of cortex begins at 4 to 6 weeks postnatally, and is complete by the age of 10 to 11 years, at which time the fascicular zone assumes the relative proportion of the gland found in the adult.

When cells are lost from the cords, by disintegration or by karyopycnosis, they are replaced by others (*cell migration*) from the glomerular zone and capsule, as is suggested by the changes in the cytology of all three types of cells from the periphery.

Whereas Greep and Deane (1949*a*, 1949*b*), on the basis of their researches, have no firm conviction concerning the concept of cell migration, they do state (1949*b*) that "it is an inescapable conclusion that cells which ultimately come to lie in the inner zone arose from the glomerulosa cells," to which we add "and capsule cells." Reese and Moon (1938) had previously found that ACTH prevented degeneration if given before and after hypophysectomy. These data suggest, in support of embryological findings, that the inner zones are dependent upon cells from the glomerular zone and capsule for their continued existence.

Jones (1948), by means of mitotic counts, found that "Mitoses occur all through the zona glomerulosa with the majority towards the inner border." Schaberg (1955), working with adrenal fragments *in vitro,* found that fragments from the peripheral area reproduced both capsule and glomerulosa with occasional fasciculate-zone cells. He doubts cell migration, but states: "ACTH added to the culture media showed an increase in the number of cells with a vacuolar cytoplasm suggesting an increase in the number of cells which differentiate from glomerulosa into fasciculate cells."

Two modes of disintegration of the cortical cells are of interest and pose a problem for further investigation. The one: internal histologic differentiation, swelling, and disintegration (p. 201) are found in the fasciculoreticular zone of the fetus and the fascicular and outer reticular zones of the adult gland. The other: hyalinization, shrinking of the cytoplasm, pycnosis of the nucleus, and phagocytosis of the cells are found during the first postnatal month (Kern, 1911, and personal observations) and in the cells of the innermost cords of the reticular zone. It is suggested, subject to further investigation, that the two phenomena have some relation to secretion or the lack of it. In the fetal gland, all the cells in the fasciculoreticular zone disintegrate by the first method, few intact cells reaching the center of the gland, whereas in the adult gland most of the cells in the fascicular and outer reticular zones disintegrate in the same manner. A few of the cells fail to change their internal structure during their passage through the fascicular zone, retaining their integrity in the attenuated cords of the adult reticular zone, where they are removed by the second mode of disintegration.

The question arises: Are these modes of degeneration in any way associated with secretion? It is not in the province of this discussion to consider that question.

ADRENAL MEDULLA

Wiesel (1902), Poll (1906), and Zuckerkandl (1912) have described the development of the neural elements and the chromaffin cells in the fetal adrenal from 10 weeks to term. Wiesel and Zuckerkandl described and named the cells which become the chromaffin cells. Wiesel called them "sympathetic formative cells," and Zuckerkandl "parasympathetic cells," a term now generally used. None of the above authors or any others of whom the present author is cognizant describe the embryonic or postnatal phases of development. The development during the embryonic period was described under "Development of the Adrenal Medulla" (pp. 202–203) and illustrated by figure 15 (pl. 2) and figures 16 and 17 (pl. 3).

The author has been unable to find in the literature a description of the movement of the medullary elements to the central portion of the gland and the formation of a definitive medulla during the early postnatal period. Kern (1911) touches upon it, but only in passing.

Other authors (Elliott, 1913; Hollinshead, 1936; Swinyard, 1937; Young, 1939) have shown by section of the nerve roots and the splanchnic nerves that the integrity of the nerve supply to the medulla is dependent upon the continuity of spinal roots from thoracic-6 through thoracic-12 or lumbar-1.

It is desirable to think of the medullary neural elements as an integral part of the great abdominal plexus from their first appearance through the fetal and early postnatal periods, since they are both derived from the same sources, pass through the same developmental stages, and have the same cellular characteristics during that time. Examination of sections caudally from figure 14 (pl. 2; embryo no. 792) and figure 17 (pl. 3; embryo no. 6758) demonstrates the continuity of the invading sympathetic nerves. Embryo no. 9226, from which figure 28 (pl. 5) was taken, also shows that neural elements in the abdominal perivertebral plexuses are in all respects identical with those in the adrenal. Throughout the fetal period, the neural elements of the adrenal are distributed in a retiform manner among the cortical cells.

Section of the last eight thoracic and first two lumbar nerve roots caused almost complete degeneration of nerves entering the adrenal (Swinyard, 1937), whereas section of the splanchnic nerves (Young, 1939) caused only partial degeneration. The inference is that both the adrenal and abdominal sympathetic plexuses are dependent upon the same nerves.

The sympathetic nerve development has periods of growth with intervening periods of quiescence. The cortical cells in the adrenal appear to have a relatively stable progressive rate of increase. When the neural elements are actively increasing, they seem to crowd the cortical cords, pushing them aside. During their lull in growth, the cortical elements fill in, and the gland expands around the nerve tracts. The two elements appear to be in active competition for the same area; phylogenetically, this could be possible. In lower vertebrates, e.g. some of the elasmobranchs, the two components are completely separate entities (Hartman and Brownell, 1949). Hartman and Brownell state that the interrenal and chromaffin tissues are usually associated all the way from mere contiguity to a mingling in the higher forms, and chromaffin cells continue to be found in the sympathetic ganglia. In *Anura,* the interrenal tissue has become an organized structure and takes up some of the area occupied by chromaffin tissue in lower forms. In reptiles and birds, the cortical substance occupies most of the area between the mesonephros and aorta during the embryonic stage and becomes thoroughly intermeshed with the chromaffin cells and nerves. In both classes, the same relation of interrenal and chromaffin tissues continues in the adult. In *Ornithorhynchus,* medullary processes extend into the cortical tissue, sometimes reaching the periphery (Hartman and Brownell, 1949). A similar condition obtains in the opossum, *Didelphis virginiana.* The hilum is very large, and the medulla is a loose network of interlacing strands of nerves and chromaffin cells with interdigitating cords of cortical cells (Crowder, unpublished). In placental mammals, there is a postnatal degeneration of the cortex subsequent to which the definitive medulla is formed, conforming more or less to the shape of the gland.

In the human, after the postnatal degeneration of the fetal cortex, the support afforded by the cords of cortical cells and the reticulum of the intervening sinusoids is lost, and the medullary tissue gravitates to the central veins. At first, the strands are loosely intertwined with degenerating cortical cells and other detritus in the interstices. By 6 weeks, it has become fairly well organized into a rather compact, highly vascularized structure. When the reticular zone begins to form, at about 12 to 18 months, cords of cortical cells are again seen interspersed among the groups of chromaffin cells. Complete adult configuration is attained at about 10 years.

BLOOD SUPPLY

The earliest organized blood supply to the primordium is a branch from each of the segmental mesonephric arteries, which is given off at the lateral, posterior border of the primordium. Each branch breaks up into a globular arborization, which collects at the anteromedial surface and is carried laterally again in a capillary vein that runs parallel to the celomic epithelium, just posterior to the layer of type C-II cells, and empties into the postcardinal vein. The blood supply and return is entirely segmental at this stage.

The pattern is disorganized by the neural invasion in horizons xvi and xvii, to be replaced by the more permanent form. During horizons xviii and xix, the cortex of the gland is reorganized, and the gland as a whole begins to assume a pyramidal shape in which the three central veins take form.

The author interprets the change in form of the adrenal as follows: The active intrusion of the metanephros, beginning during horizon xix, into the area which the adrenal would occupy if it retained its cigar-shaped form, causes it to assume a conical shape with a concave base. As growth continues, it is molded by the neighboring structures into a pyramid having a triangular base. Further development produces a lip overhanging the medial surface of the kidney. The morphogenetic forces involved are, of course, obscure.

The arterial blood supply is from the periphery of the gland after horizon xxii. The pressure, therefore, would be approximately equal from all sides, and the blood would accumulate in the center of the gland.

The following quotation from Minot *et al.* (1912) succinctly sums up the mechanism of the developing blood vessels in the adrenal: "The cause of the early appearance of vessels in a multiple capillary form is to be found in the view that this represents the fundamental method of vascular growth, and that larger vessels only come into existence secondarily when the number of capillaries induces an increased supply of blood. Such an event leads to enlargement of certain fortuitously situated capillaries into arteries and veins. The larger vessels are to be considered in the light of servants of the capillaries, for which they are but the delivering and draining pipes. Consequently, the cause for rich vascularity of a tissue cannot be sought in its possession of larger vessels, but rather in the influences which have brought about a more abundant growth of capillaries in it." In the adrenal, this influence is the prodigious growth and increase in the number of cells.

From a pyramidal exterior, three main channels to the center of the gland will be formed. The most fortuitously situated branch of the subcardinal veins must then dilate to drain the blood from this central area and thus become the adrenal vein. The tributary veins, as such, do not form until the embryo is 50 to 60 mm. in length, and then only because the shape and mass of the trilobate gland are such that one vein of exit from the three tributary veins is the most efficient.

After the three tributary veins are formed, the line of least resistance for the forming cords of cells to travel, against the pressure of the blood and the adjacent cords, is toward the channels; thus, an approximately trilobate form evolves, with the cords tending toward these veins. Gersh and Grollman (1941) imply, in their discussion of the vascular pattern of the adrenal in the mouse and rat, that the cords of cells conform to the capillary pattern. The converse appears to be true in the present material, for the cords are the dominant feature, and the capillaries conform to the ever-changing cord pattern. There is no change from this blood supply throughout life.

SUMMARY AND CONCLUSIONS

1. In the human, the adrenal cortex derives its cell components from (*a*) celomic epithelium and (*b*) the glomerular capsules of the mesonephros during the embryonic period.

2. Three distinct types of cells, defined on the basis of nuclear size and structure, are so derived: two from the celomic epithelium, and the other from the mesonephros.

3. The first evidence of the adrenal primordium is demonstrated in horizon xiv early in the 4th week (30 days±2); it consists of type C-I cells.

4. Type C-II cells begin differentiation in horizon xv, early in the 5th week. Two groups are found in the medial wall of Bowman's capsule. The dorsal group forms a nidus in the dorsolateral portion of the primordium beneath each mesonephric artery, from which cells are derived to form the adrenal capsule. At the height of migration from the ventral group, the entire medial wall of each Bowman's capsule forms new cells which migrate medially, forming a layer 4 to 6 cells thick across the ventral surface of the primordium just dorsal to the celomic epithelium. This layer of cells (C-II) does not interfere with cells of the other types entering the primordium from the celomic epithelium.

5. Type C-III cells begin to enter the primordium from the celomic epithelium together with type C-I cells during horizon xvi, early in the 5th week.

6. Migration of cells of type C-II from the nidi begins in horizon xvii, about the middle of the 5th week, and by the beginning of the 6th, horizon xxi, a definite capsule is formed around the primordium except where sympathetic nerves are entering the gland.

7. When the capsule is formed, cells of types C-I and C-III, having the same characteristics as those previously seen in the celomic epithelium, are found in the primordium just central to it. They form a layer 10 to 12 cells deep. Mitotic figures are frequent.

8. The celomic epithelium has ceased to function as a source of cortical cells by horizon xxi; the cells just beneath the capsule assume that function.

9. The invasion of the adrenal primordium by sympathetic neural elements begins about the middle of the 4th week and ends by the first of the 5th week. At this time, activation of the sympathetic ganglia from dorsal-6 to lumbar-1 results in the abdominal sympathetic plexuses, of which adrenal medullary nerves are a part. Growth is relatively slow, keeping pace with body growth from horizon xvii through horizon xxiii. At 7 weeks, a second increase in rate of growth begins, which lasts about 2 weeks; it results in an enormous development of nerve fibers and primitive chromaffin cells.

10. Chromaffin cells have begun to differentiate morphologically by 8 weeks. They continue to do so until after birth.

11. The so-called "fetal cortex" has the same cellular components as the adult cortex. The difference in appearance in the fetal gland is due only to the increased rate of maturation of the cortical cells in the central portion.

12. The fact that mitoses are found in the glomerular and subglomerular regions at all times, but rarely in the other zones, speaks for the continuous production of new cells in the glomerular zone and their migration into the deeper zones.

13. The postnatal reticular zone is composed of cells that retained their integrity during their passage through the middle zone and continue to travel within the framework of the cords. The supporting structures of the cords are the walls of the sinusoids. The connective tissue within the sinusoidal walls is continuous from the arteriolar capillaries in the capsule to the central veins. The attenuated cords lack the support of neighboring cords found in the fascicular zone, and, as a result, are forced into an irregular pattern to permit the length to adjust to the perpendicular space available.

14. The neural elements and chromaffin cells are found throughout the cortex during fetal life in a retiform pattern in all respects similar to that observed in the adrenals of adult birds. Only after the massive degeneration of the cortex during the 1st postnatal week, when they lose the support of the cortical cords, do they gravitate to the central veins, together with the reticulum of the sinusoids. After the 4th postnatal week, most of the neural tissue and chromaffin cells in the adrenal are clustered around the tributary veins. The medulla becomes adult in appearance between 12 and 18 months. In the adult medulla, there are cells among the chromaffin cells, similar in all respects to the paraganglion or primitive chromaffin cells.

ACKNOWLEDGMENTS

I wish to thank Dr. George W. Corner, former Director of the Department of Embryology of the Carnegie Institution of Washington, for making the Carnegie Collection available to me and for the many other courtesies extended to me. Without the thoughtful encouragement, patience, and inspirational criticism of Dr. George W. Bartelmez, this work could never have come to fruition. The credit for the photographs used as illustrations is due Mr. Richard D. Grill. The unstinting help given by Miss Harriet L. Caspari, in locating the histologic preparations and making data available, and by Miss D. G. Smith and Mrs. Emilie A. Littleton, in preparing the manuscript, deserve my grateful thanks.

LITERATURE CITED

Benirschke, K., E. Bloch, and A. T. Hertig. 1956. Concerning the function of the fetal zone of the human adrenal gland. Endocrinol., vol. 58, pp. 598–625.

Benner, M. C. 1940. Studies on the involution of the fetal cortex of the adrenal glands. Amer. Jour. Pathol., vol. 16, pp. 787–798.

Bloch, E., K. Benirschke, and E. Rosemberg. 1956. C_{19} steroids, 17α-hydroxycorticosterone and a sodium retaining factor in human fetal adrenal glands. Endocrinol., vol. 58, pp. 626–633.

Deane, H. W. 1955. Histophysiology of the adrenal cortex in fetal and prepuberal rats, with comments on the carbonyl reactivity of the cortical lipid droplets. Report, 13th M. and R. Pediatric Research Conference: Adrenal function in children, pp. 17–26.

Elliott, T. R. 1913. The innervation of the adrenal glands. Jour. Physiol., vol. 46, pp. 285–290.

Felix, W. 1912. The development of the reproductive glands and their ducts. *In* Keibel and Mall (eds.), Manual of human embryology, vol. 2, pp. 881–911. Philadelphia.

Gersh, I., and A. Grollman. 1941. The vascular pattern of the adrenal gland of the mouse and rat and its physiological response to changes in glandular activity. Carnegie Inst. Wash. Pub. 525, Contrib. to Embryol., vol. 29, pp. 111–125.

Gillman, J. 1948. The development of the gonads in man, with a consideration of the role of fetal endocrines and the histogenesis of ovarian tumors. Carnegie Inst. Wash. Pub. 575, Contrib. to Embryol., vol. 32, pp. 81–131.

Greep, R. O., and H. W. Deane. 1949*a*. The cytology and cytochemistry of the adrenal cortex. Ann. N. Y. Acad. Sci., vol. 50, pp. 596–615.

——— ——— 1949*b*. Histological, cytochemical and physiological observations on the regeneration of the rat's adrenal gland following enucleation. Endocrinol., vol. 45, pp. 42–56.

Hartman, F. A., and K. A. Brownell. 1949. The adrenal gland, pp. 23–33. Philadelphia.

Hollinshead, W. H. 1936. The innervation of the adrenal glands. Jour. Comp. Neurol., vol. 64, pp. 449–467.

Hunter, O. J., Jr. 1954. Personal communication.

Jones, I. C. 1948. Variation in the mouse adrenal cortex with special reference to the zona reticularis and to brown degeneration, together with a discussion of the "cell migration" theory. Quart. Jour. Microscop. Sci., vol. 89, pp. 53–74.

Jordan, H. E., and J. E. Kindred. 1948. Textbook of embryology. 5th ed., pp. 220–224. New York.

Keene, M. F. L., and E. E. Hewer. 1927. Observations on the development of the human suprarenal gland. Jour. Anat., vol. 61, pp. 302–324.

Kern, H. 1911. Ueber den Umbau der Nebenniere im extrauterinen Leben. Deut. med. Wochschr., vol. 37, pp. 971–974.

Lanman, J. T. 1953. Fetal zone of the adrenal gland; its developmental course, comparative anatomy, and possible physiologic functions. Medicine, vol. 32, pp. 389–430.

Lewis, R. W., and A. M. Pappenheimer. 1916. A study of the involutional changes which occur in the adrenal cortex during infancy. Jour. Med. Research, Bost., vol. 34, pp. 81–93. (Also quoted in part by Benner, *vide supra.*)

McClure, C. F. W., and E. G. Butler. 1925. The development of the vena cava inferior in man. Amer. Jour. Anat., vol. 35, pp. 331–383.

Minot, C. S., H. M. Evans, J. Tandler, and F. R. Sabin. 1912. The development of the blood, the vascular system, and the spleen. *In* Keibel and Mall (eds.), Manual of human embryology, vol. 2, pp. 581–582. Philadelphia.

Parkes, A. S. 1945. The adrenal-gonad relationship. Physiol. Revs., vol. 25, pp. 203–254.

Politzer, G. 1938. Ueber die Frühentwicklung der Nebennierenrinde beim Menschen. Ztschr. f. Anat. u. Entwicklungsgesch., vol. 106, pp. 40–48.

Poll, H. 1906. Die vergleichende Entwicklungsgeschichte der Nebennierensysteme der Wirbeltiere. *In* O. Hertwig, Handbuch der vergleichenden und experimentellen Entwickelungslehre der Wirbeltiere, Bd. 3, Teil 1, pp. 443–603. Jena.

Reese, J. D., and H. D. Moon. 1938. The Golgi apparatus of the cells of the adrenal cortex after hypophysectomy and on the administration of adrenocorticotropic hormone. Anat. Rec., vol. 70, pp. 543–556.

SCAMMON, R. E. 1925–1926. The prenatal growth and natal involution of the human suprarenal gland. Proc. Soc. Exper. Biol. and Med., vol. 23, pp. 806–811.

SCHABERG, A. 1955. Regeneration of the adrenal cortex in vitro. Anat. Rec., vol. 122, pp. 205–221.

SOULIÉ, A. H. 1903. Recherches sur le développement des capsules surrénales chez les vertébrés supérieurs. Jour. de l'anat. et de le physiol., vol. 39, pp. 492–533.

STREETER, G. L. 1951. Developmental horizons in human embryos. Age groups xi to xxiii. Carnegie Inst. Wash., Embryology Reprint Volume II. 196 pp.

SWINYARD, C. A. 1937. The innervation of the suprarenal glands. Anat. Rec., vol. 68, pp. 417–429.

THOMAS, O. L. 1948. The spheroid system of sympathetic neurons with special reference to the problem of neurosecretion. Quart. Jour. Microscop. Sci., vol. 89, pp. 333–350.

UOTILA, U. U. 1940. Early embryological development of the fetal and permanent adrenal cortex in man. Anat. Rec., vol. 76, pp. 183–203.

VELICAN, A. 1950. Les phases de l'évolution ontogénétique de la cortico-surrénale. Bull. histol. appl. et tech. microscop., vol. 27, pp. 79–87. (Abstract in Excerpta Med., 1951, vol. 5, sect. 1, p. 171.)

WIESEL, J. 1902. Beiträge zur Anatomie und Entwickelung der menschlichen Nebenniere. Anat. Hefte, vol. 19, pp. 481–522.

YOUNG, J. Z. 1939. Partial degeneration of nerve supply of adrenal. Study in autonomic innervation. Jour. Anat., vol. 73, pp. 540–550.

ZUCKERKANDL, E. 1912. The development of the chromaffin organs and of the suprarenal bodies. *In* Keibel and Mall (eds.), Manual of human embryology, vol. 2, pp. 157–179. Philadelphia.

Plates 1 to 8 are untouched photomicrographs of sections of embryos in the Carnegie Collection illustrating relations and cell types of adrenal primordium. Ages are estimated ovulation ages, following Streeter (1951).

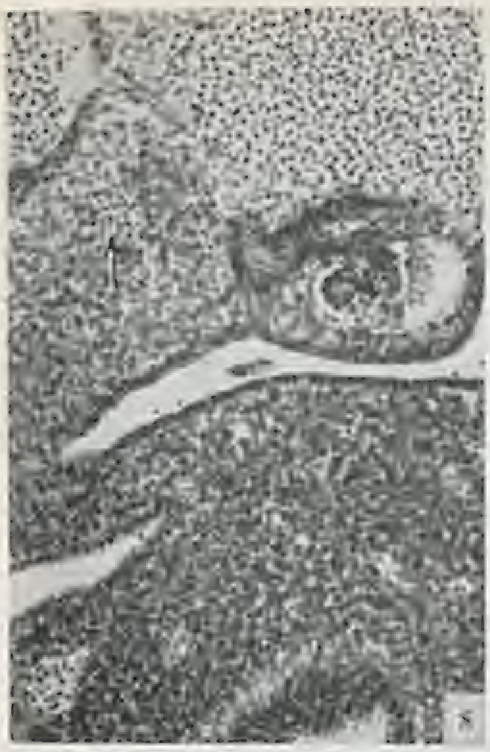

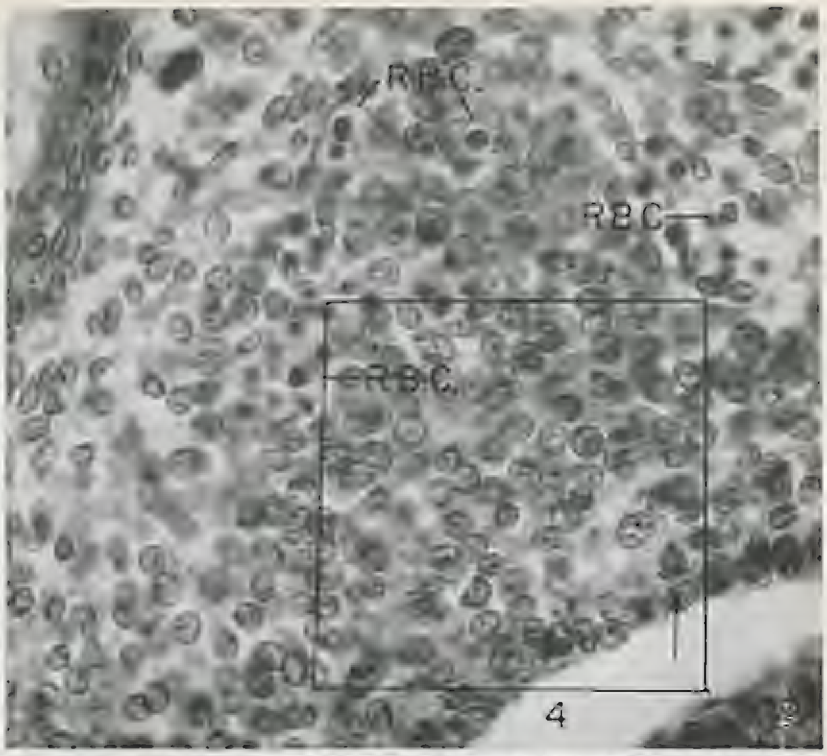

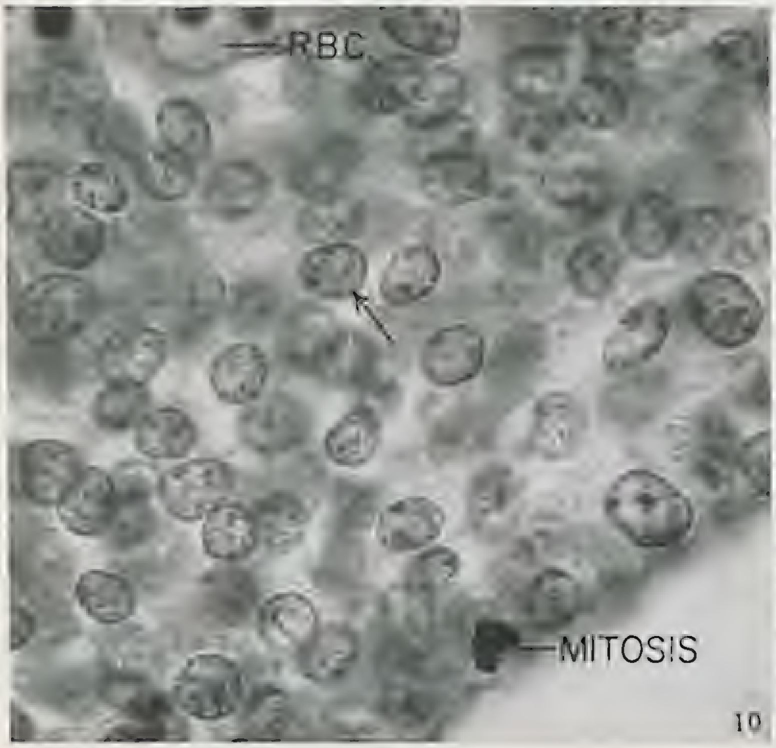

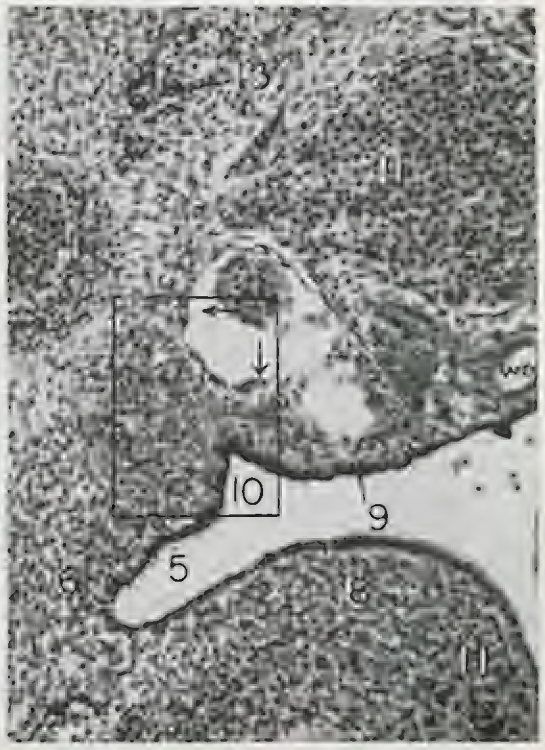

Fig. 8. Transverse section of embryo from beginning of 5th week; midgastric level. Aorta with origin of a mesonephric artery, upper left. Postcardinal vein, upper right. Beneath it, mesonephros with genital ridge on its peritoneal surface. Arrow indicates a transient vessel. Between it and mesonephros, enlarged cells define adrenal primordium. The adjacent celomic epithelium can be distinguished from other mesenchyme. No. 3385, 14-3-1. Horizon xv. ×150. 8.3 mm.

Fig. 9. From a section taken about 150 microns caudal to that of figure 8. Primordium differentiated from surrounding mesenchyme by its crowded type C-I cells (see p. 197) with large nuclei and more abundant cytoplasm. Arrow indicates a mitosis. *R. B. C.*, red blood corpuscles marking capillary plexus on medial surface of primordium. No. 3385, 15-1-5. ×500.

Fig. 10. Area enclosed by rectangle in figure 9. All cells of type C-I. Cytoplasm abundant, and nuclei large with relatively little chromatin and an eccentric nucleolus. Arrow indicates nucleus showing highly refractile spheroid body (see fig. 38, pl. 8). Zeiss 3.0 mm. apochromat, ap. 140. ×1000.

Fig. 11. From a more advanced embryo, showing primordium of adrenal protruding into celom. Mesonephros with Malpighian bodies, tubules, and Wolffian duct (*W. D.*). Increase in size of ganglion of sympathetic chain (13) due to cell division and ingrowth of nerve fibers. Two groups of cells in Bowman's capsule indicated by arrows mark a significant differentiation (see fig. 2; fig. 12, pl. 2). No. 721, 14-3-5. Horizon xv. ×150. 4, aorta; 5, celomic cavity; 6, mesogastrium; 8, stomach; 9, genital ridge; 10, adrenal groove; 11, postcardinal vein.

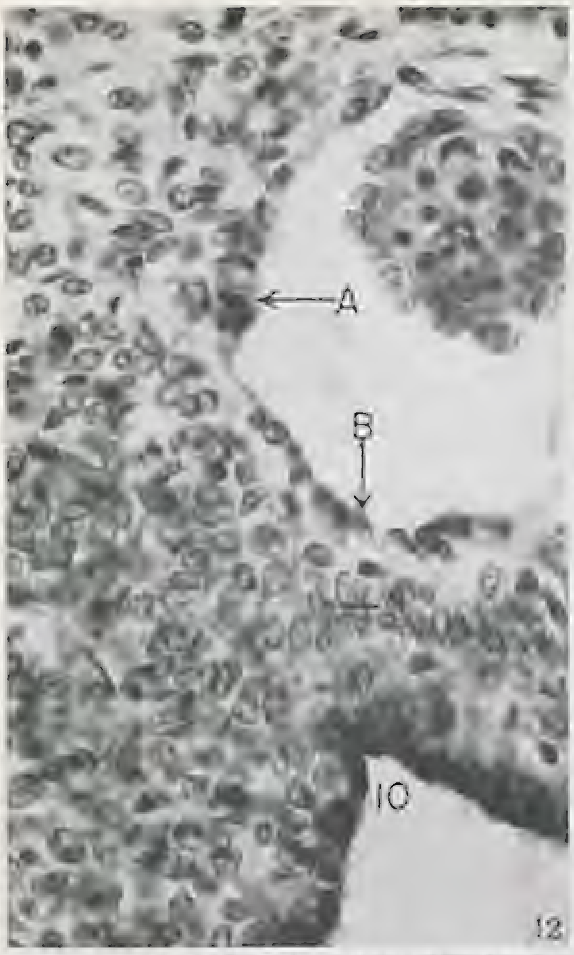

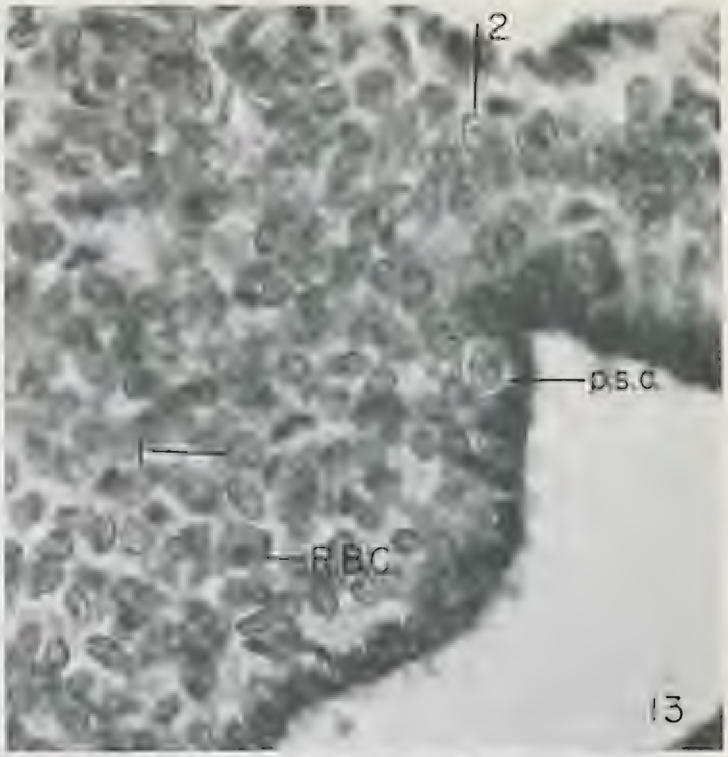

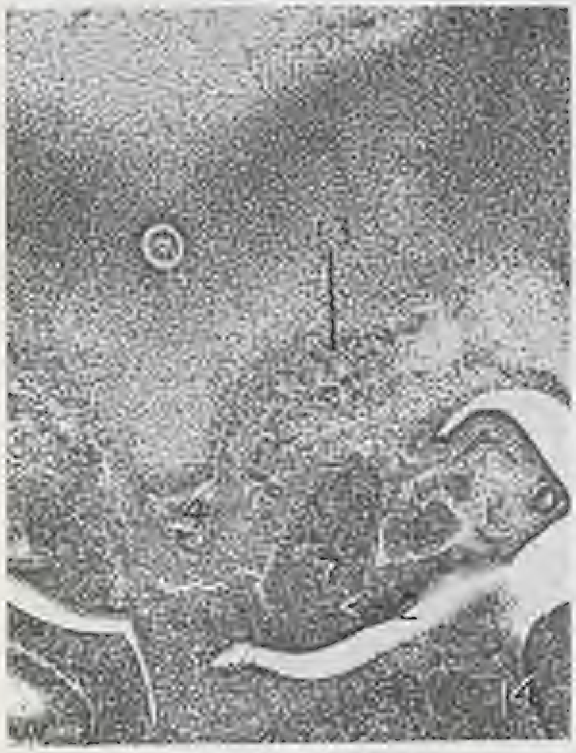

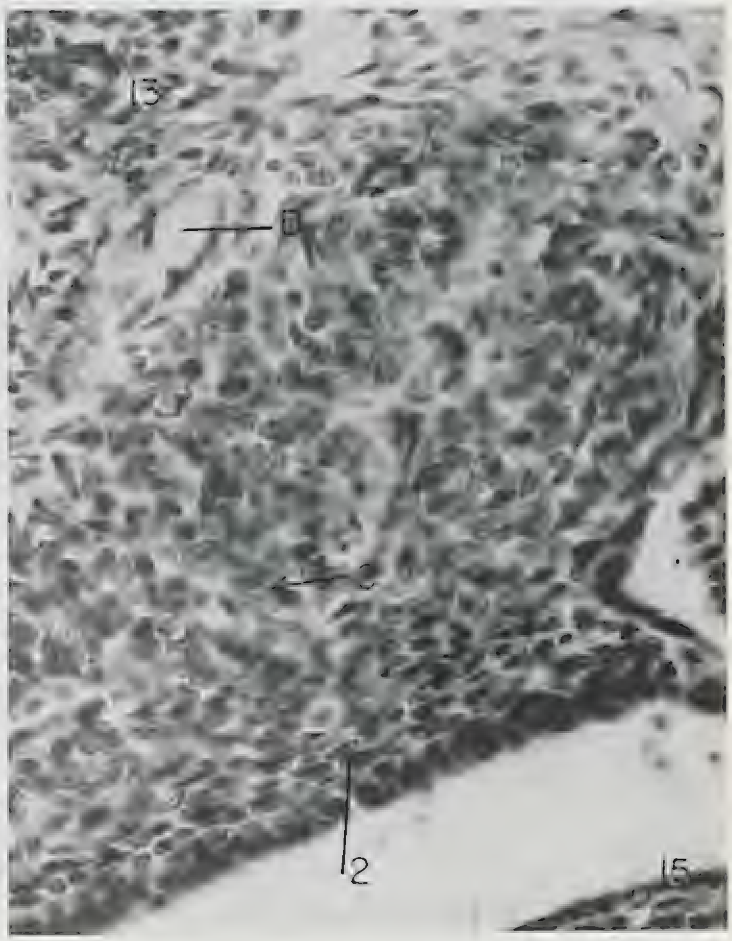

Fig. 12. Area of rectangle in figure 11, showing cells of Bowman's capsule. At arrow *A*, cells appear to be migrating into mesenchyme dorsal to adrenal primordium. At arrow *B*, they appear to be migrating into the adrenal and gonadal primordia. Small cells (*C*) with elongated nuclei are seen in the ventrolateral portion of the gland. No. 721, 14-3-5. ×500. 10, adrenal groove.

Fig. 13. From the same embryo as figure 11, 20 microns caudal to section shown in figure 12. ×600. 1, type C-I cells; 2, type C-II cell; *p. s. c.*, primordial sex cell.

Fig. 14. From an embryo of 5 weeks. Primordia of adrenal and sympathetic ganglion (13) are relatively larger, compared to mesonephros, than in figure 11 (pl. 1). Adrenal primordium in direct continuity with celomic epithelium. No. 792, 10-1-3. Horizon xvi. ×100. 8 mm. 4, aorta; 7, adrenal primordium; 12 (arrow), band of cells of mesonephric origin (type C-II).

Fig. 15. From a section near that shown in figure 14. Type C-II cells (2) appear to be migrating along ventral surface of primordium from Bowman's capsule. Invading neural elements (*C*) (arrow) from sympathetic chain spreading widely among the cells of the primordium have disturbed its homogeneity. *D*, sympathetic nerve. ×500.

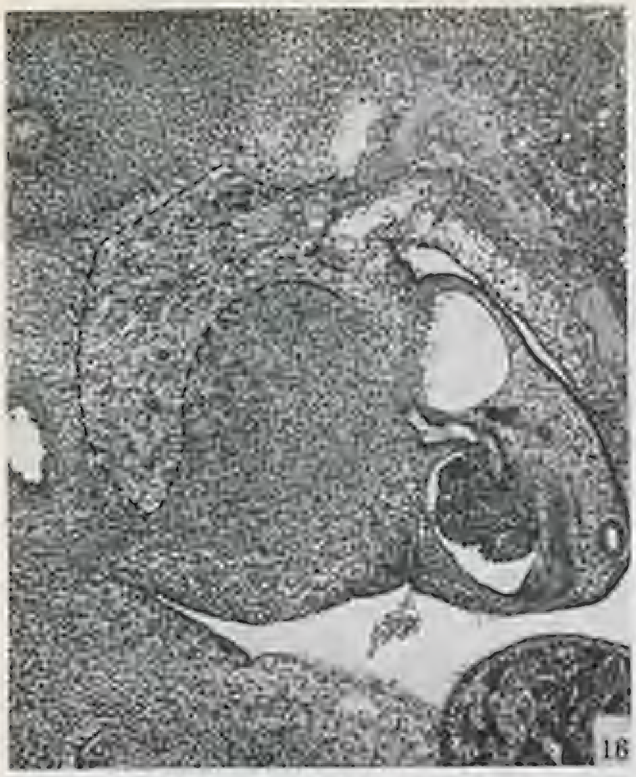

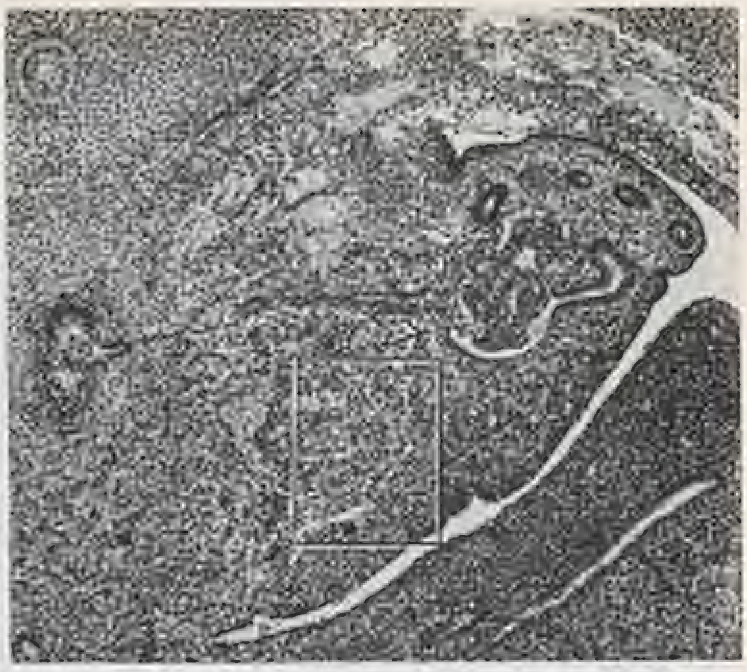

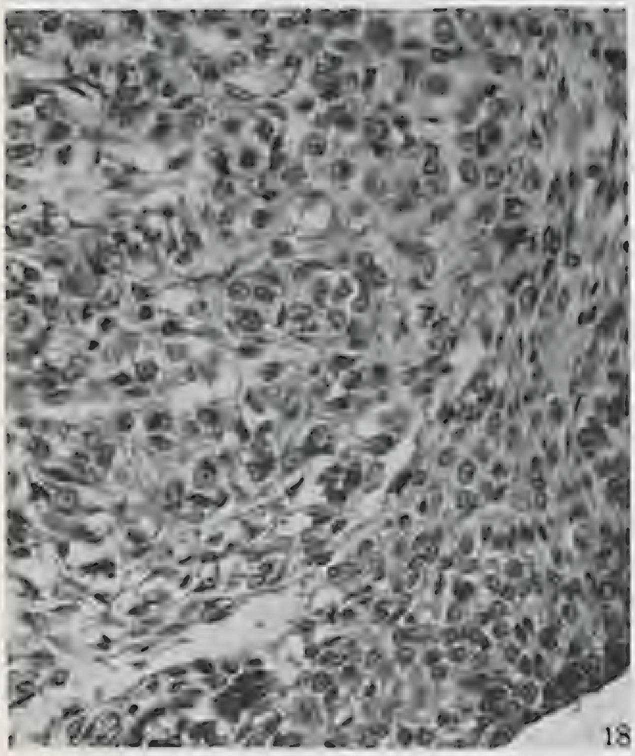

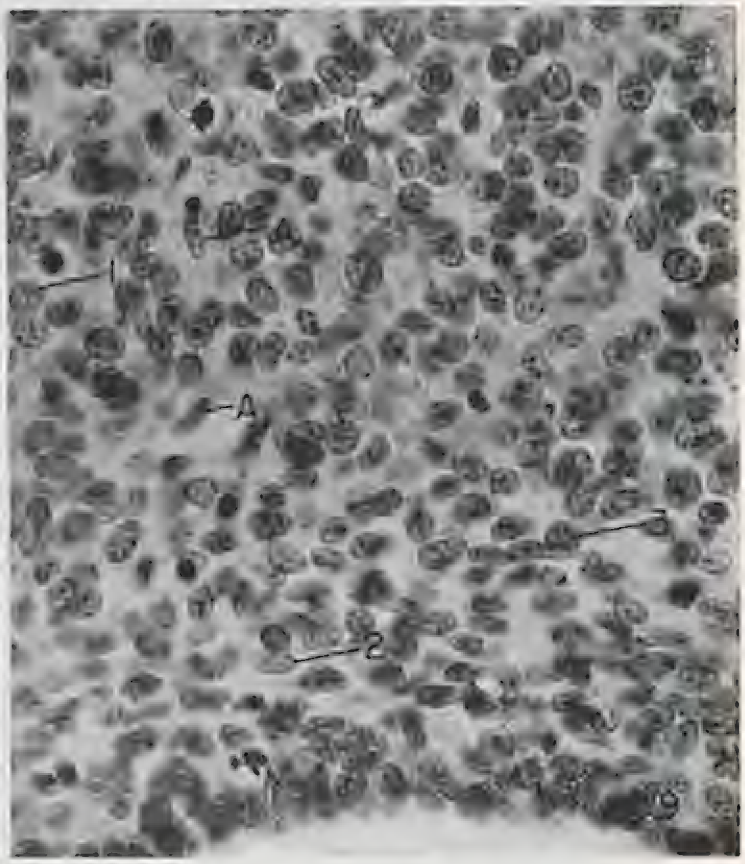

FIG. 16. Embryo from end of 5th week, showing a remarkable increase in the size of the gland and particularly in the amount of the sympathetic nerve tissue (outlined by broken line), which lies along the dorsal and medial surface of the primordium, many fibers and their cells infiltrating it. Section near the cephalic pole. No. 6742, 13-2-3. Early horizon xvii. ×100. 11 mm.

FIG. 17. Embryo more advanced than the preceding. Final stage of the invasion of neural elements into the adrenal primordium. Cortical cells are separated into islands by the neural tissue, except in the ventrolateral margin. Type C-II cells still passing from Bowman's capsule into the nidus area beneath the mesonephric artery at arrow. No. 6758, 16-5-5. Horizon xvii. ×100. 12.8 mm.

FIG. 18. Area included within rectangle in figure 17. Two regions of primordium are distinct. Above and to left, area infiltrated by neural elements which surround groups of types C-I and C-III cells. Below and to right, types C-I and C-III cells are being proliferated from the celomic epithelium. In this denser area are also many type C-II cells. ×400.

FIG. 19. Sagittal section of an embryo later in horizon xvii than the others illustrated, taken from near the center of lower pole of the gland and including the ventral third. Celomic epithelium at lower border. All the cellular elements of the adrenal. Cell types C-I (1) and C-III (3) originating in the celomic epithelium form cords in the expanding gland. Type C-II (2) cells lie parallel to the outer surface, and a few nerve cells and fibers (*A*) extend between the cortical cells. No. 6519, 16-1-3. Horizon xvii. ×600. 10.8 mm. Arrow, mitosis in celomic epithelium.

PLATE 4

FIG. 20. Embryo from early in 6th week. Cross section from middle of cephalocaudal axis of adrenal. Disorganization by neural elements not so complete as at caudal pole (fig. 17, pl. 3). Medially, cells of neural origin and nerve fibers predominate. No. 8101, 25-4-3. Late horizon xvii. × 100. 13 mm. 4, aorta; 5, celomic cavity; 6, mesogastrium; 7, adrenal gland; 8, stomach; 9, gonad; 10, adrenal groove; 11, postcardinal vein; 13, sympathetic ganglion.

FIG. 21. Embryo more advanced than preceding. Section near the caudal end of the gland. The cephalic two-thirds is similar to the previous embryo, but organization is a little further advanced. At this level, a few nerve fibers are entering the dorsomedial surface, and the gland has increased in size. Gland is completely separated from the celomic epithelium at this level. Continuity is maintained at the adrenal groove. Two new features are the beginning canalization of the body of the gland (arrow), and the beginning development of the para-aortic and visceral nerves and plexuses (*A*). The dorsomedial half at this level is composed principally of neural elements; the lateral portion, of cortical cells. The neural component is small at this level. The dark areas represent a preponderance of nerve cells; the gray areas dorsomedially, of fibers. The nerves (15) are part of the renal plexus. No. 7707, 41-2-4. Horizon xviii. × 100. 14.5 mm. 9, gonad; 10, adrenal groove; 11, postcardinal vein; 13, sympathetic nerve tissue; 14, subcardinal vein.

FIG. 22. Embryo similar in its development to the preceding. The section shows a nidus (there is one for each body segment) formed by accretion of cells from the portion of Bowman's capsule just ventral to and partly surrounding the segmental mesonephric artery as it enters the glomerular tuft. Active proliferation indicated by numerous mitoses (*M*). Nidus surrounded by broken line is medial to glomerulus. Adrenal groove (10) separates adrenal (7) and the gonad (9). No. 6524, 42-2-1. Horizon xviii. × 500. 11.7 mm. 11, postcardinal vein.

FIG. 23. Cellular details, from an embryo similar to the preceding. The type C-II (2) cells originating in the nidus (*B*) (fig. 22) have the same characteristics as those which first passed from the wall of Bowman's capsule directly into the adrenal primordium (fig. 19, pl. 3): cylindrical nuclei having scanty chromatin, a small or no discernible nucleolus, and one or more large vacuoles or inclusions. The nidus cells are beginning to penetrate between the cells of the celomic epithelium (*A*) preparatory to assuming a position outside them. Nuclei of cortical cell types C-I (1) and C-III (3) appear at the left. No. 8172, 34-2-1. Horizon xviii. × 1000. 16.5 mm. *B*, nidus.

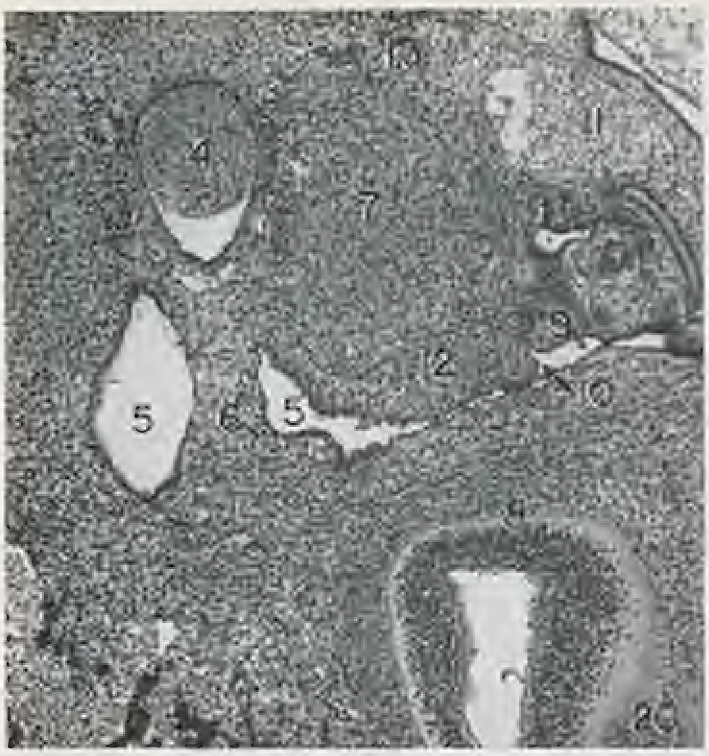
20

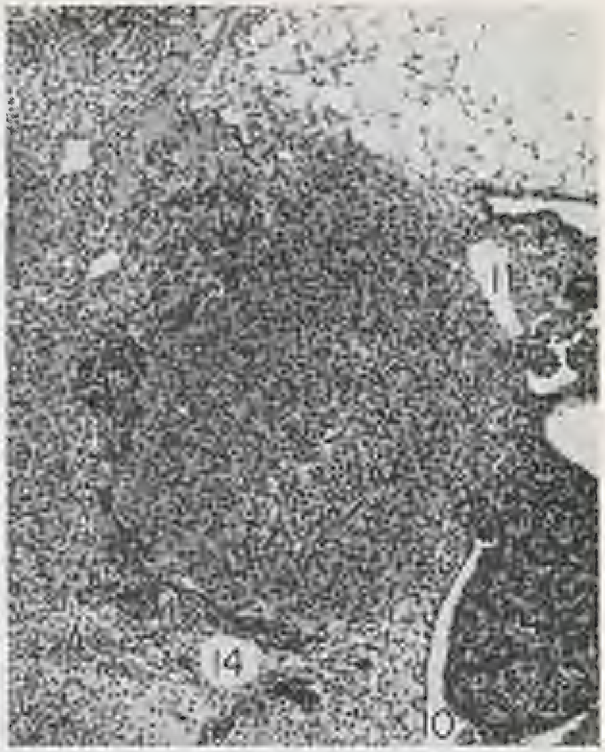

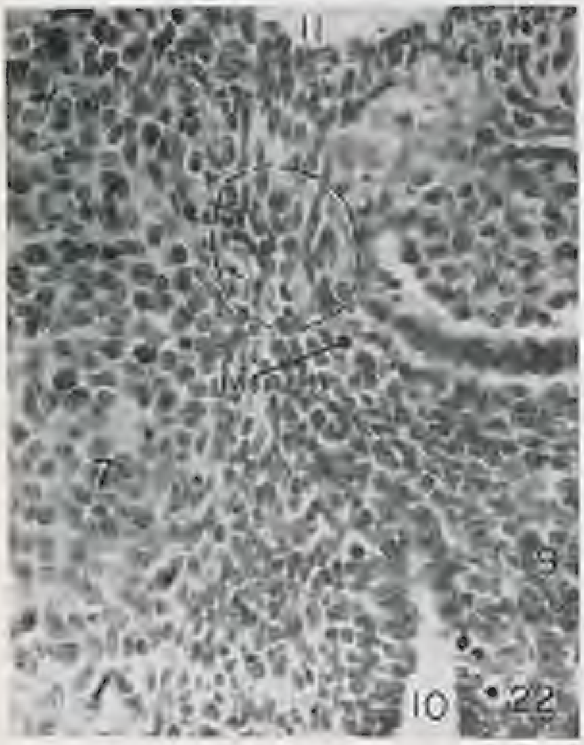
22

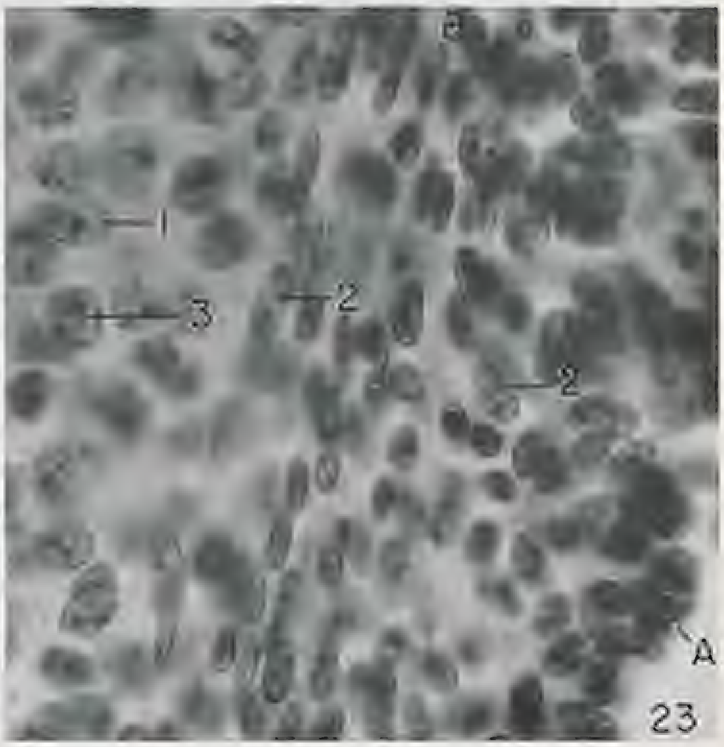
23

FIG. 24. Embryo from the 6th week. A transverse section from the lower, middle third, cephalocaudally. The gland has been completely reorganized after the neural invasion. Neuroblasts or nerve fiber bundles of significant size are seen only around the periphery of the dorsomedial surface of the caudal half of the gland (*D*). Thin strands of nerve fibers and a few accompanying large cells of neural origin (M-III) (*F*) are scattered among the cortical cells within the encircling band of cells of mesonephric origin (12).

Capillary channels have multiplied, dividing the cell mass of cortex into loose, irregular cords of cells. The venous outlet is by way of three or four of the more fortuitously situated capillaries which communicated between the postcardinal and subcardinal veins before the neural invasion. One, *A*, is seen here emptying into a portion of the inferior vena cava.

The layer of type C-II cells is well developed along the ventral and lateral surface of the gland in this section. At the cephalic end, it completely surrounds the gland and has come to be the outermost layer of cells. At the caudal end, it is fragmentary because of the presence of the rapidly developing splanchnic plexus. At this level, a small increment of cells, types C-I and C-III, is still coming through the layer from the celomic epithelium along the ventral surface. No. 6527, 38-3-2. Horizon xviii. × 150. 14.4 mm. *B*, cross sections of adrenal nerve; *C*, inferior vena cava; *E*, mesonephric glomerulus; 9, gonad.

FIG. 25. A portion of the gland on the ventral surface, cut sagittally. At this stage, the type C-II cells (12) form the outermost layer. No well defined celomic epithelium or peritoneum is present. Cell types I and III, previously proliferating in the celomic epithelium, are now found, central to the forming capsule, in a poorly defined layer 10–12 cells deep. Mitoses are frequently found in this layer but only occasionally deeper in the gland. No. 6202, 22-1-2. Horizon xx. × 600. 21 mm.

FIG. 26. From the lateral border of a frontal section of the adrenal, about its middle, in an embryo during the 7th week. The gland as a whole is very similar to that of horizon xx except that the anteromedial portion has begun to grow caudally over the kidney and the area of entrance of the sympathetic nerve tissue has become relatively much smaller. Type C-II cells (2) have become a definite capsular layer. The central mass of cells is divided into cords by capillaries (arrows) in whose walls endothelial nuclei (*A*) are seen. All the elements of the adrenal cortex are now present and in their ultimate relation to one another. Outside (capsule) are the C-II cells. Just within are types C-I (1) and C-III (3) cells found in the celomic epithelium in earlier stages. Beyond them, and derived from them, are cords of large cells extending to the central portion of the gland. No. 8394, 106-2-2. Horizon xxii. × 500. 25.3 mm.

FIG. 27. A horizontal section of the right gland along the peritoneal margin near its middle in an embryo in the 8th week. Arterial capillaries (*C*) divide the cells of the outer (germinal) layers into globular nests (*B*) as the vessels dip inward to connect with venous sinusoids (*D*), thus forming the glomerular zone of the cortex. The layer of capsule cells on the surface is partly dragged inward by the invading vessels (*E*), establishing a relation in which cells from it will pass into the cords in the substance of the gland. (See also fig. 36, pl. 8.) For the most part, the cells remain at or near the surface and form the major part of the capsule. No. 6573, 63-2-2. Horizon xxiii. × 500. 31.5 mm. *A*, endothelial cells.

FIG. 28. Embryo early in the 8th week. The cross section cuts across the lower pole of the right adrenal and at about the junction of the lower and middle third of the left. The lower pole of the right gland (*F*) is disorganized by the rapidly growing celiac plexus (*G*). The left gland, from the cephalic pole to this level, is undisturbed. (See p. 198.) No. 9226, 161-1-2. Horizon xxiii. × 45. 30.1 mm. *A*, aorta; *B*, right crus of diaphragm; *C*, splanchnic nerves; *D*, left sympathetic ganglion; *E*, right kidney.

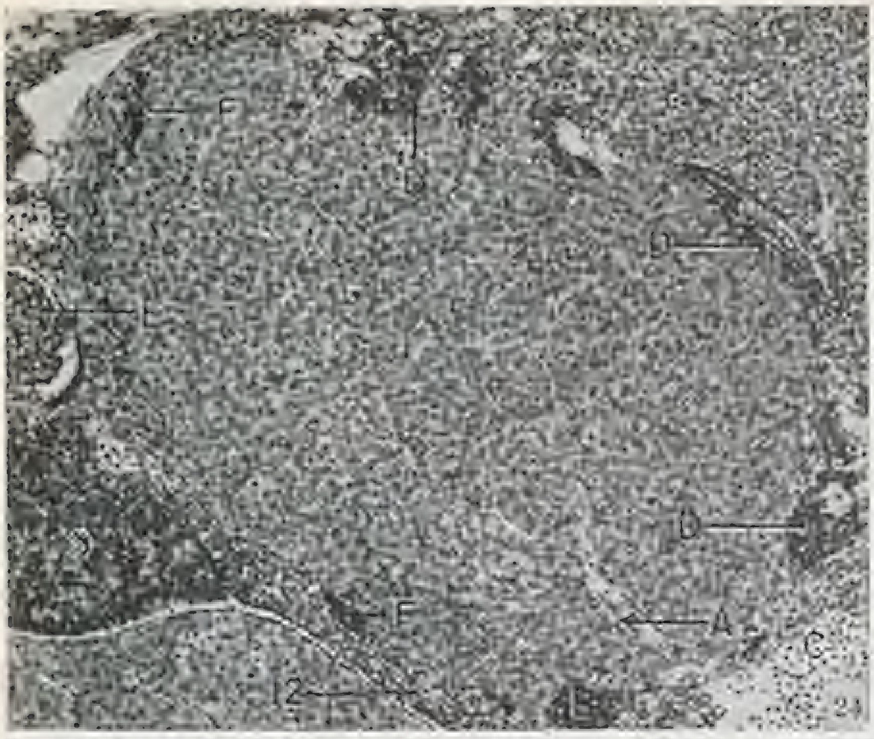

24

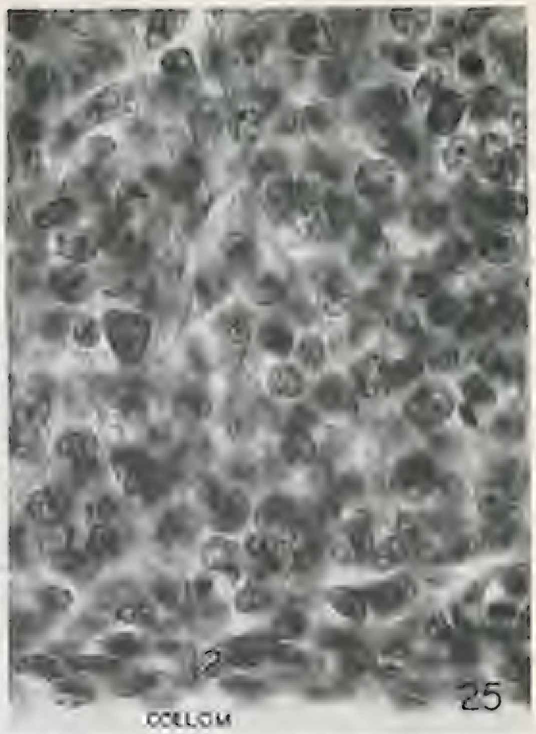

25

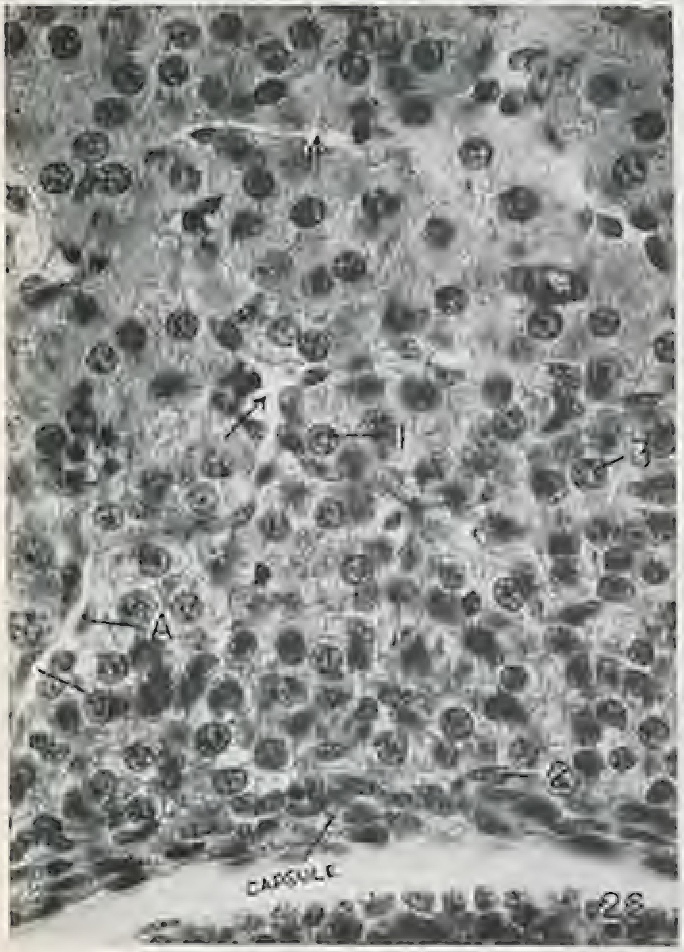

26

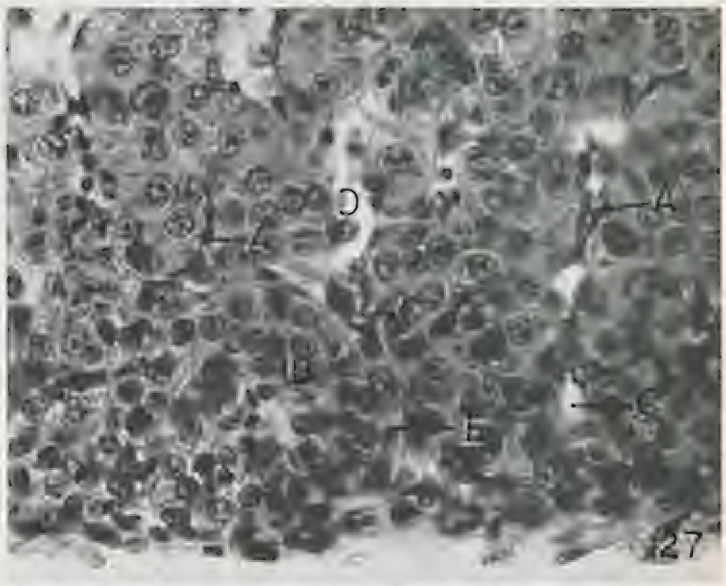

27

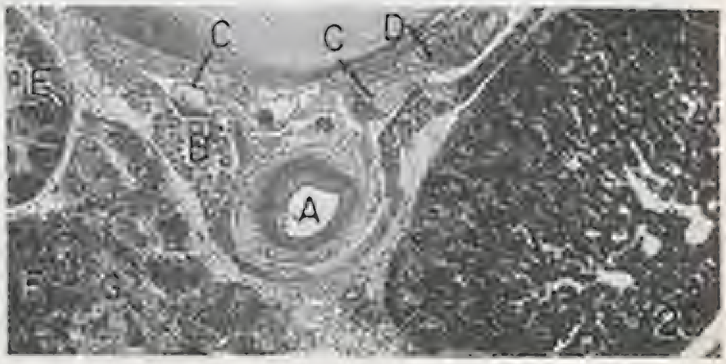

28

Plate 6

Figs. 29–30. From a horizontal section of the embryo near the level of the caudal end of the middle third of the right adrenal. The same process as is going on at the caudal pole in figure 28 (pl. 5), but shown with more clarity, since only one nerve is involved instead of the great plexuses. Figure 29 shows one of the branches of the adrenal nerve at the height of the second period of proliferation. The first was during horizons xvi and xvii (see figs. 3–5; figs. 16–18, pl. 3). The same growth is going on in all areas into which the earlier growth penetrated. M-I cells and nerve fibers together with the accompanying large M-III cells multiply at a rapid rate. The bulk of nerve tissue becomes relatively so enormous that it encroaches upon the surrounding adrenal cortex. The pressure by the neural elements pushes the cortical cords aside to make room for the nerves. The M-III cells heretofore in the interior of the nerves now begin to multiply and form into islands of various sizes throughout the cortex (*C* in fig. 30). These cells mature into the chromaffin cells (*A* through *D*, fig. 37, pl. 8). No. 301, 196-1-2. 44 mm. Figure 29, ×200. Figure 30, ×500 (blocked area). *A*, entering nerve; *B*, ramifying nerves; *C*, islands of multiplying chromaffin cell precursors.

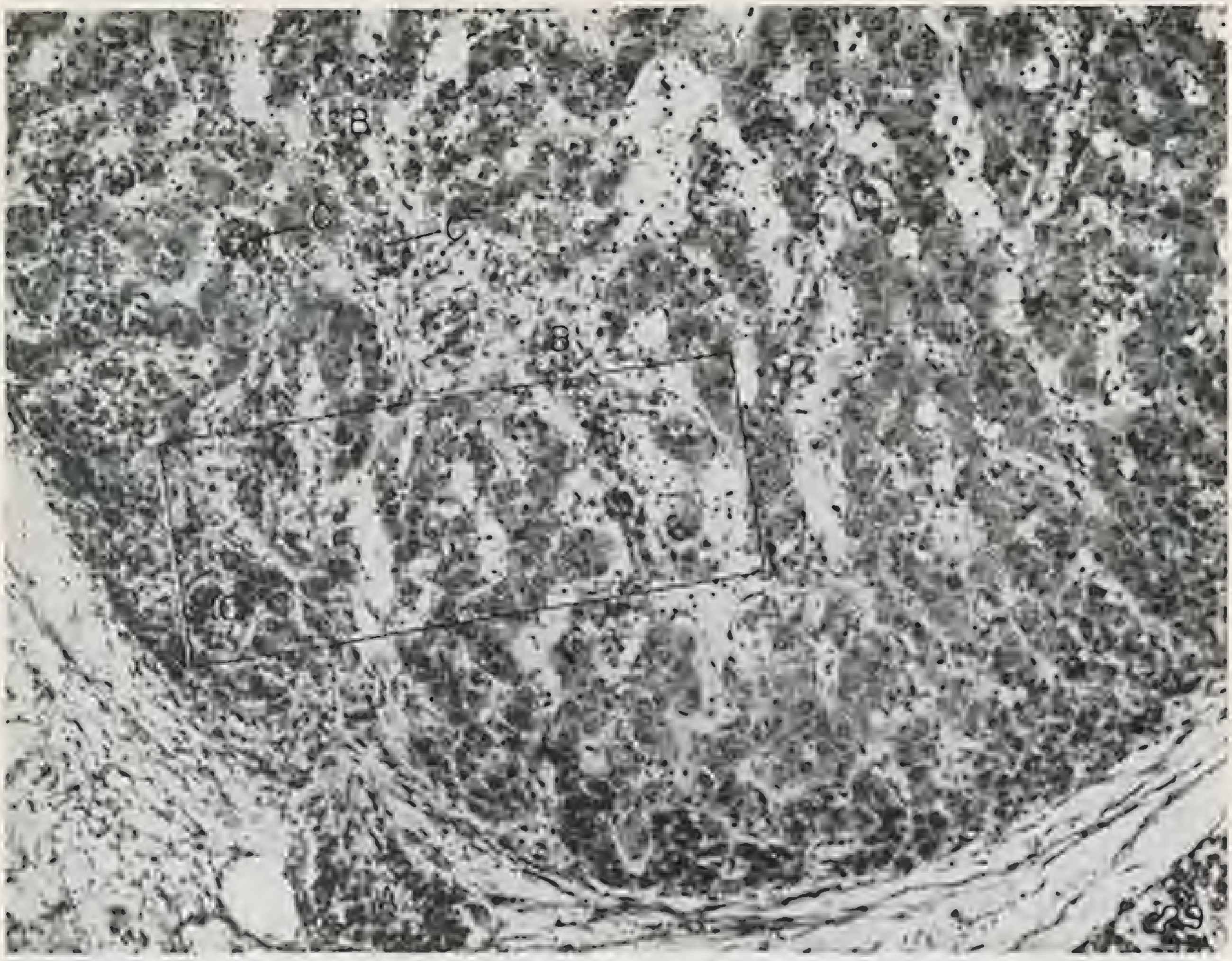

29

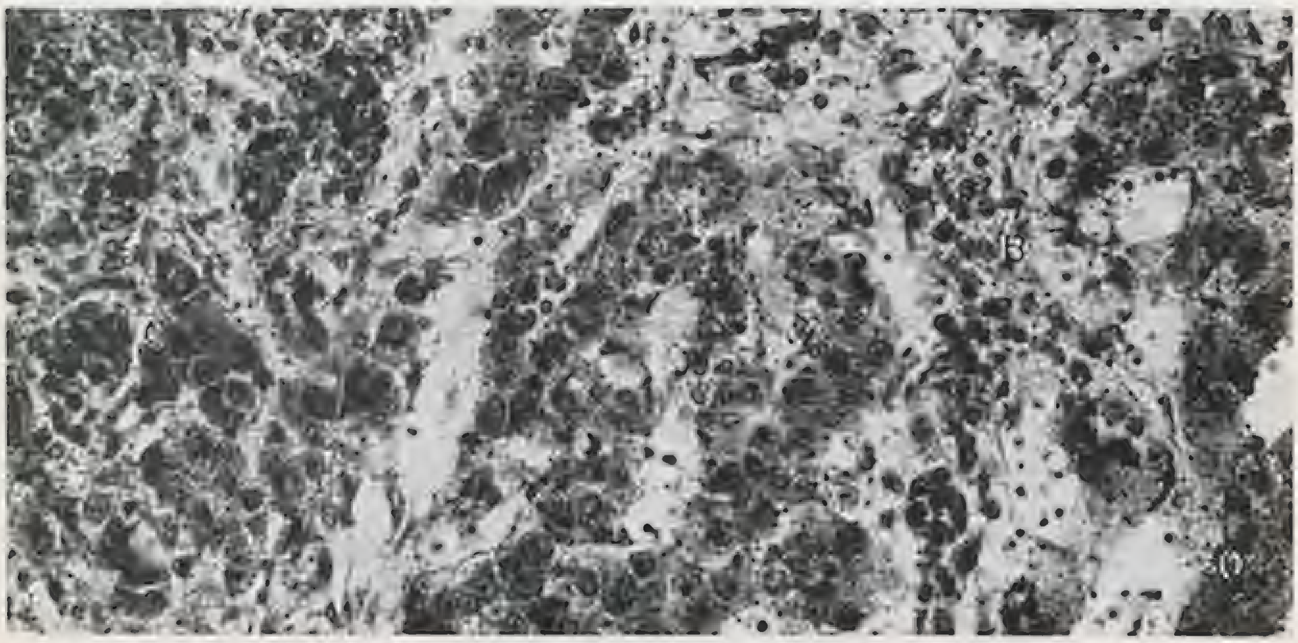

30

PLATE 7

FIG. 31. India-ink injection. Right adrenal vein (*A*) emptying into the inferior vena cava (*B*). The poorly organized venous system at this stage is clearly shown. No central vein can be demonstrated, but the outlines of the irregular main channels can be seen. The central portion is much darker than the outer zone, because of the rich blood supply in the capillaries between the cords of cells centrally and the relative anemia of the poorly vascularized glomerular area. At each side and dorsal to the aorta (*C*), the three splanchnic nerves (*D*). Sympathetic chain ganglia (*E*) are on each side of the body of the vertebra (*F*). No. 4415, 106-1-3. ×25. 37 mm.

FIG. 32. The adrenal is cut horizontally in the middle third of the gland. The wide glomerular or germinal zone (*A*) around the outside of the gland is composed of embryonal cells actively dividing. Immediately central to it is the fetal fasciculoreticular zone (*B*). The three collateral veins (*C*) drain the blood from the sinusoids and join to form the adrenal vein at a lower level. A process of degeneration (*D*), further illustrated in figures 33 and 34, is found only at this stage of fetal development. No. 84, 51-2-1. ×25. 54 mm.

FIG. 33. Boxed area in figure 32, localizing the condition found in figure 34.

FIG. 34. At a magnification of 500 diameters is shown a form of cell degeneration found during the formation of the collateral veins. After this stage, the area in which the degeneration took place is occupied by large blood sinuses.

FIG. 35. Section near the upper pole of the gland of an 80-mm. embryo. The descending collateral vein (*A*) has been cut across. The dark areas (arrows) are groups of rapidly proliferating neural cells, part of a network scattered through the cortex, which form and contain the chromaffin cells. (See also fig. 37, pl. 8.) No. 172, 50-2-1. ×25.

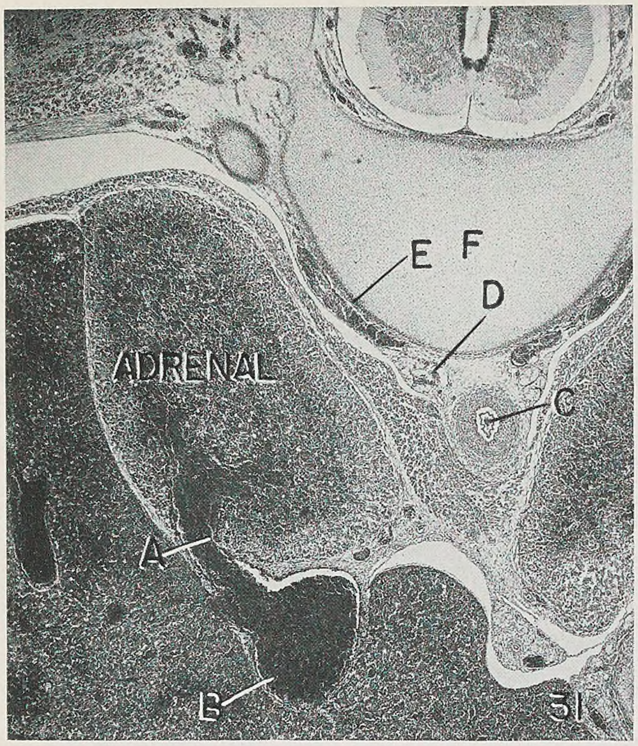
ADRENAL
E
F
D
C
A
B
31

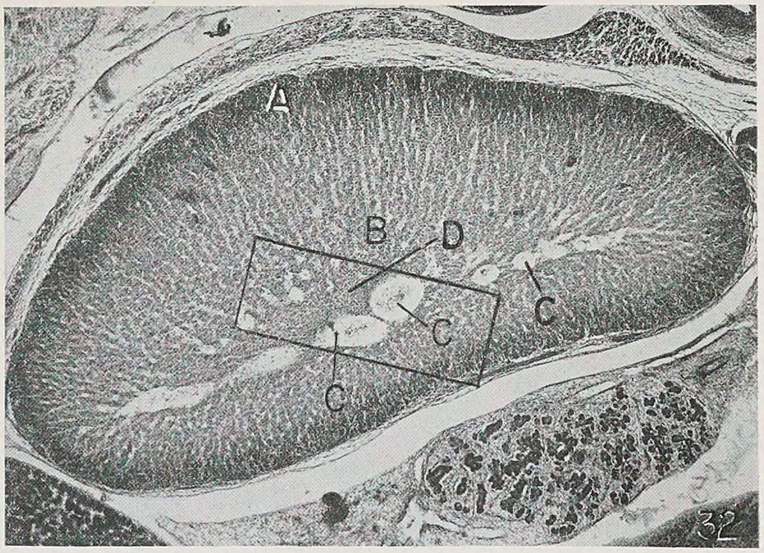
A
B
D
C
C
C
C
32

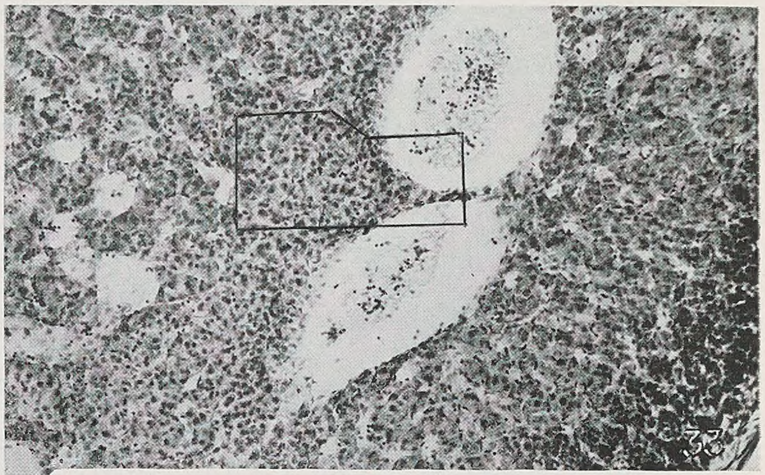
33

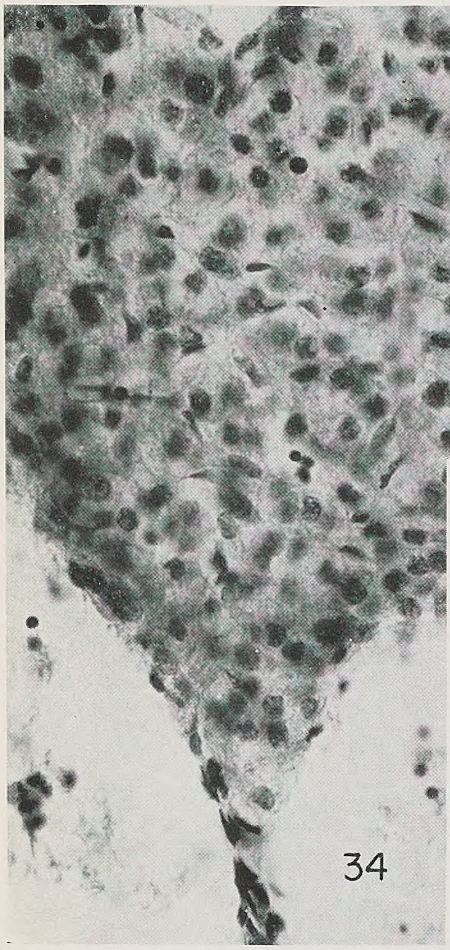
34

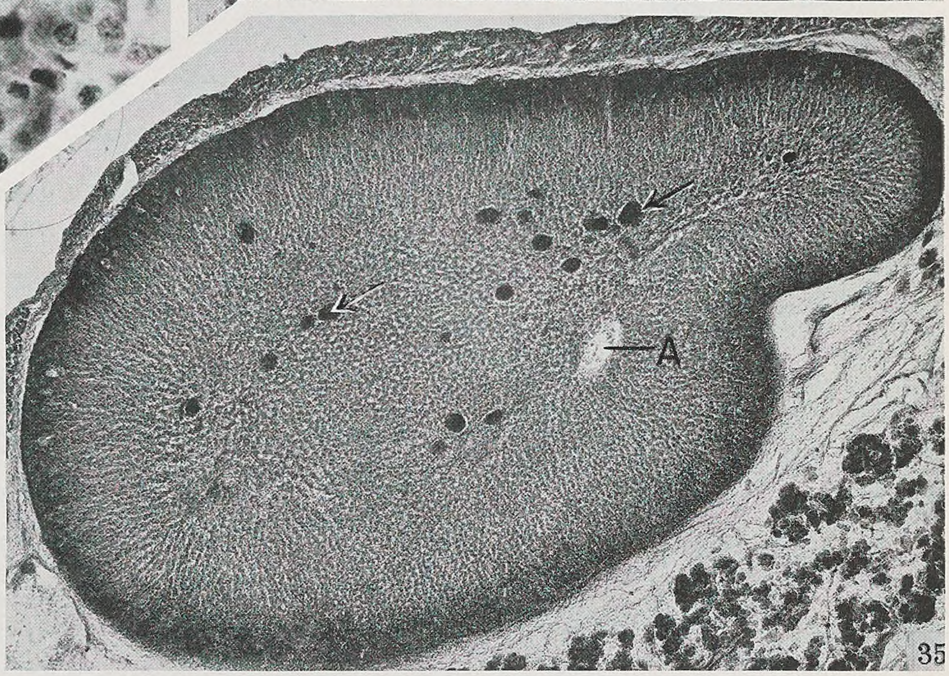
A
35

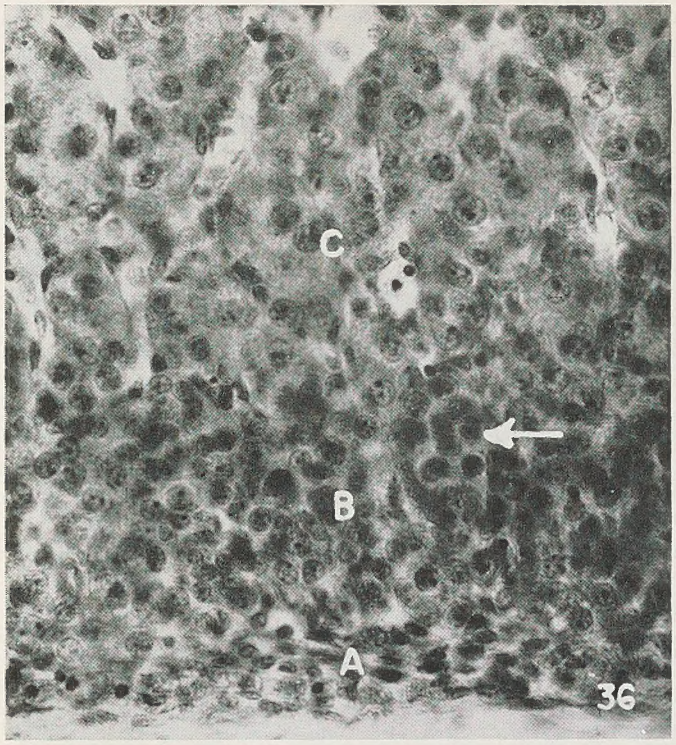

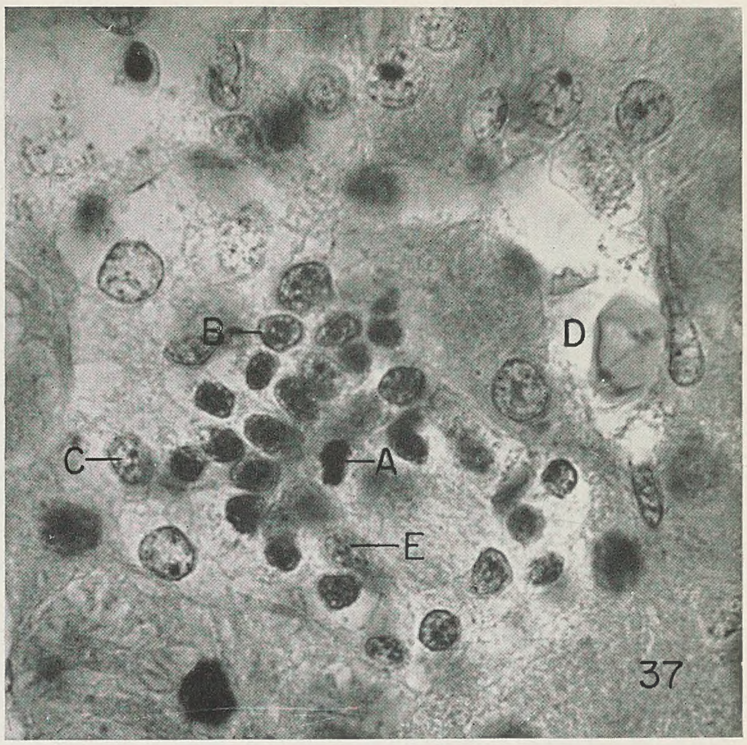

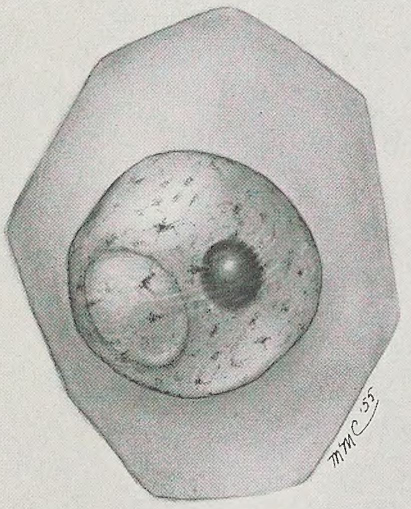

Fig. 38

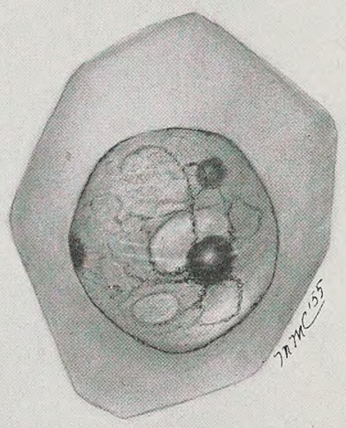

Fig. 39

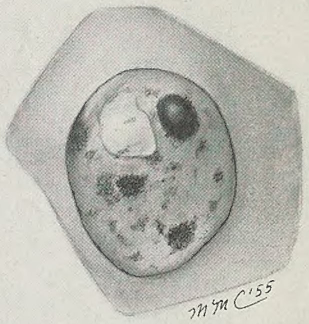

Fig. 40

Fig. 36. From the surface of a gland, about 8 weeks. The capsule (*A*) is along the lower border. The glomerular zone (*B*) is between it and the fasciculoreticular zone (*C*) at the top. The arrow indicates a group of capsule cells oriented toward the center of the gland. No. 6658, 59-1. ×500. 40 mm.

Fig. 37. Section through a nest of paraganglion cells, showing the various stages of development of the chromaffin cells from mitosis (*A*) to maturity (*D*); *E* is the undifferentiated type M-III cell from which all others are derived. No. 9226, 163-2-5. Horizon xxiii. ×1000. 30.1 mm.

Figures 38–40 are drawings of the three types of cells derived from the capsule and the glomerular zone of the adrenal of the embryo in figure 36. These cells are not limited to the fetal stages of development but are found in all adrenals examined. Nor are they species specific, having been found in all mammalian glands so far examined. The nuclei retain the characteristics of the cell type they represent until the cells' final dissolution; differentiation of cell types is based on these characteristics. Cells illustrated were found in the reticulofascicular zone.

Fig. 38. Cell type C-I, characterized by the larger size of both cytoplasm and nucleus. The nucleus is round and relatively clear; the nucleolus spherical, usually slightly eosinophilic, and eccentrically placed. The scanty chromatin is loosely disposed in fine threads and small knots. The center is occupied by a vacuole in usual paraffin-embedded material. It stains with Sudan III in frozen sections and in material chromated after fixation in an aqueous mixture. The sex chromatin was not included in this section but is shown in the other two.

Fig. 39. Type C-II cell. As a rule, there is one nucleolus and a small condensation of sex chromatin on the nuclear membrane in the female. The chromatin is distributed in threads just beneath the nuclear membrane in a spider-like formation, the nucleolus forming the body. The center of the nucleus contains two or more ovoid lipoid globules.

Fig. 40. Type C-III cell is much smaller and has a smaller nucleus than either of the other two. The nucleolus is more centrally placed, and the nucleus is much darker. The chromatin is greater in amount and condensed into large clumps. The strands are very coarse. Three or more large clumps of chromatin are irregularly disposed throughout the nucleus. The lipoid globule is eccentrically placed and usually is somewhat irregular in outline.